Regional geology of the Southern Smithton Synclinorium

Explanatory Report for the Roger, Sumac and Dempster 1:25 000 scale geological map sheets, far northwestern Tasmania

Department of Infrastructure, Energy and Resources
Mineral Resources Tasmania

Tasmania
Explore the possibilities

Mineral Resources Tasmania
Department of Infrastructure, Energy and Resources

Tasmania
Explore the possibilities

1:25 000 Scale Digital Geological Map Series
— Explanatory Report 2 —

Regional geology of the Southern Smithton Synclinorium

Explanatory Report for the Roger, Sumac and Dempster 1:25 000 scale geological map sheets, far northwestern Tasmania

by J. L. Everard, D. B. Seymour, A. R. Reed, M. P. McClenaghan, D. C. Green and C. R. Calver

September 2007

ISBN 0 7246 4019 3

Mineral Resources Tasmania PO Box 56 Rosny Park Tasmania 7018
Phone: (03) 6233 8377 ● Fax: (03) 6233 8338
Email: info@mrt.tas.gov.au ● Internet: www.mrt.tas.gov.au

Cover: *Arthur River about one kilometre upstream of the Julius River confluence (336 100 mE, 5 446 400 mN), looking southwest: undercut cliff outcrop of shallowly-dipping Black River Dolomite. The crag is capped by Julius River Member diamictite.*

CONTENTS

FIGURES

PLATES

TABLES

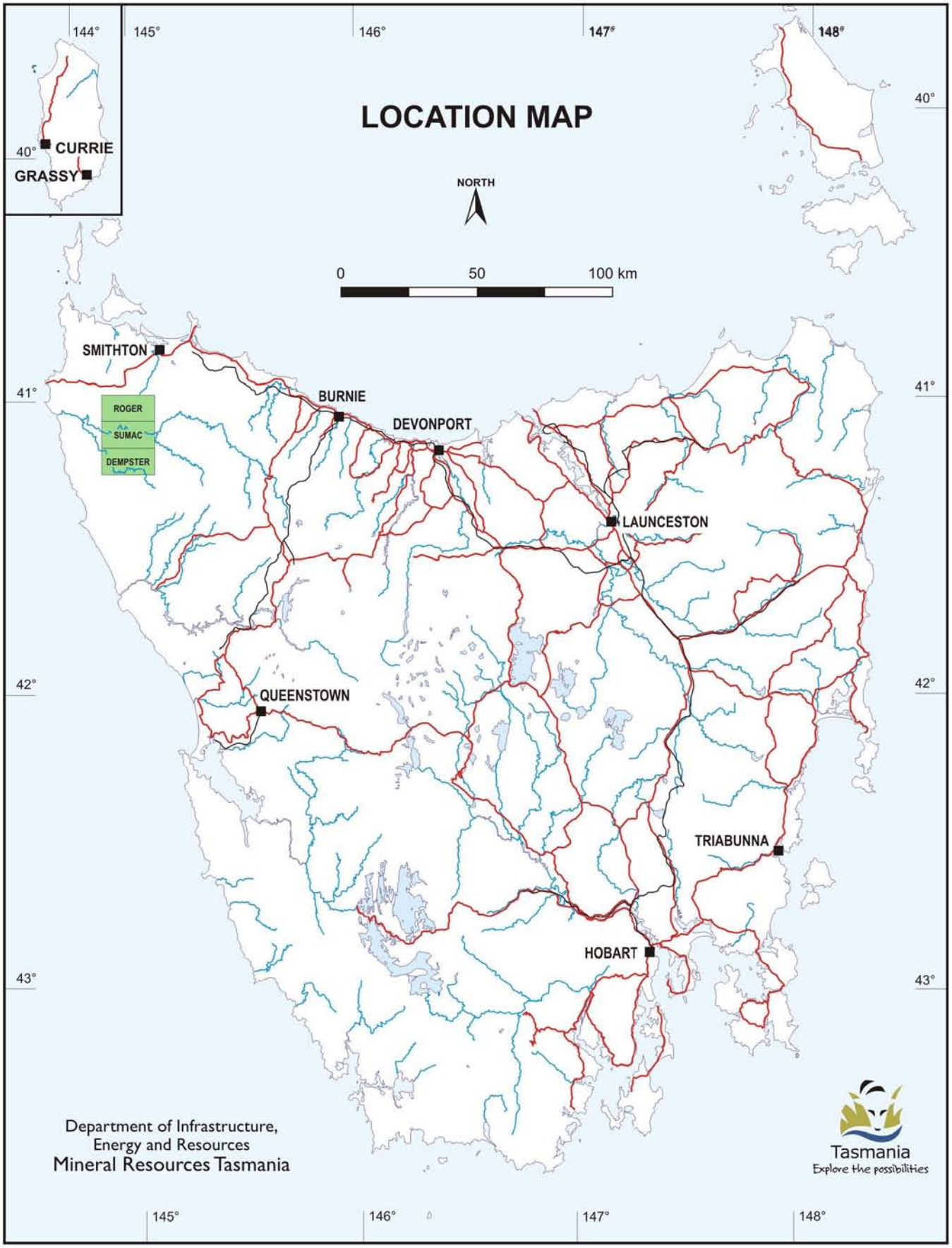
LOCATION MAP
NORTH
0
50
100 km
144°
145°
146°
147°
148°
40°
41°
42°
43°
CURRIE
GRASSY
SMITHTON
BURNIE
DEVONPORT
LAUNCESTON
ROGER
SUMAC
DEMPSTER
QUEENSTOWN
TRIABUNNA
HOBART
Department of Infrastructure,
Energy and Resources
Mineral Resources Tasmania
Tasmania
Explore the possibilities

Summary

The area covered by the Roger, Sumac and Dempster 1:25 000 scale geological map sheets includes part of the Smithton Synclinorium, a complex structure resulting from Proterozoic extension and Palaeozoic compression, and which is flanked and underlain by an early Neoproterozoic shelf sequence, the Rocky Cape Group. Within the synclinorium, a late Neoproterozoic to Early Cambrian shelf and rift sequence, the Togari Group, and overlying Middle to Late Cambrian lithic sandstone are preserved. Two early phases of syndepositional extension were followed by at least four compressional phases of deformation, the latter probably in both Cambrian and Devonian times. The only younger units present are Tertiary basalt and unconsolidated Cainozoic sediments.

Three major, wholly siliciclastic units of the Rocky Cape Group are present. The shallow marine Lagoon River Quartzite consists of cycles of trough cross-bedded quartz sandstone grading up into variably carbonaceous siltstone and shale. It is faulted against the younger Balfour Subgroup, which is about 3500 m thick and has been divided into four formations. Diverse lithologies include planar to wavy laminated and cross-bedded siliceous sandstone and siltstone, carbonaceous pyritic siltstone and shale, quartzite and green chloritic siltstone. These were probably deposited on a marine shelf near storm wave base. Clastic dykes, channel structures and (near Temma) growth faults suggest some extensional deformation during deposition of the Balfour Subgroup. In contrast, the conformably overlying hemipelagic Cowrie Siltstone is typically a monotonous planar bedded, thinly laminated, flaggy to fissile, black to paler weathering, locally pyritic and carbonaceous siltstone, with few current-generated sedimentary structures. The Cowrie Siltstone consists dominantly of quartz, sericite, detrital muscovite and carbonaceous material in variable proportions. Minor chlorite may be present.

Although younger units are present within the Rocky Cape Group further east, in this area the Cowrie Siltstone is overlain by the Togari Group with low angle unconformity or disconformity. This hiatus may be related to the Wickham Orogeny (c.760 Ma) on King Island, or alternatively be the result of block rotation ('roll-over') above listric extensional faults coeval with the onset of Togari Group sedimentation.

The basal unit of the Togari Group, the Forest Conglomerate and Quartzite, is impersistent and variable in thickness (0–120 m) in this area. Rather than the well rounded quartzite pebble-cobble conglomerate found in the north of the synclinorium, here it normally consists of an open framework chert breccia interbedded with stratified pebble conglomerate and medium-grained, locally hematitic quartzarenite. The clasts mostly resemble chert of the Black River Dolomite, and Rocky Cape Group derived clasts are usually subordinate, whereas the matrix is quartzarenite.

The Black River Dolomite, which commonly directly overlies the Rocky Cape Group, thickens from 250 m in the west of the synclinorium to 600–800 m in the east. It consists of a variety of shallow-marine dolostone types, together with thin interbeds of massive to banded, white to black chert, flaggy black siliceous siltstone, and pelitic and locally carbonaceous mudstone. The unit contains domical stromatolites and vase-shaped microfossils resembling chitinozoans. These, together with isotope chemostratigraphy, suggest a mid-Neoproterozoic age (c.750–650 Ma: Calver, 1998).

Towards the top of the Black River Dolomite, a very poorly sorted matrix-supported conglomerate (diamictite) consists of sparse to abundant angular to subrounded clasts of dolomite and chert in a dark grey dolomitic mudstone matrix. This unit, the Julius River Member, may be a mass-flow deposit, or alternatively a tillite correlating with the Sturtian glaciation. No definitive glaciogene features have been found.

The overlying Kanunnah Subgroup (c.650–575 Ma) was deposited during a period of marked basin instability, including syndepositional extensional faulting. It varies in thickness from 220–800 m, west of the major NNE-trending Roger River Fault, to up to 1400 m to the east, and consists of three interdigitating formations; the Keppel Creek Formation, the Croles Hill Diamictite and the Spinks Creek Volcanics. A rhyodacite flow on the north coast, outside the area of this report, has been dated at 582 ± 4 Ma (Calver *et al*., 2004).

The Keppel Creek Formation consists mainly of thin-bedded, cuboidally-weathering lithic sandstone and siltstone, with rare conglomerate, impure dolomite and mudstone. Clast and grain types are mainly basaltic and of local provenance, but also include felsic volcanic rocks, chert, carbonate, orthoquartzite, feldspar, clinopyroxene, chlorite, iron-titanium oxides, spinel and strained metamorphic quartz. A distinctive hematitic alteration, locally grading to ironstone, may be present, particularly near basalt.

The Croles Hill Diamictite is a massive, very poorly sorted diamictite which normally occurs below the Spinks Creek Volcanics, particularly in the south of the area. It is composed of angular clasts of basalt and subordinate felsic volcanic rocks, dolomite, chert, picrite, and clastic sedimentary rocks in a matrix of basalt-derived mudstone. Rare, associated laminated siltstone with lonestones suggests a glacial influence, although extrabasinal clasts are lacking. The Croles Hill Diamictite immediately overlies the dated rhyodacite (582 ± 4 Ma) on the north coast, suggesting a possible correlation with the c.580 Ma Gaskiers glaciation (Calver *et al*., 2004).

The Spinks Creek Volcanics occurs mainly towards the top of the Kanunnah Subgroup and is thickest east of the Roger River Fault. This formation consists mainly of massive to locally pillowed, usually fine-grained,

dominantly tholeiitic basalt with sparse plagioclase ± clinopyroxene ± olivine phenocrysts, metamorphosed up to the prehnite-pumpellyite or, rarely, greenschist facies. Together with minor associated subvolcanic intrusive rocks, the Spinks Creek Volcanics can be subdivided into at least seven tightly defined geochemical groups on the basis of parameters such as TiO_2, Nb/Zr, Mg# and REE patterns. Each group has a distinct regional distribution and stratigraphic position, and probably represents a discrete volcanic episode, triggered by the influx of fresh magma from various mantle sources into fractionating crustal magma chambers. The detailed geochemistry of tholeiitic dolerite dykes that intrude the Rocky Cape Group shows that they cannot represent feeders for the Spinks Creek Volcanics, although they may be broadly part of the same Neoproterozoic rifting episode.

The Smithton Dolomite is about 1500 m thick. In contrast to the Black River Dolomite, stromatolitic textures are absent and intercalated chert or clastic sedimentary beds are rare, although late silicification has led to local development of agate. The lower third of the formation consists of commonly thin-bedded fine-grained dolostone with minor coarser dolostone and limestone, while the upper two-thirds is massive crystalline dolostone and minor limestone. The unit is unfossiliferous, but isotope chemostratigraphy suggests a middle to late Ediacaran age (about 575–545 Ma: Calver, 1998).

The Salmon River Siltstone, locally preserved at the top of the Togari Group, comprises up to 350 m of pale to dark grey, thin-bedded to thinly planar-laminated siliceous siltstone, mudstone and shale. Inarticulate brachiopods and siliceous sponge spicules suggest an Early to Middle Cambrian age.

In the north of the area the Togari Group is overlain, with inferred unconformity, by the Scopus Formation, which consists of polymict conglomerate, lithic sandstone and siltstone/mudstone. In this area the formation contains a much greater proportion of ultramafic-derived detritus (including chrome spinel) than in previously mapped areas further north, from where Middle to Late Cambrian marine fossils have been described (Jago, 1976; Baillie, 1981).

The earliest phase (D_1) of compressional deformation has been identified from microstructures in Rocky Cape Group rocks mainly south and west of the Smithton Synclinorium, but it probably also affected the Togari Group and may be of Cambrian age.

Gently west-plunging north-vergent folds just to the south of the Smithton Synclinorium are provisionally assigned to the second deformation event (D_2). Further north, deformation of possible D_2 age is expressed as gently east or west-plunging open upright folds affecting the Togari Group east of the Roger River Fault, and adjacent areas of the Rocky Cape Group. Definite D_2 cleavage and coeval porphyroblast growth are locally present in the Rocky Cape Group west of the Smithton Synclinorium.

East of the Roger River Fault, the Togari Group and Rocky Cape Group are affected by a prominent set of upright northeast to NNE-trending folds with associated steep cleavage, which increase in intensity and become strongly southeast-vergent eastward towards the Arthur Lineament. Overprinting relationships, which are still equivocal at the current state of knowledge, suggest that these folds may be post-D_2 and pre-D_3 in relative age. Recent research in the Arthur Lineament (Holm and Berry, 2002) indicates that this phase of folding is Cambrian in age but post dates the two main metamorphic events associated with the c.510 Ma Tyennan Orogeny.

D_3, the main deformation west of the Roger River Fault, was a complex episode expressed mainly as northwest-trending, northeast-vergent folds and associated major northeast-directed thrust faulting, which disrupted and partly inverted the stratigraphy of both the Rocky Cape and Togari groups. One thrust hosts copper vein mineralisation in a breccia zone (Murrays Reward). Late-D_3 dextral transpressional reactivation of the Roger River Fault rotated nearby D_3 fold trends clockwise to almost north–south. East of Balfour, ENE to northeast-trending strike-slip faults pre-date late northwest-trending reverse faults, one of which hosts disseminated Sn-W mineralisation at Specimen Hill. In turn these are truncated and variably offset by northeast to ENE-trending splays of the Roger River Fault, which probably formed as transfer structures. Syn- to late-D_3 relationships of possibly granite-related contact metamorphic mineral assemblages suggest that D_3 is of Devonian age, although this interpretation remains somewhat equivocal.

D_4, also probably of Devonian age, is expressed mainly as open upright north-trending folds in the Scopus Formation in the core of the Smithton Synclinorium. It is also evident as minor folds of similar orientation, with associated cleavage, that overprint D_3 structures in the Rocky Cape and Togari groups, and as steeply east-dipping reverse faults near Temma.

A thin discontinuous blanket of gravel, quartz sand and clay, probably Tertiary and alluvial in origin, occurs mainly in the west of the area, usually overlying the Smithton Dolomite or Rocky Cape Group. The gravel is mostly closed-framework, and typically consists of well-sorted and rounded, sometimes aligned or imbricate, pebble to cobble-sized clasts of quartzite in a quartz sand matrix, locally cemented by silica. In places it is stratified, and grades to quartz sand, peaty sand (rarely with plant fossils), silica flour and clay.

Tertiary basalt occurs mostly as thin hill cappings in the south of the area. These are probably the dissected remnants of an extensive series of flows that once covered much of the region. Chemically the basalts are mostly moderately fractionated and range from strongly alkalic types (including a possible basal flow of basanite), through alkali olivine basalt and hawaiite, to transitional olivine basalt and tholeiite. An unusual

strongly fractionated potassic nepheline mugearite at Molompto Road contains spinel lherzolite xenoliths and may be an unrelated small plug.

Large tracts of alluvium and swamp deposits are developed on most areas underlain by Smithton Dolomite and, less commonly, Black River Dolomite. Other Quaternary deposits are limited in extent but include chert lag (overlying Black River Dolomite) and rare talus.

Small copper and tin-tungsten vein prospects, and associated tin placers, are known, mainly in the south of the area. These represent the northern end of a NNW-trending linear belt of similar deposits, about 35 km long and mostly less than 2 km wide, extending from The Clump to the Toner River area. The belt is roughly co-extensive with both a major shear zone in the Rocky Cape Group and a series of magnetic anomalies. The deposits consist of veins, fracture and breccia-fillings, replacements, disseminations and semi-massive pods occupying dilational zones such as fault splays and vein intersections, hosted by pyritic, carbonaceous and/or chloritic slate and siltstone. The primary mineralogy, although rarely seen due to severe leaching, is simple and consists of chalcopyrite, quartz ± pyrite ± carbonate ± chlorite. The largest producer, Murrays Reward (just south of the report area), contained pods of high-grade supergene enriched ore (mainly covellite and digenite). Geological and geochemical evidence, together with reconnaissance isotopic and fluid inclusion studies, suggest that the deposits were formed by metamorphic, late granitic and/or meteoric fluids that dissolved and transported copper and were focussed into faults. The source of the copper is speculative but may have been older, sediment-hosted deposits (Taheri and Bottrill, 2004).

Tin mineralisation (cassiterite-wolframite-quartz-pyrrhotite-arsenopyrite-tourmaline-chalcopyrite-pyrite) is also fracture controlled and overlaps with a segment of the copper belt, but is spatially restricted to within two kilometres of the main deposit at Specimen Hill. Together with fluid inclusion studies, this distribution indicates that tin was deposited from fluids emanating from underlying Devonian granite, inferred from gravity surveys, and is probably unrelated to nearby copper mineralisation (Taheri and Bottrill, 2004).

The area is prospective for further discoveries of small high-grade vein deposits, or magnetite lodes such as at Nelson Bay River. Exploration models for much larger sediment-hosted copper, lead-zinc and tin-tungsten deposits may be applicable, and there is also potential for larger granite-related tin-tungsten sheeted vein systems. Known potential also exists for industrial minerals, notably chromite, silica, dolomite and slate.

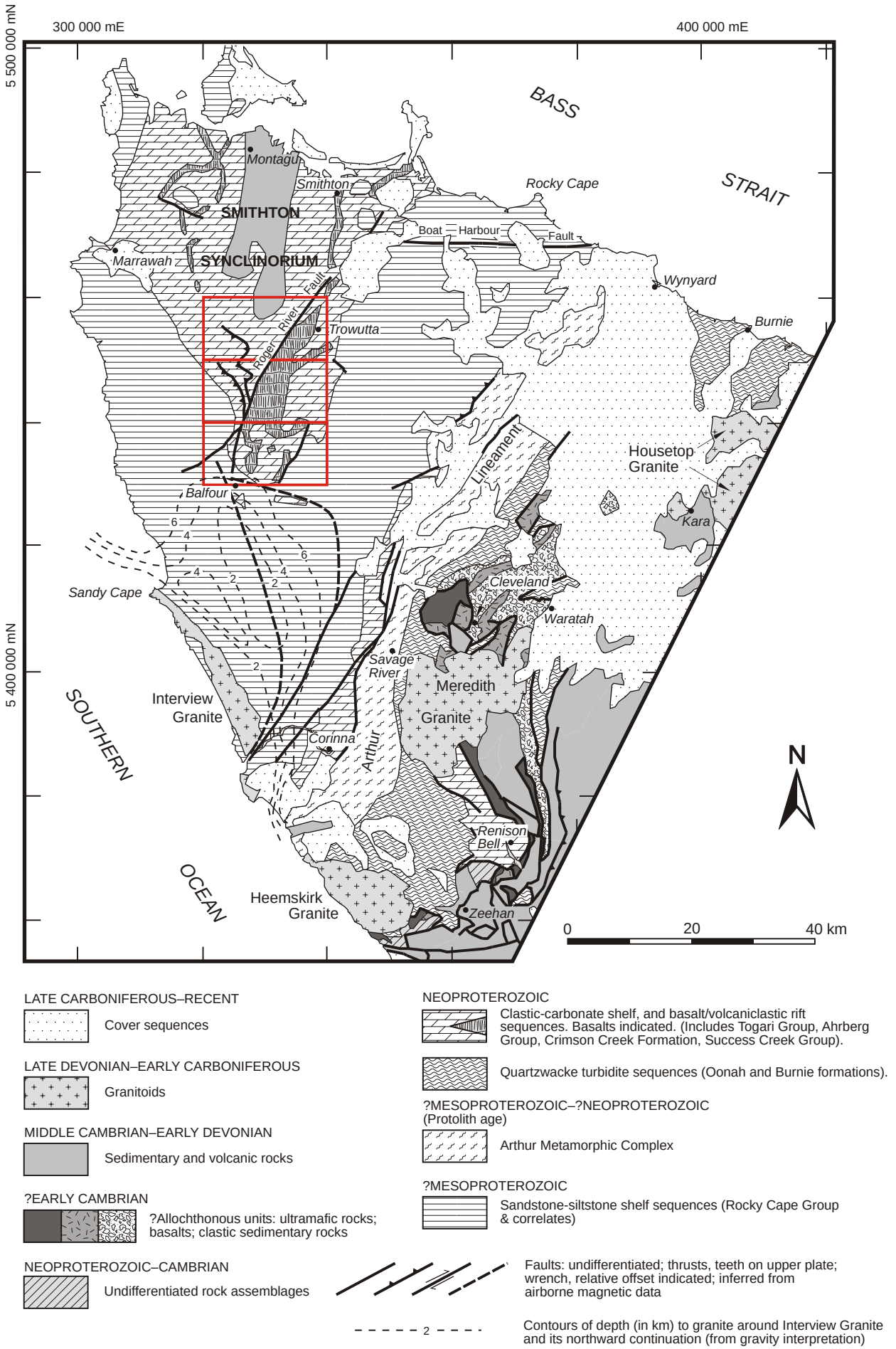

Figure 1

Location map showing simplified regional geology.

Location and scope

This report describes the regional geology of a 600 km^2 tract of northwestern Tasmania (fig. 1, 2, 3), bounded by Australian Map Grid (AMG) lines 5 430 000 mN, 5 460 000 mN, 320 000 mE and 340 000 mE. This area comprises the Roger (to the north), Sumac (middle) and Dempster (to the south) 1:25 000 scale geological map sheets.

Approximately the eastern third of the area covered by Roger, Sumac and Dempster map sheets (east of longitude 145°E, approximately 332 000 mE) overlaps with previously published geological mapping of the Trowutta 1:50 000 scale quadrangle (Everard *et al*., 1996). The northern margin of the Roger map sheet overlaps slightly with previously published mapping of the Smithton and Woolnorth 1:50 000 scale quadrangles (Lennox *et al*., 1982; Seymour and Baillie, 1992).

Field work commenced in 1986, initially for the Trowutta 1:50 000 scale map sheet (Everard *et al*., 1996). Calver and Everard (1992*a*, *b*) commenced investigations in the adjacent Bluff Point quadrangle (not published as a 1:50 000 scale sheet) with a traverse across the Smithton Synclinorium along the Arthur River. This work highlighted the stratigraphy of the Togari Group and suggested that it was disrupted by major thrusting in the western part of the synclinorium. The remainder of the Roger and Sumac map sheets was mapped in the summer of 1995/96, and the Dempster map sheet in 1997/98, by the present authors.

The southern margin of the Dempster sheet lies on the Magnet and Balfour quadrangles, which were not published as 1:50 000 scale geological map sheets.

This report also describes some observations made on Togari Group rocks in the east of the Smithton Synclinorium, which fall on immediately adjacent areas of the Tayatea and Holder 1:25 000 scale map sheets and within the Trowutta 1:50 000 scale quadrangle.

Nomenclature and grid references

Rock unit mnemonics quoted in the text are applicable to hardcopy 1:25 000 scale geological maps produced after January 2001, following a major translation of existing mnemonics to integrate more fully with the mnemonic system used on MRT 1:250 000 scale digital geological maps. Hardcopy 1:25 000 scale geological maps produced prior to January 2001 may contain superseded mnemonics for some rock units.

Rock samples are stored in the Mineral Resources Tasmania collection at Mornington. Sample numbers quoted in the text are almost exclusively current-series MRT registered sample numbers (in the form R004286). Some tables and figures also quote current-series MRT registered geophysical samples (format G401349), previous-series MRT registered rock samples (format 85/0081; first two digits are year of registration), AGSO registered samples (format 93220001; first two digits are year of registration), or samples with field numbers only (various formats with capital letter prefixes). Registered and field numbers are clearly distinguished in the tables. All new samples collected for this project are listed in Appendix 6, which shows current-series MRT registered sample numbers, corresponding field numbers, AMG locations and other information.

Clastic sedimentary rocks are classified as:

- conglomerate (mean grain size >2 mm);
- sandstone (coarse grained with mean grain size 2 mm–500 μm, medium grained 500–250 μm, fine grained 250–125 μm, very fine grained 125–62 μm);
- siltstone (coarse grained 62–31 μm, medium grained 31–16 μm, fine grained 16-8 μm, very fine-grained 8–4 μm), and
- mudstone (<4 μm).

Rock colours quoted are ISCS-NBS names used on the Geological Society of America Rock Color Chart (1991 edition).

Thirteen new stratigraphic names are formally defined herein, although some have been previously used on published maps (e.g. Everard *et al*., 1996).

The grid datum used in this report is the currently used Australian Geodetic Datum 1966 (AGD66), and all locations quoted in the text are full AMG coordinates relative to this datum. Grid references quoted in this report are in the form xxxxxx/yyyyyyy, where the first six numbers are metres east and the last seven numbers are metres north.

To convert co-ordinates to the Geocentric Datum of Australia (GDA94), which is currently being introduced, it is necessary to add 111 m to the easting and 183 m to the northing. Thus Kanunnah Bridge (330 620 mE, 5 446 340 mN) would lie at 330 731 mE, 5 446 523 mN under GDA94.

Access

The northern limit of the area (fig. 2) is located about 17 km south of the town of Smithton. Most areas north of the Arthur River are readily accessible by several sealed roads and a good network of unsealed minor roads and forestry and farm tracks. South of the Arthur River access is by two partially sealed major forestry roads, Blackwater Road and Sumac Road, which extend down the western and eastern sides of the area respectively. Although both have numerous minor spur roads, there is a large tract of densely vegetated country between them with no roads, mainly on the Dempster map sheet. This area was mapped by long day traverses from the roads, and from camps at the end of two purpose-cut walking tracks, the locations of which can be obtained on request. A forestry road

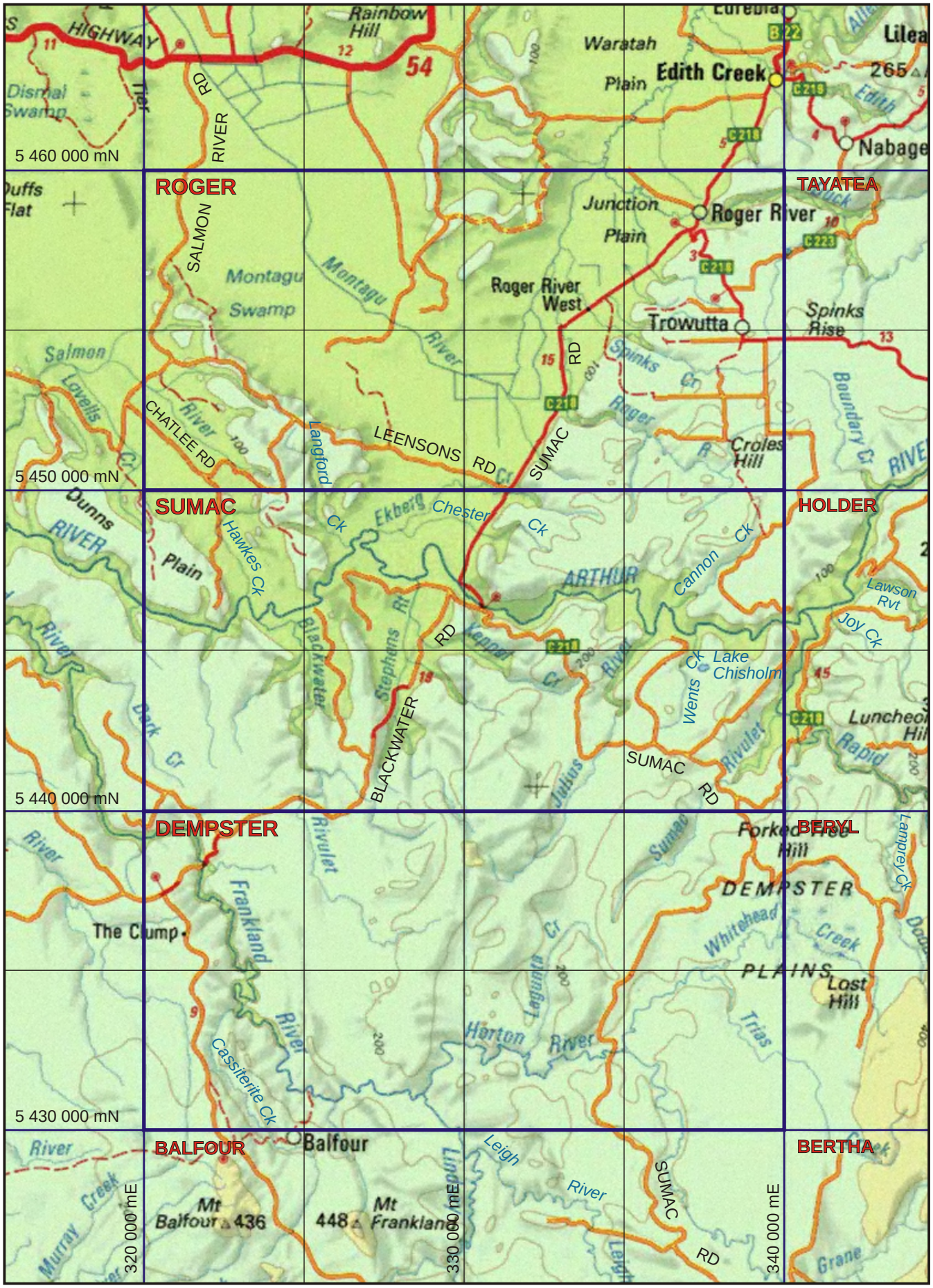

Figure 2

Topographic map of report area, showing some place names mentioned in text.

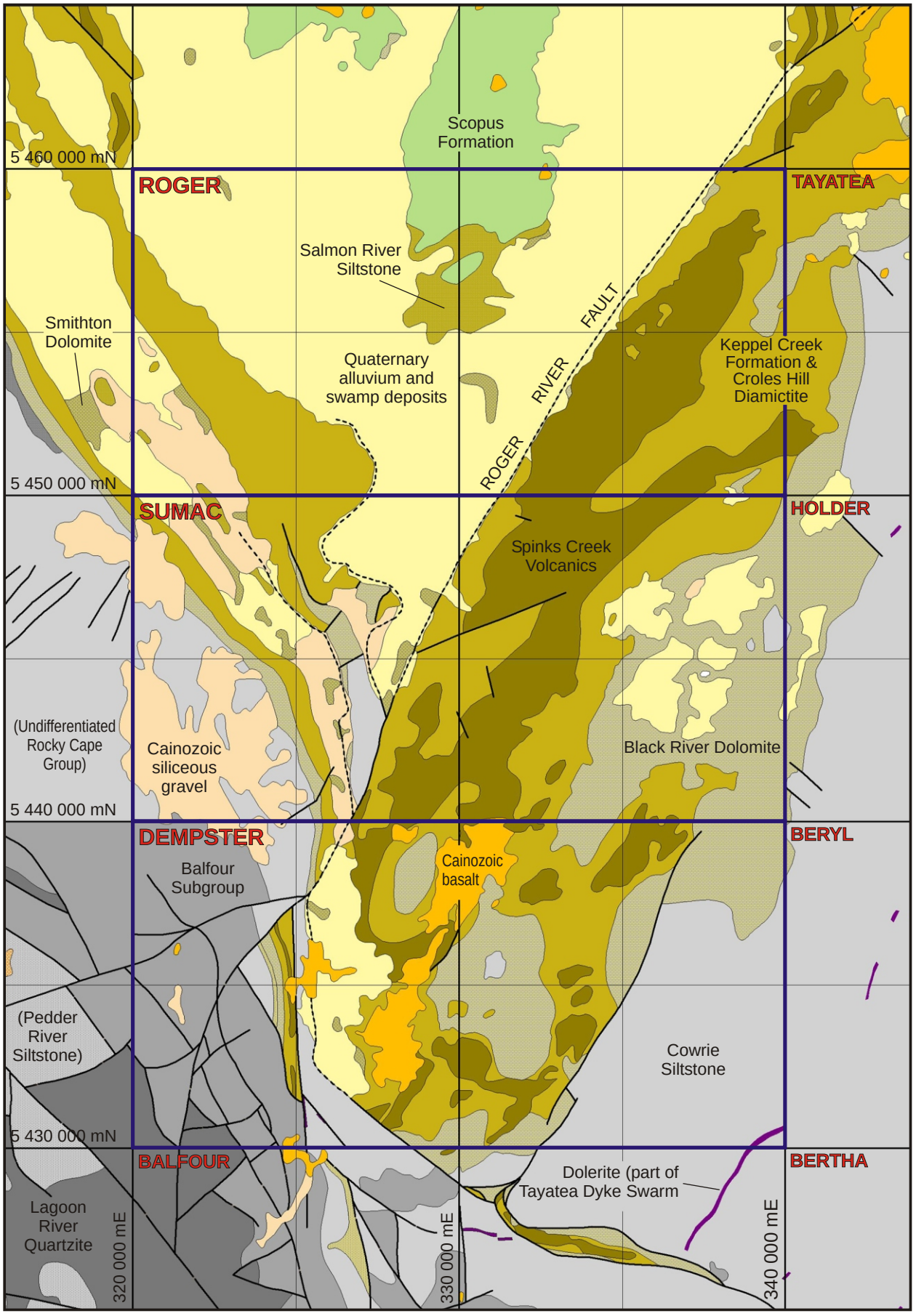

Figure 3

Simplified geological map of report area, adapted from MRT 1:250 000 scale digital data (Calver et al., 1995 as updated to 2006), showing geological units (labelled), faulted contacts (heavy), concealed faults (dotted lines), 1:25 000 scale map sheet names and five kilometre grid. The Forest Conglomerate and Quartzite (black dots on pale khaki background) and unassigned quartzite (white dots on dark grey background) are not labelled.

recently constructed southward from near 324000/5440000 has since improved access to part of this area.

Progress in densely vegetated areas may be as slow as 500 m per hour, and 2–3 km from a point of access, such as a road or cut track, is the limit of attainability by day traverses.

The old pack-saddle track to the Balfour township passed through the middle of the area, but has long been completely overgrown except for two sections. One has been rehabilitated as a tourist walk in the Balfour Forest Reserve. The other, a former vehicular track, now only walkable, provides access from Balfour to the Frankland River at the former suspension bridge site at 325120/5431350. The track continues north on the opposite side of the river but is traceable for less than a kilometre.

The Frankland, Horton and Lindsay rivers are generally wadeable, but crossing them or even smaller streams (such as Blackwater Rivulet) may be difficult or impossible after heavy rain. The Arthur River is difficult to cross in many places, even at low river levels. During mapping, most of the Horton, Frankland and Arthur rivers were traversed using an inflatable raft.

Land use and tenure

The small farming communities of Roger River and Trowutta, in the northeastern part of the area, are the only permanent settlements (fig. 2). Dairying, beef cattle and limited cropping are the main activities on the surrounding areas of mostly cleared private land, which largely lie on the Roger map sheet. Agricultural land extends to the north bank of the Arthur River around 328000/5447300. Some land in the northeast of the Sumac map sheet, mostly to the north of the Arthur River, has been subdivided but remains uncleared and mostly Crown Land.

To the west (around Montagu Swamp) and to the south (beyond the Arthur River) extensive forestry is currently the main economic activity, apart from bee-keeping and limited tourism. Most of this country is State Forest, but small areas have been set aside for recreation and conservation at the Balfour Track, Lake Chisholm and Julius River Forest reserves. Recently, as a result of the Regional Forest Agreement, a larger area lying between the Sumac and Blackwater roads and the Horton and Frankland rivers has been proclaimed as the Sumac Forest Reserve.

Dempster Plains has been used for rough grazing, and a dilapidated cattle ramp is present on the Sumac Road (near 338500/5437800).

The southwest edge of the area, in more open country near the western edge of the Dempster map sheet, is within the Arthur-Pieman Protected Area. The former mining town of Balfour, which was in its heyday around 1911, lies at the extreme southern edge of the Dempster map sheet, and now consists of a few shacks with no permanent residents. There are numerous old workings and prospects (tin and copper) in the vicinity but production in recent years has been negligible.

Mineral exploration is generally permitted throughout the area, including (subject to conditions) in the reserves.

Physiography and drainage

The area lies between 20 m (Arthur River at 320000/5446300) and 312 m (at 330100/5438500) above sea level and mainly consists of undulating low hills (fig. 2). On the Sumac and Dempster map sheets drainage is almost completely into the Arthur River and its tributaries the Horton and Lindsay, which form the Frankland below their confluence. In the north of the area, on the Roger map sheet, the hilly country is broken by an extensive, very flat, poorly drained tract containing sections of the Duck, Roger and Montagu rivers, which drain northward into Bass Strait. This tract is underlain by Smithton Dolomite, but outcrops are sparse due to extensive alluvium.

The tract extends southward across a very low watershed (near 331000/5451000) to the Arthur River (below Kanunnah Bridge) and lower Stephens Rivulet. It is likely (Nye and Blake, 1938; Fish and Yaxley, 1966, p.79–80) that the Arthur River once drained northward and deposited much of this alluvium, prior to its capture by a stream flowing westward into the Southern Ocean. Further evidence for this is seen in the distribution of the giant freshwater crayfish *Astacopsis gouldii*, which is found in northern Tasmanian rivers flowing into Bass Strait and in the Arthur River system, but not in other western Tasmanian rivers which flow into the Southern Ocean (e.g. Hamr, 1992).

Similar but smaller low flat areas underlain by dolomite occur in the lower parts of Blackwater Rivulet and Hawkes Creek (centred on 324500/5446000) and north of the Frankland River (centred on 326500/5432500). In these areas, streams (including the lower parts of Keppel Creek, Blackwater Rivulet and Stephens Rivulet) are commonly slow, muddy, frequently choked with log jams, and usually contain only limited outcrop. They are often extremely meandering and their courses are not generally depicted accurately on available topographic maps.

A creek is shown on topographic maps entering the Lindsay River at a bend at 329770/5430130 (in another dolomite area). This creek actually passes within 50 m of the river, but remains separated from it by a natural levee about 10 m high on the creek side and 20 m on the river side. The creek continues northwest to join another creek at 329540/5430200, which ultimately meets the Lindsay River at 329000/5430630, as shown correctly.

Dempster Plains, another area of low relief, is developed on Rocky Cape Group sedimentary rocks. Trias Creek and Whitehead Creek are also choked with log jams (indicating that this is not solely due to forestry activities, as this is an undisturbed area) but contain frequent outcrops.

Streams generally quicken where they flow over Proterozoic basalt. Major rapids occur on the Horton River between 331900/5431800 and 331900/5432000, and downstream (at 330390/5432440) the river drops five metres in a waterfall. Notable waterfalls developed on basalt also occur on Keppel Creek (331630/5444020, 10 m) and Stephens Rivulet (328360/5441750, 4 m).

A series of three attractive waterfalls on the upper Julius River (333600/5440800, 3 m; 333530/5440740, 6 m; 322480/5440670, 5 m) are developed over slightly more resistant black carbonaceous siltstone units within the Black River Dolomite.

A recent landslip on the steep right (east) bank of Blackwater Rivulet (at 325210/5443320) has left a hole about 25 m long, 10 m across and 5 m deep, suggesting movement of about 3000 t of Proterozoic basalt and derived soil. The slip probably occurred in the five years prior to field work in January 1996, with the debris damming Blackwater Rivulet, killing vegetation for some distance upstream. The natural dam was subsequently breached, depositing debris downstream as small alluvial flats and islands.

Relatively flat but upstanding land on the western margin of the Dempster map sheet is underlain by Rocky Cape Group sedimentary rocks, but these are partly concealed by a thin veneer of Tertiary siliceous gravel. This area slopes gently westward and drains (via the Nelson Bay River) into the Southern Ocean. It is part of an extensive, partly dissected Tertiary surface which extends south towards the Norfolk Range and Sandy Cape, the gravel being deposited by meandering or braided rivers. It is likely that prior to dissection this surface once extended much further east.

The entrenched meanders of the Frankland River, sections of the Arthur River and (to the east) the Rapid River were probably developed on flat-lying gravel (and also basalt). After erosion of the Tertiary cover, the drainage was superimposed on to the Proterozoic basement. This type of superimposed drainage appears to be very common throughout northwest Tasmania.

As noted by Ward (1911), the headwaters of Emmetts Creek (near Balfour) have been captured by Cassiterite Creek (formerly Tin Creek), which may account for the presence of alluvial tin in the valley of the former.

Some marked topographic lineaments in the area are the modern expression of old basement faults. The longest and most obvious extends from beyond the northern margin of the sheet, through 338000/5460000 and 329700/5447200 (below Kanunnah Bridge) to 327000/5447700, becoming less distinct further south, and coincides with the Roger River Fault. Others occur northeast of Balfour (327500/5430700 to 329500/5432500) and at Dempster Plains (336300/5437500 to 333800/5432400). In each case the topographic effect is almost certainly due to differential erosion of juxtaposed units (especially where one is dolomite) rather than any recent movement.

Karst and warm springs

Large scale karst features in the area include Lake Chisholm (4.5 ha, 337500/5444500) which fills a uvala or collapse doline. The much smaller Deception Pool (337600/5439300) is also a sinkhole lake. Detailed descriptions are given by Sharples (1996 and references therein). Numerous, mostly very small sinkholes are shown nearby on the Sumac and Dempster 1:25 000 scale topographic map sheets.

Just north and downstream of Sumac Road, the Julius River enters a small gorge, flows through a 9 m high arch and then disappears into a major swallet with a 25–30 m high dolomite headwall (at 335000/5443190). The river re-emerges about 170 m away (334910/5443330) from an outflow cave about three metres high and four metres wide at the base of a dolomite cliff. The former bed of the river is partly occupied by a small tributary stream. These features are described further by Sharples (1996 and references therein).

During mapping less spectacular and shorter sections of subterranean flow were discovered in Hawkes Creek (322400/5448600), Lamprey Creek (340100/5440300 — 50 m) and in an un-named tributary of the Lindsay River (328840/5430150 — 10 m).

Warm (tepid) springs vigorously upwell into the bottom of a small pool, a few metres across and about 20 m from the west side of a creek near a tributary of the Lindsay River. Soft orange ferruginous material (possibly iron hydroxides) is precipitating from the pool, which downstream drains into the creek. The area is in low-lying rainforest with peaty soil and sporadic outcrops of dolomitic diamictite (Julius River Member). An analysis of the spring water has been obtained (Table 1).

On the right bank of the Arthur River (at 336100/5446440) a spectacular large isolated crag drops directly into the river, in a slightly undercut cliff more than 50 m high (cover photo). The crag is capped by dolomitic diamictite (Julius River Member) but at river level consists of corroded massive dolomite.

Trowutta Arch (341200/5451900), lying within the Trowutta Caves State Reserve and just outside the main area of this report, consists of several vertical sinkholes, including two large and deep holes that intersect to form an arch five metres high. One holds a pond more than 20 m deep and has been considered to be Tasmania's best example of a cenote or steep-sided sinkhole pond (R. Eberhard quoted by Sharples, 1996, p.38).

All the above features, except for that in Hawkes Creek, occur in the Black River Dolomite. Few large or medium-scale karst features are known from the Smithton Dolomite, probably because of its greater purity and low topographic expression. Outcrop-scale karst features such as karren are common in both units.

Table 1

Water analysis, warm spring near Lindsay River tributary (328 900 mE; 5 430 300 mN)

pH	7.2
Conductivity (µS/cm)	570
Item (mg/L)	
Carbonate	<5
Bicarbonate	290
Chloride	28
Sulphate	<5
Calcium	52
Magnesium	34
Iron	<0.1
Aluminium	<0.2
Potassium	3.4
Sodium	29
Fluoride	<0.3
Nitrate	<10
Total dissolved solids	350
Permanent hardness	32
Temporary hardness	240
Alkalinity	240
NO_3 by Bruciene	<0.5

Mineral Resources Tasmania laboratories, analysis 980027. Analyst L. M. Hay

Vegetation

Rainforest and wet sclerophyll forest are the natural vegetation over most of the area. In well-drained areas with good soils (such as on basalt), callidendrous rainforest (i.e. with a relatively sparse and open understorey) dominated by myrtle and sassafras has often developed. On poorer soils or less well-drained areas (often on dolomite), thamnic rainforest with a dense understorey of horizontal, laurel and other minor species may be present. Progress through this latter vegetation type is commonly very slow and arduous. The rainforest in the area lacks some of the species common in colder, wetter, higher altitude areas in western Tasmania. It is interesting to note that Huon Pine is absent from the area, whilst pandani (*Richea pandanifolia*) occurs only sporadically along the lower reaches of the Lindsay River and in the Frankland River, and is absent from the Horton, Arthur and Rapid rivers.

Wet sclerophyll forest, dominated by tall eucalypts, may have a very dense, locally almost impenetrable, understorey of cutting grass and bauera if it has been recently burnt. With decreasing fire frequency this is gradually replaced by a more open tea tree understorey and then rainforest species, which after several centuries may ultimately replace the eucalypts.

The Tertiary basalt plateau in the centre of the Dempster map sheet mostly supports a fine, relatively open blackwood forest, rather than rainforest. This is probably partly due to the influence of fire.

Low robust riverine scrub dominated by tea-tree species frequently lines the banks of major rivers.

Open plains, dominated by buttongrass and heath species, occur to the southeast and southwest of the Dempster map sheet, and a smaller area mostly just west of Blackwater Rivulet extends north towards the Arthur River on the Sumac map sheet. The underlying rock types are usually Rocky Cape Group quartzite and siltstone, or sometimes chert derived from the Black River Dolomite. Rapid progress is usually possible across these plains, especially where they have been recently burnt. In the absence of fire they are gradually invaded by dense, closely-spaced tea-tree and melaleuca scrub. In a small outlying area of former buttongrass (near 331000/5435500) this process has progressed almost to the stage of impenetrability.

At the interface between areas of buttongrass and rainforest there is usually a very narrow (10–50 m) belt of very dense scrub dominated by bauera, followed by a broader zone of closely-spaced tea tree, which gradually passes into rainforest.

Complete removal (clear felling) of all trees followed by regeneration burns is a common forestry practice in the area. This initially leads to excellent access and exposure of any outcrop or float, but after a few years the subsequent regrowth may be extremely dense and difficult to penetrate, particularly if large amounts of dead timber remain on the forest floor.

Previous work

Although tin was discovered at Balfour in the 1880s, and copper in 1901, there is little recorded geological work in the area until Ward (1911). Most of Ward's bulletin deals with the economic geology and detailed description of numerous small workings. He also gave descriptions of major rock units and produced a geological sketch map of the country between the lower Arthur River and the Pieman River, to about as far east as the Frankland, Lindsay and Donaldson rivers. Only a small part of this area overlaps with that presently under discussion.

The first regional geological mapping of the Trowutta and Bluff Point quadrangles, which include most of the present area, was conducted by the Geological Survey of Tasmania in 1960 and 1961 (Matthews, 1961*a*, *b*; Everard, 1962; Longman and Matthews, 1962; Longman, 1962). Although reconnaissance in nature and hampered by dense vegetation and difficult access south of the Arthur River, for many years this work provided the only useful geological information for most of the area (e.g. compilation map of Williams and Turner, 1973).

In the 1960s, access was improved by the bridging of the Arthur River and the construction of forestry roads southward. Griffin's (1974) thesis was mainly based on work between Kanunnah Bridge, Julius River and Trowutta. Griffin and Preiss (1976) published a geological map of this area, and described stromatolites (including *Baicalia* cf. *B. burra*) occurring in diamictite

unit, now known to be the Julius River Member of the Black River Dolomite.

Most previous stratigraphic work in the Smithton Synclinorium was based on mapping in its northern part (Nye *et al*., 1934; Carey and Scott, 1952; Gulline, 1959; Gee, 1968; Lennox *et al*., 1982). The rather convoluted history of stratigraphic interpretation has been previously reviewed by Brown (1989*a*), and is briefly described below.

Modern mineral exploration in the area is briefly reviewed in the *Economic Geology* section of this report.

Acknowledgments

The authors thank numerous past and current staff members of Mineral Resources Tasmania (formerly the Tasmania Department of Mines) for field and technical assistance. Staff at Forestry Tasmania's Smithton office were very helpful, particularly with regard to field communications. Dr G. R. Green constructively reviewed the manuscript.

Early Neoproterozoic (?): Rocky Cape Group *(JLE)*

Introduction

The oldest rocks in far northwest Tasmania belong to the Rocky Cape Group, a thick, unfossiliferous, dominantly siliciclastic shelf sequence, the basement of which is unknown.

The term was introduced by Spry (1957) and originally included all "those sediments, chiefly quartzites, slates, dolomites and siltstones, outcropping intermittently between Penguin to Smithton and lying unconformably below the Dundas Group (at Penguin)." Gee (1968) more narrowly redefined the Rocky Cape Group, excluding units both within and east of the Arthur Lineament (such as the Burnie Formation) and within the Smithton Synclinorium (the Togari Group as defined below). As extended by Bell (1972) and with redefinitions herein, the Rocky Cape Group is now considered to consist of:

- Jacob Quartzite (Gee, 1968);
- Irby Siltstone (Gee, 1968);
- Detention Subgroup (Gee, 1968) (comprising the Bluff Quartzite, Port Slate and Cave Quartzite of Spry, 1957);
- Cowrie Siltstone (Spry, 1957; Gee, 1968);
- Balfour Subgroup (redefined herein);
- Lagoon River Quartzite (Gee *et al*, 1969; Bell, 1972);
- Pedder River Siltstone (Bell, 1972).

The uppermost four formations comprised the redefined Rocky Cape Group of Gee (1968). The term "Balfour slates and sandstones" was originally used by Ward (1911) but, although variants have been used by numerous other authors, the unit has not been formally defined previously. The two lowermost formations were introduced informally by Bell (1972) for units in the Sandy Cape region.

Other units have been introduced at various times by other authors. In particular, the Interview Beds (Spry and Ford, 1957) were later defined (as the Interview Slate and Quartzite) along the lower Pieman River by Spry (1962, 1964) and subsequently divided into the Interview Siltstone and an underlying unit, "Quartzite of the Lagoon River", by Gee *et al*. (1969). The Interview Siltstone is thus probably the approximate equivalent of the Balfour Subgroup. Bell (1972) introduced the term Pedder River Siltstone for "a distinctive unit of dominantly dark grey siltstones, in which slump and scour-and-fill sedimentary structures are prominent …[appearing] to conformably underlie the Lagoon River Quartzite in the Sandy Cape area…". Further mapping in the Sandy Cape–Norfolk Range region, which is still a poorly known area, is clearly required to fully elucidate the detailed stratigraphy of the lower part of the Rocky Cape Group (Everard, 2005).

The minimum age of the Rocky Cape Group is directly constrained by three minimum K-Ar ages (ranging from 584 ± 8 to 600 ± 8 Ma) of dolerite dykes intruding the Cowrie Siltstone and two K-Ar slate ages (643 ± 10 and 630 ± 10 Ma) from the Irby Siltstone, both from the north coast (Adams *et al*., 1985). The overlying Black River Dolomite is considered to be 750–650 Ma based on biostratigraphy and isotope chemostratigraphy (Calver, 1998). The Jacob Quartzite can be no older than 1000 Ma, based on the youngest detrital zircons from that unit (Black *et al*., 2004). Thus the Rocky Cape Group is broadly constrained to the early Neoproterozoic (1000–750 Ma) in age.

Only the Cowrie Siltstone, Balfour Subgroup and a limited tract of Lagoon River Quartzite occur on the Sumac and Dempster map sheets, and are discussed below.

West of the Smithton Synclinorium

Correlate of Lagoon River Quartzite (Prl) *(ARR)*

Gee *et al*. (1969) showed "Quartzite of the Lagoon River — cross-bedded and well sorted" as a unit underlying the Interview Siltstone on the northern part of the Pieman Heads map sheet. Bell (1972) described the Lagoon River Quartzite as "a distinctive white, massive, apparently 'recrystallised' quartzite, with rare shale units generally preserved in the cores of folds". These authors did not formally define the formation, most exposures of which are thought to lie in the poorly known Norfolk Range region, south of the area described in this report.

Sections through the Lagoon River Quartzite (equivalent) are exposed in road cuttings northeast of Mt Balfour in the vicinity of 322300/5430300, in the extreme southwest of the Dempster map sheet. The sequence forms part of an erosion-resistant, variably folded and faulted regional package. The unit is dissected by faults and is in part in fault contact with stratigraphically overlying sedimentary units of the Balfour Subgroup. The thickness of this unit is not known but is estimated from mapping in adjacent areas to be greater than 2000 metres.

The Lagoon River Quartzite sequence comprises packages of clean cream-coloured quartz sandstone upwardly gradational into variably carbonaceous, laminated, and fissile siltstone and shale. The base of each cycle is dominated by sandstone beds to one metre thick, with the lower contacts of individual beds normally planar, although scoured bases are also common. Trough cross bedding is common but has been variably obscured or modified by quartz recrystallisation during weathering and/or deformation. Ripple casts are rare. Rounded elongate and laminated shale clasts are rarely present (sample R004791) and form poorly-graded, upwardly-fining layers to about 50 mm thick within, but near the base of, individual sandstone beds. Matrix material comprises 95% variably recrystallised and sutured equigranular quartz (to 1 mm diameter), 1% feldspar and 3% sericite (rare flakes to 1 mm long of recrystallised muscovite).

In the upper parts of each cycle, sandstone fines upward to laminated variably carbonaceous siltstone. Siltstone is typically absent near the base of individual cycles.

This unit equates to lithofacies 1 of Heithersay (1982) in the vicinity of the Balfour mineral field. Here, the sequence was reported to contain ferruginous as well as quartzitic sandstone cemented by predominantly silica, but also iron oxides and carbonate.

Balfour Subgroup *(ARR)*

Definition

The Balfour Subgroup is herein defined as that sequence of interbedded planar to wavy laminated cross-bedded and gutter-cast siliceous sandstone and siltstone, carbonaceous pyritic siltstone and shale, quartzarenite and chloritic siltstone that conformably overlies the Lagoon River Quartzite and is conformably overlain by a correlate of the Cowrie Siltstone in the vicinity of Balfour. The type section is composite and is designated as along the access track to Balfour, and along Blackwater Road in the vicinity of the Frankland River bridge, as detailed below. It consists of four formations; the Skinners Flat Siltstone, the Cassiterite Creek Quartzite, the Emmetts Creek Shale, and the Looneys Flat Siltstone, as defined below.

It is approximately equivalent to the "Balfour slates and sandstones" of Ward (1911) and other authors.

General features

Sections through the Balfour Subgroup are exposed along Blackwater Road near the Frankland River bridge, in the Frankland River from north of Balfour through to north of Blackwater Road, and along Heemskirk Road north of Mt Balfour. The Balfour Subgroup is compositionally heterogeneous and has been subdivided into six lithological units and four formations (described separately below) with contrasting rheological characteristics. Strain, both within and at the contacts between units within the Balfour Subgroup, is greater than that in stratigraphically adjacent but compositionally more homogenous sedimentary successions. Consequently, apparent unit thicknesses vary dramatically along strike, particularly where units are transected by thrusts. The total thickness of the Balfour Subgroup is about 3500 metres.

Skinners Flat Siltstone (Prbl)

The Skinners Flat Siltstone is herein defined as that unit of variegated, laminated to gutter-cast and trough cross-bedded light grey siliceous fine-grained sandstone and siltstone, and dark grey carbonaceous siltstone, that crops out along the access tracks to Balfour between 323 300 mE, 5 429 970 mN and 323 700 mE, 5 430 040 mN, where it is abruptly and conformably overlain by the Cassiterite Creek Quartzite. The unit is about 500 m thick, and although the lower contact is faulted in the type section, it gradationally and conformably overlies the Lagoon River Quartzite near Skinners Flat at 323 400 mE, 5 428 650 mN.

Plate 1

Field photograph showing typical bedding characteristics of the Skinners Flat Siltstone (unit Prbl) (323 250 mE, 5 431 150 mN).

This unit is best exposed along the access road into Balfour township (324000/5429800), and north of Balfour at 323050/5431050, where the diversion of Cassiterite Creek by mining operations has resulted in the old stream bed being exposed. It was included in the unit informally named the Specimen Hill siltstone by Yaxley (1981), and its characteristic stripy appearance in outcrop has also earned it the name 'pyjama siltstone' (e.g. Veska, 1993).

It comprises repeated light grey fine-grained siliceous sandstone to predominantly siltstone beds upwardly gradational to dark grey weakly carbonaceous to quartzose siltstone (Plate 1). Beds are typically less than 100 mm thick and commonly less than 10 mm, and show both planar and irregular contacts. Where less than 10 mm thick, the lower contacts of strata commonly exhibit a lobate texture, possibly indicative of rapid deposition on an unconsolidated substrate. Bedding continuity in such cases is normally less than a few metres. Bed sets to 150 mm may also locally appear brecciated, with individual clasts typically tabular and elongate in shape and variably rotated. Beds greater than 50 mm thick commonly show highly irregular cuspate upper and lower contacts and are discontinuous along strike. Deeply incised (up to 0.5 m) and rounded channels are common, with individual channels undercutting underlying strata. Internal cross lamination within individual channels is common.

Quartz silt-filled clastic dykes are common to darker, finer-grained siltstone layers. These dykes are typically less than 10 mm in length, orientated orthogonal to bedding, and are variably folded, with fold axes parallel to bedding. Folding of the dykes has probably resulted from shortening through compaction and dewatering of the host shale stratum. Viewed in the plane of bedding the dykes show both preferred and random alignments at different sites. Elsewhere in the Rocky Cape region, similar clastic dykes have been described as shrinkage or syneresis cracks (Calver and Baillie, 1990; Scott, 1997). The preferred alignment of the dykes near Balfour might also indicate the influence

of syn-sedimentary extensional processes during, or shortly after, deposition.

In thin section, the siltstones are both matrix- and grain-supported and comprise sub-angular to rounded quartz (≤0.5 mm diameter) (Veska, 1993; sample R007226). The matrix comprises sericite (30%), chlorite (20%), opaque minerals (2%), and up to 15% carbonaceous matter, with carbon and chlorite content defining the colour of the beds in outcrop.

The lower contact of the Skinners Flat Siltstone with the underlying Lagoon River Quartzite (Unit Prl) in the Dempster map sheet is faulted, although it becomes conformable further south at 323400/5428650. Here, the transition from the Lagoon River Quartzite to Unit Prbl occurs over an interval of about 100 metres. The upper contact of this unit west of Balfour (323700/5430040) is less than 20 m wide, and is defined in the topography by steep slopes where Unit Prbl meets Unit Prbq. Both upper and lower contacts become progressively less defined north of Cassiterite Creek (322400/5433600).

Cassiterite Creek Quartzite (Prbq)

The Cassiterite Creek Quartzite is herein defined as that unit comprising upwardly fining packages of cream-coloured tabular-bedded quartzarenite, laminated siltstone and carbonaceous shale, that crops out along the access track to Balfour between 323 700 mE, 5 430 04 mN and near 324 200 mE, 5 430 000 mN, where it is abruptly and conformably overlain by the Emmetts Creek Siltstone. The unit is about 350 m thick in its type section but thickens northward.

The Cassiterite Creek Quartzite corresponds to the upper member of the informally named 'Specimen Hill Siltstone' of Yaxley (1981). It is best exposed along the access road into Balfour township (324000/5429800), and on Heemskirk Road at 321200/5436400. Both upper and lower sedimentary contacts along the access road are sharp, and the strata dip steeply east and west and face east, with erosion resulting in this unit forming clearly-defined ridges. Both upper and lower contacts of this unit are less clearly defined north of Cassiterite Creek (322400/5433600) where bedding dips are variable and the unit is less well defined topographically.

The Cassiterite Creek Quartzite is similar to the correlate of the Lagoon River Quartzite (Prl). It is about 350 m thick west of Balfour but appears to thicken northward. West of Balfour, the unit comprises alternating tabular-bedded cream-coloured quartzite sandstone to seven metres thick, interbedded with variably laminated siliceous (commonly also erosion resistant) grey siltstone of similar thickness. The laminated siltstone component increases relative to the sandstone further north. Beds typically lack any definable internal sedimentary structure in the road section west of Balfour, but exhibit all those structures common to the Lagoon River Quartzite where outcropping along Heemskirk Road. Hemipyramidal casts suggestive of diagenetic evaporite development were also apparent in one shale unit north of The Clump (321420/5436475).

Quartz grains in sandstone beds from west of Balfour show undulose extinction and sutured contacts indicating recrystallisation (Veska, 1993). Yaxley (1981) also noted a small amount of post-depositional tourmaline in rocks west of Balfour.

Emmetts Creek Shale (Prbg)

The Emmetts Creek Shale is herein defined as that unit of thinly laminated blue-green or green to cream siltstone with chlorite porphyroblasts, black pyritic carbonaceous shale and rare quartzarenite that crops out along Blackwater Road, near the Frankland River, between 321 100 mE, 5 438 100 mN and 321 800 mE, 5 438 600 mN. The unit is about 500 m thick, abruptly and conformably overlies the Cassiterite Creek Quartzite, and is gradationally and conformably overlain by the Looneys Flat Sandstone.

This unit is best exposed along the banks of the Frankland River (323300/5433600), along the access road into Balfour (324400/5429700), and along Blackwater Road in the vicinity of the Frankland River (321850/5438300). It is characteristically poorly outcropping and commonly defined by a low-lying topography and dense understorey of scrubby vegetation.

The transition from the stratigraphically underlying Cassiterite Creek Quartzite (Prbq) occurs over a distance of less than 20 metres. The Emmetts Creek Shale comprises monotonous sequences of laminated siltstone, characteristically azure to green in colour when fresh but typically weathering to alternating dull green and rusty brown colours. Individual laminae are typically less than 10 mm thick.

Laminated black pyritic carbonaceous siltstone and shale sequences to 50 m thick also occur at irregular intervals throughout the sequence (e.g. 321900/5438350). Crystalline pyrite is common on bedding planes in carbonaceous units. Coarser-grained units are characteristically absent although one quartzose sandstone bed to five metres thick was mapped in the Frankland River at 322959/5433600.

In thin section, the green siltstone comprises 70% rounded equigranular quartz grains to 0.15 mm diameter and 6% detrital chlorite to 0.25 mm diameter in a microcrystalline chlorite-sericite ± carbon matrix. Veska (1993) also noted up to 5% pyrite in rocks from the vicinity of Balfour township but also noted that the pyrite cut the tectonic cleavage, suggestive of a post-diagenetic origin. Consequently, the percentage of diagenetic pyrite, if any, in this unit remains uncertain.

Porphyroblasts to 2 mm diameter are common in the green siltstone and to a lesser extent the carbonaceous siltstone and shale. Porphyroblasts are typically elongate ovoid and rarely rhombohedral in shape and comprise cores of variably microcrystalline chlorite-sericite ± albite ± quartz rimmed by chlorite and sericite. The porphyroblasts overgrow and

preserve two tectonic foliations (S_1–S_2), and their formation was coincident with S_2 (See *Structural Geology* section.)

The Emmetts Creek Shale is well exposed in the lower reaches of a tributary of the Frankland River up to 500 m southeast of the Blackwater Road bridge. Typical outcrops are of thin-bedded, plane-laminated, colour-banded siltstone, with alternating cream and olive-green coloured laminae in approximately equal proportions. The pale-coloured laminae are quartz rich and may also be somewhat coarser than the olive green laminae, and in some outcrops younging is indicated by small-scale sole structures in the coarser laminae. Sample R004287 from 321940/5438190 towards the top of the unit consists of laminae ≤4 mm thick of relatively finer and coarser grain size. The fine-grained laminae are dominated by very fine-grained white mica preferentially aligned parallel to one dominant penetrative cleavage and at least one later (?crenulation) cleavage. The coarser laminae are dominated by mostly subangular quartz grains generally ≤0.06 mm in diameter, with subordinate very fine-grained white mica and ?chlorite. These layers also contain about 5% of blocky single crystals and plates ≤0.22 mm diameter of chlorite with aligned basal cleavage, and which are interpreted as due to metamorphic mineral growth (see *Structural Geology* and *Metamorphism* sections).

Looneys Flat Siltstone (Prbs, Prbsa, Prbsq)

The Looneys Flat Siltstone is herein defined as that unit of grey to buff-coloured micaceous fine-grained sandstone, interbedded with and grading up to dominant planar laminated green siltstone with chlorite porphyroblasts, that crops out along Blackwater Road between 321 800 mE, 5 438 600 mN and about 323 100 mE, 5 439 800 mN, near where it is conformably overlain by a correlate of the Cowrie Siltstone. The unit is about 1000 m thick and locally contains members of dominantly thinly bedded medium-grained sandstone (Prbsa) and thickly bedded quartzarenite (Prbsq).

The main lithological unit (Prbs) of the Looneys Flat Siltstone is best exposed along Blackwater Road east of the Frankland River at 322220/5439000, and in road cuttings along Heemskirk Road at 326350/5425450 on the Balfour map sheet to the south of the Dempster map sheet. It is more resistant to erosion than the underlying Emmetts Creek Shale (Prbg), with which it is in gradational contact.

The Looneys Flat Siltstone (unit Prbs) can be differentiated from the Emmetts Creek Shale (Prbg) by a coarsening grain size up-section. Beds typically range in thickness from less than 10 mm to about 200 mm and comprise micaceous and rarely pyritic fine-grained sandstone that may grade stratigraphically upward into laminated chloritic siltstone. Bedding planes are typically regular and internal sedimentary structures other than grading are absent. The same porphyroblastic texture that is observed in the Emmetts Creek Shale occurs at intervals throughout this unit, but is not ubiquitous. Where present, the porphyroblasts are typically restricted to the finer-grained portions of each stratum.

The Looneys Flat Siltstone (Prbs) is exposed in numerous weathered road cuttings on Blackwater Road within 1.8 km northeast of the Frankland River bridge. The sequence generally dips and faces northeast at moderate to steep angles. The most typical lithology is thin-bedded, plane-laminated, light olive-green siltstone, with prominent dark green chloritic spots ≤2 mm in diameter, which are either selectively concentrated in certain laminae or dispersed throughout the rock. In some outcrops these spots show cubic or tetragonal cross sections. Some outcrops also show rare, large dark cubic crystal shapes up to 4 mm in diameter, which may have originally been pyrite. Sequence facing is determined from small-scale basal scours in some beds. Sample R004297 from 321920/5438680, near the base of the sequence, is a siltstone laminated on a centimetre scale, with alternating relatively finer-grained and coarser-grained laminae. The fine-grained laminae consist dominantly of a very fine-grained mosaic of white mica, in part orientated parallel to a dominant cleavage oblique to bedding, but also with a pre-existing preferred orientation parallel or sub-parallel to bedding. The coarser laminae contain up to about 20% of sub-angular to sub-rounded detrital quartz grains, generally ≤0.1 mm in diameter. All laminae contain about 5% of blocky single crystals ≤0.24 mm in diameter, of chlorite with aligned basal cleavage, and which are interpreted as due to metamorphic mineral growth. A further 10% of the overall rock consists of irregular ovoids ≤2 mm in diameter, with somewhat diffuse margins, consisting of a central core of very fine-grained quartz ± albite, succeeded outwards by a concentration of single blocky crystals and platelets of chlorite with basal cleavage aligned sub-parallel to bedding, followed by a relatively thin rim zone of very fine-grained white mica. The ovoids are interpreted as porphyroblasts associated with regional metamorphism (see *Structural Geology* and *Metamorphism* sections).

Fresher outcrops of the lower half of the Looneys Flat Siltstone occur in the middle reaches of a creek extending about 0.5 to 1.3 km ESE of the Frankland River bridge. Here colour-banded, plane-laminated lithologies with prominent chloritic metamorphic spotting comprise cream-coloured laminae of quartz siltstone to fine quartz sandstone, with alternating subordinate laminae of olive green siltstone or mudstone. Sample R004288 (from 322290/5438300) is similar to R004297, but in this case the quartz-?albite-chlorite porphyroblasts are much less developed, and are ≤0.65 mm in diameter. As with R004297, the rock contains a few percent of blocky single crystals and plates ≤0.16 mm in diameter of chlorite with aligned basal cleavage, which are interpreted as due to regional metamorphic mineral growth. The coarser (and relatively more quartzose) laminae in this sample show

distinct grading from a maximum grain size of about 0.07 mm (at the base) to about 0.03 mm (at the top).

Quartz sandstone-bearing units (Prbsq) occur in the upper parts of the Looneys Flat Siltstone (e.g. 323500/5434950). These units may be up to 250 m thick but are laterally discontinuous along strike. Individual quartz sandstone beds can be greater than five metres in thickness, lack internal structure, and are typically erosion resistant.

The upper half of the Looneys Flat Siltstone is exposed in about 500 m of creek section approximately centred on 323600/5436400. Here the dominant lithology is colour-banded, cream-grey-olive green plane-laminated siltstone with distinct fine green chloritic spotting, interpreted as a regional metamorphic effect, in parts of the rock. Overall, the Looneys Flat Siltstone sequence may fine upwards.

North of Balfour (at 324900/5430900) unit Prbs grades upward into erosion resistant, but finely bedded (<150 mm), medium-grained sandstone (Prbsa). Siltstone is characteristically lacking from these rocks.

Correlates of the Cowrie Siltstone (west of the Smithton Synclinorium) (Prc)

Frankland River above Balfour *(JLE)*

A rather brief examination of this section (326800/5431400 to 325300/5431000) was made by raft. The most common lithology (samples R005596, R005597) is a medium to dark grey, thinly and diffusely laminated but not necessarily fissile, slightly micaceous and sometimes pyritic siltstone or very fine-grained sandstone. The lamination is usually planar, but slightly to markedly wavy laminated variants (samples R005595, R006600) also occur. Graded bedding is sometimes present and the unit generally dips and faces southwest. Sinistral mesoscopic folds, plunging at about 27° to 160°, were noted on the north bank of the river at 325740/5430930. Outcrop on the surrounding hills to the north and south of the Frankland River in this area is generally very poor.

In thin section a sample (R005596; 326620/5431140) of medium-grey, relatively massive, faintly and diffusely planar laminated fine to medium-grained sandstone is seen to be moderately well sorted and grain supported. It consists mainly of equant angular quartz grains, mostly100–400 μm across, with undulose extinction, with an interstitial matrix dominated by small unorientated splinters (3–10 μm long) of white to pale green mica (phengite?) and subordinate very fine-grained, low birefringence, clay material. There are rather rare larger flakes of detrital muscovite and rare pale green chlorite. Anastomosing carbonaceous seams occur parallel to bedding in places, and adjacent mica is commonly orange-brown (oxidised?). Accessory minerals include sparse small opaque grains and small rounded zircons.

Sample R005597 (326220/5431370) is, in hand specimen, a faintly planar laminated but not fissile dark grey medium-grained siltstone, with pyrite both disseminated and along joint planes. In thin section it is seen to be thoroughly metasomatised with abundant aggregates of fine-grained, pale to dark brown pleochroic tourmaline. The mineralogy is partly obscured by abundant scaly carbonaceous material, but detrital minerals include subrounded quartz grains (mostly less than 50 μm) and scattered flakes of muscovite. A streaky bedding lamination is defined by alignment of muscovite and carbonaceous material and some compositional banding.

A specimen of the wavy laminated lithofacies (R005595; 326680/5431250) is a poorly-sorted, very fine-grained sandstone with slightly wavy to convolute bedding lamination suggesting some soft sediment slumping. The thin section (Plate 2) shows that the rock is also metasomatised with abundant amber brown tourmaline aggregates comprising 10–15% of the rock, sometimes accompanied by pale green chlorite. The main detrital grains are subangular quartz anhedra (mostly less than 200 μm) and flakes of muscovite aligned parallel to the lamination, accompanied by abundant carbonaceous material. Bedding is defined mainly by compositional banding.

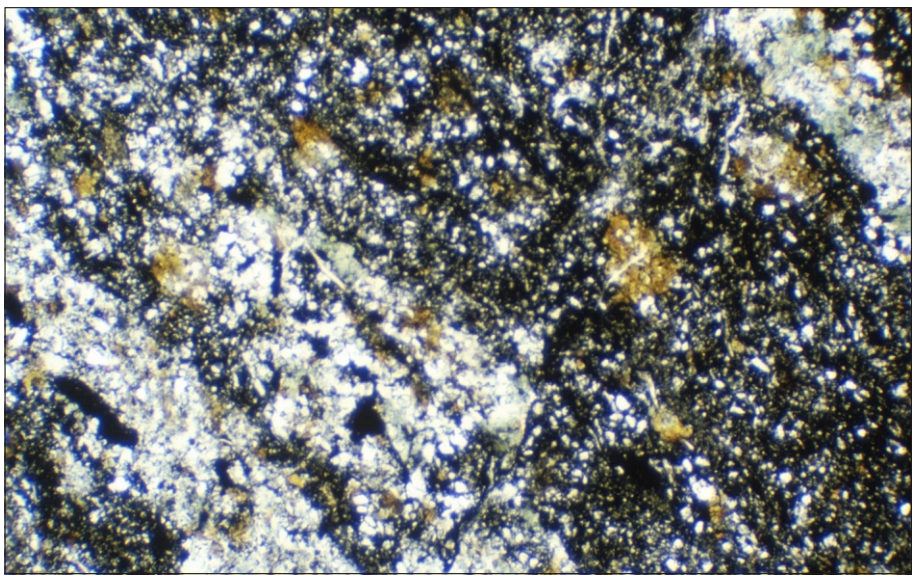

Plate 2

Photomicrograph of Cowrie Siltstone correlate, sample R005595 (Frankland River, 326 680 mE, 5 431 250 mN). Very fine-grained carbonaceous sandstone with slightly wavy lamination. Thoroughly metasomatised with abundant tourmaline (amber brown) and chlorite (pale green). Plane polarised light, field of view 4.4 × 2.9 mm.

Sample R006600 (326770/5431380) is a similar wavy laminated, tourmalinised, very fine-grained sandstone to coarse-grained siltstone. The lamination is defined mainly by compositional banding, and carbonaceous material is mainly confined to wavy, discontinuous to slightly anastomosing thin subparallel seams.

The planar bedded rocks resemble the Cowrie Siltstone to the east of the Smithton Synclinorium (see below) but the wavy laminated varieties are atypical. The tourmaline metasomatism suggests the proximity and influence of the spine of Devonian granite, inferred to underlie the Balfour mineral field a few kilometres away.

Upper Blackwater Rivulet *(DBS)*

Correlates of the Cowrie Siltstone are exposed in a steeply eastward-dipping and facing section in Blackwater Rivulet extending some two kilometres SSE from the Blackwater Road bridge (324850/5440460). As this part of the stream flows largely along strike, only perhaps 500 m of Cowrie Formation stratigraphy is exposed, commencing some 1150 m above the contact with the Balfour Subgroup (the nature of this contact has not been established). The most typical lithofacies consists of dark grey, thin-bedded, plane-laminated siltstone and/or fissile shale, with minor interbedded mid-grey, plane-laminated quartz siltstone. A representative sample is R004286 (from 324900/5440090), which is dominated in thin section by closely spaced, anastomosing sub-parallel seams consisting of extremely fine-grained black opaque ?carbonaceous material. Between these is very fine-grained mudstone and siltstone, in the coarser parts of which identifiable clastic grains, ≤0.1 mm in diameter, include subangular quartz, and detrital flakes of white mica which are commonly aligned parallel to bedding. Subordinate lithofacies in the Blackwater Rivulet section include thin-bedded mid-grey quartz siltstone to fine quartzarenite with common small-scale cross lamination, and green-grey to maroon, plane-laminated siltstone. The former lithology is typified by sample R004285 from 324930/5440140. This contains about 15% of mostly subangular quartz and rare ?albite clasts ranging up to about 0.1 mm in diameter, and about 5% of detrital white mica flakes ≤0.15 mm long showing strong preferential alignment probably parallel to bedding. These clasts are set in a very fine-grained matrix rich in white mica (sericite). The thin section also contains several large blebs up to about two millimetres in diameter, consisting of single or multiple grains of coarse-grained ?quartz (or possibly albite) poikilitically enclosing the clastic quartz and mica grains.

Cowrie Siltstone exposures stratigraphically below the Blackwater Rivulet section in this area are limited to shallow excavations beside Blackwater Road, and a few low exposures on a disused forestry investigation track leading south from the same road. The Blackwater Road exposures, which are probably close to the contact with the Balfour Subgroup, consist of dark grey to black ?graphitic shale in which some horizons are rich in pyrite cubes, and which commonly carries an upright, north-trending finely developed penetrative cleavage (correlated with regional S_4, see *Structural Geology* section). This facies is very similar to the 'classic' black shale facies typical of the extensive exposures of the Cowrie Siltstone in the Trowutta 1:50 000 scale quadrangle (Everard *et al*., 1996). Some shale beds in the Blackwater Road exposures show fine metamorphic spotting (e.g. at 323380/5439940, sample R004298); bedding in this sample is defined by parallel thin wisps of very fine-grained opaque black ?carbonaceous material.

About 1.3 km to the southeast and further up-section, a low exposure on a disused forestry track consists of grey-brown weathered quartz siltstone in beds up to 300 mm thick with subordinate black shale, and showing basal scours and small-scale trough cross lamination in some beds.

Other exposures between Blackwater Rivulet and the Frankland River *(DBS)*

Small outcrops of Cowrie Siltstone correlates occur close to the contact with basal Togari Group units between 324020/5435830 and 323820/5436180 along a disused forestry investigation track which meanders across the Togari Group boundary. The main lithology in the Cowrie Siltstone here is thin-bedded, plane-laminated light grey-weathering quartz siltstone.

Inferred Cowrie Siltstone correlates were also encountered near 325110/5436400 in the upper reaches of a tributary of the Frankland River. Lithologies include sheared blue-grey siltstone and plane-laminated mid-light grey quartz siltstone, but also present are blue-green, olive green and purple-grey laminated siltstone with small (≤1.5 mm) dark green chloritic spots, reminiscent of lithologies in the Balfour Subgroup. Some 4.5 km further south, near 325230/5431890, creek outcrops of thin-bedded, plane-laminated dark grey siltstone and shale are also correlated with the Cowrie Siltstone. Based on structural position and correlation with the Sumac map sheet, the outcrops at these two localities are interpreted as lying within a 600 m wide north-trending fault-bounded sliver of Cowrie Siltstone abutted to the east and west by younger Togari Group units. The Blackwater Road inlier (see above) is inferred to be the same feature offset some 4–5 km in a dextral sense along the northeast-trending Roger River Fault (see *Structural Geology* section for further discussion).

Lower Blackwater Rivulet *(JLE)*

Much of the large tract of Cowrie Siltstone correlate in the southwest of the Sumac map sheet is obscured by Tertiary gravel, but good exposures occur in Blackwater Rivulet downstream from the bridge (332800/5420500 to 324600/5442800).

The typical lithology is a medium to dark grey, thinly laminated, moderately fissile, medium to coarse-grained siltstone with scattered pyrite euhedra, resembling the Cowrie Siltstone to the east of the Smithton Synclinorium.

A thin section (sample R004807, 325190/5441200) consists mostly of poorly-sorted quartz anhedra (mostly ≤50 μm) and sericite, although some unrecrystallised detrital mica remains. A few large (to 1 mm) subangular quartz grains with aligned inclusions of muscovite splinters, probably of medium to high-grade metamorphic origin, are present in some beds. Subhedral pyrite euhedra may have adjacent pressure shadows of vein quartz, less commonly accompanied by minor chlorite. Rare isolated chlorite grains, very rare plagioclase fragments and traces of zircon and tourmaline are also present. Bedding is defined by compositional banding (alternating more and less sericitic material), anastomosing carbonaceous seams and grain size variations. Some paler beds lack carbonaceous material. A strong cleavage, at a high angle to bedding, is defined by alignment of sericite and/or carbonaceous material and flattening of some lenticular aggregates of opaque grains.

Similar outcrops of coarse-grained poorly-sorted siltstone, in places grading to very fine-grained sandstone, occur in small tributary creeks to the west (e.g. sample R004809, 324060/5444150).

A somewhat silicified medium-grey siltstone (R004805, 325430/5441190) is bleached to a cream colour along fractures. The thin section shows rather sparsely distributed, well-rounded quartz grains (to 100 μm) and minor detrital muscovite in a strongly-cleaved sericitic matrix. Diffusely disseminated, fine-grained opaque grains are partly oxidised and/or altered to sphene(?). There are also occasional larger grains of inclusion-ridden metamorphic quartz (to 1 mm) and opaque grains with pressure shadows of fibrous quartz.

A distinctive hard purplish-red-grey (5RP4/2), flaggy and fissile, thinly planar-laminated silicified siltstone (sample R004803) was noted in a steeply descending section of Blackwater Rivulet, stratigraphically just below the contact with the Togari Group at 325360/5440440. Similar rocks occur in a similar stratigraphic position downstream (samples R004804, 325500/5441030; R004808, 325000/5442180), and were also noted in an inlier in the Arthur River (R005034, 339970/5445940) (see above). Although distinctive in outcrop, these rocks closely resemble other Cowrie Siltstone samples in thin section. They are rather poorly-sorted coarse-grained sericitic quartz siltstones with abundant detrital mica and occasional larger grains of polycrystalline metamorphic quartz. Bedding is defined mainly by thin wispy discontinuous laminae of scaly dark oxidised material, which is translucent and pink to purple under strong illumination, accounting for the colour of the hand specimen. In sample R004808 the coloured material is more evenly disseminated throughout the rock.

Secondary silicification and local oxidation, perhaps a palaeoweathering feature beneath the unconformity and/or related to chertification of the Black River Dolomite, presumably occurred in the Proterozoic.

Dunns Plain south/lower Arthur River **(DBS/JLE)**

Correlates of the Cowrie Siltstone are well exposed in the incised valley of the Arthur River south of Dunns Plain near the western boundary of the Sumac map sheet. The sequence generally dips steeply northeast or southwest, but is consistently northeast facing, with steeply overturned bedding evident in the part of the section closest to the contact with the Togari Group. In the western part of the river section, dips become shallower due to open folding about shallowly northwest-plunging axes.

The river section mostly consists of flaggy thin-bedded, plane-laminated dark to medium grey siltstone with very planar bedding surfaces and locally common scattered small pyrite euhedra. Occasional outcrops are greenish-grey or oxidised to pinkish-purple. The top 200 m or so of the section, immediately below the Togari Group, is an indurated (somewhat silicified?) medium-grey siltstone, described in the field as 'very fine-grained quartzite'.

A thin section of 'quartzite' (sample R005082, 322370/5445620) shows that it is a somewhat poorly-sorted coarse-grained siltstone typical of the Cowrie Siltstone, although not particularly carbonaceous. Moderately angular quartz grains, rarely more than 50 μm across, and occasional splinters of white mica, grade to a finer-grained quartz-sericite aggregate. Bedding is defined by closely spaced anastomosing seams of fine-grained carbonaceous material. There are rare larger grains (up to 2 mm) of quartz and smaller sub-cubic euhedral to anhedral pyrite grains.

Similar but paler weathering, thinly-laminated pyritic siltstone and very fine-grained sandstone are exposed in a minor creek southwest of 323040/5445130. In thin section, a sample (R004810, 322940/5445200) is a much less carbonaceous but otherwise similar coarse-grained siltstone. Scattered small ragged lithic clasts (about 0.5–2 mm), generally crudely aligned parallel to bedding, of finer-grained carbonaceous siltstone and sericite schist, are also present.

Some outcrops show minor pale grey laminae of more quartz-rich fine to very fine-grained sandstone, and uncommonly this lithology may become prominent. One such occurrence is exposed in a tributary of the Arthur River at 321680/5446090, where the pale-weathering quartzose lithology forms more than 50% of the section and occurs in beds up to one metre thick. Where the pale lithology is prominent it commonly shows small-scale cross lamination, within which erosional truncations readily indicate facing, in contrast with the more typical dark grey plane-laminated siltstone in which facing is commonly indeterminate.

In thin section (sample R004265) the pale sandstone consists dominantly of a very fine-grained quartz-rich matrix with minor white mica, set within which are subangular to subrounded, generally monocrystalline quartz clasts (about 20% component, size range 20–200 μm); detrital muscovite flakes with a ?bedding-parallel preferred orientation (<3% component, ≤300 μm long); and rare, relatively little altered feldspar clasts ≤1 mm in size, some polycrystalline and some with simple twinning, and which are probably K-feldspar. This clast population may indicate a granitic provenance, although the fact that the maximum feldspar grain size exceeds that of quartz suggests that some of the former may be diagenetic.

These lithologies are similar to one of the facies typical of the Cowrie Siltstone in the Smithton, Woolnorth and Trowutta 1:50 000 scale quadrangles (Lennox *et al*., 1982; Seymour and Baillie, 1992; Everard *et al*., 1996).

East of the Smithton Synclinorium

Cowrie Siltstone (Prc, Prcs) *(JLE)*

The Cowrie Siltstone flanks the eastern margin of the synclinorium, along which it extends northward, roughly along strike, to its type area on the north coast (Spry, 1957; Gee, 1968). To the east it extends, repeated by folding and faulting, for about 20 km, until it is overlain by the Detention Subgroup (mainly quartzite) or, in the upper Rapid River area, grades into a phyllite transitional to the Arthur Metamorphic Complex (Everard *et al*., 1996). As mapping has now established lateral and stratigraphic continuity of the formation over this large area, previous local terms such as Lawson River Siltstone and Neasey Quartzites and Slates (McNeil, 1961; Matthews, 1961*a*, *b*; Longman and Matthews, 1962) are considered redundant.

Only a small part of this large tract lies on the Dempster map sheet (where it is mostly poorly exposed) and, together with a few immediately adjacent exposures to the north on the Holder map sheet, is described in this report.

The following lithologies are present in the Cowrie Siltstone in this area, but are both gradational and commonly interbedded on outcrop or even thin section scale. It is doubtful whether the unit can be divided into regionally mappable members, even in areas of better exposure.

Dark grey to black, thinly planar laminated, pyritic siltstone

This is the most characteristic lithology in the unit and can readily be examined in the Mt Bertha Road quarry (342440/5437380) on the adjoining Beryl map sheet. The best and most accessible exposures within the Dempster map sheet are along the Sumac and Sumac 7 spur roads near their junction (334000/5430600). The rock is a rather brittle, flaggy, fissile, shaly carbonaceous siltstone, sooty to the fingers, which readily splits along bedding laminae into sheets up to a metre across and a centimetre or less thick. Mesoscopically it consists of alternating black, dark to pale grey, or occasionally off-white planar laminae, less than 0.5 mm to about 10 mm thick. Penetrative cleavage is commonly visible, particularly when etched out on weathered surfaces. Yellow pyrite euhedra are common and locally abundant, being typically scattered on particular bedding planes, but also disseminated throughout the rock or occasionally concentrated into discoid nodules a few centimetres across. Oxidation of pyrite may impart a slight yellow-green staining or produce thick brown weathering crusts along bedding or joint planes.

Within the Dempster map sheet, similar rocks crop out in the beds of the Horton River and its tributaries Whitehead and Trias creeks, but are not the dominant lithology there.

In thin section typical specimens (e.g. R005228, Trias Creek at 338430/5433330; R006586, Horton River at 336820/5429780) are fine to very fine-grained carbonaceous siltstones (Plate 3). A pale aggregate of small (≤20 μm) splinters of sericite and fine-grained quartz may be visible between dark streaky to slightly anastomosing carbonaceeous laminae typically 50–100 μm apart. There are rare narrow flakes of detrital muscovite up to 100 μm long but very few quartz grains more than 25 μm across.

A sample (R005186) from the Mt Bertha Road quarry is a similar but darker and more carbonaceous fine to very fine-grained siltstone. Samples R005212 (Lamprey Creek at 340220/5441070) and R005200 (Horton River at 335120/5432460) are mineralogically typical samples. In the thin sections, cut parallel to bedding, there are diffusely blotchy domains, a few hundred micrometres across, of darker carbonaceous and paler quartz-sericite material.

A sample from Sumac 7 spur (R006584, 333760/5430490) is notable for pale grey, diffusely and faintly laminated sericitic beds up to 25 mm thick, which alternate with more typical dark grey to black carbonaceous beds (0.5–10 mm thick) with a stronger planar fabric (Plate 4). In thin section (Plate 5) the paler beds are seen to be composed of weakly orientated sericite splinters (≤10 μm), tiny opaque blebs (≤5 μm) and probably submicroscopic silica, together with occasional larger (mostly 200 μm–1 mm) subrounded grains of polycrystalline quartz. Some of the larger quartz grains appear to be overgrowths on a core of an opaque mineral (pyrite?), and do not disturb or deflect the laminated fabric of the matrix, and thus may be diagenetic rather than detrital in origin.

Other samples differ only slightly. Sample R005218 (Horton River at 333730/5432440) is less carbonaceous, with rather thin diffuse anastomosing seams in a siliceous, possibly silicified matrix (mostly ≤25 μm) with minor detrital mica and relatively little sericite. In sample R005240 (Whitehead Creek at 335050/5432990) the anastomosing carbonaceous seams are thicker and wider spaced (100–200 μm), between which is very

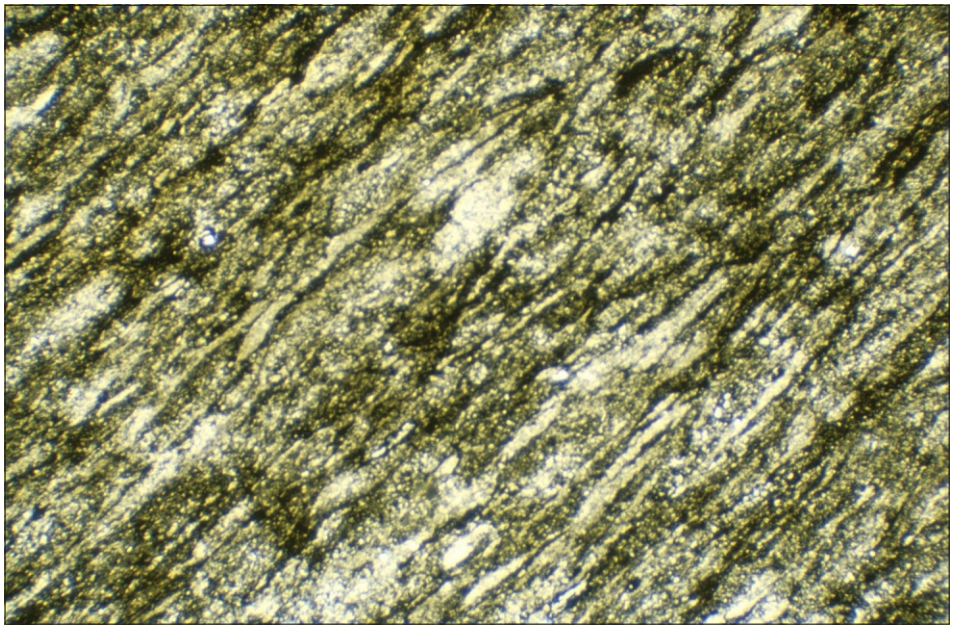

Plate 3

Photomicrograph of typical Cowrie Siltstone, sample R005228 (Trias Creek, 338 430 mE, 5 433 330 mN). Fine-grained quartz-sericite aggregate with streaky to very finely anastomising carbonaceous laminae. Plane polarised light, field of view 4.4 × 2.9 mm.

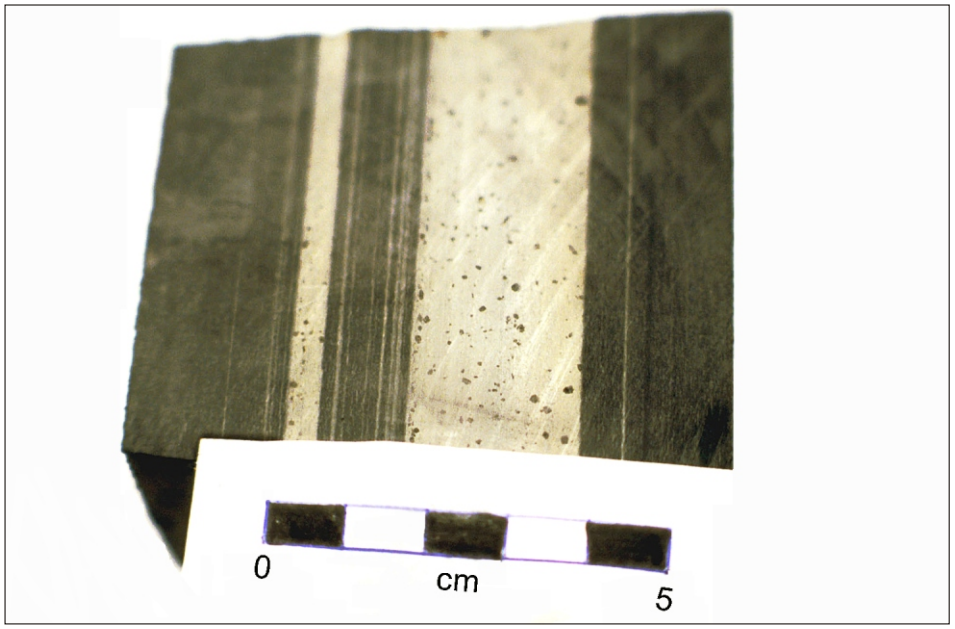

Plate 4

Cowrie Siltstone sample R006584 (Sumac 7 road, 333 760 mE, 5 430 490 mN). Planar laminated siltstone with alternating dark carbonaceous and pale sericitic beds.

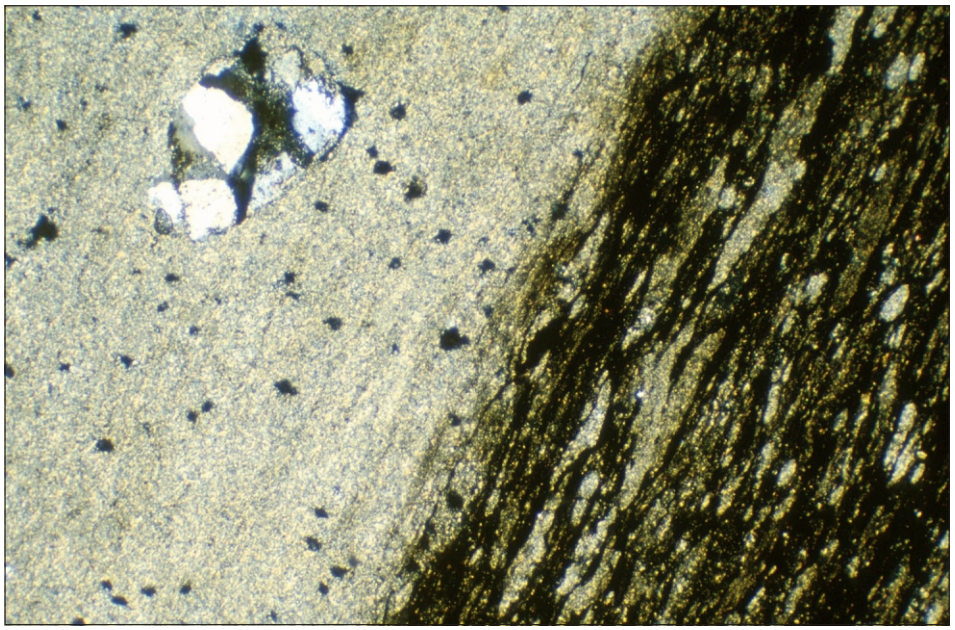

Plate 5

Photomicrograph of Cowrie Siltstone sample R006584. Dark carbonaceous bed at right (cf. Plate 3) and pale sericitic bed with polycrystalline quartz grain (overgrowth?) at left. Crossed nicols, field of view 4.4 × 2.9 mm.

fine-grained quartz (partly attributable to some secondary silicification) with relatively less sericite than most other samples. Sample R005217 (Horton River at 334360/5432250) is also relatively siliceous.

Pale grey, thick bedded to diffusely planar laminated, very fine-grained quartz sandstone to siltstone

This is the dominant lithology in the Horton River upstream of the Sumac Road bridge (334560/5432440) to and beyond the edge of the Dempster map sheet, and is also commonly exposed in the bed of Trias Creek. Most of the rare small low outcrops on Dempster Plains are similar. Typical hand specimens are hard, tough, flaggy and sometimes diffusely planar laminated but not fissile, thickly bedded, pale grey (N7) or sometimes slightly greenish, orange-brown weathering very fine-grained sandstone or coarse-grained siltstone. Small pyrite euhedra, or voids left by them, may be scattered throughout the rock.

In thin section typical specimens (e.g. R005211, Dempster Plains, 336450/5435690; R006588, Horton River, 336420/5430560; R006590, Horton River, 336300/5431170) are poorly-sorted coarse-grained siltstone with equant angular quartz grains (typically 40–80 μm across) grading to a microcrystalline to almost cryptocrystalline siliceous matrix with variable amounts of fine-grained sericite. There are typically also subordinate aligned detrital muscovite flakes (mostly ≤100 μm long) generally aligned parallel to bedding, ragged very pale green to yellow chlorite grains, scattered small (mostly ≤50 μm) irregular opaque grains and rare plagioclase fragments, together with accessory tourmaline and zircon. A few samples also contain minor red-brown biotite, partly altered to chlorite. The very fine-grained sandstones (e.g. R005241, Whitehead Creek at 337940/5435120; R005199, Horton River at 335100/5432450) are mineralogically similar, but contain quartz grains up to 150 μm across.

Some paler (grey to cream-coloured) samples (e.g. R005198, Horton River bridge at 334560/5432440; R005201, Horton River at 335930/5432050) have a very fine-grained, probably recrystallised and/or silicified matrix, and are transitional to silicified siltstone (Prcs) described below.

A coarse-grained siltstone sample from the Horton River (R006591, 336310/5431260) contains numerous irregularly-shaped lithic clasts (mostly 0.5–3 mm) of darker, much finer grained and more pelitic laminated siltstone (Plate 6). These are randomly orientated throughout the rock, and the more elongate ones show only a weak alignment. Similar but less abundant clasts of dark pelitic siltstone were noted in several other samples (R006597, Dempster Plains, 339450/5430140; R005237, Whitehead Creek at 336560/5434220; R006587, Horton River at 336690/5430640). The last contains much less detrital muscovite than other samples. Two samples (R005252, 342020/5445560; R005253, 342140/5444550), from Joy Creek on the Holder map sheet, also contain clasts of dark pelitic siltstone and some sparry secondary carbonate in a matrix of medium to coarse-grained siliceous siltstone.

A large (0.8 × 0.4 m) massive concretion of tough dark grey siltstone, containing some pyrite euhedra, was noted at a bend in the Horton River at 336040/5430700. It is orientated discordant to bedding in the enclosing well-bedded paler grey siltstone. In thin section (sample R006589) the concretion is seen to consist of a fine intergrowth of angular quartz (25–150 m) and pale grey-green chlorite.

Pale, thinly planar laminated pelitic siltstone

Relatively massive to faintly and diffusely planar-laminated, hard, well-jointed medium-grey to olive greenish-grey (5GY6/1, 5GY7/2, 10GY6/2) or rarely bluish-grey (5BG5/2) siltstone crops out in Lamprey Creek. Secondary silicification was suspected from mesoscopic observations, but in thin section samples (R005214, 340230/5441400; R005222, 340100/5440460; R005223, 340090/5440390) are quite sericitic and not obviously silicified. They are medium-grained siltstones with sparse small (up to 50 μm), mostly angular to subangular quartz grains and scattered muscovite flakes, in a strongly foliated fine-grained sericitic matrix. Equant, often euhedral pyrite grains (up to 100 μm) are relatively common. Sample R005223 contains a few oblong zones of sericite up to one millimetre long, probably pseudomorphs after feldspar.

Further north near Red Hat Hill, sample R005242 (340910/5443740) is a similar rock, interbedded with very fine-grained quartz sandstone. To the south on Sumac Road, sample R005206 (334520/5432010) is a pale grey medium to coarse-grained siltstone with distinct thin (1 mm) alternating medium-grey and paler less sericitic greenish-cream laminae. In thin section it consists of subangular quartz grains (mostly 50 m), strongly aligned detrital muscovite, some pale chlorite, and sparsely disseminated fine-grained scaly to bleb-like opaque minerals.

Several other samples from Lamprey Creek (e.g. R005230, 340130/5440340; R005224, 340100/5440260) are mesoscopically similar but more sericitic, and quartz grains are small and very sparse, to absent. Sample R005224 contains numerous diffuse ovoid aggregates about 500 m across of translucent red-brown hematite (after pyrite?), around which the matrix consists of cryptocrystalline siliceous material, without sericite.

Similar fine-grained to schistose pelitic siltstone, with few quartz grains, is a fairly common lithology elsewhere within the Cowrie Siltstone. At 342130/5432970 on Dempster Plains, a pale greenish-grey, hard, well-jointed, diffusely planar-laminated siltstone (sample R005215) resembles R005214 in hand specimen. The thin section (Plate 7) consists mostly of randomly orientated sericite splinters (20 m) and microcrystalline quartz, but there is some coarsely polycrystalline quartz in large

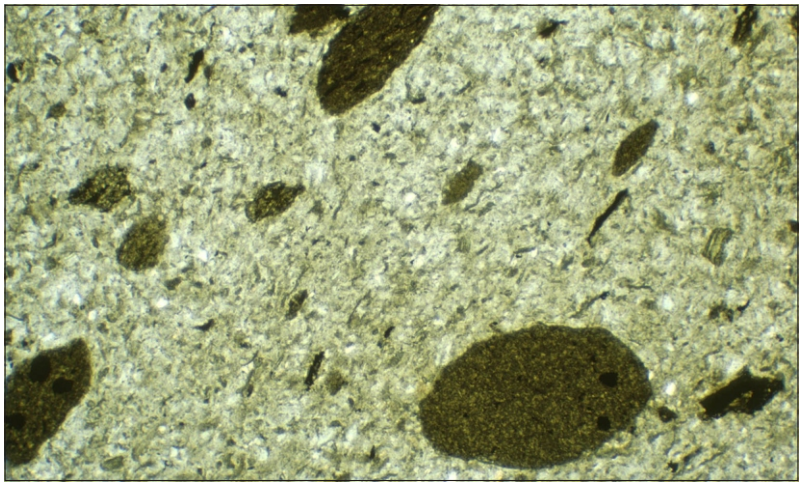

Plate 6

Photomicrograph of Cowrie Siltstone sample R006591 (Horton River, 336 310 mE, 5 431 260 mN). Pale coarse-grained siliceous siltstone with lithic clasts of darker, finer-grained and more pelitic siltstone. Plane polarised light, field of view 4.4 × 2.9 mm.

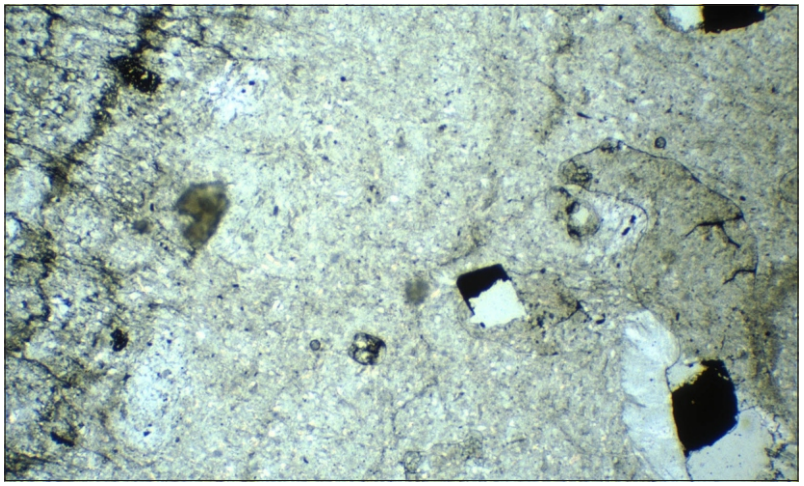

Plate 7

Photomicrograph of Cowrie Siltstone sample R005215 (Dempster Plains, 342 130 mE, 5 432 970 mN). Pale pelitic siltstone with polycrystalline quartz in pressure shadows around pyrite euhedra (right). Note also interlaminated cleaved carbonaceous siltstone (left). Plane polarised light, field of view 4.4 × 2.9 mm.

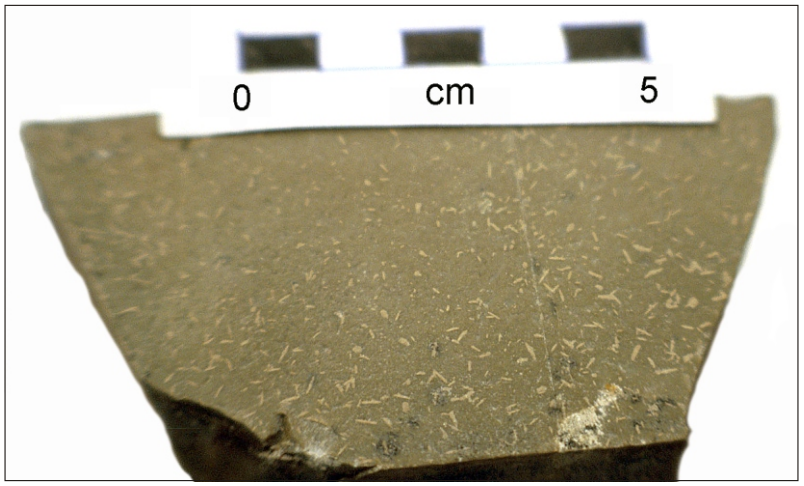

Plate 8

Cowrie Siltstone sample R005185 (Sumac Road, 337 490 mE, 5 437 420 mN), showing probable casts after anhydrite on bedding surface.

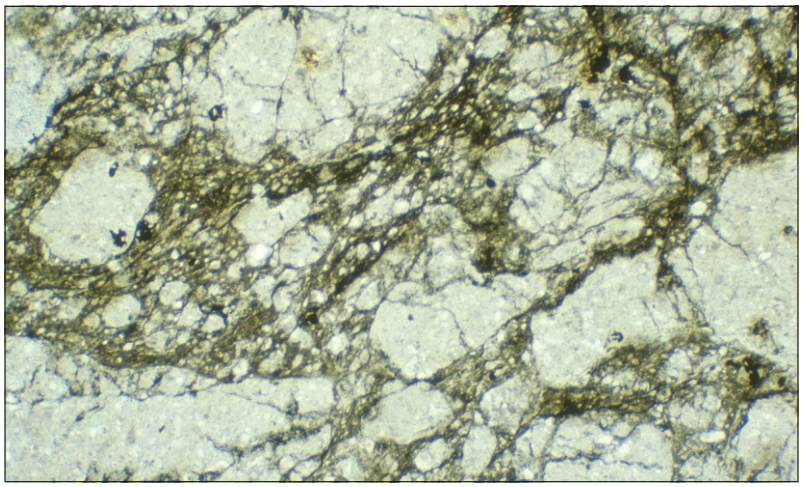

Plate 9

Photomicrograph of Cowrie Siltstone sample R005238 (Whitehead Creek, 336 380 mE, 5 434 290 mN). Pale coarse-grained sericitic siltstone with anastomising chloritic veinlets producing pseudobreccia texture. Plane polarised light, field of view 4.4 × 2.9 mm.

pressure shadows up to several millimetres across, around scattered pyrite euhedra. The rock resembles the paler laminae of sample R006584 (see above) and is interlaminated on thin section scale with typical dark laminated carbonaceous siltstone.

A fissile planar laminated pale siltstone (sample R006585) from Sumac 7 spur (333500/5430290) contains abundant very fined-grained (20 m) sericite, crudely aligned parallel to bedding, subordinate larger (to 75 m) flakes of pale green chlorite, and microcrystalline to cryptocrystalline quartz. Bedding is also defined by slightly coarser-grained, less sericitic planar laminae (up to 2 mm thick) with some small detrital quartz grains (to 25 m).

Pale massive silicified siltstone (Prcs)

This lithology is a secondary silicified variant of the Cowrie Siltstone, usually found close to the contact with the overlying Black River Dolomite. Some areas where this silicification is common to dominant are depicted on the Dempster map sheet (known outcrop) and Holder map sheet (partly inferred from known outcrop in the Rapid River, Lamprey Creek and small creeks west of Colemans Hill). It is most readily accessible in a large road cutting on Sumac Road near 336000/5436500. Typical samples (R005185, R005207–8) from this locality are tough, hard, well-jointed, pale grey to yellowish-grey (5Y8/1) or greenish-grey (5GY6/1), massive to diffusely planar-laminated siltstones. Small (up to 5 × 0.5 mm) rod-shaped structures, randomly orientated on bedding planes, are interpreted as anhydrite pseudomorphs (Plate 8), suggesting a locally shallow and evaporitic depositional environment for the Cowrie Siltstone.

In thin section sample R005208 contains a few scattered aligned muscovite flakes and sparse small subangular to subrounded quartz grains (mostly 50 m) in a microcrystalline to cryptocrystalline siliceous matrix. There are also sparse small opaque grains and accessory tourmaline.

Float of similar silicified fine-grained siltstone occurs at Dempster Plains (337110/5432150). The thin section (sample R005216) is a siliceous aggregate with few quartz grains more than 20 m, a few small sericite splinters and scattered equant opaque grains (pyrite?) 20–80 m across.

Another sample (R005213) from Lamprey Creek (340190/5441130) is a weathered pale pinkish to pinkish grey (10R8/2, 5R8/2) silicified siltstone with thin, darker pink, planar laminae. In thin section it is similar to the other silicified siltstones. Quartz grains, rarely more than 25 m across, grade to a microcrystalline siliceous matrix with subordinate small splinters of sericite. Detrital muscovite is rare. The pink colour is due to diffuse aggregates, 250 m to 1 mm across of fine-grained, scaly, nearly opaque ferruginous material, which is partly translucent and pinkish-purple under strong illumination.

Pseudobreccia

An unusual lithology occurs in Whitehead Creek at 336380/5434290, within a sequence of typical medium-grey coarse-grained siltstone. The rock (sample R005238) consists of cream-coloured lenticular pseudoclasts 15 mm to less than 1 mm in size. The larger ones are transected by, and the smaller ones grade into, a 'matrix' of anastomosing to reticulate blue-grey veinlets. In thin section (Plate 9) most of the rock (the 'clasts') is seen to be a coarse-grained siltstone or very fine-grained sandstone, similar to samples described above. It consists of rather sparsely distributed subangular to subrounded quartz grains up to 100 m and occasional detrital muscovite in a silicified and sericitic matrix. The seams and veinlets consist of fine-grained chlorite and abundant opaque material.

Inliers within the Smithton Synclinorium

Inliers of Cowrie Siltstone in the Arthur River area *(JLE)*

Two inliers of Rocky Cape Group rocks were encountered whilst traversing the Arthur River. The larger inlier, centred near 339700/5446000 just below the confluence with the Rapid River, is exposed over an area of about 0.8 km^2. Outcrops in the Arthur River typically comprise tough, somewhat silicified, medium to thick-bedded siltstone and very fine-grained sandstone ('quartzite'), occasionally with some fine streaky laminae. The rocks are medium to dark-grey or grey-green when fresh, but weather paler, sometimes with a pink tint. Bedding dips fairly consistently and moderately (19° to 50°) to the east or north throughout the river section, suggesting that the western contact with the younger Black River Dolomite is a west-side-down fault. On the north bank at 339700/5446030, generally easterly dipping 'quartzite' is disturbed by later gentle, ESE-plunging (115°) upright mesoscopic folds, with a wavelength of about 400 mm.

In thin section, sample R005033 (340080/5445960) consists of beds of rather poorly-sorted coarse-grained siltstone, up to 25 mm thick, alternating with very fine-grained sericitic siltstone to mudstone. Subangular to subrounded quartz grains up to 80 m across and splinters of detrital muscovite are abundant in the coarser beds, but very sparse and smaller in the finer ones. Cleavage, defined by closely spaced subparallel to slightly anastomosing thin stringers of brown sericite, is better developed on the finer-grained beds, which also contain scattered small square pyrite euhedra (20–100 m across). Small flame structures are locally developed at the base of some of the coarser beds.

Sample R005034 (339970/5445940) is a distinctive purplish-grey (approximately 5RP6/2, 'pale red-purple') hard silicified siltstone, with thin (1 mm) rather faint dark grey planar laminae, mostly 4–20 m

apart. In thin section the rock is seen to be poorly sorted, and consists of sparse (<10%) subrounded quartz grains (up to 100 m but mostly <50 m) and scattered splinters of detrital muscovite in a matrix of almost cryptocrystalline siliceous material with abundant sericitic shreds, aligned to define cleavage. There is also a pervasive dissemination of scaly opaque to slightly translucent material, accounting for the mesoscopic colour. These tend to be clumped into irregular aggregates (probably altered detrital iron-titanium oxide grains) or concentrated into diffuse bands 500 m to 1 mm wide.

Sample R005035 (339590/5445990) is a medium-grey, massive, very fine-grained silicified sandstone consisting of well-sorted angular to subangular quartz grains (50–100 m), very sparse opaque grains and occasional flakes of detrital muscovite in a mainly low birefringence quartzose matrix with abundant irregular, diffuse patches of fine-grained brown secondary carbonate. There are also rare small rounded grains of zircon and pale green to orange tourmaline.

The second and smaller inlier is exposed on a river bend near 338900/5445400 and consists of similar east-dipping, thick-bedded, medium-grey to pinkish-weathering very fine-grained quartz sandstone. A few hundred metres downstream, at 338750/5445730, medium-grey 'thick-bedded chert' was noted underlying or passing laterally into dolomite. However a thin section (sample R005038) of the 'chert' shows that it is a very fine-grained Rocky Cape Group sandstone similar to, but slightly more micaceous than, R005035 (see above). It consists of angular quartz grains (up to 150 m), aligned flakes of detrital muscovite and fairly densely disseminated opaque grains (40 m), with diffuse bedding defined by slight compositional variations. Bedding in the vicinity dips very gently NNW, and this outcrop is probably an extension of the inlier near 338900/5445400.

Inlier of Cowrie Siltstone near Blackwater Road *(JLE)*

A four kilometre long, north-trending inlier of Cowrie Siltstone correlate, centred near 327200/5443000, forms a flat-topped ridge between the lower catchments of Stephens Rivulet and Blackwater Rivulet. The inlier is mostly fault-bounded, by the Roger River Fault to the southeast and by two inferred east-directed thrusts to the northeast and west. Dips are fairly consistently moderately to steeply west dipping, and part of the western part of the inlier is overlain, probably conformably, by chert and dolomite correlated with the Black River Dolomite. To the north the inlier is truncated by a probable cross fault, against chert also correlated with the Black River Dolomite.

Good exposures occur along Blackwater Road between 327660/5443360 and 326810/5440660, along Blackwater 4 spur, and in small gullies to the north. Fresh outcrops are of hard, dark grey to nearly black, thinly planar-laminated, fissile to flaggy siltstone, frequently containing a few small yellow pyrite euhedra. These weather to pale grey, cream or off-white, sometimes with a pink to purplish tint or a yellow-green staining from alteration of pyrite. Very weathered exposures may have a pale brown skin and a soft off-white interior. Lithologically the inlier is identical with the most common facies of the Cowrie Siltstone, exposed to the east of the Smithton Synclinorium.

In thin section a typical sample (R004801, 326860/5443060) is a medium to coarse-grained siltstone, consisting of mainly angular quartz grains (mostly 25–75 m) and abundant splinters of detrital muscovite (up to 150 m long) with a crude preferred orientation. Muscovite has partly recrystallised to, and is not always clearly distinguishable from, shreds of sericite. There is also abundant opaque material, probably both scattered small pyrite euhedra and diffuse discontinuous bands of finely scaly carbonaceous(?) material which, together with detrital muscovite, define the bedding lamination. Cleavage, as defined by sericite, is parallel to bedding. Some of the larger quartz grains are polycrystalline and strongly elongate parallel to the fabric.

Sample R004802 (326840/5440730) is a less fissile and more weathered, dark olive-green to brown flaggy siltstone, but in thin section is very similar to R004801.

Two other samples are much less carbonaceous but otherwise similar in thin section. Sample R004806 (326660/5444100) is a dark greenish-grey, flaggy but not fissile, planar-laminated siltstone. R004811 (326610/5444170) is a more weathered, tawny-coloured (pale orange-pink, 5YR7/2) soft fissile siltstone, which retains a thin planar lamination, visible when wet.

Inferred inlier of Rocky Cape Group north of the Horton River *(JLE, ARR)*

A zone of high total counts on radiometric data around 331100/5435600, near the centre of a domal structure in the Black River Dolomite, suggests that pelitic material, probably an inlier of Cowrie Siltstone, occurs in the vicinity. Field traverses across this area failed to locate any outcrop of Rocky Cape Group lithologies. As discussed below, chert breccia cropping out on an arcuate ridge immediately to the east (331500/5435560) may represent, or be transitional to, the Forest Conglomerate and Quartzite. The area (c. 0.4 km^2) of inferred Cowrie Siltstone depicted on the Dempster map is consistent with field and geophysical evidence.

Geochemistry of the Rocky Cape Group *(JLE)*

Six samples of the Cowrie Siltstone were chemically analysed to provide background geochemical information. Data are given in Table 2, together with previous data obtained by J. W. Hudspeth and R. G. Richardson during petrophysical studies, which include a further two analyses of the Cowrie Siltstone, and four from the Balfour Subgroup. More chemical

Table 2. *Chemical analyses, Rocky Cape Group*

	Cowrie Siltstone								Balfour Subgroup			
Unit/Field No.	Prc/TJ71	Prc/TJ148	Prc/TJ571	Prc/TJ1332	Prc/TJ2711	Prc/AR1	Prc/-	Prc/-	Prbs/-	Prbg/-	Prbq/-	Prbq/-
Reg. No.	R005186	R005187	R005197	R005232	R005276	R005025	G401352	G401353	G401354	G401355	G401356	G401357
Anal. No.	941139	941138	941145	941142	941141	941159	891865	891866	891867	891868	891869	891870
AMG (mE)	359230	342710	344100	345630	353540	343760	327120	324320	322120	321800	320820	321700
AMG (mN)	5437260	5435160	5441850	5441780	5435700	5450150	5442330	5440170	5439240	5438440	5437600	5435800
Sheet	Beryl	Beryl	Holder	Holder	Beryl	Tayatea	Sumac	Sumac	Dempster	Dempster	Dempster	Dempster
Lithology	siltstone	siltstone	siltstone	sandstone	siltstone	'quartzite'	siltstone	siltstone	'hornfels'	siltstone	siltstone	siltstone
SiO_2 (%)	76.50	80.28	68.90	69.16	67.89	80.56	63.06	60.59	64.72	68.84	73.01	63.52
TiO_2	0.45	0.40	0.71	0.52	0.65	0.19	0.82	0.72	0.40	0.82	0.62	0.72
Al_2O_3	11.52	10.25	16.16	12.96	15.26	10.64	18.20	21.54	12.31	16.98	13.97	18.35
Fe_2O_3	0.61	0.79	1.06	2.78	2.95	0.74	2.22	1.06	2.94	1.40	1.50	0.01
FeO	1.52	0.86	2.18	3.77	0.30	0.56	3.31	2.78	6.75	1.59	2.31	5.28
MnO	0.02	0.01	0.02	0.04	0.02	0.11	0.08	0.02	0.10	0.06	0.06	0.06
MgO	2.57	0.81	2.34	2.43	1.52	0.35	2.39	1.76	4.94	1.05	0.93	1.28
CaO	0.04	0.01	0.07	0.11	0.13	0.10	0.01	0.01	0.05	0.05	0.01	0.01
Na_2O	0.09	1.00	0.10	0.69	1.38	1.96	0.27	0.23	0.21	0.21	0.20	0.21
K_2O	3.23	2.27	4.11	2.73	4.24	3.60	4.96	5.80	1.62	5.13	3.98	4.44
P_2O_5	0.06	0.05	0.06	0.12	0.12	0.05	0.04	0.02	0.12	0.01	0.01	0.01
H_2O^+	2.30	2.00	3.09	3.16	4.06	0.80	4.12	4.62	4.69	2.95	2.73	4.81
CO_2	0.27	0.29	0.21	0.08	0.30	0.46	0.76	0.72	0.82	0.51	0.52	1.23
SO_3	0.06	0.04	0.03	0.05	0.05	0.04	0.09	0.05	0.11	0.04	0.10	0.24
TOTAL	**99.24**	**99.06**	**99.04**	**98.60**	**98.87**	**100.16**	**100.33**	**99.92**	**99.78**	**99.64**	**99.95**	**100.17**
LOI	[2.41]	[2.19]	[3.06]	[2.82]	[4.33]	[1.19]	[4.53]	[5.05]	[4.80]	[3.30]	[3.03]	[5.55]
Sc (ppm)	11	<9	11	12	11	<9	20	18	9	13	13	15
V	39	35	64	45	70	10	71	51	50	55	45	70
Cr	56	69	49		88	120	105	59	50	91	120	105
Co	<8	<8	<8	12	<8	8	<5	<5	10	<5	<5	8
Ni	9	15	15	16	11	5	13	16	15	15	17	22
Cu	<5	12	7	<5	<5	9	5	13	14	15	38	35
Zn	24	22	43	69	23	77	23	32	84	<5	7	26
Ga	11	7	19	14	18	10	16	20	14	15	12	16
As	<20	<20	<20	<20	<20	<20	8	<5	7	11	11	14
Rb	140	120	250	120	170	140	220	260	70	230	180	210
Sr	29	22	37	32	43	65	15	11	<5	19	14	17
Y	40	30	37	40	43	29	28	43	5	22	27	26
Zr	470	470	270	250	220	175	165	230	175	240	210	180
Nb	17	16	20	15	18	10	18	16	6	16	14	12
Mo	<5	<5	<5	<5	29	<5	<5	<5	<5	<5	5	<5
Ag	nd	nd	nd	nd	nd	nd	<5	<5	<5	<5	<5	<5
Sn	<9	<9	<9	<9	<9	<9	<5	<5	<5	<5	8	<5
Sb	nd	nd	nd	nd	nd	nd	<5	<5	<5	<5	<5	<5
Ba	120	270	860	560	480	1150	660	800	220	630	500	700
La	34	59	38	38	28	35	70	73	46	37	61	70
Ce	72	93	81	70	59	66	145	170	115	83	125	140
Nd	31	53	41	52	33	40	38	46	34	25	41	33
W	<10	<10	<10	<10	<10	<10	5	7	10	17	9	10
Pb	13	<10	<10	<10	17	12	<5	<5	<5	5	10	6
Bi	<5	<5	<5	<5	<5	<5	6	5	7	6	5	5
Th	23	26	25	<10	27	13	22	16	7	6	9	14
U	<10	<10	<10	<10	15	<10	7	8	<5	<5	<5	5

Analyses by Mineral Resources Tasmania laboratories

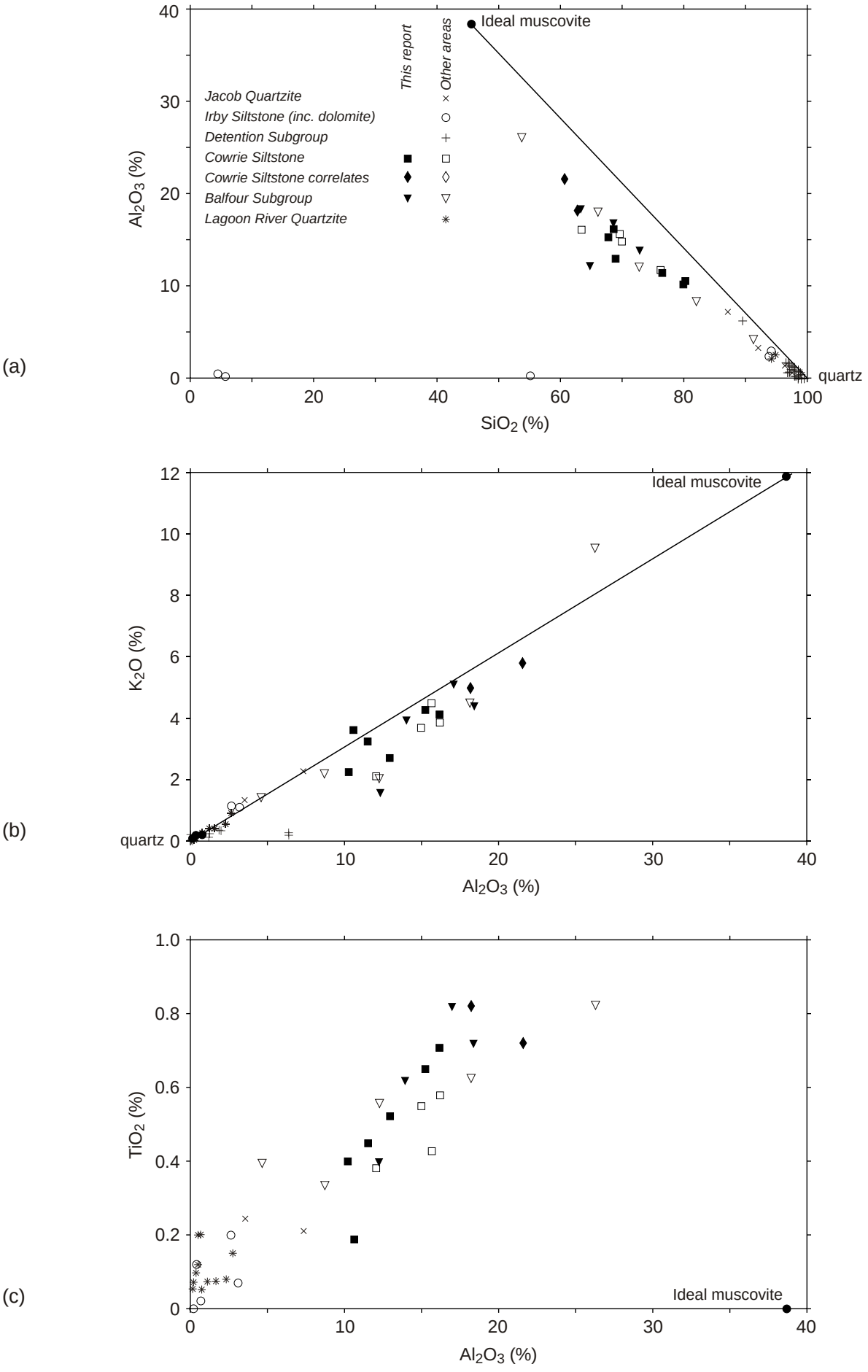

Figure 4

Geochemical plots of whole rock analyses, Rocky Cape Group: (a) Al_2O_3 against SiO_2; (b) K_2O against Al_2O_3; (c) TiO_2 against Al_2O_3

analyses of Rocky Cape Group samples, from outside the Roger–Sumac–Dempster area, are available in the MRT ROCKCHEM database.

All these samples, including dark carbonaceous siltstone (R005186, R005276), greenish siltstone (R005197, R005232) and pale fine-grained sandstone (R005232), are fairly typical pelites comprising mainly SiO_2, Al_2O_3 and K_2O, and have low Na_2O and very low CaO. Significant MgO and iron occur in some samples, mainly reflecting the presence of chlorite (particularly sample 401354, from the Balfour Subgroup unit Prbs with porphyroblastic chlorite). It is also noteworthy that the indurated pale, apparently silicified 'quartzite' (sample R005025) near the base of the Togari Group is also compositionally pelitic and similar to the other samples, even carbonaceous siltstone such as R005186. H_2O+, which is lowest in R005025, was calculated by difference from loss-on-ignition, and would therefore also include any organic carbon.

The total geochemical data from the Rocky Cape Group presently available comprises about 52 analyses, excluding two dolomites and an ironstone from the Irby Siltstone. About half of these analyses are quartzites, with well over 90% SiO_2. In this total data set, a strong positive correlation is apparent between Al_2O_3 and K_2O (fig. 4*a*), with most of the data lying close to a mixing line between the compositions of ideal muscovite ($KAl_2.AlSi_3O_{10}(OH)_2$) and quartz, the principal minerals in these rocks.

A strong negative correlation exists between SiO_2 and Al_2O_3 (fig. 4*b*). As these are the most abundant elements in these rocks, this is partly due to the 'sum effect' (e.g. Rollinson, 1993), but it is noteworthy that the most of the pelites lie near but just below the mixing line between muscovite and quartz. This reflects the presence of other minerals lower in both SiO_2 and Al_2O_3, probably mainly chlorite, iron-titanium oxides and carbonaceous matter. Note that Al_2O_3 also correlates with TiO_2 (fig. 4*c*), total iron and (rather poorly) with MgO. There are no systematic correlations involving CaO (which is always low), MnO, Na_2O or P_2O_5.

Of the trace elements, Rb, Ba, Ga, Sc, V (rather poorly) and Nb correlate well with K_2O and Al_2O_3. Apart from Nb, these elements have geochemical affinities to K, Al or Fe. The light rare earth elements (La, Ce and Nd) and Y are generally lower in quartzite than pelite but, within these two groups, do not show any convincing correlation with either Al_2O_3 or K_2O. The remaining trace elements show quasi-random behaviour, or are close to detection limits.

Depositional environments of the Rocky Cape Group *(ARR, JLE)*

The Lagoon River Quartzite has many of the sedimentary features seen in other orthoquartzite units of the Rocky Cape Group, such as the Jacob Quartzite and those that form the major formations of the Detention Subgroup (e.g. Gee, 1967). These include supermature composition (>95% quartz), upwardly fining cycles commonly with scoured bases, common trough cross bedding, rare ripple casts, and the presence of interbedded lutite. A tectonically stable, shallow marine, sub-littoral to neritic depositional environment, similar to that inferred by Gee (1967, p.123–124) for the other quartzites, seems likely. The fine-grained carbonaceous siltstone towards the top of some cycles probably represents spatially-restricted episodes of restricted sedimentation. The thickness of the unit probably requires a slowly and gently subsiding basin. Most of the Lagoon River Quartzite remains unmapped and no detailed sedimentological, provenance or palaeocurrent studies to compare it with the younger orthoquartzites have been undertaken. Its significance is probably that it records an earlier period of shallow marine sedimentation, prior to the deposition of Cowrie Siltstone which was thought by Gee (1967) to be the oldest unit in the region.

Although some units of the Balfour Subgroup, notably the Cassiterite Creek Quartzite, are lithologically similar to the Lagoon River Quartzite, the subgroup as a whole is lithologically more diverse and characterised by rapid lateral facies changes. Chemically reducing, carbonaceous and sometimes pyritic siltstones are more common than in the Lagoon River Quartzite, suggesting longer periods of slower sedimentation in temporarily isolated local sub-basins, although common small-scale cross bedding shows that the conditions were not as quiet as in the overlying Cowrie Siltstone. Although common trough cross bedding in sandier units suggests that the environment was probably still shallow marine, possible evaporite casts in the Cassiterite Creek Quartzite suggest local emergence. Deeply incised channels, gutter-cast structures, and clastic dykes previously thought to have formed in syneresis cracks, may be related to tectonic extension (see *Structural Geology* section below). These features suggest that the Balfour Subgroup was deposited in an unstable, dominantly shallow marine basin influenced by syn-sedimentary growth faulting.

In contrast, the Cowrie Siltstone is a monotonously fine-grained, finely planar-laminated unit, with few tractional sedimentary structures and without graded bedding, indicating deposition in a very quiet, low energy environment. Much of it is carbonaceous, and sedimentary pyrite is very common, indicating reducing conditions. Gee (1967, p.122–123) suggested deposition by fall-out from suspended clay and fine silt in a relatively deep, euxinic marine environment, starved of coarse-grained detritus. He considered that the Cowrie Siltstone represents the earliest, deep water phase of sedimentation in the Rocky Cape Group, after which the younger orthoquartzite formations represent a change to shallower water, free circulation and higher energy environments. The recognition that a similar orthoquartzite unit, the Lagoon River Quartzite, lies below the Cowrie Siltstone makes a deep water environment for the latter less likely. It is suggested instead that the Cowrie Siltstone was deposited in a large shallow, stagnant lagoonal environment, largely

isolated from marine currents. The presence of likely anhydrite casts in the unit (Sumac Road near 336000/5436500) is consistent with shallow water, locally evaporitic conditions. The carbonaceous facies may represent periodic algal blooms. As for the orthoquartzites, slow subsidence is required to account for the apparently great thickness of the formation. Some of the orthoquartzite units may, in part, be facies equivalents, representing bars enclosing the lagoon.

Metamorphism in the Rocky Cape Group *(ARR, JLE)*

Regional metamorphism

Bladed to tabular green chlorite, commonly forming aggregates to one millimetre across, is the most common preserved regional metamorphic mineral. Brown pleochroic cores to chlorite in rocks from the Temma coastline (samples R007214, R007215) indicate probable retrogression (at least locally) of biotite to chlorite.

Although the presence of chlorite in cleavages of all generations suggests a number of thermal events, the timing of peak metamorphism remains unclear. Bladed chlorite (± biotite) commonly forms cores to the D_2 porphyroblasts. The bladed chlorite cuts the S_1 cleavage but, in turn, is cut and deformed by S_3, making it of probable D_2 age (see *Structural Geology* section for further discussion). The origin of the elongate ovoid to pseudo-rhombohedral spots in Rocky Cape Group sedimentary rocks remains enigmatic.

Contact metamorphism and/or metasomatism

Pale blue to brown, euhedral to subhedral tourmaline to 0.25 mm in length is common in Rocky Cape Group rocks near Balfour. Tourmaline crystals overgrow the S_1 and S_2 cleavages, but show a conflicting timing relationship with respect to S_3, both cross cutting and also cross cut by the S_3 cleavage. South of Mt Balfour (322290/5425570) on the Balfour map sheet, rounded shale clasts in sandstone beds from the Lagoon River Quartzite (sample R004791) contain up to 98% tourmaline, with crystals arranged in a herringbone pattern suggestive of mimetic overgrowth of at least two pre-existing cleavages. Tourmaline is also present in mylonite (sample R004800) from the Waratah Creek thrust (327400/5424800), also on the Balfour map sheet.

Pseudo-hexagonal porphyroblasts and aggregates were noted by A. R. Reed near the Blackwater Road–Heemskirk Road junction (320900/5437750, Dempster map sheet), near the Lindsay River and in the vicinity of D_3 thrusts (330190/5427770, Balfour map sheet), and on the coast near Temma (306875/5432935). The porphyroblasts are up to 5 mm in diameter and, in hand specimen, comprise a matted to radiating, fibrous pale green to brown mineral. In thin section (samples R007219, R007216) they typically comprise matted chlorite (± tourmaline) which, together with the hexagonal shape and radiating fabric observed in hand specimens, was thought to be indicative of pseudomorphs after cordierite (A. Reed). The pseudomorphs cross cut S_3 but are also weakly deformed by S_3. This, and the inclusion of tourmaline in mylonite of D_3 age, suggests a syn- to late-D_3 timing for granite intrusion, if these minerals are of contact metamorphic origin. The nearest outcropping granite, the Interview Granite at Sandy Cape, has recently yielded a U-Pb SHRIMP age from zircon of 362.4 ± 1.9 Ma (Black *et al.*, 2005). Intrusion of the granite late during the D_3 event is consistent with granite-related fluids being channelled into D_3 faults.

Euhedral bladed chlorite to one millimetre diameter, and anhedral poikiloblastic epidote of similar proportions, have also been observed in thin sections (e.g. sample R007214) of rocks located on the Temma coastline (306875/5432215). The chlorite is commonly poikiloblastic, enclosing bladed chlorite (± biotite) of probable regional metamorphic origin. If intrusion of granite has resulted in chlorite crystallisation, it is unlikely that the earlier-formed biotite is also the product of the same contact metamorphism. A locally higher grade of contact metamorphism may have enabled preservation of regional metamorphic biotite that elsewhere has almost entirely retrogressed to chlorite.

A more detailed mineralogical study of porphyroblasts in spotted metasedimentary rocks from several localities near Balfour was made by Bottrill (2004*a, b*), after the first compilation of this report. Although they are nearly always retrogressed to fine-grained sericite, quartz and sometimes chlorite, several types of porphyroblasts were distinguished on morphological criteria. One equant, possibly cubic, dodecahedral or trapezohedral type, commonly with a radial structure, was thought to be after garnet. This was confirmed in samples from near the junction of the Heemskirk and Blackwater roads (320760/5437640, near one of Reed's localities), in which electron microprobe analyses showed relict Ca-Mn garnet (spessartine-grossular) to be present. A second, bladed type of porphyroblast is completely replaced by quartz, sericite and locally cores of chlorite, and was thought to be most likely after chloritoid or ottrellite (a Mn-rich member of the chloritoid group). A third type, consisting of irregular aggregates of quartz and leucoxene, was thought to be pseudomorphs after ilmenite or sphene. Mineral compositions were used to tentatively suggest temperatures of 320–360°C and pressures of 4.9–6.9 kb (490–690 MPa). It was concluded that neither the porphyroblasts nor tourmaline provided definite evidence of granitic influence, but the composition of the garnet in particular was "typical of that in the alteration zones about Broken Hill-style stratabound Pb-Zn deposits" (Bottrill, 2004*a*). This casts doubt on Reed's arguments for the timing of successive deformations relative to granite intrusion.

Proterozoic dolerite: Tayatea dyke swarm (Pmd; Pmf where foliated)

Definition *(JLE)*

The Tayatea Dyke Swarm is herein defined as the series of mainly tholeiitic, generally NNE to NE-trending dolerite dykes that intrude the Rocky Cape Group within a zone approximately 100 km long and up to 30 km wide, east of the Smithton Synclinorium and west of the Arthur Metamorphic Complex. The swarm crops out on the north coast between Black River (357600/5476700) and two kilometres west of Boat Harbour (382200/5468300) and extends to near the west coast between south of the Pieman River (at 333000/5385200) and the Norfolk Range area (e.g. 331200/5408000). The name replaces the informal and invalid term 'Rocky Cape Dyke Swarm'.

Only a few poorly-exposed dykes occur in the area under discussion, on the Dempster map sheet.

Dempster Plains *(JLE)*

Field relationships

A poorly-exposed NE-trending dolerite dyke (Pmd) occurs in the upper Trias Creek area on Dempster Plains, in the extreme southeast of the Dempster map sheet. On the ground it is marked by a zone of characteristic orange-red soil, which supports a narrow belt of trees in an area of otherwise mainly buttongrass and heath. Sporadic dolerite float, mostly deeply weathered but with a few fresh kernels of larger boulders, was noted at 339130/5430170 and 339780/5430480. Because of poor exposure, the thickness of the dyke is difficult to judge; the mapped thickness (100–150 m) may be an overestimate. The dyke is associated with a weak aeromagnetic anomaly, and on colour images it can be traced four kilometres southwest towards the Horton River to similar exposures at 337910/5428260 and 336960/5426970 on the Balfour map sheet. Five kilometres to the northeast, orange-red soil and deeply weathered dolerite on minor logging roads near Lost Hill (at 342340/5435500 and 342320/5435260; Everard *et al*., 1996) are probably exposures of the same dyke. However large segments of the dyke have little or no surface expression due to peaty regolith.

Petrography

In thin section (Plates 10, 11) a sample (R006778) consists mainly of interlocking slightly elongate subhedral plagioclase (500 µm–1.5 mm) and subhedral clinopyroxene (500 µm–1 mm), in an even-grained, consertal to slightly subophitic texture. In their interstices are anhedra of clear quartz, and micrographic to microgranophyric intergrowths of quartz and feldspar. Angular to skeletal opaque grains (500 µm–1 mm) are rather sparsely scattered throughout the rock.

The clinopyroxene is colourless, biaxial positive with moderate 2V and is probably augite. It is somewhat turbid, and partly replaced around its rims by amphibole, which ranges from probable actinolite (fibrous and pleochroic from sea-green to colourless) to well crystallised brown hornblende. Rare biotite (pleochroic from dark yellow-brown to colourless) is locally associated with amphibole. Plagioclase is probably albite, and potash feldspar is probably also present. Both show partial to incipient alteration to a scaly colourless phyllosilicate, probably sericite. Only a trace of chlorite is present. Some skeletal opaque grains outline apparent pseudomorphs, closely associated with amphibole, and may be metamorphic in origin.

No foliation is present.

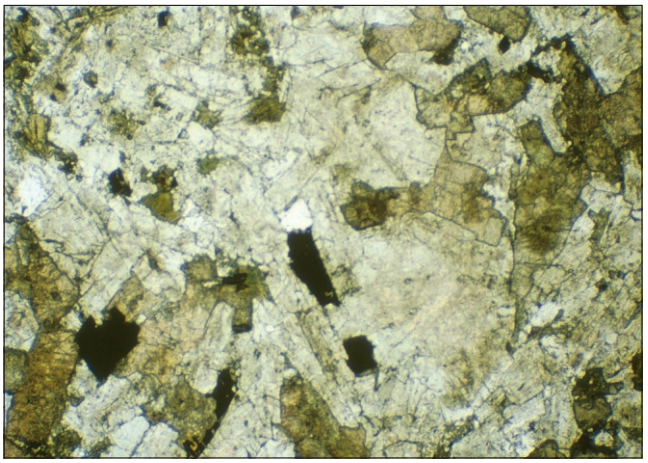

Plate 10

Photomicrograph of Proterozoic dolerite (Pmd) dyke sample R006778 (Dempster Plains, 339 130 mE, 5 430 170 mN). Interlocking plagioclase (light, with patchy alteration to sericite) and clinopyroxene (dark, partly altered to amphibole), with minor quartz (centre) and opaque grains. Plane polarised light, field of view 4.4 × 2.9 mm.

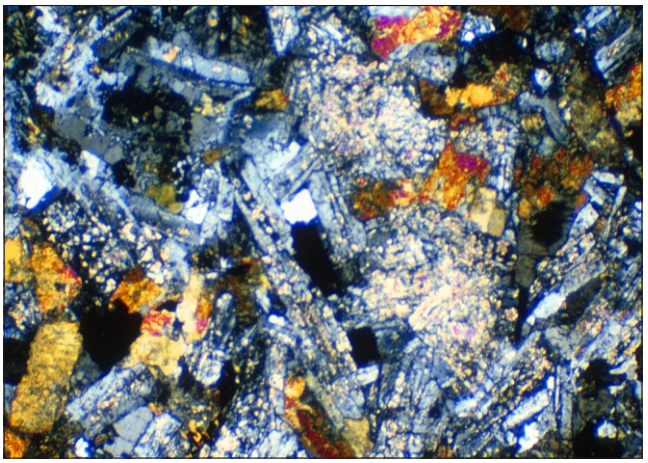

Plate 11

Photomicrograph of Proterozoic dolerite (Pmd) dyke sample R006778. Same view as Plate 10, crossed nicols.

North of Sumac 7 Spur Road *(JLE)*

On coloured images derived from the 1996 Arthur–Pieman geophysical survey (flown for the Regional Forestry Agreement by MRT and AGSO), a moderate positive magnetic anomaly, elliptical with a north to NNE elongation, is centred near 333200/5430600, about one kilometre west of Sumac Road and 1.5 km south of the Horton River. The anomaly is within an area mapped as Cowrie Siltstone (Prc), although close to the faulted contact with the Togari Group. During ground checking, soft deeply-weathered orange-brown float (sample R006779), with a possible relict igneous texture, was collected from the roots of a fallen tree near 333110/5430540. In thin section this rock consists of unorientated plagioclase laths, mostly 500 μm–1 mm but up to 2 mm long, largely replaced by prehnite, together with much dark brownish-red altered ferromagnesian material and minor interstitial anhedral quartz (up to 400 μm). It is probably a Proterozoic dolerite intrusion and is petrographically similar to fresher samples from the Tayatea Dyke Swarm. The presence of quartz makes assignment to the Spinks Creek Volcanics (or Tertiary basalt) unlikely. Although the sample has low magnetic susceptibility ($<0.4 \times 10^{-3}$ SI), this may be due to weathering, and fresher material is probably the source of the anomaly.

Frankland River near Balfour *(ARR)*

Two dolerite dykes have been mapped intruding correlates of the Cowrie Siltstone along faults northeast of Balfour. The easternmost dyke, which crops out in the Frankland River at 325800/5430900, is relatively massive and has a northwesterly trend. The other dyke, about 500 m further west, is foliated and has a northerly trend parallel to the Balfour Shear Zone.

Geochemistry *(JLE, ARR)*

Chemical analyses of the westernmost of the Frankland River dykes (analysis 980096) and the Dempster Plains dyke (R006778, analysis 980397) are presented in Table 3. Both rocks have a tholeiitic chemistry, indicated by relatively low total alkalis ($Na_2O + K_2O$), low P_2O_5 and a low Nb/Y ratio (<1).

The Dempster Plains dyke and, probably, the Frankland River dykes are assigned to the Tayatea Dyke Swarm on the basis of field relationships and geochemistry. A detailed discussion of the geochemistry of the swarm will be given elsewhere, based on a large data set of more than 100 samples mainly from the Trowutta and Smithton quadrangles (J. L. Everard, A. V. Brown and D. B. Seymour, unpublished data). When compared to this data set, virtually all major and trace elements in both of these dykes fall within typical ranges. It is perhaps noteworthy that, in the Frankland River dyke (analysis 980096), MgO, Ni and Cr are within the higher part of the range, indicating a relatively unfractionated composition, whilst CaO is relatively low in the Dempster Plains dyke (R006778). The only unusual feature of either analysis is the anomalous As (45 ppm) in the former. This suggests weak mineralisation, but Pb, Zn, Cu, Bi and S are not elevated.

The relatively high K_2O content is a characteristic feature of the Tayatea Dyke Swarm dolerites, and suggests that they are not the direct feeders for the Spinks Creek Volcanics, as previously suggested by Brown (1989*a*, p.68).

Table 3

Chemical analyses, Proterozoic dolerite dykes and miscellaneous mafic rocks

Field No.	MJ925	480	71	585
Reg. No.	R006778	R004744	R004772	R004762
Anal. No.	980397	980096	980095	980097
AMG (mE)	339130	325320	321180	327880
AMG (mN)	5430170	5431010	5436260	5439210
SiO_2	51.53	50.61	60.71	53.75
TiO_2	1.46	1.17	4.25	0.62
Al_2O_3	14.28	14.36	20.77	15.00
Fe_2O_3	1.85	1.42	0.13	1.70
FeO	9.23	9.23	0.00	6.91
MnO	0.18	0.14	0.00	0.22
MgO	6.29	8.41	0.15	6.76
CaO	9.02	5.85	0.02	6.61
Na_2O	1.97	3.13	0.03	2.44
K_2O	1.61	1.45	0.02	2.48
P_2O_5	0.22	0.16	0.07	0.14
SO_3	0.11	0.07	0.03	0.08
CO_2	0.43	0.10	2.05	0.19
H_2O^+	1.76	3.93	10.92	3.06
TOTAL	**99.94**	**100.04**	**99.15**	**99.96**
LOI	[1.17]	[3.01]	[12.97]	[2.48]
Sc	32	34	16	42
V	330	280	170	200
Cr	97	480	760	270
Co	34	43	9	34
Ni	76	185	75	62
Cu	87	92	43	28
Zn	150	98	27	82
Ga	20	18	28	16
As	<20	45	<20	<20
Rb	59	44	<5	115
Sr	165	185	<5	110
Y	26	26	21	32
Zr	120	120	370	105
Nb	11	9	100	12
Mo	<5	<5	7	<5
Sn	<9	<9	<9	<9
Ba	300	380	<23	460
La	<20	<20	63	20
Ce	40	36	135	31
Nd	21	<20	62	23
W	<10	<10	<10	<10
Pb	12	21	49	21
Bi	<5	<5	<5	<5
Th	17	15	74	16
U	<10	<10	<10	<10

MJ925: massive, unfoliated coarse-grained dolerite dyke, Dempster Plains.
R004744: Folded and foliated dolerite dyke, up to 100 m wide, striking ~150°, Frankland River.
R004772: Pale brown, weathered, deformed dyke, near The Clump.
R004762: Gabbro boulder in diamictite, Blackwater Rivulet tributary.
Analyses at Mineral Resources Tasmania laboratories.

Late Neoproterozoic–Early Cambrian: Togari Group

Definition *(JLE)*

The Togari Group is herein defined as that sequence, up to four kilometres thick, of principally conglomerate, dolomite and chert, diamictite, volcaniclastic and siliceous sedimentary rocks and basalt, that unconformably or disconformably overlies the Rocky Cape Group and is overlain by the Scopus Formation. The constituent formations are the Forest Conglomerate and Quartzite (0–120 m thick), Black River Dolomite (≤800 m), Kanunnah Subgroup (≤1400 m), Smithton Dolomite (≤1500 m), Salmon River Siltstone (≤350 m) and their members. The type section is composite and designated as that of these constituent formations, as defined or referred to herein. In a tributary of Blackwater Rivulet, between 324140 mE, 5444240 mN and 324930 mE, 5445040 mN, there is a well-exposed, unfaulted, consistently east-facing section extending through the Black River Dolomite (at the base of the group) and Kanunnah Subgroup to the middle of the Smithton Dolomite. The age of the Togari Group is considered to be mid-Cryogenian (c.750 Ma) to Early (–Middle?) Cambrian.

Previous work *(JLE)*

Nye *et al*. (1934) divided the rocks in the Smithton area into a number of 'Stages', which roughly correspond to the formations as now recognised, in their correct stratigraphic order:

(6) 'Upper Slate and Breccia Stage' (now Scopus Formation).

(5) 'Dolomite Stage' (now Smithton Dolomite).

(4) 'Slate, Breccia and Limestone Stage' (now Kanunnah Subgroup in part).

(3b) 'Cherts, Slates &c., Sub-stage'; and

(3a) 'Dolomite Sub-stage' (together now Black River Dolomite).

(2) 'Grey-green Quartzite Stage' (now part of Cowrie Siltstone).

(1) 'White Quartzite Stage' (now part of Cowrie Siltstone, and Forest Conglomerate and Quartzite).

The (usually low angle) unconformity between the Cowrie Siltstone and Togari Group was not recognised, and the basalts of what are now known as the Spinks Creek Volcanics were thought to be a later (Devonian) dolerite intrusion.

Carey and Scott (1952) recognised the extrusive nature of the basalts, and grouped them with Stage 4, which they regarded as Cambrian and assigned to the Dundas Group of western Tasmania. However they miscorrelated the dolomite of the Duck River plains (Stage 5) with the dolomite and chert near Irishtown (Stages 3a and 3b), terming both Smithton Dolomite, and likewise combined Stage 4 and Stage 6.

Gulline (1959) extended this correlation, assigning all dolomite between Redpa and Black River to the Smithton Dolomite.

Spry (1964) introduced the terms Forest Conglomerate and Quartzite and Black River Dolomite for units successively overlying the Cowrie Siltstone "without angular discordance" (sic) at the Black River bridge on the Bass Highway. He regarded the Black River Dolomite as a correlate of the Rapid Dolomite of McNeil (1961) and the Smithton Dolomite of Carey and Scott (1952), and suggested further correlations with the Corinna and Zeehan areas.

McNeill (1961) and Matthews (1961*b*) used the term Rapid River Dolomite for dolomite, chert, cherty slate and breccia occurring in the Arthur River area (the Black River Dolomite as described in this report). They considered that it appeared to conformably overlie the Lawson River Siltstone (equivalent to part of the Cowrie Siltstone) and correlated it with the Smithton Dolomite. Longman and Matthews (1962), summarising the geology of the same area, apparently considered the term Rapid River Dolomite to be redundant, and suggested that the dolomite ('Smithton Dolomite') overlay the 'Bryant Hill Quartzite' of the 'Older Precambrian', possibly unconformably.

Gee (1968) defined the Rocky Cape Group (including the Cowrie Siltstone), and described the unconformity at the mouth of Black River between the Cowrie Siltstone and the Forest Conglomerate and Quartzite. He also correlated the overlying Black River Dolomite with the Smithton Dolomite.

The stratigraphy of far northwest Tasmania remained confused until Large (1982) re-established the presence of two separate major dolomite units. This interpretation was published by Baillie and Crawford (1984) and applied to the Trowutta map sheet, together with the first usage of several stratigraphic names including Togari Group and Kanunnah Subgroup, by Everard *et al*. (1996).

The Smithton 1:50 000 scale geological map (Lennox *et al*., 1982) depicts only a single dolomite unit, but the correct stratigraphy is outlined in the subsequent explanatory notes (Brown, 1989*a*).

Forest Conglomerate and Quartzite (Pscb)

This unit was defined at the Black River bridge (357300/5476700) on the Bass Highway east of Smithton (Spry, 1964). Oddly, Spry appears not to have recognised the unconformity with the underlying Cowrie Siltstone there, and grossly mis-correlated the Forest Conglomerate and Quartzite with the Bluff Quartzite (the lower formation of the Detention Subgroup).

The Forest Conglomerate and Quartzite is well developed at the base of the Togari Group in the Smithton area and at some localities near Marrawah. In these areas it comprises a siliciclastic conglomerate with well-rounded pebble to cobble-sized clasts of Rocky Cape Group type quartzite (e.g. P. W. Baillie,

K. D. Corbett, E. B. Corbett and P. G. Lennox *in* Brown, 1989*a*, p.20–21). It is generally absent to the south, and at most localities the Black River Dolomite rests directly on Rocky Cape Group basement.

East of the Frankland River *(DBS)*

An inferred correlate of the Forest Conglomerate and Quartzite is intermittently exposed along a disused forestry investigation track between approximately 323920/5436120 and 324330/5434700 on the Dempster map sheet. It is terminated to the north by one of the main splays of the Roger River Fault, and to the south by an inferred northwest-trending fault which is probably a component of the major northeast-directed thrust system which dominates the western parts of the Dempster and Sumac map sheets. The unit is about 120 m thick, and comprises interbedded chert breccia, distinctly stratified lithic pebble conglomerate, and pale grey-weathering distinctly laminated medium-grained quartzarenite which may show hematitic staining. Clasts up to 100 mm in diameter vary from subangular or angular in the breccia to subrounded in the conglomerate, and commonly form an open framework. Clast lithologies are dominantly black, grey and white chert (similar to that forming much of the Black River Dolomite), but the matrix appears to be quartzarenite.

In thin section (sample R004295), pebble conglomerate from 324330/5435300 displays clasts of chert with a variety of characteristics. These include massive microcrystalline chert (grain size ≤10 μm), slightly coarser chert in which grain size variations delineate ghost textures suggestive of relict peloidal or ooidal fabrics, and massively recrystallised chert with grain size ≤150 μm. All of these chert types are typical of silicified parts of the Black River Dolomite. The remainder of the rock is quartzarenite comprising a moderately well-sorted population of subangular to subrounded clastic grains averaging 300 μm in diameter, with an open to closed fabric, consisting dominantly of quartz but with rare possible plagioclase, in a very fine-grained siliceous matrix. Rarely the quartz clasts show embayments suggestive of volcanic quartz, and some have the appearance of phenocryst fragments, so there may be a volcanic component in the clast population.

Sample R004296 (324290/5435350) is a closed framework quartzarenite with an average grain size of about 300 μm, in which the original texture is largely obscured by pressure solution processes (possibly both diagenetic and tectonic). These have resulted in the formation of sutured grain boundaries and optically continuous overgrowths on the original clastic grains. Original clastic grain boundaries are commonly difficult to see, but where evident the original grains were well rounded. The original clastic fabric was probably well sorted. Some grain flattening due to tectonism is evident.

Blackwater Road *(DBS)*

Similar lithologies form lenses at the base of the Togari Group north of the Roger River Fault, and are exposed in Blackwater Rivulet near 325410/5437940 and on Blackwater Road near 325600/5439890. Clasts in the breccia and conglomerate at the latter locality include black, grey and white chert, vein quartz, dark grey siltstone and pale quartzite. The latter two clast types are most likely derived from the Rocky Cape Group. Indistinctly laminated pale grey quartzarenite again forms a significant part of the section.

A thin section of breccia (sample R004299 from 325600/5439890) shows a semi-closed framework of angular fragments (which in outcrop range up to 100 mm in diameter), consisting of very fine-grained chert which varies in texture from finely banded, to largely recrystallised but showing a shadowy relict ?peloidal texture, to a completely recrystallised mosaic of very fine-grained anhedral quartz. The chert fragments show signs of jigsaw fit in places. There are also <3% of generally subangular monocrystalline to polycrystalline quartz clasts ranging up to about 1.5 mm diameter. The matrix is very fine-grained and siliceous, and appears to be largely recrystallised. Overall, this rock is similar to the chert breccia commonly associated with the Black River Dolomite. Its assignment to the Forest Conglomerate and Quartzite is based mainly on the quartzarenite associated with it at this locality. A sample of the latter (R004300) is a quartzarenite similar to sample R004296, but more fine grained, with a mean grain size of about 130 μm.

Blackwater Rivulet *(JLE)*

An isolated possible conglomerate outcrop occurs on the east bank of Blackwater Rivulet at 325050/5442080, close to the contact of the Togari and Rocky Cape groups. The conglomerate is poorly sorted, clast supported, and consists of subrounded pebbles and cobbles (mostly 20–100 mm across) of hard brittle medium-grey chert.

A moss-encrusted outcrop of an unusual clast-supported granule-pebble conglomerate occurs about 50 m downstream (325050/5442130). Elongate to platy, mostly pale orange-brown clasts (mostly 5–15 mm across and a few millimetres thick) are crudely aligned in a reddish-grey matrix (sample R004821, Plate 12). In thin section (Plate 13) the clasts are seen to be well rounded to subrounded and mainly of fine to coarse-grained, sometimes diffusely laminated siltstone, but a few are of polycrystalline quartz (orthoquartzite?), partly disaggregated to angular to rounded grains. The matrix is mineralogically similar to, but slightly coarser grained than, the siltstone clasts, from which it is not always clearly distinguished. Both consist of fine-grained quartz and scaly sericite with minor detrital mica. A thin but pervasive purplish-red dissemination of wispy oxidised hematitic material is present. The rock

Plate 12

Forest Conglomerate (unit Pscb), sample R004821 (Blackwater Rivulet, 3250 50 mE, 5 442 130 mN). Clast-supported, flat-granule-pebble conglomerate with pervasive hematitic oxidation. The specimen is about 100 mm long.

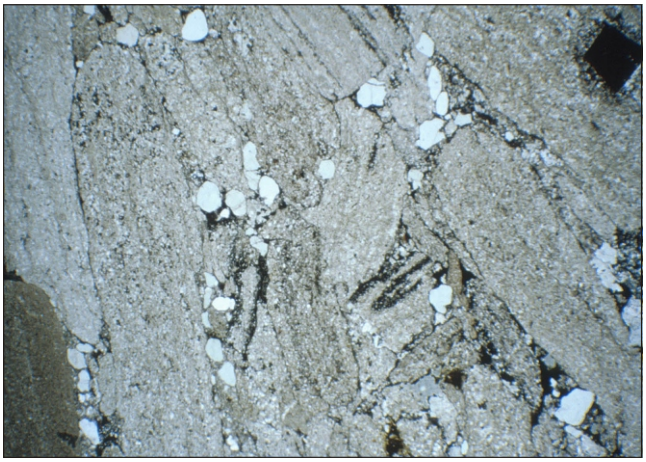

Plate 13

Photomicrograph of Forest Conglomerate (unit Pscb), sample R004821. Clasts of diffusely laminated siltstone and polycrystalline quartz, in a similar siliceous matrix. The clast at the top right contains a pseudomorph after pyrite. Field of view 11 × 7.3 mm.

appears to be wholly derived from the underlying Rocky Cape Group.

Unequivocal Rocky Cape Group siltstone crops out 100 m upstream (south) of the first locality and 27 m downstream (west) of the second. During mapping and compilation these outcrops were considered to be a variant of the chert of Black River Dolomite (Pssc), but they are perhaps better correlated with the Forest Conglomerate and Quartzite (Pscb).

South of the Horton River *(JLE)*

Float boulders (up to 2 m) and probable near-outcrop of similar breccia were noted in two areas (near 331900/5429900 and 332200/5430400) towards the southern margin of the Dempster map sheet. The breccia is massive, very poorly sorted and unbedded, and consists of very angular clasts, a few millimetres to 100 mm across, of black, grey and white chert, white quartz, and rare better rounded small cobbles of orthoquartzite, in a fine-grained medium-grey cherty matrix.

These localities are shown on the map as part of an area of Black River Dolomite-derived chert (unit Pssc) but assignment to the Forest Conglomerate and Quartzite (Pscb) (see *Discussion* section) would be more consistent with mapping in the Blackwater Road–Frankland River areas. Because of the very poor outcrop in this area of buttongrass, it would be difficult to map Pssc and possible Pscb as separate units in this area.

Rapid River bridge area *(JLE)*

At a locality on the Holder map sheet (340500/5442090) on the south side of the Rapid River, just upstream of the Rapid River Road bridge, pale coloured, rather flaggy, well-bedded quartzite (probably a silicified variant of the Cowrie Siltstone) is folded into an open anticline. Ripple marking is present on bedding planes at one point (Plate 14). High up on the river bank the quartzite is overlain by a breccia, up to a few metres

Plate 14

Ripple marks in Forest Conglomerate correlate, near the Rapid River bridge (340 500 mE, 5 442 090 mN). The lens cap is 50 mm across.

thick, consisting of angular, pebble to small boulder-sized quartzite clasts in a pale, also very silicified matrix. The contact with the underlying folded quartzite is sharp but irregular and transgressive to bedding, and represents the unconformity at the base of the Togari Group (Plate 15). The breccia may have been formed by the more-or-less *in situ* disaggregation of the underlying quartzite, with little or no lateral transport, followed by recementation and silicification. It is overlain by peaty soil containing chert granules, probably representing lag from Black River Dolomite-derived chert.

Plate 15

Unconformity near the Rapid River bridge (340 500 mE, 5 442 090 mN). The hammer rests on silicified Cowrie Siltstone (Prcs) which dips to the right on the limb of an open anticline. The contact with the overlying Forest Conglomerate correlate lies just above the hammer, and to the right is transgressive downward.

Typical unsilicified Black River Dolomite crops out less than 150 m away, both on the left bank of the river immediately downstream from the bridge (340400/5421900), and in Lamprey Creek (340510/5442010).

Discussion *(JLE)*

At all these localities, lithologies are atypical of the Forest Conglomerate and Quartzite at its type locality. There, and elsewhere east of Smithton, the unit consists of angular to well-rounded pebbles, cobbles and boulders of dominantly orthoquartzite (rather than chert) in a sandy matrix, passing upward to cross-bedded orthoquartzite and minor shale (e.g. P. W. Baillie, K. D. Corbett, E. B. Corbett and P. G. Lennox *in* Brown, 1989*a*, p.20–21).

An alternative approach would be to regard the chert breccias of this area as variants or sub-units of the Black River Dolomite. However, the presence of subordinate but significant interbedded quartzarenite is uncharacteristic of the Black River Dolomite, and the chert breccias described above are considered to be correlates of the Forest Conglomerate and Quartzite.

Black River Dolomite (excluding Julius River Member) (Pss, Pssd, Pssc, Pssm, Pssf)

Previous work *(JLE)*

This term was first used informally by Spry (1957) for "the thin (50 feet) grey to buff dolomite which outcrops at the bridge where the Bass Highway crosses the Black River". He initially considered that the Black River Dolomite underlay the Cowrie Siltstone but overlay "unnamed siltstones which occur to the south up the Black River". Gulline (1959) correlated the dolomite at Black River with the Smithton Dolomite, and considered that it belonged to the 'Carbine Group' as opposed to 'Older Precambrian undifferentiated slates, cherts and quartzites'. Spry (1964) later recognised that, at its type locality, the Black River Dolomite overlay the Forest Conglomerate and Quartzite (see above) which rests on Cowrie Siltstone, but adhered to the correlation with the Smithton Dolomite.

Following the recognition that there are two distinct dolomite units within the Togari Group (see above), the recommendation of Brown (*in* Brown, 1989*a*, p.11), that the lower unit be termed the Black River Dolomite, is adopted in this report. Equivalent and redundant terms include Rapid (River) Dolomite (McNeil, 1961; Matthews, 1961*b*) and Irishtown Dolomite (Nye *et al.*, 1934).

Exposures of the Black River Dolomite in the Smithton Quadrangle, to the north of the area covered here, are described by various authors in Brown (1989*a*, p.21–23).

Calver (1998) briefly reviewed the formation and presented strontium, carbon, and oxygen isotope data that suggested a time correlation with the lower Akademikerbreen Formation (Spitzbergen) and the Skillolagee Dolomite of the Burra Group (Adelaide Geosyncline, South Australia). This implies a Torrensian to early Sturtian (mid-Cryogenian) age (c.750–650 Ma). Vase-shaped microfossils were first recorded from the Black River Dolomite by Saito *et al.* (1988) and are consistent with that age (Porter and Knoll, 2000).

General features *(JLE)*

This formation is the basal unit of the Togari Group over most of the area. At the western margin of the Smithton Synclinorium, where it is steeply dipping, its thickness (including the Julius River Member) is

readily estimated at 250 to 450 metres. The thickness is more difficult to estimate in the poorly exposed probable thrust slices near the synclinorium axis. In the east of the synclinorium, where the unit is gently to moderately folded, it is probably 600 to 800 m thick.

Natural outcrops are sparse except in streams, and in large areas its presence is indicated by abundant cherty lag. This has led Brown (*in* Everard *et al.*, 1996) to map a separate member (Pssc) of chert, laminated siltstone and minor dolomite. However in most areas the dominant lithology in stream outcrops is usually dolomite, with chert, siltstone and mudstone occurring mostly as thin interbeds. In addition, the lower part of a drill hole at Forest, near Smithton (Brown, 1989*a*; Calver, 1998), penetrated the upper part of the Black River Dolomite, but encountered very little chert in a thickness of 103 m of dominantly carbonate below the Julius River Member. Thus the extensive surficial chert lag is probably derived from thin, but highly resistant, beds within a dominantly carbonate succession.

Common primary lithologies in the Black River Dolomite include massive pure dolomite, thinly laminated and/or stromatolitic dolomite, stromatolitic dolomitic breccia (flakestone), pale pelitic mudstone and black carbonaceous siltstone. In turn many of these have silicified equivalents, including massive, banded, blotchy or thinly laminated white, grey or black chert and flaggy black siliceous siltstone. At least some of the chert formed soon after carbonate deposition, as clasts of chert occur in the overlying Julius River Member, and some may be primary (i.e. directly precipitated from seawater) rather than a diagenetic replacement of carbonate.

Some of these lithologies are depicted on the map as point localities, but it is not usually possible, because of the discontinuous nature of the outcrop, to map them out as separate units.

Western flank of the Smithton Synclinorium

Dunns Plain–Arthur River area **(DBS, JLE)**

Sections through the Black River Dolomite are exposed in the Arthur River (Calver and Everard, 1992*a*) and in a southward-flowing tributary near Dunns Plain. The sequence is sub-vertically dipping and between 350 and 450 m thick in total, with the dolomitic diamictite of the Julius River Member (see below) comprising the upper 150–200 metres.

Discontinuous small outcrops in the Arthur River between 322610/5445860 and 322620/5445760 consist of medium to thin-bedded black chert (Pssc) and black, possibly sheared, mudstone (Pssf). Neither the top nor the bottom of the unit is exposed.

In a small creek south of the river the Black River Dolomite (excluding the Julius River Member) is about 250 m thick. The approximate base of the unit is marked by the appearance of chert boulders (322980/5445290) in the creek. About 50 m downstream (roughly up section) the stratigraphically lowest outcrop (323000/5445320) is a tough, hard, very fissile, faintly laminated dark grey to black chert. Both fissile and massive dark chert and dark grey puggy dolomitic siltstone crop out sporadically for about 100 m up section, and soft-sediment deformation in well laminated medium to dark grey chert was noted at 323050/5445440. The first outcrop of massive cream-coloured dolomite occurs about 100 m below the Julius River Member, but another massive chert outcrop occurs just below this.

The base of the Togari Group is not exposed in a creek section north of the river (near 321850/5446380), and there is an 80 m gap in exposure between the Black River Dolomite and the underlying Rocky Cape Group. However bedding data indicate a close approach to structural concordance across the contact. Further up section, but below the Julius River Member, the sequence comprises a variety of lithologies, including mottled black, grey and white chert, dark grey thin-bedded dolomite, interbedded light to dark grey and black mudstone and siltstone, and buff-weathering thin-bedded laminated dolomitic siltstone. These facies are typical of the Black River Dolomite in the Woolnorth and Trowutta quadrangles. A chert outcrop near the base of the section is coarsely brecciated, but it is not clear whether the breccia is of tectonic or regolith origin. Some of the angular blocks of chert comprising the breccia internally show chaotically disrupted lamination. Nearby, an unusual lithology (sample R004250) consists of large ovoids of translucent grey chert up to several centimetres in diameter in a pale grey siliceous matrix. In thin section, the ovoids consist of a mosaic of microcrystalline quartz with some variations in grain size up to about 0.1 mm. The ovoid boundaries are generally quite sharp and smoothly curved, but have fine irregularities in places. The matrix is darker in colour and much more fine grained than the ovoids. It comprises 5–10% of orientated detrital white mica flakes ≤75 μm in size, rare quartz clasts ≤200 μm, and about 5% of semi-opaque crystalline grains below 20 μm, in a dark grey, very fine-grained probably siliceous matrix.

Lower Blackwater Rivulet area **(JLE)**

A partial section through the unit is exposed in a small tributary west of Blackwater Rivulet between 324140/5444240 and 324540/5444400. This section consists of isolated outcrops of irregular alternating fissile or massive to blotchy, usually dark grey chert and usually massive cream-coloured dolomite, with minor dark to medium-grey fissile pyritic siltstone (e.g. at 324530/5444400) which may superficially resemble the Cowrie Siltstone. In some outcrops (324260/5444450, 324220/5444420) chert can be observed as interbeds, lenses and pods within massive dolomite. Mesoscopic folding occurs in fissile platy chert at 324190/5444420.

Sporadic outcrops in a tributary creek between 323700/5444870 and 324270/5444550 comprise a near strike section, towards the top of the unit, of mostly massive pale grey to cream-weathering dolomite, with

occasional thin lamination due to pelitic interbeds. Little interbedded chert is present. Rather poorly preserved stromatolitic flakestone was noted at 324250/5444580 (sample R004831, see *Petrography* section).

Exposures in Blackwater Rivulet downstream of 324570/5442860, where the unit may be 400 m thick, are poor. In the stratigraphically lower part of the section, massive to blotchy black to white chert occurs only as boulders, and the only definite outcrop is intruded by picrite (see *Igneous Rocks* section). A corroded outcrop at 324780/5442940 consists of coarsely crystalline dolomite beds (0.2–1 m) and numerous outweathering thin interbeds (0.1–0.3 m) apparently of black carbonaceous mudstone, which in thin section (R004824) is seen to be talcose. Similar outcrops of corroded well-bedded dolomite with thin talcose(?), pelitic and black cherty interbeds crop out downstream (up section) to 324860/5443150. There is then a gap in exposure of 160 m before the Kanunnah Subgroup is encountered (a small basalt outcrop at 325000/5443170 not shown on the map), and the presence of the Julius River Member cannot be proven.

The Black River Dolomite crops out sporadically in both branches upstream of a major creek junction at 325430/5441190. Most outcrops are off-white to grey massive chert, but banded black carbonaceous chert (325510/5440530) was also noted. The only unsilicified outcrop (325620/5440960) consists of cream-coloured dolomite (even and fine-grained dolomicrosparite) with thin (5–100 mm) planar interbeds of pale grey chert. The sequence in this area is disrupted by minor gabbroic intrusions and a southeast-side-down and/or dextral cross fault.

Gently folded, pale to medium-grey, thinly laminated fissile chert is exposed in a cutting near the end of Blackwater 5-1 spur (325590/5441460).

Blackwater Road–Frankland River (DBS)

A correlate of the Black River Dolomite forms a poorly outcropping unit some 200 m thick on Blackwater Road near 325700/5439820, and continues south to 325500/5437950 where it is intersected by the Roger River Fault. The corresponding unit south of one of the main splays of the Roger River Fault is 200–300 m thick and extends from a creek section near 324100/5436480 to near 324500/5433400 where it is intersected by an inferred northwest-trending, northeast-directed thrust fault. Even in this well-incised creek most outcrops of the Black River Dolomite are of massive, mottled dark grey/light grey chert similar to the most common lithology in the formation in areas north of the Roger-Sumac-Dempster map sheets (e.g. Woolnorth Quadrangle, Seymour and Baillie, 1992). The creek section does contain some unsilicified outcrops, consisting of thin-bedded buff-weathering grey fine-grained dolomite. In thin section (sample R006007, 324140/5436490) this rock shows an almost totally recrystallised texture, consisting of an even-grained mosaic of fine-grained anhedral dolomite with grain size ≤100 μm. Faint traces of bedding can be discerned in plane polarised light, as well as definite traces of a relict possible peloidal grainstone fabric (clasts ≤1 mm in diameter). Rarely these relict grains have a slightly coarser, clearer dolomite core, and may have originally been ooids.

Central tracts

A number of structural domes and fault slices of Black River Dolomite occur near the axis of the Smithton Synclinorium.

Leensons Road south–Arthur River (DBS, CRC, JLE)

In the area between the southern end of Leensons Road and the Arthur River, the Black River Dolomite (including possible correlates of the Julius River Member) is preserved in a narrow structural sliver. The dolomite here is considered to face westward and is bounded on its eastern side by an inferred thrust fault.

A spectacular outcrop of dolomite occurs on the northern bank of the Arthur River near 325320/5447180. Very finely crystalline, off-white dolomite contains very rough-weathering granular flakestone with a partly silicified matrix, concentrated in particular horizons. The intraclasts are uniformly fine grained rather than stromatolitic. Shelter porosity indicates west facing. About one metre above river level, some flat clast grainstone is fairly pure and relatively free of outweathering detrital material. The eastern end of the outcrop consists of alternating thick (3–4 m) beds of prominently outweathering crystalline dolomite and subordinate corroded inweathering beds of very fine-grained limestone with grainstone texture.

Fine-grained massive grey dolomite is interbedded with black chert about 100 m downstream (325270/5447090).

The top of the Black River Dolomite appears to be exposed on the right (northwest) bank of the Arthur River at 325250/5446920. Thin-bedded pale dolomite with strongly outweathering impure silty beds is overlain by 0.7 m of weathered sulfide-bearing vesicular basalt, which is in turn overlain by massive dark grey basalt. Although very weathered, a chemical analysis of the basalt indicates a picritic composition (see *Igneous Rocks* section).

Away from the river to the north-northwest, lithologies include sheared grey dolomite, dolomitic siltstone, possible dolomitic diamictite, mottled black-grey-white chert, and at least two occurrences of chert with a well-preserved original ooidal or peloidal grainstone texture.

Sample R004248 of the latter facies (325150/5447500) consists of a closed framework of dark grey, silicified, sub-rounded peloids and probable ooids up to about 5 mm in diameter, and which consist internally of a mosaic of microcrystalline quartz. Some of the grains show distinct signs of relict concentric layering, and some are composites of two or more earlier-formed grains. The pore space of the grainstone fabric is filled

with clear crystalline quartz with a grain size up to 0.8 mm. Sample R004245 (324920/5448210) is a chert consisting almost entirely of a mosaic of fine-grained clear crystalline quartz ranging in grain size up to about 0.25 mm. The finer grained parts of this rock show suggestions of a relict peloidal grainstone fabric. An even more recrystallised fabric is represented by sample R004247 (324770/5448420), a chert which consists entirely of a mosaic of fine to medium-grained crystalline quartz varying in grain size up to about one millimetre. This sample shows little evidence of the original sedimentary fabric.

Blackwater Road (spur 1) area *(JLE)*

Detailed traverses were required to map this structurally complex area, due to several major thrusts, cross faults and poor outcrop. Isolated exposures and float of chert and dolomite are not always possible to unequivocally distinguish from the Smithton Dolomite, which occurs both to the east and west. The geology of this area, as shown on the Sumac map sheet, is necessarily partly interpretative.

A tract of Black River Dolomite near the end of Blackwater Spur 1 and on the ridge to the south represents the southern extension of the Leensons Road tract. Much of the tract has been mapped from float and rare outcrops of white, grey and black, massive to banded or blotchy chert. Fissile, thinly laminated to platy, grey to black cherty siltstone (lithology Pssf) also crops out sporadically (e.g. 326150/5446040, 326480/5445470). These lithologies are typical of the Black River Dolomite, rather than the pale, massive, sandy-textured chert derived from the Smithton Dolomite (see below).

To the south the tract is probably faulted against an inlier of Cowrie Siltstone correlate, but chert also occurs south of the fault on the western side of the inlier. Unsilicified outcrops in a small creek near 326420/5444780 are dolomicrosparites with remnant patches of dolomicrite, more akin to the Black River Dolomite than Smithton Dolomite in the area. Chert float occurs in an apparently unfaulted sequence, above the Cowrie Siltstone correlate and below the Julius River Member, in another small creek about 500 m further south (at 326510/5444210).

Float of mainly pale to off-white chert is scattered on a small hill around 327500/5446600, but small outcrops of mostly soft, friable, sandy-textured, off-white leached dolomite occurs in some adjacent road cuttings. The only relatively fresh outcrop (327570/5446850) is a massive to vaguely banded, pale grey peloidal grainstone (sample R004936, see below) which could belong to either the Black River Dolomite (as shown) or the lower part of the Smithton Dolomite.

Blackwater road (spur 5) area *(JLE)*

Massive blotchy chert overlies well-laminated, medium-grey flaggy chert, resembling that derived from the Black River Dolomite, in a partly rehabilitated gravel pit at 326690/5442010. Further exposures of similar chert occur in a larger gravel pit further north (326700/5442200).

Unsilicified dolomite crops out in a small creek above Blackwater 5-2 spur (326210/5443140) for about 730 m to 326620/5442830. Much of the section consists of very pale grey, cream weathering massive dolomite, which is very difficult to unequivocally assign to either the Black River Dolomite or Smithton Dolomite. Mapping of the surrounding area indicates that the lower part of the section is almost certainly the latter. In the upper part of the section, the presence of chloritic lithicwacke (326550/5442790) and chert interbeds suggests Black River Dolomite, overlying the inlier of Cowrie Siltstone correlate to the east. A major east-directed thrust has been inferred, and may be marked by cataclastic dolomicrosparite noted at 326420/5442820.

East of upper Blackwater Rivulet *(ARR)*

The Black River Dolomite is poorly exposed along the margins of a shallow-plunging dome (329000/5439300). Two facies of the Black River Dolomite are common as float but rarely crop out. The most common facies consists of interbedded dark grey/black and white, commonly laterally discontinuous chert beds up to several centimetres thick. Beds are typically massive although oolitic textures are evident at 328380/5437200. The chert-dominated units are interbedded with units comprising massive, well-bedded pale brown to buff-coloured siltstone beds to 150 mm thick. A third facies of monomictic conglomerate, restricted to the uppermost portions of the unit, is assigned to the Julius River Member (see below).

North of the Horton River *(JLE, ARR)*

The Black River Dolomite occupies a large tract centred near 331000/5435000 (Dempster map sheet). Outcrops are rare, even in major streams, and most of the area is mapped from float of off-white to grey, massive, blotchy or irregularly-banded chert. Very few bedding readings were obtained but this tract probably represents the crest of a large structural dome. The overlying Julius River Member occurs, possibly discontinuously, around its margins, and residual outliers of the overlying Keppel Creek Formation occur on two low hills (330000/5434300, 331000/5434200) within the tract.

In the northern part of this tract 'ball and pillow' textures were noted in chert at 330730/5438000.

Sporadic outcrops of chert and chert breccia occur on a small but well defined arcuate ridge near the centre of the tract (331500/5435560). The breccia consists of angular white clasts in a medium-grey matrix, and may be transitional to the Forest Conglomerate and Quartzite (see above). The possible inlier of Rocky Cape Group has been interpreted in this area from geophysical data, but only chert float could be found around 331350/5435400 (in an area of extremely dense low bauera).

The only unsilicified outcrop known within this tract is on the Horton River, just below the mouth of Lagunta Creek (331940/5432420). This is a massive, medium grey, slightly impure, partially recrystallised peloidal grainstone (sample R005115 — see *Petrography*) which lies stratigraphically near the top of the unit, as stylolitised diamictite (Julius River Member) crops out about 120 m downstream.

Roger River and Trowutta areas

Relatively small tracts of chert and dolomite were mapped near Roger River township (centred on 337000/5458000) and Faheys Creek, northeast of Trowutta (around 339500/5456000) by A. V. Brown (*in* Everard *et al*., 1996). He assigned them to the Black River Dolomite but no detailed descriptions are available. A small, partly fault-bounded area of chert at 333400/5453000 was also assigned to the unit.

Eastern flank of Smithton Synclinorium *(JLE, CRC)*

The largest tract of Black River Dolomite in the area occurs on the eastern flank of the Smithton Synclinorium, between and around Dempster Plains and the Julius, Rapid and Arthur rivers. This tract, which extends on to the adjoining Tayatea, Holder and Beryl 1:25 000 scale map sheets, was previously mapped by Everard *et al*. (1996), although further traverses enabled slight modifications to be made during preparation of the Sumac 1:25 000 scale map sheet.

The greater extent of the Black River Dolomite in the east of the synclinorium is partly due to the more gentle dips, but the unit is also thicker here (perhaps about 500 m) than in the west.

Contacts with Cowrie Siltstone

The lowermost beds of the Black River Dolomite are exposed in Lamprey Creek (Holder map sheet), where both pale grey-green leached Cowrie Siltstone ('quartzite') and the overlying dolomite dip gently west. The Forest Conglomerate and Quartzite is absent, and the contact is a disconformity or very low angle unconformity. At one locality (340100/5440460) the contact is almost exposed, with shallowly dipping 'quartzite' cropping out on the right bank and well laminated dolomite 2–3 m away on the left. A similar exposure occurs about 50 m upstream (340090/5440390), just below a small section of underground creek flow.

The contact appears brecciated and is possibly faulted in a cutting on Mt Bertha Road (339730/5437660). Deeply-weathered Cowrie Siltstone dips steeply southwest, discordant to the northerly trend of the mapped boundary. Immediately west of the contact, bedding is not preserved in cherty lag derived from the Black River Dolomite.

Arthur River section

Good exposures of the Black River Dolomite occur in the Arthur River between a faulted contact at 342600/5448600 and the mouth of the Julius River (335900/5445500), but detailed stratigraphic work is not possible because of the discontinuous nature of outcrop, gentle folding and possible faulting. Bedding is generally gently dipping with highly variable strikes, and two inliers of Cowrie Siltstone correlate are present.

Stromatolitic dolomite is common in the lower part of the unit. A spectacular outcrop of well-bedded stromatolitic dolomite and well-preserved stromatolitic flat-pebble breccia (flakestone) occurs on the left (west) bank at 342570/5448410. These beds are a few metres thick and crop out for about 100 m, striking parallel to the river. Off-white dolomite at 342600/5448510 is dominantly a grainstone, with a faintly intraclastic or coarsely oolitic to pisolitic texture that is more conspicuous on weathered surfaces. Domal hemispherical stromatolitic structures about 100 mm in diameter are developed in places (Plate 16). Similar structures occur at 342510/5448290, where they are overlain by several metres of fine-grained dolomite.

Plate 16

Domal hemispherical structure, viewed from above, in stromatolitic flakestone. Black River Dolomite (unit Pss), outcrop on the Arthur River at 342 570 mE, 5 448 410 mN. The lens cap is 50 mm across.

Near the base of a large outcrop on the right bank just above the mouth of Lawson Rivulet (342010/5446890), a thick in-weathering bed contains large hemispherical stromatolitic domes, surrounded and overlain by flat-pebble breccia (flakestone) and underlain by massive fine-grained dolomite. Less well-preserved stromatolitic flakestone and coarse grainstone was noted near the mouth of the Rapid River (e.g. 341260/5446360, 340710/5446350).

These stromatolitic outcrops may be part of the same unit. They appear to be overlain at 342450/5448220 by hard, well-bedded thick to thin-bedded, fissile and flaggy black mudstone (lithology Pssf) and subordinate interbedded, thickly-bedded chert. Similar rocks, together with massive black chert, crop out sporadically downstream to 341910/5447010, downstream from the mouth of the Rapid River (e.g. at 340450/5446070), and between two inliers of Cowrie Siltstone (339380/5445870, 339300/5445740).

The westernmost Cowrie Siltstone inlier is overlain by finely crystalline to micritic dolomite with some stromatolitic flakestone and minor chert lenses (338940/5445660 to 338750/5445730). More black chert and thin-bedded mudstone crop out sporadically further downstream in another section of river (338210/5445610 to 337870/5445810). At the latter locality, mesoscopic, gently northeast-plunging folds appear to be parasitic on a larger anticline.

The upper part of the section, below the Julius River Member, is dominated by thick to thin-bedded fine-grained dolomite, with occasional strongly outcropping beds of black chert (e.g. at 337160/5445790 and near the mouth of Wents Creek). At 337330/5445920 a large dolomite outcrop has a faint, gently-domed stromatolitic lamination, although it lacks the rhythmic banding seen lower in the sequence. Numerous irregular vugs are filled with coarse-grained black spar. Similar poorly preserved stromatolitic lamination forms small gently-domed structures at 336850/5445540.

The base of the Julius River Member is exposed (although not very accessible) in a spectacular 60 m overhanging cliff at 336100/5446440 (cover photo). Sub-horizontally bedded, thick-bedded dolomite crops out at river level, whilst diamictite occurs at the top of the crag (A. V. Brown). In the river section near the mouth of the Julius River, massive fine-grained creamy-white dolomite with thinly interbedded, steeply west-dipping, pale shaly siltstone and some massive chert is followed 50 m downstream by diamictite.

Rapid River–Julius River–Dempster Plains area

Karstic outcrops of mostly thick-bedded dolomite occur sporadically in the lower Rapid River downstream from near the bridge (340420/5442180). Stromatolitic breccia (flakestone), concentric banding and domal structures are locally abundant (340210/5442740, 340260/5442890). Pale grey dolomite contains irregular, subrounded clasts up to 50 mm across of darker dolomite at 340500/5443000.

Stromatolitic flakestone, interbedded with pale grey massive dolomite, was also noted in lower Lamprey Creek (e.g. 340460/5441750).

Corroded outcrops of pale grey thick-bedded to massive dolomite occur, near the base of the Black River Dolomite, in small creeks northwest of Colemans Hill (e.g. 340710/5443750, 340790/5444350, 340940/5444300, Holder map sheet). A faint thin lamination is occasionally evident and possible stromatolitic fragments were noted at the last locality.

Outcrops in Sumac Rivulet near the bridge (337930/5440920) consist of thinly laminated (5–20 mm) dolomite with some slump folding, overlain by massive dolomite. Thinly laminated dolomite predominates upstream, stratigraphically near the top of the unit, whilst downstream outweathering irregular patches (50–100 × 10–20 mm) of silicification (e.g. 338010/5440970) and massive black chert interbeds were noted in dolomite. Concentric stromatolitic structures, up to 250 mm across, occur in grey chert at 339560/5442440.

Thin to medium-bedded dolomite, with occasional interbeds of black chert, crops out in the Julius River downstream of the outflow cave (334910/5443330). Individual beds may be massive or thinly laminated, locally with some wavy to convolute lamination, but no stromatolitic dolomite was noted. Although both mesoscopic to megascopic folding is present, the section probably generally faces west towards the top of the unit. The transition into the Julius River Member, marked by the appearance of thick (1 m) beds of diamictite near 334500/5443570, is probably gradational over a few tens of metres.

Two waterfalls (4–6 m high) on the Julius River, about one kilometre south of Sumac Road (333530/5440740, 333480/5440670), occur over beds of thinly bedded (5–20 mm) and faintly laminated, dark grey to black carbonaceous siltstone (lithology Pssm). The rock (samples R005112, R005117) is hard but brittle, with a well-developed, closely-spaced conchoidal to lenticular fracture. These beds are associated with massive dolomite and are stratigraphically just below diamictite of the Julius River Member (Pkx). Similar dark grey to black carbonaceous and pyritic siltstone occurs in a similar stratigraphic position on a tributary at 333890/5439430.

Natural outcrops are rare away from major streams and the presence of the unit is indicated by lag of white, pale to dark grey or black chert. Several textural varieties are present, including massive, irregularly blotchy and crudely banded chert, and chert breccia. Chert breccia is commonly matrix supported and consists of unsorted, unorientated mostly angular clasts (typically 5–20 mm but up to 100 mm) of white and/or grey to black chert in a fine-grained chert matrix that may be either paler or darker than the clasts. Stromatolitic textures are locally preserved, usually in otherwise

massive white or cream chert (e.g. in partly rehabilitated gravel pits on Sumac Road near 334800/5442200, and at Dempster Plains near 338480/5437780).

Outcrops of unsilicified dolomite are rare in road cuttings and gravel pits, and commonly leached to a soft brown pug, but small outcrops of both chert and thinly laminated, fissile, medium grey to black siliceous siltstone (lithology Pssf) are common. Near Dempster Lookout (337990/5437810), gently folded beds of banded chert (50–150 mm thick) are interbedded with thinner (50 mm or less), less competent and more deformed beds of very thinly laminated fissile siltstone. These are less competent and more deformed than the chert beds. Similar lithologies are also well exposed in the Rapid quarry (339900/5440830).

Horton River

A small inlier of pale grey, poorly-bedded dolomite crops out on a bend of the Horton River (334260/5432420) about 300 m below the Sumac Road bridge, and occupies the core of a downfolded structural basin in the Cowrie Siltstone. A relict conglomeratic texture is evident, both in outcrop and thin section (see below). Off-white, slightly outweathering, irregularly shaped clasts (up to 100 mm) of off-white dolomite lie in a pale grey matrix. Wavy, light to dark grey stylolitic veinlets up to 10 mm wide are also present.

The main contact between the Togari and Rocky Cape groups is probably a fault in this area, in places juxtaposing the Kanunnah Subgroup against the Cowrie Siltstone. The Black River Dolomite is present as massive black chert outcrops in the Horton River (333410/5432220) immediately west of the fault. Mostly off-white chert float was also noted in minor creeks and on a small knoll north of the river.

South of the Horton River, where the fault is offset westwards, sporadic chert float occurs on the buttongrass plains west of Sumac 7 spur road. Boulder-sized (≤2 m) float and possible outcrop of unbedded, very poorly-sorted chert breccia with occasional more rounded quartzite clasts (e.g. near 331900/5429900) may represent the Forest Conglomerate and Quartzite (see above).

In this area the upper diamictite (Julius River Member) of the Black River Dolomite appears to be absent. Diffusely laminated to banded chert, corroded massive dolomite (331470/5430340), Keppel Creek Formation and basalt all crop out intermittently in the headwaters of a tributary of the Lindsay River which flows subparallel to the contact.

Lower Lindsay River and Leigh River areas *(JLE)*

The base of the Black River Dolomite crops out in the lowermost reaches of the Leigh River (Balfour map sheet). Wavy laminated grey to black chert forms resistant beds up to 300 mm thick at 330490/5429440, and corroded massive dolomite, with only minor pods of silicification, crops out at 330350/5429420. Cowrie Siltstone crops out about 50 m away at the confluence with the Lindsay River. There is no sign of the Forest Conglomerate and Quartzite. Sporadic chert float is scattered on the arcuate ridge to the north.

The Black River Dolomite is encountered as irregularly blotchy black and white chert, in a bar across the Lindsay River at 329950/5429600, and also occurs as float on a small hill to the west (329770/5429480). Similar chert is associated with fissile, thinly-laminated black to dark grey siltstone (lithology Pssm) nearby at 329920/5429640. Basalt and associated Keppel Creek Formation rocks occur in the river near 329800/5430000, but there are more chert outcrops further downstream (to the north). A corroded outcrop of well-bedded dolomite is interbedded with fissile, thinly-laminated siltstone below a bend in the river (329680/5430040), and corroded massive dolomite occurs at 329440/5430030.

Diamictite constituting the Julius River Member is well developed in this area, and comprises most of the small isolated outcrops in an un-named tributary that enters the Lindsay River at 329000/5430600. Other rock types noted include massive chert, lead-grey massive dolomite (330430/5429950) and thinly and faintly laminated dolomite with a cuboidal fracture (329720/5430310, 329850/5430470). Small corroded outcrops of extremely tough, dense, diffusely laminated, orange-brown ferruginous chert occur at 329750/5430380 and 331750/5430020.

In small creeks west of the Lindsay River, pale grey chert, massive grey dolomite (328620/5430030, 329480/5430000), well-bedded dolomite (328790/5430170), ferruginous chert (329460/5429970) and diamictite (Julius River Member) were noted in the Black River Dolomite.

A probably fault-bounded inlier of Black River Dolomite is present about one kilometre south of the Leigh River/Lindsay River confluence, and just north of the end of Sumac 10 spur road (Balfour map sheet). Most of the inlier has been mapped from chert float, but corroded outcrops of massive dolomite occur in the Leigh River (331000/5428730) and Lindsay River (330560/5428680). There are also probable fault slivers of Keppel Creek Formation and basalt in this structurally complex area.

There is an elongate east-trending inlier of Togari Group rocks, principally basalt, in the Sumac 10 spur road area (Balfour map sheet). On the northern side of the inlier, massive to irregularly blotchy, off-white to dark grey chert occurs as sporadic outcrop and float in the Leigh River (334020/5427330 to 333770/5427530, 333170/5427530) and on a prominent hill (near 335100/5427100). Thinly laminated grey to off-white siltstone is interbedded with similar chert in a large gravel pit at the start of Sumac 10 spur road (336600/5426400). No unsilicified dolomite was encountered in these areas but the chert is lithologically typical of the Black River Dolomite.

There is a small outcrop of steeply-dipping, well-laminated pale to medium grey dolomite in the Leigh River on the southern side of the inlier (at 333750/5426730), and dark grey massive chert nearby at 333830/5426700. These outcrops, and sporadic chert float elsewhere along the southern margin of the inlier, are probably also assignable to the Black River Dolomite, but the unit is probably very thin or partly faulted out. An alternative correlation with the Smithton Dolomite would imply a major fault against Rocky Cape Group rocks to the south.

Petrography *(JLE, CRC)*

Detailed petrographic descriptions are given in Appendix 1. Sample locations are listed in Appendix 6.

Dolomite

In outcrop and hand specimen, most dolomite samples are medium to pale grey, less commonly cream coloured, bone-white or with a faint olive-green or brown tint; weathered surfaces are generally cream coloured. A usually faint planar to streaky bedding lamination may be present, but many samples are apparently massive. Less often bedding is well defined, sometimes by thin interbeds of pelitic mudstone or by orientated tabular stromatolitic fragments. Many samples are mottled by usually diffuse, irregular to wispy blotches of paler (often cream coloured) remnant dolomicrite. Irregular patches of white calcite are present in a few samples. An irregular to anastomosing stylolitic network of thin to hair-line, dark grey seams may be present.

About fifty samples were examined in thin section (Appendix 1, Plates 42–53). The primary fabric, well preserved in only a minority of samples, is most commonly a peloidal (Plates 43, 44) to intraclastic (Plates 46, 47) grainstone. The peloids are usually dolomicrite or very fine-grained dolomicrosparite, sometimes with recognisable ooids, and may be strongly flattened. A few samples are flakestones with large fragments of laminated stromatolitic dolomicrite (Plate 42). The matrix is sometimes dolomicrite, but more commonly has recrystallised to fine-grained to coarse-grained dolomicrosparite (Plates 48–51). In many samples recrystallisation has left only diffuse relict patches of micrite or fine-grained dolomicrosparite, probably remnants of original peloids or intraclasts.

Most dolomite samples have little or no siliciclastic debris, but a few contain thin planar interbeds of pelitic mudstone (Plate 52). Others, usually from near the base of the unit, contain a few per cent scattered quartz anhedra and rare lithic fragments.

Clastic sediments intercalated within the Black River Dolomite

Pelitic mudstone or fine-grained siltstone, with little or no carbonate, occurs sporadically interbedded with dolomite, particularly towards the top of the main part of the unit (i.e. below the Julius River Member). Many samples are pale khaki-green or brown-green, weathering pale grey to off-white, or oxidising to brown-red. More carbonaceous beds are dark grey to black, and may superficially resemble Cowrie Siltstone. Some beds display a very fine planar bedding lamination. Cleavage is variably but usually poorly developed. In thin section samples typically consist of splinters of sericite and sometimes chlorite, variable amounts of fine-grained opaque minerals (including carbonaceous matter and pyrite), and very fine-grained to cryptocrystalline quartz.

One distinctive lithology, transitional to chert, is flaggy black siliceous mudstone and siltstone (unit Pssf; Plates 54–56). Typically this contains numerous chitinozoan-like microfossils, as previously described in the Black River Dolomite by Saito *et al*. (1988). They are ovoid or flask-shaped, 60–120 μm long, with thin clear, colourless, possibly chalcedonic shell-like walls about 2 μm thick, and a dark interior (Plate 55). Many show brittle compaction fracture, and in some samples there are numerous curved or crescent-shaped fragments.

Chert

Chert interbedded within the Black River Dolomite may be black, grey, bone-white or less commonly brown, but displays a wide variety of textures, including massive, thinly diffusely laminated, banded and irregular blotchy variants (Plates 57–60). In thin section they consist of microcrystalline to cryptocrystalline silica, variable amounts of opaque and/or carbonaceous material, and sometimes small patches of relict carbonate. In some less recrystallised samples, chitinozoan-like microfossils, similar to those described above, are recognisable.

Geochemistry *(JLE)*

Nine chemical analyses of the Black River Dolomite from the Roger-Sumac-Dempster and immediately surrounding areas are quoted in Table 4.

Four of the samples (R005094, R005101, R005030, R005041) are relatively pure dolomite, and probably consist of 97–98% carbonate, with only small amounts (<1%) of quartz and apatite. The Ca/Mg ratio indicates that the carbonate is near-stoichiometric dolomite, and little calcite is present, either as a separate mineral phase or in solid solution.

Sample R005091 contains excess Mg, which together with significant SiO_2 and Al_2O_3 and negligible K_2O, suggests that the main impurity is chlorite (possibly 4–5%), although none was observed in thin section. Small amounts of quartz (1–2%) and apatite (about 1%) are also probably present.

The two most impure samples (R005122 and R006660), with the highest SiO_2 and Al_2O_3, also contain significant K_2O, indicating substantial amounts (20–25%) of pelitic material (quartz and muscovite/sericite).

Most trace elements are low or below detection limits, especially in the more pure samples. The main

Table 4. *Chemical analyses of dolomite units*

	(a) Black River Dolomite									*(b) Smithton Dolomite*				
Field No.	TJ502	TJ516	TJ942	TJ1095	TJ3394	AR84	AR38	MJ151	-	AR122	T7	T8	T9	T10
Reg. No.	R005091	R005094	R005101	R005112	R005122	R005040	R005030	R006660	G401347	R005054	-	-	-	-
Anal. No.	941144	941143	941148	941137	941146	941162	941165	941166	891860	941161	-	-	-	-
AMG (mE)	338010	339750	340420	333610	333370	336100	341580	333750	336940	326480	322600	323400	324000	324000
AMG (mN)	5440980	5443170	5441660	5440810	5440170	5446440	5446540	5426730	5458060	5448500	5459100	5459000	5459000	5459800
Sheet	Sumac	Sumac	Holder	Sumac	Sumac	Sumac	Holder	Balfour	Roger	Sumac	Roger	Roger	Roger	Roger
Lithology	dolomite	dolomite	dolomite	mudstone	dolomite	dolomite	dolomite	dolomite	chert	dolomite	dolomite	dolomite	dolomite	dolomite
SiO_2 (%)	3.17	0.97	1.47	68.55	17.34	0.57	1.16	13.84	94.93	1.67	0.19	0.17	0.21	0.04
TiO_2	0.04	0.00	0.00	1.09	0.21	0.00	0.00	0.14	0.09	0.00	<0.01	0.01	<0.01	<0.01
Al_2O_3	0.98	0.19	0.45	13.85	3.40	0.93	0.59	2.07	0.57	0.49	0.07	0.08	0.09	0.09
Fe_2O_3	0.34	0.11	0.05	0.86	0.70	0.13	0.11	0.49	0.48	0.09	0.05	0.09	0.13	0.10
FeO	0.03	0.03	0.03	0.10	1.12	0.07	0.07	0.71	0.40	0.03	0.00	0.00	0.00	0.00
MnO	0.04	0.04	0.02	0.01	0.07	0.02	0.04	0.05	0.01	0.02	0.01	0.01	0.01	0.01
MgO	22.03	20.33	20.69	1.42	16.36	21.34	20.87	17.90	0.81	21.29	19.75	20.90	20.79	20.22
CaO	28.90	29.14	29.08	0.04	23.50	30.18	30.08	25.74	0.91	30.31	32.43	31.98	33.10	32.10
Na_2O	0.00	0.00	0.00	0.03	0.01	0.00	0.00	0.08	0.27	0.00	0.16	0.21	<0.01	<0.01
K_2O	0.02	0.02	0.02	4.20	0.88	0.00	0.02	0.63	0.03	0.02	<0.01	0.02	<0.01	<0.01
P_2O_5	0.41	0.25	0.34	0.04	0.25	0.40	0.32	0.21	0.02	0.23	0.02	0.02	0.01	0.00
H_2O^+	0.83	0.01	0.00	8.73	0.83	0.01	0.01	0.05	0.26	0.00	nd	nd	nd	nd
CO_2	44.60	47.10	46.90	0.52	35.90	46.90	47.30	39.30	1.14	47.20	nd	nd	nd	nd
SO_3	0.04	0.04	0.04	0.03	0.20	0.02	0.04	0.24	0.05	0.04	0.23	0.38	0.08	0.08
LOI	[45.43]	[47.10]	[46.90]	[9.24]	[36.60]	[46.91]	[47.30]	[39.27]	[1.37]	[47.20]	46.60	46.79	46.33	46.79
TOTAL	**101.43**	**98.23**	**99.09**	**99.47**	**100.77**	**100.57**	**100.61**	**101.45**	**99.97**	**101.39**	**99.51**	**100.66**	**100.75**	**99.43**
Sc (ppm)	<9	<9	<9	20	<9	<9	<9	<9	<5	<9	nd	nd	nd	nd
V	19	<5	11	270	36	<5	<5	24	10	6	nd	nd	nd	nd
Cr	24	13	33	105	38	13	18	26	71	15	nd	nd	nd	nd
Co	<8	<8	<8	<8	8	<8	<8	<8	6	8	nd	nd	nd	nd
Ni	18	12	10	<5	24	9	14	17	16	6	nd	nd	nd	nd
Cu	<5	<5	18	5	<5	<5	<5	<5	24	<5	nd	nd	nd	nd
Zn	70	60	29	19	48	31	155	32	16	24	nd	nd	nd	nd
Ga	<5	<5	<5	18	<5	<5	<5	5	<5	<5	nd	nd	nd	nd
As	<20	<20	<20	<20	<20	<20	<20	<20	9	<20	nd	nd	nd	nd
Rb	<5	<5	<5	220	36	<5	<5	<5	<5	5	nd	nd	nd	nd
Sr	610	57	65	21	69	97	105	145	11	4	nd	nd	nd	nd
Y	<5	<5	<5	47	9	<5	<5	9	<5	5	nd	nd	nd	nd
Zr	10	13	14	230	44	17	19	50	13	11	nd	nd	nd	nd
Nb	<3	<3	<3	24	4	5	5	7	<5	<3	nd	nd	nd	nd
Mo	<5	<5	<5	7	<5	<5	<5	<5	5	<5	nd	nd	nd	nd
Ag	nd	nd	nd	nd	nd	nd	nd	nd	<5	nd	nd	nd	nd	nd
Sn	<9	16	<9	<9	14	<9	58	<9	6	<9	nd	nd	nd	nd
Sb	nd	nd	nd	nd	nd	nd	nd	nd	<5	nd	nd	nd	nd	nd
Ba	27	<23	<23	620	65	<23	<23	54	86	<23	nd	nd	nd	nd
La	<20	<20	<20	48	<20	<20	<20	<20	7	<20	nd	nd	nd	nd
Ce	<28	<28	<28	87	<28	<28	<28	<28	22	<28	nd	nd	nd	nd
Nd	<20	<20	<20	42	24	<20	<20	<20	<5	<20	nd	nd	nd	nd
W	<10	<10	<10	<10	<10	<10	<10	<10	7	<10	nd	nd	nd	nd
Pb	<10	<10	<10	25	<10	<10	<10	<10	6	<10	nd	nd	nd	nd
Bi	10	11	9	<5	7	11	7	8	6	9	nd	nd	nd	nd
Th	<10	<10	<10	35	<10	60	<10	<10	<5	<10	nd	nd	nd	nd
U	<10	<10	<10	10	<10	<10	<10	<10	<5	<10	nd	nd	nd	nd

Analyses by Mineral Resources Tasmania laboratories, analyses T7–T10 from Threader (1992)

exceptions are Sr (which is anomalously high in sample R005091) and Zn. These elements are probably held in the dolomite lattice, as they have the same charge and similar ionic radius to Ca and Mg.

Sample 401347, a chert from near Roger River, is mainly silica, probably with 2–3% remaining dolomite, and is very depleted in all trace elements, except possibly Ba and Cu.

Sample R005112, a carbonaceous siltstone from the Julius River, contains very little carbonate and is essentially pelitic, with high K_2O, SiO_2 and Al_2O_3. The high H_2O^+ (8.73%), calculated from loss-on-ignition after correcting for CO_2, SO_3 and FeO, may be misleading and probably also includes several per cent carbon. Many trace elements are much higher than in the carbonates, notably Ba, Rb, V, Cr, Zr, Y and REE. This probably indicates the presence of both mica and heavy accessory minerals such as zircon.

Julius River Member (Pssr)

Definition *(JLE)*

The Julius River Member is herein defined as that unit of about 200 m of dolomitic diamictite, occurring at the top of the Black River Dolomite, that crops out in the Arthur River between 50 m below the mouth of the Julius River (335 860 mE, 5 445 530 mN) and 334 760 mE, 5 446 890 mN, near where it is conformably overlain by the Keppel Creek Formation (Kanunnah Subgroup). It contains boulder- to granule-sized clasts of dolomite, stromatolitic dolomite and chert in an unbedded to diffusely laminated dolomitic matrix. Although the middle of the type section is concealed by alluvium, further exposures occur in the Julius River and tributaries, between 333 710 mE, 5 441 510 mN (near where it is overlain by the Croles Hill Diamictite) and 334 420 mE, 5 441 960 mN, and downstream of 334 460 mE, 5 443 670 mN.

The term was first used on the Trowutta map sheet (Everard *et al*., 1996) but has not previously been formally defined.

The Julius River Member is probably equivalent to the 'Salmon River Dolomitic Breccia' of Matthews (1961*b*), a rarely used term that was never formally defined. Matthews showed it as cropping out mainly in the Julius River and near Maguires Road (Trowutta), areas where the Julius River Member has more recently been mapped. The older term is abandoned mainly because Matthews considered it part of the 'Trowutta Group' (roughly synonymous with the Kanunnah Subgroup), and thus may have confused it with another diamictite unit, the Croles Hill Diamictite (see below). In addition, it was never mapped at or near Salmon River. It should be noted that the new term Salmon River Siltstone has been recently applied to a quite different and younger unit of the Togari Group.

Although formally part of the Black River Dolomite, the Julius River Member is considered sufficiently distinctive to warrant separate treatment in this report.

Previous work *(JLE, CRC)*

Griffin and Preiss (1976) described a "possibly late Precambrian diamictite", now known to belong to the Julius River Member. The clasts, of dolomite and subordinate chert, were shown to have been already lithified when they were incorporated into the diamictite, and not necessarily locally derived from the underlying 'Smithton Dolomite', which they did not distinguish from the Black River Dolomite. Because of the absence of striated or faceted clasts, limited range of clast lithology, and crude bedding in one outcrop, Griffin and Preiss (1976) favoured a mass-flow rather than glacial mechanism of deposition. They described in detail two types of stromatolite occurring in dolomite clasts at localities at Faheys Creek (Trowutta) and on the Arthur and Julius rivers. The first type, in dark grey dolomite, is well preserved and falls into the group *Baicalia*, particularly resembling *B. burra*. The second, in pale grey rather recrystallised dolomite, consists of stratiform and column layered stromatolites.

In the Forest-1 diamond-drill hole (352740/5480110), Brown (1985) logged an interval of about 125 m that included units of 'mixtite (calcareous pebble conglomerate)', 'pyritic pebbly black mudstone' and 'calcareous pebbly mudstone', interbedded with 'bedded carbonate' and 'laminated pyritic mudstone'. The interval, also described as including 'stromatolitic breccia units', is underlain by 'a lateral continuation of the Black River Dolomite' and overlain by 'the correlate of the Crimson Creek Formation in the Smithton Basin' (i.e. Kanunnah Subgroup).

Calver (1998) re-logged the Forest drill hole, and assigned his 'unit 2' (about 95 m of dolomitic diamictite) and 'unit 4' (about 32 m of 'diamictite with limestone clasts, and minor beds of limestone and black mudstone') to the Julius River Member. These are separated by a thin (about 12 m) interval of fine-grained microsparitic limestone with minor black shale interbeds, giving a total thickness of about 140 metres. He also quoted a thickness of about 200 m for a similar diamictite in the Arthur River section. Calver (1998) suggested correlation of the Julius River Member with the Sturtian glacials (c. 700–650 Ma) of South Australia, based on isotope chemostratigraphy and other considerations.

General features *(JLE)*

In fresh outcrop and hand specimen the Julius River Member is a medium to dark-grey, very poorly-sorted, matrix-supported diamictite. It contains sparse to abundant, angular to subrounded clasts (commonly up to 25 mm) of usually paler grey to cream-coloured carbonate, white to black out-weathering chert, and less commonly darker grey mudstone. Bedding is usually absent, but a diffuse streaky lamination and/or a weak anastomosing stylolitic cleavage may be present. The unit weathers to a dull khaki-brown or sometimes olive-green (e.g. 5Y4/4 to 5Y5/6), but fresh

samples generally lack the dark green colour of the younger Croles Hill Diamictite (see below).

Both matrix and most carbonate clasts are usually dolomite (effervescing feebly in dilute HCl), but limestone clasts to 20 mm are present in samples R004839 and R004840, from a small tributary of the Arthur River (near 322900/5445800), and the matrix of the latter also contains abundant calcite. Sample R006675 (Lindsay River at 329330/5430170) is also dominantly calcite.

Field relationships

Dunns Plain–lower Arthur River–Blackwater Rivulet areas (DBS, JLE)

Chert-dolomite-siltstone lithologies give way to dolomitic diamictite of the Julius River Member some 130 m above the base of the Black River Dolomite in the creek section near 321850/5446380. Sample R004251 of the diamictite from near the base of the section has a disorganised fabric comprising about 10% of subangular to subrounded pale to mid-grey rock fragments ranging up to about 17 mm in diameter in a very fine-grained light grey-buff matrix. In thin section most of the fragments consist of fine to medium-grained dolomite, and some are partially silicified. The fragments show a continuous range of sizes down to <30 μm, and the fine-grained matrix is also strongly dolomitic. These characteristics are similar to those of the Julius River Member in its type area in the Trowutta Quadrangle (Everard *et al.*, 1996).

The Julius River Member forms an extensive platform on the northwest bank of the Arthur River at 322680/5446000. Sparse (about 10%) granule to pebble-sized dolomite clasts lie in a matrix of medium-grey dolomitic mudstone. Here the diamictite is strongly cleaved. About 50 m downstream, strongly outcropping and vertically dipping beds of sandy dolomitic diamictite contain more abundant, rounded, pebble-sized clasts, and locally approach a clast-supported (closed framework) fabric.

The unit also crops out sporadically in a small tributary creek south of the Arthur River. The best outcrop, at 322890/5445760, is a very poorly sorted, matrix-supported diamictite comprising subrounded to subangular clasts, a few millimetres to 50 mm in diameter, of mostly fine-grained medium grey chert set in a darker matrix. Elsewhere in this creek similar massive diamictite alternates with thinly laminated dolomite with few clasts.

About two kilometres to the southeast and along strike, corroded outcrops of mostly very weathered diamictite, with up to cobble-sized clasts, crop out in a tributary of Blackwater Rivulet between 324570/5444410 and 324570/5444490. The diamictite is interbedded with planar laminated medium grey dolomite and dark grey, flaggy, carbonaceous and siliceous siltstone (lithology Pssf). The unit here is about 50 m thick and is overlain by the Keppel Creek Formation. On the Sumac map sheet it is depicted as lensing out southward, but this is difficult to verify due to lack of outcrop (e.g. in Blackwater Rivulet near 324900/5443200).

A small tract of the Julius River Member is depicted in a similar stratigraphic position near the southern edge of the Sumac map sheet, where tough black to dark grey-green diamictite with sparse small chert clasts crops out sporadically in a small creek. In thin section, samples (R004836, 325700/5440500; R004837, 325690/5440460) appear to be highly altered, carbonated diamictites with some mafic clasts. This tract therefore probably belongs to the adjacent Croles Hill Diamictite (see below).

Leensons Road south–Arthur River area (DBS)

Sample R004249 from 325150/5447500 is a breccia comprising a rather chaotic closed framework of dominantly angular to sub-angular fragments, ≤6 mm in diameter, of grey-brown, slightly silty fine-grained dolomite, in a fine-grained dark grey-brown dolomitic matrix. Most of the dolomite fragments contain a few per cent of fine-grained sub-angular quartz clasts. Considerable flattening of the fragments has accompanied the development of a moderate to strong tectonic foliation at this locality. This lithology may represent a variant of the open-framework dolomitic diamictite, which elsewhere is typical of the Julius River Member.

Julius River–Arthur River area (JLE)

The lowermost part of the Julius River Member crops out sporadically on the south bank the Arthur River, just below the mouth of the Julius River (e.g. 335660/5445630). The diamictite contains clasts up to boulder size (400 mm), apparently all of dolomite, in a dark grey, brown-weathering matrix of fine-grained dolomitic siltstone/mudstone. Diamictite was also reported (A. V. Brown, pers. comm.) capping a large crag on the north side of the river (at 336000/5446400), the base of which is sub-horizontally bedded massive dolomite.

The base of the unit also crops out about two kilometres further south in the Julius River. The contact with underlying, mostly thinly laminated to medium-bedded, clast-free dolomite appears to be transitional over a few tens of metres. Thick (1 m) beds containing angular chert clasts were first noted at 334500/5443570, but they are overlain by more thinly laminated dolomite. Massive diamictite with abundant granule, pebble and (rare) cobble-sized chert clasts crops out in rapids at 334460/5443670.

Tracts of diamictite also occur in the Julius River upstream of the Sumac Road bridge, and extend southward onto the Dempster map sheet to about 332660/5439030. The abundance and size of clasts is highly variable, but typically subangular granule to pebble-sized clasts of off-white chert and less commonly massive dolomite lie in a medium to dark grey, generally unbedded matrix. Clasts of stromatolitic dolomite were noted at 332240/5441800,

and granular white sulfide at 334110/5441280. At 332770/5439160, the diamictite contains exceptionally abundant clasts, ranging from subrounded boulders (up to 300 mm) to typically angular granules.

Sumac Rivulet (JLE)

Similar diamictite, containing generally small (≤50 mm) subrounded to subangular clasts of mostly chert in a medium-grey dolomitic matrix, crops out poorly in Sumac Rivulet between about 337510/5440330 and 337200/5439250.

East of upper Blackwater Rivulet (ARR)

Near 329000/5439500 a laterally discontinuous tract of monomictic conglomerate near the top of the Black River Dolomite is assigned to the Julius River Member. It comprises angular to sub-rounded chert and rarely friable (possibly originally containing carbonate) siltstone clasts to 10 mm diameter, within a matrix of cream-coloured fine-grained sandstone or siltstone.

North of Horton River (JLE)

A few low corroded, sometimes pedestal or mushroom-shaped outcrops of diamictite occur in Lagunta Creek, as indicated individually on the Dempster map sheet. Typically they contain sparse, mostly small (few millimetres) angular to subrounded clasts in a pale grey-green, light brown to tan-weathering dolomitic matrix. The most clast-rich outcrop (332550/5434500) contains numerous (20–25%) fragments of white and black chert, and minor granular sulfide.

Diamictite overlies moderately south-dipping black shale in an outcrop on the south bank of the Horton River (at 331900/5432290). Downstream, a low outcrop at 331200/5432600 contains scattered chert and dolomite clasts in a blue-grey muddy dolomitic matrix. A similar outcrop on a major tributary at 330190/5433570 contains occasional sulfide clasts in a diffusely bedded, hard blue-grey matrix.

In these areas, on the Dempster map sheet, the Julius River Member is shown flanking the southern, eastern and extreme northern margins of a large structural dome. The unit crops out poorly and may be more continuous than shown, possibly also occurring on the western side of the structure.

Lower Lindsay River area (JLE)

A relatively large but poorly exposed tract of the Julius River Member occurs towards the southern end of the Smithton Synclinorium.

On the right (northeast) bank of the Lindsay River at 329330/5430170, about three metres of river gravel overlies a low corroded outcrop of matrix-supported diamictite, containing about 25% clasts of mainly dolomite, including well-rounded pebbles (≤50 mm) and smaller angular granules. The medium-grey dolomitic matrix contains traces of yellow sulfide. The diamictite is associated, a few metres upstream, with 'fretted', fissile to cuboidally-weathering, thinly-laminated medium-grey siltstone.

The unit also crops out intermittently in tributary creeks east of the Lindsay River (e.g. at 330390/5430270, 329620/5430300, 330500/5430980). These typically contain sparse (5–10%), small (5–20 mm but occasionally ≤50 mm), angular clasts of mainly white and/or black chert in a lead-grey to blue-grey, occasionally diffusely laminated matrix.

Petrography (JLE)

All samples are very poorly sorted, matrix-supported (open-framework) diamictites, with little or no suggestion of bedding, but sometimes with an anastomosing stylolitic cleavage. In thin section (Plates 61–68) they consist essentially of angular to subangular clasts (5–40%) of dominantly sparry to micritic dolomite and subordinate chert in a finely sparry to micritic, grey to pale yellow-brown weathering impure carbonate matrix. Detrital quartz and siliciclastic rock fragments are rare. Detailed petrographic descriptions are given in Appendix 1.

Discussion (JLE)

Two possible interpretations for the Julius River Member are a mass-flow deposit or a tillite. Most of the clasts could have been locally derived from the immediately underlying main member of the Black River Dolomite, with a minor siliciclastic component from the Rocky Cape Group. The only possible exceptions are the rare basaltic clasts. This tends to favour a mass-flow origin, the preferred interpretation of Griffin and Preiss (1976).

Calver (1998) considered that there was no clear evidence for the mode of origin of the diamictite, but suggested correlation with the Sturtian glaciation of the Adelaide Geosyncline (South Australia). If the remainder of the Black River Dolomite is a correlate of the Skillolagee Dolomite (lower Burra Group), a significant disconformity at the base of the Julius River Member is implied, corresponding to the 2–3 km of upper Burra Group rocks beneath the Sturtian Glacials in South Australia.

Kanunnah Subgroup

Definition (JLE)

The Kanunnah Subgroup is herein defined as that sequence of intercalated lithicwacke, basalt, diamictite and minor conglomerate, lithicarenite, hematitic ironstone, mudstone and impure carbonate that conformably overlies the Black River Dolomite and is conformably overlain by the Smithton Dolomite. Its type section is the composite of its three constituent, interdigitating formations, the Keppel Creek Formation, the Croles Hill Diamictite and the Spinks Creek Volcanics, as defined herein. A supplementary type section is designated in a tributary of Blackwater Rivulet between 324 570 mE, 5 444 510 mN and 324 750 mE, 5 444 640 mN, where the subgroup is about 220 m thick and the Croles Hill Diamictite is absent. Elsewhere the subgroup reaches a maximum thickness of about 1400 metres.

The Kanunnah Subgroup is equivalent to the rarely used term 'Trowutta Group' of Matthews (1961*b*). This term was not formally defined and is avoided here because Jago (1981) also used the term 'Trowutta Breccia' for some of the diamictite units. Other equivalent, informal terms are 'Crimson Creek Formation correlates in Smithton Basin' (e.g. Brown, 1986, p.98–102) and 'Smithton-Trowutta basalt-sedimentary rock association' (e.g. Brown, 1989*a*, *b*). Griffin and Preiss (1976) incorrectly correlated the sequence with the Dundas Group.

The age of the Kanunnah Subgroup is constrained by a SHRIMP U/Pb zircon age of 582.1 ± 4.1 Ma from a rhyodacite exposed on the foreshore at Robbins Passage, west of Montagu (320270/5487030) and well north of the area described in this report. The rhyodacite overlies Keppel Creek Formation and is overlain by the Croles Hill Diamictite, which in turn is overlain by the Spinks Creek Volcanics (Calver *et al*., 2004). This age is consistent with previous, indirect age estimates for the Black River Dolomite (650–750 Ma) and Smithton Dolomite (545–580 Ma), which enclose the Kanunnah Subgroup (Calver, 1995, 1998).

Kanunnah Subgroup: Keppel Creek Formation (Psvw, Psvwl, Psvwi, Psvwd)

Definition *(JLE)*

The Keppel Creek Formation is herein defined as that unit of olive green, blue-grey or maroon to orange-brown weathering, thinly bedded to massive, commonly cuboidally fracturing volcaniclastic lithicwacke sandstone, lithicwacke siltstone and subordinate conglomerate, lithicarenite, hematitic ironstone, mudstone, impure limestone, dolomitic siltstone and laminated dolomite that occurs between the Black River Dolomite and Smithton Dolomite. The composite type section comprises a lower part along the Arthur River between 334 640 mE, 5 446 800 mN, where the unit overlies the Julius River Member of the Black River Dolomite, and 334060 mE,/5446660, where it is overlain by the Croles Hill Diamictite; and an upper part, stratigraphically overlying the Spinks Creek Volcanics, along Blackwater Road between 330 300 mE, 5 446 400 mN and 329 600 mE, 5 446 900 mN. The top of the formation is faulted out here, but a conformable upward transition to the Smithton Dolomite is observed northeast of Balfour at 327 100 mE, 5 432 600 mN. The Keppel Creek Formation has an interdigitating relationship to both the Croles Hill Diamictite and Spinks Creek Volcanics.

This term, resurrected and adapted from the 'Kepple Creek Siltstone' (sic) of Matthews (1961*b*), is adopted for the dominantly clastic sedimentary component of the Kanunnah Subgroup.

The unit is poorly exposed, and outcrops are largely restricted to small discontinuous stream outcrops and road cuttings.

Western tracts

General features *(JLE)*

The stratigraphic position of the unit, above the Black River Dolomite and below the Smithton Dolomite, is seen most clearly in the tract parallel to the western margin of the Smithton Synclinorium, where the Togari Group dips steeply. The Spinks Creek Volcanics occurs as a lens, or as isolated flows, within the unit. Incomplete sections are exposed through the Keppel Creek Formation in the Arthur River (between 322900/5446500 and 322800/5446100), and in an un-named tributary of Blackwater Rivulet (between 324770/5444650 and 324560/5444490).

The most common lithology in this area is an indurated, pale olive-green to grey (10G6/2, 5GY7/2, 10Y6/2) lithicwacke siltstone or very fine-grained lithicwacke sandstone, with a faint diffuse, planar to slightly wavy bedding lamination, spaced typically at one to five millimetres. Streaky bedding is less commonly present. Sometimes the rock is mesoscopically massive and may be difficult to distinguish from weathered basalt.

Cleavage is usually poorly developed. The unit is usually well jointed on hand specimen scale and this, together with parting along bedding planes, may impart a closely spaced (10 mm or less) cuboidal fracture to the rock, and a crumbly 'fretted' appearance to outcrops. Otherwise fracture is conchoidal, subconchoidal or uneven.

No systematic difference in lithology appears to exist between exposures stratigraphically above and below the intercalated basalt. However where closely associated with basalt, the unit is greyish-red to brownish-red ('maroon': 5R4/2, 10R3/4, 5YR2/1) in colour, due to hematitic alteration.

South Chatlee Road–Dunns Plain north (north of the Arthur River) *(DBS)*

The Kanunnah Subgroup occurs at the southern end of Chatlee Road, and in several northeast-flowing creeks between there and the northwestern corner of the Sumac map sheet, north of the Tertiary gravel cover of Dunns Plain. The sequence is probably a maximum of about 800 m thick, including one discontinuous unit of basalt (correlated with the Spinks Creek Volcanics), which is about 60–100 m thick. The sedimentary part of the sequence is dominated by siltstone, of which there are two common facies variants:

- Brown-weathering, thinly bedded, very distinctly plane-laminated grey or grey-green siltstone, rarely with discontinuous pyritic laminae;
- Thinly or indistinctly bedded, faintly laminated to massive grey or blue-grey siltstone, which may include thin lithic pebble and lithicwacke horizons, the latter commonly showing small-scale graded bedding. Rarely, lithicwacke and siltstone may be interbedded in roughly equal proportions in this facies.

At 321320/5448880, in the most complete creek section, the uppermost unit below the Smithton Dolomite is a rather red-weathering, grey-green siltstone.

Arthur River section (CRC, JLE)

Probably the best exposure of the formation in the area is over a distance of more than 60 m, approximately perpendicular to strike, along the south bank of the Arthur River below 322920/5446300. This exposure is towards the top of the Keppel Creek Formation, near the base of the Smithton Dolomite. The sequence, which is steeply dipping, consists of mainly thin-bedded, mostly laminated, pale to dark grey-green or blue-grey siltstone and shale, and some beds of fine to very coarse-grained greyish blue-green lithicwacke sandstone. The sandstone beds have sharp bases (i.e. western contacts) but less sharp tops. Graded bedding is present but not particularly common. Facing can also be obtained from erosional truncation and low-angle cross lamination and is consistently eastward.

At the stratigraphic bottom of the section (near 322890/5446240), two basalt flows, separated by 4–5 m of conglomerate, are intercalated in the sequence. The upper flow is 10–15 m thick and massive, except for a slightly vesicular top. Sharply overlying the basalt is an apparently conformable but discontinuous layer of ironstone, 0.5–1 m thick, containing small nested turbinate structures resembling stromatolites. The ironstone forms discrete pods, surrounded and overlain by the thin-bedded sedimentary sequence. The conglomerate is massive and has a closed framework (or nearly so). It consists of well-rounded pebble to cobble-sized clasts (up to 250 mm) in a matrix of coarse lithic greenish sandstone. The clasts are typically grey-green to purplish with green mantles, and some are clearly basaltic. The lower basalt flow at the bottom of the continuous section is the thicker of the two, as sporadic outcrops occur downstream.

Further downstream, stratigraphically below the basalt flows, are two small isolated outcrops of medium to dark-grey siltstone, mudstone and black laminated pyritic mudstone. These are intruded by dolerite (Psbz) and underlain by dolomitic diamictite (Julius River Member, Pssr) but contacts are not exposed.

Lower Blackwater Rivulet area (DBS, JLE)

The western tract extends southeastward and southward from the Arthur River for about nine kilometres to near 325600/5438100 on the Dempster map sheet, where it is offset by the Roger River Fault.

In an un-named tributary of Blackwater Rivulet, between 324770/5444650 and 324560/5444490, the formation rests on dolomictic diamictite (Julius River Member) and dips and faces steeply ENE. It is less than 30 m thick below the intercalated basalt, and between 90 and 130 m thick above the basalt. Typical lithologies (samples R004853, R004854) are pale grey, well laminated and sometimes wavy laminated, fine to coarse-grained lithicwacke siltstone, sometimes with small-scale cross bedding or sub-cuboidal fracture.

In Blackwater Rivulet, downstream from about 324900/5453200, generally brown to maroon poorly-sorted laminated lithicwacke siltstone, with lenses of lithicwacke sandstone containing grains to granule size, is interbedded with thin basalt (at 325000/5443170, not shown on the map) and basaltic tuff (?). The contact with the overlying basalt is almost exposed at 325130/5443210.

Exposures of the Keppel Creek Formation are very poor along Blackwater 5-1 road, although fresh, massive, bluish-grey very fine-grained lithicwacke sandstone crops out in a small cutting at 325730/5442120. The orange-brown soil developed on the formation contrasts very markedly with the pale cherty soils associated with the enclosing dolomite units.

The formation is exposed in a short creek section southeast of a bridge on Blackwater Road at 325960/5439940. Here it is steeply eastward dipping and facing, and includes blue-grey, greenish-grey and maroon plane-laminated to massive siltstone, with some interbedded dark grey-green lithicwacke containing rare clasts of red mudstone. Facing was determined from small sole structures on the bases of coarser laminae in some of the siltstones. The upper part of the section is probably missing due to truncation by the Roger River Fault.

Blackwater Road–Frankland River (DBS, JLE)

The Keppel Creek Formation is mapped southward for a further six kilometre south of the Roger River Fault. This tract probably conformably overlies the Black River Dolomite to the west, but is faulted against a block the Rocky Cape Group to the east. Near 325200/5431400, just short of the Frankland River near Balfour, it is wedged out by a thrust fault.

Outcrop is very poor in much of this area. Intermittent exposures occur in a westward-flowing tributary of the Frankland River between 324210/5436500 and 324900/5436440. At the latter locality the unit is truncated by a north-trending inferred fault which may lie close to the line of the original, extensional Roger River Fault at the time of Togari Group deposition (see *Structural Geology* section). The sequence dips and faces eastward. Exposures between the top of the Black River Dolomite and the base of a thin basalt unit are poor, the best outcrops being of the Croles Hill Diamictite (see below). More common exposures stratigraphically above the basalt include plane-laminated to massive, pale green, olive green and grey-green siltstone, and a notable, conspicuously red-weathering, hematitic siltstone at 324740/5436520.

Central northern tracts

Leensons Road (DBS)

The Kanunnah Subgroup is exposed in an area up to about one kilometre wide, between a bifurcating pair of northwest-trending faults extending from near

323250/5450400 on Black Jay Road, to the Arthur River some 4.5 km southeast of this point. On the eastern side of this fault-bounded block, the Kanunnah Subgroup appears to rest conformably on the Black River Dolomite, but on the western side it is inferred to be in faulted contact with the Smithton Dolomite. Observed and inferred facings suggest that the Kanunnah Subgroup forms a tight syncline within the fault block.

Sedimentary facies within the Kanunnah Subgroup here are similar to those recorded in the South Chatlee Road–Dunns Plain north area (see above). Very clear truncated cross-lamination in siltstone provided reliable facing evidence in the creek section at 323610/5449420. Just east of this point an occurrence of hematitic ironstone lies less than 100 m stratigraphically below basalt of the Spinks Creek Volcanics correlate. An occurrence of similar ironstone in road cuttings at 324020/5448990 on Leensons Road is about 600 m away to the southeast along strike and within 50 m stratigraphically below the basalt. These two occurrences suggest that the hematitic ironstone represents a thin stratigraphic unit or horizon, perhaps a hydrothermal precursor to the mafic volcanism.

Lerunna Road–Langford Creek area *(DBS)*

This large area of Kanunnah Subgroup rocks is enveloped by two inferred northeast-directed thrust faults. One is a steep northwest-trending fault which intersects both ends of Leensons Road at the southwestern margin of the area, and the other an inferred shallowly southwest-dipping major thrust forming the northeastern margin of the area, and which appears to have structurally emplaced the Kanunnah Subgroup over the Smithton Dolomite. Within this area, sedimentary rocks of the Kanunnah Subgroup are strongly folded about shallowly northwest-plunging axes.

Sedimentary rocks in the Kanunnah Subgroup here are similar to those in the south Chatlee Road–Dunns Plain north area. There are two main facies, the first of which is the more dominant:

- Brown-weathering, generally thin-bedded, dark grey or grey-green, laminated siltstone or interbedded laminated siltstone and mudstone. Facing is commonly evident from small scale sedimentary structures in some of the siltstone laminae — particularly basal scour and flame structures, grading and cross lamination. Rarely, soft sediment deformation is evident in the form of small-scale convolute folding of laminae.
- Brown to red-brown weathering, indistinctly bedded, fine to medium-grained massive lithicwacke, commonly in graded beds (?turbidites) up to 0.5 m thick. Less commonly (particularly on Leenson 2 Road between 326420/5450790 and 326220/5449410), the grain size of this facies increases to pebble conglomerate in graded beds up to one metre thick, with clast compositions including siltstone, red mudstone, cream and grey chert, milky quartz, and probable weathered volcanic rock (?basalt).

No basalts were encountered in the numerous ground traverses carried out in the Kanunnah Subgroup in this area. The conclusion that equivalents of the Spinks Creek Volcanics are absent here is reinforced by a lack of the typical narrow, linear, strongly positive magnetic anomalies which are associated with the basalt in the south Chatlee Road–Dunns Plain north and Leensons Road areas (see above).

Blackwater 1 Road area *(JLE)*

Several very poorly exposed, probably fault-bounded areas assigned to the Keppel Creek Formation occur just south of the Arthur River, in the vicinity of Blackwater 1 spur.

Weathered, soft, pale orange siltstone, characteristically with a cuboidal fracture, occurs in road cuttings near 327500/5446800, 327600/5446300 and 328100/5446800. Thin, slightly wavy bedding lamination, dipping moderately west, is locally recognisable. This area is depicted on the map as a slice enclosed by a bifurcation of a major east-directed low angle thrust, but given the poor outcrop other interpretations are possible.

Keppel Creek Formation further along Blackwater-1 (west of 326900/5447300) was mapped mainly from soil type, and is an extension of the Lerunna Road–Langford Creek area described above. Finely laminated, fissile to cuboidal, pale brown to orange-weathering mudstone was noted on a track cutting near 326400/5447700. Sporadic poor outcrops of soft orange to khaki-brown weathered, cuboidally-fracturing siltstone (in thin section very fine-grained lithicwacke sandstone, see below) occur along a minor creek between 326150/5446770 and 325840/5446770. Better, although infrequent, outcrops occur in the Arthur River between 326160/5447870 and 325560/5447130. Lithologies are thin bedded or laminated greenish to khaki-coloured fine-grained lithic sandstone and lithicwacke, and medium to dark grey or grey-green siltstone and mudstone. Spheroidal and 'fretted' cuboidal weathering is characteristic. A large outcrop on the south bank at 325680/5447030 is sheared into irregular slickensided lozenges. This tract is probably bounded by low angle east to northeast-directed thrusts.

Similar thinly laminated khaki-coloured calcareous siltstone (sample R005065), medium-grey to black sometimes pyritic mudstone and minor lithic sandstone crops out in the Arthur River at 325340/5446490. Sporadic float and rare outcrop of cuboidal weathered brown siltstone occurs on the hillside to the southeast. This is an extension of the Leensons Road tract (see above). To the southwest, the unit is faulted against concealed Smithton Dolomite by an inferred northwest-directed thrust. It cannot be traced further southeast than about 326000/5446000, where it is probably truncated by a cross fault.

Eastern tracts

General features (JLE, MPM)

These include areas on the Sumac map sheet, east of the Roger River Fault.

Here the formation consists of generally similar lithologies of finely and diffusely laminated lithicwacke sandstone, lithicwacke siltstone and rare mudstone, all with a cuboidal or subconchoidal fracture. Siltstones often have only very faint and thin banding, whereas the fine-grained sandstones generally have more obvious thin banding, and beds up to a metre thick. Some hard, tough, dark greenish-grey rock varieties are present, but commonly the rocks are less indurated and purplish-grey, purplish-red ('maroon') to brick-red in colour (10R4/2, 5RP4/2). This is probably due to oxidation, and as hematitic granules occur in some of the lithicwackes, this may be a primary feature rather than a recent weathering effect. The maroon colour is most commonly seen in exposures stratigraphically below basalt, and may be a hydrothermal effect. This would also explain why it is much less common west of the Roger River Fault, where the basalts are thinner.

On weathering, the rocks become pale green, or oxidise to sepia-brown to pale yellow-orange. With further weathering, the rocks decompose to an orange-red to orange-brown soil, similar to that developed on basalt.

In thin section, mineral grains and clasts noted (MPM) include both strained and unstrained quartz, opaque minerals, chlorite (possibly after clinopyroxene), plagioclase, serpentine (probably after olivine), rare muscovite and chert (one sample). Abundant intergranular chlorite may be after clay minerals and is difficult to distinguish from clasts. Fine-grained siltstone at 329300/5445750 contains abundant clasts of carbonate. This suggests derivation from a dominantly basalt provenance, probably the associated Spinks Creek Volcanics, with subordinate components from the underlying Black River Dolomite (chert, carbonate), metamorphic terrain (muscovite, strained quartz) and possibly felsic volcanic rocks (unstrained quartz). More detailed petrographic descriptions are given below.

Two small areas near lower Keppel Creek (329960/5444250, 329310/5445170) are of impure limestone (unit Psvwl) with abundant clasts of opaque minerals and sparse quartz clasts. In thin section the rock appears to be a partly recrystallised clastic carbonate.

Arthur River exposures (JLE, CRC)

Medium to dark-grey or khaki-coloured, thinly-laminated very fine-grained siltstone and mudstone crops out sporadically downstream from 334640/5446800 to 334060/5446660, where it is overlain by basaltic diamictite (Croles Hill Diamictite).

Further downstream (near 332040/5446030 and 331580/5445890), well-bedded grey-green to maroon siltstone and mudstone are interbedded with minor lithicwacke.

Between 500 m and 1200 m downstream of Kanunnah Bridge, flaggy thinly bedded purplish-grey siltstone and mudstone with parallel lamination contains occasional pyrite nodules and cuboidal fracture and weathering pattern. Further away from the basalt exposed near Kanunnah Bridge, the unit is green to grey rather than maroon, and contains fine-grained lithicwacke sandstone in addition to siltstone and mudstone.

Blackwater Road cuttings (JLE)

The Keppel Creek Formation is well exposed in numerous cutting in Blackwater Road between 330300/5446400 and 328300/5443900, but is usually deeply weathered. The main lithology is a soft pale orange-brown, thinly and faintly laminated, cuboidally-fracturing siltstone. Open mesoscopic folding is recognisable in several places (plunging at 30° to 300° with sinistral vergence at 328440/5444100) but as the exposures are very close to the Roger River Fault the regional significance is doubtful.

Stephens Rivulet area (JLE)

The Keppel Creek Formation outcrops sporadically in Stephens Rivulet and its tributaries upstream from 327900/5443300, where it crosses the Roger River Fault. Fine-grained lithicwacke sandstone and siltstone, similar to those in the unit elsewhere, are lithologically dominant, but some degree of maroon hematitic alteration is usual, perhaps due to the proximity and thickness of the basalt. This is particularly strong in a small creek near 328600/5442900, where diffusely laminated, hematitic lithicwacke sandstone is noticeably dense, and approaches hematitic ironstone. Similar dense, although better sorted and more massive, lithic arenite at 328520/5442480 contains pebble to cobble-sized clasts of fresh basalt bearing native copper.

Upper Keppel Creek (JLE)

Much of the Keppel Creek Formation around 333000/5441000 is mapped from float of weathered soft pale orange-brown siltstone. Good outcrops of tough, dark green, thinly planar laminated siltstone occur in small waterfalls in Keppel Creek upstream from 331900/5440210 (shown within unit Psvx on the Sumac map sheet). About 200 m upstream the siltstone passes into a tough, faintly laminated, maroon, dense and very hematitic lithicwacke sandstone, depicted as a separate unit (Psvwi – hematitic ironstone) on the Sumac map sheet. The unit dips shallowly south and is immediately overlain by basalt.

Southern tracts

Apart from deeply weathered orange-brown siltstone exposed in a cutting on Sumac Road near 334700/5434400, the Keppel Creek Formation on the Dempster map sheet occurs in dense, relatively inaccessible rainforest with few good exposures, even on major streams.

Blackwater Rivulet–Julius River headwaters (ARR)

The Kanunnah Subgroup exposed in and between the headwaters of Blackwater Rivulet (327800/5436300) and Julius River (332000/5438300) comprises a gently folded sequence of interbedded siltstone and diamictite horizons overlain by predominantly massive basalt. Siltstone units to about 250 m thick are poorly exposed and comprise rusty brown to yellow-coloured beds commonly less than 50 mm thick. Joints with manganiferous surfaces are common to laminated units, typically masking bedding and giving the unit a blocky appearance in outcrop. Fine-grained volcanic detritus is rarely evident in hand specimen.

Horton River–Frankland River outcrops (JLE, CRC)

Thinly and faintly laminated, grey-green to maroon siltstone weathers to a soft orange-brown brittle rock with a cuboidal fracture in the Horton River downstream from 333150/5432320. Maroon siltstone with occasional thin sandy interbeds occurs near 332500/5431600.

On the northern bank of the Horton River (near 331060/5432600) planar-bedded fissile khaki-brown to maroon siltstone, with some more resistant tough dark grey beds up to 100 mm thick, is exposed in a seven to eight metre high cliff. Similar maroon siltstone and intercalated coarse-grained lithicwacke sandstone, exposed near river level a few metres upstream, is overlain by basalt; the contact dips very shallowly south, subparallel to bedding. Sporadic outcrops occur for about 150 m downstream, where the siltstone becomes pebbly and grades into the Croles Hill Diamictite. Further downstream, past a bend, the river section passes stratigraphically upward through the siltstone unit, and back into basalt.

Similar outcrops of maroon lithicwacke siltstone, generally shallowly dipping and underlying or apparently intercalated with basalt, occur in the Horton River at several localities further downstream. On the right (northern) bank at 327130/5431460, mesoscopic gently WNW-plunging open folds with a wavelength of four to five metres occur in planar-bedded, medium-grey to pale-brown to purplish cuboidal siltstone. On the major bend about 100 m downstream (327080/5431550), similar cuboidal medium-grey siltstone contains ellipsoidal to irregular, football-sized concretions of paler carbonate. This locality is stratigraphically close to the top of the formation, near the contact with the overlying Smithton Dolomite.

A fine outcrop of thinly laminated, very cuboidal, purplish siltstone, with thin (20–40 mm) interbeds of coarser pale siltstone spaced at intervals of 0.5 to 1 m, occurs on the south bank just downstream at 326990/5431440.

Other southern areas (JLE)

The occasional isolated outcrops in small streams (as in a small tributary entering the Horton River at 329200/5432800) are generally of thinly laminated grey to brown-weathering soft siltstone, with few lithicwacke sandstones.

The transition with the overlying Smithton Dolomite is intermittently exposed in a creek near 327100/5432600. Thinly laminated, medium to fine-grained lithicwacke siltstone passes up-sequence into thicker and planar-bedded, very fine-grained sandstone with impure dolomite interbeds, and thence into well-bedded lead-grey dolomite. The transition occurs in about 100 m of creek section, but after allowing for the dip of the strata and the gradient of the creek, the stratigraphic thickness of the transitional interval is probably twenty to thirty metres.

Petrography (JLE, MPM)

More than fifty samples were examined in thin section. Full descriptions are given in Appendix 2 and photomicrographs of representative samples are presented as Plates 69–75.

Most samples are poorly sorted, mineralogically immature lithicwackes, with a few moderately well-sorted lithic arenites. The most common lithologies are fine to very fine-grained lithicwacke sandstone and coarse-grained lithic siltstone. There is some medium to very fine-grained siltstone, but little true mudstone. Because of poor sorting, and weathering of some samples, this grain size classification may be difficult to apply.

The most common clast type is fine-grained basalt resembling, but usually more feldspathic than, the basalt of the Spinks Creek Volcanics. Other clast types noted, mainly in the coarser-grained lithicwackes and arenites, are felsic volcanic rocks (resembling the clasts in the Croles Hill Diamictite, see below), chert, both fine-grained and sparry carbonate, orthoquartzite, quartz sandstone, finer grained lithicwacke and mudstone. Common grain types include usually turbid to sometimes clear feldspar, chlorite, opaque grains partly altered to hematite and/or sphene, and frequently strained monocrystalline or polycrystalline quartz.

The formation is therefore of dominantly local and basaltic provenance, although fresh clinopyroxene is present in only a few samples, usually those very proximal to basalt. Chromite (chrome spinel) is an accessory mineral in many samples. The most obvious source for the chromite is also the basalt, but it has not been seen in thin sections of the basalts, and its mineral chemistry suggests an ultimate ultramafic or possibly picritic source (see below).

The presence of detrital quartz in most samples, and detrital white mica in a few, suggests a subordinate component from the Rocky Cape Group. Samples with significant carbonate or chert are usually those stratigraphically close and transitional to the enclosing Smithton Dolomite and Black River Dolomite.

Geochemistry *(JLE)*

Only limited geochemical data is available from the Keppel Creek Formation (Table 5).

Three analysed samples, described as tuff, were collected by J. W. Hudspeth during petrophysical investigations from 330580/5446280 near Kanunnah Bridge, in an area subsequently mapped as basalt (Psb). Although the analyses are remarkably similar to the Group C basalts in that area for most major and trace elements, they are lower in CaO, K_2O and Sr and higher in Na_2O and H_2O^+.

A 'greywacke' (sample 401351) collected by Hudspeth from mapped Keppel Creek Formation about one kilometre to the west (346200/5429300) is oxidised, depleted in CaO, Na_2O and MgO, and relatively enriched in some immobile elements including Al_2O_3, Cr, Zr and Nb, probably due to weathering.

Two analysed samples of ironstone (Psvwi) from near the base of the Spinks Creek Volcanics are probably lithicwackes that have been hydrothermally impregnated with up to 50% hematite. On the limited basis of these data there is no evidence for base metal or gold anomalism.

Table 5

Chemical analyses, Keppel Creek Formation

Field No.	MRS22	MRS32	-	-	-	-
Reg. No.	R002864	R002874	G401351	G401348	G401349	G401350
Anal. No.	961074	961075	891864	891861	891862	891863
AMG (mE)	328510	331920	329300	330580	330580	330580
AMG (mN)	5442320	5449320	5446200	5446280	5446280	5446280
Sheet	Sumac	Sumac	Sumac	Sumac	Sumac	Sumac
Lithology	ironstone	ironstone	'greywacke'	'tuff'	'tuff'	'tuff'
SiO_2 (%)	53.86	25.63	45.47	50.50	46.04	47.84
TiO_2	1.67	1.19	2.69	1.60	1.65	1.59
Al_2O_3	13.56	6.96	23.17	13.40	14.35	13.82
Fe_2O_3	19.27	49.60	15.26	4.06	4.60	3.97
FeO	1.60	3.68	0.33	9.33	9.79	9.33
MnO	0.10	0.15	0.01	0.12	0.20	0.13
MgO	1.15	1.97	0.91	5.86	8.50	5.61
CaO	2.25	1.85	0.07	3.53	5.25	4.44
Na_2O	4.13	1.29	0.43	4.94	4.15	5.44
K_2O	0.39	0.05	2.13	0.05	0.03	0.05
P_2O_5	0.21	1.20	0.17	0.14	0.13	0.16
H_2O^+	1.60	2.77	9.36	5.15	4.95	5.62
CO_2	0.11	0.11	0.68	1.70	0.59	1.95
SO_3	0.08	0.09	0.29	0.27	0.13	0.35
TOTAL	**99.98**	**96.54**	**100.97**	**100.65**	**100.36**	**100.30**
LOI	[1.53]	[2.48]	[10.11]	[5.88]	[4.50]	[6.61]
Sc (ppm)	44	24	69	49	51	49
V	460	1100	270	230	290	240
Cr	115	610	820	115	120	120
Co	38	80	8	36	43	40
Ni	52	150	36	60	70	59
Cu	16	92	41	200	145	155
Zn	150	150	15	74	88	68
Ga	18	8	16	13	14	14
As	<20	24	<5	8	<5	<5
Rb	15	22	43	<5	<5	<5
Sr	135	91	7	22	71	16
Y	23	47	11	25	22	24
Zr	105	210	185	92	93	95
Nb	8	24	25	6	5	7
Mo	<5	<5	<5	<5	<5	<5
Ag	nd	nd	<5	<5	5	<5
Sn	<9	<9	<5	<5	<5	<5
Sb	nd	nd	<5	6	9	<5
Ba	105	110	165	84	89	92
La	<20	41	15	10	<5	8
Ce	<28	120	61	46	46	37
Nd	<20	31	7	17	17	15
W	<10	46	<5	9	8	<5
Au	<0.05	<0.05	nd	nd	nd	nd
Pb	16	11	18	<5	<5	<5
Bi	7	18	5	5	6	<5
Th	<10	<10	6	<5	<5	<5
U	<10	<10	<5	<5	<5	<5

Analyses by Mineral Resources Tasmania laboratories

Kanunnah Subgroup: Croles Hill Diamictite (Psvx)

Definition *(JLE)*

The Croles Hill Diamictite is herein defined as that discontinuous unit of dark green, massive to rarely diffusely bedded diamictite, containing clasts of basalt and subordinate felsic volcanic rocks, carbonate and fine-grained clastic sedimentary rocks, that occurs as lenses within the Kanunnah Subgroup in the southern Smithton Synclinorium. It typically interdigitates with or overlies the Keppel Creek Formation and underlies the Spinks Creek Volcanics. The type section is designated as the Arthur River between 334 060 mE, 5 446 750 mN, and 333 880 mE, 5 446 880 mN, where it is overlain by the Spinks Creek Volcanics.

It is synonymous with the term Croles Hill Mixtite, as used by Everard *et al*. (1996) on the 1:50 000 scale Trowutta map sheet.

General features *(JLE)*

The Croles Hill Diamictite is best developed south of the Arthur River and east of the Roger River Fault. The few bedding readings within it are very variable but are usually shallowly dipping in this area, and its maximum thickness is probably about 250 metres. The Croles Hill Diamictite has also been recorded near Forest in the northeastern part of the Smithton Synclinorium (unit Csm of Lennox *et al*., 1982), and from the north coast at Robbins Passage (Calver *et al*., 2004).

Field relationships *(JLE, ARR)*

This unit is a massive, unbedded, very poorly sorted, frequently very tough, dark blue-grey to green basaltic diamictite. Outweathering granule to pebble-sized (and less often cobble to small boulder-sized) clasts are conspicuous.

The Croles Hill Diamictite typically crops out poorly and weathers to a brown soil, similar to that produced by other units within the Kanunnah Subgroup. It is thus difficult to map from float, and may be somewhat more extensive than mapped. Most of the unit occurs in relatively inaccessible, dense rainforest, but it can be readily examined as mainly float boulders along Sumac 3 spur road at 337700/5441300 and 336300/5441400.

There are excellent, although relatively inaccessible, polished outcrops of this unit in the Lindsay and Horton/Frankland rivers near their confluence (328700/5431100). Here, the diamictite contains 20 to 30% clasts in a blue-grey, diffusely streaky groundmass, with alternating darker and lighter lenticular bands defining bedding. The clasts are mostly angular to subangular, very poorly sorted and up to 300 mm across, but typically 2–50 mm. Mesoscopically identifiable clast lithologies included basalt, felsic volcanic rocks, and various sedimentary rocks including lithicwacke and relatively rounded clasts of coarse-grained grey dolomite. In an otherwise similar outcrop 100 m downstream of the confluence, clast abundance is only 5 to 10%.

In the area between the headwaters of Blackwater Rivulet (327500/5443800) and Julius River (332000/5438300), diamictite units comprise rounded to angular clasts to 200 mm diameter of basalt and, near the base of the unit, angular clasts of fine-grained siltstone and sandstone, possibly Black River Dolomite. Boulders to one metre diameter of medium-grained gabbro (equigranular pyroxene, amphibole and feldspar) were also noted at 327870/5439200. Clast size is greatest nearer the Roger River Fault. The matrix to the diamictite typically comprises dark grey, poorly sorted and variably ferruginous siltstone to sandstone. The diamictite is typically erosion resistant and forms an upstanding topography.

The Croles Hill Diamictite is poorly developed to the west of the Roger River Fault. It is apparently absent in the Arthur River below Hawkes Creek and in the western tributary of Blackwater Rivulet around 324600/5444500. In both these areas, the Keppel Creek Formation directly underlies relatively thin basalt flows. The unit was recognised further south in tributaries of Blackwater Rivulet at 325570/5441990 (float), and near 325900/5441200 and 325900/5440000 (outcrop). The last locality is incorrectly shown as Julius River Member (Pssr) on some versions of the Sumac map sheet.

There are a few outcrops of Croles Hill Diamictite in a small gully at 326450/5444230, apparently overlying a thin sequence of Black River Dolomite-type chert, which in turn rests on steeply west-dipping Cowrie Siltstone. These outcrops may represent one or more thrust slices, as Smithton Dolomite occurs nearby to the west; if interpreted as a continuous section, both the Black River Dolomite and Kanunnah Subgroup would be anomalously thin and incomplete.

Petrography *(JLE)*

In hand specimen, freshly broken surfaces have an irregular to hackly fracture. The matrix is typically a medium to dark green (5G3/2) or dark yellowish-green (10GY3/2) against which most clasts are a somewhat paler greyish-green (10GY5/2) or pale olive-green (10Y6/2). Less often the clasts are slightly darker than the matrix. A few off white or cream-coloured dolomite clasts, and occasional oxidised dark red clasts, may be present. The rock weathers to pale olive-green (10Y6/2) or yellowish-orange (10YR7/6) to light brown (5YR5/6).

When seen in thin section, samples (about 35 examined) are more-or-less similar (e.g. sample R004929, Plate 17). Most consist of 30% to 85% of irregularly shaped angular clasts, mainly of basalt. Other common clast lithologies include fine to coarse-grained recrystallised dolomite, spherulitic felsic volcanic rocks, fine-grained sedimentary rocks including laminated siltstone and fine-grained wacke resembling lithologies in the Keppel Creek Formation, and carbonaceous and calcareous mudstone

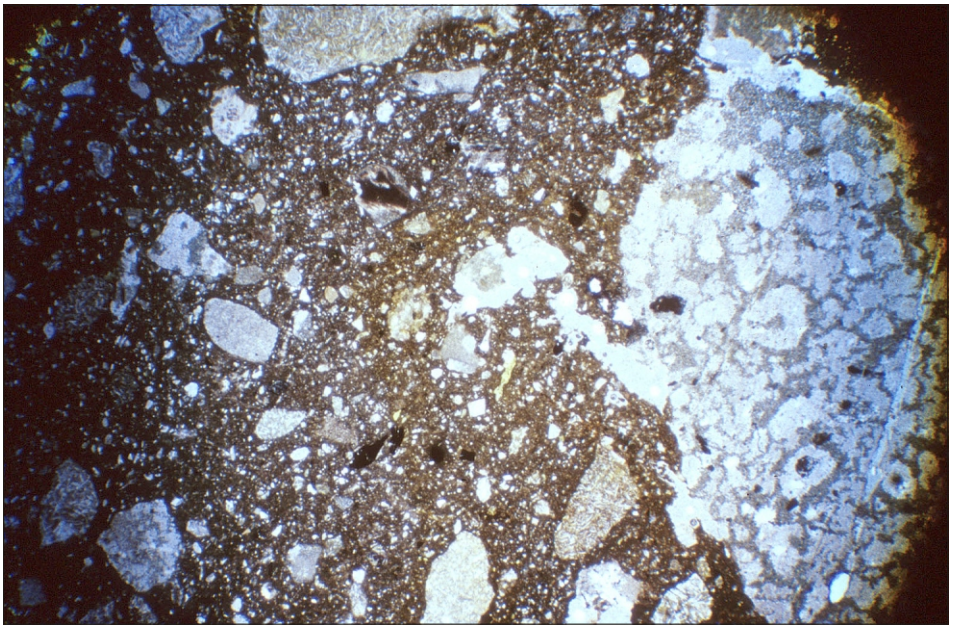

Plate 17

Photomicrograph of sample R004929 (329 530 mE, 5 439 800 mN), typical of Croles Hill Diamictite (unit Psvx). Plane polarised light, field of view 11.0 × 7.3 mm. Note clasts of fine-grained basalt (e.g. top edge) and spherulitic felsic lava (right).

resembling certain lithologies (Pssm) in the Black River Dolomite. Rarer clast lithologies include fine-grained white or black chert. Probable picrite clasts (consisting of coarse-grained chloritised olivine, clinopyroxene and minor sphene) were noted in samples R005152 and R004926. In addition, monomineralic grains of plagioclase, clinopyroxene and carbonate (dolomite?) and irregular aggregates of opaque minerals (magnetite?) may be present. Chromite is rare (observed in five thin sections), and occurs as mostly subhedral red-brown isotropic grains.

Small clasts of quartzite and quartz mudstone, with minor sericite, were noted in a single sample (R005583, Horton River at 328800/5431200). Elsewhere quartz-rich clastic sedimentary rocks, such as those dominating the Rocky Cape Group, are notably absent. Quartz is extremely rare, and is present in appreciable quantities in only one sample (R005150) from the upper Julius River, although samples R005144, R005560, R005583, R006717 and R006721 also contain rare quartz. In most cases quartz grains are small, angular, monocrystalline and unstrained, and are probably volcanic rather than metamorphic in origin.

The matrix of the diamictite usually consists of fine-grained basaltic material (mostly plagioclase fragments) grading down to an extremely fine-grained unresolvable low birefringence material. Primary matrix carbonate is absent in nearly all samples, in contrast to the matrix of the Julius River Member of the Black River Dolomite. Sample R005570, from the Horton River (331090/5432530), is atypical in containing some primary carbonate in the matrix, and may be transitional to the Julius River Member, which directly underlies the unit at this locality.

The unit is typically unbedded and uncleaved, but diffuse bedding lamination is visible at some localities. A thin section of such a rock (R005586) from near the Lindsay River/Horton River confluence shows that the lamination is both mineralogical and due to variation in grain size, with coarser laminae having a more dolomitic matrix (of probably clastic grains). This sample is also atypical in containing sparser and smaller clasts.

The basalt clasts display a wide variety of grain size, texture and alteration states, even on thin section scale, but generally they are fine-grained and intergranular. Most are leucocratic and richer in plagioclase than usual in typical basalts from the Spinks Creek Volcanics. A few basalt clasts are coarser grained to gabbroic, and ophitic. Usually they are aphyric, but some clasts contain sparse phenocrysts of plagioclase and, less commonly, clinopyroxene. Others are unusually rich in disseminated opaque grains and particularly poor in pyroxene, and may be late-stage differentiates. Fresh groundmass pyroxene is visible in many clasts, but most show some degree of alteration, particularly replacement by carbonate (e.g. sample R005583). Some contain amygdales filled with chlorite. In others, pyroxene and opaque minerals are replaced by chlorite and sphene respectively. None of the clasts show glassy margins or any evidence for hyaloclastic fragmentation.

The felsic volcanic (rhyolite?) clasts are present in about 70% of the thin sections examined and may be the second most abundant clast type, after basalt. They may be very fine grained and featureless, but more commonly they display a well-developed snowflake texture consisting of abutting diffuse spherulitic structures typically 200–250 μm across. They contain sparse opaque minerals, and are aphyric or less commonly contain a few squat plagioclase phenocrysts. Sample R005152 (Plate 18) (from northeast of Lagunta Creek, 334330/5436900), contains a clast (5 mm) with well-developed flow banding, defined by diffuse, slightly coarser-grained bands containing pale grey-green chlorite, minor epidote and resolvable (up to 40 μm) angular quartz grains. A single grain (within the clast) of red-brown biotite is also present. Similar flow-banded felsic clasts are present in sample R005561 (Horton River, 333220/5432190).

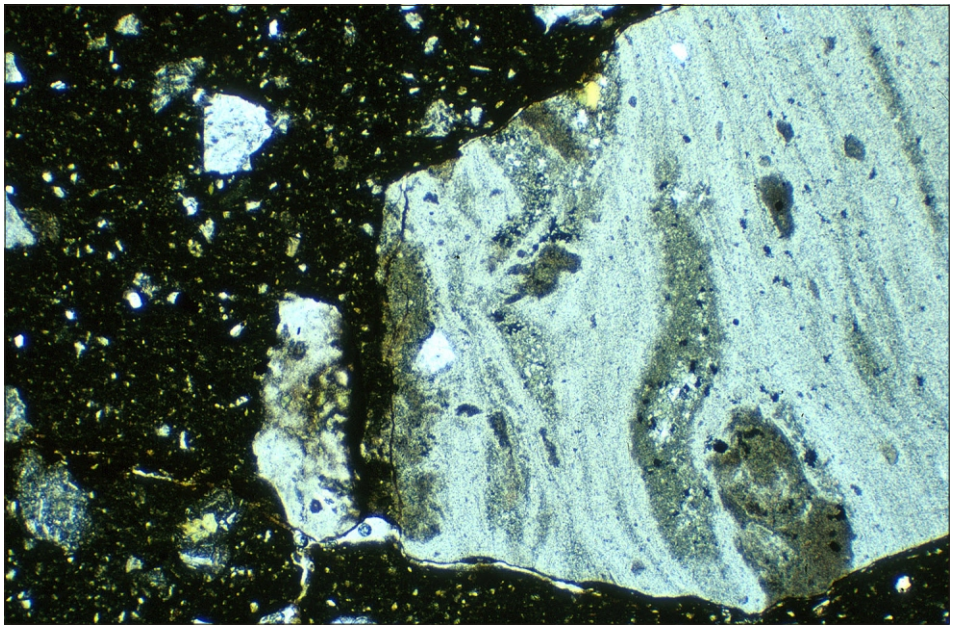

Plate 18

Photomicrograph of sample R005152 (334 330 mE, 5 436 900 mN), Croles Hill Diamictite (unit Psvx), showing clast of flow-banded rhyolite/ trachyte (?). Plane polarised light, field of view 4.4 × 2.9 mm.

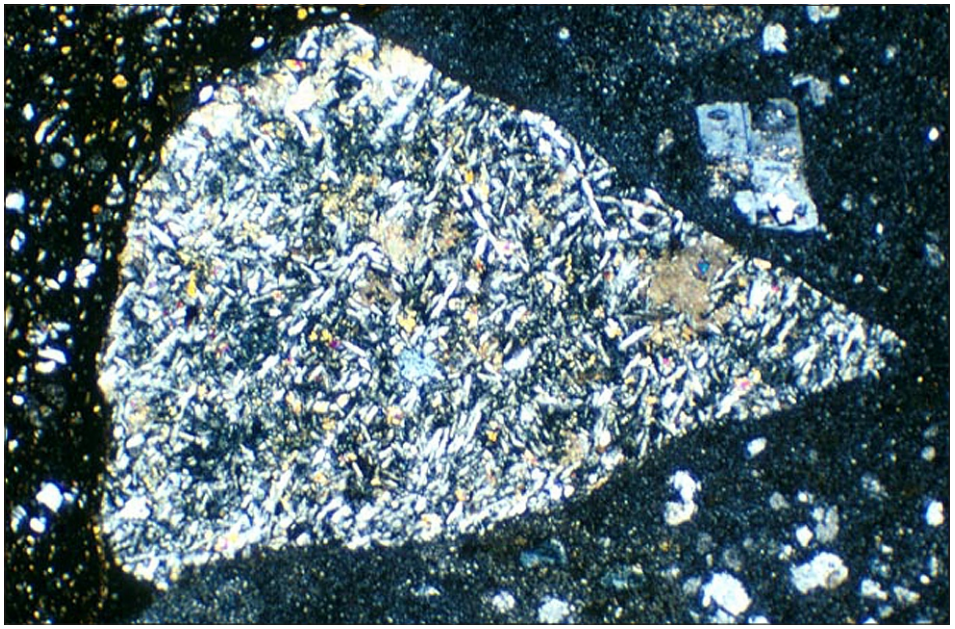

Plate 19

Photomicrograph of sample R005143, Croles Hill Diamictite (unit Psvx) (Julius River, 332 520 mE, 5 438 730 mN), showing clast of rhyolite/ trachyte(?) with an annealed, wedge-shaped inclusion of basalt. The matrix of the diamictite is at the far left. Crossed nicols, field of view 4.4 × 2.9 mm.

Sample R005585 (Horton River, 328630/5431120) also contains a clast of flow-banded rhyolite, but original textures are otherwise obscured by the spherulitic recrystallisation.

An observation in sample R005143 (Plate 19) from the upper Julius River (332520/5438730) suggests that the felsic magmatism that was the source of these clasts was coeval with Kanunnah Subgroup deposition. In this rock a 10mm long clast of a typical snowflake-textured felsic volcanic rock contains a wedge-shaped inclusion of medium-grained basalt, typical of the basaltic clasts also present in the sample and the Spinks Creek Basalts in general. The boundary between the clasts is clear, slightly wavy and sharp, and clearly an igneous contact. There is no sign of either magma mixing or chilling of either magma against the other, but the geometry suggests that the felsic magma incorporated a small accidental inclusion of already solidified basalt, possibly from the wall rock of a vent. It therefore seems likely that the felsic volcanism is local, and was at least partly later than, but probably closely associated with, the dominant basaltic volcanism of the Kanunnah Subgroup.

On a regional scale the felsic volcanic clasts appear to be more abundant in the east of the area, such as in samples from the Julius River, and have not been recorded from samples west of the Roger River Fault. No in situ felsic volcanic rocks were observed in the mapped area, although two thin (<20 m) autobrecciated rhyodacite flows are known from Robbins Passage on the north coast, immediately below and within the Croles Hill Diamictite. The lower flow is dated at 582 ± 4 Ma (Calver *et al*., 2004).

A sample (R004926) from the east tributary of Blackwater Rivulet (325900/5441130) contains a clast of altered picrite. Much of the thin section consists of pale yellow, nearly isotropic fine-grained chlorite/serpentine and fine-grained (5–20 μm) sphene, and retains a relict igneous texture. Very abundant pseudomorphs (200 μm–1 mm), probably

after olivine, are replaced by chlorite and/or carbonate with little sphene, and stand out against a much more sphene-rich groundmass. This is veined and partly replaced by coarse-grained sparry carbonate, with a locally dense dissemination of irregular to sub-cubic opaque grains, probably pyrite.

Sample R004925 (east tributary of Blackwater Rivulet) is unusual in being monomict (only basalt clasts noted) with a coarse-grained matrix, suggesting that it is proximal to its source. On the other hand two samples from the Julius River area may be distal; R005150 is fine grained with significant quartz, and R005149, with only 10% clasts and vague bedding, may be lithologically transitional to the Keppel Creek Formation.

Miscellaneous samples from southern tributary of Blackwater Rivulet

Although shown on the Sumac map sheet as dolomite diamictite of the Julius River Member (unit Pssr), these samples are petrographically more akin to the Croles Hill Diamictite.

Sample R004836 (325700/5440520) is a very poorly sorted diamictite with clasts of mainly sparry carbonate and dark, well-laminated basaltic volcaniclastic siltstone ('tuff'). There are also subordinate clasts of glassy basalt, quartz mudstone with minor sericite, opaque aggregates and sparse to rare detrital plagioclase, quartz and spinel. At least some of the sparry carbonate clasts are secondary after basaltic material. The matrix is very fine grained, nearly isotropic, and probably basaltic.

Black pebbly, pyritic diamictite crops out at a small waterfall at 325690/5440460. A clast of altered basalt (sample R004837) contains abundant pseudomorphed phenocrysts (up to 1 mm), probably after olivine but now replaced by carbonate, and mostly turbid, recrystallised and albitised plagioclase phenocrysts. These grade down into a groundmass which also contains abundant colourless to pale green, nearly isotropic chlorite and abundant ?sub-cubic to irregular opaque grains (up to 400 μm), partly altered to sphene.

Chemical composition of felsic clasts *(JLE)*

An attempt was made to determine the composition of the felsic clasts in the diamictite by relatively broad area (about 0.8 × 0.6 mm) scans on the electron microprobe (Table 6). Two separate clasts in sample R005137 have an apparent trachytic composition (e.g. on the total alkali-silica diagram of Le Maitre, 1989). However the very high BaO and K_2O/Na_2O ratios are unlikely in primary magmatic compositions, and some modification by potassic hydrothermal alteration seems likely. This is even more true of the apparently phonolitic analysis from a clast in sample R004929 (which has high MgO, unlikely in an evolved rock). A coastal outcrop of in situ rhyodacite (SiO_2 69.3–70.1%) from west of Montagu, in the northern part of the Smithton Synclinorium, may preserve the phase of felsic volcanism which has been reworked into the diamictite (Calver *et al*., 2004).

Table 6

Felsic clasts in Croles Hill Diamictite: estimated chemical composition by electron microprobe analysis (scan mode)

Sample	TJ785Y	TJ785Y	FJ828
Reg. No.	R005137	R005137	R004929
Analysis	R1	R3	R1
AMG (mE)	336740	336740	329530
AMG (mN)	5440760	5440760	5439800
SiO_2 (%)	65.634	65.555	52.754
TiO_2	0.001	0.173	0.094
Al_2O_3	13.479	13.261	17.878
Cr_2O_3	0.000	0.000	0.000
FeOt	2.242	5.540	6.547
ZnO	0.000	0.000	0.000
MnO	0.099	0.001	0.018
NiO	0.000	0.000	0.000
MgO	1.191	2.365	5.369
CaO	2.094	1.821	2.270
BaO	1.108	0.588	0.403
Na_2O	3.125	2.530	1.593
K_2O	10.898	8.161	13.007
P_2O_5	0.127	0.001	0.064
F	0.001	0.002	0.001
Cl	0.000	0.000	0.000
TOTAL	**100.000**	**100.000**	**100.000**
Original total	30.892	23.054	30.228

Analyses by Cameca SX50 microprobe, Central Science Laboratory, University of Tasmania.

Discussion *(JLE)*

As for the Julius River Member of the Black River Dolomite, possible interpretations of the Croles Hill Diamictite are a glacial diamictite (tillite), or a mass-flow deposit in an unstable, rapidly subsiding basin. While the lack of any clearly extrabasinal clasts militates against a glacial origin, local developments of laminated siltstone with pebble-sized dropstones do suggest a glacial influence (Calver *et al*., 2004). The Croles Hill Diamictite is probably the same age, or very close in age, to the 580 Ma Gaskiers glaciation of eastern North America. Although it occurs stratigraphically below the Spinks Creek Volcanics, the abundance of basaltic clasts in the diamictite indicates that it is coeval with at least the early stages of volcanism. Instability and rapid subsidence of the basin may have foreshadowed the onset of volcanism.

Kanunnah Subgroup: Spinks Creek Volcanics (Psb, Psba, Psbb, Psbc, Psbd, Psbe, Psbf, Psbz, Psbzp, Psbzf)

Definition *(JLE)*

The Spinks Creek Volcanics is herein defined as that unit of commonly massive or occasionally pillowed, usually fine-grained, aphyric or sparsely plagioclase-clinopyroxene ± olivine metabasalt, and minor intercalated volcaniclastic sedimentary rocks, that crops out along the Arthur River in a composite section, between 333 900 mE, 5 446 900 mN (where the unit conformably overlies the Croles Hill Diamictite) and 332 350 mE, 5 446 150 mN; and 331 300 mE, 5 446 300 mN and 330 300 mE, 5 446 400 mN (where the unit is conformably overlain by the upper part of the Keppel Creek Formation). A composite type section is necessary because of a major fault at 331 300 mE, 5 446 300 mN and the uncertain nature of the contact with Keppel Creek Formation at 332 350 mE, 5 446 150 mN. The Spinks Creek Volcanics is of the order of 500 m thick here. A supplementary type section is designated in a tributary of Blackwater Rivulet between 324 600 mE, 5 444 530 mN and 324 710 mE, 5 444 520 mN, where the unit is about 110 m thick.

The term was introduced by Matthews (1961*b*) as the Spinks Creek Basalt, but not formally defined, and until recently has rarely been used.

General features *(JLE, MPM, DBS)*

This unit of mainly fine-grained massive basalt usually occurs well up in the Kanunnah Subgroup, usually overlying the Croles Hill Diamictite or, less commonly, Keppel Creek Formation lithologies.

On the western limb of the Smithton Synclinorium, west of the Roger River Fault, the Spinks Creek Volcanics is relatively thin (e.g. probably about 150 m stratigraphic thickness in the Blackwater Rivulet, and 90 m in the Arthur River below Hawkes Creek) and locally is probably absent. The unit is more widespread and much thicker east of the Roger River Fault. Due to lack of bedding in the unit and in some underlying and overlying units, stratigraphic thicknesses are difficult to determine, but are probably of the order of 500 m to one kilometre. The Roger River Fault, which is now downthrown to the west, may have been active at the time of volcanism, possibly as an east-downthrown half-graben against which the lavas were ponded.

The Spinks Creek Volcanics is a topographically resistant unit, particularly with respect to the Black River and Smithton dolomites. It forms moderately hilly country and slight ridges through which major streams, such as the Arthur River and Blackwater Rivulet, have cut modest gorges. Smaller streams may form small waterfalls within the unit; notably Keppel Creek (331770/5439950 and 331630/5444040), Stephens Rivulet (328360/5441750), and an un-named tributary of the Julius River (near 335700/5440000). The unit usually supports a relatively open, callidendrous rainforest, particularly in well-drained areas. Much of the unit has been mapped from sparse float on the rainforest floor.

The same unit (designated Csp) was described to the north in the Smithton Quadrangle as an amygdaloidal spilite, commonly with pillows, notably on the foreshore at Duck Bay, Smithton (Lennox *et al*., 1982; Brown, 1989*a*). Small (0.2–0.3 m) closely packed pillows occur in basalt outcrop in the Horton River at 328070/5431120, in the south of the area described in this report. Pillows indicate that the basalt was at least locally intruded subaqueously, but elsewhere few megascopic or mesoscopic features, other than jointing, were noted. This may be a function of poor exposure, as there are relatively few large or continuous exposures, apart from the Arthur River section above Kanunnah Bridge where the unit is massive. Its apparently massive character may possibly indicate subaerial extrusion. An intrusive interpretation (except for the rare doleritic to gabbroic outcrops) seems precluded by the usual fine to very fine grain size, and the occasional presence of amygdales.

In the field and in hand specimen, fresh samples are hard, often extremely tough, fine-grained, grey-green to blue-grey rocks with an angular to subconchoidal fracture. Most samples are aphyric, massive and featureless; less often there are visible small, sparsely distributed phenocrysts of plagioclase (generally ≤1 mm) and/or small, generally subspherical amygdales (commonly less than 1 mm but occasionally ≤3 mm) filled with either off-white carbonate or dark green chlorite. Basaltic breccia was noted in some places (e.g. near Kanunnah Bridge at 330500/5446450 and 330500/5446300). Minor possible crystal lithic tuff with hematite alteration occurs near Keppel Creek at 331170/5444460 and 331140/5444030.

At several localities the lower contact of the basalt with the Keppel Creek Formation or the Croles Hill Diamictite is marked by a hematitic ironstone (e.g. near Ekberg Creek at 331800/5449500, near the upper Montagu River at 332200/5450500, upper Keppel Creek at 331800/5440100). Just north of Stephens Rivulet (at 328500/5443400), basalt near the contact is strongly mineralised with hematite, suggesting that ironstone may have developed in this area as well.

Native copper is locally present, either as very sparse disseminations or as a very thin lining of fractures. Localities noted during field work include those near Chester Creek (332000/5448000 and 332150/5448800), Keppel Creek (331000/5444550), several in the upper Stephens Rivulet area (328290/5441880 – sample R004896; 328470/5441050; 328160/5440460; 330790/5440360; 330810/5440470), an outcrop on a tributary of Blackwater Rivulet (327190/5439490 – sample R004910) and two localities north of the Horton River (333230/5433200 – sample R005172; 330220/5433080 – sample R006735). Native copper within basalt has also been long known from Copper Mine Point and elsewhere near Smithton (Nye *et al*., 1934; Carey and Scott, 1954).

In several localities near the western edge of the Smithton Synclinorium, much coarser grained, doleritic to gabbroic bodies occur at a particular stratigraphic horizon within the Black River Dolomite. Notable localities are on the Arthur River (322800/5446100), Blackwater Rivulet (325500/5440500) and a tributary thereof (325600/5441200), and Blackwater Road (325700/5439800). These are interpreted as shallow sub-volcanic intrusions. Typically the rocks are also massive, but with a grain size of two to three millimetres. Diffuse centimetre-sized compositional layering, with in particular some more leucocratic banding, is present in the Blackwater Road outcrop. In the Arthur River there are outcrops of an associated micropegmatitic phase, with pyroxene crystals up to 10 mm (sample R005079).

Several well-defined geochemical suites may be distinguished in the Spinks Creek Volcanics (see below) but these are very difficult or impossible to distinguish in the field.

Field relationships

South Chatlee Road–Dunns Plain north (DBS)

Aeromagnetic data suggest that the single thin basalt unit within the Kanunnah Subgroup in this area is remarkably continuous from near 326000/5441500 (within 1.5 km of the southern boundary of the Sumac map sheet) to a point just southeast of Chatlee Road, where it climbs onto the plateau southwest of the Hawkes Creek valley. Northwest of this point, aeromagnetic and ground data suggest a pronounced thinning (or absence) of the unit over a strike length of about 900 m, beyond which it resumes its thickness before intersecting the northwestern corner of the Sumac map sheet.

The basalts vary considerably in texture, from prominently amygdaloidal (with up to 15% amygdales ≤6 mm in diameter), to sparsely porphyritic and massive even grained. Sample R004253 is typical of the more porphyritic samples, containing up to 5% blocky clinopyroxene phenocrysts ≤0.65 mm in diameter and a few per cent of plagioclase laths ≤1 mm in length. This sample also contains 3–5% of blocky to prismatic phenocrysts which are pseudomorphed by fine-grained chlorite (?after olivine). The groundmass of R004253 is also typical, comprising an interlocking network of elongate plagioclase microlaths generally ≤0.25 mm in length, showing suggestions of flow alignment in places, and about 10% of blocky clinopyroxene microphenocrysts ≤0.1 mm in diameter. Some of the samples have a very fine-grained, non-porphyritic texture, and one sample (R004256) has a groundmass which probably had a substantial glass component prior to alteration. All of the samples show some alteration, to assemblages comprising various combinations of chlorite-albite-epidote-quartz-carbonate-actinolite. The alteration minerals (particularly, radially sheathed fine-grained chlorite) commonly fill amygdales, but alteration is more pervasive in some samples. As well as alteration observed in thin section, substantial hematitic alteration was noted in the field at the top of the basalt in the creek section near 322100/5447450, and near the base of the basalt in the creek section near 321200/5448700.

Leensons Road (DBS)

The discontinuous unit of basalt in this area is probably between 60 and 90 metres thick, similar to that in the South Chatlee Road–Dunns Plain north area, and it is probably the same unit. The two disjunct bodies of basalt here have strike lengths of about 900 m and about 1600 m respectively, and they may occur on opposite limbs of a tight syncline in the Kanunnah Subgroup. The more southern of the two bodies crops out poorly, and its distribution has been determined mainly by interpretation of aeromagnetic data. Two samples from the northern body show textural similarities to the basalts from South Chatlee Road–Dunns Plain north. Amygdales ≤4 mm in size form a 3–5% component, and are filled with sheathed chlorite ± albite ± ?actinolite. Clinopyroxene as phenocrysts ≤0.5 mm in diameter (and glomerocrysts ≤0.9 mm across) comprise ≤3%, and in similar proportion are altered, tabular plagioclase phenocrysts ≤1.2 mm in diameter. Sample R004259 also contains about 3% blocky to prismatic phenocrysts ≤0.45 mm in diameter with hexagonal cross sections, and which are pseudomorphed by chlorite (?after olivine). The groundmass is comparable to those of the basalts from South Chatlee Road–Dunns Plain north, although the proportion of groundmass clinopyroxene may be somewhat higher, up to 15–20% in the case of sample R004259.

Blackwater Road–Frankland River (DBS)

Between Blackwater Road near 325900/5439900 and a point just north of the Frankland River at 324950/5431550, the Spinks Creek Volcanics is represented by a single unit of basalt of notable continuity and constant thickness (100–140 m), although at one point there is a net dextral horizontal offset of the unit of about two kilometres across one of the main splays of the Roger River Fault. Aeromagnetic data indicate two 500–800 m gaps in the unit's lateral continuity in a strike length of over seven kilometres in this area. The basalt is commonly a dense fine-grained grey, blue-grey or olive-green rock, in many cases with scattered small (≤3 mm), ovoid, chlorite-filled amygdales. A deep maroon colour in some outcrops is caused by hematitic alteration.

In thin section the basalts commonly show substantial alteration, to assemblages of fine-grained chlorite ± sericite ± albite ± sphene ± hematite. The southernmost sample (R006011 from 324950/5432050) has a greenschist facies metamorphic texture in thin section, with a mineralogy of actinolite-epidote-albite-chlorite-sphene. Sparse amygdaloidal texture is common, with up to 5% of amygdales up to 3 mm in diameter filled with radially-sheathed fine-grained

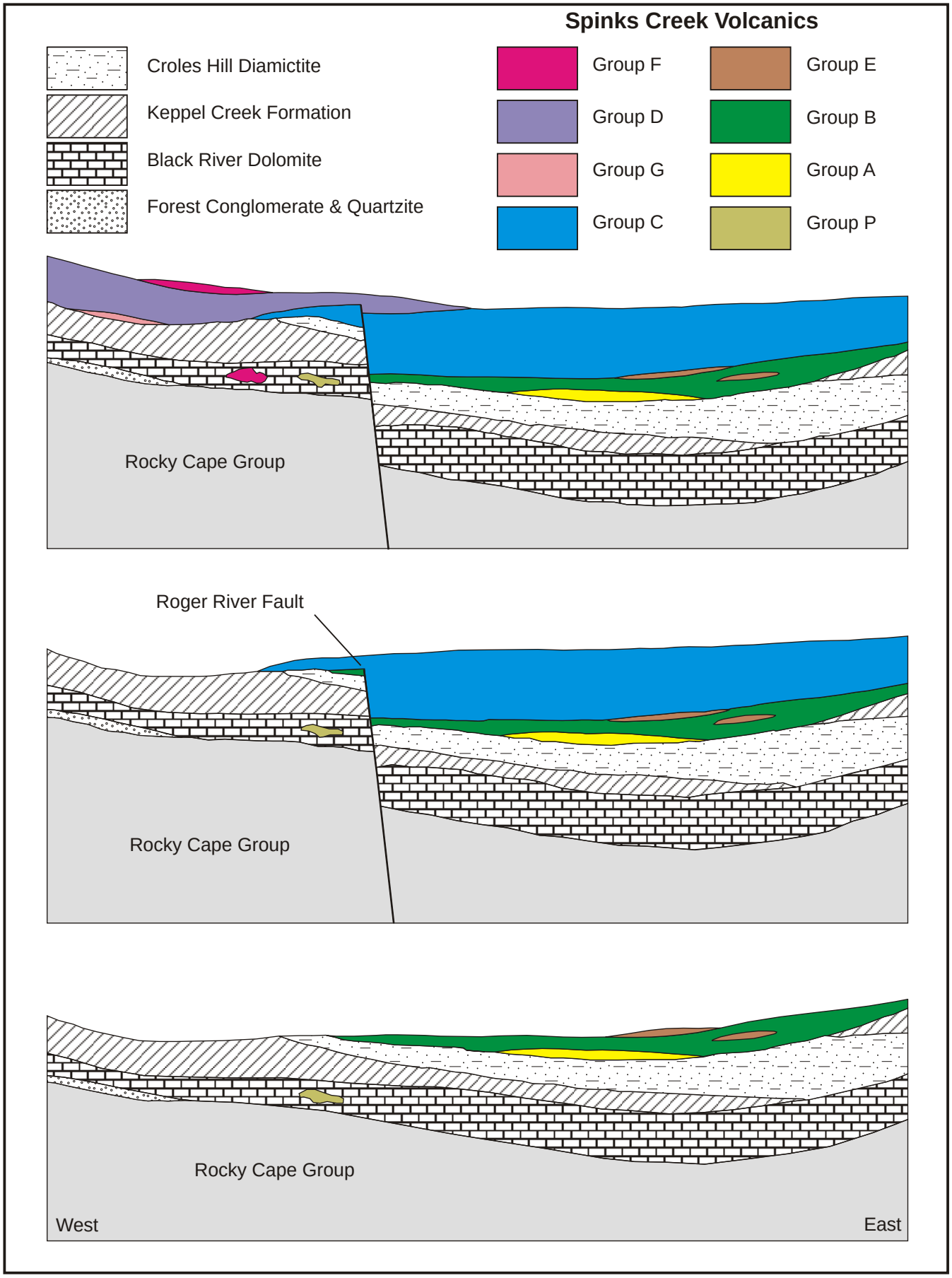

Figure 5

Schematic cross section across the Smithton Synclinorium, showing inferred stratigraphic relationships and sequential emplacement relative to the Roger River Fault for chemically defined groups (probably major flows and shallow intrusions) of the Spinks Creek Volcanics. The Group G basalts occur in the Welcome River and Redpa areas in the west of the synclinorium, and are not discussed in this report.

chlorite, or with mixtures of chlorite, albite, epidote and opaline silica or zeolite. Some of the basalts are aphyric and evenly fine grained, but more commonly they contain up to about 7% of partially to completely altered (to fine-grained chlorite-sericite) blocky phenocrysts and laths ≤3.5 mm in diameter of plagioclase, in some cases forming glomerocrysts up to 5 mm in diameter. One sample (R006002 from 325850/5439880 on Blackwater Road) also contains 3–5% of relatively little altered blocky clinopyroxene phenocrysts up to 0.5 mm in diameter, which also form glomerocrysts up to 1 mm across. The groundmass of most samples is commonly an interlocking mesh of partially to completely altered feldspar microlaths up to 500 μm long, with up to 15% of less altered, blocky clinopyroxene crystals up to 200 μm in diameter, and 5–20% of opaque grains ≤0.2 mm in diameter. The opaque grains commonly show 3, 4, or 6-sided cross sections and a reddish tinge, and are probably magnetite or possibly ilmenite, partially altered to hematite.

Several of the basalt samples (R004291 from 324470/5436520; R004292 from 324630/5436230; R004293 from 324650/5436200) show petrographic similarities to nearby samples which have been chemically analysed and assigned to Chemical Group C (about 1.6% TiO_2). Sample R006002 (325850/5439880) is similar to a previous nearby sample which was assigned to Chemical Group B (1.0–1.1% TiO_2) (see *Igneous Rocks* section).

Near 324270/5436560, in a tributary of the Frankland River south of Blackwater Road, several low outcrops consist of a disorganised open-framework breccia comprising subangular to subrounded fragments, mostly of grey-green basalt, ranging up to 100 mm in diameter, in a medium grey 'matrix'. In the field these outcrops have a similar appearance to typical lithologies of the Croles Hill Diamictite, but a thin section (sample R006006) shows a disorganised fabric of somewhat indistinct, subangular to ragged fragments of very altered vesicular to amygdaloidal aphyric fine-grained basalt in a 'matrix' of similar composition and texture. Amygdales are irregular and chlorite filled, while the rest of the rock is probably mostly albitised plagioclase, epidote, chlorite and sparse unaltered opaque minerals. This is probably a primary autobreccia or a flow-top/flow-front breccia, which formed due to cracking of a vesicular crust during further lava movement prior to complete solidification. It therefore belongs to the Spinks Creek Volcanics rather than the Croles Hill Diamictite, even though it occurs down section of the main basalt unit in this area. Petrographically it is similar to a low-Ti basalt of Chemical Group A (see *Igneous Rocks* section).

A distinctive breccia on a nearby disused forestry investigation track (at 324450/5436560) consists of subangular fragments of dark purple-black strongly hematite-altered basalt, up to several centimetres in diameter, in a dark grey fine-grained matrix. The thin section (sample R004289) shows an open to closed framework of tectonically flattened angular fragments of hematite-altered fine-grained amygdaloidal and massive basalt, in a 'matrix' of similar composition in which flow texture defined by altered thin feldspar laths wraps around the large fragments in some places. The overall composition is mainly altered plagioclase and opaque minerals, with a suggestion of flattened plagioclase phenocrysts in places. This is probably a hematite-altered primary volcanic breccia similar in origin to sample R006006, and is thus best assigned to the Spinks Creek Volcanics.

Headwaters of Blackwater Rivulet and Julius River *(ARR)*

In the area between the headwaters of Blackwater Rivulet (327500/4438000) and Julius River (332000/5438300), the basalt of the Spinks Creek Volcanics is typically massive to variably jointed dark to mid-green, commonly limonite stained and chloritic. The basalt is magnetic relative to other units of the Togari Group, with 23 magnetic susceptibility readings returning an average of 41×10^{-3} SI units. Demagnetisation and intense sericitisation/chloritisation of the basalt is common near faults. Where present, vesicles to two millimetres diameter within the basalt contain chlorite and, more rarely, native copper. The basalt typically shows little internal variation, although a limonitic siltstone unit containing rounded cobbles of basalt and capped by ferricrust at 328400/5436200 is interpreted as an intraflow sedimentary rock. The underlying poorly exposed basalt contains irregular zones of breccia, individual clasts to 100 mm being angular and forming a mosaic pattern. The matrix to the breccia is fine grained and cryptocrystalline, suggestive of a hyaloclastite.

Further petrographic descriptions of the Spinks Creek Volcanics, discussed in a geochemical context, are given below.

Geochemistry and Petrography *(JLE)*

The Spinks Creek Volcanics, and the related gabbroic to doleritic rocks which are interpreted as shallow intrusives, can be divided into a number of discrete suites (fig. 5–8) on the basis of whole rock geochemistry. The petrographic and petrophysical features of each suite are described, and comments made on petrogenesis and tectonic implications. Analyses of Spinks Creek Volcanics rocks (Tables 15 to 24) are given in Appendix 4.

Previous work

The earliest petrographic and petrological work on the basalts of the Smithton area was that of Nye *et al*. (1934), who interpreted them as Devonian dolerite and obtained seven major element analyses. Later petrographic descriptions can be found in Carey and Scott (1952), who showed that they were mainly extrusive, Scott (1954) and Everard (1962). Longman (1962) briefly described samples of 'tholeiitic basalt'

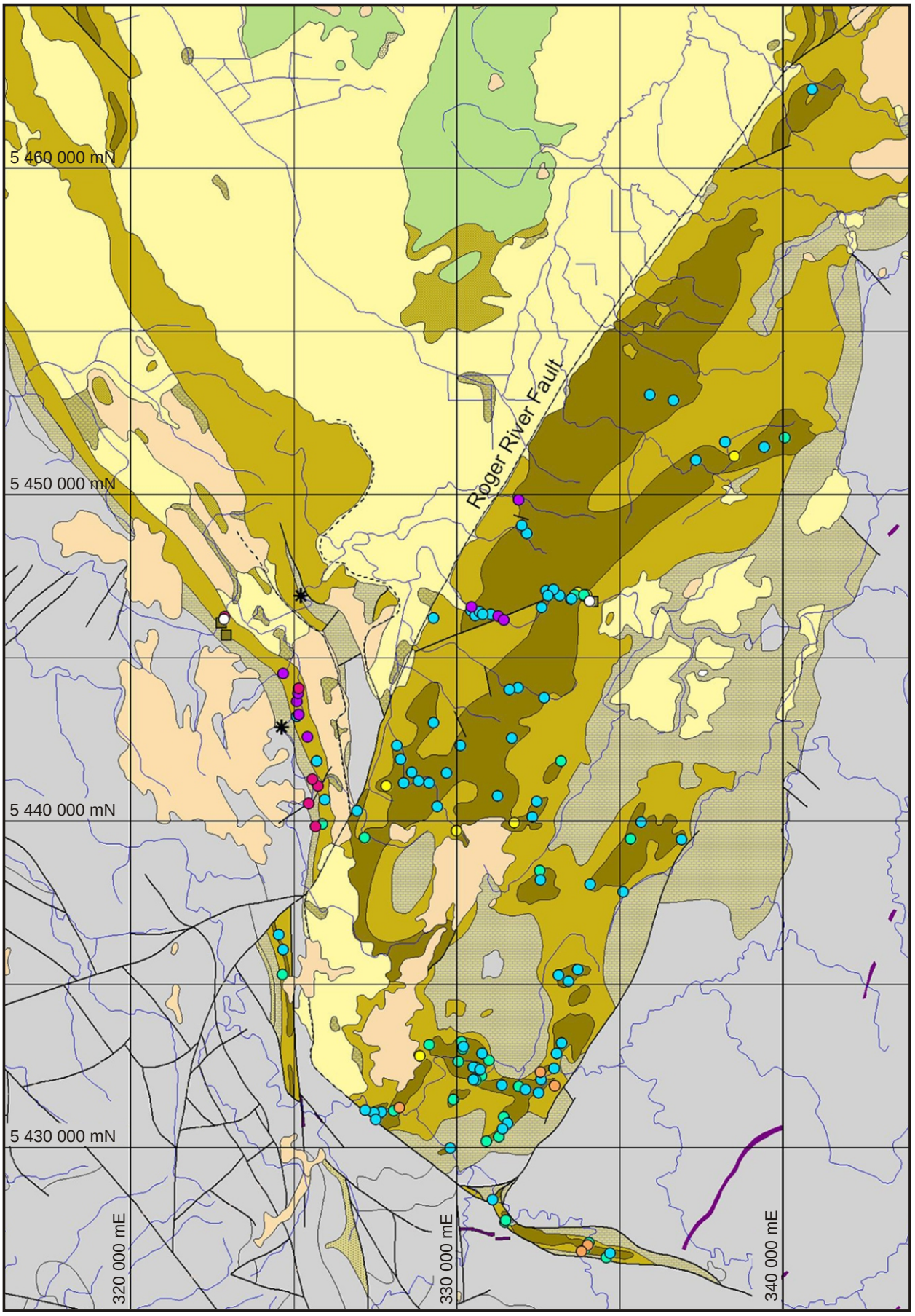

Figure 6

Map of report area, showing location of analysed samples of Spinks Creek Volcanics, classified by chemical group (as for Figure 5): Group P – dark khaki squares; Group A – yellow; Group B – green; Group E – pale brown; Group C – blue; Group D – blue; Group F – crimson; picrites – black stars; miscellaneous samples – white. Rock units modified after Figure 3.

from the Arthur River, and basalt and 'gabbro' from Blackwater Rivulet.

Griffin (1974) described the petrography and geochemistry of the 'Smithton–Trowutta Volcanics' in the Trowutta area and along the Arthur River upstream of Kanunnah Bridge. He divided the basalts into two types, a low-TiO_2 (0.5–1.0%) olivine-phyric type at the base of the sequence, and a more widespread high-TiO_2 (1.5–2.0%), mainly clinopyroxene-plagioclase-phyric type, which he thought was related by crystal fractionation, mainly of olivine. His 24 chemical analyses are given in Table 15*b*, and are now thought to include representatives of at least five distinct groups.

Fourteen analyses from the Smithton Quadrangle and four from the Montagu area (Table 15*b*) were briefly discussed by Brown (1986, 1989*a*). He identified three 'magma groups', again principally on the basis of TiO_2 content, which were attributed to different degrees of partial melting and fractional crystallisation.

Baillie and Crawford (1984) and Crawford and Berry (1992) briefly described the basalts and classified them as low K_2O tholeiites. The most likely tectonic setting was considered to be an ensialic back arc basin, erupted during attenuation and aborted rifting of thin continental crust over a subduction zone.

Sampling and analytical methods

During and following mapping, a suite of 118 samples of Neoproterozoic basalt and related rocks was collected and analysed for major and trace elements by X-ray fluorescence (XRF). FeO and CO_2 were determined classically (Table 15*a*). Of these samples, 59 were from the Sumac map sheet, a further 49 from the Dempster map sheet adjoining to the south, and ten from an outlier on the Balfour map sheet at the southern end of the Smithton Synclinorium. The petrography of all samples is summarised in Table 16.

This data set is supplemented by 14 analyses from the Smithton Quadrangle (Brown, 1989*a*), four from near Montagu in the Woolnorth Quadrangle (Brown, 1985), 24 from Griffin (1974) and six collected by J. W. Hudspeth and R. G. Richardson during geophysical investigations (unpublished data in ROCKCHEM database). Some of this older data (Table 15*b*) is less complete (in particular it is unfortunate that Griffin did not analyse for Nb) and there are several clusters of very similar analyses from virtually the same locality.

Although all new XRF analyses were done at the Department of Mines (Mineral Resources Tasmania) laboratories, there are some differences in certain trace element values that suggest systematic analytical error between batches analysed at different times. In particular the earlier TJ series samples (R005141–R005172) gave somewhat lower V and Zn values than other geologically similar samples subsequently analysed. In addition, later TJ series and AR series samples gave lower Sc and higher Ni and Pb values than the remainder. A review of sample locations and other geochemical features strengthens the conclusion that these differences are due to analytical error. In addition the three lava samples of Richardson and Hudspeth gave lower P_2O_5 than other similar samples.

Rare earth elements and Nb, Ta, Hf and Th (Table 15*c*) were determined for a selected subset of 17 by the inductively coupled plasma mass spectrometry (ICPMS) method at Analabs, WA. Some REE and Ta, Hf and Th data (14 samples, seven of which were published by Brown, 1986) were obtained by instrumental neutron activation analysis (INAA) at Becquerel Laboratories, NSW. Unfortunately, the Ta and Hf data obtained by the ICPMS method are unrealistically high, particularly when compared to the INAA data for similar samples. The XRF data for Nb are likewise preferred to the ICPMS data.

Further analyses of additional samples from the Woolnorth Quadrangle will be published shortly (Seymour and Everard, in prep.). However the essential features of the Spinks Creek Volcanics are apparent from the data presented here.

General comments

Most analysed samples are moderately evolved tholeiites, with low K_2O (nearly all <1% and mostly much lower), and have Na_2O of typically 3–4%. Because of the likelihood of some modification of major element chemistry during low-grade metamorphism, CIPW norms are not tabulated. Most samples are probably olivine-hypersthene normative tholeiites, whilst a few (mainly with high or low Na_2O respectively) are apparently nepheline or quartz normative. The high Fe_2O_3/FeO ratio of many samples suggests secondary oxidation. (This affects the CIPW norm calculation; note that the norms of Cainozoic basalts are commonly calculated at $Fe_2O_3/FeO = 0.20$). Samples R005063, R005075 and R004911 have high H_2O and CO_2, together with petrographic features indicative of severe alteration, and are treated with particular caution.

Particular emphasis is placed on high field strength elements (HFSE) such as Ti, P, Zr, Nb, Y and the rare earth elements (REE), which are relatively immobile during metamorphism, alteration and weathering.

The distinctive geochemical characteristics of the various components of the Spinks Creek Volcanics are most readily seen in simple binary plots of HFSE elements and element ratios. Examples are Nb against TiO_2 (fig. 7*a*), Nb against Zr (fig. 7*b*), Nb/Zr against TiO_2 (fig. 7*c*) and Mg# against TiO_2 (fig. 7*d*). Chondrite-normalised REE patterns (fig. 8*a–j*) are also useful.

When considered this way, they can be divided into six, possibly seven, very well defined groups. Each occurs in a distinct stratigraphic and/or geographic position within the Smithton Synclinorium (fig. 5, 6).

Group P (low-Ti, primitive) (Psbz in part)

This suite is known from seven analysed samples from three areas. Two samples (samples R005078 and R004904) are from a gabbroic intrusion within the Black

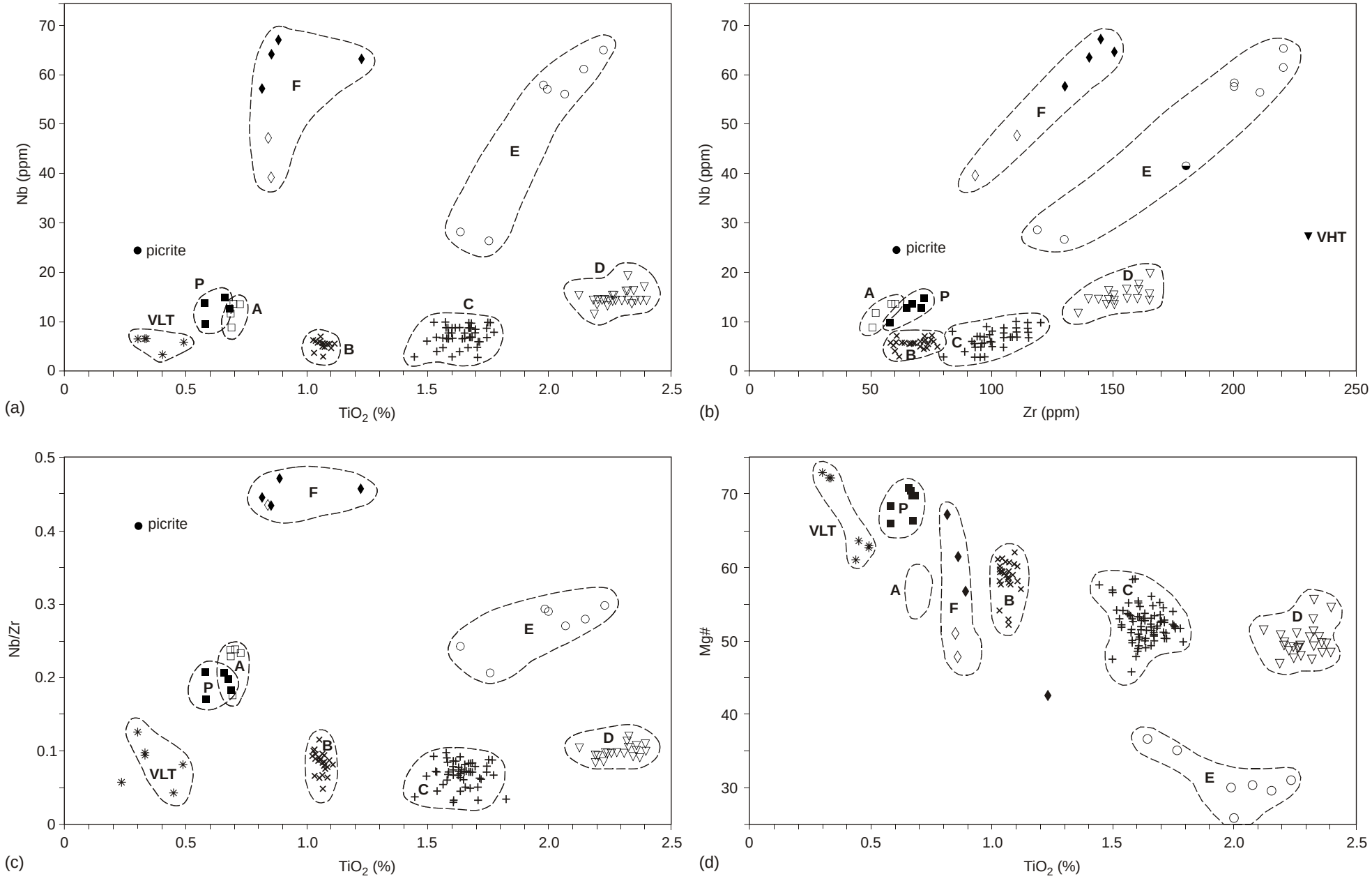

Figure 7

Geochemical plots, Spinks Creek Volcanics: (a) Nb against TiO_2; (b) Nb against Zr; (c) Nb/Zr against TiO_2; (d) MgO against TiO_2.

River Dolomite, cropping out in the Arthur River at the western limb of the Smithton Synclinorium. Another two are also from the Arthur River but from the eastern limb of the synclinorium (Griffin's samples 42167 and 42168). Three samples (ABS36 to 38) are from the Smithton foreshore (Brown, 1989*a*).

These are mildly tholeiitic, but are rather unusual for continental tholeiites in being near primitive, with Mg numbers (molar 100Mg/(Mg + Fe^2) calculated at Fe_2O_3/FeO = 0.20) of 66–71, and high levels of Ni (150–310 ppm) and Cr (440–960 ppm). They can also be distinguished from the other groups by low TiO_2 (0.58–0.68%). Total iron (FeO_T: 9.1–9.6%) is lower than in most other groups, and MgO (8.6–11.0%) distinctly higher. CaO is also relatively high (7.5–12.2%, but mostly >9.8%) but overlaps with that of the other groups. Trace elements indicate mildly enriched affinities, with relatively high Nb (10–15 ppm) given the low Zr (58–93 ppm); thus Nb/Y (0.5–1) and Nb/Zr (0.16–0.25) are relatively high.

PETROGRAPHY

The fresher of the two thin sections available (R004904, Plate 20) displays a relatively coarse-grained, locally subophitic, doleritic texture. It consists of mainly subhedral colourless clinopyroxene (augite) grains (mostly <500 μm but up to 1 mm), colourless to pale yellow serpentinised pseudomorphs after olivine (mostly <1 mm, occasionally to 4 mm) and plagioclase, grading into a feldspathic mesostasis. Very pale yellow-green chlorite is also present. Opaque grains (≤200 μm) are rather sparsely distributed and frequently partly replaced or rimmed by turbid sphene.

Sample R005078, from outcrop in the Arthur River of the same body, is coarser grained, with clinopyroxene subhedra commonly 1 mm or more, and has a higher proportion of fine-grained feldspathic mesostasis. Opaque grains are almost completely altered to sphene, and clinopyroxene frequently has a brown turbid appearance suggesting incipient alteration to amphibole (uralitisation). The main metamorphic mineral is very pale yellow chlorite. Pumpellyite (pleochroic from blue-green to very pale yellow, anomalous birefringence to lower second order) also occurs as aggregates of fibrous to radiating sheaves up to 100 μm long. A narrow (≤200 μm), irregular crooked veinlet consists mainly similar pumpellyite and minor chlorite.

A pegmatoidal variant (R005079, Plate 21) is mineralogically similar, but consists of large (≤10 mm) interlocking crystals of mainly plagioclase and partly uralitised pyroxene, with little finer-grained mesostasis. In parts of the section these large crystals are almost anhedral and the texture approaches that of an adcumulate. Aggregates of chlorite and pumpellyite, optically and texturally similar to those in R005078, are present.

This body is not a true gabbro, but probably a shallow hypabyssal intrusive rock with locally developed cumulate textures.

Group A (low Ti, evolved) (Psba)

This group is known from ten analysed samples from widely dispersed localities, all of which are east of the Roger River Fault. These are (from north to south) from near Trowutta township (samples 42176, 42181), the Arthur River on the eastern side of the Smithton Synclinorium (samples R005046, 42159, 42165, 42169), Blackwater 6 spur road (R004875), upper Stephens Rivulet (R004908), near upper Keppel Creek (R004922) and from a small creek just north of the Horton River (R006740). At each locality the samples are fine-grained basalt from or close to the base of the Spinks Creek Volcanics, and just above the lower contact with the Croles Hill Diamictite (or in the case of R006740, the Keppel Creek Formation). No gabbroic examples are known, and the sampled rocks are probably lavas.

Group A is chemically similar to Group P in being a low-TiO_2 tholeiite, but is distinguished from that group by its lower MgO (7.3–8.2%), Cr (120–165 ppm) and Ni (100–165 ppm). It is thus more evolved (Mg# = 54.6–59.2), but its distinctly higher total iron (FeO_T = 11.2–12.6%) suggests that it was not derived directly from group P magma by simple low pressure crystal fractionation of olivine ± pyroxene ± plagioclase. It also has very slightly higher TiO_2 (0.68–0.73%), V (270–370 ppm) and possibly Co (46–60 ppm) and MnO (0.20–0.28%), and lower Ba (90–165 ppm), than group P samples. Incompatible element abundances and ratios (Zr/Nb, Ti/Zr, Nb/Y) are similar to group P.

PETROGRAPHY

In thin section a typical specimen (R004875, Plates 22, 23) contains sparse to rare euhedral microphenocrysts (500 μm–1 mm) of former olivine, replaced by pale yellow-green pumpellyite, together with a few narrow microphenocrystal laths of altered plagioclase (≤1 mm) and rare microphenocrysts of clinopyroxene (≤500 μm). The fine-grained groundmass consists of colourless clinopyroxene granules (typically 50–200 μm), altered plagioclase, minor altered olivine, and irregularly jagged opaque grains (probably magnetite), together with aggregates of very pale yellow-green chlorite ± pumpellyite. Some pale yellow epidote is present. There are also occasional coarser-grained segregations consisting of ophitically intergrown plagioclase and clinopyroxene, also associated with minor altered olivine.

Other samples examined in thin section (R005046, R004908, R004922, R006740) are similar. Minor secondary sphene may be present, and a few amygdales are filled with chlorite. Samples R004922 and R006740 are more oxidised, with hematite occurring as an alteration of opaque grains and olivine. In the latter sample olivine is replaced by colourless rather than yellow-green chlorite, together with hematite and rare fibrous anthophyllite(?).

Group B (intermediate Ti) (Psbb)

This is the second most abundant suite, being identified on the basis of thirty analysed samples. Most were

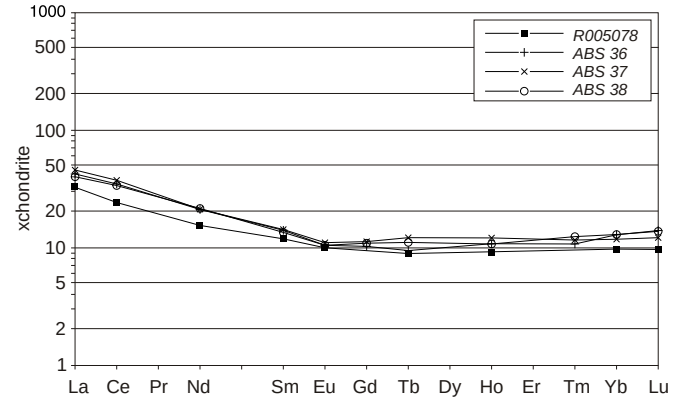

(a) Group P – INAA data

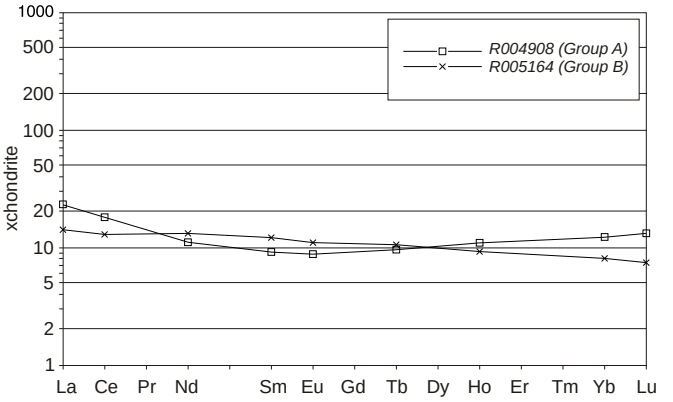

(b) INAA data

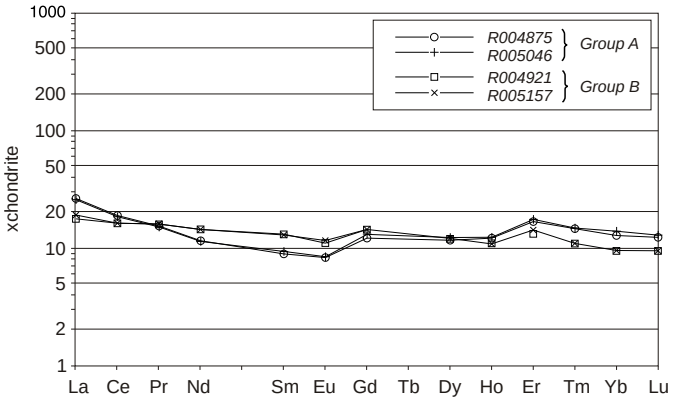

(c) Groups A and B — ICPMS data

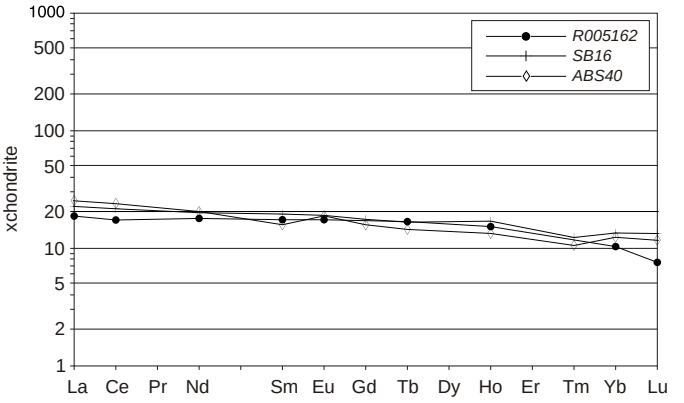

(d) Group C – INAA data

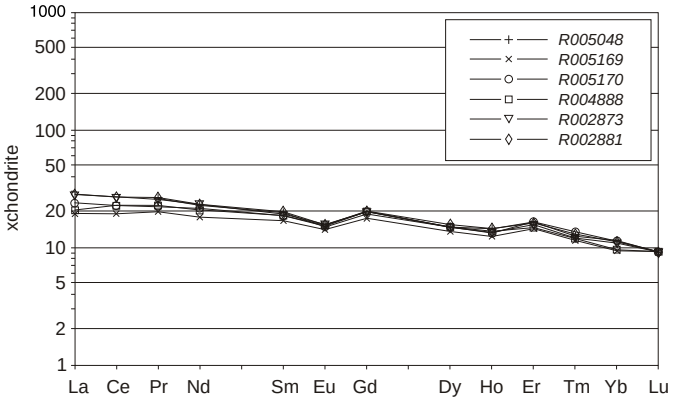

(e) Group C – ICPMS data

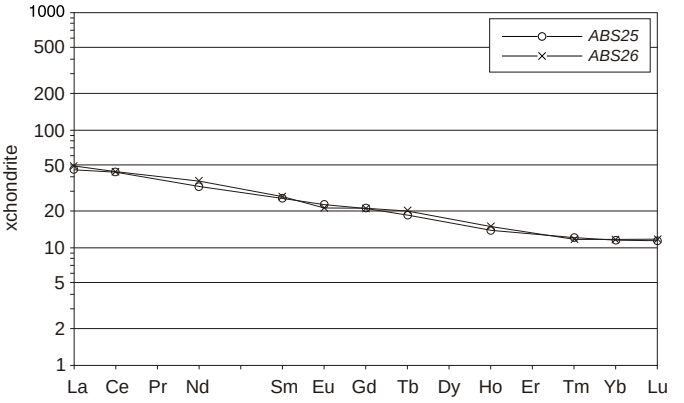

(f) Group D – INAA data

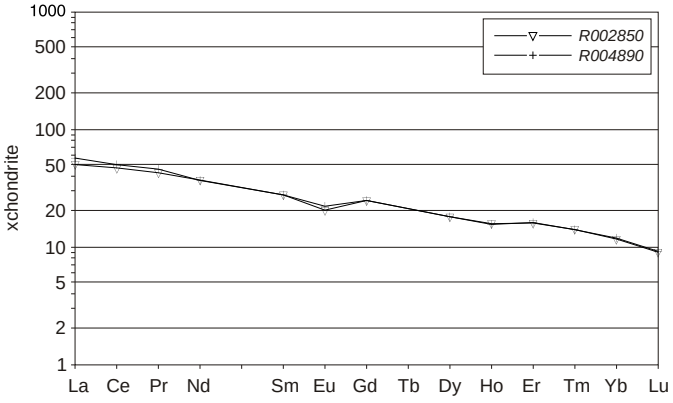

(g) Group D — ICPMS data

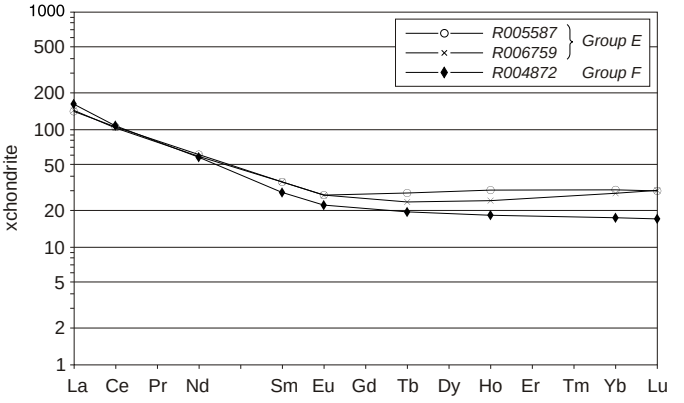

(h) Groups E and F — INAA data

Figure 8

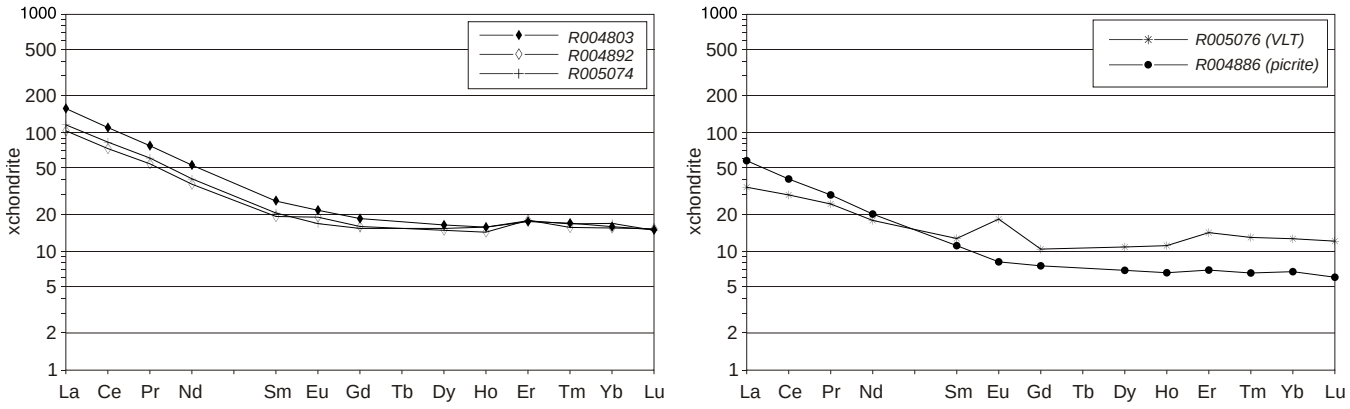

(i) Group F – ICPMS data *(j) ICPMS data*

Figure 8

Chondrite-normalised rare earth diagrams, Spinks Creek Volcanics: (a) Group P, INAA data, (b) Groups A and B, INAA data, (c) Groups A and B, ICPMS data, (d) Group C, INAA data, (e) Group C, ICPMS data, (f) Group D, INAA data, (g) Group D, ICPMS data, (h) Groups E and F, INAA data, (i) Group F, ICPMS data, (j) picrite and very-low-Ti sample R005076, ICPMS data.

collected in and around the Horton and Leigh rivers, from the southern part of the Dempster map sheet and the outlier on the adjoining Balfour map sheet respectively. In this area group B lavas are closely associated with and probably underlie group C, probably at or near the base of the Spinks Creek Volcanics (as in this area group A is generally absent). To the north they have has also been identified at isolated localities in a similar stratigraphic position, both in the western (samples R004882, R004871, R004910) and eastern (R005171, R005175, R004921 — see Table 16, Appendix 6 for locations) limbs of the Smithton Synclinorium. Two of Griffin's samples (42144, 42171) from the Arthur River at the eastern limb belong to group B; these appear to overlie, and possibly partly interfinger with, group A basalts. Griffin also sampled this suite at Gun Road, Trowutta (42185 from 340060/5451720), while further afield, J. W. Hudspeth sampled it between Smithton and Stanley (401285).

This group is most characterised by its TiO_2 content, which falls into a narrow range of 1.02–1.12%. All samples appear to be relatively evolved, with MgO of 5.99–8.26% and Mg# of 52.6–62.1, although Ni (92–115 ppm, except for 175 ppm in R005175) and Cr (185–230 ppm apart from two of Griffin's samples) have a narrow range and do not correlate with Mg#. Other major elements are similar to levels found in groups A, C and D, although CaO (6.92–12.66%) extends to rather high values. K_2O is mostly less than 0.35%, but exceeds 1% in two samples (R006725, R006752). High field strength elements are consistently low, most significantly Zr (55–77 ppm), Nb (7 ppm or less) and P_2O_5 (<0.20%).

PETROGRAPHY

All suite B basalts (23 samples examined in thin section) are plagioclase-clinopyroxene-(olivine)-phyric, with minor textural differences in grain size and rank (intensity) of metamorphism.

A typical specimen (R004910) has a porphyritic to seriate texture, with abundant phenocrysts and glomerocrysts of turbid plagioclase (3 mm) and smaller microphenocrysts of fresh colourless clinopyroxene (1 mm), also frequently clumped in glomerocrysts. The plagioclase has well spaced multiple twinning with small extinction angles, is optically positive, and is probably albite. Euhedral pseudomorphs after olivine phenocrysts (1 mm) are much less abundant. Most are replaced by yellow-green chlorite and minor iron oxide, but a few retain zones of high birefringence, suggesting that alteration is incomplete. The mineralogy of the groundmass is similar to the phenocrysts, and comprises clinopyroxene granules (typically 50–100 μm), altered plagioclase, yellow-green chlorite and/or pumpellyite, minor epidote, and also equant angular opaque grains with some alteration to turbid sphene. Rare ellipsoidal amygdales (1 mm) are filled with very pale yellow-green fine-grained chlorite with anomalous blue-grey birefringence colours.

Other samples are generally similar. Secondary turbid sphene rims opaque grains in some samples (e.g. R005171, R006752) and has completely replaced the opaque phase in others (e.g. R005175, R005567, R005574, R005579, R006729, R006732 and R006745). In R004921 the plagioclase phenocrysts are extremely turbid although the opaque phase in the groundmass is little altered. In contrast other samples (e.g. R005573, R005574) have a relatively well preserved intergranular groundmass with little alteration of plagioclase laths, but opaque phases are mostly replaced by sphene. Olivine phenocrysts are completely replaced by pale green to pale yellow chlorite in all samples. Prehnite is sometimes recognisable as a replacement of plagioclase. Groundmass chlorite is ubiquitous, but its abundance and colour (colourless to pale yellow or green) is rather variable between samples. Some of the more strongly coloured 'chlorite' may in fact be pumpellyite.

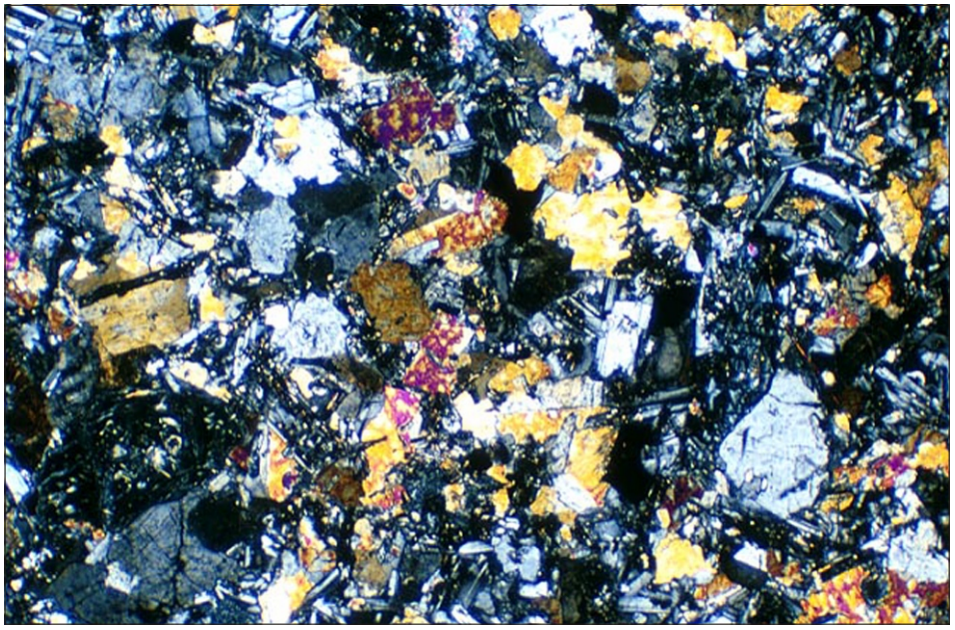

Plate 20

Photomicrograph of Spinks Creek Volcanics related Group P microgabbro (Psbz), sample R004904 (322 940 mE, 5 445 700 mN). Interlocking, locally subophitic texture of mainly plagioclase, clinopyroxene and altered olivine. Crossed nicols, field of view 4.4 2.9 mm.

Plate 21

Photomicrograph of Spinks Creek Volcanics related Group P pegmatoidal gabbro (Psbz), sample R005079 (Arthur River, 322 800 mE, 5 446 070 mN). Interlocking plagioclase and clinopyroxene with little mesostasis, approaching adcumulate texture. Crossed nicols, field of view 4.4 × 2.9 mm.

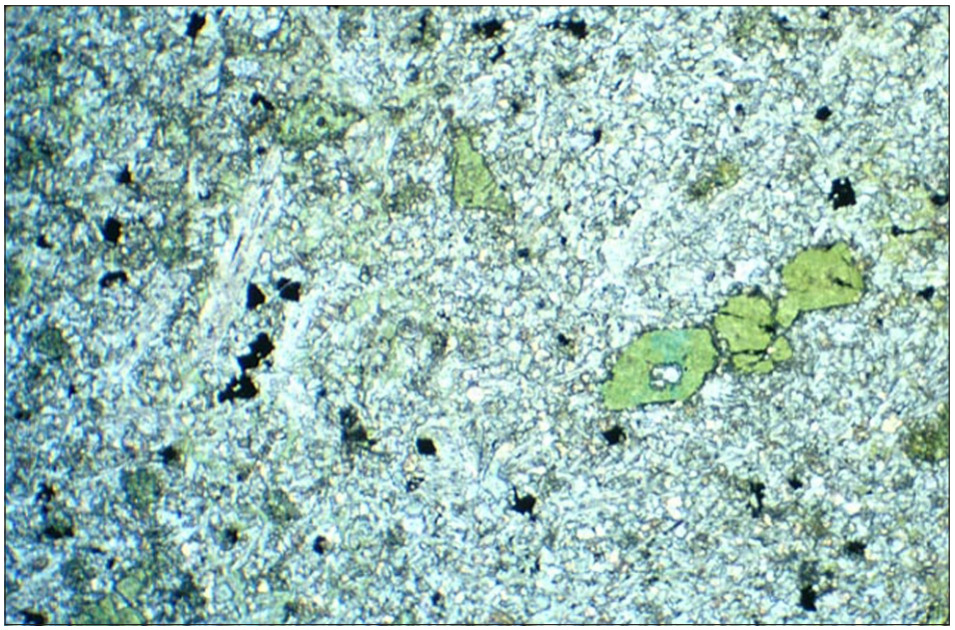

Plate 22

Photomicrograph of Spinks Creek Volcanics Group A lava (Psba), sample R004875 (327 850 mE, 5 441 060 mN). Microphenocrysts of plagioclase and former olivine (?) pseudomorphed by pumpellyite, in a fine-grained groundmass of mainly plagioclase, clinopyroxene and opaques. Plane polarised light, field of view 4.4 × 2.9 mm.

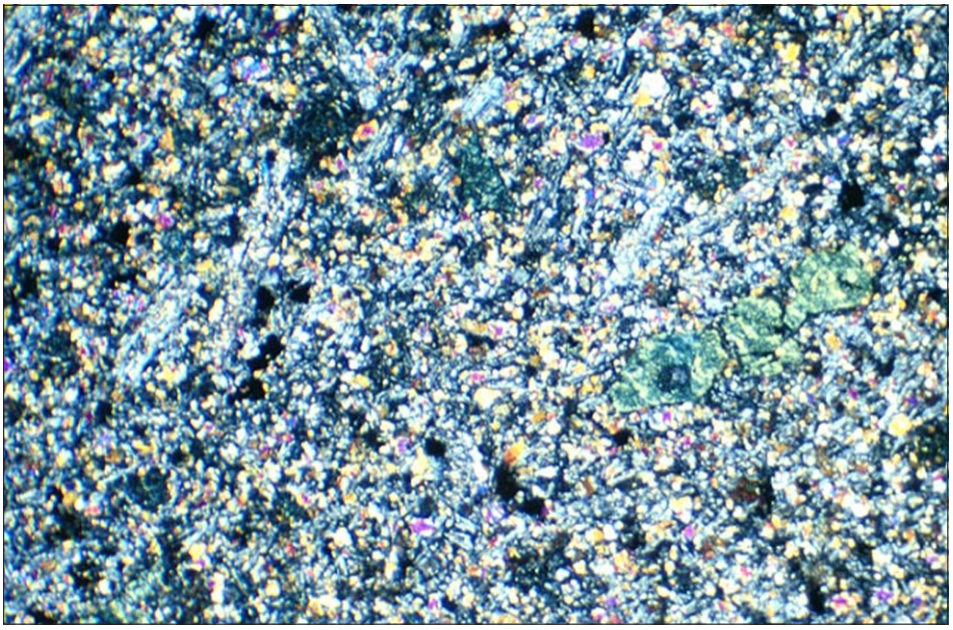

Plate 23

Photomicrograph of Spinks Creek Volcanics Group A lava (Psba), sample R004875. Same view as Plate 22, crossed nicols.

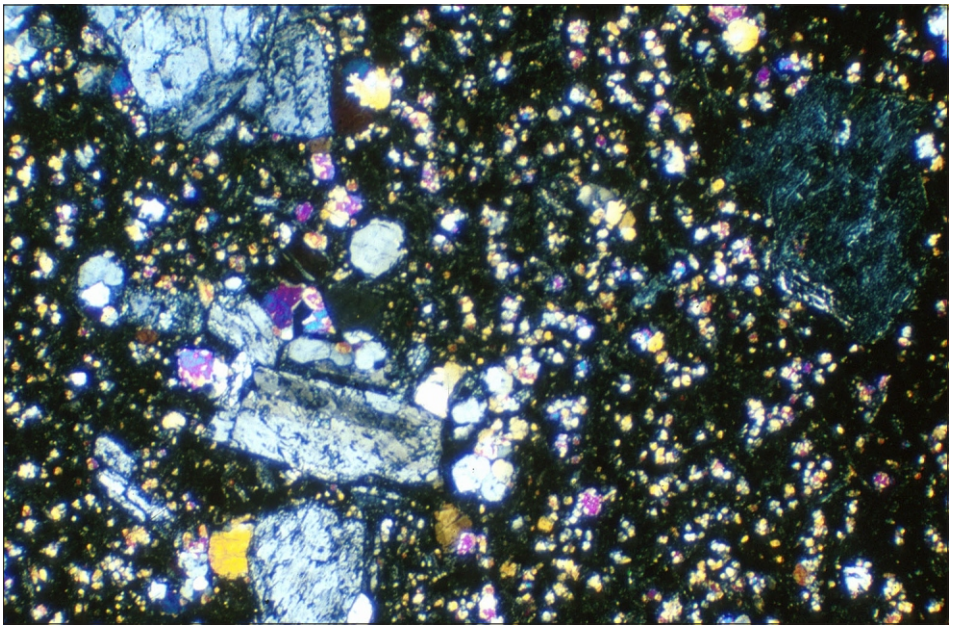

Plate 24

Photomicrograph of Spinks Creek Volcanics Group B lava (Psbb), sample R004871 (325 880 mE, 5 439 890 mN). Microporphyritic texture with glomerocrysts (left) of plagioclase and clinopyroxene, and phenocrysts of chloritised olivine (upper right). Crossed nicols, field of view 4.4 × 2.9 mm.

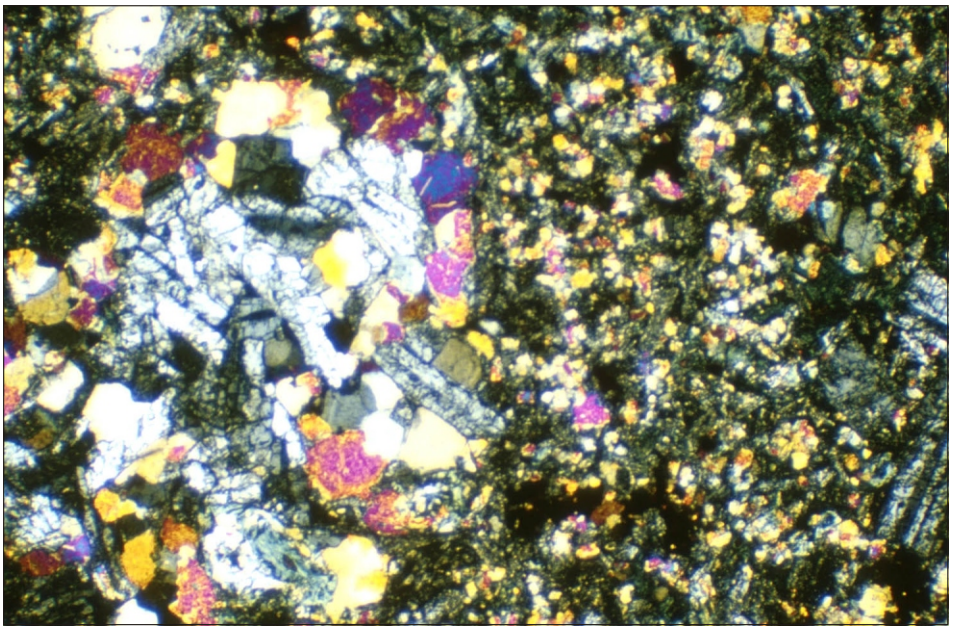

Plate 25

Photomicrograph of Spinks Creek Volcanics Group C lava (Psbc), sample R005162 (Horton River, 332 110 mE, 5 431 750 mN). Glomerocryst of plagioclase and clinopyroxene (left) and plagioclase phenocrysts (right) in a relatively coarse-grained intergranular groundmass. Crossed nicols, field of view 4.4 × 2.9 mm.

Some samples have a well developed microporphyritic groundmass. One such sample (R004871, Plate 24) contains abundant phenocrysts (≤2 mm) of mostly fresh plagioclase, clinopyroxene (150–500 μm, biaxial positive) and less abundant euhedral olivine phenocrysts (≤1 mm), completely pseudomorphed by pale green chlorite. Glomerocrysts are common and are mostly entirely clinopyroxene or plagioclase, but a few are composite, and may display ophitic intergrowths of the two minerals. Some plagioclase phenocrysts are partly altered to a blue-green pleochroic mineral with higher relief and birefringence than chlorite, probably pumpellyite. The medium-grained microporphyritic groundmass consists of abundant clinopyroxene granules (≤80 μm) and small equant opaque grains in a fine-grained turbid mesostasis of mainly plagioclase, together with chlorite and rare epidote. Ellipsoidal amygdales (≤1 mm) are filled with pale green chlorite, and may have an outer lining of fine-grained epidote. Chlorite veinlets also transect the slide.

Sample R004882 has a microporphyritic groundmass similar to R004871, but is more altered with very turbid plagioclase. Samples R006724 and R006739 also have a microporphyritic, but slightly coarser-grained groundmass with abundant greenish chlorite.

Several thin sections contain interesting amygdales. R005157 contains a large (6 mm) amygdale filled with nearly colourless chlorite, subordinate amounts of a finely fibrous, higher relief, pleochroic bluish-green mineral (pumpellyite?) and minor epidote. An ellipsoidal (4 × 3 mm) amygdale in R005579 contains three generations of chlorite. Pale yellow low birefringence chlorite occurs in its core, surrounded by a mantle of finer grained pale green chlorite with slightly higher birefringence, and another generation of pale yellow but fine-grained chlorite in the rim. In R005580 an ellipsoidal (3 × 2 mm) amygdale is filled by very fine-grained pale green chlorite in the core and rim, with a mantle of coarser grained radiating sheaves of prehnite.

Group C (high Ti) (Psbc)

This group of lavas is by far the most common (about half of all analysed samples), and includes the bulk of the thick pile to the east of the Roger River Fault. It also occurs to the west of the fault, where groups A and B are less common. In the Blackwater Rivulet section Group C lavas appear to form the base of the unit. This group extends at least as far south as the Horton River, and as far north as South Forest and Smithton.

This suite has TiO_2 of 1.44–1.78%, but typically about 1.6%. All samples are moderately evolved, and some quite strongly so (Mg# = 45.9 to 58.6), and both MgO (4.65–8.50%) and CaO (3.53–11.29%) extend to lower values than in groups A and B, suggesting differentiation by olivine and/or clinopyroxene fractionation. Within the group Ni only correlates weakly with Mg#, and neither Ni nor Cr correlate well with MgO. Incompatible elements such as K_2O, P_2O_5, Rb, Zr (80–120 ppm, excluding Griffin's samples) and Nb (up to 10 ppm) are more variable than in the other groups and extend to slightly higher values. Total iron (FeO_T 11.31–13.93%), V, Zn and Ga are also slightly higher than in groups A and B.

PETROGRAPHY

About sixty thin sections were examined. Their petrographic features are summarised in Table 16. They vary widely in grain size, from relatively coarse grained (groundmass grains mostly 100–300 μm) to almost glassy. About 85% contain distinct phenocrysts and glomerocrysts of plagioclase (rounded and broadly oblong in outline), although these are often very altered. About 55% also contain phenocrysts and glomerocrysts of clinopyroxene, and about 30% usually sparse to rare phenocrysts of olivine. All three phenocryst phases may be present in the same thin section, and mineralogically composite phenocrysts are common. A few samples (notably R005160, R005182, R004876, R004906, R004912, R004917, R005051, R002851, R002873) have a strongly speckled appearance in hand specimen, due to the large size (≤500 μm and sometimes more than 1 mm) of their opaque grains.

A typical, relatively coarse-grained sample from the Horton River (R005162: Plate 25) contains scattered phenocrysts of plagioclase (≤2 mm) and colourless clinopyroxene (≤500 μm), sometimes singly, but more commonly in composite glomerocrysts. Both minerals grade down in size into an intergranular groundmass of turbid plagioclase laths (mostly 150–400 μm), clinopyroxene granules, pale yellow to sea-green chlorite and irregularly angular grains of former opaque minerals, now mostly altered to fine-grained turbid sphene.

A typical, relatively fresh, fine-grained sample (R004894) is plagioclase-clinopyroxene-minor olivine phyric. The plagioclase phenocrysts are broadly oblong (≤2 mm) to irregularly polygonal in section. Most are fresh with well-spaced multiple twinning, but a few are partly replaced (especially in their cores) by pale green chlorite. Many are clumped together in glomerocrysts. Equant phenocrysts (≤750 μm across) of colourless clinopyroxene are less abundant and occur singly or in composite glomerocrysts with plagioclase. Rare olivine phenocrysts occur as euhedra (≤750 μm) completely replaced by pale green to pale yellow pleochroic chlorite. The groundmass is intergranular with plagioclase laths (mostly ≤200 μm), clinopyroxene granules, and opaque grains (typically equant and 50 μm across). Metamorphic minerals are chlorite, minor pale yellow epidote and small turbid grains of sphene. A few round amygdales (≤200 μm) are filled with radiating green chlorite.

Sample R004900 contains sparse plagioclase phenocrysts, grading down to microphenocrysts in a fine-grained groundmass. There are some nearly glassy zones in the groundmass with a dense dissemination of very small opaque grains.

The finest-grained sample (R004880) is aphyric with groundmass grains up to 50 μm; clinopyroxene and opaque grains (≤20 μm) are resolvable. Numerous, irregular to slightly flattened, ellipsoidal amygdales (≤1 mm) are filled with pale green, nearly isotropic chlorite. There is a single, irregular, angular (crudely triangular in outline) coarser grained granophyric segregation, 2 mm across, of mainly altered feldspar with a mottling of turbid blebs of sphene (10–20 μm).

Most samples have an overall green, grey-green or yellow-green colour in thin section, but a few (notably R005141, R005160, R004905, R004906, R004907, R005047, R005048) are grey with little or no greenish tint. Under the microscope the greenish colour is seen to be due to chlorite, whilst in the grey samples the chlorite is colourless (presumably low in iron) and associated with secondary hematite. This suggests that the grey samples are affected by secondary oxidation. This is supported by the relatively high Fe_2O_3/FeO ratio in many of them.

Pumpellyite (pleochroic from pale yellow to sea green) was confirmed by microprobe analysis in one sample (R006735 from 330220/5433080).

Amygdales are usually small and range from spherical to highly flattened. Chlorite is the most common filling, but fine-grained prehnite (e.g. R004869, R005051, R002873) and carbonate are also common. In sample R005177 (not analysed but probably belonging to Group C), amygdales up to 3 mm across commonly have rims of radiating coarse-grained prehnite, mantles of finer grained unorientated prehnite, and may have cores of very fine-grained green chlorite. In sample R004869, a round amygdale 3 mm across is filled with a mosaic of coarse-grained prehnite and minor epidote in the core, and quartz in its rim. Another in the same sample is filled with carbonate, apart from a discontinuous rim of albite. Sample R005172 contains an interesting ovoid amygdale about 6 mm in diameter. The core (about 3 mm in diameter) consists of interlocking quartz anhedra (0.5–1 mm), and is surrounded by a mantle of turbid zeolite(?), anhedral, equant to elongate grains of an unidentified mineral, possibly pumpellyite, and minor carbonate.

Group D (very high TiO_2) (Psbd)

These lavas are closely associated with Group C in the Arthur River near Kanunnah Bridge (R005050, R002850, 42147). All other samples are from west of the Roger River Fault, as in the middle Blackwater Rivulet area (R004870, R004889, R004890, R004891, R004893), and in Ekberg Creek (R002877 from 331900/5449830). Outside the Roger–Sumac–Dempster area, Brown (1985, 1989*a*) has sampled these lavas at Montagu in the Woolnorth Quadrangle (ABS22–25) and preliminary data from samples collected by D. B. Seymour suggests that they are the most abundant basalt group in that area. They also occur at Copper Mine Point near Smithton (ABS26 and 401287 collected by J. W. Hudspeth).

Their relative stratigraphic position is not completely clear, but in Blackwater Rivulet they probably overlie Group C and underlie Group F lavas. Near Togari (in the Woolnorth Quadrangle where Group C is apparently absent) they appear to overlie a single analysed Group B sample.

In this group of evolved tholeiites (Mg# = 47.3–55.9), TiO_2 falls within a narrow range of 2.12–2.39%. Other major elements are mostly similar to group C, although CaO extends to lower levels (5.4–10.5%) and MnO is higher (to 0.42%) in a few samples. A clear difference with groups C, B and A can be seen in higher levels of some incompatible high field strength elements, notably P_2O_5 (0.25–0.33% except for one sample), Zr (135–200 ppm), and Nb (12–20 ppm). V, Ga, Y and possibly Zn also show a progressive but slight increase, with much overlap between groups, from group A, through B and C, to group D.

PETROGRAPHY

Representatives of this suite (eight thin sections examined) are aphyric or nearly so.

In thin section a typical sample (R005050, Plate 26) contains a single isolated euhedral clinopyroxene phenocryst, and glomerocrysts of two clinopyroxene grains, both one millimetre across. The remainder of

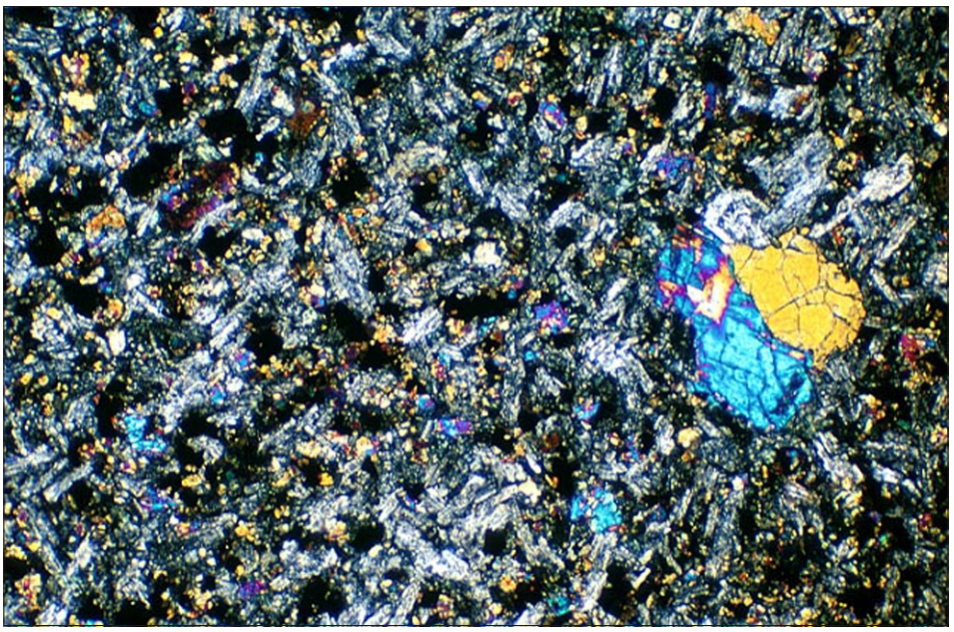

Plate 26

Photomicrograph of Spinks Creek Volcanics Group D lava (Psbd), sample R005050 (Arthur River, 331 280 mE, 5 446 260 mN). Clinopyroxene glomerocryst (right) in a medium to coarse-grained groundmass. Crossed nicols, field of view 4.4 × 2.9 mm.

the rock is relatively medium to coarse-grained and consists mainly of turbid plagioclase laths (mostly 200–400 μm long), intergranular clinopyroxene granules (100–200 μm) across, pale yellow-green chlorite and very abundant opaque grains. There are also small grains of secondary sphene, and minor epidote.

Two samples from close to the stratigraphic top of the Spinks Creek Volcanics, just below Kanunnah Bridge (R002850) and in Ekberg Creek (R002877), are very similar virtually aphyric basalts. The latter contains a large (13 mm) flattened amygdale filled with randomly-orientated sheaves of colourless prehnite.

Samples from Blackwater Rivulet (R004889, R004890) are slightly finer grained, with plagioclase laths mostly ≤200 μm long and clinopyroxene granules less than 200 μm across; both contain rare clinopyroxene phenocrysts (≤1 mm). Sample R004870 from nearby is similar and also contains very rare turbid plagioclase phenocrysts (≤1 mm) in addition to clinopyroxene. Sample R004891, from near the top of Group D in the Blackwater Rivulet section, also contains a few clinopyroxene and plagioclase phenocrysts and composite glomerocrysts (≤1 mm) in a slightly coarser grained, rather turbid altered groundmass. Some of the secondary chlorite in the groundmass is strongly pleochroic from deep sea-green to very pale yellow.

Sample R004893 is intermediate in grain size, with scattered plagioclase microphenocrysts (≤600 μm), but most groundmass plagioclase is between 150–200 μm long. The sample contains amygdales filled with pale yellow-green chlorite, pleochroic (grass green to colourless) actinolite, and subordinate epidote and clear albite.

Group E (evolved, weakly alkalic) (Psbe)

This group is tentatively defined on the basis of five samples from the southern part of the Smithton Synclinorium, where they are associated with group B and C lavas near the probable base of the Spinks Creek Volcanics. Three samples (R006750, R006751 and R005587) are from the Horton River area in the Dempster map sheet, and a further two (R006759, R006760) from the Leigh River outlier in the Balfour map sheet.

All are strongly evolved tholeiites (Mg# = 26.1–31.2) with low MgO (2.45–3.18%), Ni (8–15 ppm) and Cr (11–13 ppm), and somewhat low V (170–185 ppm) and Co (14–31 ppm). Most also have low CaO (4.34–8.26%). They have TiO_2 values (1.98–2.22%) most similar to Group D, but otherwise are quite different, with higher P_2O_5 (0.65–0.74%) and mostly higher K_2O and total FeO_T. The incompatible trace elements Rb, Y, Zr, Ce, Nb and Ba are also as high as, or higher than, group D. Probably of most significance is the very high Nb (57–66 ppm) and Nb/Zr (0.27–0.30 ppm), suggesting a more enriched mantle source.

Two samples (ABS6, ABS44), including one from a drill hole, were collected by Brown (1989*a*) from North Forest, in the northern part of the Smithton Synclinorium. These have some similarities to the Horton River samples and are tentatively also assigned to Group E. However they are less evolved, with higher Mg# (35.3, 36.9), and are less depleted in compatible trace elements (e.g. Ni, Cr and V). They are also less enriched in incompatible elements (e.g. TiO_2 1.63, 1.75%) and have slightly lower Nb/Zr (0.208, 0.244).

PETROGRAPHY

Sample R006751 contains fairly common elongate plagioclase phenocrysts (≤2 mm, grading to groundmass) and rare equant clinopyroxene phenocrysts (≤1 mm). Both occasionally contain altered melt inclusions and plagioclase often shows signs of resorption. There are also rare olivine phenocrysts, completely altered to fine-grained yellow-green chlorite. The rather turbid, mostly medium-grained intergranular groundmass consists of plagioclase laths (typically 100–300 μm long), clinopyroxene granules, abundant pale yellow-green chlorite and opaques, largely altered to sphene.

Sample R006750 is broadly similar, consisting of common plagioclase phenocrysts (up to 4 mm), sparse smaller clinopyroxene phenocrysts and glomerocrysts (some composite) in a very turbid groundmass with abundant dark yellow-green chlorite but mostly fresh opaques. Another sample (R005587) is another plagioclase-clinopyroxene phyric basalt with a somewhat finer grained groundmass containing relatively minor dark yellow-green chlorite, and a dark turbid indeterminate mesostasis, perhaps once partly glassy.

Sample R006759, from the Leigh River inlier, contains common euhedral phenocrysts of clear plagioclase (up to 3 mm) which grade into the groundmass. There are also rare phenocrysts of former olivine (e.g. 2 × 1.5 mm, anhedral, replaced by fine-grained yellow-green chlorite) and weakly coloured clinopyroxene (1.5 mm). The groundmass is medium-grained and consists of clear plagioclase laths (150–400 μm) with intergranular clinopyroxene, irregularly shaped but generally equant opaques (mostly ≤100 μm across), and minor yellow-green chlorite and fine-grained secondary sphene. There are also traces of epidote and probable pumpellyite (pleochroic from blue-green to pale yellow with anomalous birefringence colours). Sample R006760 is texturally similar, but only plagioclase phenocrysts are present in the thin section, and the groundmass is relatively oxidised.

Group F (alkalic) (Psbf, Psbzf)

Group F occurs mainly as coarser grained, doleritic to gabbroic intrusions within the Black River Dolomite near the western limb of the Smithton Synclinorium, as in Blackwater Rivulet (R004878 from 325460/5440520) and an eastern tributary (R004883, R004884, near 325600/5441200). Another coarse-grained outcrop from a similar stratigraphic position on Blackwater Road (R004872 from 325670/5439830) differs slightly

in chemistry, in particular having a higher TiO_2 content. Probable flows assigned to group F are exposed in the Arthur River section (R005074, lower flow at 322900/5446240), and in Blackwater Rivulet (R004892 from 325160/5444050). At the latter locality group F appears to occur near the top of the Spinks Creek Volcanics, overlying group C and D lavas.

This group differs from all others in its high Nb (40–68 ppm), P_2O_5 (0.36–0.73%), Rb, Nb/Y (>1) and Nb/Zr (~0.45), indicating alkalic affinities. To some extent this is reflected in major element chemistry, notably K_2O (from 0.46%, to 2.43% in one of the Blackwater Rivulet intrusions). Another feature distinguishing group F from all other groups is higher Al_2O_3 (16.90–18.63%). Although based on only six samples, this is a relatively heterogeneous group, with a wide range of MgO (4.00–8.75%) and CaO (5.84–10.84%) suggesting appreciable olivine and clinopyroxene fractionation (or accumulation?) in some samples. TiO_2 falls within a low, narrow range (0.83–0.91%), intermediate between the ranges of groups A and B, except for one sample (R004872) with 1.26% TiO_2. This particular sample also has the lowest MgO and Ni, highest CaO, V, Zn and Y, and may be unique.

PETROGRAPHY

The intrusion exposed in the Blackwater Rivulet tributary (samples R004883: Plate 27, R004884) has an ophitic texture, with abundant large (3–4 mm) subhedra of clinopyroxene and former olivine, often in interlocking glomerocrysts, between which is a turbid greenschist facies groundmass. Clinopyroxene grains are colourless augite (optically positive with moderate optic angle) and poikilitically enclose or partly enclose numerous lath-like inclusions of turbid altered plagioclase. Olivine is less abundant and invariably altered to pale yellow-green chlorite; some grains are nearly euhedral. The groundmass consists mainly of turbid altered plagioclase (albite?), chlorite and sea-green fine-grained tremolite-actinolite. Iron-titanium oxide minerals are almost totally altered to angular grains of sphene (≤400 μm). Minor secondary carbonate is present.

The Blackwater Rivulet intrusive rock (R004878) is similar but coarser grained (≤5 mm) and consists mainly of interlocking, poikilitic augite and olivine grains with relatively little groundmass.

The outcrop on Blackwater Road (sample R004872) is also a coarse-grained intrusive rock but has a higher proportion of groundmass. The large clinopyroxene grains are partly altered (uralitised) to yellow-green fibrous amphibole. Epidote is present in the groundmass in addition to altered plagioclase, chlorite, tremolite-actinolite and large (≤1 mm) grains of sphene.

A group F lava (sample R004892, Plate 28) contains a few large (≤5 mm) rounded, strongly resorbed plagioclase phenocrysts, largely altered to a fibrous cleavage-slow phyllosilicate resembling sericite. The groundmass has a fluidal, ophitic texture, consisting of aligned plagioclase laths (≤200 μm) largely enclosed by augite granules, together with yellow-green chlorite, minor epidote and small (≤150 μm) angular opaque grains (probably titanomagnetite).

Sample R005074, the lower flow from the lower Arthur River section, is aphyric and slightly finer grained, but otherwise similar to R004892, with a relict fluidal, ophitic texture. It is slightly more metamorphosed, with conspicuous epidote and some replacement of opaque grains by sphene.

Longman (1962) described a similar 'gabbro' from Blackwater Rivulet (sample 61/83). Although the thin section has not been relocated and the exact locality is uncertain, it was probably from one of these bodies. He reported that it contained accessory zircon and acicular apatite, associated with chlorite replacing diallage (i.e. clinopyroxene), in addition to saussuritised plagioclase, ilmenite altered to leucoxene, and actinolite. Zircon was not observed during the current

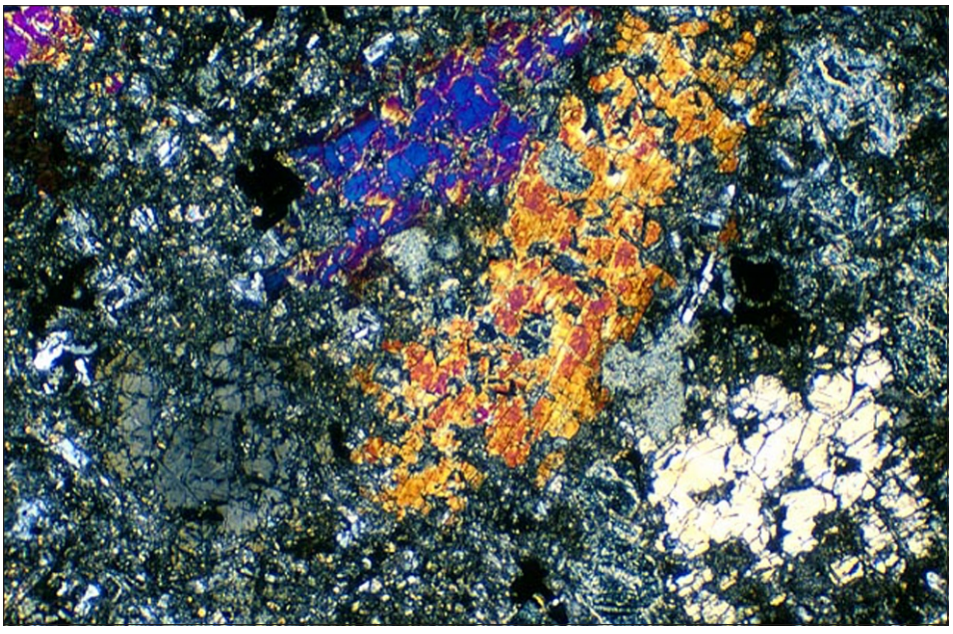

Plate 27

Photomicrograph of Spinks Creek Volcanics related Group F microgabbro (Psbzf), sample R004883 (325 750 mE, 5 441 070 mN). Note large clinopyroxene subhedra, ophitically enclosing some plagioclase laths. Crossed nicols, field of view 4.4 × 2.9 mm.

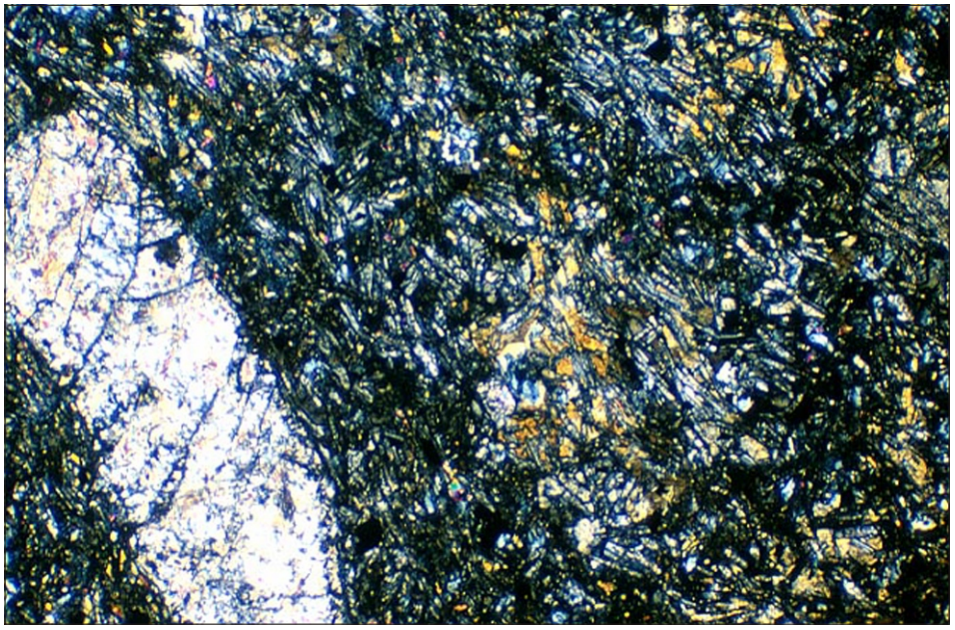

Plate 28

Photomicrograph of Spinks Creek Volcanics Group F lava (Psbf), sample R004892 (Blackwater Rivulet, 325 160 mE, 5 444 050 mN). Partly altered plagioclase phenocryst (left) in a fluidal, ophitic-textured groundmass. Plane polarised light, field of view 4.4 2.9 mm.

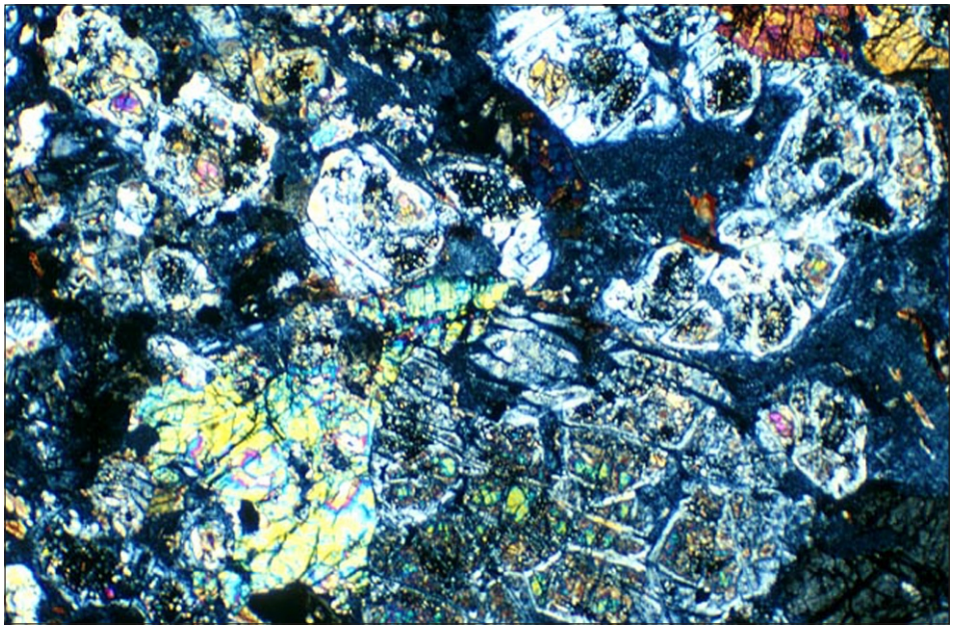

Plate 29

Photomicrograph of Spinks Creek Volcanics related picrite (Psbzp), sample R006799 (Blackwater Rivulet, 324 640 mE, 5 442 890 mN). Interlocking mosaic of partly serpentinised olivine and titanaugite (lower left, upper centre, top right) with minor red-brown biotite and kaersutite. Plane polarised light, field of view 4.4 × 2.9 mm.

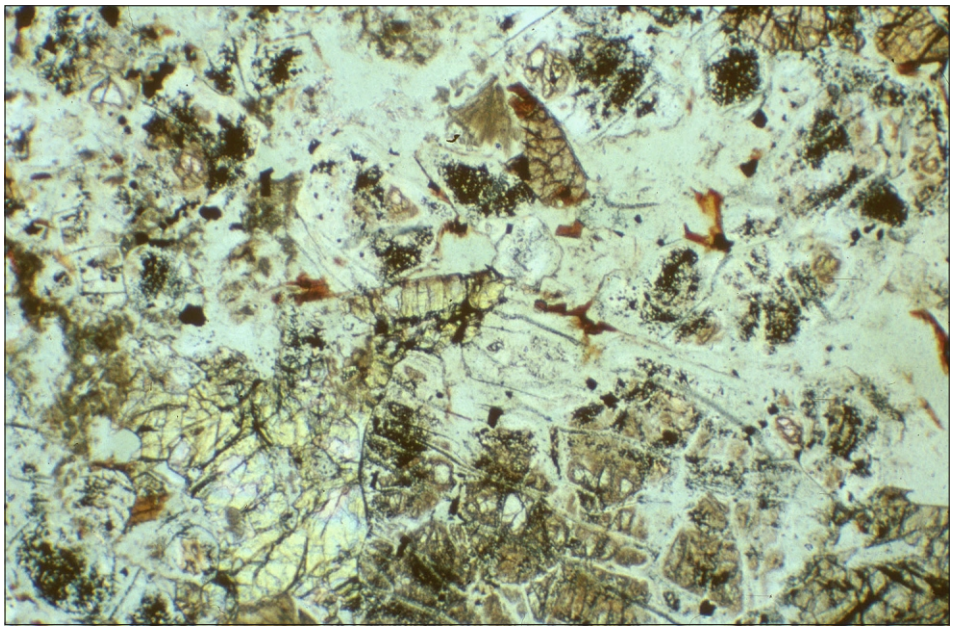

Plate 30

Photomicrograph of Spinks Creek Volcanics related picrite (Psbzp), sample R006799. Same view as Plate 29, crossed nicols.

study, and it seems possible that it was a misidentification of sphene.

Picrites (Psbzp)

BLACKWATER RIVULET

A dark grey-green massive coarse-grained mafic rock apparently intrudes massive black chert assigned to the Black River Dolomite on the steep undercut left bank of Blackwater Rivulet at 324640/5442890. The contact, about two metres above normal water level, appears subhorizontal and the topographically overlying chert is more resistant and overhanging. Similar weathered mafic rock forms a small bar across the rivulet nearby.

Samples from the bank (R006799, Plates 29, 30; R004886) consist mainly of an interlocking mosaic of partly altered olivine, and colourless to pale pinkish augite/titanaugite grains up to 4 mm across. Rare, well-crystallised grains (≤250 μm) of deep red-brown to pale pink, strongly pleochroic kaersutite overgrow titanaugite. The olivine is largely replaced by serpentine and fine-grained opaque aggregates (secondary magnetite?), but some relict cores remain. There is relatively little intergranular material, but ragged splinters (≤200 mm long) of deep to pale red-brown pleochroic biotite (comprising less than 1% of the rock) and primary opaque grains (50–200 μm) are present, in addition to very fine-grained serpentine and/or chlorite. There are also a few radiating clustered sheaves (≤400 μm) of colourless prehnite.

Samples from the bar across the creek (R004885, R006800) are similar but more altered, with a pervasive yellow-brown staining. They contain a little more biotite, as well developed oblong laths up to one millimetre long.

Chemically the rock (sample R004886 analysed, Table 15*a*) is picritic with 28.85% MgO and elevated Cr and Ni. The rock formally classifies (Le Bas, 2000) as a komatiite (e.g. MgO > 18%; 30% < SiO_2 <52%; Na_2O + K_2O <2%; TiO_2 <1%). Despite the low K_2O (0.21%) and Na_2O (0.11%), alkalic affinities (possibly to Group F basalts) are suggested by the presence of biotite and kaersutite, and trace element geochemistry (notably high Nb, P and light rare earths).

ARTHUR RIVER AT 325250/5446920

On the right (locally west) bank of the river at this locality, weathered basaltic rock rests directly on well-bedded Black River Dolomite. The basal 0.7 m is weathered vesicular and sulfide-bearing, but is overlain by massive dark grey (but carbonate-altered) picrite. Although in a similar stratigraphic position to the Blackwater Rivulet picrite, field relationships here suggest that the picrite may be extrusive.

In thin section the rock (sample R005063) consists largely of very abundant (probably >60%) euhedra (500 μm–1 mm) of former olivine and clinopyroxene. They are replaced by pale yellow-green chlorite, finely disseminated secondary opaque minerals and abundant carbonate, except for rare relict cores of colourless clinopyroxene. The groundmass consists of mainly chlorite, small sphene grains (25–50 μm) with some relict opaque cores, and fairly abundant (3–5%) ragged splinters (mostly ≤100 μm) of pleochroic red-brown biotite. Veinlets of carbonate are present.

A chemical analysis shows that the rock is very altered (e.g. 8.08% CO_2) but high MgO (17.19%), Ni and Cr, and low Al_2O_3 suggest that it is an altered picrite. It differs from the fresher Blackwater Road picrite in having much higher TiO_2 (2.95%). Relatively high Nb, P_2O_5, Ce and other light rare earths suggest mildly alkalic affinities. The rock may represent a lower degree partial melt of the same mildly enriched source that produced Group A.

Miscellaneous basalt samples

A few samples appear chemically unique, and do not readily fit into any of the suites.

R005076 (ARTHUR RIVER AT 322870/5446160)

This is a very fine-grained pale grey-green rock and was thought in the field to be possibly a felsic lava. In thin section it is seen to be a leucocratic basalt, consisting of mainly small plagioclase laths and clinopyroxene granules, with very little opaque minerals. It is aphyric apart from very sparse small (≤400 μm) microphenocrysts of clinopyroxene. It is essentially non-magnetic (X about 0.6×10^{-3} SI). A chemical analysis shows a tholeiitic composition with unusually low TiO_2 (0.45%) and a positive europium anomaly. The rock is probably a late-stage differentiate of Group P, possibly by plagioclase resorption and titanomagnetite fractionation. One of Griffin's samples (42145) is comparable (but more altered) and spatially associated with Group A lavas.

R005075 (ARTHUR RIVER AT 322900/5446240, THIN UPPER FLOW)

This rather altered rock consists in thin section of mainly chlorite, turbid plagioclase laths, carbonate and opaque minerals, although the basaltic texture is well preserved. Chemically it appears to have mildly alkalic affinities (e.g. moderately high P_2O_5, Nb and Ce), but has intermediate TiO_2, and is unlike any other sample.

FOREST-1 DDH

One of Brown's samples from the Forest-1 drill hole (ABS52) has extremely high TiO_2 (3.59%), but is also rather altered.

Metamorphism *(JLE)*

Petrographic examination (see Table 16) indicates a low but variable degree of metamorphism in basalts of the Spinks Creek Volcanics.

In most samples plagioclase, both as microphenocrysts and in the groundmass, is turbid and in some samples completely altered to fine-grained prehnite. Preliminary microprobe data (see above) indicates that the composition of plagioclase is bimodal, with both metamorphic albite and relict igneous labradorite being present.

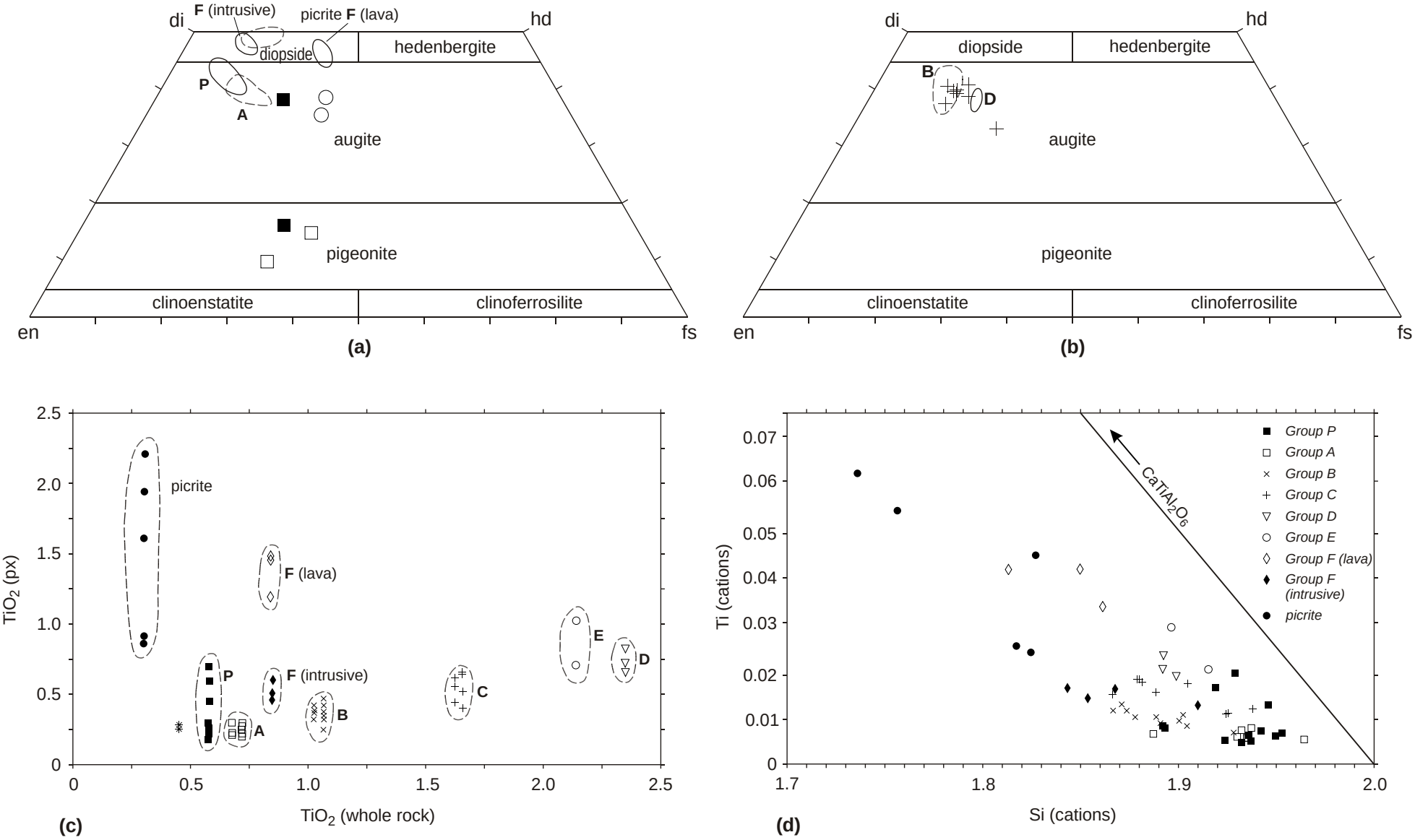

Figure 9

Plots of pyroxene analyses, Spinks Creek Volcanics: (a) en:fs:wo quadrilateral plot, Groups P, A, E, F and picrite (b) en:fs:wo quadrilateral plot, Groups B, C and D (c) TiO_2 partitioning between whole rock and pyroxene (d) Si-Ti (cations) plot.

Chlorite is usually abundant in the groundmass, and is highly variable in grain size and colour (colourless, very pale yellow or green, to quite dark yellow-green).

Pumpellyite, which is much less common, can usually be distinguished from chlorite by its strong pleochroism (pale blue-green or yellow-green to very pale yellow) and higher relief and birefringence. Some very finely granular material is very difficult to identify optically, and may be an intergrowth of both minerals. It is possible that some yellow-green pumpellyite has been petrographically misidentified as chlorite, and more microprobe work is required.

Clinopyroxene is typically fresh and actinolite uncommon. Epidote is rare, and occurs more often in amygdales or veinlets than in the groundmass. Quartz, probably of metamorphic origin, is present in the groundmass of some samples (e.g. R004904).

The grade of metamorphism is thus probably prehnite-pumpellyite facies, but preservation of igneous clinopyroxene and some igneous plagioclase suggests that the rank (intensity) is low.

In one sample (R006011 from 324950/5432050) from a fault sliver north of the Frankland River, replacement of clinopyroxene by actinolite indicates metamorphism is more complete, and probably of greenschist facies.

Mineral chemistry *(JLE)*

The mineralogy of fifteen samples of the Spinks Creek Volcanics, representative of all chemical groups including picrite, was studied at reconnaissance level using the Cameca SX-50 electron microprobe at the Central Science Laboratory, University of Tasmania.

Pyroxenes

In the classification of Morimoto (1988) all are quadrilateral pyroxenes (Table 17, fig. 9*a, b*).

The majority of pyroxenes from the tholeiitic groups P and A to E are augites. In most groups there is a substantial range in pyroxene Mg# due to fractional crystallisation, and there is a slight tendency for late-crystallising granule pyroxenes to be more iron-rich than phenocrysts. The most magnesian pyroxene composition from each group correlates with whole rock Mg#. Thus pyroxenes from Group B (pyroxene Mg# 83.3–87.6) range up to more magnesian compositions than those from the successively more fractionated Groups C (72.2–81.9) and Group D (Mg# up to 79.2). Likewise pyroxenes from Group P intrusions (pyroxene Mg# 68.3–88.8), the possibly related Group A lavas (Mg# 62.0–82.6) and strongly evolved Group E lavas (Mg# 60.5–61.8) become more iron-rich as whole rock Mg# decreases.

Pyroxenes from the relatively alkalic Group F are more calcic and classify as diopside. Groundmass pyroxenes from the group F lava (R004892) have lower Mg# (66.0–69.5, plotting as salites in the older classification of Deer *et al*., 1963) than the larger grains from the gabbroic intrusion R004883 (Mg# 85.7–90.4). Pyroxenes in the alkali picrite (R004885, R006799) are also highly magnesian, calcic diopsides (Mg# 82.2–90.3). The tendency for clinopyroxene from alkali basalts to have higher Ca, relative to tholeiites, has long been known (e.g. Deer *et al*., 1963; Carmichael *et al*., 1974, p.271–274).

Three pigeonites were analysed from two samples. Sample R004904, from a coarse-grained subvolcanic intrusion assigned to Group P, contains pigeonite granules, whilst in sample R004875, a Group A lava, both microphenocrysts and granules are present. All these grains have lower Mg# than coexisting augites.

There are also systematic differences between and within basalt groups in minor element chemistry of pyroxene. In the tholeiitic basalts, TiO_2 in pyroxenes increases from Group A (0.20–0.31%), through Group B (0.26–0.48%) and C (0.41–0.66%), to Group D (0.69–0.85%), obviously reflecting whole rock chemistry (fig. 9*c*). In each case the ratio between TiO_2 in the most magnesian pyroxene phenocryst and the whole rock suggests a pyroxene/melt partition coefficient of 0.25–0.40. This also applies to sample R005076 (with very low TiO_2 in both pyroxenes and whole rock), and the strongly evolved Group E. A single granule pyroxene analysed from the latter is particularly titaniferous (1.03%), reflecting fractionation. Some pyroxenes from the coarser grained Group P rocks are anomalously titaniferous relative to whole rock TiO_2.

In the more alkalic Group F rocks, particularly the lava (R004892) and also in the picrite, the pyroxenes are relatively titaniferous compared to whole rock composition. These titaniferous pyroxenes also have lower Si (and therefore higher tetrahedral Al^{iv}) (fig. 9*d*). In part this is due to the coupled substitution ($Mg \leftrightarrow Ti$, $2Si \leftrightarrow 2Al$; i.e. solid solution to $CaTiAl_2O_6$) common in clinopyroxenes from alkalic rocks due to lower silica activity in the melt (e.g. Carmichael *et al*., 1974). These pyroxenes are also relatively high in Fe^{III} and Na, both of which also correlate negatively with Si, and other substitutions (e.g. $Mg \leftrightarrow Fe^{III}$, $Si \leftrightarrow Al$; i.e. solid solution to $CaFe^{III}AlSiO_6$) may also be important. Most Al appears to be held in the tetrahedral sites, and octahedrally co-ordinated Al^{vi} shows no correlation with Na.

Mn correlates well with Fe^{II} (i.e. negatively with Mg#), and Cr is an important cation only in some pyroxenes with high Mg# (>80), mainly from Group B, the group P and F intrusive rocks, and the picrite (sample R004886).

Feldspars

Feldspars from the basalts are commonly turbid, and were difficult to analyse by microprobe due to widespread patchy alteration to prehnite and the presence of iron oxides. About twenty reasonably 'clean' analyses of plagioclase were obtained from representative samples of each chemical group (Table 18).

These fall into two distinct populations. Ten analyses are albite ($An_{1.1–5.1}$), consistent with a metamorphic, lower greenschist (prehnite- pumpellyite) facies origin. Relict igneous calcic plagioclase (predominantly

labradorite, $An_{46.0–70.1}$) appears to be best preserved in the Group P sample R004904, from a coarse-grained Group P subvolcanic intrusion. Labradorite ($An_{49.6–62.3}$) was also analysed from four lava samples, from Groups A, C, E and F. Given the reconnaissance nature of this work, it seems likely that both metamorphic (albite) and igneous plagioclase are widespread in all the basalts.

Potash feldspar is present in the Group F rocks, reflecting their relatively potassic whole-rock chemistry, but no good analyses were obtained.

Iron-titanium oxides

Attempts to obtain reconnaissance data on the opaque phases in the basalts (Table 19) were frustrated by widespread partial to complete alteration to sphene. Two large grains from the Group P intrusive rock R004904 are ilmenite with about 7% $MnTiO_3$ (pyrophanite) and 5–6% hematite in solid solution. Two analyses from the Group F lava R004892 are probably titanomagnetites with 32–40% ulvospinel ($Fe^{II}_2TiO_4$) and 9–11% hercynite ($Fe^{II}Al_2O_4$) in solid solution. The remaining analyses (from Groups A, B, C and D) contain appreciable amounts of Ca and Si, suggesting the presence of sphene impurities, but are probably also essentially titanomagnetite.

Epidote

Only three microprobe analyses of epidote were obtained (Table 20). In sample R006740 (a Group A lava), pseudomorphed phenocrysts apparently after olivine contain approximately 25–30% clinozoisite in solid solution. Nearly stoichiometric epidote containing inclusions of native copper occurs in Group C lava R006735, surrounded by chlorite, in the core of a large amygdale.

Pumpellyite

Nine pumpellyite analyses (Table 21) from five samples were calculated to 16 cations, and iron distributed to Fe^{III} and Fe^{II} by assuming $O_{21}(OH)_7$ per formula unit (Coombs *et al*., 1976). All are typical 'pumpellyite-Al' (Deer *et al*., 1997, p.201–247), because of the predominance of Al over Fe in both the X and Y sites (e.g. $100*Al/(Al + Fe^{III})_Y$ varies from 57.0 to 82.0).

The majority of the analysed pumpellyites are close to the ideal composition $Ca_4(Mg,Fe^{II})Al.Al_3Fe^{III}.Si_6O_{21}(OH)_7$, and have a fairly restricted range of Mg# ($100*Mg/Mg + Fe^{II}$) from 38.8–56.0. In thin section these grains are pleochroic from colourless to pale blue-green, or less commonly apple green (sample R004875). The more magnesium-rich varieties (from sample R005171) are the less strongly coloured. Birefringence ranges to upper first order with anomalous interference colours. Although the fine grain size precludes detailed determination of optical properties, at least some grains are optically negative, as is usual for pumpellyites with more than about 9% iron as Fe_2O_3 (e.g. Deer *et al*., 1997, p.216).

Pumpellyite from Group D lava R004891 is much more magnesian (Mg# 82.8), deficient in Ca and Si, and the W sites cannot be filled even if all the available Fe^{II}, Mn, Na and K is allocated to them. Optically this grain is strongly pleochroic from nearly colourless to khaki-green, biaxial negative and has birefringence up to lower second order blue. These are anomalous characteristics for pumpellyite.

Chlorite

Reconnaissance studies of chlorites (eleven analyses from four samples, Table 22) suggest that they are typical, compositionally rather uniform chlorites with negligible alkalis and TiO_2, and low CaO. The slightly low cation totals (9.82 to 9.90 per formula unit), compared with the ideal ten cations, suggests that Fe^{III} is also not a significant component. Aluminium occupies just under a quarter of the tetrahedral sites (0.83–0.95 cations per formula unit) and Mg# ranges from 39.9 to 57.0.

The most iron-rich chlorites (Mg# 39.9–40.6) of those analysed are from Group C sample R006735. They are mostly finely granular aggregates of deep 'khaki' yellow-green groundmass chlorite, in which optical properties are obscured by the strong colour and fine grain size. Crudely radiating length-slow chlorite (analysis R006735/R4/1) from a 2.5 mm diameter amygdale, which also contains minor epidote and traces of native copper, is compositionally similar. These chlorites fall in or near the field of brunsvigite in the nomenclature of Hey (1954).

An analysis (R005078/R1/4) of a pale yellow, nearly isotropic, rather large grain adjacent to a pumpellyite veinlet in a coarse-grained intrusive rock is slightly more aluminous than the other samples and relatively iron rich (Mg# 48.5).

The remaining analyses, of pale yellow-green to very pale yellow chlorites, are compositionally very similar (Mg# 53.8–57.0) and straddle the pycnochlorite (Si < 3.1) and diabantite (Si > 3.1) fields of Hey (1954). There is no apparent difference between finely granular chlorite associated with pumpellyite in pseudomorphed phenocrysts and groundmass chlorite.

Olivine, biotite and kaersutite (from picrite)

Olivine is completely replaced by chlorite, pumpellyite and other secondary minerals in all basalt samples examined from the Spinks Creek Volcanics, although rare fresh olivine occurs in the Blackwater Rivulet picrite (see above). Reconnaissance electron microprobe analyses (Table 23*b*) show that it is too iron-rich (about $Fo_{80–84}$) to have been in equilibrium with normal mantle olivine ($Fo_{88–92}$).

Amphibole (Table 23*a*) from the picrite is classified as kaersutite in the scheme of Leake *et al*. (1997). It is probably an oxyhornblende (containing excess oxygen at the expense of hydroxyl groups) and may also contain significant ferric iron. Constraints imposed by cation site occupancy do not allow these to be

independently estimated from electron microprobe analyses. The structural formula given in Table 23*a* is a modified '13eCNK' formula (Leake *et al*., 1997) which assumes no ferric iron and that cations other than Ca, Na, K (and Ba) total 13, to fill the T and C sites. If ferric iron is present, less H (partial substitution of OH by oxygen) is required to maintain charge balance.

Both kaersutite (Mg# 69.7, 6.81% TiO_2) and biotite (Mg# 66.0–75.8, 6.46–9.01% TiO_2) in the picrite are remarkably titaniferous, but the earlier crystallising titanaugite (Mg# 73.9–83.9, up to 2.20% TiO_2 and 7.16% Al_2O_3) is not especially so. The presence of significant BaO (up to 1.98%) in the biotite is also notable.

Magnetic susceptibility *(JLE)*

The susceptibility of hand specimens of the basalts (Table 16) is generally high but variable, and broadly correlates with the TiO_2 content in analysed samples, and proportion of fresh titanomagnetite, as seen in thin section.

Group P, represented in this area by a coarse-grained doleritic intrusive body in the lower Arthur River area, is weakly magnetic (both samples about 0.56×10^{-3} SI). Four samples representative of the low Ti, tholeiitic Group A, all have relatively moderate susceptibility, between 13 and 20×10^{-3} SI.

Samples of groups B, C and D mostly have susceptibility between 20 and 50×10^{-3} SI, the highest measurement of a hand specimen being 105×10^{-3} SI from R005052, a Group C basalt from Kanunnah Bridge. Twenty field measurements taken from fresh bedrock at this locality yielded an average of 55.5×10^{-3} SI (range 15.4–84.0), indicating substantial natural variation of susceptibility on an outcrop scale. Likewise twenty measurements from outcrop in Keppel Creek (at 331630/5444020) yielded an average of 32.5×10^{-3} SI (range 5.66–77.9); an analysed sample (R004918) is a Group C basalt with a susceptibility of about 8×10^{-3} SI. A few samples from elsewhere with much lower values (less than 1×10^{-3} SI) show petrographic evidence of either destruction of titanomagnetite by alteration to sphene (e.g. R005567, R005573, R005574, R005577, R005588, R006729, R006732, R006747, R005162, R005175, R005179) or secondary oxidation (e.g. R005565, R005160, R005162, R004906).

The coarse-grained gabbroic representatives of Group F (R004872, R004878, R004883, R004884) have low susceptibilities ($0.4–1.8 \times 10^{-3}$ SI), but the lavas have higher values (R005074, 45×10^{-3} SI; R004892, 9×10^{-3} SI). Again this reflects the replacement of titanomagnetite by sphene, which seems to be more advanced in the intrusive rocks.

Copper anomalies *(JLE)*

The Spinks Creek Volcanics display an overall weak regional anomaly for copper. The most anomalous sample (590 ppm Cu) is R006747, a group B lava from upper Ekberg Creek. Further details are given in Table 24. Copper appears to vary erratically from sample to sample, is not correlated with any other element, and is unrelated to the particular suite. The presence of native copper in some samples suggests a very low sulfur content, as otherwise chalcopyrite and/or other sulfides would probably form instead.

In contrast the Tasmanian Tertiary basalts have copper contents of usually less than 100 ppm, and typically 40–60 ppm (MRT ROCKCHEM database).

Rare-earth element data *(JLE)*

Representative samples of groups A, B, C, D and F were analysed by either the INAA or ICPMS methods. Only INAA data were obtained for group P and E samples. The very low-Ti sample (R005076) and picrite R004886 were analysed by the ICPMS method (Table 15*c*, fig. 8*a–j*).

Although it is possible to analyse all fourteen naturally occurring REE by the ICPMS method, these data, although internally consistent, appear less reliable. Chondrite-normalised plots of the ICPMS data mostly have a kinked pattern, with in particular usually substantial positive terbium anomalies, and also sometimes small positive erbium anomalies. This is not seen in the INAA data for similar samples. The kinked patterns are unlikely to be real in these rocks of magmatic origin (e.g. Bau, 1996), and are attributed to analytical problems with the ICPMS method, perhaps related to the lanthanide tetrad effect seen in REE in aqueous solution.

Nevertheless if ICPMS terbium data are ignored, the ICPMS and INAA results, for different samples but from the same group, are broadly consistent.

Groups B (fig. 8*b, c*), C (fig. 8*d, e*) and D (fig. 8*f, g*) each have linear chondrite-normalised rare earth patterns with normalised values decreasing evenly from La to Yb. Each group is successively more light-rare earth enriched, with La_N increasing markedly from B (13.9–18.8) through C (20.3–29.3) to D (47.5–59.4), whilst Yb_N and the other heavy rare earths show little change (at 7 to 12 × chondrite). Thus the patterns become progressively more tilted, with $(La/Yb)_N$ increasing from 1.86–1.92 in Group B, to 1.96–2.50 in Group C, and 3.79–4.86 in Group D. This suggests successively smaller degrees of partial melting of a similar mantle source, with the incompatible heavy rare earths strongly partitioning into the melt and the heavy rare earths being buffered, possibly by clinopyroxene, in the residue. It is also noteworthy that the INAA patterns have no, or negligible, Eu (europium) anomalies, suggesting that plagioclase fractionation is insignificant. The small negative Eu anomalies seen in most of the ICPMS patterns are probably analytical artifacts.

The INAA data of Brown (1986) for the primitive low-TiO_2 Group P from the Smithton foreshore show a distinctly different, flat to slightly concave chondrite-normalised REE pattern (fig. 8*a*). La_N is about 40 to 44, but the pattern slopes steeply downward to about 10 × chondrite for Eu and Gd, and is nearly flat

or rises slightly in the HREE. The gabbroic intrusion in the Arthur River (sample R005078) has a very similar shaped pattern, subparallel at slightly lower abundances (e.g. La_N = 32.5), supporting its assignment to the same group. Again there are no definite Eu anomalies.

The evolved low-TiO_2 group A samples also have a concave pattern, but are less enriched in the light rare earths, with La_N at about 26 and $(La/Yb)_N$ of 1.94–2.00 (fig. 8*b, c*). The very low-TiO_2 sample R005076 (fig. 8*j*) may be a fractionated representative of this group, or possibly of Group B. It has a marked positive Eu anomaly, suggesting plagioclase accumulation, consistent with its slightly high Al_2O_3 and leucocratic petrography. The fractionated Group E lavas have a concave pattern similar to Group A, but at much higher relative levels (fig. 8*h*).

The alkalic Group F rocks have more strongly LREE-enriched (La_N = 115 to 163) but also strongly concave patterns (fig. 8*h, i*). Heavy rare earths are also slightly more abundant than groups P and A (and indeed than groups B, C and D). The intrusive rocks (R004883, R004872) have higher relative levels, particularly of LREE ($(La/Yb)_N$ = 9.3–9.5) than the lavas (R005074, R004892; $(La/Yb)_N$ = 6.7–6.8). The alkali picrite R004886 shows a parallel pattern at lower abundances (fig. 8*h*).

Petrogenesis *(JLE)*

To test whether at least some of the basalt groups were related by crystal fractionation (e.g. Griffin, 1974), the fractionation paths of the average group B, C and D compositions (normalised to 100%) were calculated at 10 MPa (1 kb), using the method of Grove *et al*. (1992). These calculations suggest that the average Group B composition initially precipitates olivine, but after only 1.2% fractionation it is joined by plagioclase, and after 9.4% fractionation by clinopyroxene. When the calculated liquid line of descent is projected on a Mg# versus TiO_2 plot (fig. 10), it is clear that it does not pass through the Group C field, which lies at higher Mg# and/or TiO_2. In other words, crystal fractionation only cannot account for the large increase in TiO_2 between Group B (c. 1.1%) and Group C (c. 1.7%) without conflicting with other major element data such as Mg#. This problem is even more evident if fractionation of Group C is modelled to derive Group D. Attempts to improve the model by calculating the fractionation paths at higher or lower pressures were unsuccessful. The main effect of increasing or decreasing pressure is to respectively hasten or delay the onset of clinopyroxene fractionation, with only a slight effect on the Mg#–TiO_2 paths.

A simple fractionation model also has difficulty in explaining the tight clustering of data into groups (fig. 10), and the absence of lavas with intermediate compositions (e.g. between groups B and C, or C and D).

Brown (*in* Brown, 1989*a*, p.76–78) suggested that the progressively increasing TiO_2 content from groups A and P (his Group 1), through Group C (his Group 2) to Group D (his Group 3) was due primarily to a batch melting process. Crystal fractionation (clinopyroxene + plagioclase ± olivine) was thought to have played a subordinate role in the formation of some groups. This model appears to assume that the groups were derived from a common mantle source. It is not immediately obvious why the successively younger lavas with higher TiO_2 (presumably generated by successively lower degrees of partial melting) should be progressively more fractionated (lowest Mg#).

To test whether the various groups could have been derived from the same mantle source, incompatible element ratios such as Nb/Zr and Ti/Zr were considered. Unless the degree of partial melting is very small, such ratios change little with increasing degree of partial melting, and are virtually unaffected by low pressure fractionation of common near liquidus mineral phases. Thus they resemble isotope ratios in closely reflecting mantle source characteristics (e.g. Weaver, 1991).

A plot of Nb against Zr (fig. 7*b*) shows that the analysed samples fall on one of three, possibly four linear trends. Each group plots as a cluster on one of the trends. This is interpreted as indicating various degrees of partial melting of three, possibly four distinct mantle sources. On each trend, groups with higher Zr and Nb probably represent smaller degrees of partial melting than those groups that are lower in these elements. Each trend extrapolates back towards the origin, or to a small intercept on the Zr axis (since Zr is a less incompatible element than Nb).

In this model the high and very high TiO_2 groups C and D are interpreted as being derived from a mantle source relatively depleted in Nb, and probably represent moderately-low and low degrees of partial melting, respectively. Sample ABS52 from the Forest drill hole lies on an extension of this trend and may represent a still lower degree partial melt of the same source. The intermediate TiO_2 Group B may be derived from the same source by a higher degree of partial melting, or may define a fourth, very slightly enriched mantle source, as it has slightly higher Nb/Zr.

The low TiO_2 groups A and P, and the mildly alkalic, high TiO_2 Group E, are also approximately mutually colinear on Figure 7*b*, and are probably derived from a mildly Nb-enriched source. The altered sample R005063 lies on an extrapolation of this trend and may also represent a low degree partial melt.

The third, most enriched mantle source is defined by Group F and may also include the alkali picrite R004886.

This is summarised on a plot of Nb/Zr against TiO_2 (fig. 7*c*), which clearly defines the six groups. Essentially the vertical axis represents increasingly enriched mantle sources, and the horizontal axis decreasing degrees of partial melting. Clearly Group F

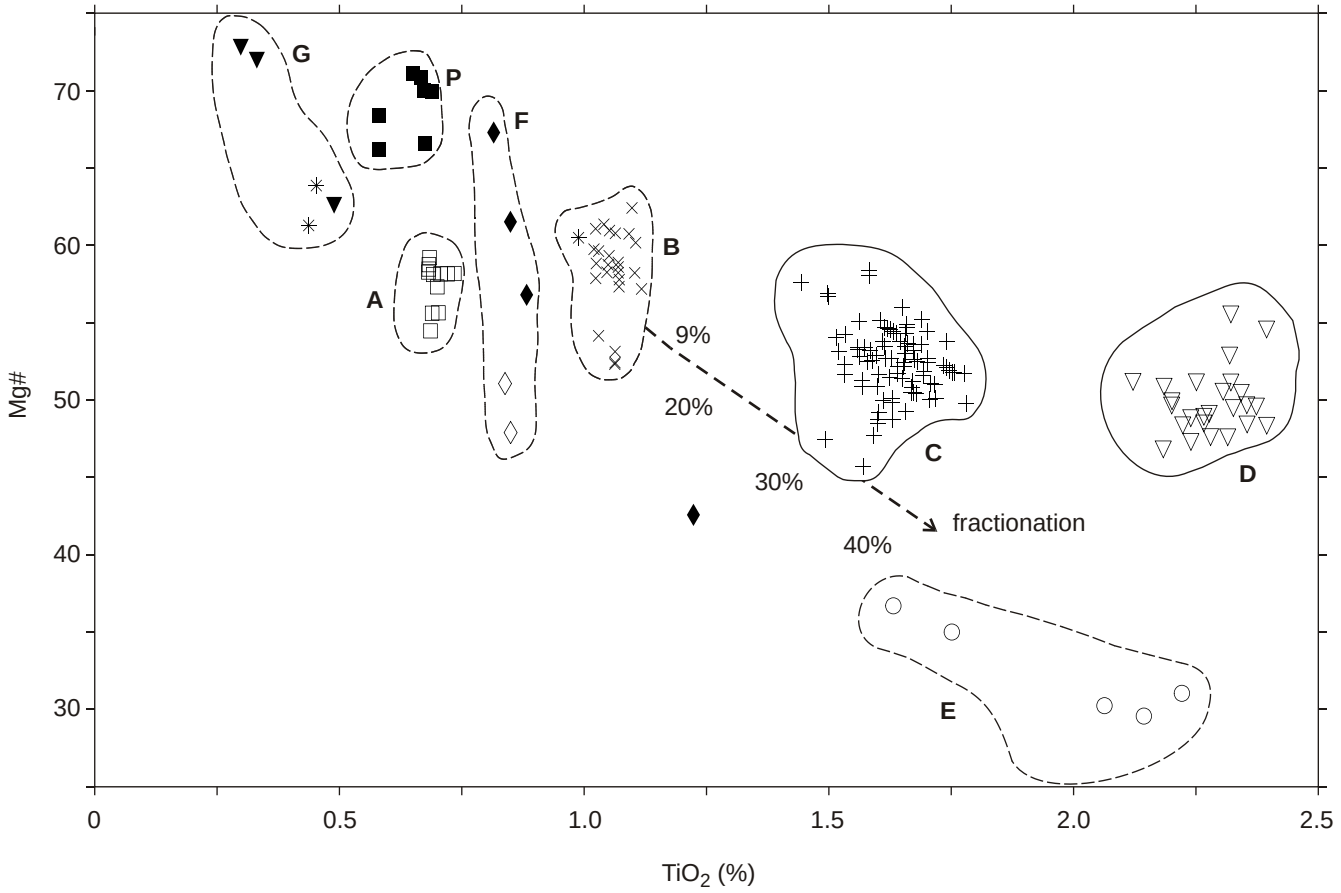

Figure 10

MgO-TiO_2 plot outlining petrogenetic model for the Spinks Creek Volcanics.

is derived from the most enriched source (with Nb/Zr of about 0.45), with groups A, P and probably E from a mildly enriched source (with Nb/Zr of about 0.20). The other groups (B, C and D) are derived from a relatively depleted source (with Nb/Zr of 0.10 or less). The slightly higher Nb/Zr of Group D could be caused by a lower degree of partial melting, as Zr is a less incompatible element than Nb.

Nb/Y varies between the groups in a similar manner to Nb/Zr, and also reflects the relative degree of source enrichment. Ti/Zr is similar in groups B, C and D, consistent with their derivation from the same source by different degrees of partial melting, but the lower values in groups A, P and F again suggest different sources.

These three or four inferred mantle source signatures are interpreted in terms of two components. The first is a relatively depleted, probably asthenospheric component, and is the source of groups B, C and D. The second is an enriched plume component originating in the deep mantle, and is dominant in Group F. The source of groups A and P is inferred to be a mixture of these two components.

The heavy REE and Y increase slightly from Group P, through B and C to Group D, consistent with mildly incompatible behaviour and decreasing degrees of partial melting. They are significantly higher in groups A and F. None of the groups has depleted Y and HREE, or high Zr/Y, which would be expected if garnet had been a residual phase. Thus the partial melting events were either large enough to completely remove garnet from the residue, or took place at lower pressures in the stability field of spinel lherzolite. If the latter is correct, this constrains the depth of melting to less than about fifty to sixty kilometres.

A model for the petrogenesis of the Spinks Creek Volcanics is summarised in Figure 10. The spatial and stratigraphic location of the analysed samples suggest that the oldest flows were the low-TiO_2 Group A, representing a high degree of partial melting of a mildly-enriched mantle source. They evolved by crystal fractionation (olivine-clinopyroxene-plagioclase) mainly in the crust, and Group P rocks are probably, at least in part, complementary cumulates.

The next major group of lavas, Group B, was generated from a more depleted source, also by a relatively high degree of partial melting, and also fractionated in crustal magma chambers before eruption. After the Group B eruptions, some magma remained stagnant at depth, and continued to fractionate. Eventually the magma chamber was replenished by a fresh pulse of primitive magma from the mantle, produced by a relatively low degree of partial melting and thus high in TiO_2. Influx of the fresh primitive magma caused both mixing with the stagnant fractionated magma and a new eruption, to produce the voluminous Group C lavas.

This magma chamber process of stagnation and fractionation, followed by replenishment, mixing and eruption, was repeated, producing the Group D lavas. By now the degree of partial melting in the mantle was low, and the new fresh magma was quite rich in TiO_2.

In contrast, the relatively rare Group E lavas are probably differentiates of Group A magmas, and do not appear to have mixed with another mantle melt. This is supported by the similar shape of their REE pattern, albeit at higher levels (fig. 8*b, h*).

The final phase of volcanism produced the alkalic Group F from a strongly enriched source. Only two Group F lava samples are known, and the remaining intrusive rocks may include some cumulates.

Note that not all the groups are present in any one stratigraphic section. It is particularly noteworthy that the alkalic Group F occurs only west of the Roger River Fault. The relative age of Group P, and to a lesser extent Group F, is poorly constrained, as many of these samples are intrusive rocks.

This geochemical progression of magmatism, erupted in a rift setting, may have been induced by a rising mantle plume. Initially the plume, which was enriched in LREE and other HFSE, but which had entrained LREE-depleted asthenosphere from the deep mantle, impinged against the bottom of the lithosphere, and induced lithospheric stretching and thinning. This enabled the upwelling hybridised mantle to reach depths within the stability field of spinel lherzolite, at which partial melting commenced. The resulting early and relatively deep-sourced, mildly enriched melts thus had a mixed plume and asthenosphere signature. Their characteristic concave REE patterns had LREE dominated by the plume component and the HREE by the asthenospheric component. They produced, after some fractionation, the Group A (and E) lavas and complementary Group P intrusive rocks. Later the thermal anomaly associated with the rising plume reached shallower depths, and relatively voluminous and tholeiitic melts, such as those that fractionated to form Group B lavas, resulted. As the lithosphere stretched and thinned further, the zone of melting rose to still higher levels and successive batches of melt were produced, at lower pressure and temperature, from lower degrees of partial melting. These higher TiO_2 melts rose into the crust and mixed with fractionated magma remaining in magma chambers, and erupted as Group C and ultimately Group D lavas. The final stage of magmatism saw a return to possibly deeper seated alkalic partial melts dominated by the plume component, which produced strongly enriched alkalic Group F lavas.

There is little petrographic or geochemical evidence for contamination by continental crust in the available data; for example K_2O, Rb, Th and U are low (apart from K_2O in Group F). The presence of felsic clasts coeval with basalt in the Croles Hill Diamictite suggests that some associated crustal melts were generated locally.

Studies of radiogenic isotopes (Nd, Sr, Pb), and more high quality analytical data for trace elements such as Nb, Ta, Hf, Th and U, are required to better constrain the model suggested above.

Smithton Dolomite (Psd, Psdc)

Previous work *(JLE, CRC)*

This unit corresponds to the 'Dolomite Stage' or 'Duck River dolomite' described by Nye *et al*. (1934). They considered that two dolomite types were present near Smithton: a fine to very fine-grained type, and a possibly overlying crystalline type. Spry (in Hughes, 1957*a*) formally defined the term 'Smithton Dolomite' and gave the type locality as "immediately west of the Duck River just north of the Smithton–Marrawah Road", an area of limited outcrop. Following Carey and Scott (1952), he correlated tracts now assigned to the older Black River Dolomite with the Smithton Dolomite.

Calver (1995, 1998) divided the Smithton Dolomite, in the lower Montagu River and Smithton areas, into a lower member (500 m) of often thinly bedded dolomicrite with minor dolograinstone and limestone, and an upper member (1000 m) of massive crystalline dolostone with minor limestone. He used Sr, C and O isotope data to suggest early (syndepositional to early diagenetic) dolomitisation of the lower member, and late (burial diagenetic) dolomitisation, possibly by seawater convection, of the upper member. He also suggested a middle to late Ediacaran age (about 580–545 Ma) for the Smithton Dolomite on the basis of strontium isotope stratigraphy.

General features *(JLE, CRC)*

In this area the Smithton Dolomite occurs mostly west of the Roger River Fault. It has a generally negative topographic expression and outcrops are mostly confined to less mature streams and a few road cuttings. Large tracts are concealed beneath alluvium.

The Smithton Dolomite is lithologically much less variable than the Black River Dolomite. The dominant lithology is a grey massive recrystallised dolomite, in which bedding is not always recognisable. Stromatolites and stromatolitic fragments are not known. Intercalated clastic sediments, well bedded or laminated chert, and blotchy black and white chert, characteristic of the Black River Dolomite, are rare. In the main mapped area of silicification in the Smithton Dolomite (indicated Psdc), the derived chert is cream to off-white, and massive with local development of white agate.

Both the lower member, in which sedimentary features are relatively well preserved, and upper crystalline member (Calver, 1995, 1998) are present in this area, but there are few good sections through the unit.

In thin section, the Smithton Dolomite is generally a recrystallised coarse to very fine-grained dolomicrosparite, or less commonly a laminated

dolomicrite. In contrast to the Black River dolomite, peloids or other intraclasts are rare (observed in only about six out of more than thirty thin sections) and poorly preserved. This is the case even in less recrystallised samples from the lower part of the formation.

Field relationships and petrography

Montagu Swamp and Junction Plains area (MPM)

The Smithton Dolomite underlies the low ground flanking the southern Christmas Hills in the Montagu Swamp and Junction Plain area, where it is largely covered by a thin layer of Quaternary alluvial sand. It is probably conformable on the Kanunnah Subgroup and conformably overlain by the Salmon River Siltstone. Outcrop is largely confined to the bottom of deep drainage ditches near 331000/5453000 where there is massive buff to white crystalline dolomite (R002860).

Lower Stephens Rivulet–Lower Keppel Creek area (JLE, CRC)

This tract is a southern continuation of that at Montagu Swamp and Junction Plain. Because the tract is fault bounded, by the Roger River Fault to the east and an inferred thrust to the west, and the dolomite is very poorly exposed and largely silicified, internal stratigraphy is uncertain.

Unsilicified dolomite with well developed karren crops out semi-continuously in Stephens Rivulet for a distance of about 800 m above the Blackwater Road bridge (327830/5443930), up to a creek junction near the inferred position of the Roger River Fault. Typically the rock is medium grey with a cream weathering rind. Most outcrops are massive with only a vague suggestion of bedding, but at 327890/5463620 the dolomite is well laminated with silty to sandy outweathering beds 5–50 mm thick, traceable for several metres. A thin section (sample R004953) consists of very coarse-grained (500 μm–1 mm) pseudopleochroic dolospar, partly replaced by a mosaic of much less even-grained (<20–500 μm) crystalline chert.

Outcrops are very sporadic and mostly submerged in Stephens Rivulet below the bridge. The dolomite is mostly massive and bedding is rarely recognisable. Sample R004944 (from about 328000/5444500) is seen in thin section to consist wholly of recrystallised medium (about 200 μm) and even-grained pseudopleochroic dolospar.

A small low outcrop of very pale grey to off-white, mesoscopically massive dolomite occurs at the base of a road cutting on Blackwater Road opposite the start of spur 3A (327780/5443870). In thin section a sample (R004943) is seen to be an impure dolomite, composed of crystalline, medium and even-grained (mostly 100–200 μm) dolospar (about 75%) and detrital quartz (about 25%) of about the same grain size. Diffuse thin bands of finer and less even-grained dolospar, also with detrital quartz, may define bedding. In other nearby road cuttings, up to five metres of pale grey to off-white cherty lag and white silica sand overlie occasional outcrops of chert and rare dolomite.

Medium-grey corroded carbonate rock, with off-white weathering rinds, crops out sporadically in the meandering bed of lower Keppel Creek for at least 500 m below Blackwater Road. Bedding is usually clear and dips gently to steeply (15° to 70°) to the west. In thin section a sample (R004956 from 328680/5445270) is seen to consist of commonly graded laminae (100–400 μm) of pure fine-grained limestone, often with a faint pelletal texture, interlaminated with less pure, darker but also fine-grained limestone. Thin (≤20 μm) very wavy laminae, rich in a fine-grained opaque mineral, are also present. All are cut by veinlets (up to 1.5 mm, but mostly less than 200 μm wide) of coarse-grained sparry carbonate.

On a low hill near 328300/5445100 there is abundant pebble to cobble-sized float of cream, off-white and pure white chert, derived from the Smithton Dolomite. Some is relatively coarse grained, well crystallised and sparkling, with botryoidal texture and vugs of quartz crystals. This rock approaches agate, but the colourfully banded semi-precious variety prized by gem collectors was not observed.

Exposures of Smithton Dolomite along Blackwater 1 spur road (around 329300/5447000) are very poor and mainly of cream to white, coarse-grained and largely silicified dolomite, with associated chert lag.

A small outcrop of crystalline dolomite on the north bank of the Arthur River (at 326480/5448500) displays faint, irregular, possible cross bedding (dipping at about 30° to the west and right way up) on weathered surfaces. In thin section a sample (R005054) is a pure dolomite (see also Table 4 and *Geochemistry* section), composed of medium to coarse (200–400 μm) and even-grained brownish pseudopleochroic dolospar, with straight grain boundaries. The only obvious impurities are traces of deep red-brown detrital hematitic material. A similar outcrop of crystalline dolomite downstream at 326270/5447990 has fairly good bedding, defined by variations in grain size.

Although the stratigraphic position of these samples cannot be determined from their field relationships, their petrography suggests that they may belong to the upper crystalline member of Calver (1995, 1998).

Upper Salmon River valley (DBS)

Much of the Salmon River valley is believed to be underlain by Smithton Dolomite, mostly obscured by an extensive superficial cover of Tertiary gravel and sand. This northwest-trending belt of dolomite is enclosed by two inferred major faults, one against the Salmon River Siltstone to the southwest, the other against the Kanunnah Subgroup to the northeast. The dolomite apparently wedges out towards the Arthur River to the southeast, due to convergence of these two faults.

Intermittent small outcrops of the dolomite occur in the bed of a westward-flowing tributary of Hawkes Creek, to which access can be gained via a dilapidated bridge on Bark Hut Road at 323080/5449390. Lithologies are similar to those in the Hawkes Creek section (see below), and bedding mostly dips steeply to the southwest (facing direction unknown).

Samples R004276 and R004278 are from low creek outcrops near 322800/5449340, just east of the contact with the Salmon River Siltstone. The former is very recrystallised, consisting of a mosaic of fine-grained sparry dolomite with an average grain size of about 150 μm, with a few areas of coarser spar up to about 1 mm grain size. Some systematic variations in grain size visible in thin section may reflect original bedding, but there is little sign of original sedimentary textures. Sample R004278 is much finer grained and considerably less recrystallised. The thin section shows distinct bedding lamination, and a distinct relict grainstone texture, in the form of rounded possible peloids (≤330 μm in diameter) composed of dark microcrystalline carbonate, which are clearly distinguishable from the paler coloured fine-grained sparry dolomite matrix.

Hawkes Creek valley (DBS)

The Smithton Dolomite is probably about 1050–1100 m thick in the Hawkes Creek valley area, depending on where the concealed, assumed conformable upper contact with the Salmon River Siltstone is judged to be. The lower contact is probably conformable on the Kanunnah Subgroup. Substantial parts of the section are obscured by a superficial cover of Tertiary gravel and sand. The dolomite is well exposed in the bed of the main trunk of Hawkes Creek upstream and downstream of the Chatlee Road bridge. Most outcrops show small to medium-scale karst development, and Hawkes Creek flows temporarily underground through a small flooded cave about 110 m downstream of the Chatlee Road bridge.

Bedding mostly dips steeply to the northeast or southwest. Younging evidence is generally absent, but there is little evidence of mesoscopic folding, and stratigraphic considerations indicate that the whole section probably faces continuously northeast. The most continuous exposure is preferentially along strike, and accounts for a total of probably only about 450 m of stratigraphic thickness in about the middle of the formation. The lower 200 m of the formation is intermittently exposed in the bed of a northeast-flowing tributary of Hawkes Creek (near 321400/5448950). Most outcrops consist of buff-weathering, unsilicified buff to grey massive crystalline dolomite, in which distinct thin bedding and/or lamination is commonly visible. In some outcrops, bedding is defined by thin dolomitic stringers, which show positive relief on weathering. Otherwise, bedding is indistinct or undetectable.

Sample R004266, from an unbedded outcrop underneath the Chatlee Road bridge, is a breccia. It consists of a closed framework of angular fragments, up to 20 mm in diameter, of mostly an even-grained mosaic of crystalline dolomite with an average grain size of 1 mm, in a matrix of finer and less even-grained crystalline dolomite. Some of the fragments still show a jigsaw fit with their neighbours. Internally many of them show definite signs of a relict, possible oolitic grainstone fabric, defined by circular to ovoid cross-sections up to 1 mm in diameter of distinctly darker and finer-grained dolomite. Some of the ovoids show relict finely developed concentric layering, indicating that they were probably ooids.

Lower Blackwater Rivulet area (JLE, CRC)

The Smithton Dolomite crops out poorly in this area, an extension of the Hawkes Creek tract, extending for about seven kilometres south of the Arthur River. The Smithton Dolomite here is also probably conformable on the Kanunnah Subgroup to the west, generally steeply dipping and probably at least one kilometre thick. The top is not exposed as to the east the tract is faulted against other units, probably by a major east-directed thrust fault. This tract is truncated to the south by the Roger River Fault, along which the unit is offset dextrally to reappear in the Upper Blackwater Rivulet area (see below).

Several well-spaced outcrops occur in the Arthur River, including a 100 m long platform, cut into islands by deep solution channels, of massive crystalline dolomite near 323900/5446400. Semi-continuous dolomite outcrops occur along some sections of lower Blackwater Rivulet and some of its tributaries, notably downstream from 327490/5444680, and between 326200/5443130 and 326340/5442710. Away from streams (and in some streams) the unit is usually silicified to a white to pale grey, massive sandy chert, although a few outcrops of unsilicified carbonate rock occur along Blackwater 5 road and its spurs.

LOWERMOST BEDS

The lowermost few hundred metres of the unit are intermittently exposed in Blackwater Rivulet between 325220/5444430 and 325080/5444910, and in a nearby tributary creek between 324790/5444680 and 324930/5445040. These outcrops are of creamy white to pale grey, often well-bedded dolomite with well developed karren and occasional grey-brown outweathering silty patches. A sample (R004949 from 325190/5444440) from about 100 m above the base is seen in thin section to be a dolomicrite or very fine-grained dolomicrosparite with a faint diffuse well-spaced bedding lamination. It contains about 1% detrital iron oxides and is traversed by veinlets (to 1 mm wide) of coarse spar, sometimes with a central zone of quartz. Nearby, at the end of Blackwater 5-3 spur (near 325360/5444560), similar laminated dolomicrite contains minor detrital quartz (sample R004940, Plate 31). Another sample (R004952, Plate 32 from 324820/5444720) from the tributary creek is a very

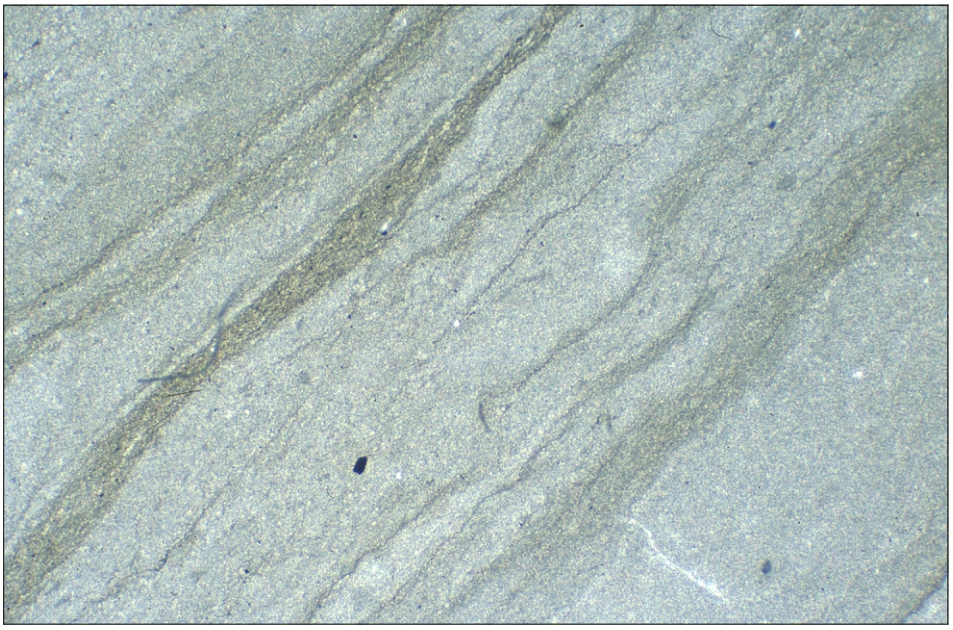

Plate 31

Photomicrograph of sample R004940 (325 360 mE, 5 444 560 mN), lower part of Smithton Dolomite (unit Psd). Laminated dolomicrite. Plane polarised light, field of view 4.4 × 2.9 mm.

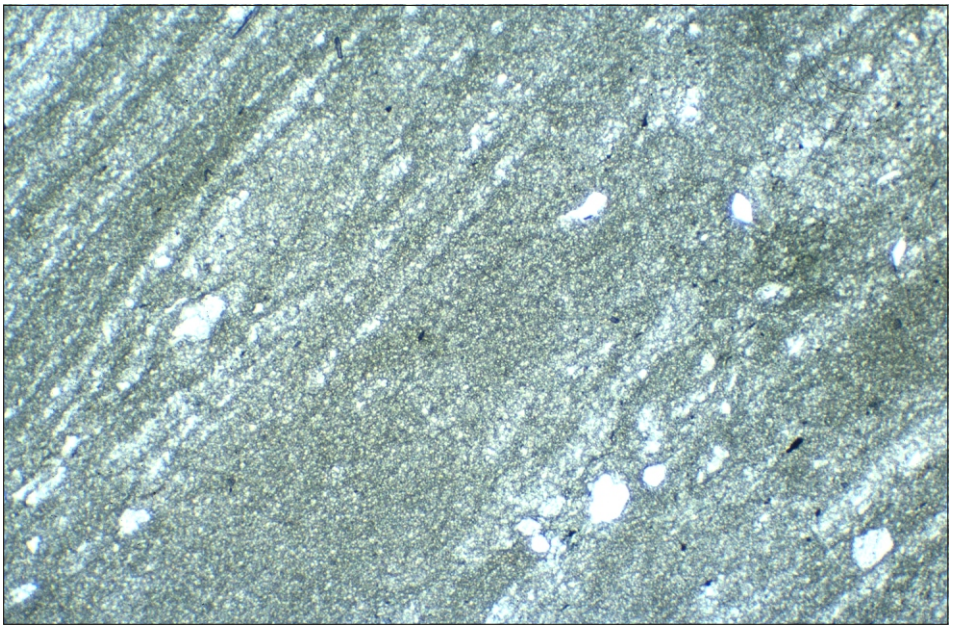

Plate 32

Photomicrograph of sample R004952 (324 820 mE 5 444 720 mN), lower part of Smithton Dolomite (unit Psd). Laminated, very fine-grained, microsparite with minor detrital quartz. Plane polarised light, field of view 4.4 × 2.9 mm.

well laminated, slightly coarser, very fine-grained dolomicrosparite (5–10 μm) containing about 1% detrital quartz sand and silt (polycrystalline and possibly from a metamorphic provenance) and a tenuous dissemination of opaque grains (2–10 μm).

Further south, well-bedded unsilicified dolomite is exposed in a similar stratigraphic position in another tributary of Blackwater Rivulet between 326240/5441260 and 326070/5441350. A thin section (sample R004948 from 326190/5441350) shows a faintly laminated dolomicrite with spar-filled fractures and a very tenuous dissemination of iron oxide.

A 100 m long outcrop of mainly thick bedded to massive dolomite on a bend of the Arthur River (at 323470/5446010) includes, in places, a dolomite-in-secondary dolomite breccia.

Small, near-basal outcrops of bedded dolomite occur in lower Blackwater Rivulet (at 323970/5445630) and submerged in the Arthur River around 323000/5446600.

REMAINDER OF UNIT

Elsewhere in this tract, unsilicified outcrops of the Smithton Dolomite are usually massive to thickly bedded crystalline dolomite. Thin sections mostly consist of usually even-grained pseudopleochroic dolospar, (generally) xenotopic with curved or irregular grain boundaries, to (occasionally) idiotopic with straight grain boundaries. Grain size varies between samples from medium grained (about 60–250 μm) to coarse grained (250 μm–1 mm). Many samples are very pure, but sample R004939 (325470/5444520) contains about 10% detrital quartz. A few samples (R004943, R004953, R004946) show partial replacement of dolomite by a mosaic of commonly very uneven-grained (<20–500 μm) quartz.

Remnant sedimentary textures are rare, but partly leached (porous) and partly silicified grainstone forms prominently outcropping beds in the Arthur River at 323240/5446740. Rare remnant patches of relict catagraphic grainstone can also be seen in thin section in sample R004947 (Plate 33) (326350/5440990). Sample

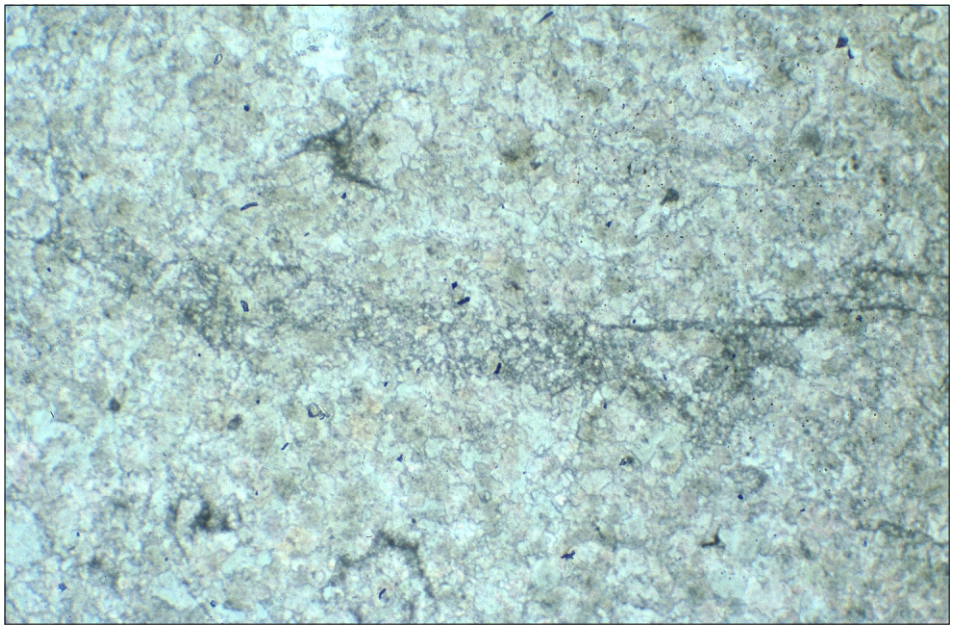

Plate 33

Photomicrograph of sample R004947 (326 350 mE, 5 440 990 mN), Smithton Dolomite (unit Psd): crystalline dolomite with relict catagraphic grainstone texture. Plane polarised light, field of view 4.4 × 2.9 mm.

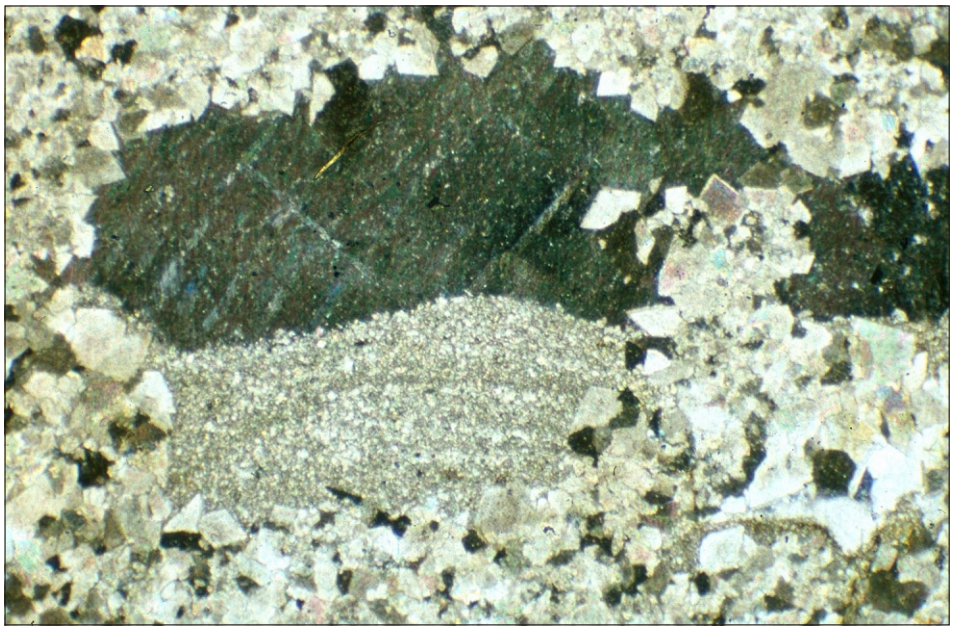

Plate 34

Photomicrograph of sample R004951 (Blackwater Rivulet, 324 420 mE, 5 445 770 mN), Smithton Dolomite (unit Psd). Medium-grained crystalline dolomite; note geopetal vug with fill of fine-grained dolosparite (lower) and coarse-grained calcite spar (upper, in extinction). Crossed nicols, field of view 4.4 × 2.9 mm.

R004958 (326340/5442710), consisting of dark coarse-grained turbid dolospar, has a possible relict peloidal texture in places.

Saddle dolomite (probably non-stoichiometric with undulose extinction) was noted in a very coarse-grained sample (R004941) from Blackwater 5-2 spur (326310/5443170). A medium-grained (100–200 μm) sample (R004951, Plate 34) from an isolated outcrop in Blackwater Rivulet (324420/5445770) contains geopetal vug fills about 3 mm across. These comprise a lower fill of fine-grained diffusely laminated dolosparite, and an upper fill of coarse-grained calcite spar.

Upper Blackwater Rivulet area (DBS)

A correlate of the Smithton Dolomite crops out intermittently in Blackwater Rivulet between about 325400/5437530 and 325960/5437220, immediately east of the Roger River Fault system. Where unsilicified, the common lithology is buff-weathering, light to medium grey crystalline dolomite. Bedding is indistinct or indeterminate, and outcrops commonly have small-scale karst weathering characteristics.

In thin section (sample R006004 from 325400/5437530) the rock consists of completely recrystallised even-grained sparry dolomite with a grain size of about 600 μm, in which evidence of the original sedimentary fabric has been totally obliterated. At some outcrops heavy secondary silicification has resulted in the formation of a thick crust of banded crystalline silica in which textures reminiscent of banded agate are common, completely obscuring evidence of the original lithology.

North of Frankland River (JLE, CRC)

A southerly continuation of the upper Blackwater Rivulet tract occupies a broad flat-bottomed valley, almost extending to the Frankland River near 326600/5432000. Due to difficult access this area was not thoroughly traversed, but bedrock seems to be almost completely covered by alluvium. Good dolomite outcrops are rare and restricted to streams.

The tract is truncated to the west by an inferred thrust and is probably underlain by the lower part of the Smithton Dolomite.

Corroded karstic outcrops of massive to thickly bedded grey dolomite, dipping west at 40° to 50°, occur in the undercut banks of the major creek between at least 326230/5433700 and 326330/5433610, and may extend further downstream. In thin section a sample (R006766 from 326350/5433670) consists of mostly fine but not even-grained (mostly 15–100 μm) dolospar with a diffuse bedding lamination. Sparsely distributed, diffuse ovoid patches about 250 μm across of finer grained and darker carbonate may be poorly preserved peloids. Sample R006764 (326200/5433690) is a massive dolomite which in thin section consists of medium to coarse-grained (mostly 150–250 μm) pseudopleochroic dolospar and probable peloids. The rock is pure apart from a few thin narrow sinuous veinlets of red-brown hematite. Sample R006765 (326230/5433700) is similar but fine to medium-grained (40–200 μm), and also contains probable peloids.

In a minor tributary to the west there are sporadic outcrops of off-white to orange-stained, sandy textured silicified dolomite and white massive to banded agate.

Near 326500/5432600, a 900 m chain-and-compass traverse of the meandering main creek covered a net distance of only 350 m without finding outcrop, but a corroded probable outcrop of cream-coloured, apparently massive dolomite occurs further south at 326550/5432000. In thin section this rock is seen to be completely silicified, and consists of a very uneven-grained mosaic of allotriomorphic quartz (400 μm–1 mm), with a vague banding defined by grain size variations. The next outcrop at 326780/5431570, less than 200 m from the Frankland River, is a bluish grey siltstone assigned to the Keppel Creek Formation, suggesting that the Smithton Dolomite tract does not reach the river.

The transition between the Smithton Dolomite and the underlying Keppel Creek Formation occurs within a discontinuous 400 m long creek section between about 326960/5432880 and 327320/5432940. Typical massive pale grey to brown corroded dolomite passes eastward upstream and stratigraphically downwards to diffusely laminated lead-grey impure dolomite and dolomitic siltstone, and thence to Keppel Creek Formation rocks (see *Field relationships: other southern areas*). The stratigraphic thickness of the transitional sequence is probably about twenty to thirty metres. In thin section, a sample (R006670B, 327040/5432890) of the basal impure dolomite consists of fine (10–40 μm) to very fine-grained (5–10 μm) dolospar and abundant (5–10%) small (5–15 μm) blebs of an opaque mineral, which locally coalesce into larger aggregates. The finer-grained laminae also contain 5–15% detrital quartz silt.

Geochemistry *(JLE)*

Only one sample (R005054) of Smithton Dolomite was analysed during this project (Table 4). This was a relatively pure, nearly stoichiometric dolomite with small amounts of impurities, probably mainly silica (1.7%) and apatite (0.5%). The low Sr (54 ppm) is more typical of values reported by Calver (1998) from the lower member (70 ± 15 ppm) than the upper member (122 ± 41 ppm). Apart from Zn (24 ppm), other elements are close to or below XRF detection limits.

This sample is less pure than four (T7–T10) dolomite samples collected from limited outcrops in the Montagu Swamp near the northern margin of the Roger map sheet (Threader, 1992), but is comparable to some samples from the Black River Dolomite (see above and Table 4).

Isotope chemostratigraphy of the Smithton and Black River dolomites *(CRC)*

The Black River and Smithton dolomites are juxtaposed by faulting in the western part of the Sumac map sheet, and may be lithologically difficult to distinguish. Six dolomite samples from this area were analysed for stable isotopes (Table 7) in order to provide an additional check on the identity of some outcrops. Isotope-stratigraphic studies of the Black River and Smithton dolomites (Calver, 1995, 1998) showed that the two formations can, in part, be distinguished by their stable isotopic compositions. The lower part of the Black River Dolomite is characterised by more ^{13}C-enriched compositions (greater than +3‰) than younger horizons. The upper part of the Smithton Dolomite is characterised by relatively ^{18}O-depleted compositions, at least in part a diagenetic overprint

Table 7

Isotope analyses, selected dolomite samples

Reg. No.	Field No.	Anal. No.	AMG (mE)	AMG (mN)	$^{13}C_{PDB}$	$^{18}O_{PDB}$	Rock unit
R004936	FJ36	7274	327570	5446850	0.204	-7.568	Black River Dolomite
R004954	FJ1034	7275	326340	5444270	0.536	-4.828	Smithton Dolomite
R004834	FJ1079	7276	326420	5442820	0.789	-7.990	Black River Dolomite
R004976	FJ1135	7277	326410	5444750	-0.981	-4.829	Black River Dolomite
R004957	FJ1175	7278	326430	5442600	-1.382	-5.815	Smithton Dolomite
R004959	FJ1177	7279	326580	5443580	-0.186	-7.509	Smithton Dolomite

Analyses at Central Science Laboratory, University of Tasmania
Analyst: M. Power

(Calver, 1998). There is considerable overlap in the isotopic compositions between the upper Black River Dolomite and the lower Smithton Dolomite.

Carbon isotopic compositions of the analysed samples lie between -1.4 and +0.8‰, with oxygen between -4.8 and -8.0‰ relative to PDB (Table 7). Unfortunately, none of the six analysed samples can be unequivocally assigned to a formation based on the results. Samples R004957, R004976 and R004954 may belong to either the upper part of the Black River Dolomite or the lower part of the Smithton Dolomite, on the basis of the previous work. The remaining three samples could also belong to the upper part of the Smithton Dolomite. None of the six samples is from the lower part of the Black River Dolomite.

Early Cambrian: Salmon River Siltstone (Psr)

Definition

The Salmon River Siltstone is herein defined as that unit of black to dark grey, pale grey to green weathering thin-bedded, fissile, planar laminated siliceous siltstone, mudstone and shale that crops out on a spur of Molompto Road (southern Christmas Hills area) south of 331 200 mE, 5 457 800 mN, where it is probably unconformably overlain by the Scopus Formation, to about 331 300 mE, 5 457 400 mN. The lower contact is nowhere exposed but is probably conformable on the Smithton Dolomite. The formation is probably up to 350 m thick and contains inarticulate brachiopods and sponge spicules suggesting an Early to Middle Cambrian age.

Field relationships and petrography

The Salmon River Siltstone is a newly recognised formation that occurs, probably discontinuously, at the top of the Togari Group in the Roger and Sumac map sheets.

Hawkes Creek–Salmon River area (DBS)

Between the Hawkes Creek and Salmon River valleys the Salmon River Siltstone crops out intermittently along the crest of a low narrow ridge which extends southeastward for some 6.5 km from near 352000/5420000, at the western edge of the Roger map sheet, to about one kilometre northwest of the Arthur River. Along the length of this ridge the unit is commonly obscured by a blanket of ?Tertiary siliceous gravel and quartz sand. The formation may be up to about 350 m thick in this area, although the position and nature of the inferred conformable lower boundary with the Smithton Dolomite is uncertain due to lack of outcrop, and the upper boundary is an inferred fault.

The most common lithology in the Salmon River Siltstone in this area is pale grey-weathering, silicified, thin-bedded, finely plane-laminated siltstone. This facies is well exposed in a large gravel pit around 322380/5449840. Sample R004273 from this locality has a distinct lamination in thin section, enhanced by a component (about 5%) of thin elongate silicified objects (?spicules), ≤400 μm long and composed of microcrystalline quartz; these show a strong preferred orientation parallel to bedding and are set in a siliceous microcrystalline matrix. Sample R004267, float from a small pit beside Bark Hut Road at 323410/5448390, is similar in thin section but also contains about 10% of quartz clasts ≤40 μm in diameter.

A less common facies variant is represented by sample R004270 from another shallow pit beside Bark Hut Road at 323910/5447420, close to the southeastern limit of exposure of the Salmon River Siltstone in this area. This lithology is a dark grey-black siliceous shale with prominent plane lamination and bedding fissility, the latter partially due to the presence of a high percentage of microscopically unresolvable dark material which forms thin, wispy, discontinuous layers parallel to bedding. The rock contains a <3% component of scattered quartz clasts generally ≤80 μm in diameter. In addition, scattered throughout the rock are black spine-shaped bodies up to about 500 μm long, and their equivalent circular and ellipsoidal cross sections. These objects are probably spicules. There are also a few small elongate to ovoid, shell-like cross sections up to 300 μm long, and which consist of a thin outer layer of microcrystalline quartz surrounding a translucent brown cryptocrystalline (phosphate?) filling. These objects are also almost certainly organic in origin, possibly juvenile inarticulate brachiopods.

The best exposures of the Salmon River Siltstone occur along strike from the outcrops in the Hawkes Creek–Salmon River area, in a large quarry at 319120/5453220 near the eastern margin of the Bluff map sheet. Several small fossils collected from this quarry have been identified as inarticulate brachiopods, suggesting an Early to Middle Cambrian age (J. R. Laurie, Australian Geological Survey Organisation, pers. comm.). An independent examination of samples from this quarry yielded two species of inarticulate brachiopods, a few cruciform stauract sponge spicules, and elliptical blobs about 20 mm in diameter which may be sponge bodies (J. B. Jago, University of South Australia, pers. comm.).

Christmas Hills area (MPM)

The Salmon River Siltstone is poorly exposed on the lower slopes of the southern part of the Christmas Hills. The formation is believed to rest conformably on the poorly exposed Smithton Dolomite, which is mostly covered by Quaternary alluvial sand in the low ground of the Montagu Swamp and Junction Plain area south of Christmas Hills. The contact between the two units is not exposed. It is overlain, probably unconformably, by Scopus Formation, which forms the higher parts of Christmas Hills.

The best exposures of the unit are found in road cuttings on logging tracks and at a quarry at 331320/5457630 in the Molompto Road area. The rock type in the quarry is a pale grey to pale green-weathering, well-bedded silicified siltstone. The siltstone is finely laminated with thin mudstone

interbeds. In thin section a sample (R002843) from this locality has abundant small quartz grains (≤30 μm) set in a fine-grained siliceous matrix with fine opaque grains and mica flakes. Bedding lamination is present and fine quartz veining is common.

A single small macrofossil, possibly a phosphatic brachiopod (J. R. Laurie, pers. comm.) was recovered from this quarry. Also present at this locality are sparse small (≤2 mm) oval or rod-shaped structures, consisting of an outer zone of microcrystalline quartz and an inner zone of fibrous quartz or translucent brown cryptocrystalline (phosphatic?) material. These structures may represent some organic body in different orientations.

Elsewhere the rock type has been mapped based on the presence of a pale grey sandy soil with abundant small angular chips of pale grey to white silicified siltstone. This soil and float type contrasts with the rich red/brown soil and siltstone/sandstone fragments found in the areas of the overlying Scopus Formation.

Middle to Late Cambrian: Scopus Formation (Cm)

Definition *(JLE, MPM)*

The Scopus Formation is herein defined as that unit of turbiditic, thin to thick-bedded, coarse to fine-grained lithicwacke sandstone, granule conglomerate, siltstone and mudstone that lies in the core of the Smithton Synclinorium. It crops out between Stony Point (329 300 mE, 5 487 600 mN) near Montagu and 331 200 mE, 5 457 800 mN in the Christmas Hills area, where it probably overlies, probably unconformably, the Salmon River Siltstone. The type section is formally designated as the Bass Highway between Brittons Swamp (328 900 mE, 5 469 000 mN), where it is inferred to unconformably overlie the Smithton Dolomite, to a road junction at 331 300 mE, 5 470 100 mN, near where it is overlain by a minor Tertiary basalt flow. No stratigraphic top to the formation is known. Its age is constrained by Late Middle and Early Late Cambrian marine fossils.

This unit has long been recognised but has not previously been formally named. It is equivalent to 'Stage 6: Upper Slate and Breccia' of Nye *et al*. (1934). An inferred Cambrian age was confirmed by the discovery of macrofossils at Christmas Hills by A. B. Gulline in 1956 (Gulline, 1959; Banks, 1962), and several other fossil localities have since been discovered (Jago and Buckley, 1971; Jago, 1976; Baillie, 1981; Rickards *et al*., 1990; Jago and Baillie, 1992).

The incorrect correlation of the Black River Dolomite and Smithton Dolomite (see *Togari Group: previous work*) led many authors (e.g. Lennox *et al*., 1982) to group all clastic sedimentary and volcanosedimentary successions in the Smithton 'Trough' into a single (Cambrian) unit, thus combining the Scopus Formation and the Kanunnah Subgroup. The re-recognition of two major dolomite units in the Togari Group implies that two clastic sedimentary successions are also present.

Field relationships and petrography *(MPM)*

Christmas Hills area

In the higher areas of the Christmas Hills, in the central northern part of the Roger map sheet, the Scopus Formation is very poorly exposed and generally very weathered. Outcrops are confined to creeks and road cuttings, and elsewhere the unit was mapped from float and the presence of a rich red to brown soil. The formation consists of generally well-bedded, red to brown weathering, polymict lithic conglomerate, lithicwacke and siltstone/mudstone.

In this area, the mapped distribution of the Scopus Formation and the underlying Salmon River Siltstone suggests that the boundary between them is gently dipping. Both formations are poorly exposed and deeply weathered in low road cuttings near 329500/5456600, but contrasting attitudes of bedding readings suggest an unconformity between them. Because of this relationship, and a significantly younger fauna, the Scopus Formation is excluded from the Togari Group.

The best outcrops of conglomerate, although very weathered, occur on a track at 331300/5458000 where there are rounded pebbles of up to 50 mm. The freshest rock was found in small creeks draining east near 332480/5458890. In thin section, samples R002870, R002871 and R002872 (Plates 35–37) from this area are poorly sorted, lithic sandstone and siltstone. Lithic clasts are of various sorts and include fine-grained mudstone of different types, serpentinite and sparse fine-grained felsic lava, quartzite and chert. Monomineralic clasts include quartz, opaque mineral and rare plagioclase. The clasts are subangular to subrounded.

A late middle Cambrian marine fossil fauna at Christmas Hills (331200/5467900) (Jago and Buckley, 1971; Jago, 1976) indicates that at this locality the unit is a biostratigraphic correlate of the Trial Ridge Beds (Adamsfield Trough) and, probably, the topmost lower Dundas Group near Zeehan (e.g. summary of Jago and Brown, 1989). An early Late Cambrian marine fossil fauna at Scopus (333500/5480600) (Baillie, 1981; Rickards *et al*., 1990) indicates biostratigraphic correlation with the Singing Creek Formation (Denison Group, Adamsfield Trough) and the upper Dundas Group. Both localities are in the more northern part of the Christmas Hills, outside the area described in this report.

Two lithofacies associations have been recognised in the Scopus Formation on the north coast at Stony Point, where there is more complete exposure (Baillie and Jago, 1995). These are a thin-bedded association of fine or very fine-grained sandstone, siltstone and mudstone, and a coarse-grained association of thick-bedded coarse to very coarse-grained sandstone, pebbly sandstone and granule conglomerate. The rocks were considered to have been deposited within a submarine basin-floor turbidite-fan complex. Palaeocurrents from both associations are directed north.

The rocks in the area under discussion belong dominantly to the coarse-grained association, and are distinguished from those to the north by having a much larger component of ultramafic-derived detritus in the form of conspicuous clasts of serpentinite. The nearest present-day outcropping ultramafic body which could have provided such clasts is the Early Cambrian (?) Heazlewood Complex, 55 km southeast of Christmas Hills (Brown, 1986). The greater ultramafic-derived component in the rocks of the southern Christmas Hills compared to those at Stony Point, together with the palaeocurrent directions, are consistent with a source to the southeast. Analysis of detrital spinel grains in the Scopus Formation has provided further constraints on possible source rocks (see Appendix 3).

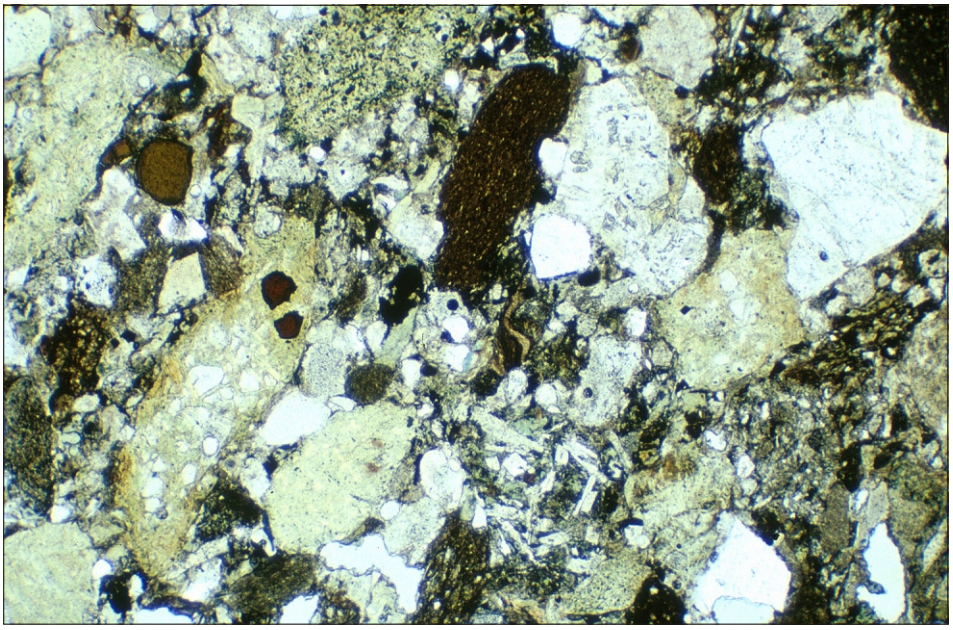

Plate 35

Photomicrograph of sample R002872, Scopus Formation (unit Cm) (from near 331 300 mE, 5 458 000 mN). Poorly sorted polymict lithic sandstone. Note grains of very dark red-brown chrome spinel (central and upper left), plagioclase (lower middle) and quartz. Plane polarised light, field of view 4.4 2.9 mm.

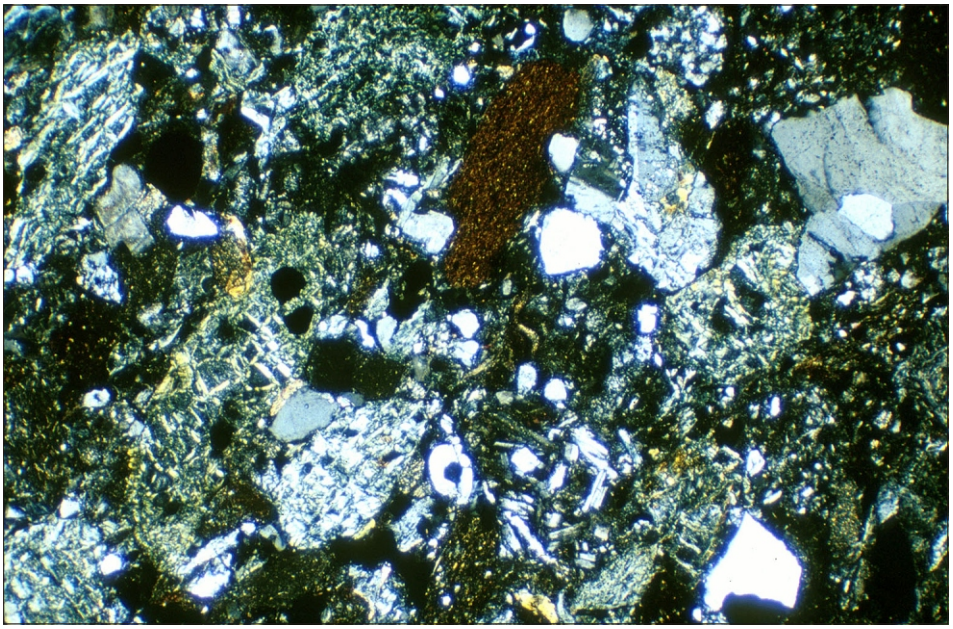

Plate 36

Photomicrograph of sample R002872, Scopus Formation (unit Cm). Same view as Plate 35, crossed nicols.

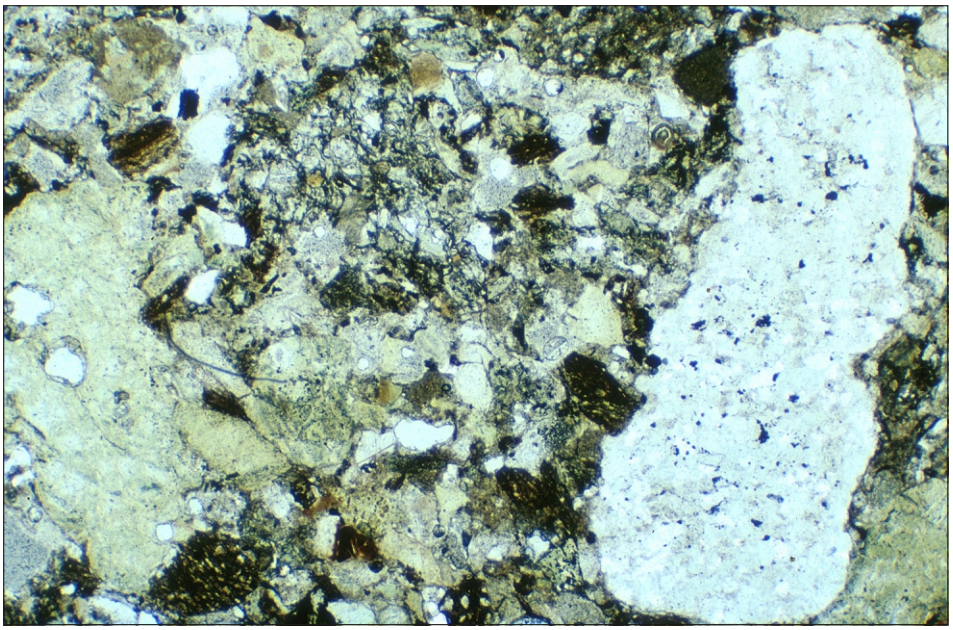

Plate 37

Photomicrograph of sample R002872, Scopus Formation (unit Cm). Note large serpentinite clast at right. Plane polarised light, field of view 4.4 2.9 mm.

Alkalic dykes of unknown age (south of The Clump)

Field relationships *(ARR)*

Weathered pale grey-green to orange-coloured dykes occupy northeast-trending faults along the Heemskirk Road near The Clump (at 321150/5436150), and also further south at 321900/5432000. The faults are syn to post-D_3 in age and link to the northeast with the regional-scale Roger River Fault (see *Structural Geology* section). The dykes are up to about one metre wide and contain angular inclusions to 200 mm wide of country rock. Despite weathering, the dykes still show an aligned porphyritic texture in hand specimen.

Petrography *(ARR)*

Thin sections of the dyke material reveal angular to pseudo-hexagonal and tabular phenocrysts to 3 mm in length of microcrystalline quartz after what was probably originally amphibole and feldspar, respectively. The phenocrysts are poorly preserved and commonly fractured, and rarely show remnant zoning. The matrix is of a mottled pale brown and cryptocrystalline nature.

Geochemistry *(ARR, JLE)*

The analysed sample (R980095, Table 3) is so altered that the chemical analysis needs to be considered with extreme caution. Major elements, other than SiO_2, Al_2O_3 and TiO_2, have been leached out to almost negligible levels. The high H_2O^+ (10.92%) is indicative of the severity of alteration, whilst CO_2 (2.05%) may indicate analytical difficulties (possibly trapped air rather than CO_2 driven off) as there are virtually no major elements (e.g. CaO, MgO, FeO) with which it could be combined.

Relatively high Cr (760 ppm) may indicate an originally mafic or ultramafic composition.

Probably the only other potentially diagnostic elements are the relatively immobile high field strength elements such as Ti, Zr, Nb and Ce, and also perhaps Pb and Th. Their high abundance in The Clump dyke, although probably further enhanced due to mass loss of major elements during alteration, suggests strongly alkalic affinities. Table 8 compares the ratios of these elements, which are more likely to be little modified during alteration, with those of some other mafic rocks in western Tasmania.

The mainly tholeiitic dykes of the Rocky Cape Dyke Swarm, together with the bulk of the Spinks Creek Volcanics, have much lower Nb/Zr and Nb/Y and are therefore unlikely correlates. Similar considerations apply to the widespread but rare Devonian lamprophyres, which in addition are demonstrably post tectonic (Baillie and Sutherland, 1992). Some alkalic suites, such as rare dykes on Hunter Island (Everard *et al*., 1997), the Cooee Dolerite further east in the Rocky Cape Region, and the Group F phase of the Spinks Creek Volcanics, also have considerably lower Nb/Y but higher Nb/Zr. A hornblende-phyric dyke of unknown age on Councillor Island (near King Island) also differs radically in these ratios and in Ti/Zr.

The Clump dyke has particularly high Ce/Y, Pb/Ce and Th/Ce, but some of these elements may not be completely immobile under such extreme alteration. In addition, Pb and Th are difficult to determine reliably by XRF at low concentrations.

Geochemically, the most similar rocks are some Tertiary alkali basalts (e.g. sample WB17), but field evidence (mode of occurrence, foliation and possibly the severe alteration of The Clump dykes) precludes any relationship.

Discussion *(ARR, JLE)*

The dykes are foliated, faulted, and variably silicified, and were probably emplaced during the latter stages of faulting. They probably represent a previously unrecognised igneous phase of Neoproterozoic or Early Palaeozoic age.

Fresh dyke material crops out on the coast near Temma (306850/5430850) in apparent extensions (from regional aeromagnetics) of the Roger River Fault splay near The Clump. This rock is massive, fractured and variably silicified in outcrop. In thin section, pseudomorphed phenocrysts up to 1.5 mm long of former euhedral hexagonal amphibole are replaced by quartz and lie in a fine-grained (to 25 μm) aggregate of pale brown biotite (phlogopite). The Temma rock is probably related to the dykes near The Clump, but no chemical analysis is yet available.

Table 8

Immobile trace element ratios, alkalic dyke near The Clump: comparison with other western Tasmanian dyke and/or mafic rocks

Suite	Sample		Ti/Zr (ppm)	Nb/Zr (ppm)	Nb/Y (ppm)	Ce/Y (ppm)	Pb/Ce (ppm)	Th/Ce (ppm)	Cr (ppm)
	Reg. No.	Field No.							
The Clump dyke	R004772		68.9	0.27	4.8	6.4	0.36	0.55	270
Devonian lamprophyre	R101698		26.7	0.05	0.36	4.5	0.36	0.14	830
Devonian lamprophyre		MH111	41.3	0.04	0.27	4.2	>0.04	0.18	560
Devonian lamprophyre		MH258	72.8	0.10	1.21	4.6	0.06	0.06	580
Hornblende porphyry dyke		CN3	14.5	0.10	1.25	4.9	0.13	0.14	39
Cooee Dolerite	93220001*		67.8	0.32	2.21	2.32	0.08	0.09	151
Cooee Dolerite	93220002*		60.8	0.40	2.49	2.86	0.03	0.07	91
Rocky Cape dyke swarm		TJ377	54	0.09	0.52	1.48	<0.32	<0.32	330
Rocky Cape dyke swarm	R006778	MJ925	72.9	0.09	0.42	1.54	0.3	0.43	97
Spinks Creek Volcanics (Group F)	R004872	FJ145	52.2	0.46	1.68	2.76	<0.10	<0.10	11
Spinks Creek Volcanics (Group F)	R004884	FJ363	37.4	0.45	1.93	2.63	<0.13	0.13	390
Spinks Creek Volcanics (Group F)	R004892	FJ481	45.8	0.44	1.6	2.13	<0.16	0.17	12
Tertiary basalt		WB17	76.4	0.25	3.22	5.44	0.17	0.19	195

* AGSO Registered Numbers

Data sources:

R004772 Weathered deformed dyke near The Clump (Table 3, this report)
R101698 Prince Lyell mine, dated at 363 3 Ma (Baillie and Sutherland, 1992)
MH111 Varna Bay, Macquarie Harbour quadrangle (McClenaghan and Findlay, 1993)
MH258 Near Nielsen River, Macquarie Harbour quadrangle (McClenaghan and Findlay, 1993)
CN3 Hornblende porphyry, unknown age, Councillor Island, near King Island (Everard *et al*., 1997)
93220001 Cooee Dolerite (Black *et al*., 1997)
93220002 Cooee Dolerite (Black *et al*., 1997)
TJ377 Dolerite dyke, Rapid River, 344150/5440660 (J. L. Everard, unpublished data)
MJ925 Dolerite dyke, Dempster Plains, 339130/5430170 (this report)
FJ145 Gabbroic intrusive, 325670/5439830 Blackwater Road (this report)
FJ363 Gabbroic intrusive, 325590/5441260, Blackwater Rivulet tributary (this report)
FJ481 Lava, 325160/5444050, Blackwater Rivulet (this report)
WB17 Nepheline hawaiite, Montagu, 327830/5484120 (Everard and Seymour, in prep.)

Siliceous gravel with interbedded quartz sand and clay (Tsgs)

Salmon River–Dunns Plain area *(DBS)*

Large parts of the Salmon River and Hawkes Creek valleys, and most of the Dunns Plain area surrounding the southern part of Lovells Creek Road, are covered by an extensive blanket of mostly unlithified, white to pale grey siliceous gravel and quartz sand, of probable Tertiary age. Some of the gravels are closed-framework and moderately to well sorted, as shown in exposures on Chatlee Road between the intersections with Chatlee 1 spur road and Black Jay Road, but this fabric type merges into sandy gravel and pebbly sand. Clasts in the gravel are rounded and ≤50 mm in diameter, and consist of quartzite, white quartz and uncommonly, black chert, in a white to pale grey well-sorted quartz sand matrix. Distinct stratification may be present, and the clasts commonly show a tendency towards alignment parallel to bedding, with suggestions of imbrication in some places. Well-sorted, fine, medium and coarse-grained, white to pale grey quartz sand is interbedded with the gravel. Some of the very fine-grained sand is almost flour-like in texture. On Dunns Plain, just west of the western boundary of Sumac map sheet (at 319920/5447700), a side track leading west off Lovells Creek Road exposes at least 1.5 m of white siliceous gravel overlying dark brown-black semi-indurated sandy peat which may represent a palaeosol.

The sediments are silicified at a number of localities, for example at 322330/5449290 on Chatlee Road where large bouldery float of silicified gravel occurs in grey sandy soil by the roadside. Sample R004280 from this locality is essentially a siliceous conglomerate, but texturally it represents a more poorly-sorted variant of the gravel facies. It consists of an open framework of subrounded to subangular clasts ≤35 mm in diameter, composed of metaquartzite (dominant) and quartz (subordinate), together with rare tabular clasts of black chert or siliceous shale up to 10 mm in length. The matrix is a poorly to moderately sorted quartz sandstone with a microcrystalline siliceous cement. Silicification of quartz sand along a low, broken, northwest-trending ridge which crosses Chatlee Road near 322220/5448250 has resulted in patchy development of banded agate and quartz crystal-lined vugs and geodes. Field relationships suggest the partial development of a silicified cap rock in the sand and gravel along the crest of this ridge.

These sediments are similar to those occurring intermittently beneath and intercalated within Tertiary basalt successions in the Trowutta 1:50 000 scale quadrangle (Everard *et al*., 1996), to the east of the Roger and Sumac map sheets. The combination of lithology, facies relationships and sedimentary structures suggests that the sediments are of alluvial origin.

Arthur River–Blackwater Road area *(DBS)*

Between the Arthur River near the western margin of the Sumac map sheet and Blackwater Road, some seven kilometres to the southeast, Rocky Cape Group correlates are largely obscured by a superficial veneer of unlithified white siliceous gravel and quartz sand of probable Tertiary (?pre-basalt) age, the same unit as that in the Salmon River–Dunns Plain area (see above). On Blackwater Road the unit shows rapid variations in thickness up to a maximum of about five metres. Some of the sand in the sequence weathers to a dark brown-black colour and is probably peaty.

The Clump–Balfour area *(ARR)*

The plains in the Balfour area, west of the Frankland River, are largely covered by a veneer (typically less than one but up to five metres thick) of loose to poorly indurated white to pale grey gravel and, more rarely, variably organic-bearing quartz sand and clay. The gravel is comprised of up to 80% rounded sub-spherical quartz pebbles to cobbles, to 100 mm diameter, in a well-sorted unconsolidated to poorly indurated sand matrix. Discrete bedding planes are typically not apparent, with stratification of the gravel beds evident as variation in the ratio of clasts to matrix. Sand-rich layers contain variable quantities of organic matter (up to about 10%) and rarely grade into organic-rich clay.

Deposits of variably indurated organic-rich sand and clay interfingering with poorly-sorted gravel are incised into the Proterozoic basement southwest of Balfour (e.g. at 324030/5427150). The deposits are dendritic in plan and are interpreted as Tertiary channels originally draining the slopes of Mt Frankland and Mt Balfour. Channel margins are commonly defined by silicified grey-billy talus that comprises poorly-sorted angular quartzite and shale clasts to 200 mm diameter in a sandstone matrix. Layering, apparent as variation in clast size, dips at angles of up to 30° towards the channel centre. Channel centres typically comprise poorly indurated and variably organic-rich sandstone and less common quartz pebble conglomerate.

Headwaters of Blackwater Rivulet and Julius River *(ARR)*

Well-sorted cream to orange-coloured poorly to well-indurated and commonly vuggy quartzose sandstone locally underlies Tertiary basalt. This unit is poorly outcropping and is typically evident only as float and within streams. It is not present everywhere, and Tertiary basalt commonly rests directly upon Proterozoic basement.

Indurated quartz sand with plant fossils (Tqs)

A small tract (about 20 ha) of deposits of this description was mapped by Brown (*in* Everard *et al*., 1996), capping a small hill (337200/5447200) north of Cannon Creek on the Sumac map sheet. The deposit rests on Black River Dolomite and is apparently overlain by cherty lag (unit Qhl).

Basalt (Tb, etc.) *(JLE)*

Most areas of Tertiary basalt occur in the Dempster map sheet, as usually thin dissected flow remnants. The basalt is thicker near 330100/5438500, suggesting a possible feeder nearby. A small area of basalt at Molompto Road (332650/5459800), on the northern margin of the Roger map sheet, is petrologically dissimilar and may be an unrelated plug or small flow remnant.

In the following section the classification scheme of Johnson and Duggan (1989), based on CIPW norms calculated at $Fe_2O_3/FeO = 0.20$, is applied to those Tertiary basalts for which chemical analyses are available.

Molompto Road

Field relationships

This small area (about 12 ha) of basalt rests on Scopus Formation rocks, capping a small hill (332600/5459800) at an elevation of 100–130 m, close to the northern margin of the Roger map sheet. It lies in the extreme southwest corner of the Smithton Quadrangle, but is not depicted on the 1:50 000 scale Smithton geological map.

The basalt is fine grained and black in hand specimen, and contains sparse small (up to 5 mm) lherzolite nodules. It has a magnetic susceptibility of about 12×10^{-3} SI (mean of twenty field measurements, range 6.5 to 24.8) and is associated with a small positive aeromagnetic anomaly.

Petrography

In thin section (sample R005373 from 332470/5459770) (Plate 38), there are abundant euhedral microphenocrysts of olivine (≤500 μm) and pale yellow augite (mostly ≤200 μm, often zoned and twinned) in a fine-grained groundmass of abundant equant opaque blebs (mostly 10–50 μm) and a low birefringence, indeterminate mesostasis. Plagioclase is absent. X-ray diffraction shows that this groundmass consists of alkali feldspar (probably sanidine), nepheline, analcite and apatite.

Rare anhedral xenocrysts of olivine (≤1 mm, surrounded by fine-grained recrystallised reaction rims) and pale yellow-brown spinel (≤250 μm, with opaque reaction rims) represent disaggregated lherzolite debris.

Pale yellow-brown to darker, more oxidised alteration products of olivine and augite occur patchily throughout the slide.

This rock resembles a nepheline hawaiite occurring in a similar situation about three kilometres to the NNW on Poilinna Road (Everard and Seymour, in prep.), but contains generally larger and more abundant augite grains and a finer grained mesostasis.

Geochemistry

An analysis of this rock (Table 9) shows that it is normatively a strongly undersaturated nepheline mugearite, similar to, but even more evolved than, the Poilinna Road rock. Very few known Tasmanian basalts are as alkalic, and especially as potassic, as these samples. Probably the most similar are the mafic nepheline benmoreites of Lower Sandy Bay and Droughty Hill near Hobart (Aurousseau, 1926; Spry, 1955; Sutherland, 1976).

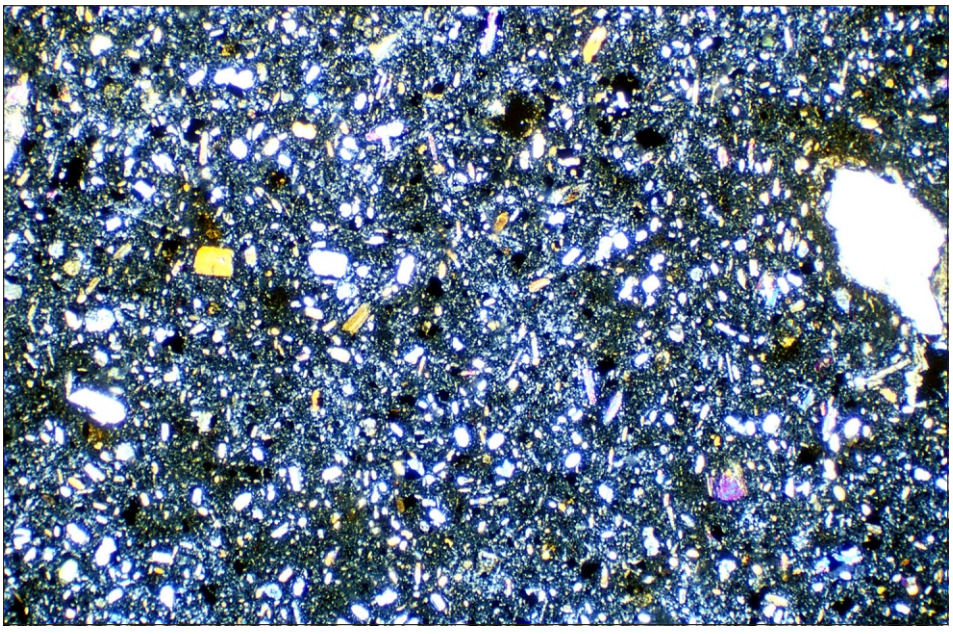

Plate 38

Photomicrograph of Tertiary basalt, potassic nepheline mugearite, sample R005373 (Molompto Road, 332 470 mE, 5 459 770 mN). Olivine and augite microphenocrysts in a fine-grained, opaque-rich, mesostasis. Plagioclase absent. Olivine xenocryst at right. Crossed nicols, field of view 4.4 2.9 mm.

Table 9

Chemical analyses, Tertiary basalt

Reg. No.	R005373	R006791	R006793	R004965	R006798	R004964	R004962	-
Field No.	TJ3600	MJ729	MJ763	FJ1113	MJ2173	FJ321	FJ30	Y1
Analysis No.	930731	980393	980394	961107	990468	961106	961103	-
AMG (mE)	332470	328380	327840	331360	330270	324360	325000	324800
AMG (mN)	5459770	5432200	5434370	5439990	5438630	5435260	5430320	5430000
SiO_2 (wt %)	45.20	43.57	44.27	45.46	46.99	47.24	48.10	49.66
TiO_2	2.02	2.96	2.67	2.09	2.05	2.01	1.75	1.70
Al_2O_3	15.35	13.28	13.60	14.34	14.26	13.92	15.19	14.19
Fe_2O_3	6.98	3.42	3.41	3.09	2.66	3.84	1.89	#12.96
FeO	4.56	10.78	9.75	8.83	8.77	8.55	8.96	nd
MnO	0.18	0.20	0.19	0.17	0.19	0.18	0.16	0.19
MgO	5.49	9.16	9.28	9.32	9.12	9.31	7.94	8.66
CaO	6.59	8.96	9.30	8.74	8.06	8.04	8.61	8.30
Na_2O	6.14	3.33	3.14	2.66	3.69	2.57	2.94	2.78
K_2O	3.02	1.81	1.70	1.73	0.87	1.29	1.14	1.02
P_2O_5	1.08	0.80	0.75	0.57	0.49	0.39	0.33	0.27
H_2O^+	3.08	1.59	1.96	2.32	2.43	1.85	1.88	nd
CO_2	0.07	0.09	0.05	0.12	0.09	0.14	0.06	nd
SO_3	0.10	0.11	0.12	0.09	0.04	0.16	0.13	nd
LOI	-	-	-	-	-	-	-	1.02
TOTAL	**99.86**	**100.04**	**100.22**	**99.53**	**99.70**	**99.49**	**99.08**	**100.75**
FeO*	10.84	13.84	12.82	11.61	11.16	12.01	10.66	11.66
Mg#(0.20)	51.58	58.20	60.35	62.80	63.22	61.99	61.04	60.97
Sc (ppm)	4	18	21	18	21	20	20	nd
V	156	220	230	185	210	185	190	nd
Cr	80	175	200	250	210	290	260	nd
Co	27	50	49	56	41	58	47	nd
Ni	86	195	200	210	185	240	140	nd
Cu	21	54	56	43	33	32	24	nd
Zn	140	155	125	115	105	105	100	nd
Ga	31	26	24	23	23	24	25	nd
As	<20	<20	<20	<20	<20	<20	<20	nd
Rb	33	21	22	34	24	30	18	nd
Sr	1400	970	920	730	540	480	490	nd
Y	22	22	21	21	23	23	20	nd
Zr	575	350	290	240	210	185	155	nd
Nb	110	58	47	37	32	31	18	nd
Mo	10	8	6	<5	<5	<5	<5	nd
Sn	<9	<9	<9	<9	<9	<9	<9	nd
Ba	200	185	180	180	220	290	165	nd
La	50	39	30	<20	28	24	<20	nd
Ce	135	100	89	68	51	58	42	nd
Nd	75	48	41	29	<20	23	<20	nd
W	<10	<10	<10	<10	<10	<10	<10	nd
Pb	<10	<10	<10	<10	<10	<10	<10	nd
Bi	<5	<5	<5	<5	<5	<5	<5	nd
Th	16	21	16	13	10	12	10	nd
U	<10	<10	<10	<10	<10	<10	<10	nd
CIPW norms (calculated at $Fe_2O_3/FeO = 0.20$)								
or (wt %)	18.55	10.87	10.28	10.57	5.29	7.85	6.97	6.08
ab	13.49	12.28	13.86	19.05	28.64	22.42	25.63	23.86
an	5.62	16.27	18.36	22.76	20.38	23.28	25.65	23.57
ne	21.97	8.88	7.20	2.28	1.90	0.00	0.00	0.00
di	17.38	19.31	19.33	14.73	14.23	12.35	13.19	13.41
hy	0.00	0.00	0.00	0.00	0.00	9.96	7.69	17.36
ol	13.59	21.25	20.80	22.19	21.53	16.23	13.95	8.89
mt	2.76	3.46	3.21	2.94	2.82	3.03	2.69	2.89
il	3.98	5.73	5.18	4.10	4.00	3.93	3.41	3.26
ap	2.55	1.86	1.75	1.34	1.14	0.91	0.77	0.61
Total	**99.89**	**99.91**	**99.97**	**99.96**	**99.93**	**99.96**	**99.95**	**99.93**
an/plag*	28.19	55.53	55.53	52.96	40.14	49.46	48.54	48.21

R005373	nepheline mugearite	R004965	alkali olivine basalt	R004962	transitional olivine basalt
R006791	basanite	R006798	hawaiite	Y1	olivine tholeiite
R006793	basanite	R004964	transitional olivine basalt		

* molar 100/(an/an + ab) in normative plagioclase

totals are less than 100% due to rounding errors in computer program

total iron expressed as Fe_2O_3

Analysis Y1 from Yaxley (1981). Remainder are new analyses by MRT laboratories. Analyst L. M. Hay

The low Mg#, CaO, Ni and Cr of both rocks, but especially the occurrence at Molompto Road, indicates that they are not primary magmas (i.e. unmodified partial melts of mantle), but rather have been modified by a substantial amount of crystal fractionation. The low Cr, CaO and also Sc suggests that the fractionating assemblage included clinopyroxene as well as olivine, and the presence of lherzolite xenoliths implies rapid ascent from the mantle; thus fractionation occurred within the mantle prior to xenolith entrainment, rather than at crustal levels. The very high levels of high field strength elements (P_2O_5, Zr, Nb, Ce) and also Sr are probably partly attributable to a relatively low degree of partial melting of the parental magma, but have been further enhanced by crystal fractionation. Despite their potassic character neither rock is especially rich in Rb or Ba.

Lower Julius River

Matthews (1961*b*) and Longman and Matthews (1962) showed a very small area of Tertiary basalt on the eastern bank of the Julius River, just upstream from the arch (at about 334800/5443000). The basalt was not relocated during the recent field project, despite a short search, perhaps because it represents a single, very small outcrop (W. L. Matthews, pers. comm.).

A thin section (61/20) was described by Longman (1962) as an intergranular to subophitic basalt consisting mainly of plagioclase (partly as small phenocrysts up to 1 mm) and titanaugite. Re-examination of the thin section reveals that a few small euhedra of altered olivine are also present. The presence of distinctly purplish titanaugite and the freshness of the plagioclase suggest that the rock is an alkali olivine basalt of Tertiary age. It is coarser grained and more altered than the alkali olivine basalt west of the Keppel Creek headwaters, about five kilometres to the southwest, but is probably chemically similar. It probably represents a tiny flow remnant.

Upper Julius River–Horton River

Field relationships

The largest tract (about 10 km^2) of Tertiary basalt in the area is on the central Dempster map sheet, and extends almost continuously SSW for more than eight kilometres from 331400/5440200 to 328300/5431700. In the south of the tract the basalt appears to be fairly thin, with a base at an elevation of mostly 200–230 m, and it forms a cap to a small plateau at an elevation of about 240 metres. Further north its base is not much higher (typically about 240 m) but it is locally much thicker, and rises to 312 m at 330100/5438500 (the highest point in the whole area). This may indicate a nearby feeder, although no special features (such as lherzolite xenoliths) were noted there. Near its northern limit (near 330100/5440000), in dense rain forest at the extreme southern edge of the Sumac map sheet, the basalt cap appears to be no more than about 30 m thick.

In most places the basalt has been erupted directly on to basement, mostly Kanunnah Subgroup units, although it is locally underlain by Tertiary sandstone. In the field it is usually massive and rarely vesicular. It somewhat resembles the basalt of the Spinks Creek Volcanics, but can be distinguished by its medium to dark-grey colour, without any greenish tint, and the sparkling, rather than dull lustre of fresh surfaces. The basalt is less tough, less well jointed and has a hackly fracture, rather than angular to conchoidal fracture characteristic of most Neoproterozoic basalts.

Outcrop is generally poor and most of the tract is mapped from float. Fresh boulders can be found in the roots of fallen trees. Small amygdales, variously filled with calcite, white zeolites and green to bluish grey talcose material, were noted. Good outcrops occur where streams leave the plateau, often in small waterfalls. In a four metre high waterfall at 327840/5434370, fine-grained grey basalt, with scattered soft grey-green talcose amygdales, displays moderately well developed vertical columnar jointing. At 327570/5432680, in a 2.5 m high waterfall, similar basalt displays more irregular 'knobby' jointing.

Columnar joints are rare but where present are orientated near to vertical. Horizontal alignment of vesicles in basalt located immediately above the contact with Proterozoic rocks at 330970/5438560 may be flow banding. Eleven magnetic susceptibility readings returned an average of 5×10^{-3} SI, considerably less than that for the stratigraphically underlying Proterozoic basalt.

Magnetic susceptibility of the Tertiary basalt, measured in the field, ranges from 4 to 8.2 ($\times 10^{-3}$ SI), whilst the Neoproterozoic basalt has values of 12 to 105. On aeromagnetic images any response by the Tertiary basalt is swamped by that of the underlying and thicker Neoproterozoic basalt.

Basanites (Tbb)

The chemically most undersaturated analysed sample (R006791), from 328380/5432200 near the southern edge of the plateau, is a fine-grained aphyric basalt. In thin section it consists of abundant olivine euhedra (generally less than 500 μm, and typically about 200 μm across) and sparsely distributed plagioclase laths (typically 200–300 × 20–30 μm), in a mesostasis in which purplish titanaugite, abundant small equant opaque grains (10–40 μm across) and clear zoned nepheline (?) can be discerned. Acicular apatite is present as an accessory mineral. A diffuse globular zone, about one millimetre across, of mostly fine-grained, colourless clinopyroxene may represent a digested xenolith. There are some patches of orange to brown ferruginous alteration (goethite?) in the mesostasis.

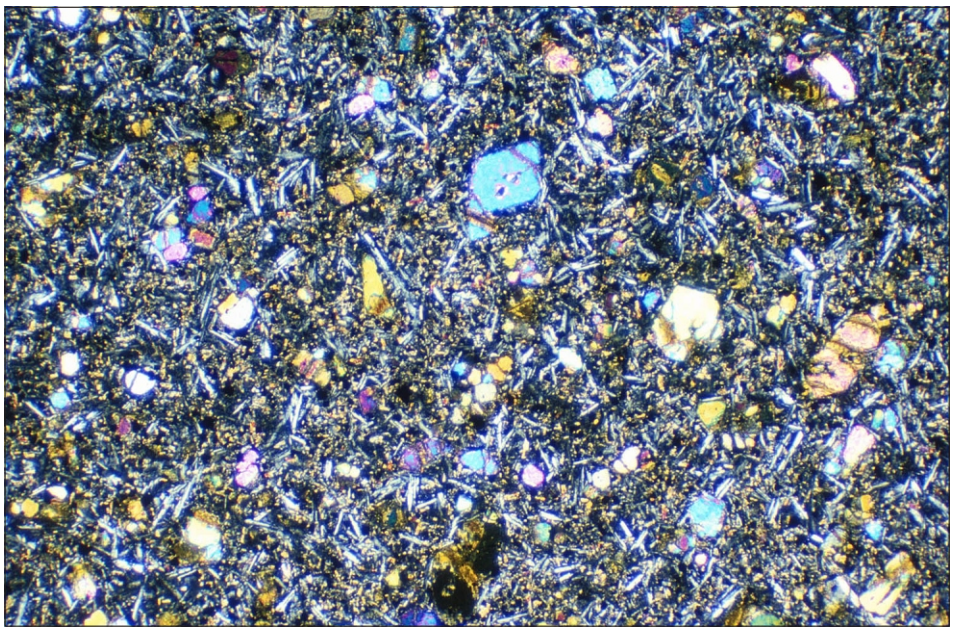

Plate 39

Photomicrograph of Tertiary basanite (Tbb), sample R006793 (327 840 mE, 5 434 370 mN). Partly altered olivine microphenocrysts in a groundmass with relatively sparse plagioclase laths. Crossed nicols, field of view 4.4 2.9 mm.

Another sample (R006793, Plate 39), from the waterfall at 327840/5434370, is similar, but contains somewhat more abundant plagioclase laths (typically 150–200 μm long), in addition to olivine euhedra (mostly ≤250 μm) and mesostasis. There are some irregular, probably late crystallised, zones in the mesostasis which lack titanaugite or opaque minerals, and consist of mainly clear fine-grained probable nepheline. There is some orange to greenish-brown partial alteration of olivine euhedra, whilst the mesostasis is generally fresh. Sample R006794 (327570/5432670) is very similar but more altered than R006793, with complete replacement of some olivine euhedra by khaki-brown material.

Alkali olivine basalts (Tba)

Alkali olivine basalt has been sampled from the northern limit of this tract. A thin section of a sample (R004966) collected from the crest of a ridge (330960/5440020) just west of the headwaters of Keppel Creek consists of abundant, mostly fresh olivine microphenocrysts in a fine-grained fluidal intergranular groundmass of mainly plagioclase, titanaugite and opaque minerals. The olivine microphenocrysts are typically equant, slightly rounded but not strongly embayed euhedra and subhedra, up to 400 μm across and grading down to a few small groundmass granules. Narrow plagioclase laths (typically 100–200 × 20–40 μm, but a few attaining the dimensions of microphenocrysts) are closely packed and crudely aligned, defining the fluidal fabric. Irregularly shaped clinopyroxene granules display the pinkish colour characteristic of titanaugite and do not enclose plagioclase laths. Opaque minerals occur as angular equant to irregular grains up to 100 μm across. Traces of minute splintery grains of bright red-brown pleochroic biotite are also present in the groundmass, usually accompanying titanaugite. Acicular apatite is also an accessory mineral. A bright green to blue-green chloritic alteration rims many olivine microphenocrysts. A few round amygdales, up to 500 μm across, are filled with a fibrous radiating zeolite.

A second thin section (R004965) collected from 400 m to the east (331360/5439990) is broadly similar, but the groundmass is finer grained. The olivine microphenocrysts (≤500 μm) are more euhedral and are here accompanied by similar sized euhedral phenocrysts of titanaugite, and a few of plagioclase. Two larger (≤2 mm) olivine phenocrysts were intersected by the section; one is an irregularly shaped, strongly embayed euhedron and may be a xenocryst. In the groundmass plagioclase laths are rarely more than 100 μm long and grade down in size to microlites. Pyroxene granules are also present, as are minute (≤10 μm) equant opaque grains. Much of the mesostasis is colourless with low birefringence and may include alkali feldspar, nepheline and/or zeolite. Some of the olivine phenocrysts are altered to an orange-red material, but most of the rock is remarkably fresh.

Hawaiite (Tbh)

A sample (R006798) from the highest point in the area (330270/5438630) is a coarse-grained olivine-clinopyroxene-plagioclase phyric basalt. It contains abundant, mostly fresh, equant and slightly rounded olivine phenocrysts (typically 500 μm to 1 mm), euhedral colourless clinopyroxene phenocrysts (≤1.5 mm) and elongate plagioclase phenocrysts (≤1 mm), grading down to an intergranular groundmass which also contains irregularly angular opaque minerals (mostly 40–100 μm) and traces of apatite. Minor green chlorite is present in the groundmass as a peripheral alteration of olivine. The rock petrographically resembles transitional olivine basalt R004962 from Balfour (see below), but the CIPW norm shows that it is an hawaiite.

Transitional olivine basalt (Tbr)

Sample R006792, from a small local topographic high (328350/5434010), contains slightly rounded to quite strongly embayed olivine phenocrysts (≤1 mm), frequently clumped in glomerocrysts, in a well crystallised intergranular groundmass. This consists of

locally aligned plagioclase laths (200–400 μm), colourless clinopyroxene granules, minor olivine, irregularly angular to markedly elongate opaque minerals (≤100 μm) and accessory apatite. There is some very minor peripheral orange-brown alteration of olivine. The rock was not chemically analysed, but petrographically resembles transitional olivine basalt R004964 (see below).

Upper Blackwater Rivulet

An area of about 1.2 km^2 of basalt occurs around 325500/5435500, on the watershed between the upper Blackwater Rivulet and the Frankland River, and straddling the locally thrusted contact between the Togari and Rocky Cape groups.

A sample (R004964) from a small outlier to the west (324360/5435260) is chemically a transitional olivine basalt (see below). In thin section it contains abundant, equant, slightly resorbed and rounded subhedra and anhedra of olivine (mostly 500 μm–1 mm), in a fluidal intergranular to intersertal groundmass. In the groundmass, plagioclase laths (typically 150–300 μm) are locally aligned, but have no overall alignment even on thin section scale. Colourless clinopyroxene granules, equant (50–100 μm), irregularly angular to almost acicular (to 200 × 10 μm) opaque minerals, relatively minor olivine granules and accessory acicular apatite are also present. Much yellow-green chlorite is present, both in the groundmass and as an alteration to olivine phenocrysts. The rock is very similar to, although more altered than, sample R006792. It differs from alkali olivine basalt R004965 and transitional olivine basalt R004962 in lacking clinopyroxene (and plagioclase) phenocrysts, and in grain size.

The Clump

A small area (about 300 × 125 m) of orange-red soil centred at 321400/5436100 supports a conspicuous patch of forest known as The Clump, and is almost certainly derived from Tertiary basalt. However no outcrop or even float of basalt could be found. There is no obvious associated magnetic anomaly, although in the vicinity there are strong anomalies sourced in the Rocky Cape basement. The soil probably results from weathering of a very thin flow remnant.

Balfour *(JLE, ARR)*

Basalt stratigraphically overlies Tertiary gravel west of the Frankland River but is evident only as rounded boulder float, or as weathered basalt chips, contained within a deep red to brown-coloured and fertile soil.

A small area (about 0.8 km^2) of basalt caps a low forested ridge at the southern margin of the Dempster map sheet, including the Balfour town site, and extends on to the adjoining Balfour map sheet. The basalt has a probable maximum thickness of less than 20 m and rests on Rocky Cape Group units. It was deposited within a north-draining alluvial channel, clearly demonstrating the link between Tertiary drainage patterns and flow distribution.

Fresh basalt float west of Balfour (324700/5430050) is massive, grey and crystalline in hand specimen. Equant olivine phenocrysts to 3 mm diameter are rare. Outcrops are poor and much of the basalt is mapped from float and soil. Previous petrographic descriptions are given by Ward (1911) and Yaxley (1981).

In thin section a similar sample (R004962, Plate 40) from just north of Balfour (325000/5430320) has a glomeroporphyritic to seriate texture, with abundant phenocrysts of olivine and plagioclase, and relatively sparse clinopyroxene phenocrysts, grading down to an intergranular groundmass. Olivine phenocrysts (≤2 mm) are typically equant subhedra and anhedra, embayed due to partial resorption, but lack reaction rims. Plagioclase phenocrysts (elongate and typically 500 μm–3 mm × 100–300 μm) are fresh. Clinopyroxene phenocrysts are colourless to pale yellow, sometimes twinned euhedra and anhedra, and are probably augite

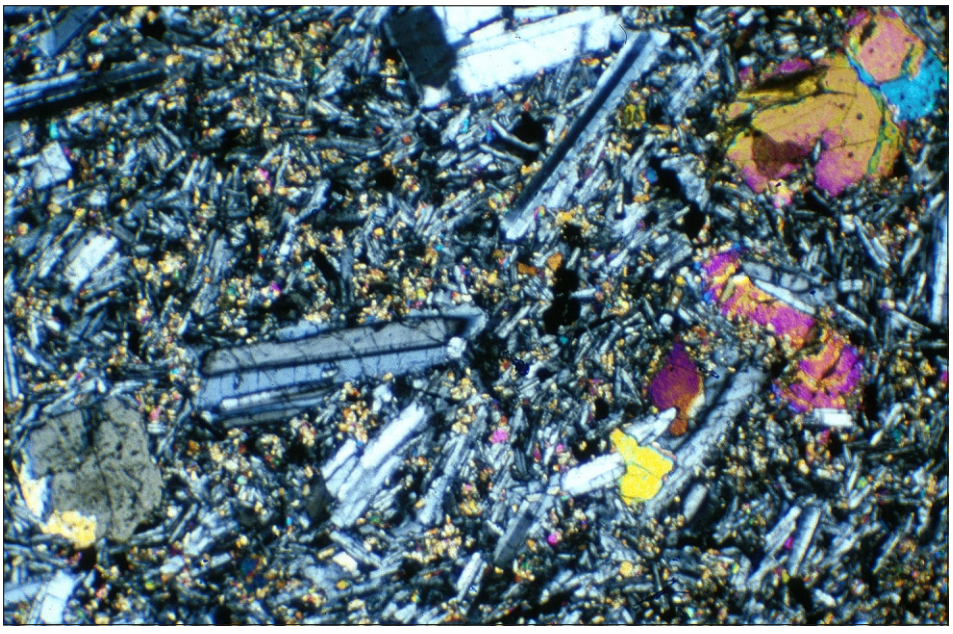

Plate 40

Photomicrograph of Tertiary transitional olivine basalt (Tbr) sample R004962 (near Balfour, 325 000 mE, 5 430 320 mN). Plagioclase, olivine (right) and clinopyroxene (lower left) phenocrysts in an intergranular groundmass. Transitional olivine basalt (Tbr). Crossed nicols, field of view 4.4 2.9 mm.

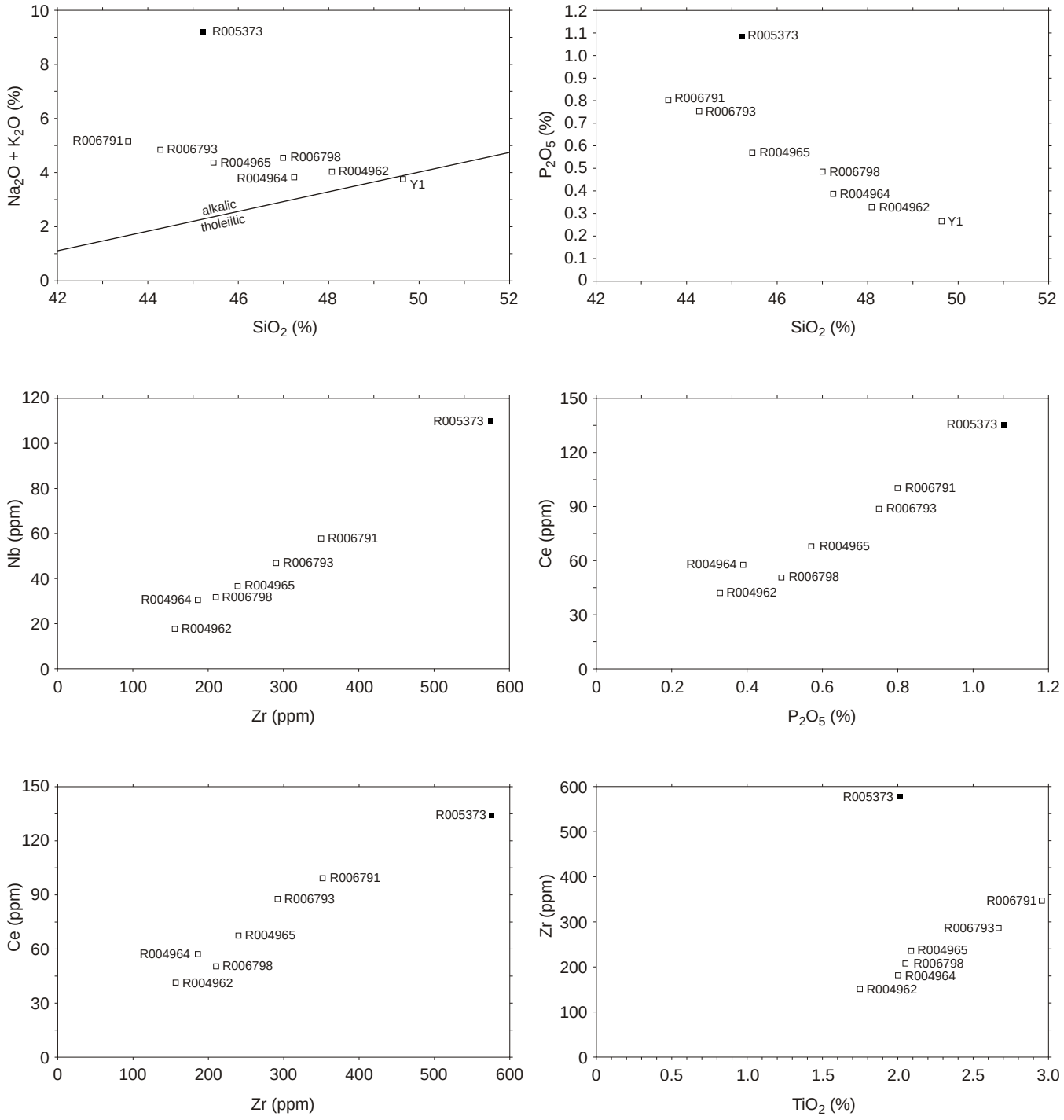

Figure 11

Geochemical plots, Cainozoic basalts: (a) total alkalis ($Na_2O + K_2O$) against SiO_2; (b) P_2O_5 against SiO_2; (c) Nb against Zr; (d) Ce against P_2O_5; (e) Ce against Zr; (f) Zr against TiO_2.

(biaxial positive). Some have a distinctive mottled or poikilitic appearance due to abundant small (melt?) inclusions. The groundmass is well crystallised and consists mainly of plagioclase laths (mostly 100–300 μm long), pale yellow clinopyroxene and angular, equant to irregularly shaped opaque grains (typically 20–150 μm across). Finely acicular apatite is a common accessory mineral. The rock is fresh apart from some slight marginal yellow-green to orange alteration of olivine.

Geochemistry and petrogenesis

Seven Tertiary basalt samples were chemically analysed at the Mineral Resources Tasmania laboratories (Table 9). These are considered together with a further major element analysis (Y1) from Yaxley (1981). The Molompto Road sample (R005373) is a nepheline mugearite, very different from the other samples, and its geochemistry and petrogenesis is discussed separately (see above).

The remaining analysed samples range from basanite (R006791, R006793), through alkali olivine basalt (R004965), hawaiite (R006798) and transitional olivine basalt (R004964, R004962) to an olivine tholeiite (Y1). On a total alkali-silica diagram (fig. 11*a*), all except Y1 lie in the field of alkali basalts, above the line of Macdonald and Katsura (1964). All are moderately fractionated, with Mg# (atomic $Mg/(Mg + Fe^2)$, calculated at $Fe_2O_3/FeO = 0.20$) of 58–63 and Ni of 140–240 ppm, well below values (68–75 and >300 ppm respectively) considered typical of unfractionated primary magmas.

A remarkably good negative correlation is present between SiO_2 and relatively incompatible minor elements such as P_2O_5 (fig. 11*b*), TiO_2 and K_2O. Na_2O also decreases with increasing SiO_2 from R006791 to R004964, but is slightly higher in the two less undersaturated samples from Balfour (R004962 and Y1). CaO and total FeO show a slight crude negative correlation with SiO_2, and Al_2O_3 a crude positive correlation with appreciable scatter.

The Molompto Road rock plots well off these trends with higher P_2O_5, K_2O and Na_2O and lower CaO (and MgO) given its SiO_2 content.

Excellent positive correlations exist between all pairs of the incompatible high field strength elements (HFSE), Zr, Nb, light rare earth elements (e.g. Ce), TiO_2 and P_2O_5 (e.g. fig. 11*c, d, e, f*). The divalent elements Sr and Zn can also show a similar pattern of variation and appear to have also behaved incompatibly. K_2O shows similar behaviour, but is slightly higher relative to other elements in sample R004965 (consistent with the presence of traces of groundmass biotite in the nearby thin section R004966). In contrast the large ion lithophile elements (LILE) Rb and Ba correlate poorly with both K_2O and HFSE.

Compatible elements such as Ni, Cr, V, Sc and Co are much lower in the Molompto Road sample (R005373), consistent with its strongly fractionated nature, but in the other samples they vary over only a small range. Given the limited range of Mg#, this is not surprising.

Ga and Y also show very little variation. These elements are compatible in garnet and may have been buffered during partial melting of a garnet lherzolite source, but would behave incompatibly during low pressure olivine fractionation.

Similar major and trace element trends are typical of Tasmanian Tertiary basalts in general (e.g. Everard, 1989 and unpublished data).

The main cause of the geochemical variation in these basalts is probably a variable degree of partial melting of a common mantle source, in the order R006791 (least melting), R006793, R004965, R006798, R004964, R004962, Y1 (most melting). As the incompatible trace elements Zr, Nb, Ce, Sr and P_2O_5 mostly vary by a factor of 2 to 2.5, the percentage of partial melting may have ranged from about 8% (basanite) to around 20% (transitional olivine basalt and tholeiite), broadly consistent with the model advocated by Frey *et al*. (1978).

Superimposed on this variation has been that caused by crystal fractionation. About 13–20% fractionation, mainly of olivine, could account for the relatively low Mg# and Ni contents, and would slightly raise incompatible element contents by a factor of 1.15 to 1.25.

Discussion

Further Tertiary basalt outliers occur to the west, near Rebecca Creek and 'Kaywood', and to the south, seven kilometres southeast of Balfour (J. L. Everard, unpublished data; Seymour and Reed, 2003). It is likely that all are dissected remnants of a once extensive sheet-like flow or series of flows that once covered much of the region.

On the basis of the limited sampling it appears that, in at least the southern part of the large Upper Julius River–Horton River tract, a basal flow of basanite may be present, and the overlying flows may become progressively less undersaturated up sequence. A similar basalt stratigraphy, with thin basal basanites, is present to the east in the Lyons River–Keith River area (J. L. Everard, unpublished data). Correlates of only the possibly younger less undersaturated basalts have been recognised at Balfour and in the Upper Blackwater Rivulet area.

The precise age of the Tertiary basalt remains obscure. The nearest basalts that have been radiometrically dated are at:

- Mt Cameron West (14.5 ± 0.2 Ma, 15.5 ± 0.2 Ma, Seymour and Baillie, 1992);
- The Nut (12.5 ± 0.2 Ma, Baillie, 1986); and
- Green Hills, also near Stanley (8.5 ± 0.1 Ma; Baillie, 1986).

These are amongst the youngest recorded dates in Tasmania, and in view of the inferred degree of erosion, the Tertiary basalts in the Roger–Sumac–Dempster area

(except perhaps the Molompto Road nepheline mugearite) may be considerably older. The palynological ages (latest Eocene to early Oligocene, perhaps c. 35–40 Ma) obtained for the thick Tertiary basalt pile east of Waratah (Brown and Forsyth, 1984; R. Morgan quoted by Seymour, 1989 and references therein) may be of more relevance, particularly if these basalts represent a dissected extension of that volcanic episode.

Quaternary deposits

Lag of dominantly chert, with associated silt and sand (Qhl)

This unit was used by Brown (*in* Everard *et al*., 1996) for deposits overlying the Black River Dolomite, mostly on low drainage divides, around Lake Chisholm, Wents Creek and adjacent areas north of the Arthur River, on the Sumac map sheet.

Talus (Qpt) *(DBS)*

Because of the generally subdued topography, mappable slope deposits are rare in far northwest Tasmania. A small area of talus derived from the Salmon River Siltstone has been mapped near Chatlee Road around 322300/5449700 on the Sumac map sheet.

Alluvium and swamp deposits (Qha) *(JLE)*

There are large tracts of alluvium and swamp deposits, particularly in the north of the Roger-Sumac-Dempster area. Most are developed on, or closely associated with, usually poorly outcropping Smithton Dolomite bedrock. Extensive deposits overlie Black River Dolomite on both sides of the Arthur River near 335500/5446500, near Howitzer Creek (339000/5447000) and beside the lowermost reaches of the Rapid River.

The deposits are poorly exposed and were not examined in detail. In a cutting on the Rapid River Road at 340360/5443630 (Holder map sheet) they consist of cobbles and pebbles (mostly 10–100 mm) of quartz (well rounded), quartzite (less well rounded) and laminated siltstone in a grey-brown matrix of fine sand and silt. Similar deposits at 340670/5444920 overlie chert lag, and may represent the remnant of an older terrace. A five metre high cliffy bank on the Arthur River at 335440/5446230 consists of a lower half of cobbles, overlain by an upper half of sand. Similar sand and gravel is exposed downstream (at 335340/5446980) in a ten metre cliff. Gravel and sand is at least five metres thick on the Arthur River at 329150/5448310 and similar exposures occur for several kilometres downstream without any bedrock outcrops. Drilling further north in the lower Duck River area (Smithton Quadrangle) indicates that the Quaternary deposits are up to 21 m thick and rest on Smithton Dolomite (Lennox *et al*., 1982). As noted above (*Physiography and drainage* section), it is likely that much of the deposits in the present Montagu River and lower Duck River drainages were deposited by the ancestral Arthur River at times when it flowed north into Bass Strait.

Introduction

The Roger, Sumac and Dempster map sheets cover the central southern part of the Smithton Synclinorium (fig. 1), a large structure encompassing sequences belonging to the early Neoproterozoic Rocky Cape Group, the late Neoproterozoic–?Early Cambrian Togari Group and the late Middle–early Late Cambrian Scopus Formation.

The area is structurally complex, having undergone at least two extensional and four compressional deformation events. It has been possible to establish a precise sequence of compressional events only in the southwestern part of the Dempster map sheet and in neighbouring areas on the Balfour and Temma map sheets, to the south and west of Dempster. The northern, central and southeastern parts of the main area of interest of this report have been affected by additional compressional deformation events. Structural data from these areas have been analysed statistically, enabling some correlations to be made with the four-fold sequence of compressional structures recognised in the southwestern Dempster, Balfour and Temma map sheets.

Although deposition of parts of both the Rocky Cape Group and Togari Group was partly controlled by syndepositional deformation, including extensional faulting, the major phases of compressional deformation post-dated their deposition. It seems likely that the Togari Group represents one structurally preserved portion of an originally more extensive Neoproterozoic shelf sequence, that may have encompassed the Ahrberg Group near Corinna and perhaps other similar sequences in western and southwestern Tasmania. Thus the term Smithton Synclinorium is preferred to previous terms such as Smithton Basin (e.g. Brown, 1989*b*) and Smithton Trough (e.g. Williams, 1979).

Extensional deformation

Late to early Neoproterozoic syn-sedimentary extension *(ARR)*

The identification of syn-sedimentary faults is important from an economic viewpoint, in that such structures are ideal conduits for commonly metal-rich brines derived during basin de-watering. They are also important for their controlling influence on deposition and, in combination with the stratigraphic contrasts which may develop across such faults, their influence on the formation of later compression-related structures. No syn-sedimentary faults that were active during Rocky Cape Group deposition have yet been identified in the Roger, Sumac and Dempster map sheets, although extensional structures and the results of their influence on sedimentation are preserved in Rocky Cape Group rocks on the coastline at Temma, 15 km west of the Dempster map sheet (Seymour and Reed, 2003). Rocky Cape Group sequences in the Temma area show lithological and sedimentological similarities to parts of the Balfour Subgroup sequence in the southwestern part of the Dempster map sheet, and so brief descriptions of some of the Temma outcrops are included here.

Syn-sedimentary faulting in the Rocky Cape Group occurs near the hinge of an anticline, inland of the Temma coast at 307230/5431200. The fault can be traced across outcrop for twenty metres. A parallel-bedded siltstone forms the footwall to the fault, whereas hanging wall strata form a fan-shaped prism of sedimentary rock. An upward-increasing concordance of bedding in the prism with overlying stratigraphy and truncation of the fault by overlying beds attest to a syn-sedimentary timing for this structure. Development of a fan-shaped sedimentary prism in the hanging wall to the fault indicates progressive movement during sedimentation. The angle between bedding and the growth fault is about 64°, close to optimal for a normal fault. A well-developed slaty foliation parallels the fault in the immediate hanging wall. Both the fault and related foliation are cut by a compressional fold-related cleavage. Wedge-shaped and sand-filled sedimentary dykes to several centimetres depth parallel the strike of the growth fault in footwall siltstone, and are consistent with formation during active extension. Incised trough cross-laminated channels in rocks hanging-wall to the growth fault are also aligned parallel to the strike of the growth fault, suggesting that extensional tectonism influenced palaeocurrents, channel formation and sediment migration.

Effects of syn-sedimentary deformation are also evident 500 m east of Temma at 307560/5433180. Angular clasts, ≤200 mm in diameter, of laminated siltstone in a massive siltstone matrix, overlie convolute-folded bedding, and have subsequently been refolded during compressional deformation. Clast size increases to greater than 500 mm at 307100/5433120, indicating the possibility of an even larger syn-sedimentary structure nearby. Here, the increase in clast size is matched by an increase in strain and development of the overprinting compression-related foliation. Larger syn-sedimentary faults may have been ideal structures for failure during subsequent deformation, complicating their identification as growth structures.

Clastic dykes, like those adjacent to syn-sedimentary faults on the coastline at Temma, are also common to Balfour Subgroup sedimentary rocks in the Dempster map sheet. The dykes are cut by foliations of compressional origin and are clearly of syn or early post-sedimentary origin. Although similar structures elsewhere in the Rocky Cape Group have been previously described as shrinkage or syneresis cracks (Calver and Baillie, 1990; Scott, 1997), these dykes commonly show a preferred alignment on bedding surfaces, more consistent with their formation during

extension. Deeply incised sediment-filled channels, like those in the hanging wall to growth faults at Temma, are also common in Balfour Subgroup sedimentary rocks, further indicating the likely influence of growth faulting in controlling sedimentation.

In contrast with the Cowrie Siltstone which stratigraphically overlies it, the Balfour Subgroup contains common current-generated erosional and depositional sedimentary structures and shows marked facies variations, both along strike and up-section. Such features are consistent with deposition of the Balfour Subgroup in a compartmentalised sedimentary system influenced by syn-sedimentary growth faulting. That such faults have not yet been recognised in the Dempster map sheet might simply be the result of their subsequent reactivation, and recognition as compressional structures only.

Late Neoproterozoic to Early Cambrian extension *(ARR, DBS)*

Regional setting

An angular unconformity separating Rocky Cape Group rocks from the overlying Togari Group is exposed along the eastern margin of the Smithton Synclinorium, near the mouth of the Black River east of Smithton (Lennox *et al*., 1982; Brown, 1989*a*) (Plate 41). At other exposures around the margin of the Smithton Synclinorium, the Rocky Cape Group–Togari Group contact is erosional but commonly near to concordant. Regional mapping has shown that the Togari Group overlies different stratigraphic levels within the Rocky Cape Group at different points around the margin of the synclinorium (Seymour and Baillie, 1992; Everard *et al*., 1996). These observations indicate a period of significant erosion between deposition of the Rocky Cape and Togari groups.

The angular unconformity between the Rocky Cape and Togari groups was historically attributed to the Penguin Orogeny of Spry (1962) (Williams, 1979; P. W. Baillie *in* Brown, 1989*a*), an event suggested to have caused open folding of Rocky Cape Group rocks prior to deposition of the Togari Group. The event originally known as the Penguin Orogeny has since been recognised as Middle Cambrian in age (Turner *et al*., 1995; 1998), consequently some recent interpretations have correlated the suggested pre-Togari Group open folding with a tectonothermal event at c. 760 Ma which affected Mesoproterozoic rocks on King Island (Turner *et al*., 1995; Berry, 1995; Seymour and Calver, 1995*b*).

The unconformity between the Rocky Cape and Togari groups may alternatively be a consequence of Neoproterozoic extension. If normal faulting accompanied the onset of Togari Group sedimentation, then deposition into graben was possibly accompanied by erosion of topographically upstanding blocks of Rocky Cape Group. Juxtaposition of Togari Group sedimentary rocks with different levels in the Rocky Cape Group stratigraphy might therefore be the product of contemporaneous erosion of the Rocky Cape Group during Togari Group deposition. The angular unconformity between the Rocky Cape and Togari groups could be the product of block rotation or 'roll-over' of hanging-wall strata above non-planar extensional faults. The irregular distribution of the basal Forest Conglomerate and the predominance of quartzite pebbles within this unit are consistent with basin compartmentalisation by normal faulting during early Togari Group deposition.

Roger River Fault

The Roger, Sumac and Dempster map sheets are bisected by the Roger River Fault, a regionally extensive and steeply dipping fault that now shows perhaps 750 m of west-side-down net offset (based on the cross section in Everard *et al*., 1996, and revised stratigraphic thicknesses determined in this project). Although the Roger River Fault was an active structure

Plate 41

The best known exposure of the unconformity between the basal unit (Forest Conglomerate & Quartzite) of the late Neoproterozoic Togari Group and the underlying Cowrie Siltstone of the ?Mesoproterozoic Rocky Cape Group, at the Black River bridge near the northeastern margin of the Smithton Synclinorium (357 240 mE, 5 476 740 mN).

Table 10

Average thickness of Togari Group units, east and west of the Roger River Fault

Unit	Estimated thickness west of Roger River Fault (m)	Estimated thickness east of Roger River Fault (m)
Smithton Dolomite	~ 1075	Max. >900?
Spinks Creek Volcanics	0–120	?200–>750?
Kanunnah Subgroup (including Spinks Creek Volcanics & Croles Hill Diamictite)	220–800	Max ?1400
Croles Hill Diamictite	0–?190	0–?350
Julius River Member	0–200	0–>170
Black River Dolomite	150–450	?550

during at least two compressional deformations, there is evidence in the stratigraphy to suggest that this structure originated as an extensional fault and formed the western boundary of a half-graben into which Togari Group sedimentary and volcanic rocks were deposited.

Extension during Togari Group deposition is indicated by marked variations in the thicknesses of stratigraphic units across the Roger River Fault within the area covered by Sumac and Dempster map sheets (Table 10).

An accurate estimate of the extent to which syndepositional normal faulting has affected unit thickness is complicated by the varying response of units either side of the Roger River Fault to subsequent compressional events. Consistently steep dips in the lower part of the Togari Group northwest of the Roger River Fault on the Sumac map sheet, together with a good density of bedding orientation data, enable accurate calculation of unit thicknesses from the map. In contrast, the same rocks southeast of the Roger River Fault on the Dempster and southernmost Sumac map sheets dip gently within a somewhat irregular dome and basin geometry, and structural data are more sparse, so estimates of stratigraphic thicknesses are less reliable. Nonetheless, the data show a clear pattern of greater stratigraphic thicknesses southeast of the Roger River Fault compared with northwest of the fault, particularly in the Kanunnah Subgroup and its constituent formations, the greatest difference being in the Spinks Creek Volcanics. The pattern of thickness variations suggests that syn-sedimentary rifting may have been initiated during Black River Dolomite deposition (but may have been only incipient at that time), and commenced in earnest at the start of Kanunnah Subgroup deposition (i.e. with the Croles Hill Diamictite). It reached a peak during eruption of the Spinks Creek Volcanics, and may have largely ceased by the time of deposition of the Smithton Dolomite, which appears to show little difference in thickness across the Roger River Fault.

Subsidiary structures to the Roger River Fault

A northeast-trending fault at 329650/5436000 does not crop out, but is inferred from aeromagnetic data and its separation of basalt of the Spinks Creek Volcanics to the northwest, from interfingered basalt, volcaniclastic siltstone and diamictite to the southeast. There is a significant increase in the complexity of the interfingering diamictite and siltstone facies, with diamictite units both coarser grained and less sorted southeast of the fault. The more varied geology to the southeast of the fault suggests a higher energy proximal depositional environment, consistent with southeast-side-down syn-depositional faulting. Such a sense of movement matches that inferred for the nearby Roger River Fault.

The along-strike continuation of this fault, traceable in the magnetic data, coincides with a hematitic ironstone unit (Psvwi) at 331770/5440000. If the fault were active during deposition then this unit may be exhalative in origin and of potentially economic importance.

A major northeast-trending fault system traverses the eastern half of the Dempster map sheet, from the southern boundary of the sheet at 332400/5430000 to about 337440/5439750. Along most of its trace, this fault juxtaposes Togari Group rocks to the west with Cowrie Siltstone to the east. It also appears to be spatially associated with mapped patches of a silicified facies variant of the Cowrie Siltstone (unit Prcs), which may represent a palaeoregolith developed close to the unconformity surface with the Togari Group. Post-Togari Group movement probably initiated at the unconformity, and was possibly influenced by an earlier, extensional basement fault that existed at the time of Togari Group deposition.

Compressional deformation *(ARR, DBS)*

A sequence of at least four phases of compressional deformation has been recognised within an area comprising the western parts of the Roger, Sumac and Dempster map sheets, together with more recently mapped areas in the Balfour and Temma map sheets (Everard *et al.*, 2003; Seymour and Reed, 2003) to the south and west of the Dempster map sheet, respectively. Evidence for the first two deformations (D_1 and D_2) comes largely from early foliations observed in orientated thin sections made of samples collected from the Balfour and Temma map sheets. These two events are considered likely to have affected at least part of the area covered by the Roger, Sumac and Dempster map sheets, and so are included within the overall structural sequence presented here. Additional compressional folding events affecting the

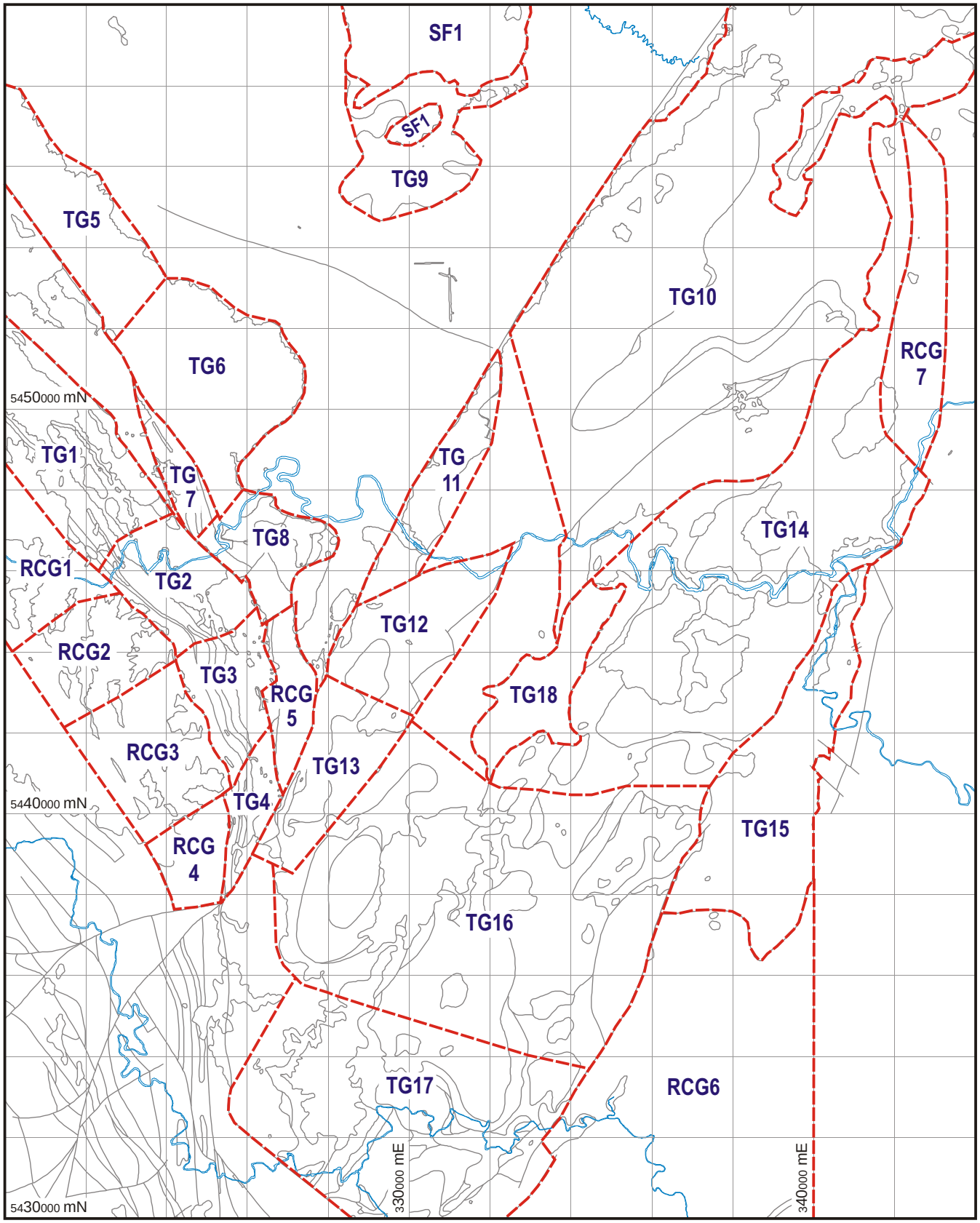

Figure 12

Map of domains used in statistical analysis of structural data.

central and eastern parts of the Roger, Sumac and Dempster map sheets cannot be precisely correlated with the D_1–D_4 sequence, but are described at their most likely position in the sequence.

First compressional deformation (D_1)

No mesoscopic structures have been observed associated with D_1 deformation. The S_1 cleavage has only been observed in thin section and is preserved only in areas of low D_3 strain and/or within porphyryblasts of probable syn-D_2 age.

S_1 has been measured in orientated thin sections made from samples collected from the Temma coastline (samples R007216, R007214, R007215), Heemskirk Road (sample R007226), Lindsay River area (samples R007218, R007219, R007220), and Waratah Creek area (sample R007227). In thin section, S_1 is a continuous to spaced disjunctive cleavage defined by alignment of chlorite between variably sutured quartz and feldspar grains. Chlorite grains are typically less than 0.2 mm in length and orientated at an angle of greater than 30° to bedding. S_1 in weakly deformed rocks from east of Mt Frankland (samples R004795, R004797) strikes about E-W and dips between 20° and 45°N (pre-D_3 orientation).

S_1 is also preserved as a preferred alignment of chlorite within chlorite-sericite ± albite porphyroblasts of ?D_2 age. S_1 may not always be apparent outside of the porphyroblasts, where D_3 has had a greater effect in re-orientating pre-existing micas.

The absolute age of D_1 is unknown. Existing thin sections of Togari Group sedimentary rocks are not orientated, and foliations within these rocks cannot be correlated with certainty with those orientated sections from the Rocky Cape Group. However thin sections of Keppel Creek Siltstone from 330510/5428550 (sample R006716), less than two kilometres from rocks known to preserve S_1, show three to four foliations. The morphology and orientation of these foliations relative to bedding is consistent with the presence of the earliest cleavage (S_1) in Togari Group sedimentary rocks. Multiple foliations are also evident in Keppel Creek Siltstone from northwest of the Roger River Fault (samples R005070, F5757). D_1, therefore, is likely to post-date deposition of Togari Group rocks. As D_1 pre-dates several known or inferred Devonian-age compressional deformation events (including D_3 and D_4 of the sequence presented below), it is most likely to be Cambrian in age.

Second Compressional Deformation (D_2)

Folding

No folds of unequivocal D_2 age have been identified from the Roger, Sumac and Dempster map sheets, although more recent mapping of the Balfour map sheet (Everard *et al*., 2003) has delineated D_2 structures preserved in rocks of low D_3 strain east of Mt Frankland, five kilometres south of the Dempster map sheet. Aeromagnetic data and preliminary regional mapping of rocks southeast of the southern closure of the Smithton Synclinorium (334000/5427000) have delineated a set of almost east-trending structures of probable D_2 age within partially fault-bounded Togari Group rocks, and also in adjacent Rocky Cape Group siltstone (Everard *et al*., 2003). D_2 folds at these localities are typically open to closed, plunge less than 30°W and verge north. Folding was accompanied by thrusting, with mineral lineations on the surface of one thrust deforming Black River Dolomite at 336500/5426450 showing reverse transport towards 028°.

Further north, folding of possible D_2 age is expressed as shallowly east or west-plunging open upright folds, identified from secondary girdle patterns in bedding data from Togari Group areas near the southern and southeastern margins of the Smithton Synclinorium and adjacent areas of the Rocky Cape Group (domains TG14, 15 and 17 and RCG6; fig. 12, 14, 19, 20). Some development of steep east-striking cleavage associated with the folding is evident (e.g. domain TG17, fig. 19). In most of these areas the ?D_2 folding is weaker than dominant NNE to NE-trending open folds of probably Cambrian but late or post-Tyennan age (see below), although a relative overprinting relationship cannot be established with certainty from the mesoscopic data.

Foliation and porphyroblasts

S_2 cleavage has been recognised in thin sections of Rocky Cape Group rocks from within the Roger, Sumac and Dempster map sheets, and also from east of Mt Frankland south of the Dempster map sheet, and on the coast at Temma. The S_2 cleavage is similar in form to, but typically cross-cuts S_1. S_2 is a continuous to closely spaced disjunctive cleavage defined by preferred alignment of chlorite grains typically less than 0.03 mm long. In orientated thin sections from weakly strained rocks east of Mt Frankland (samples R004795, R004797), S_2 strikes east-west and dips about 20°to 45°S (pre-D_3 orientation), consistent with mapped north-facing and east-trending folds.

S_2 is also preserved within porphyroblasts in Balfour Subgroup siltstone (Prbg) on Blackwater Road in the vicinity of 322130/5438850. Porphyroblasts are typically elongate, ovoid and rarely rhombohedral in shape and are up to about 2 mm in length (e.g. sample R004297, 321920/5438680). The porphyroblasts comprise cores of bladed chlorite and microcrystalline sericite ± albite ± quartz, and are rimmed by chlorite and sericite. The S_2 foliation is continuous from within the porphyroblasts to outside them, although the foliation developed internally is consistently rotated with respect to S_2 outside the porphyroblasts. The coincident rotation and preservation of S_2 through the porphyroblasts is inferred to indicate a syn-D_2 timing for porphyroblast growth.

Sample R006009, from a creek section at 323490/5436440 in unit Prbs, consists dominantly of very fine-grained white mica preferentially aligned parallel to a dominant cleavage (correlated with regional S_3, see below), and subordinate very

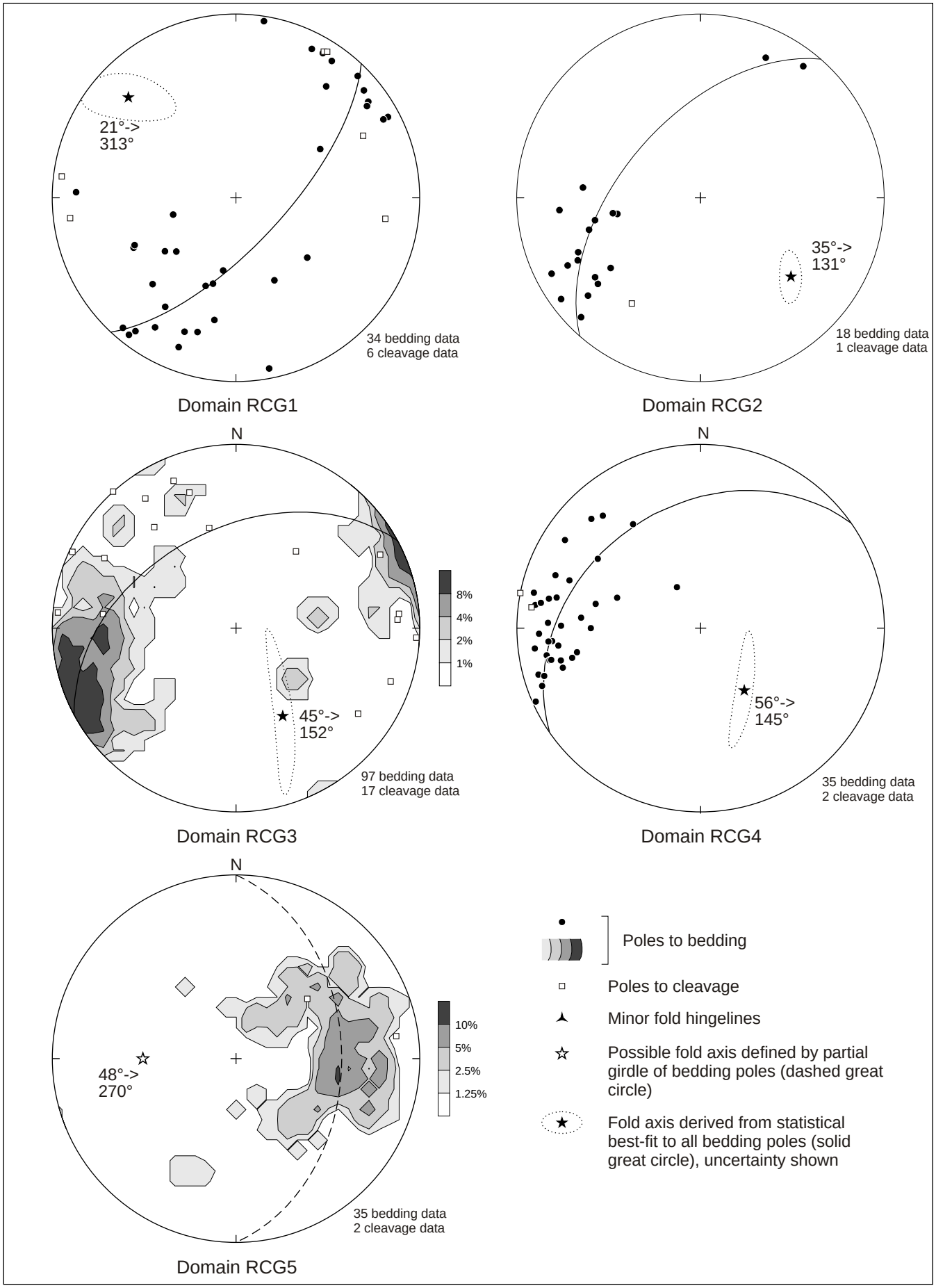

Figure 13

Stereograms of mesoscopic structural data, Cowrie Siltstone domains RCG1–5 west of the Roger River Fault.

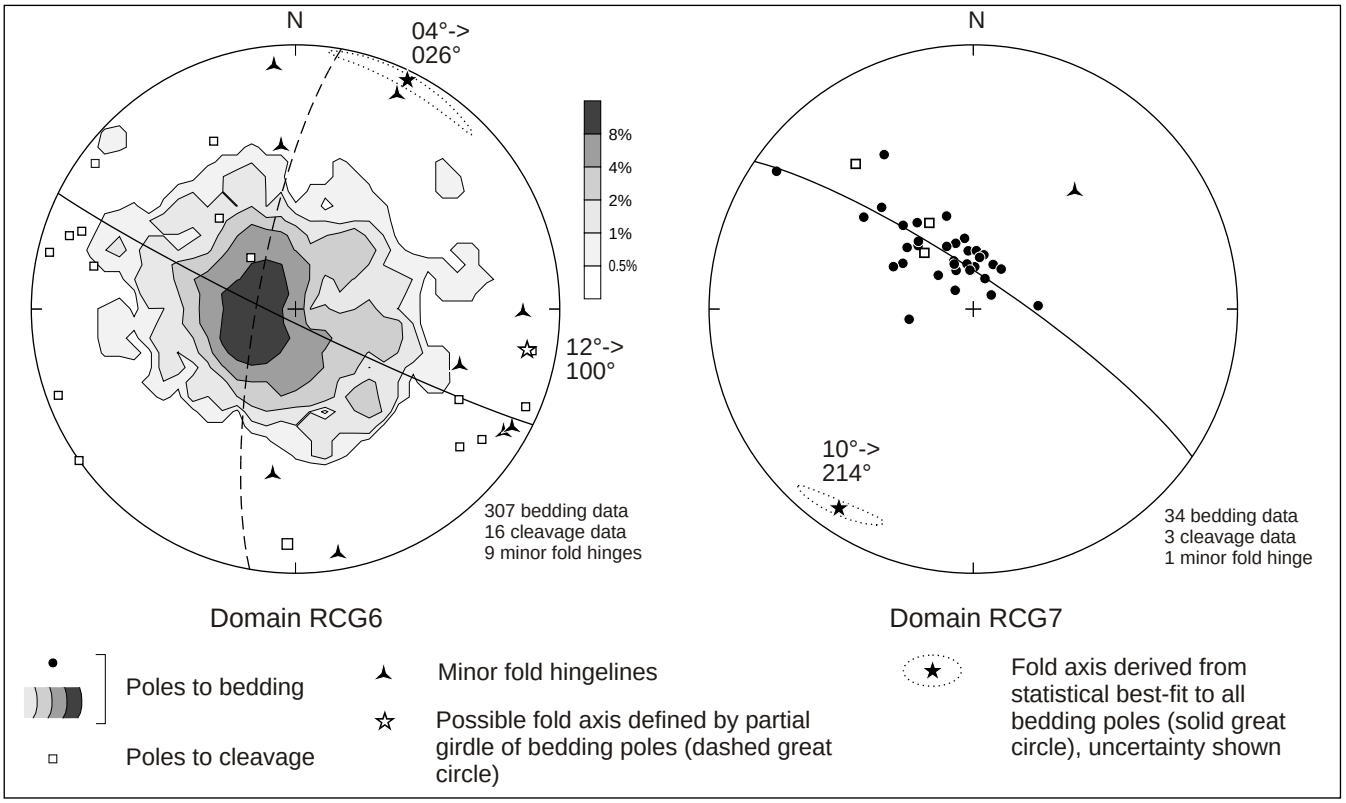

Figure 14

Stereograms of mesoscopic structural data, Cowrie Siltstone domains RCG6–7 east of the Roger River Fault.

fine-grained quartz. There is a subsidiary preferred orientation of the white mica about 30° oblique to the dominant cleavage, and which appears to define an earlier cleavage, interpreted to be regional S_2. A folded thin quartz vein in the thin section shows evidence of having been folded during both cleavage-forming events. The rock contains some 3–5% of ovoid porphyroblasts ≤1 mm in diameter, consisting mostly of a mosaic of fine-grained quartz, but with a thin rim of fine-grained white mica preferentially orientated parallel to the earlier of the two cleavages (S_2) in the rock. The porphyroblasts are commonly flattened in the plane of the dominant (S_3) cleavage, but because their rims preserve the S_2 fabric, the porphyroblasts grew either syn or post-D_2.

Sample R004298, of pelitic shale from the Cowrie Siltstone at 323380/5439940 on Blackwater Road, contains about 7% of ovoid porphyroblasts ≤1 mm in diameter. These pre-date the dominant semi-penetrative cleavage (probably regional S_4 based on its steep, N-S orientation) in the rock, as dark seams have developed on the sides of the spots which are parallel to this cleavage. The porphyroblasts commonly consist of a core of coarsely crystalline ?albite and an outer zone rich in fine-grained white mica, the latter showing a strong preferred orientation oblique to bedding which represents an earlier tectonic foliation (interpreted as regional S_2) preserved within the spots. White mica aligned in this earlier foliation is also present outside the porphyroblasts, but the fabric is much enhanced within the spots and progressively rotated counterclockwise within the spots compared to outside them. Outside the porphyroblasts the S_2 fabric is still oblique to bedding. The porphyroblasts also preserve at least two other preferred orientations of white mica, of unknown association.

Summary

The origin and absolute age of D_2 remain enigmatic. The presence of syn-D_2 porphyroblasts with composition and character consistent with a regional metamorphic event suggests that D_2 is related to one of the main phases of the Tyennan Orogeny. The folds are of an orientation that matches neither the northwest-trending folding and thrusting of D_3 age that dominates the western parts of the Sumac and Dempster map sheets, nor the NE-NNE trend that typifies Tyennan structures within the Arthur Lineament and ?late Tyennan or younger Cambrian folds east of the Roger River Fault in the Roger, Sumac and Dempster map sheets (see below).

Late(?) or post-Tyennan, Cambrian(?) folds east of the Roger River Fault

A minimum age for prograde metamorphism in the Arthur Lineament is provided by K-Ar (amphibole) dating of three amphibolite bodies, yielding a consolidated age of 500 ± 10 Ma (Turner, 1993). This event was assigned to a re-defined Tyennan Orogeny by Turner *et al*. (1998). Mapping by Everard *et al*. (1996) suggested that schistosity in the metamorphic core of the Arthur Lineament shows a gradual westward decrease in strain and metamorphic grade, apparently grading into axial plane cleavage associated with a belt

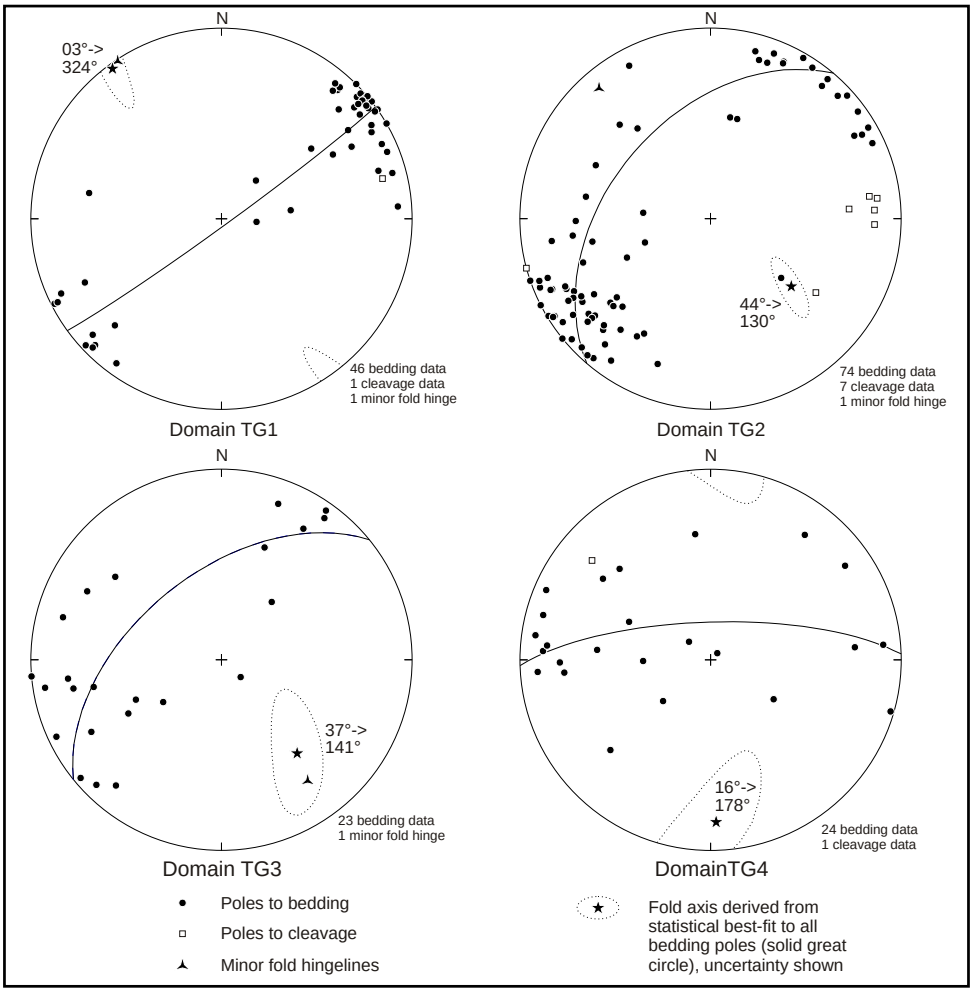

Figure 15

Stereograms of mesoscopic structural data, Togari Group domains TG1-4, west of the Roger River Fault.

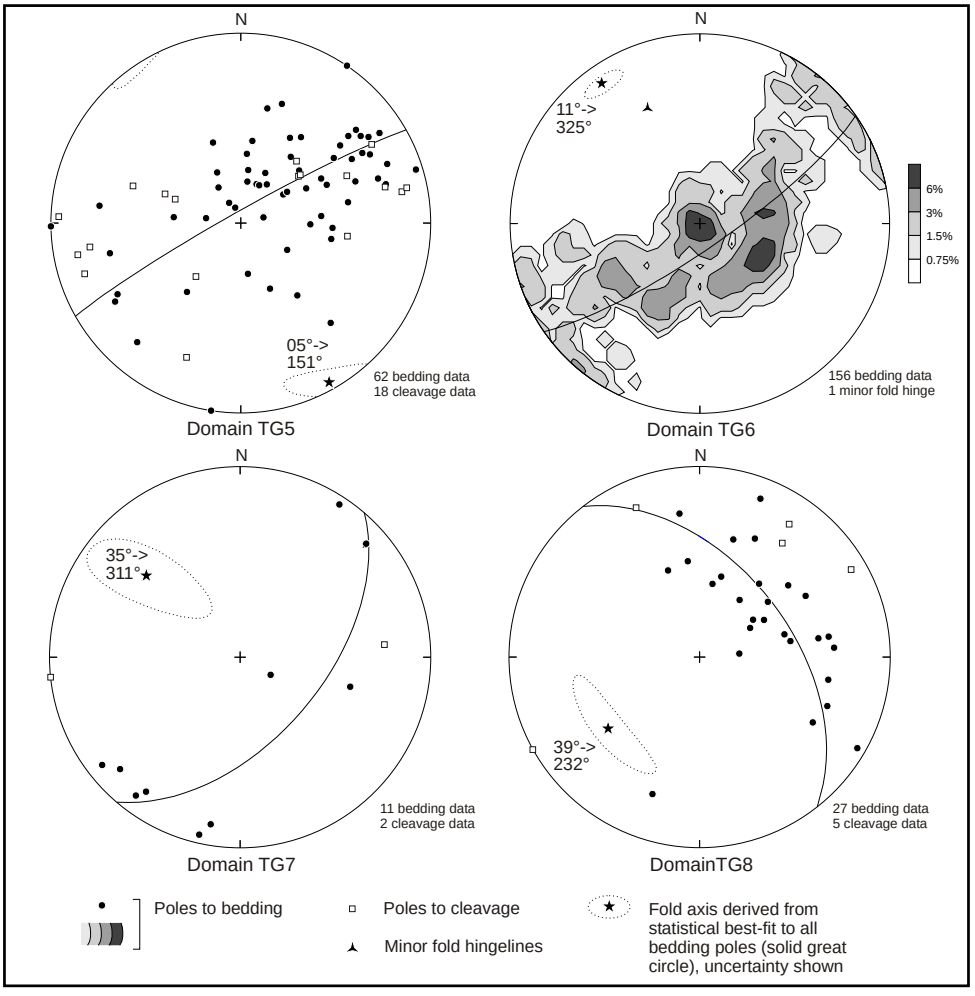

Figure 16

Stereograms of mesoscopic structural data, Togari Group domains TG5-8, west of the Roger River Fault.

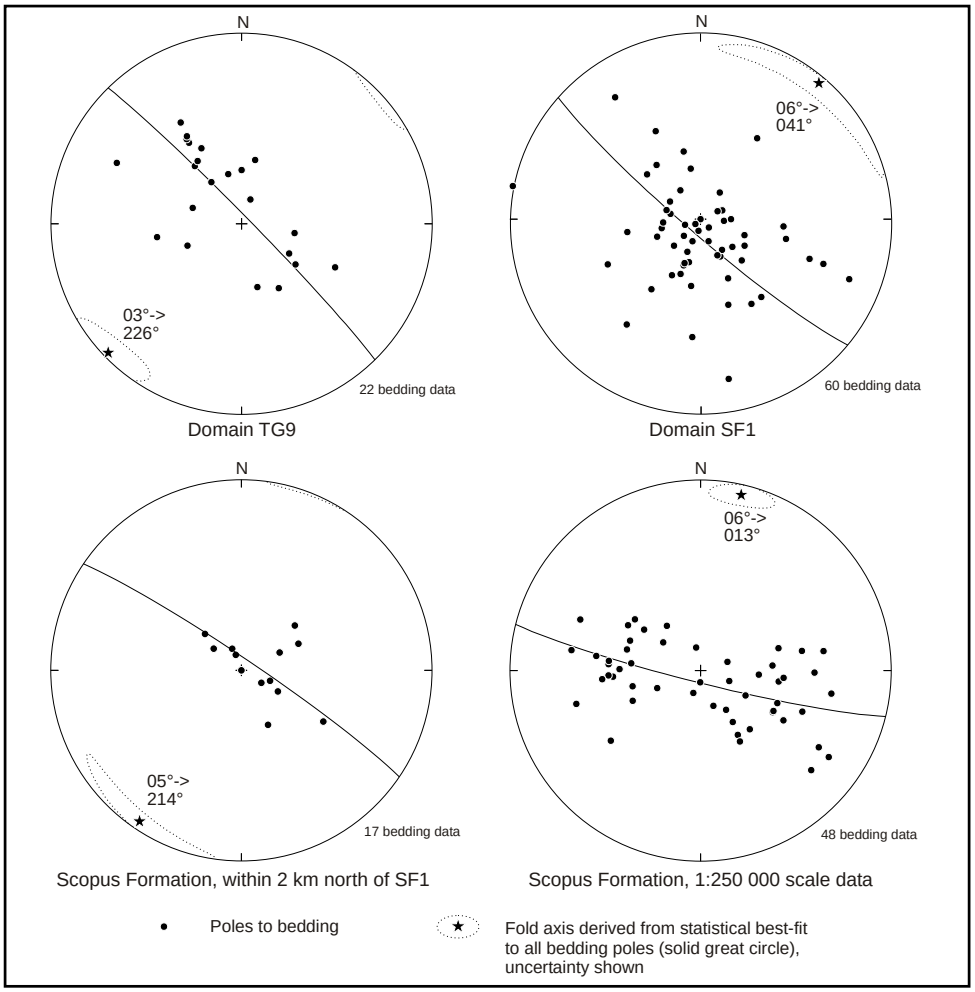

Figure 17

Stereograms of bedding data, domains TG9 (Togari Group) and SF1 (Scopus Formation), southern Christmas Hills area, west of the Roger River Fault. Also Scopus Formation bedding data from within two kilometres of domain SF1, and from the whole Christmas Hills–Stony Point region.

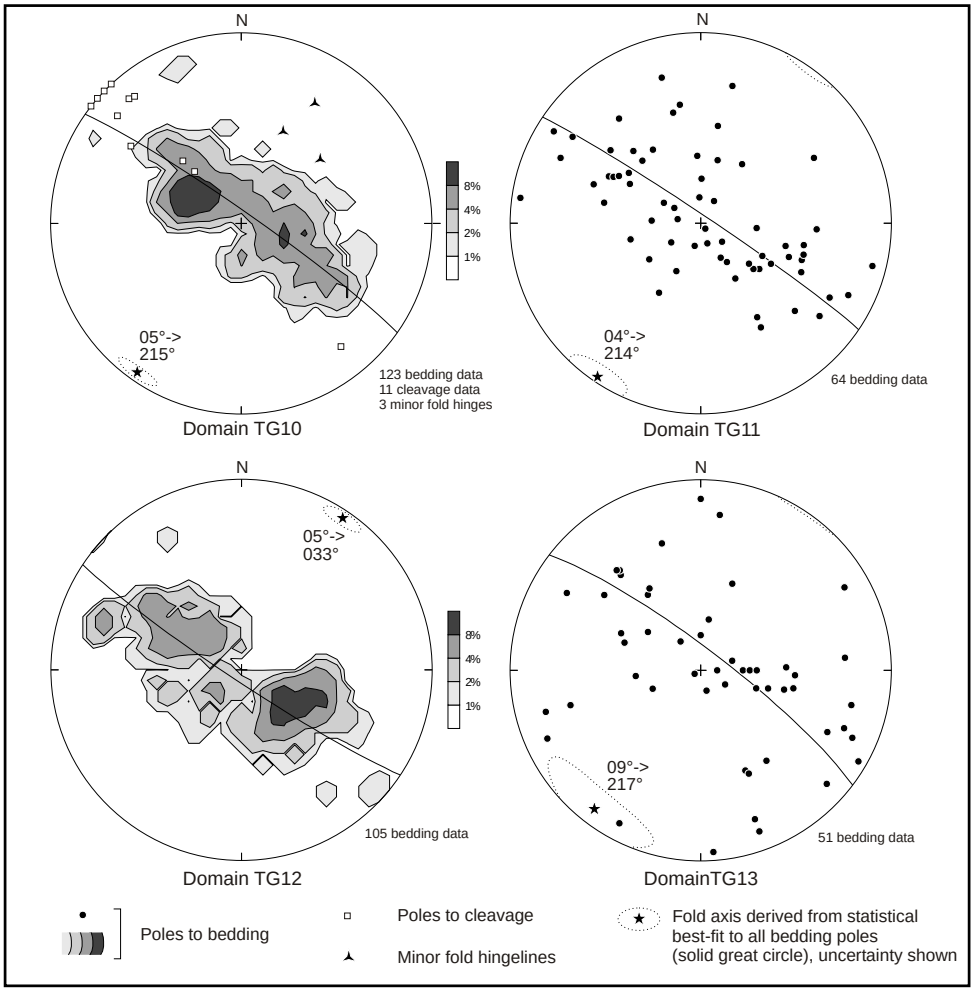

Figure 18

Stereograms of mesoscopic structural data, Togari Group domains TG10–13 east of the Roger River Fault.

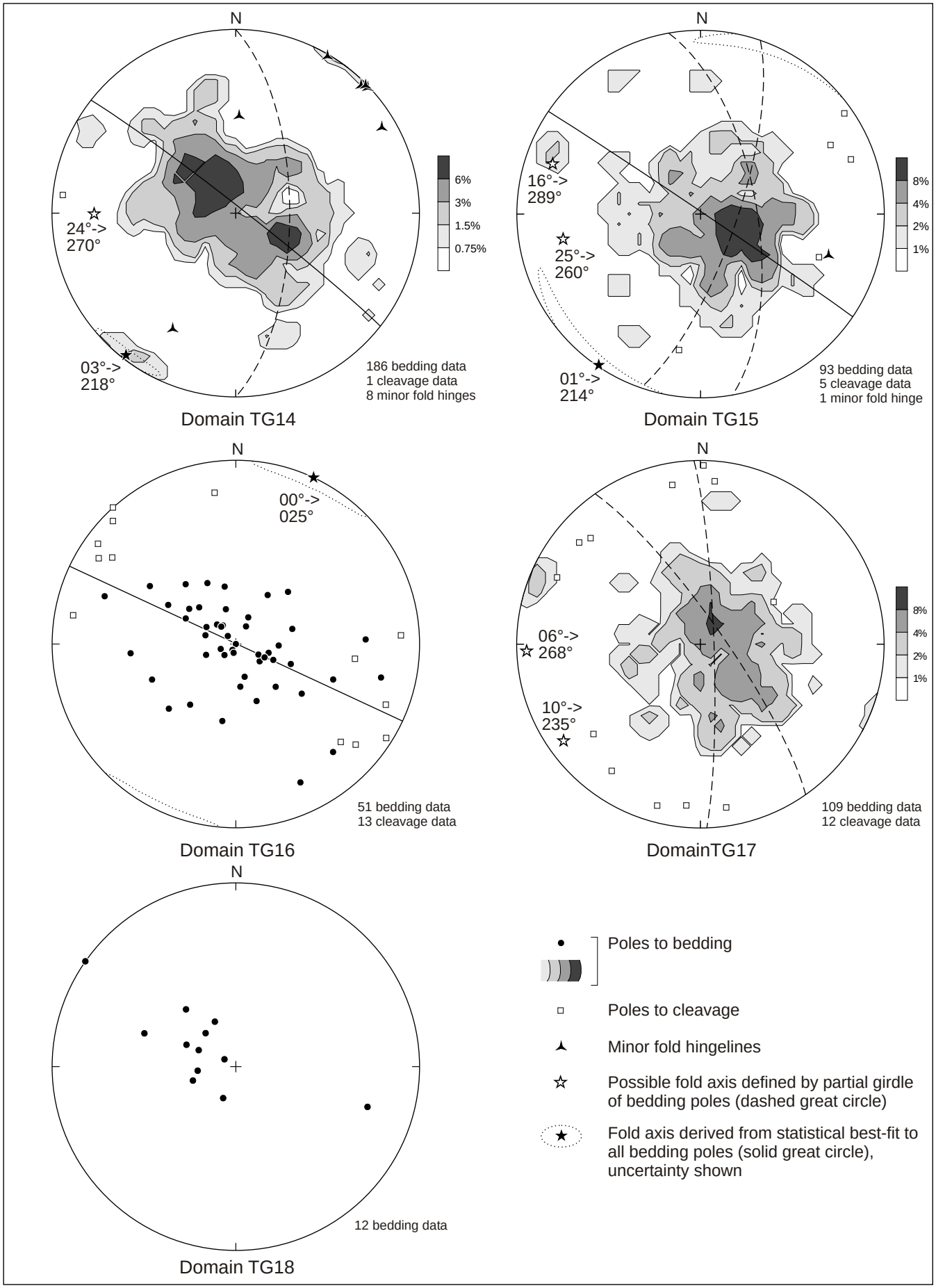

Figure 19

Stereograms of mesoscopic structural data, Togari Group domains TG14–18 east of the Roger River Fault.

of NE to NNE-trending folds in the Rocky Cape Group. Such a relationship would infer a Tyennan age for the latter folds, which are tight and strongly southeast-vergent with associated northwest-dipping thrusts close to the Arthur Lineament, but become gradually more open and upright with proximity to the eastern margin of the Smithton Synclinorium.

Later research in the Arthur Lineament (Holm and Berry, 2002) has demonstrated a complex metamorphic history, with two sequential high-strain deformation events and associated schistose textures. Both events were assigned to the Tyennan Orogeny by Holm and Berry (2002), but the southeast-vergent folds in the Rocky Cape Group were assigned to the Late Cambrian, on the basis that they refold the earlier schistose fabrics but do not penetrate Ordovician strata in the Duck Creek Syncline, at the intersection of the Arthur Lineament and the west coast (fig. 1). A Late Cambrian age for this substantial folding event is somewhat difficult to reconcile with the known stratotectonic history of western Tasmania, unless perhaps it correlates with the unconformity at the base of the Owen Group and correlates. Nonetheless, a late-Tyennan or post-Tyennan, Cambrian age for the event is consistent with the presently known constraints on its age.

Mapping by Everard *et al*. (1996), which overlapped the eastern half of the Roger map sheet, suggested that this ?Cambrian generation of folds also affects the Togari Group east of the Roger River Fault in the Smithton Synclinorium, although here the folds are open and almost upright in style. Penetration of these folds into the Togari Group in the eastern part of the Smithton Synclinorium is evident in Figure 21. Dominant gently southeast-plunging folds in the two easternmost Togari Group domains are similar in axial orientation (fig. 21) and style (Everard *et al*., 1996) to ?Cambrian folds which dominate Rocky Cape Group domains further east, and they are almost certainly of the same generation.

In the Togari Group east of the Roger River Fault within the Smithton Synclinorium, areas furthest away from the fault show rather diffuse patterns of bedding data on the stereograms (domains TG14–17, fig. 12, 19). This is believed to be due in part to the presence of more than one generation of folding in several of these domains, as inferred from secondary partial girdle patterns in the bedding data (fig. 19), the significance of which is discussed further below. Despite the diffuseness of the bedding data, statistical analysis in three of these four domains (TG14–16) yields inferred dominant fold axes which are close in orientation to the major folds of ?Cambrian age affecting the Rocky Cape Group east of the Smithton Synclinorium, albeit with broad uncertainty limits on the fold axial azimuths in TG14–16. This is consistent with the conclusion that the major generation of ?Cambrian folds east of the Smithton Synclinorium penetrates well into the Togari Group east of the Roger River Fault. The strain associated with the ?Cambrian folding in domains TG14–16 is not high, and only in domain TG16 is there evidence of any significant associated axial plane cleavage development (fig. 19).

Togari Group areas closest to the Roger River Fault on its eastern side (domains TG10–13, fig. 12) show well-developed girdle patterns in bedding data on the stereograms (fig. 18), indicating dominant fold axes plunging shallowly to about 035°/215°, with relatively small uncertainties on the axial orientations. These folds are virtually identical in orientation to ?Cambrian folds further east. The dominant folds in domains TG10–13 show evidence of higher strain, in better-defined girdle patterns and steeper limb dips, although axial plane cleavage development associated with the folds has only been recorded in domain TG10 (fig. 18). This zone of higher strain close to the Roger River Fault is interpreted to be a result of coaxial overprinting and/or tightening of the ?Cambrian folds during dextral transpression associated with late-D_3 strike-slip reactivation of the Roger River Fault (see below).

Immediately southeast of the Smithton Synclinorium, regional airborne magnetic data show patterns which suggest that these NE to NNE-trending ?Cambrian folds are truncated by arcuate major faults (McClenaghan and Seymour, 1996; fig. 1 herein) which are most likely thrust faults of D_3 age (see below) — although locally the truncation actually juxtaposes the ?Cambrian folds to the north against east to ESE-trending D_2 structures to the south.

Summary

The new research by Holm and Berry (2002) appears to have constrained this folding event to a Cambrian, but possibly post-Tyennan age, the implications of which need further work to resolve in the area studied by Everard *et al*. (1996). The known evidence suggests that the event is post-D_2 (and therefore perhaps late or post-Tyennan, consistent with the conclusions of Holm and Berry, 2002), and pre-D_3. There is a need for further work to tighten the relative age constraints, and so the event is not currently assigned a definite place in the structural sequence herein.

Third Compressional Deformation (D_3)

Rocky Cape Group and Togari Group units in the western parts of the Roger, Sumac and Dempster map sheets are dominated by a prominent belt of northeast-directed thrust faults and associated north to northwest-trending, northeast-vergent asymmetric folds, of D_3 relative age.

First order folding and thrusting

WEST OF THE ROGER RIVER FAULT

West of the Roger River Fault on the Sumac map sheet, and in the southwestern corner of the Roger map sheet, the Cowrie Siltstone and units of the Togari Group are involved in a major northeast-directed D_3 thrust system with associated gently to moderately northwest and southeast-plunging, northeast-verging folds. The main

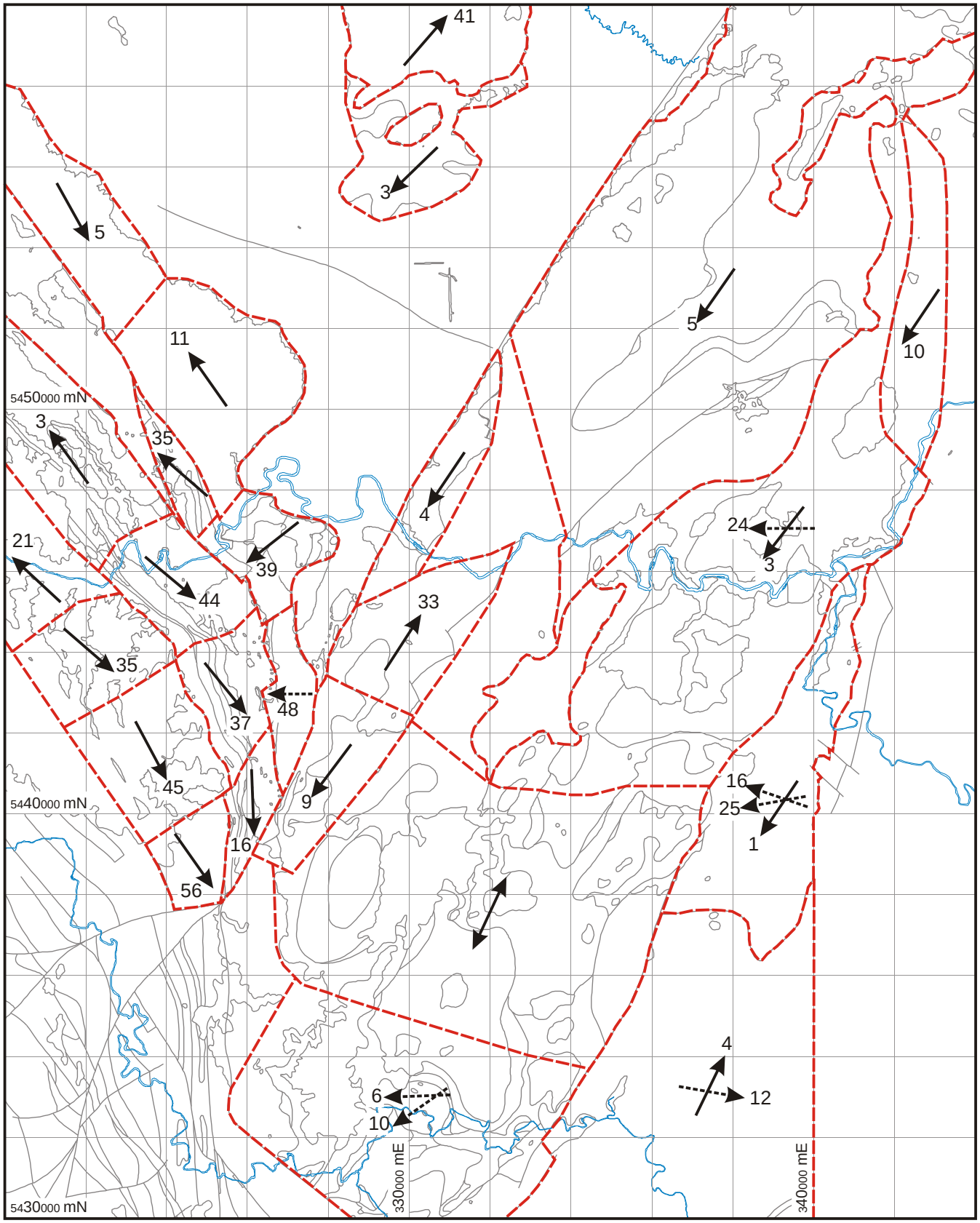

Figure 20

Summary results of domain analysis of bedding data, showing main and subsidiary interpreted fold axial orientations.

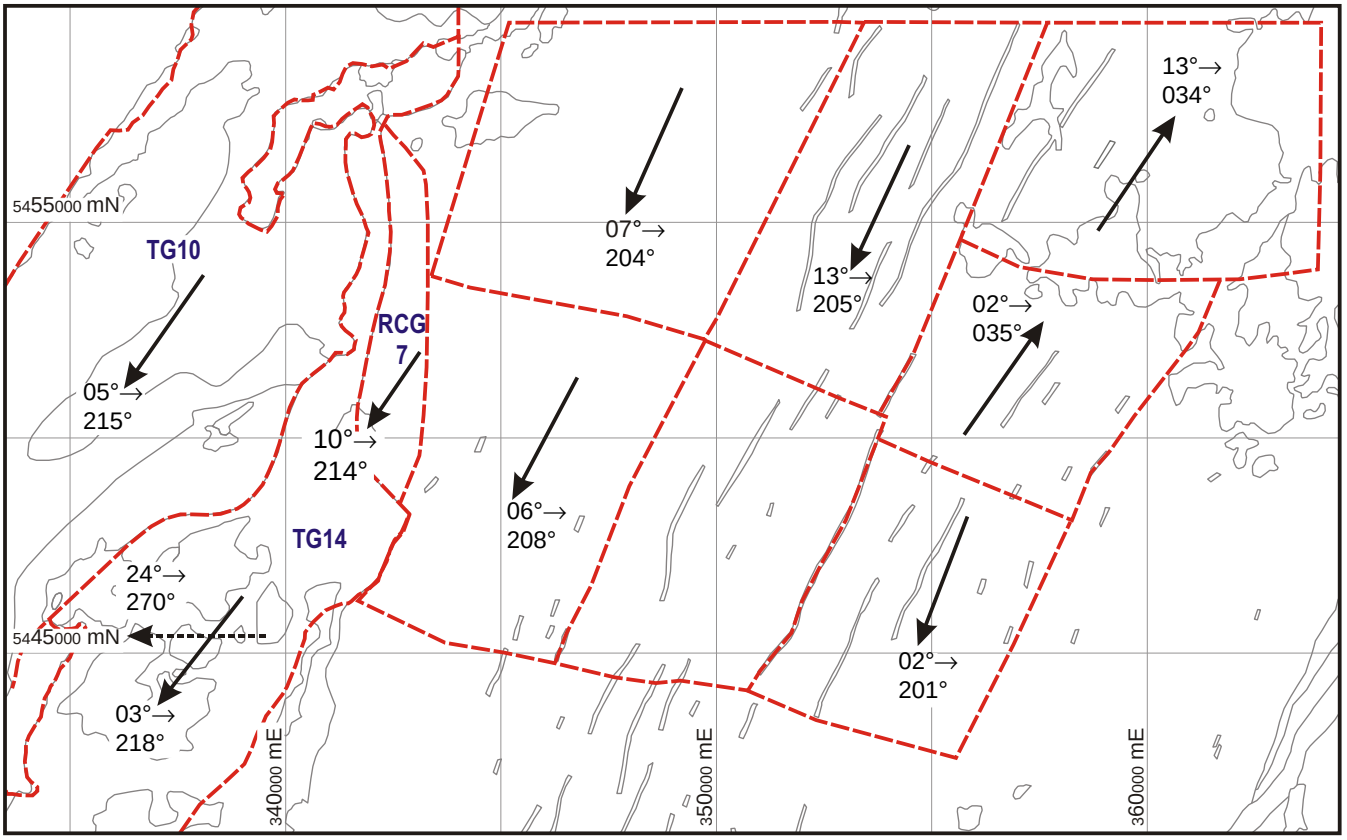

Figure 21

Comparison of interpreted dominant fold axial orientations between domains TG10, TG14 and RCG7, and Cowrie Siltstone domains east of the Smithton Synclinorium.

thrust faults in this system vary in orientation at ground level from steep to shallowly southwest-dipping, and the system includes one fault-bounded block comprised dominantly of Cowrie Siltstone but completely surrounded by Togari Group units. The major sole thrust of the system in this area is shallowly southwest-dipping at ground level and has a markedly curvilinear trace, crossing the Arthur River at 326245/5447910. This fault has locally inverted the stratigraphic order by placing sedimentary units of the Kanunnah Subgroup and Black River Dolomite structurally above the Smithton Dolomite.

Map patterns suggest that the dominantly northwest structural trends in this area show progressive clockwise rotation into almost north–south trends with proximity to the Roger River Fault, the effect being first evident some five kilometres northwest of the fault. Domain analysis shows that the rotation is also evident in the azimuths of D_3 fold axes (fig. 20, supporting data in fig. 13, 15 and 16), and that there is concomitant steepening or reversal of D_3 fold plunges, from sub-horizontal to shallow northwest plunges away from the fault, to intermediate southeast to south plunges close to the fault (fig. 20). These rotations comprise one of several effects considered to have resulted from late-D_3 dextral transpression on the Roger River Fault (see further discussion below).

Strong asymmetry of the D_3 folds is evident within the thickest block in the thrust system in this area (encompassing domains RCG1-4 and TG1-4, fig. 12), which includes a 2.65 km thick section of Cowrie Siltstone unconformably overlain by an almost complete section of Togari Group units. Many of the domains in this block show bedding dominantly steeply northeast to east-dipping and facing, but with partial girdle patterns defining the effect of D_3 folding (fig. 13, 15). Axial plane cleavage development associated with the D_3 folds is apparently scant, but some domains show development of steep north-striking cleavage apparently overprinting the D_3 folds (domains RCG1 and RCG3, fig. 13; TG2, fig. 15), and which is correlated with D_4 (see below).

Togari Group units which immediately overlie the main D_3 sole thrust show greater development of D_3 folding, evident in moderately to well-developed girdle patterns in bedding data on the stereograms (domains TG5-7, fig. 12, 16). Cleavage data from domain TG5 tend to cluster around the somewhat diffuse bedding girdle, suggesting some of these are S_3 cleavages. Domains TG8 and RCG3, along strike from TG5-7 but closer to the Roger River Fault, show evidence of folds plunging moderately to the southwest and west respectively, but these are interpreted as late-D_3 structures which have overprinted the first-order D_3 folds, as discussed below.

WESTERN PART OF THE DEMPSTER MAP SHEET, AND TEMMA–BALFOUR AREAS

West of the Frankland River, in the western part of the Dempster map sheet, a northwest-trending D_3 anticline with a half-wavelength exceeding five kilometres deforms Balfour Subgroup sedimentary rocks. The anticline verges northeast, and has a sub-vertical, in places overturned, northeast limb truncated by southwest-dipping thrusts. Reverse movement on thrusts has placed older over younger Balfour Subgroup rocks and Balfour Subgroup rocks over younger Togari Group sedimentary and volcanic rocks. Exposure of the thrusts is typically poor. One structure cropping out in Cassiterite Creek (322590/5433760) is manifest as an intensely brecciated and silicified zone separating older sandstone (Prbq) in the hanging wall from younger chloritic siltstone (Prbg) in the footwall. The along-strike continuation of this structure hosts the Murrays Reward deposit at Balfour (324500/5429500).

The southern continuation of one of the thrusts placing Rocky Cape on Togari Group rocks crops out south of the Dempster map sheet at the intersection of the Heemskirk Road with Waratah Creek, south of Mt Frankland (327400/5424800). This thrust is here named the Waratah Creek Thrust. The fault is not a discrete structure but rather a zone of highly foliated and moderately veined schist, the boundaries of which are transitional with adjacent sedimentary rocks. This has made it difficult to ascertain an accurate dip. Elongate ovoid porphyroblasts of D_2 age are recognisable in hand specimen from outcrops in the creek but are flattened (about 90% shortening) into the prominent S_3 foliation. Nearby, the rocks are mylonitic, with tails to rotated clasts and S-C fabrics (samples R007201, R004800) indicating reverse movement. C-C′ fabrics and ultramylonites are also common. Thrust fabrics are overprinted by an S_4 crenulation cleavage, the formation of which may have accompanied fault reactivation (sample R004799).

The Waratah Creek Thrust separates predominantly steeply east-dipping Balfour Subgroup rocks in the west from gently folded Cowrie Siltstone and Togari Group rocks further east. West of the fault, both D_3 folds and cleavage strike north, but east of the fault they strike northwest. This discordance is consistent with progressive development of a northwest-trending fold, followed by thrusting and rotation of hanging-wall structures into a north-south orientation near the southern limits of an arcuate thrust system. Juxtaposition of upper Balfour Subgroup and Cowrie Siltstone rocks either side of the Waratah Creek Thrust also suggests minimal disruption of the stratigraphic sequence and displacements of probably less than 500 metres. In contrast, the strike continuation of the same structures on the Dempster map sheet place Balfour Subgroup rocks over Togari Group (324500/5433500). Comparing the difference between the northwest projection (parallel to the original fold trend, preserved in rocks east of the Waratah Creek Thrust) of the Waratah Creek locality with the same thrust on the Dempster map sheet, indicates a minimum eastward horizontal displacement of Rocky Cape Group rocks (southwest of the Roger River Fault) of 3500 metres.

The age of movement on the Waratah Creek Thrust has been constrained relative to the intrusion of granite at depth (see granite isobaths, fig. 1). Pseudohexagonal porphyroblasts of chlorite and tourmaline (possibly after cordierite) overprint flattened D_2 porphyroblasts within the Waratah Creek Thrust, and other thrusts of similar age, but are themselves weakly deformed by the S_3 cleavage. Brecciated tourmaline is also present as rotated clasts within D_3 mylonites. The tourmaline is most likely associated with the granite, although a sedimentary origin is not discounted. Contemporaneous overprinting and deformation of a granite-related mineral assemblage indicates a syn to late-D_3 age for granite intrusion. The nearest outcropping granite, the Interview Granite at Sandy Cape, has yielded a U-Pb zircon age of crystallisation of 362.4 ± 1.9 Ma (Black *et al*., 2005), making D_3 Devonian in age.

D_3 folding and thrusting of Rocky Cape Group sedimentary rocks was accompanied by development of a slaty cleavage, or less commonly a crenulation cleavage. Foliations formed prior to D_3 are commonly obliterated or significantly masked by S_3, and thin section examination is required for their resolution. In general, cleavages are poorly preserved in more arenaceous sedimentary units, with S_3 commonly evident in these rocks only as preferential dissolution along grain boundaries. The orientation of the S_3 cleavage varies between northwest–southeast and north–south, with both folds and cleavage rotated consistent with varying displacement above D_3 thrusts.

Second order thrusting

Northwest-trending reverse faults dissect the core of the northeast-verging anticline west of the Frankland River on the Dempster map sheet. The largest of these faults separates the Lagoon River Quartzite from stratigraphically overlying Balfour Subgroup sedimentary rocks, and hosts the Specimen Hill Sn-W deposit at Balfour (324000/5428500). Field observations and IP-based geophysical cross sections (Menpes, 1995*b*) show the faults dipping steeply both northeast and southwest, with the Specimen Hill Fault dipping moderately to the southwest. Faulting is commonly accompanied by doubly-plunging mesoscopic open to tight northwest-trending folds. The increased frequency of reverse faults towards the anticlinal hinge is consistent with their formation as accommodation structures resulting from space restrictions during folding and thrusting. These hinge-related structures probably link with thrusts emergent east and west of the Frankland River and which have resulted in Rocky Cape Group rocks being placed over younger Togari Group rocks.

Early strike-slip faulting

As well as being folded and dissected by northwest-trending thrusts, Balfour Subgroup rocks west of the Frankland River on the Dempster map sheet

are deformed by ENE to NE-trending faults. These faults are particularly common in coarser-grained, more competent sedimentary units, and are especially well developed in the Lagoon River Quartzite. The apparent offset at surface is typically no greater than a few hundred metres. These faults are almost everywhere truncated by D_3 age thrusts, implying their formation early during folding, prior to initiation of thrusting. These faults probably provided a mechanism for the compartmentalisation of strain by segmentation of the regional-scale D_3 folds, prior to thrusting.

Late strike-slip faulting and reactivation of the Roger River Fault

Northwest-trending D_3 folds and thrusts are truncated by NE to ENE-trending splays off the Roger River Fault. Two splays cross the Heemskirk Road at 321120/5436150 and 321850/5432100 and are clearly identifiable from aeromagnetic data. The faults are manifest in outcrop as complexly folded, faulted, brecciated and variably veined zones. Neither dip nor movement sense are clearly apparent, with subsidiary structures that parallel and lie adjacent to the southernmost splay showing both sinistral and dextral offset of bedding. This contrasting offset is also apparent at the map scale, with an apparent sinistral offset of the Specimen Hill fault and Lagoon River Quartzite but an apparent dextral offset of similarly northwest-trending and southwest-dipping thrusts northeast of the Frankland River.

A steep northwest dip of the southernmost splay is evident in geophysical IP cross sections (Menpes, 1995*b*). Such an orientation at first seems unusual, given the strike continuation of this fault with the originally southeast-side-down, normal and presumably southeast-dipping Roger River Fault on the Roger and Sumac map sheets. Aeromagnetic data show the southward continuation of the southernmost splay linking with a southwest-dipping and northwest-trending thrust south of the Dempster map sheet. The contrasting offset of these splays, and their late development relative to D_3 folding and thrusting, suggest their formation as transfer structures or oblique ramps linking northwest-trending thrusts with the Roger River Fault. The variation in offset across the splays is therefore probably due to variation in the degree of movement on the northwest-trending thrusts. Northwest-trending D_3 thrusts located east of the Frankland River on the Dempster map sheet have experienced relatively greater movement northwest of the Roger River Fault splay. In contrast, the sinistral offset of the Specimen Hill Fault suggests relatively greater movement on this structure on the southeast side of the Roger River splay fault.

The formation of the splays to the Roger River Fault as transfer structures not only accounts for the geometric and timing relationships of structures on the Dempster map sheet, but also implies late-D_3 dextral strike-slip transpressional reactivation along the length of the Roger River Fault. This fault, within the Roger–Sumac–Dempster area, varies in trend between about 023° and 035°, 20–32° anticlockwise from the approximate D_3 thrust transport direction of about 055°. Northwest of the Roger River Fault, northwest-striking D_3 thrusts appear to have been refolded about northeast-trending axes, e.g. in domain TG8 (fig. 12, 16, 20), and open folds apparent in map patterns within the area of domains TG2–4 (fig. 12). Up to about 45° clockwise rotation of originally NW–SE D_3 structural trends is apparently associated with proximity to the Roger River Fault in the same area. Such folding and distortion is consistent with local rotation of principal stress orientations adjacent to a reactivated Roger River Fault. A similar origin could be suggested for gently northeast or southwest-plunging open folds which affect the upper unit of the Togari Group and the overlying late Middle to early Late Cambrian Scopus Formation at the southern end of Christmas Hills on the Roger map sheet (domains TG9, SF1, and Scopus Formation within 2 km north of SF1; fig. 12, 17, 20). These areas are close enough to the Roger River Fault to be possibly affected by deformation associated with that structure. The large belt of northeast-trending open folds and elongate dome and basin structures in the Togari Group east of the Roger River Fault, while almost certainly owing part of its geometry to pre-D_3 ?Cambrian folds, may also partially reflect deformation which occurred during late-D_3 reactivation of the Roger River Fault — particularly in areas closest to the fault (domains TG11–13 and probably part of domain TG10, fig. 12, 20).

Northeast of the area covered by the Roger–Sumac–Dempster map sheets, geophysical data indicate the northeast continuation of the surface trace of the Roger River Fault into a series of east–west trending structures. These structures parallel the Boat Harbour Fault, a major east-trending structure located about five kilometres south and west of Rocky Cape. Refolding of northeast-trending folds of inferred Cambrian age adjacent to the Boat Harbour Fault, together with direct evidence from offsets of major quartzarenite units in the Rocky Cape Group, indicate dextral movement (Seymour, 1997). If the Boat Harbour and Roger River faults are linked, as the geophysical data suggest, then dextral movement on the Boat Harbour Fault is consistent with dextral transpression on the Roger River Fault. Combined, the Roger River and Boat Harbour faults, and subsidiary structures, may have transferred strain from the Dempster area as far northeast as the Bass Strait coast.

Inversion of extensional structures

Variation in the thickness of the Togari Group either side of an inferred thrust at 325000/5434000 indicates thrust reactivation of an originally extensional fault, possibly the modified surface trace of what was originally part of the Roger River Fault system. The presence of foliated and folded dolerite dykes in this and nearby parallel thrusts (e.g. 325280/5431000) also indicates an extensional history pre-dating thrusting. The age of the dykes is unknown, although dykes

located elsewhere in the Rocky Cape Group, on the Bass Strait coast east of the Smithton Synclinorium, have yielded late Neoproterozoic K-Ar ages of 584 ± 8 Ma, 600 ± 8 Ma and 588 ± 8 Ma (Brown, 1989*a*). These thrusts continue south of the Dempster map sheet and lie adjacent to Togari Group conglomerate (326500/5427100), again consistent with their having an early influence on sedimentation.

Not all structures linking with the Roger River Fault are considered to have been extensional. Northeast and east-striking faults on the Dempster map sheet (e.g. 322350/5434000) that link with the Roger River Fault at about 325000/5437700 clearly cut a major northwest-trending fold in Balfour Subgroup rocks, making them of late D_3 or later age. These structures may link at depth with the unthrusted portions of the Roger River Fault (but now overlain by folded and thrusted Rocky Cape Group).

Fourth Compressional Deformation (D_4)

In the core of the Smithton Synclinorium, the Scopus Formation of late Middle to early Late Cambrian age is affected by open, upright folds with a preferred axial orientation plunging at 6° to 013° (fig. 17). This generation of folds also appears to have affected the Togari Group in most of the northern half of the Smithton Synclinorium, and its offshore continuation in Bass Strait (visible in airborne magnetic data, e.g. Gunn *et al*., 1996). Interference with earlier (or possibly later) folds may have contributed to the presence of two basement-cored domal structures in the northeastern and northwestern parts of the synclinorium (Lennox *et al*., 1982; Brown, 1989*a*; Seymour and Baillie, 1992).

West of the Roger River Fault on the Sumac and Roger map sheets, D_4 structures are mainly manifest as steep north-trending cleavages and some associated minor folds, which appear to overprint structures associated with the dominant northwest-trending D_3 fold and thrust system. Examples include steeply west-dipping cleavages in domain TG2 that are clearly unrelated to the D_3 folding in that domain (fig. 15), and steep north-trending cleavages in Rocky Cape Group domain RCG3 (fig. 13).

The effects of D_4 on rocks west and south of the Frankland River on the Dempster map sheet are not considered great. Folding and a second spaced crenulation cleavage, clearly overprinting S_3, were noted at only one location in the Dempster map sheet (at 321800/5437900). The post-S_3 cleavage strikes 015° and dips 80° east, and accompanies folds that plunge 74° to 210°. The deformation is of an orientation consistent with open folding of upper Togari Group rocks, but may also simply be the result of local faulting.

An S_4 foliation is better preserved in rocks located east of the Waratah Creek thrust, south of the Dempster map sheet. Here, regional mapping has shown that D_4 is manifest as open upright folds, commonly showing a preferential vergence towards the west. Microscopic to mesoscopic reverse kink bands with axial planes dipping moderately east and northeast are common. A weakly developed spaced crenulation cleavage is rare.

Steeply east-dipping D_4 faults have also been recognised along the coast on the Temma map sheet (Seymour and Reed, 2003), where they deform earlier D_3 structures. *En echelon* tension fractures in rocks adjacent to the D_4 faults indicate reverse movement.

Aeromagnetic and radiometric data were acquired over the Roger–Sumac–Dempster area by the Bureau of Mineral Resources (now the Australian Geological Survey Organisation) in 1984, as part of the Northwest Tasmania Survey (500 m line spacing). A more detailed survey with 200 m line spacing was flown over most of the area (excluding those parts of the Roger and Sumac map sheets east of about 336000 mE) by MRT and AGSO in 1996 for the Tasmanian Regional Forest Agreement. The qualitative interpretation of colour images derived from these surveys (total magnetic intensity, fig. 22 and radiometrics, fig. 23, 24) is briefly discussed below.

Parts of the Dempster and Sumac map sheets (318000 to 330500 mE and as far north as 5430000 mN) were flown in more detail (100 m line spacing) by CRA in 1993. This survey has not been incorporated into the MRT data set.

Magnetics

The total magnetic intensity image (fig. 22) is dominated by anomalies sourced from Neoproterozoic basalt (Spinks Creek Volcanics), which has magnetic susceptibilities an order of magnitude higher than other major units, including most Tertiary basalt (see *Igneous rocks* section).

The thick pile of basalt immediately east of the Roger River Fault broadly accounts for the large NNE-trending zone of intense short wavelength anomalies immediately east of the Roger River Fault, although the magnetic image does not exactly coincide with the surface distribution of the basalt within this zone. The zone includes some large areas of outcropping Keppel Creek Formation (e.g. in the lower Keppel Creek area) which presumably conceal basalt at shallow depth. There are also areas of strong negative anomalies over confirmed basalt outcrops (e.g. Stephens Rivulet near 328300/5441300, south of Ekberg Creek near 333300/5448700, Horton River at 328000/5431200), raising the possibility of locally reversed remanent magnetisation. Another possible influence is metamorphism of the basalt (in particular, replacement of magnetite by sphene) which reduces its magnetic susceptibility (see above). It is unclear if this is locally consistent enough to be reflected in the regional total magnetic intensity data.

A strongly positive linear anomaly, corresponding to a thin, nearly continuous unit of steeply-dipping basalt, extends parallel to the western margin of the synclinorium from 326000/5441600 to 320000/5449800 (Sumac map sheet), where it is slightly offset by a small cross fault. A similar linear anomaly, also due to basalt, is present further east in the Leensons Road area (324800/5447000 to 323100/5450300). Several smaller anomalies in this area (321500/5447100, 322200/5446400 and 325600/5441300) are associated with gabbroic intrusions related to the basalt. These anomalies are not much larger than the mapped extents of the intrusions.

The magnetic data proved useful in mapping the basalt distribution in areas of dense rainforest in the south of the region, but all areas shown have been confirmed by field checking. Particularly evident on the image, but poorly outcropping in the field, are the linear north-trending unit of basalt north of Balfour (324400/5436800 to 324900/5431600) and the Lindsay River exposure (329700/5430000).

A positive 'bullseye' anomaly just south of the Arthur River (327700/5447000) lies over poorly outcropping Black River Dolomite, and may be sourced in underlying basalt in the footwall of an inferred east-directed thrust. A similar anomaly nearby at 326550/5447250 may have a similar origin.

The Croles Hill Diamictite (Psvx) has a weakly magnetic signature due to the presence of basalt clasts whilst the Keppel Creek Formation (Psvw) is normally magnetically quiet in character, where not closely associated with basalt. Positive magnetic anomalies in outliers of the latter unit at 330900/5434200 and 330100/5434600 (Dempster map sheet) suggest some associated basalt may be present. A small anomaly at 322700/5451800 (Roger map sheet) coincides with mapped ironstone, and nearby similar anomalies (320100/5454900, 320300/5454600) may indicate ironstones near the top of the Keppel Creek Formation, concealed beneath thin Tertiary gravel.

Tertiary basalt at Molompto Road (332600/5459800) is associated with a small positive anomaly. A similar anomaly at 329700/5459600, which probably has not been field checked, may be caused by a similar plug. The Tertiary basalt on the Dempster map sheet is apparently too thin to have a magnetic response clearly distinguishable from that of the adjacent, thicker and more magnetic Neoproterozoic basalt.

Although the Black River Dolomite is usually magnetically quiet, it contains a NNE-trending series of weak positive magnetic anomalies, extending northward of 337800/5440000 (southeast of the Sumac map sheet). These do not coincide with the radiometric total count anomalies in the same area (see below). Seymour (1997) noted that a possible extension of this magnetic trend ('Tipunah Road Anomaly') north of the Arthur River continues for 22 km into the Cowrie Siltstone before terminating against the Boat Harbour Fault. He suggested that the feature is caused by limonitic alteration along an east-directed thrust fault. To the south, on the Dempster map sheet, the magnetic trend may coincide with the faulted eastern margin of the Togari Group (through 335000/5434500). An alternative view is that the trend bends southeastward, extending to a small high-amplitude anomaly near the headwaters of Nugget Creek (340100/5445400), but not continuing into the Cowrie Siltstone.

The Cowrie Siltstone to the east of the Smithton Synclinorium is represented by a magnetically quiet area, interrupted in the extreme southeast of the

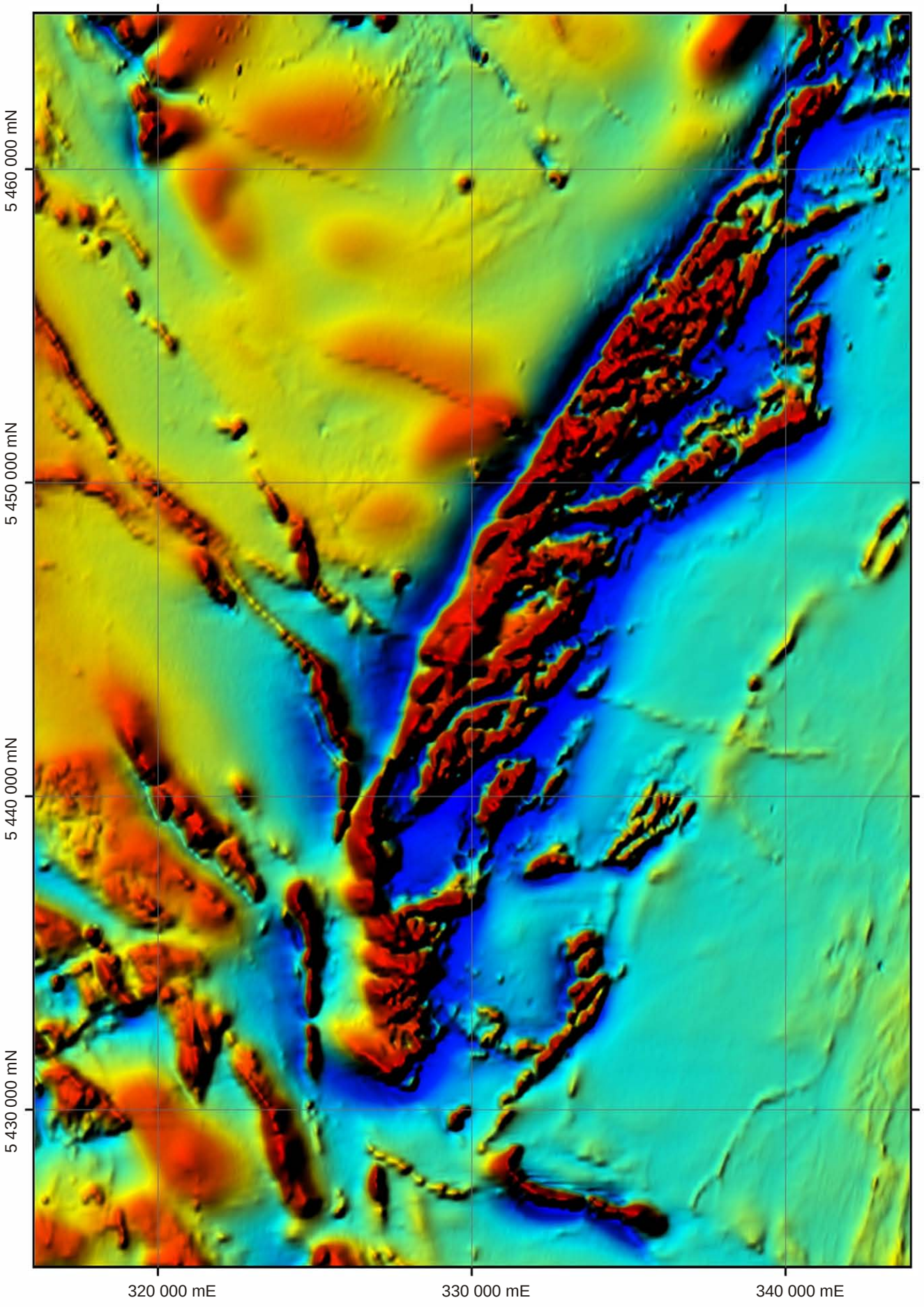

Figure 22

Total magnetic intensity image for the Roger, Sumac and Dempster map sheets and immediately adjacent areas.

Dempster map sheet (339300/5430300) by a rather weak linear anomaly coinciding with a dolerite dyke. There is much more magnetic relief over the Rocky Cape Group to the west of the synclinorium. In particular, there are several NW-trending anomalies parallel to strike in Balfour Subgroup units. There is also an unexplained 'bullseye' anomaly at 322600/5440200, where Tertiary gravel overlies Cowrie Siltstone correlate.

A large, poorly understood, WNW-trending magnetic lineament on the Roger map sheet extends as a 'magnetic ridge' from 323800/5455000 to 332000/5451500, where it terminates against the Roger River Fault. The surface geology is entirely Quaternary alluvium, probably mainly resting on Smithton Dolomite. A small, strongly positive peak on this lineament (331170/5451800), and a similar double anomaly about 1.7 km to the southwest near Leensons Road (330050/5450450; 330160/5450200), were drilled by Ashton Mining. In each case, magnetic mafic rocks (susceptibility 3–15 $\times$ 10^{-3} SI) were encountered at depths of 21 to 25 metres. Although highly weathered, microprobe analyses of chromite separates suggested an alkali basalt composition (Gunn, 1999).

A similar WNW-SSE lineament, about 7.5 km to the south and mainly on the Sumac map sheet, consists of a series of aligned positive linear and point magnetic anomalies. It extends WNW from 335800/5442600 in the Cowrie Siltstone to 320000/5449000, and continues to 309300/5453700 near Sky Creek on the unmapped Bluff map sheet. As it cuts, without deflection or offset, across all major Togari Group units and the Roger River Fault, it is probably a relatively young, or recently re-activated, structure.

Several long wavelength positive magnetic anomalies in the Montagu Swamp area (e.g. 321400/5459000, 322300/5457800, 326400/5457500 and 327300/5449000) probably have deep (≥1 km) sources.

Radiometrics

The total count image (fig. 23) predominantly reflects rock type, but physiographic, vegetation and cultural effects are also present.

The unit most consistently associated with areas of high total counts is the Cowrie Siltstone (Prc), reflecting its pelitic character (high K and presumably Th and U). The Blackwater Road inlier (centred on 327300/54430000 on the Sumac map sheet) is very obvious. The Balfour Subgroup has a locally strong but very variable radiometric signature north and northwest of Balfour.

The Scopus Formation (Cs) is also relatively high in total counts, and its mapped boundaries on the Roger map sheet closely correspond with the boundaries of an associated radiometric high. The mapped outlier at 333000/5457000 is also evident, but the image suggests that it extends further northeast and may be continuous with the main tract.

The Keppel Creek Formation (Psvw) is also associated with high total counts on the Roger map sheet. In particular, the topographically relatively upstanding northwest-trending tract in the Lerunna Road area is very obvious on the total count image, which here closely coincides with mapped geology. The Keppel Creek Formation appears to become less radioactive southward towards the Dempster map sheet, where it has only a subdued signature. This may partly be a vegetation and/or topographic effect, as the Keppel Creek Formation is poorly exposed in dense rainforest in this area.

Many areas of very low total counts are underlain by the Black River Dolomite (including the Julius River Member) or associated chert lag (unit Qhl). The folded trace of the Black River Dolomite/Rocky Cape Group boundary is clearly apparent near Dempster Lookout (338500/5436500), as is the linear faulted contact between these units further south and the inlier around 328500/5438500. The small tracts of Black River Dolomite on the Roger map sheet near Faheys Creek (339500/5456000) and south of Roger River township (337000/5458000) are not clearly expressed on the total count image. This could be due to unmapped colluvial cover, but these are also regions of relatively poor data quality. The radiometric high near 331100/5435700 (Dempster map sheet) suggests an inlier of Rocky Cape Group, but no field evidence for this was found in this area of poor exposure and low dense vegetation.

The Smithton Dolomite is too poorly exposed to have much direct effect on the radiometric image, but some relatively resistant areas of silicification (unit Psdc) also give low total counts (e.g. 329100/5446900, 328300/5445100 on the Sumac map sheet).

Siliceous units, such as the Lagoon River Quartzite (Dempster map sheet) and Salmon River Siltstone (mostly on the Roger map sheet), also give low to very low total counts. Tracts of Neoproterozoic basalt (Spinks Creek Volcanics) also have low values, although slightly higher than the Black River Dolomite. The large tract of basalt immediately east of the Roger River Fault on the Roger map sheet has a rather varied total count signature. There are unmapped areas of Keppel Creek Formation in this area (Justin Legg, pers. comm.), but some of the variation (e.g. radiometric highs at 333200/5451600, 334600/5454200, 334600/5453400) may be cultural, as these highs correspond to isolated patches of cleared land.

Tracts underlain by other units of the Kanunnah Subgroup (Croles Hill Diamictite and southern tracts of the Keppel Creek Formation) are characterised by intermediate levels of total counts.

The large area of Tertiary basalt on the Dempster map sheet is characterised by intermediate to low total counts, slightly but appreciably higher than Neoproterozoic basalt, reflecting its more alkalic and potassic character. The small area of unusually potassic Tertiary basalt (nepheline mugearite) on Molompto Road (332600/5459800) has little contrast even against

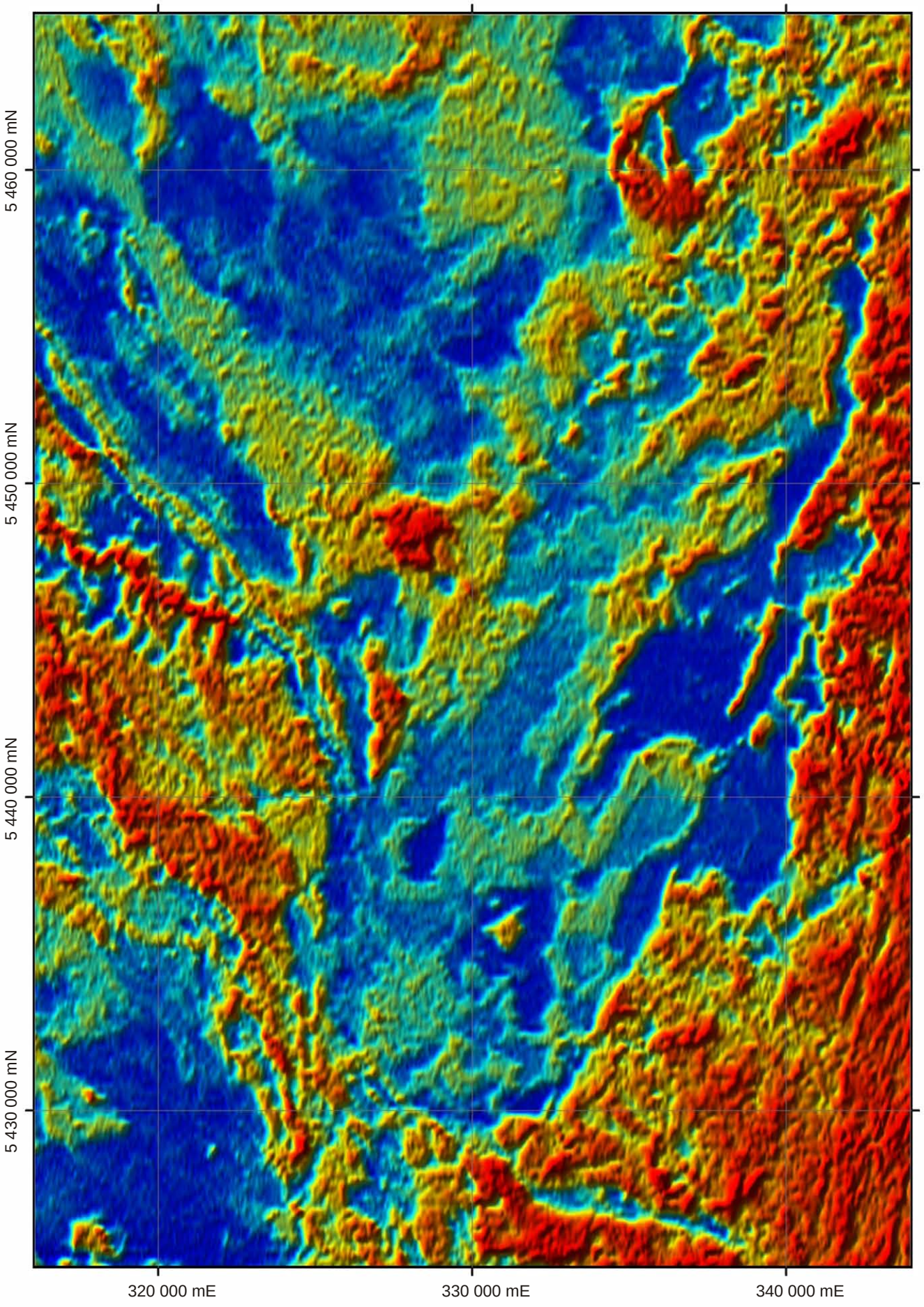

Figure 23

Radiometric image of total counts (K, Th and U) for the Roger, Sumac and Dempster map sheets and immediately adjacent areas.

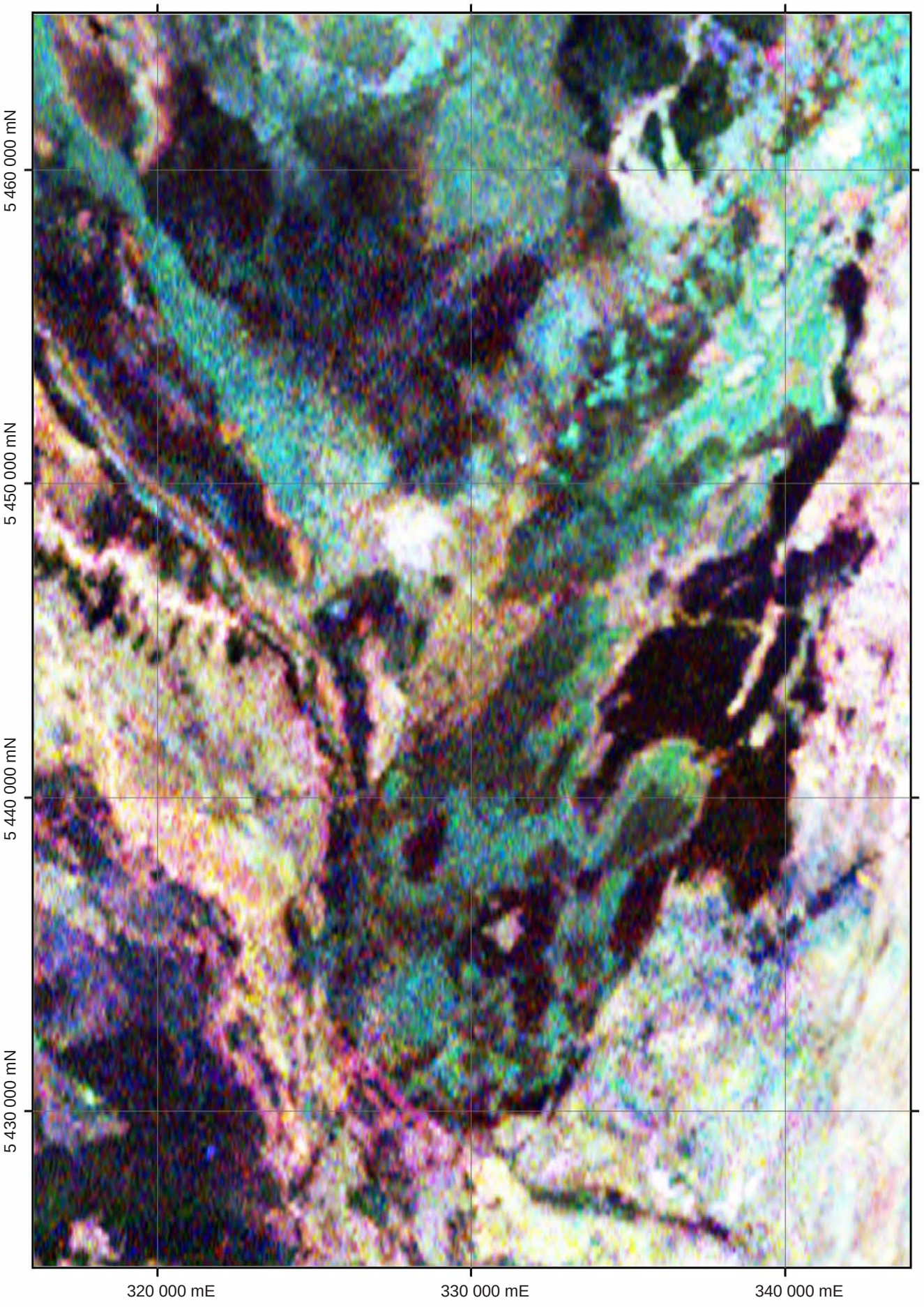

Figure 24

Radiometric (RGB) image for the Roger, Sumac and Dempster sheets and immediately adjacent areas (red = potassium, green = thorium, blue = uranium).

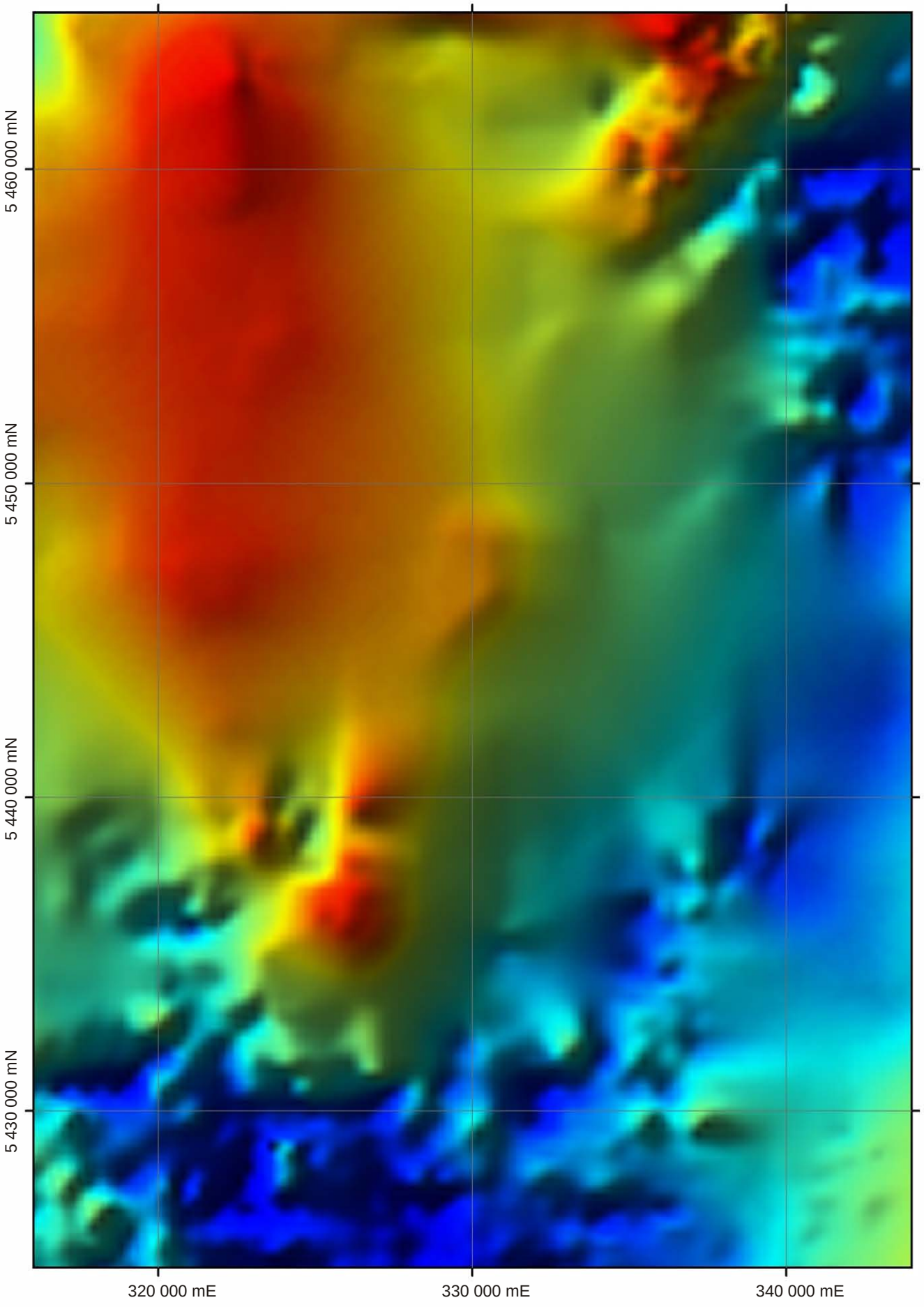

Figure 25

Gravity image of far northwestern Tasmania (red = positive Bouguer anomaly; blue = negative Bouguer anomaly).

the surrounding area of high total counts associated with the Scopus Formation.

Tertiary siliceous gravel (unit Tsgs), where developed on Smithton Dolomite and other Togari Group lithologies, gives very low total counts (e.g. Salmon River area). Where the gravel rests on the Cowrie Siltstone, notably in the southwest of the Sumac map sheet, the radiometric signature is very variable, suggesting the presence of a locally-derived pelitic component.

The signature of Quaternary alluvium (Qha) is also very variable. Alluvial flats along the Arthur River are associated with areas of high total counts, suggesting the dominance of pelitic Rocky Cape Group derived material, whilst low counts over alluvium in the lower Stephens Rivulet suggest locally derived cherty alluvium. Much of the very large Montagu Swamp–Junction Plain tract (Roger map sheet), which mostly overlies Smithton Dolomite, has low total counts. Areas of high to very high total counts occur along parts of the Duck River (336000/5459000), Styx and Roger rivers (332500/5454500), and west of the Montagu River (331600/5450800, 331400/5451800), immediately west of the Roger River Fault. These may represent alluvial fans deposited by the rivers emerging from the hilly country to the east of the fault, but they also partly coincide with areas of cleared land.

Structurally-controlled lineaments are apparent in the radiometric image where there is strong contrast between the radiometric character of adjoining units. Examples are northwest trends parallel to strike in steeply-dipping Togari Group strata in the Blackwater Rivulet–Chatlee Road area, the Roger River Fault in places (e.g. 324000/5436500), and the ENE-trending cross fault just south of Kanunnah Bridge.

Notable physiographic effects include the ESE-trending linear (through 322000/5445900) of very high total counts, coincident with good bedrock exposure, in the lower Arthur River, and a similar but weaker effect along parts of the Frankland River.

One unexplained feature is the SSW-trending radiometric high, or series of highs, east of the lower Sumac Rivulet (339000/5441800, 338300/5443000 to 339300/5445000). Further north it is coincident with a Cowrie Siltstone inlier exposed in the Arthur River, but the main part of the anomaly lies in an apparently well-mapped area of Black River Dolomite and associated chert. The feature possibly continues north of the river to a similar unexplained high at 339600/5447500.

Gravity

Gravity coverage in most of the area is regional quality, with five to eight kilometre station spacing; only ten stations lie on the Roger map sheet and most of the Sumac map sheet. Coverage is more detailed (about one kilometre station spacing) in the west, extreme south and some eastern parts of the Dempster map sheet, mainly in areas of road access and/or open country.

Even with this sparse data, the Smithton Synclinorium is clearly evident on the coloured image (fig. 25) as a region of positive residual Bouguer anomaly, corresponding to the relatively dense carbonate and mafic rocks of the Togari Group. The southwest margin of this positive area runs parallel to and slightly west of the Frankland River on the Dempster map sheet. This is well to the west of the limit of outcropping Togari Group rocks, but consistent with their presence at depth, overthrust by the Rocky Cape Group (see cross section on the Dempster map sheet). Little detail can be resolved in this area, apart from a possible 'hole' (relative gravity low) near 325000/5439000, an area of outcropping Cowrie Siltstone near the upper Blackwater Rivulet. There is a strong positive gravity anomaly at the northern margin of the area near 338000/5460000, close to the Roger River Fault and just north of Roger River township. There is some suggestion that a positive ridge continues northward, parallel to the mapped trend of outcropping basalt (Spinks Creek Volcanics), to Duck Bay near Smithton.

The area of slight negative residual Bouguer anomaly near the southern margin of the Dempster map sheet extends southwest to Sandy Cape and southward to the lower Pieman River. There is some suggestion of a narrow NNW-trending trough, roughly coincident with the 'Balfour Copper Trend', which has been attributed to a spine of Devonian granite (Leaman, 1988; Leaman and Richardson, 1992; 2003).

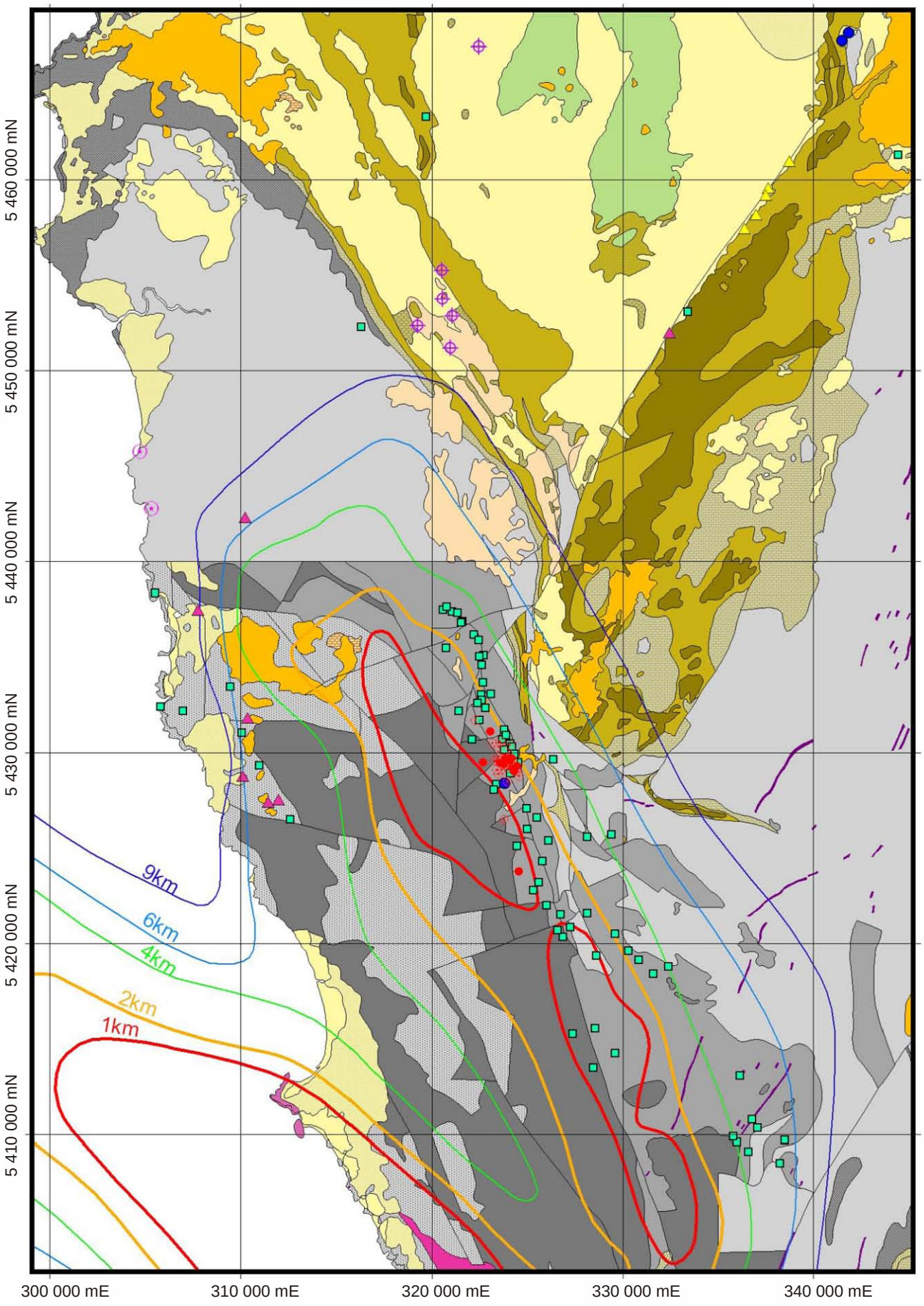

Figure 26

Map showing mines, prospects and mineral occurrences in far northwest Tasmania (metallic commodities only). Rock units as for Figure 3, with addition of Devonian granite (pink). Principal commodities: tin (lode) – filled red circles; tin (alluvial) – open red circles; copper – green squares; zinc – blue circles; gold – yellow triangles; iron (lode) – magenta triangles; chromite (detrital) – open purple circles; titanium (beach sand) – open magenta circles.

Metallic Minerals

Existing workings and known prospects *(ARR, JLE)*

Recorded mines, prospects and mineral occurrences in the area covered by the Roger, Sumac and Dempster map sheets, and adjoining sheets, are listed in Table 13 (adapted from the MRT MIRLOCH database) and depicted in Figure 26. Most of the known localities for metallic commodities (chiefly copper and tin) lie near the western margin of the Dempster map sheet, where they comprise the northern part of the Balfour Mineral Field. Ward (1911) described most of the old workings, many of which are now inaccessible. The most recent study of the metallogenesis of the copper and tin lode deposits is that of Taheri and Bottrill (2004), to which the reader is referred for more detailed information.

Copper

Approximately sixty copper vein prospects lie along a NNW-trending corridor about 35 km long and mostly less than two kilometres wide, from north of The Clump (320760/5437640) to the Toner River area (338230/5408500). This belt roughly coincides with a series of magnetic anomalies, which in turn lie along a major shear zone in the Rocky Cape Group. Only the northern part of this zone, with about 27 prospects, falls within the area covered by this report (on the Dempster map sheet). Most prospects are hosted by pyritic, carbonaceous and/or chloritic slate within the Balfour Subgroup.

In general, the copper prospects occur as fracture fillings, breccia fillings, replacements, disseminated or semi-massive pods. They are transgressive to stratigraphy and occupy dilational zones such as fault splays and vein intersections. The strike of the veins, where known, is usually NNW (commonly 160°). The primary mineralogy, although rarely seen because of severe leaching, is simple and consists of chalcopyrite, quartz ± pyrite ± carbonate ± chlorite. Geological and geochemical evidence, together with reconnaissance isotopic and fluid inclusion studies, suggests that the deposits were formed by metamorphic, late granitic and/or meteoric fluids that dissolved and transported copper and were focussed into faults. The origin of the copper is speculative, but it may have been re-dissolved and transported from older, sediment-hosted deposits. If this is correct, there are implications for the exploration potential of the region (Taheri and Bottrill, 2004).

Copper mineralisation near Balfour occupies steep northwest-trending faults developed on the steep to overturned limb of a dissected antiform. The deposits are supergene enriched and typically occur as chalcopyrite, chalcocite, covellite and digenite in quartz-dolomite veins. The main copper producer was Murrays Reward (324500/5429500; Balfour map sheet), which produced about 6000 tonnes of ore in the early twentieth century. Small tonnages mined in the early 1990s included parcels containing 12–35% Cu (P. Laan, pers. comm.). Drilling by ACI Ltd in the 1970s defined a (pre-JORC) resource of 0.5 Mt @ 0.8% Cu (McIntyre, 1972; Taheri and Bottrill, 2004).

Several old copper workings in the Dempster map sheet, including The Clump, Balfour Mines Development, Balfour Blocks and Premier prospects, were recently briefly described by Taheri and Bottrill (2004). Contemporary descriptions may be found in Ward (1911).

During field mapping it was noted that a large adit had been driven into the western bank of the Frankland River near 322770/5435100, possibly to meet shafts sunk about 300 m further west near 322480/5435040 ('Gully Prospect A'). Ward (1911, p.97) mentioned that "the intention of the owners [of Section 3955] is to drive a tunnel [from the Frankland River] to cut the lode at a depth of about 100 feet below the outcrop [in a short deep trench]….of a width of 6 feet of massive quartzose ore…..The quartz is mineralised with pyrite and chalcopyrite…Thin film of bornite and covellite are present with the copper pyrites…"

Tin-(tungsten)

About eleven known occurrences of cassiterite (-wolframite) vein mineralisation are known from Rocky Cape Group rocks in the vicinity of Balfour (MRT MIRLOCH database). All except one are within two kilometres of the main deposit on the crest and western slopes of Specimen Hill (323800/5429400) on the Balfour map sheet and only 700 m west of the Murrays Reward copper workings. The southern outlier is about six kilometres south of Balfour at 324600/5423780. The northernmost, and only record on the Dempster map sheet, is an un-named prospect at 323100/5431100; this is poorly documented and has not been validated (M. Vicary, pers. comm.). The restricted spatial extent of the tin mineralisation is in marked contrast with that of the adjacent copper vein mineralisation.

Tin was probably discovered at Balfour in the early 1880s, as alluvial workings are known to have been in existence in 1884, and a reward claim of 22 acres on Specimen Hill was granted in 1889 (Ward, 1911). Early production is poorly recorded but was probably small. According to Department of Mines records, the field produced 126 tonnes of Sn (metal) between 1907 and 1942, and small-scale production continued until the early 1980s (Taheri and Bottrill, 2004). Most production has been from derived alluvial deposits in Cassiterite Creek (formerly Tin Creek) and tributaries, as at 323500/5443000, 324000/5428500 and 323000/5429500. Alluvial tin has also been worked in Emmetts Creek (324100/5431000), the headwaters of which have relatively recently been captured by Cassiterite Creek (Ward, 1911). This accounts for the absence of alluvial tin in the lower part of Cassiterite Creek (Laan, 1985).

The primary mineralisation at Specimen Hill has been described by several authors including Ward (1911), Langsford (1982) and Taheri and Bottrill (2004). It is hosted by siltstone, sandstone, quartzite and shale, assigned by Reed (*in* Everard *et al*., 2003) to the Cassiterite Creek Quartzite, a unit within the Balfour Subgroup. At Specimen Hill the sequence is folded into a broad SSW-plunging anticline and truncated to the west by a major NNW-trending fault which may have acted as a conduit for hydrothermal fluids (Taheri and Bottrill, 2004). The fault was described as east dipping by these authors but interpreted as a west-dipping thrust (against the Skinners Flat Siltstone) by Reed. The mineralisation occurs as a swarm of thin (10–500 mm), apparently randomly-orientated quartz-cassiterite-wolframite ± muscovite veins, formed along shear and tension joints and faults. In outcrop the veins are porous, apparently due to leaching of sulfides and carbonate, as those intersected in drill core also contain pyrite, chalcopyrite, arsenopyrite, pyrrhotite, galena, sphalerite and siderite. Tourmalinisation is the most pervasive style of wall-rock alteration, but there is also minor sericitisation and silicification. Work by BHP (1963–1965) and CRA Exploration (1978–1985) at Specimen Hill suggests that the bulk tin grade is too low for open-cut mining, whereas the veins, although averaging 0.8% Sn and 1.02% WO_3, are too narrow for underground mining. Similar mineralisation occurs at Tatlows and Robbies prospects, 600–700 m further ESE of Specimen Hill (Taheri and Bottrill, 2004).

The mineralogy and restricted spatial distribution of the tin mineralisation suggests that it was deposited from fluids emanating from Devonian granite. Tin appears to have been deposited later than the copper and is possibly associated with a second phase of regional deformation. This is supported by fluid inclusion studies which suggest that the tin was deposited from high temperature (≤400°C), low salinity (~7 wt% equivalent NaCl) granite-derived fluids, and is probably unrelated to nearby copper mineralisation (Taheri and Bottrill, 2004).

The nearest outcropping granite to Balfour is at Sandy Cape, about 20 km distant, but underlying granite has long been inferred (e.g. Ward, 1911; Collins and Williams, 1986). Early interpretations of gravity data (e.g. Leaman and Richardson, 1989) were hampered by wide station spacing (~7 km) and failed to provide definite evidence for any shallow concealed body. Interpretation of a subsequent infill (~1 km spacing) survey (Leaman, *in* Hofto and Morrison, 1989) suggests that a concealed elongate spine-like granite body, about 40 km long and trending NNW roughly parallel to the coast, extends from the Mt Sunday area in the south (~333000/5403000) to west of The Clump (~317000/5437000). Most of the crest of the spine appears to lie at a depth of less than one kilometre below sea level (Leaman and Richardson, 2003). In the south, in the upper Lagoon River valley, the spine roughly coincides with the Balfour Shear Zone, suggesting a structural control, but north of Mt Hazelton (~327000/5421000) it diverges westward. The tin mineralisation at Specimen Hill lies over the eastern shoulder of the inferred granite, which appears to be shallowest three to four kilometres to the west, roughly beneath Mt Balfour (~322500/5427000). The reason for this off-set, or the apparent lack of tin mineralisation to the south in the upper Lagoon River area, is unclear.

Lead isotope comparison of copper and tin mineralisation

A lead isotope study of samples from both the Cu and Sn mineralisation at Balfour was conducted for Soloriens Mining Pty Ltd. The Pb isotope composition of pyrite from the Murrays Reward copper deposit at Balfour is quite variable (e.g. $^{206}Pb/^{204}Pb$ of 18.36–19.00), but was initially thought to be most consistent with a Cambrian age (Carr and Dean, *in* Morrison, 1991*b*). Similar work on pyrite and galena from the nearby Tatlows tin mineralisation (324400/5429300), presumably related to Devonian granite, showed it to have much less variable ratios (Dean, *in* Morrison, 1992). In particular, $^{206}Pb/^{204}Pb$ (~18.32) is not only lower than the nearby copper mineralisation, but is also lower than typical western Tasmanian Devonian mineralisation (e.g. at Queen Hill), which is generally >18.4. Tin and copper mineralisation at Balfour lies on the same linear trends on lead isotope plots (fig. 27*a, b*), which was thought to suggest a common, presumably Devonian, origin. Both have higher $^{208}Pb/^{204}Pb$ than typical Cambrian mineralisation in western Tasmania, suggesting high Th/U lower crustal high-grade metamorphic rocks were the ultimate source of the lead. It was suggested that this Pb isotope signature should also be present in the Interview Granite (Dean, *in* Morrison, 1991*b*), but recent Pb isotope data (Black *et al*., 2005) shows that granite at Sandy Cape has much higher initial $^{206}Pb/^{204}Pb$ than either the copper or tin mineralisation at Balfour.

The lead isotope data at Balfour are rather enigmatic and are not easily reconciled with other evidence for the age and origin of the mineralisation.

Minor fault-related epithermal(?) gold and base metal mineralisation

Turner (2003) described an alteration zone of extensive silicification, up to 300 m wide, extending along the Roger River Fault near Roger River (336300/5457400 to 337900/5460000). Weaker silicification extends northward to near Edith Creek (339700/5462200). The silicified rocks are usually massive or brecciated, but are also locally vughy. Weakly anomalous gold (≤5 ppb), Sb and As (~100 ppm but locally >1000 ppm) were detected in soil near five localities, termed the Quarry, Church, South Whitewater, North Whitewater and Birthday Creek prospects (Table 13). At a disused quarry at Roger River West (Quarry prospect, 336400/5457500), saccharoidal quartz was reported to contain a patch of well crystallised barite and ochreous iron minerals, with anomalous Au (1 ppb), As (102 ppm), Sb (22 ppm), Ba (5.97%) and Hg (1.48 ppm).

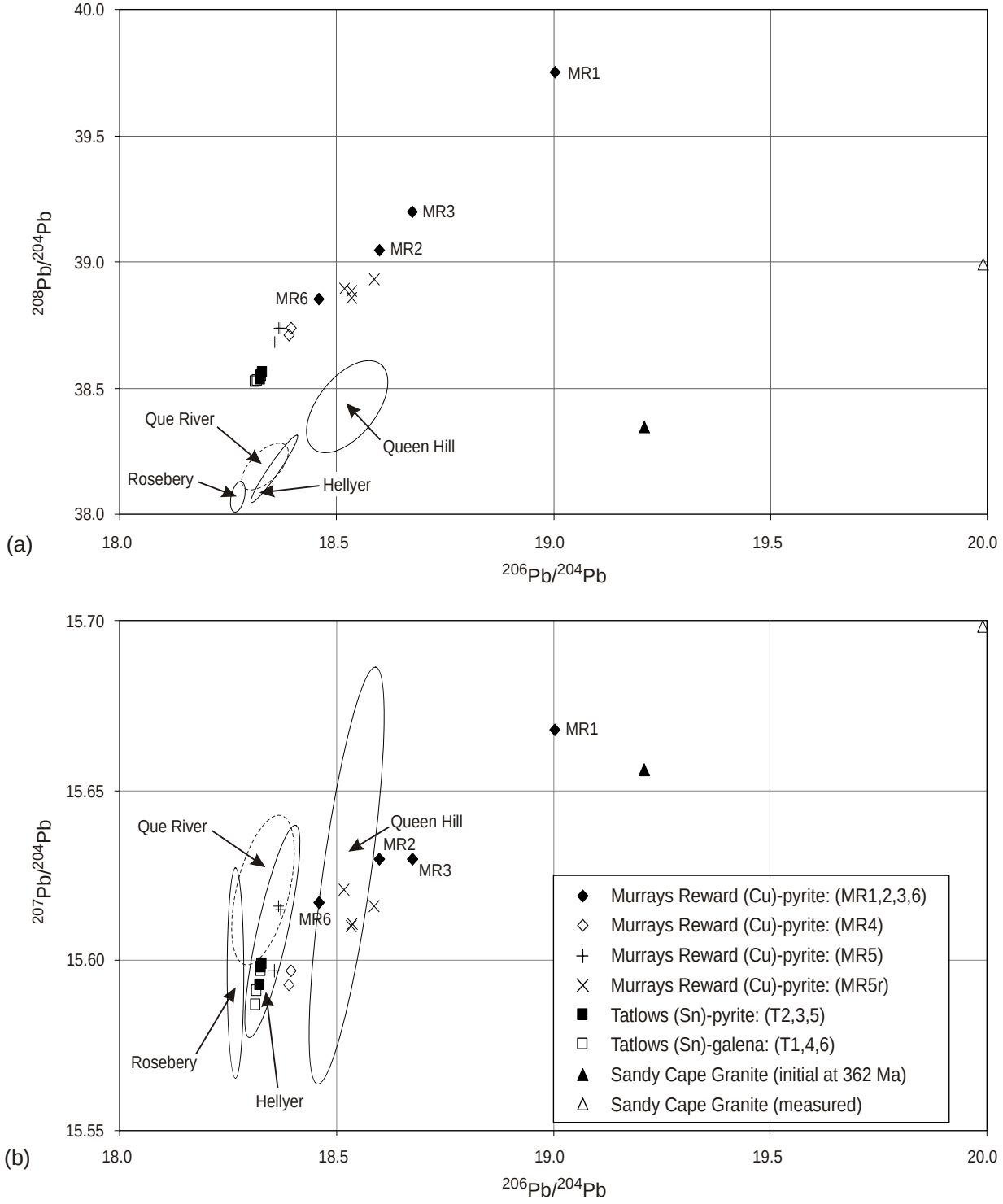

Figure 27

Lead isotope plots for tin and copper mineralisation at Balfour. (a) $^{208}Pb/^{204}Pb$ versus $^{206}Pb/^{204}Pb$; (b) $^{207}Pb/^{204}Pb$ versus $^{206}Pb/^{204}Pb$. Data from Carr and Dean (in Morrison, 1991b); Dean (in Morrison, 1992) and L. P. Black (data and in prep.).

These elements were considered characteristic of the upper parts of an epithermal alteration system. The metallogeny resembles that of deep auger samples from spring mound systems further north at Smokers Bank, Pulbeena and Copper Creek (Turner, 2003).

The Canadian Creek ironstone prospect consists of a hematite-magnetite-pyrite horizon, just east of the Roger River Road and adjacent to the Roger River Fault (332775/5452000). C-horizon soil sampling returned some anomalous assays (maxima 7120 ppm Pb, 541 ppm Cu, 140 ppm Zn, 3.1 ppm Ag, 8 ppb Au) (Westbrook, 1999*a*), but these were not followed up further.

The Roger River Copper prospect, located in 'volcanosedimentary rock' near a minor splay of the Roger River Fault (333410/5453080), is described as malachite-azurite mineralisation in epidote-quartz gangue. Rock chip samples in the vicinity returned up to 1200 ppm Cu (Reid and Westbrook, 1998).

Modern Exploration *(JLE)*

Only exploration within or overlapping with the area covered by the Roger, Sumac and Dempster map sheets is briefly reviewed here, although many of the same companies have also explored in the northern parts of the Smithton Synclinorium.

In 1965–1966, Pickands Mather International conducted a regional stream sediment survey within EL12/65 which covered much of northwestern Tasmania, including the Smithton area (Anon, 1966).

Later, Australian Consolidated Industries Ltd held much of the Arthur–Pieman area as EL16/68. Most of their exploration (including drilling) focussed on known deposits in the Balfour area, including The Clump (Jackaman, 1972), Murrays Reward (McIntyre, 1972) and Specimen Hill (Davies, 1969; Davies and McIntyre, 1973; Anon., 1972*a*, 1972*b*).

The Australian and New Zealand Exploration Company considered dolomitic rocks in far northwest Tasmania to be prospective for tungsten, by analogy to the King Island scheelite deposits, although they noted the absence of outcropping granite in this area. They conducted a stream sediment and panned concentrate survey (94 sites) over an area (EL6/72) between the Arthur River and Smithton, partly on the Roger and Sumac map sheets. The results were difficult to interpret because of the sampling method, but W and Mo results were generally disappointing. Some anomalous results for Cr, Sn and Zn were attributed to heavy minerals in recent gravel and sand. Anomalous values for Cu and Pb appeared to be related to areas of pyritic black shale and dolomite respectively, but no follow up work was done (Kinnane, 1972).

Esso Exploration conducted an airborne geophysical survey over a large area of northwest Tasmania (EL2/73), targeting base metals, and identified numerous EM (INPUT) anomalies. Most were field checked and attributed to conductive black 'slates', including two on the Dempster map sheet within areas now mapped as Cowrie Siltstone (Neale, 1974).

CRA Exploration explored a large area (EL1/77) in and around the lower Arthur and Pieman rivers. Earlier stream sediment data was collated and a regional infill survey conducted (Weir, 1982). Most Sn and W anomalies were isolated and outside the Roger–Sumac–Dempster area, but some in the Blackwater Rivulet area (Sumac map sheet) were attributed to detrital minerals derived from Tertiary gravel. A series of magnetic anomalies east of the Frankland River (roughly 325000/5432500 to 325000/5434000) were gridded and sampled (Porter, 1980*a*). Magnetic anomalies near Balfour were attributed to pyrrhotite in black shale, with a possible contribution from a deeper source. Induced polarisation (IP) anomalies were shown to coincide with Sn-Zn anomalies near the contact between quartzite and green chloritic shale (Mackay and Flis, 1980). Although the Specimen Hill mineralisation was examined (Langsford, 1982), it was concluded that the main potential for tin-tungsten mineralisation was at the margins of Devonian granite (Weir, 1983*c*).

Later, in a joint venture with Geopeko, CRA shifted the target in EL1/77 to shale-hosted lead-zinc (SEDEX) deposits, noting similarities in regional geology with the Selwyn Basin of Canada (Legge, 1980). Stream sediment lead-zinc anomalies in the Julius River (335200/5434200) and Meryanna Road areas were followed up by detailed gridding. The former was attributed to a possible disseminated source or shears within dolomite and the latter to limonitic remnant basalt (Weir, 1983*b*). A similar program of stream sediment, soil and rock sampling and mapping was undertaken in EL12/80, which included the southeast of the Dempster map sheet and areas to the south (Weir, 1983*a*; Dickson, 1985). CRA concluded that black shale at the eastern margin of the synclinorium was too thin to have generated brines sufficiently metal-rich to produce this style of mineralisation, and any metals deposited in carbonate were considered likely to have been leached out during subsequent silicification (Weir, 1983*b*).

Detailed exploration around Balfour by CRA and Geopeko between 1979 and 1983 was mainly for tin, and included mapping, geophysics (magnetic and IP), geochemistry and drilling (Porter, 1980*a*, *b*; Heithersay, 1982; Langsford, 1982; Dickson, 1983). Most of this work focussed on areas just south of the Dempster map sheet, and is not reviewed here.

Laan (1985) concluded that alluvial wash in the lower reaches of Cassiterite Creek was devoid of tin-bearing gravel.

BHP briefly explored EL18/83, roughly corresponding to the eastern half of the Sumac map sheet, for cassiterite-sulfide replacement deposits in carbonate (Anon., 1984). Some regional stream sediment (panned concentrate) and rock-chip geochemistry was done, but the main area of interest was around 339000/5443500, southeast of Lake Chisholm, where previous exploration by Esso and Anzeco (see above) had detected geophysical (magnetic and EM) and stream sediment tin anomalies near the extrapolation of a topographic lineament aligned with the Rapid River. Geological mapping, soil sampling and ground EM were conducted over a 2 km^2 grid. The geophysical anomalies were attributed to a narrow dipping conductor, probably black shale, and a small plug of weathered possible amphibolite. Weak base metal anomalies were attributed to contamination near river banks, or from heavy minerals in local gravel. The lack of evidence for shallow granite in the area was noted.

A later Landsat study (Duncan, 1986) drew the attention of the Tasmania Department of Mines to the Lake Chisholm area, which was considered not adequately tested for Carlin-style gold deposits. A field program of HUMINEX water and A-horizon soil geochemistry, rock-chip geochemistry and petrography within a 25 km^2 exempt area failed to find any gold anomalism (Duncan and Bottrill, 1997).

Aureole Resources Pty Ltd held much of the ground in the southern Smithton Synclinorium in the late 1980s. They reviewed previous exploration and geophysical data but did little 'grass roots' exploration in the area (e.g. Cromer, 1988; Morrison, 1991*a*).

Soloriens Mining Pty Ltd explored the Balfour Mineral Field between the Norfolk Range and north of The Clump, including the western part of the Dempster map sheet. A gravity survey suggested a probable northerly extension of the Interview Granite, at a depth of less than one kilometre, to the Balfour area. Known copper mineralisation was thought to lie at the intersections of magnetic and air photo linears in a NNW to NW-trending corridor, and to be probably associated with gravity highs. A lead isotope study of sulfides from both the copper and the tin mineralisation at Balfour suggested that both were produced by the same, probably Devonian, hydrothermal event (Morrison, 1991*b*, 1992).

Geopeko Limited held large exploration licences in northwest Tasmania, including much of the area covered by the Sumac and Dempster map sheets, in the early 1990s. Their main exploration technique was HUMINEX stream water geochemistry for gold and base metals, but the program was frustrated by analytical problems, particularly for gold, and they had relinquished the ground by 1991 (e.g. Virgoe and Mathison, 1990, 1991).

BHP Gold Ltd (later merging with Newmont Australia to become Newcrest Mining Ltd) briefly explored EL29/90 (Trowutta), which lay mainly on the Roger and Lileah map sheets, for Carlin-style gold mineralisation in dolomite. Widely spaced rock chip and stream sediment sampling showed low level base metal and gold anomalism (up to 9 ppb bulk leached enriched gold, BLEG) clustered along the Roger River Fault. These were attributed to high background levels in the 'Crimson Creek Formation' (i.e. Kanunnah Subgroup) rocks in the stream catchments east of the fault (McEwen, 1992).

CRA Exploration (later Rio Tinto) Pty Ltd again held much of the southern Smithton Synclinorium (EL19/92) and Balfour–Mt Frankland (EL18/92) areas between 1992 and 1997. This time the principal target was stratiform/stratabound or fault-related copper mineralisation, and solution collapse structures in carbonates. Work done in the Togari Group rocks included stream sediment, rock chip and soil geochemistry and a detailed (100 m line spacing) aeromagnetic survey (Parkinson, 1994). Again the focus shifted to the Balfour area, where detailed geological mapping (Turner, 1994*a*) and geophysics was used to identify possible fluid conduits and sedimentary contacts in the Rocky Cape Group favourable to redox copper deposition. These were followed up by ground geophysics and geochemistry, in particular at the Nelson prospect (near 321200/5430500 on the Dempster map sheet), a broad Pb-Zn soil and IP anomaly (Menpes, 1995*b*; Tear, 1996). The Murrays Reward deposit was also re-examined (Turner, 1994*b*; Menpes, 1995*a*). The potential for large copper ore bodies was considered to remain when the licence was relinquished.

Several large exploration licences were taken out by Morritt Holdings Pty Ltd in 1997/98 over much of the Smithton Synclinorium, including most of the area covered by the Roger, Sumac and Dempster map sheets. These were explored partly under arrangements with Pacific-Nevada Pty Ltd, Ashton Mining Ltd, and later Greenstone Resources. Proterozoic iron-formation hosted gold (Homestake) and copper-gold pipes (cf. Selwyn/Starra), and sediment-hosted copper (cf. Kupferschiefer/White Pine) were considered potential target deposit types. Work done included an airborne EM and magnetic survey (150 m line spacing) over much of the area, and regional stream sediment and rock-chip geochemistry. Several copper-zinc-gold anomalies in the Smithton Synclinorium, mainly in ironstones or silicified zones adjacent to the Roger River Fault, were followed up by soil geochemistry (Reid and Westbrook, 1998; Westbrook, 1999*a*; Turner, 2003). Stratiform copper, fault-related stratabound Cu-Au, Sedex Pb-Zn and carbonate replacement deposits were targetted in the Balfour/Frankland River licence (EL4/98). Gold and base metal values were of generally low order, but this was partly attributed to the effects of leaching, quartz lag cover and a weakly incised drainage system. Anomalous and visible gold was present in a panned concentrate from Cassiterite Creek (Westbrook, 1999*b*).

Ashton Mining briefly explored some of these tenements for diamonds, mainly in the Roger River area. Six magnetic anomalies, not explicable by either cultural features or exposed mafic rocks, were investigated by ground magnetics, heavy mineral sampling and/or shallow drilling which encountered highly weathered mafic rocks (see *Magnetics* section). It was concluded, mainly from chromite compositions, that these did not have kimberlitic affinities (Gunn, 1999).

Ausvaal Projects Pty Ltd held much of the Balfour–Temma–Norfolk Range region from 2002 to 2005, including some areas immediately east and north of Balfour on the Dempster and Sumac map sheets (EL10/2002). Data from the WTRMP helicopter-borne magnetic and EM surveys were processed and targets for ground investigation were identified, but no field work was done (Jenke, 2004; Anon., 2004).

Possible exploration models *(JLE, ARR)*

Seven styles of metallic mineralisation, considered to be most applicable to the Roger–Sumac–Dempster area, are briefly discussed below. Only the first two styles are known to be present in the area, but the remainder may represent potential for larger economic deposits. In particular, Proterozoic rocks in the Rocky Cape region exhibit many of the features characteristic of sedimentary environments containing base-metal mineralisation, either distal or unrelated to igneous bodies. Much of this region remains unmapped and

under-explored, despite increasing interest world-wide in seeking large sediment-hosted base-metal deposits. Consequently, the potential for these rocks to host giant SEDEX and stratabound copper deposits, similar to those in northern Australia, remains largely untested.

Copper vein deposits

There is probably potential for the discovery of more small but locally high-grade copper vein deposits, similar to Murrays Reward, particularly along the 'Balfour copper trend' between the Toner River and The Clump.

Tin (± tungsten) vein deposits

Known deposits are small and occur in a limited area near the main deposit, Specimen Hill near Balfour. The potential for significant economic discoveries is probably small and may be confined to the Balfour area, where shallow (<1 km) subsurface granite is inferred.

Stratiform/stratabound Cu deposits

Typical examples of this style of mineralisation are the large, late Proterozoic, Central African Copper Belt deposits of Zambia and Zaire, and the Permian Kupferschiefer deposits of Germany and Poland. Both occur near the margins of shallow intracratonic marine basins, mainly as disseminated sulfide mineralisation, in anoxic marine or paralic sedimentary units, sometimes associated with evaporites. The ultimate source of the copper is often obscure, but in some cases may have been underlying mafic volcanic rocks or red beds. Low temperature, oxidised connate brines or acid groundwater, which are capable of dissolving and transporting copper, may have been the mineralising fluids. The mineralisation is possibly diagenetic, and often occurs where redox boundaries (chemical traps) intersect with faults or coincide with basement highs (structural traps; e.g. Jackson, 1996 and references therein).

The Rocky Cape region has some similarities in geological setting, although red beds are lacking. Pyritic black shale is a major component of the Rocky Cape Group (Cowrie Siltstone and parts of the Balfour Subgroup), and is also present in the Togari Group (e.g. within the Black River Dolomite). There is some evidence (anhydrite casts) for locally evaporitic environments during deposition of the Cowrie Siltstone. Ironstones locally developed in the Togari Group (e.g. in the Keppel Creek Formation) are also potential redox traps for copper (± gold)-bearing mineralising fluids. The original limits of the Rocky Cape Group are unknown, but marked variations in the thickness of the Togari Group indicate the presence of basement highs and suggest the proximity of basin margins. Numerous small vein deposits between The Clump and the Toner River indicate that copper-bearing fluids have infiltrated the Balfour area. Syn-sedimentary faults, particularly in the Balfour Subgroup and Togari Group, are potential fluid conduits.

The vein mineralisation at Balfour, which lies within a compressional structure, may have formed by remobilisation of copper from the Spinks Creek Volcanics, which contain widespread native copper. This is an awkward explanation, because the volcanic rocks are younger than the Rocky Cape Group rocks that host the veins. A more plausible explanation is that copper in both units represents leakage from another, possibly larger, source at depth. It is unlikely to be mere coincidence that the Balfour copper mineralisation also lies close to an extensional structure. The extensional structures represent pre-existing crustal weaknesses that were later reactivated during compressional tectonic and mineralising events.

CRA Exploration considered the Rocky Cape Group, particularly in the Balfour area, to be prospective for stratiform replacement copper deposits, similar to Kupferschiefer and White Pine (Parkinson, 1994; Tear, 1996). The Lagoon River Quartzite and several major faults were suggested as possible fluid conduits. Potential redox traps for copper were identified at sedimentary contacts between the quartzite and the overlying pyrrhotitic siltstone at the base of the Balfour Subgroup, and between carbonaceous and iron oxide bearing siltstone units within the Balfour Subgroup (Menpes, 1995*a*). A difficulty with this model is the apparent lack of red beds, or other potential source rocks for copper, lower in the sequence.

As mentioned above, Morritt Holdings Pty Ltd and Pacific-Nevada Pty Ltd considered the area prospective for several styles of Proterozoic ironstone-hosted or structurally controlled copper-gold mineralisation.

Sedimentary exhalative (SEDEX) lead-zinc deposits

This style of layered or stratiform syn-sedimentary to syn-diagenetic deposit typically occurs in reduced sedimentary facies rocks (e.g. black shale) near the edge of rift-related intra-continental or continental margin sedimentary basins. It accounts for most of the world lead and zinc reserves, including in northern Australia (Mt Isa, Century, HYC) and western Canada (Sullivan, Selwyn Basin; e.g. Large, 1996).

Weir (1982) noted some similarities between far northwest Tasmania and the Palaeozoic Selwyn Basin, which contains numerous lead-zinc deposits. The latter contains a thick sequence of mainly black carbonaceous shale, bounded by carbonate platforms. Other lithologies include calcareous shale, chert, limestone, mudstone and coarser-grained clastic rocks, but felsic volcanic rocks are absent. Sedimentation was partly controlled by coeval rift faulting. The deposits appear to be controlled by changes in basin thickness and the style of sedimentation. They are thought to have formed from metalliferous brines that were produced by simple diagenetic compaction, and then moved upward until they were trapped or released on to a quiet seafloor environment, to deposit sulfide minerals.

The Rocky Cape Group contains a similar thick sequence of black shale (the Cowrie Siltstone) whilst

sedimentation in the underlying Balfour Subgroup (also with a shale component) was partly controlled syn-sedimentary faulting. No laterally equivalent carbonate platform is known, as the Togari Group is considerably younger. The Togari Group shows some similarities to the Selwyn Basin sequence, although black shale is a minor component, mainly within the Black River Dolomite, and sedimentation was interrupted by a major volcanosedimentary episode, represented by the Kanunnah Subgroup.

Carbonate-hosted lead-zinc deposits (Mississippi Valley and Irish style)

This style occurs within stable continental interiors, typically as irregularly cross-cutting, coarse-grained epigenetic breccia or vein mineralisation in limestone or dolomite sequences which may also contain evaporites. The Irish-style deposits occur in similar host rocks but may be stratiform, exhalative and syngenetic. The deposits tend to occur in clusters near the edge of sedimentary basins, proximal to a facies change to shale, or near a carbonate onlap to a basement high. Karst, faults or unconformities may have provided fluid pathways, but there is no obvious link with igneous activity (e.g. Large, 1996).

The Black River and Smithton dolomites may be suitable host rocks for this type of deposit, but they contain no known prospects and few indications of lead-zinc anomalism. Little exploration relevant to this target has been done in the area. However the Mississippi Valley style of deposit generally gives poor geophysical and geochemical responses, and grid drilling of prospective areas has been advocated as the most appropriate exploration technique (Muhling, 1996).

Carbonate replacement tin deposits (Renison style)

The cassiterite-wolframite mineralisation at Specimen Hill is thought to occur over a subsurface spine of the Interview Granite, inferred from gravity data (e.g. Leaman, 1988). The local Rocky Cape Group (principally Balfour Subgroup) country rocks appear to lack the carbonate horizons necessary for skarn development or Renison-style ('distal skarn') mineralisation. The nearest outcropping Togari Group rocks occur about 2.5 km to the northeast, just north of the Frankland River (325200/5431500), where they comprise Kanunnah Subgroup rocks. A major but very poorly exposed and relatively inaccessible tract of Smithton Dolomite occurs about four kilometres to the northeast (e.g. 326500/5432000). More detailed gravity work may be necessary to determine if these areas are too distal to granite to have provided traps for granite-derived hydrothermal fluids. The western limit of the Togari Group in this area is a west-dipping thrust, and carbonate units such as the Smithton Dolomite may be present at depth, closer to the spine of granite.

Carbonate-hosted gold-silver deposits (Carlin style)

The 'type area' of this important style of epithermal to mesothermal mineralisation is in Nevada and Utah (USA), but similar deposits exist in southeast China. In both areas the deposits occur in mostly Palaeozoic marine sedimentary rocks within a complex continental margin, affected by overthrusting and subsequent deep-seated extensional faulting. High fineness gold and silver (± As, Hg, Sb, W, Tl) occur as disseminations and in veins within silty carbonaceous impure dolomite and calcareous shale, associated with carbonate dissolution, silicification ('jasperoid') and illite-kaolinite alteration. Carlin-style deposits in the USA are spatially related to felsic magmatism and an analogy with modern geothermal systems (Taupo, Yellowstone) has been suggested, but in China there is no apparent relationship to igneous rocks (Arundell, 1996, and references therein).

In the Smithton Synclinorium, the Togari Group, and perhaps especially the Black River Dolomite, has many of these general sedimentological and structural characteristics, although the region was never a typical active continental margin, and major plutons (apart from the inferred spine of Devonian granite in the extreme south of the area) are absent. Minor felsic magmatism is indicated by clasts in the Croles Hill Diamictite. BHP and Newcrest Mining Ltd briefly explored for Carlin-style gold deposits in the north of the area (McEwen, 1992; see above). Duncan and Bottrill (1997) unsuccessfully tested the Lake Chisholm area, and considered that the potential of the Smithton Synclinorium to host Carlin-style gold mineralisation remains unproven. As noted above, Pacific-Nevada Mining noted that weakly anomalous Au-As-Sb ± Hg geochemistry, associated with silicification adjacent to the Roger River Fault, was suggestive of the upper levels of an epithermal alteration system (Turner, 2003).

Basalt-related copper deposits

The historically important copper deposits of the Keeweenaw Basin, Michigan, USA occur within a very thick, rapidly deposited sequence that filled a late Proterozoic intracratonic rift, accompanied by syn-sedimentary folding and thrusting. A thin (200 m) basal sedimentary sequence is overlain by nine kilometres of mainly tholeiitic basalt and subordinate andesite and rhyolite (Portage Lake Lava Series). Native copper occurs, with few sulfide minerals, in amygdaloidal flow tops and in the interstices of interbedded oxidised felsic conglomerate. The mineralisation is mainly restricted to constrictions in permeable units, which appear to have funnelled upwardly migrating hydrothermal fluids. The Portage Lake Lava Series is overlain by red bed conglomerate and sandstone, and a minor black unit which hosts the White Pine stratiform copper sulfide deposit (see

above), about 100 km southwest of the native copper districts (Brown, 1974).

The native copper occurrences in the Spinks Creek Volcanics show some similarities to those of the Keeweenaw Peninsula, both in geological setting and style of mineralisation.

Industrial Minerals *(JLE)*

Chromite

Chromite, together with 'lesser amounts of cassiterite, rutile and gold', was discovered within Tertiary siliceous gravel southwest of Montagu Swamp, probably in the 1950s, and was prospected by A. A. Walker (Hughes, 1957*b*; Jennings, 1970). Most of these chromitiferous deposits lie on the Roger map sheet.

Quest Exploration Pty Ltd and Ocean Mining NL drilled 73 holes, totalling 260 m, into Tertiary and Quaternary sediments in six areas between Montagu Swamp and Lovells Creek Road (Volker, 1969). Only two holes, both near Walkers quarry (320300/5455200) on Salmon River Road, returned values considered of economic interest (15.5 m averaging 30.4 kg/m^3 magnetic concentrate with 54.5% Cr_2O_3, and 20.1 m averaging 38.0 kg/m^3 at 48.8% Cr_2O_3).

The deposits were later explored by BHP (Kosseris, 1988) and two cycles of Tertiary alluvial deposition were identified. The 'first cycle' alluvial sediments, which mainly occur as perched remnants on ridges, are poorly sorted, matrix supported, massive and of gravel to sand grade. The second cycle sediments, formed by reworking of the first, are better sorted, fine upward and are locally cross bedded. The best chromite concentrations were found in 'second cycle' deposits (Walkers quarry; Salmon River Road at 320700/5453700; 'Section KL' roughly between 319100/5452500 and 320500/5450800), but some chromite also occurs in deposits classified as 'first cycle'. In contrast, examination of the Quaternary deposits of the Montagu River valley suggested that they were only two to three metres thick with negligible heavy mineral content.

A potential *in situ* resource of 8000–13 000 tonnes of contained Cr_2O_3 was established but considered too small to interest BHP, and the ground was taken up by C. H. Whitehead (1989, 1990). He termed the first and second cycle alluvial sediments as consolidated and unconsolidated respectively. The Walkers Quarry deposit was considered to be too low in grade to be viable, and the Salmon River Road and 'Chromite Spur' (320800/5453300) gravels were found to be unexpectedly thin (≤3.25 m). Two anomalous platinum values (best 0.60 ppm from the Salmon River at 316700/5453300) were recorded from stream sediment samples. As Tasmanian ultramafic rocks are generally associated with Os-Ir-Ru (rather than Pt-Pd) anomalism (Ford, 1981), this may suggest another source for the ultramafic detritus, including chromite (see below).

Hughes (1957*b*) assumed a Pleistocene age for the gravel, and suggested that the chromite was transported northward by rivers from 'ultrabasic intrusions' in the then virtually unknown area between Balfour and Waratah. Nye (1975) noted that most of the chromite areas lie near the contact between the Smithton Dolomite and the 'Cambrian formations' and suggested a source in the latter. His suggestion is supported by the petrographic observations herein, that detrital chromite occurs in both the Neoproterozoic Kanunnah Subgroup (specifically the Keppel Creek Formation and Croles Hill Diamictite) and Cambrian Scopus Formation (in which it is probably more abundant). Although the ultimate igneous source of the chromite is obscure (see Appendix 2), it is likely that the most of the detrital chromite in the Tertiary gravel (unit Tsgs) has been concentrated through at least two, and up to three, sedimentary cycles.

The current mapping has shown that siliceous Tertiary gravel, similar to those bearing chromite in the Salmon River Road area and also associated with Kanunnah Subgroup units, extends south of the Arthur River at least as far as 326400/5439300. These gravel deposits have not yet been explored for chromite.

Dolomite

About 60 000 tonnes/year of Smithton Dolomite is quarried about two kilometres west of Smithton by the Circular Head Dolomite and Trading Company Pty Ltd, for both agricultural and metallurgical use. Potentially large resources exist in this unit in the Roger–Sumac–Dempster area, west of the Roger River Fault. Poor exposure due to Cainozoic cover, poor drainage, and greater transport distances are possible difficulties.

Mineral Holdings Ltd explored for dolomite in two areas, near Montagu (EL32/90) and Brittons Swamp (EL33/90) (Threader, 1992). In the latter area, which falls partly on the Roger map sheet, ten surface samples of relatively pure dolomite from the Montagu River and adjacent drains were analysed for major elements.

The Black River Dolomite probably has less potential, because of more commonly interbedded cherty or pelitic impurities. In contrast to the Smithton Dolomite, this unit is usually thin west of the Roger River Fault, and any potential as a source of dolomite in this area probably lies in the eastern part of the Sumac map sheet.

Silica flour and sand

Potential for high purity silica flour or sand exists in some areas underlain by carbonate rocks, particularly the Smithton Dolomite. Deposits are exposed in road cuttings along Blackwater Road on the Sumac map sheet. About three metres of fine and very even-grained off-white sand (sample R004974) is exposed beneath an overburden of about one metre of pebbly gravel at 326420/5440160. About four to five metres of angular off-white cherty float contains patches of white sand at

327730/5443480, and about 170 m further north (327720/5443650) there is a pod of pure white sand (sample R004975) about four metres thick and four metres wide.

It appears that the fine-grained silica sand has been left as a residual material after leaching and dissolution of weakly silicified carbonate. A similar origin has been proposed for silica flour deposits near Corinna (Turner, 1992, p.23).

Major element chemical analyses of these samples are presented in Table 11. Sample R004975 in particular is quite pure, with only 0.42% elements other than SiO_2, but at this locality the deposit is almost certainly too small (and too close to the road) to be economically viable. Better potential exists north of the first locality, in areas mapped as interbedded siliceous gravel, quartz sand and clay (Tsgs) overlying Smithton Dolomite (Psd). This gravel may have acted as a protective capping that prevented erosion or contamination of the silica sand. This area is one of poor exposure in rainforest and regrowth, and shallow drilling beneath soil and gravel cover would be necessary to identify any resource.

This area has recently been explored for silica flour by Cominex and a further three samples analysed (Turner, 2000). Eight auger holes in the Blackwater No. 1 Spur Road area delineated a possible resource of 90 000 tonnes (Turner, 2001).

Seven samples of silica sand from the Salmon River area returned a maximum of only 91.7% SiO_2 (Whitehead, 1990).

Table 11

Chemical analyses, silica sand samples

Field No.	FJ138	FJ200
Reg No.	R004974	R004975
Anal. No.	961104	961105
AMG (mE)	326420	327720
AMG (mN)	5440160	5443650
SiO_2	94.75	97.96
TiO_2	1.65	0.02
Al_2O_3	0.74	0.10
Fe_2O_3	0.26	0.12
FeO	0.00	0.00
MnO	0.01	0.00
MgO	0.12	0.02
CaO	0.02	0.02
Na_2O	0.00	0.00
K_2O	0.05	0.01
P_2O_5	0.01	0.00
H_2O^+	0.01	0.00
CO_2	0.10	0.08
SO_3	0.06	0.05
TOTAL	**97.78**	**98.38**

Analyses at MRT laboratories. Analyst: L. M. Hay

Lump silica

Some of the Rocky Cape Group quartzite units are sufficiently pure to be considered as a source of lump silica, the generally preferred feed for metallurgical use (Summons, 1981; Bacon, 1989). Almost all of these units lie outside the Roger–Sumac–Dempster area, in which the only significant tract of true quartzite is in the extreme southwest of the Dempster map sheet (unit Prl, a correlate of the Lagoon River Quartzite).

Construction materials *(JLE)*

Slate

The fissile black carbonaceous facies of the Cowrie Siltstone has been extracted for slate at a former road metal quarry at Wedge Plains (350500/5455300), ten kilometres to the east in the Tayatea map sheet. The mining lease for the site lapsed in 1999. The slate appears to have been used mainly for paving and cladding. Sharples (1990, p.82–90) noted that the material from this site and elsewhere includes both 'uniform dark grey-black slate' and a 'rustic' variety with brown iron oxide markings and abundant pyrite. The latter was used in the Tall Timbers Hotel at Smithton.

Here and elsewhere in the Cowrie Siltstone and correlates (except close to the Arthur Lineament), the main fissility is parallel to bedding rather than cleavage, so the material is a 'sedimentary slate' rather than a true or metamorphic slate.

Similar rocks occur on the Sumac and Dempster map sheets, notably around 334000/5430600 at Sumac 7 road. There are more potential sites further south around 338000/5424500, near a large hill on the Balfour map sheet.

Most of the Cowrie Siltstone, including larger tracts of the fissile black facies, lies further east. Sharples (1990, p.87–90) examined the 'Lawson River Siltstone', which is now known to be a correlate of the Cowrie Siltstone, at several sites from Wedge Plains to the Horton River. He considered the whole area to be prospective for good quality slate, with large slabs being procurable. Pyrite is common and, whilst normally detrimental in slate, was considered to have some ornamental value if treated to inhibit tarnishing and staining. In contrast the Balfour Slates and Sandstones (roughly equivalent to the Balfour Subgroup as defined above) were considered unprospective due to interlaminated sandstone, undulose cleavage and closely-spaced fractures.

'Marble' (building stone)

In this context, the term 'marble' is used in the stone industry sense for a partly or wholly recrystallised carbonate rock, whether or not this is due to metamorphism. Desirable attributes for dimension stone marble (Sharples, 1990, p.18–30, 213–217) include widely spaced jointing (>2 m), uniform colour (preferably white) and texture, strength, and dimensional stability. The absence of hard impurities (e.g. quartz, chert nodules), unstable minerals (e.g. pyrite, siderite, chlorite, smectite) and commonly fossils, bedding, cleavage, stylolites or veins is also usually desirable. These criteria are more likely to be fulfilled in finely crystalline (<1 mm) carbonate rocks. Requirements for interior use and tiles may be less stringent, particularly with regard to uniformity.

Sharples (1990, p.226–228) briefly considered both the Black River Dolomite and Smithton Dolomite as potential sources of marble, rating both as having low to moderate prospectivity. The field and petrographic descriptions made during this project suggest that in this area the Smithton Dolomite, particularly its more massive middle to upper parts, has the greater potential. This is due to its greater purity, relative lack of chert or clastic interbeds, extensive recrystallisation and relative lack of intraclasts. Its poor outcrop, common jointing and commonly drab grey colour are discouraging features, but the unit has probably never been systematically examined as a source of marble.

'Black granite' (building stone)

Dark igneous rocks may be valuable as a building stone, and marketed as 'black granite', if sufficiently massive and capable of taking a polish (e.g. Sharples, 1990, p.145). Sharples (p.158–160) considered the 'spilite basalts' (i.e. the Spinks Creek Volcanics) of this area as having a low to moderate prospectivity, with the main problem being insufficiently wide (0.1–0.5 m, but locally >1 m) open joint spacings. A test sample took a 'fair polish', but mineralogical analysis was recommended to ensure that amygdaloidal minerals present were not deleterious to durability.

Potential may also reside in the coarse-grained gabbroic intrusive phase (Psbz) of the Spinks Creek Volcanics. In addition to the need for satisfactory jointing and mineralogical attributes, the limited size of these bodies could be restrictive.

Sharples (1990, p.153) further considered the dolerite dykes of the Rocky Cape region to have low prospectivity due to their relatively light colour and closely-spaced jointing. Although a major dyke transects the extreme southeast corner of the Dempster map sheet, the main area of these dykes lies to the east of the Roger–Sumac–Dempster area.

Tasmanian Tertiary basalts, particularly young and thick flows likely to have well-spaced tectonic and cooling joints, were considered to have high prospectivity as 'black granite' (Sharples, 1990, p.186–191). The occurrences in the Roger–Sumac–Dempster area probably do not meet these criteria and are mostly poorly accessible. Well developed columnar jointing (<0.5 m) was noted in some of the few well exposed outcrops.

Gravel

Gravel has been extensively extracted within the Roger–Sumac–Dempster area, mainly for forestry roads (Table 12). The preferred material has been chert derived from the Black River Dolomite, although this produces very dusty road surfaces in dry weather, which may be loose and prone to liquefaction under load. There are also large pits in the Salmon River Siltstone at 322380/5449840 and 331300/5457600. Cowrie Siltstone correlate was quarried near Blackwater 6 spur (326900/5440800) and at the Mt Bertha Road quarry (342500/5437300) on the adjacent Beryl map sheet. Sandstone (unit Prbq) within the Balfour Subgroup has been quarried at three localities near The Clump. Many of these gravel pits are disused and several have been rehabilitated. A large operation continues in chert at the Sumac 11 turnoff (336500/5426400), to the south on the adjoining Balfour map sheet.

Parts of the Heemskirk Road south of The Clump towards Balfour were constructed directly on an existing thin veneer of Tertiary gravel.

Table 12

Gravel pit locations, Roger, Sumac and Dempster map sheets and adjacent areas

Name	Location	AMG (mE)	AMG (mN)	Sheet	Unit	Status
-	Brodies Road	335500	5459900	Roger	Qha	abandoned
-	Salmon River Road spur	322750	5459780	Roger	Qha?	new area
Togari	Salmon River Road spur	323000	5459750	Roger	Qha?	abandoned
-	Roger River	337600	5459500	Roger	Qha	abandoned
Lees Pit	Roger River	337700	5459150	Roger	Pssc?	abandoned
-	Roger River	336600	5458100	Roger	Qha	abandoned
-	Roger River	336850	5457900	Roger	Pssc	abandoned
-	Molompto Road spur	331310	5457600	Roger	Psr	occasional
Roger River West	Roger River West	336300	5457400	Roger	Pssc	occasional
-	O'Neills Road	339840	5456550	Roger	Pssc	abandoned
Victor Creek	Lerunna Road	320250	5455000	Roger	Qha	abandoned
-	Chromite Road	320600	5453700	Roger	Qha	abandoned
-	Roger River West	333390	5453140	Roger	Psb	abandoned
-	Chatlee Road	322380	5449840	Sumac	Psr	abandoned
-	Blackwater 5 spur	326700	5442200	Sumac	Pssc	in use
Julius Quarry	Sumac Road	334800	5442180	Sumac	Pssc	occasional
Sumac Quarry	Sumac Road	336120	5442070	Sumac	Pssc	rehabilitated
Rapid Quarry	Rapid River Road	339930	5440870	Sumac	Pssc	rehabilitated
Blackwater Road	Blackwater 6 spur	326900	5440800	Sumac	Prc	rehabilitated
Deception Pool	Deception Pool	337600	5439600	Dempster	Pssc	unknown
-	Blackwater Road	320990	5437790	Dempster	Prbq	abandoned
Blackwater Road Quarry	Blackwater Road	320530	5437590	Dempster	Prbq	abandoned
Mt Bertha Quarry	Mt Bertha Road	342500	5437300	Beryl	Prc	unknown
Sumac 6A	Sumac 6A	335700	5436800	Dempster	Pssc	unknown
Horton quarry	Sumac Road	335000	5434800	Dempster	Pssc	rehabilitated
-	Sumac 11 spur	336500	5426400	Balfour	Pssc	in use
-	Heemskirk Road	335000	5422000	Balfour	Prbq	rehabilitated

Table 13

Mineral occurrences on the Roger, Sumac, Dempster and adjoining map sheets (adapted from MRT MIRLOCH database)

25k sheet	*Name*	*mE*	*mN*	*Main commodity*	*Other commodities*	*Type*	*Status*	*Form*	*Host unit*
Roger	Walkers Pit	320571	5455262	Cr		Mine or prospect	Mineralised area	Placer	Cainozoic
Roger	Salmon River Road Quarry	320580	5453770	Cr		Mine or prospect	Mineralised area	Placer	Cainozoic
Roger	Sapling Road	321000	5451200	Cr		Mineral occurrence	Mineralised area	Placer	Cainozoic
Roger	Chromite Spur	321100	5452900	Cr		Mineral occurrence	Mineralised area	Placer	Cainozoic
Roger	Roger River Copper	333410	5453080	Cu		Prospect			Spinks Creek Volcanics
Roger	Quarry	336400	5457450	Au	Sb, As, Hg, barite	Prospect		Replacement	Black River Dolomite
Roger	Church	337000	5458200	Au	As	Prospect		Replacement	Black River Dolomite
Roger	South Whitewater	337500	5459200	Au	As	Prospect		Replacement	Black River Dolomite
Roger	North Whitewater	337650	5459600	Au	As	Prospect		Replacement	Black River Dolomite
Roger	Canadian Creek Ironstone	332475	5452000	Iron ore	Pb	Prospect			
Roger	Roger River Dolomite	333500	5452300	Dolomite		Mine or prospect	Non-operating	Stratiform	
Sumac	Blackwater Road	326923	5440757	Silica		Mineral occurrence		Replacement	Rocky Cape Group
Sumac	Hawkes Creek	322400	5448500	Silica		Mine or prospect	New area	Residual	Cainozoic
Sumac	Blackwater West	327500	5446900	Silica		Prospect		Residual	Cainozoic
Sumac	Blackwater East	329100	5447000	Silica		Mine or prospect	New area	Residual	Cainozoic
Sumac	Blackwater Spur Road No. 1	329100	5447000	Silica		Mineral occurrence		Replacement	Smithton Dolomite
Dempster	Un-named	320590	5437475	Cu		Mineral occurrence		Vein	Balfour Subgroup
Dempster	Section 4758M	320740	5435495	Cu		Prospect		Vein	Balfour Subgroup
Dempster	Un-named	320760	5437640	Cu		Mineral occurrence		Vein	Balfour Subgroup
Dempster	North Mt Balfour A	321050	5437390	Cu		Prospect		Vein	Balfour Subgroup
Dempster	North Mt Balfour B	321340	5437340	Cu		Unknown		Vein	Balfour Subgroup
Dempster	Un-named	321420	5432200	Cu		Prospect		Vein	Balfour Subgroup
Dempster	Mt Balfour Copper	321540	5436820	Cu		Mine or prospect	Unknown	Vein	Balfour Subgroup
Dempster	The Clump	321594	5436885	Cu		Prospect		Vein	Balfour Subgroup
Dempster	Un-named	322100	5430700	Cu		Prospect		Vein	Rocky Cape Group
Dempster	Un-named	322200	5436200	Cu		Prospect		Vein	Balfour Subgroup
Dempster	Un-named	322400	5432600	Cu		Prospect		Vein	Balfour Subgroup
Dempster	Un-named	322450	5435900	Cu		Prospect		Vein	Balfour Subgroup
Dempster	Gully Prospect A	322480	5435040	Cu		Prospect		Vein	Balfour Subgroup
Dempster	Un-named	322500	5431700	Cu		Prospect		Vein	Balfour Subgroup
Dempster	Balfour Mines Development	322570	5433050	Cu		Prospect		Vein	Balfour Subgroup
Dempster	Balfour Consolidated	322600	5432750	Cu		Prospect		Vein	Balfour Subgroup
Dempster	Un-named	322600	5434600	Cu		Prospect		Vein	Balfour Subgroup
Dempster	Gurr and Herrings	322680	5433680	Cu		Prospect		Vein	Balfour Subgroup
Dempster	Gully Prospect B	322700	5435100	Cu		Mine or prospect	Abandoned	Vein	Balfour Subgroup
Dempster	Balfour Blocks	322790	5432340	Cu		Prospect		Vein	Balfour Subgroup
Dempster	Section 4169M	323080	5433060	Cu		Prospect		Vein	Balfour Subgroup
Dempster	Section 4078M	323700	5430700	Cu		Unknown		Vein	Balfour Subgroup
Dempster	Premier	323780	5431200	Cu		Prospect		Vein	Balfour Subgroup
Dempster	Un-named	323800	5430150	Cu		Prospect		Vein	Balfour Subgroup

25k sheet	Name	mE	mN	Main commodity	Other commodities	Type	Status	Form	Host unit
Dempster	Emmets Cu	323900	5430900	Cu		Unknown		Vein	Balfour Subgroup
Dempster	Harpers Tunnel	324100	5430460	Cu		Prospect		Vein	Balfour Subgroup
Dempster	McGowans Tunnel	324200	5430300	Cu		Prospect		Vein	Balfour Subgroup
Dempster	Tin Creek North	322300	5431700	Sn		Prospect		Placer	Cainozoic
Dempster	Un-named	323100	5431100	Sn	Cu	Unknown		Vein	Balfour Subgroup
Dempster	Un-named	323200	5430500	Sn	Cu	Unknown		Placer	Cainozoic
Dempster	Tin Creek South	323500	5430300	Sn		Prospect		Placer	Cainozoic
Dempster	Un-named	323600	5430600	Sn		Prospect		Placer	Cainozoic
Dempster	Balfour Mineral Field	324000	5430000	Sn	Cu	Mineral field	Mineralised area	Placer, residual, vein	Rocky Cape Group
Dempster	Emmetts Creek	324100	5430400	Sn		Prospect		Placer	Cainozoic
Balfour	Un-named	323250	5428070	Cu	Pb, Sn	Prospect		Vein	Rocky Cape Group
Balfour	Un-named	323380	5428340	Cu		Prospect		Vein	Rocky Cape Group
Balfour	Section 4132M	324100	5428900	Cu		Prospect			Balfour Subgroup
Balfour	DDB7	324300	5429500	Cu	Sn, Zn	Mineral occurrence		Disseminated, vein	Balfour Subgroup
Balfour	Central Mt Balfour	324335	5429945	Cu		Prospect		Vein	Balfour Subgroup
Balfour	Section 3802M	324470	5425115	Cu		Prospect		Vein	Balfour Subgroup
Balfour	Murrays Reward	324505	5429480	Cu		Mine or prospect	Abandoned	Vein	Balfour Subgroup
Balfour	Pierpont Morgan	324980	5427080	Cu		Prospect		Vein	Balfour Subgroup
Balfour	The Gap	325000	5426000	Cu		Prospect		Vein	Balfour Subgroup
Balfour	Section 4419M	325300	5422800	Cu		Prospect		Vein	Balfour Subgroup
Balfour	Un-named	325500	5426600	Cu	Sn	Prospect		Vein	
Balfour	Section 3640M	325600	5423200	Cu		Prospect		Vein	Balfour Subgroup
Balfour	Waratah	325800	5424300	Cu		Prospect		Vein	Balfour Subgroup
Balfour	Un-named	326000	5422000	Cu		Prospect		Vein	Balfour Subgroup
Balfour	Section 4609M	326100	5425400	Cu		Prospect		Vein	Balfour Subgroup
Balfour	Un-named	326360	5429640	Cu		Prospect		Vein	Rocky Cape Group
Balfour	Un-named	326600	5420700	Cu		Prospect		Vein	Rocky Cape Group
Balfour	Balfour South	326730	5421500	Cu		Prospect		Vein	Balfour Subgroup
Balfour	Mt Hazleton	326860	5420330	Cu		Prospect		Vein	Rocky Cape Group
Balfour	Section 3798M	327250	5420840	Cu		Prospect		Vein	Rocky Cape Group
Balfour	Section 4360M	328140	5421580	Cu		Prospect		Vein	Cowrie Siltstone
Balfour	Section 4302M	328150	5425580	Cu		Mineral occurrence		Vein	Rocky Cape Group
Balfour	Section 4281M	329400	5425700	Cu		Prospect		Vein	Rocky Cape Group
Balfour	Section 3607M	329600	5420500	Cu		Unknown		Vein	Cowrie Siltstone
Balfour	Un-named	322700	5429500	Sn	W	Prospect		Vein	Balfour Subgroup
Balfour	Matrix Creek	323300	5429600	Sn		Area of alluvial workings	Prospect	Placer	Cainozoic
Balfour	Un-named	323400	5429100	Sn		Mine or prospect	Abandoned	Placer, residual	Cainozoic
Balfour	Un-named	323500	5428900	Sn		Mine or prospect	Abandoned	Placer, residual	Cainozoic
Balfour	Un-named	323500	5429800	Sn		Mine or prospect	Abandoned	Placer, residual	Cainozoic
Balfour	Un-named	323600	5429450	Sn	W	Mine or prospect	Abandoned	Residual, vein	Balfour Subgroup
Balfour	Un-named	323600	5429600	Sn	W	Prospect		Placer, residual, vein	Balfour Subgroup
Balfour	Un-named	323700	5429150	Sn		Mine or prospect	Abandoned	Placer, residual	Cainozoic
Balfour	Un-named	323700	5429700	Sn		Mine or prospect	Abandoned	Placer, residual	Cainozoic

25k sheet	Name	mE	mN	Main commodity	Other commodities	Type	Status	Form	Host unit
Balfour	Un-named	323800	5426500	Sn		Mine or prospect	Abandoned	Residual	Cainozoic
Balfour	Specimen Hill (Western Tas)	323800	5429400	Sn	W	Prospect		Vein	Balfour Subgroup
Balfour	Un-named	323900	5429700	Sn		Mine or prospect	Abandoned	Vein	Balfour Subgroup
Balfour	Tin Creek A	324000	5428500	Sn		Area of alluvial workings	Prospect	Placer	Cainozoic
Balfour	Un-named	324050	5429200	Sn		Mine or prospect	Abandoned	Placer, residual	Cainozoic
Balfour	Un-named	324100	5429350	Sn		Mine or prospect	Abandoned	Placer, residual	Cainozoic
Balfour	Peters Flat	324100	5429600	Sn	Cu, W, Zn	Mine or prospect	Mineralised area	Residual, vein	Balfour SGp, Cainozoic
Balfour	Un-named	324150	5429500	Sn		Mine or prospect	Abandoned	Placer, residual	Cainozoic
Balfour	Un-named	324200	5429450	Sn		Mine or prospect	Abandoned	Placer, residual	Cainozoic
Balfour	Peters Ridge	324200	5429700	Sn	As	Prospect		Vein	Balfour Subgroup
Balfour	Un-named	324250	5429250	Sn		Mine or prospect	Abandoned	Placer, residual	Cainozoic
Balfour	Un-named	324300	5429600	Sn		Mine or prospect	Abandoned	Placer, residual	Cainozoic
Balfour	Robbies	324335	5429005	Sn	Cu	Prospect		Other, vein	Balfour Subgroup
Balfour	Tatlows South shaft	324350	5429150	Sn		Mine or prospect	Abandoned	Vein	Balfour Subgroup
Balfour	Tatlows Costean	324350	5429170	Sn	As, Cu, W, Zn	Prospect		Vein	Balfour Subgroup
Balfour	Un-named	324450	5429150	Sn		Mine or prospect	Abandoned	Placer, residual	Cainozoic
Balfour	Tatlows (main shaft)	324490	5429290	Sn	As, W, Zn	Prospect		Vein	Balfour Subgroup
Balfour	Un-named	324500	5429050	Sn		Mine or prospect	Abandoned	Placer, residual	Cainozoic
Balfour	Un-named	324600	5423780	Sn	Cu	Mine or prospect	Unknown	Placer, vein	Balfour Subgroup
Balfour	Un-named	324600	5428777	Sn		Area of alluvial workings	Prospect	Placer, residual	Cainozoic
Balfour	Section 4238M	323820	5428360	Zn	Pb	Prospect		Vein	Balfour Subgroup
Balfour	Un-named	324200	5420500			Prospect			
Lily	Section 4197M	327380	5415250	Cu		Prospect		Vein	Lagoon River Quartzite
Lily	Section 4307M	328450	5413480	Cu		Prospect		Vein	Lagoon River Quartzite
Lily	Section 4451M	328560	5415560	Cu		Prospect		Vein	Balfour Subgroup
Lily	Section 3483M	328630	5419350	Cu		Prospect		Vein	Balfour Subgroup
Lily	Poseidon	329590	5414250	Cu		Prospect		Vein	Balfour Subgroup
Lily	Mt Lyell Pr-3	330300	5419600	Cu		Unknown		Vein	Balfour Subgroup
Lily	Section 3483M	330850	5419130	Cu		Prospect		Vein	Balfour Subgroup
Lily	Un-named	331600	5418400	Cu		Prospect		Vein	Balfour Subgroup
Lily	Un-named	332400	5418800	Cu		Prospect		Vein	Balfour Subgroup
Lily	Section 4003M	336140	5413080	Cu		Prospect		Vein	Balfour Subgroup
Lily	Section 3485M	336770	5410780	Cu		Prospect		Vein	Balfour Subgroup
Lily	Copper Reward	337070	5410350	Cu		Prospect		Vein	Balfour Subgroup
Lagoon	Section 3487M	335800	5409900	Cu		Prospect		Vein	Balfour Subgroup
Lagoon	Section 3596M	336000	5409600	Cu		Prospect		Vein	Balfour Subgroup
Lagoon	Section 3598M	336600	5409100	Cu		Prospect		Vein	Balfour Subgroup
Lagoon	Section 3752M	338230	5408500	Cu		Prospect		Vein	Balfour Subgroup
Lagoon	Section 3595M	338500	5409700	Cu		Prospect		Vein	Balfour Subgroup
Marrawah	Dismal Swamp	319700	5463300	Cu	Co, Au, Zn	Prospect			Keppel Creek Formation
Marrawah	Carbonate Hills B	312500	5462800	Dolomite		Prospect		Stratiform	Smithton Dolomite
Marrawah	Un-named	302820	5467430	Limestone		Mine or prospect	Abandoned	Stratiform	Cainozoic
Marrawah	Un-named	303780	5468000	Limestone		Mine or prospect	Abandoned	Stratiform	Cainozoic

25k sheet	Name	mE	mN	Main commodity	Other commodities	Type	Status	Form	Host unit
Marrawah	Un-named	304500	5467360	Limestone		Mine or prospect	Abandoned	Stratiform	Cainozoic
Marrawah	Carbonate Hills C	312400	5464330	Limestone		Prospect		Stratiform	Cainozoic
Marrawah	Un-named	312500	5466300	Limestone		Mine or prospect	Abandoned	Stratiform	
Marrawah	Carbonate Hills A	312800	5464000	Limestone		Prospect		Stratiform	Cainozoic
Marrawah	Un-named	313000	5466400	Limestone		Mine or prospect	Abandoned	Stratiform	
Marrawah	Marrawah	301400	5465500	Silica		Mineral occurrence	Mineralised area	Stratiform	Detention SGp correlate
Marrawah	Marrawah Beach	305370	5469570	Ti	Zr	Area of alluvial workings	Mineralised area	Placer	Cainozoic
Bluff	Section Kl	319300	5452400	Cr		Mineral occurrence	Mineralised area	Placer	Cainozoic
Bluff	Salmon	316300	5452300	Cu		Prospect		Vein	Rocky Cape Group
Bluff	Dismal	316100	5458500			Construction materials	Unknown		
Bluff	Lovell Creek	319300	5451300			Construction materials	Unknown		
Bluff	Lovell Borrow Pits	319300	5452000			Construction materials	Unknown		
Sundown	Nelson Bay River	310250	5442320	Iron ore	Cu, magnetite	Prospect		Replacement	Rocky Cape Group
Sundown	Nelson Bay River Silica	309800	5442200	Silica		Mineral occurrence		Stratiform	Rocky Cape Group
Sundown	Sardine Creek	304750	5445750	Ti	Cr, Zr	Area of alluvial workings	Mineralised area	Placer	Cainozoic
Sundown	Nelson Bay	305340	5442760	Ti	Cr, Zr	Area of alluvial workings	Mineralised area	Placer	Cainozoic
Temma	Couta Mine	305536	5438347	Cu	Ag	Prospect		Vein	Pedder River Siltstone
Temma	Richardsons Point	305800	5432400	Cu	Iron ore, Pb	Prospect		Vein	Pedder River Siltstone
Temma	Little Eel	307000	5432200	Cu	Iron ore, Ag	Prospect		Vein	Pedder River Siltstone
Temma	Strickland	309460	5433467	Cu	Au, iron ore, Pb, Sn	Prospect		Vein	Pedder River Siltstone
Temma	No Mans Creek	310070	5431040	Cu	Iron ore	Prospect		Vein	Pedder River Siltstone
Temma	Rebecca	307800	5437500	Iron ore	Cu, Pb	Prospect		Vein	Pedder River Siltstone
Temma	Un-named	310400	5431850	Iron ore	Cu	Prospect		Vein	
Temma	Temma Farm	306800	5430900			Mineral occurrence		Vein	Rocky Cape Group
Temma	Log Dump	315900	5437000			Construction materials	Unknown		
Ordnance	Section 4438M	310980	5429320	Cu	Cu	Prospect		Vein	Pedder River Siltstone
Ordnance	Un-named	312600	5426500	Cu	Cu	Mine or prospect	Mineral occurrence	Vein	Pedder River Siltstone
Ordnance	Possum Creek	310140	5428800	Iron ore	Cu, Ag	Prospect		Other	Pedder River Siltstone
Ordnance	Dawson River	311480	5427430	Iron ore	Magnetite, pyrite	Prospect		Vein	Pedder River Siltstone
Ordnance	Grace Creek	312000	5427550	Iron ore	Cu	Prospect		Vein	Pedder River Siltstone
Togari	Montagu Swamp	322500	5467000	Cr		Mineral occurrence	Mineralised area	Placer	Cainozoic
Togari	Birthday Creek	338750	5461000	Au	As	Prospect		Replacement	
Lileah	Johns Hill	344800	5468300	Coal – lignite		Prospect		Stratiform	
Lileah	Edith Creek	346000	5461400	Coal – lignite		Prospect		Stratiform	
Lileah	Un-named	344400	5461300	Cu		Mineral occurrence		Disseminated	Black River Dolomite
Lileah	Gentle Annie Creek	348500	5462300	Au		Area of alluvial workings	Mineralised area	Placer	
Lileah	Gorgey Creek =?Harbour Creek	349000	5464000	Au		Prospect		Placer	
Lileah	Copper Creek	341518	5467257	Zn	As	Mineral occurrence		Other	Cainozoic
Lileah	McLachlans Road Ironstone	341844	5467666	Zn		Mineral occurrence		Other	
Holder	Tayatea Quarry	348800	5445200	Cu		Mineral occurrence			Cowrie Siltstone

References

ADAMS, C. J.; BLACK, L. P.; CORBETT, K. D.; GREEN, G. R. 1985. Reconnaissance isotopic studies bearing on the tectonothermal history of Early Palaeozoic and Late Proterozoic sequences in Western Tasmania. *Australian Journal of Earth Sciences* 32:7–36.

ANON., 1966. *Interim report for the northwest Tasmanian exploration project for the period ending April, 1966*. Pickands Mather and Company International [TCR 66-439].

ANON., 1972*a*. *EL16/68: Balfour reports*. Australian Consolidated Industries Ltd [TCR 74-1070].

ANON., 1972*b*. *Geology of the Specimen Hill area, Balfour*. Australian Consolidated Industries Ltd [TCR 74-1070B].

ANON., 1984. *Exploration Licence 18/83, Lake Chisholm, Tasmania. Final report*. BHP Minerals Limited [TCR 84-2145].

ANON., 2004. *EL8/2002 and EL10/2002 Balfour–Temma area. Annual Report to 20.12.2004*. Ausvaal Projects Pty Ltd [TCR 04-5096].

ARUNDELL, M. 1996. *Carlin-type Au deposits*. Master of Economic Geology Ore Deposit paper, University of Tasmania.

AUROUSSEAU, M. 1926. Analyses of three Australian rocks. *Proceedings Linnean Society NSW* 51:614–626.

BACON, C. A. 1989. Silica. *Mineral Resources of Tasmania* 12.

BAILLIE, P. W. 1981. A new Late Cambrian fossil locality from the Smithton quadrangle. *Unpublished Report Department of Mines Tasmania* 1981/47.

BAILLIE, P. W. 1986. Radiometric ages for Circular Head and the Green Hills basalt, north-western Tasmania. *Unpublished Report Department of Mines Tasmania* 1986/39.

BAILLIE, P. W.; CRAWFORD, A. J. 1984. Smithton Trough excursion, *in:* BAILLIE, P. W.; COLLINS, P. L. F. (ed.). *Mineral exploration and tectonic processes in Tasmania.* Abstracts and excursion guide, Geological Society of Australia (Tasmanian Division). 59–64.

BAILLIE, P. W.; JAGO, J. B. 1995. Sedimentology of an Upper Cambrian turbidite succession, Smithton Basin, northwest Tasmania. *Australian Journal of Earth Sciences* 42:75–82.

BAILLIE, P. W.; SUTHERLAND, F. L. 1992. Devonian lamprophyres from Mt Lyell, western Tasmania. *Papers and Proceedings Royal Society of Tasmania* 126:19–22.

BANKS, M. R. 1962. Cambrian System, *in:* SPRY, A.; BANKS, M. R. (ed.). 1962. The geology of Tasmania. *Journal of the Geological Society of Australia* 9(2):127–145.

BAU, M. 1996. Controls on the fractionation of isovalent trace elements in magmatic and aqueous systems: evidence from Y/Ho, Zr/Hf and lanthanide tetrad effect. *Contributions to Mineralogy and Petrology* 123:323–333.

BELL, D. H. 1972. *1971–72 Annual Report, EL48/70 and EL49/70, north-western Tasmania joint venture exploration*. Australian Consolidated Industries Ltd, Consolidated Goldfields Australia Ltd, Mt Lyell Mining and Railway Company Ltd, Renison Ltd [TCR 72-876].

BERRY, R. F. 1995. Tectonics of western Tasmania: Late Precambrian–Devonian, *in:* COOKE, D. R.; KITTO, P. A. (ed.). Contentious issues in Tasmanian geology. *Abstracts Geological Society of Australia* 39:6–8.

BERRY, R. F.; CRAWFORD, A. J. 1988. The tectonic significance of Cambrian allochthonous mafic-ultramafic complexes in Tasmania. *Australian Journal of Earth Sciences* 35:523–533.

BERRY, R. F.; MEFFRE, S.; JENNER, G.; FULTON, R. 1997. Heavy minerals, provenance and stratigraphy, *in:* Structure and mineralisation of western Tasmania. *AMIRA project Centre for Ore Deposits and Exploration Studies University of Tasmania* P291A:1–33.

BLACK, L. P.; CALVER, C. R.; SEYMOUR, D. B.; REED, A. 2004. SHRIMP U-Pb detrital zircon ages from Proterozoic and Early Palaeozoic sandstones and their bearing on the early geological evolution of Tasmania. *Australian Journal of Earth Sciences* 51:885–900.

BLACK, L. P.; MCCLENAGHAN, M. P.; KORSCH, R. J.; EVERARD, J. L.; FOUDOLIS, C. 2005. Significance of Devonian-Carboniferous igneous activity in Tasmania as derived from U-Pb SHRIMP dating of zircon. *Australian Journal of Earth Sciences* 52:807–829.

BLACK, L. P.; SEYMOUR, D. B.; CORBETT, K. D.; COX, S. E.; STREIT, J. E.; BOTTRILL, R. S.; CALVER, C. R.; EVERARD, J. L.; GREEN, G. R.; MCCLENAGHAN, M. P.; PEMBERTON, J.; TAHERI, J.; TURNER, N. J. 1997. Dating Tasmania's oldest events. *Record Australian Geological Survey Organisation* 1997/15.

BOTTRILL, R. S. 2004*a*. Garnet-bearing and other spotted porphyroblastic metasedimentary rocks from the Balfour area. *Record Tasmanian Geological Survey* 2004/02.

BOTTRILL, R. S. 2004*b*. Miscellaneous mineral analyses from near Balfour and Temma. *Record Tasmanian Geological Survey* 2004/06.

BOYNTON, W. V. 1984. Cosmochemistry of the rare earth elements: meteorite studies, *in:* HENDERSON, P. (ed.). *Rare earth element geochemistry*. 63–114. Elsevier.

BROWN, A. C. 1974. The copper province of northern Michigan, USA, *in:* BARTHOLOME, P. (ed.). *Gisements Stratiformes et Provinces Cupriferes*. 317–330. Societe Geologique de Belgique, Liege.

BROWN, A. V. 1985. Preliminary report on the Forest No. 1 diamond-drill hole and chemical analyses of associated tholeiitic basalts in the Smithton and Woolnorth quadrangles. *Unpublished Report Department of Mines Tasmania* 1985/62.

BROWN, A. V. 1986. Geology of the Dundas–Mt Lindsay–Mt Youngbuck region. *Bulletin Geological Survey Tasmania* 62.

BROWN, A. V. 1989*a*. (comp.). Geological Atlas 1:50 000 Series. Sheet 21 (7916S). Smithton. *Explanatory Report Geological Survey Tasmania*.

BROWN, A. V. 1989*b*. Eo-Cambrian–Cambrian, *in:* BURRETT, C. F.; MARTIN, E. L. (ed.). Geology and mineral resources of Tasmania. *Special Publication Geological Society of Australia* 15:47–83.

BROWN, A. V.; FORSYTH, S. M. 1984. Chemistry of Tertiary basalt and palynology of interbedded sediments from BHP drill holes, EL33/79. *Unpublished Report Department of Mines Tasmania* 1984/39.

CALVER, C. R. 1995. *Ediacaran isotope stratigraphy of Australia*. Ph.D. thesis, Macquarie University.

CALVER, C. R. 1998. Isotope stratigraphy of the Neoproterozoic Togari Group, Tasmania. *Australian Journal of Earth Sciences* 45:865–874.

CALVER, C. R.; BAILLIE, P. W. 1990. Early diagenetic concretions associated with intrastratal shrinkage cracks in an upper Proterozoic dolomite, Tasmania, Australia. *Journal of Sedimentary Petrology* 60:293–305.

CALVER, C. R.; EVERARD, J. L. 1992*a*. Arthur River: detailed traverse below Hawkes Creek. *Plan Department of Mines Tasmania* 5432A.

CALVER, C. R.; EVERARD, J. L. 1992*b*. Arthur River traverse : Smithton Basin. *Plan Department of Mines Tasmania* 5432B.

CALVER, C. R.; BLACK, L. P.; EVERARD, J. L.; SEYMOUR, D. B. 2004. U-Pb zircon constraints on late Neoproterozoic glaciation in Tasmania. *Geology* 32:893–896.

CALVER, C. R.; CORBETT, K. D.; EVERARD, J. L.; GOSCOMBE, B. D.; PEMBERTON, J.; SEYMOUR, D. B. (compilers). 1995. *Geological Atlas 1:250 000 digital series. Geology of Northwest Tasmania*. Mineral Resources Tasmania.

CAREY, S. W.; SCOTT, B. 1952. Revised interpretation of the geology of the Smithton district of Tasmania. *Papers and Proceedings Royal Society of Tasmania* 86:63–70.

CAREY, S. W.; SCOTT, B. 1954. Native copper at Smithton — a correction. *Papers and Proceedings Royal Society of Tasmania* 88:271–272.

CARMICHAEL, I. S. E.; TURNER, F. J.; VERHOOGEN, J. 1974. *Igneous petrology*. McGraw Hill : New York.

COLLINS, P. L. F; WILLIAMS, E. 1986. Metallogeny and tectonic development of the Tasman Fold Belt System in Tasmania. *Ore Geology Reviews* 1:153–201.

COOMBS, D. S.; NAKAMURA, Y.; VUAGNAT, M. 1976. Pumpellyite-actinolite facies schists of the Taveyanne Formation near Loèche, Valais, Switzerland. *Journal of Petrology* 17:440–471.

CRAWFORD, A. J.; BERRY, R. F. 1992. Tectonic implications of Late Proterozoic–Early Palaeozoic igneous rock associations in western Tasmania. *Tectonophysics* 214:37–56.

CROMER, W. C. 1988. *Exploration Licence 21/87 — Balfour. Annual report : year 1 (20 January, 1988–19 January, 1989)*. Aureole Resources Pty Ltd [TCR 88-2900].

DAVIES, H. G. 1969. *EL16/68 — progress report, December, 1968–August, 1969.* ACI Ltd [TCR 69-577].

DAVIES, H. G.; MCINTYRE, M. H. 1973. *Assorted reports, EL16/68, Balfour area*. ACI Ltd [TCR 73-950].

DEER, W. A.; HOWIE, R. A.; ZUSSMAN, J. 1963. *Rock-forming minerals. Volume 2. Chain silicates*. Longmans.

DEER, W. A.; HOWIE, R. A.; ZUSSMAN, J. 1997. *Rock-forming minerals. Volume 1B (Second Edition). Disilicates and ring silicates*. The Geological Society : London.

DICK, H. J. B.; BULLEN, T. 1984. Chromian spinel as a petrogenetic indicator in abyssal and alpine-type peridotites and associated lavas. *Contributions to Mineralogy and Petrology* 86:54–76.

DICKSON, T. W. 1983. *Final report, mineral leases 20M/76, 72M/77, 103M/77, 104M/77, 8M/78, 57M/78 and SPL's 774 and 781, L and B Syndicate, Balfour*. CRA Exploration Pty Ltd [TCR 83-1934].

DICKSON, T. W. 1985. *EL12/80 Leigh River — relinquishment report*. CRA Exploration Pty Ltd [TCR 85-2476].

DUNCAN, D. McP. 1986. Interpretation of Landsat imagery of western Tasmania, *in:* LARGE, R. R. (ed.). *The Mount Read Volcanics and associated ore deposits*. Geological Society of Australia (Tasmanian Division) : Hobart.

DUNCAN, D. McP.; BOTTRILL, R. S. 1997. The Lake Chisholm Exempt Area. *Record Tasmanian Geological Survey* 1997/06.

EVERARD, G. B. 1962. Petrological notes on specimens from various localities. *Technical Reports Department of Mines Tasmania* 6:85–92.

EVERARD, J. L. 1989. Petrology of the Tertiary basalt. Appendix B *in:* SEYMOUR, D. B. (comp.). Geological Atlas 1:50 000 Series. Sheet 36 (8015S). St Valentines. *Explanatory Report Geological Survey Tasmania* 79–142.

EVERARD, J. L. 2005. Reconnaissance geology of the Norfolk Range–Sandy Cape area, northwest Tasmania. *Record Tasmanian Geological Survey* 2005/02.

EVERARD, J. L.; CALVER, C. R.; PEMBERTON, J.; TAHERI, J.; DIXON, G. 1997. Geology of the islands of southwestern Bass Strait. *Record Tasmanian Geological Survey* 1997/03.

EVERARD, J. L.; REED, A. R.; SEYMOUR, D. B. 2003. *Geological Atlas 1:25 000 scale digital series. Sheet 3242. Balfour*. Mineral Resources Tasmania.

EVERARD, J. L.; SEYMOUR, D. B.; BROWN, A. V. 1996. *Geological Atlas 1:50 000 Series. Sheet 27 (7915N). Trowutta*. Mineral Resources Tasmania.

FISH, G. J.; YAXLEY, M. L. 1966. Behind the scenery: the geological background to Tasmanian landforms. *Publication Teaching Aids Centre, Education Department, Tasmania* 62.

FORD, R. J. 1981. Platinum-group minerals in Tasmania. *Economic Geology* 76:498–504.

FREY, F. A.; GREEN, D. H.; ROY, S. D. 1978. Integrated models of basaltic petrogenesis: a study of quartz tholeiites to olivine melilitites from south eastern Australia utilizing geochemical and experimental petrological data. *Journal of Petrology* 19:463–513.

GEE, R. D. 1967. *The tectonic evolution of the Rocky Cape Geanticline in NW Tasmania*. Ph.D. thesis, University of Tasmania.

GEE, R. D. 1968. A revised stratigraphy for the Precambrian of north-west Tasmania. *Papers and Proceedings Royal Society of Tasmania* 102:7–10.

GEE, R. D.; GULLINE, A. B.; BRAVO, A. P.; LEGGE, P. J.; GROVES, D. I. 1969. *Geological Atlas 1 Mile Series. Sheet 42 (7814N). Pieman Heads*. Department of Mines Tasmania.

GRIFFIN, B. J. 1974. *Cambrian tectonism and vulcanism in the Smithton Basin*. B.Sc. (Hons) Thesis, University of Tasmania.

GRIFFIN, B. J.; PREISS, W. V. 1976. The significance and provenance of stromatolitic clasts in a probable late Precambrian diamictite in northwestern Tasmania. *Papers and Proceedings Royal Society of Tasmania* 110:111–127.

GROVE, T. L.; KINZLER, R. J.; BRYAN, W. B. 1992. Fractionation of mid-ocean ridge basalt (MORB), *in:* MORGAN, J. P.; SINTON, J. M.; BLACKMAN, D. K. (ed.). Mantle flow and melt generation at mid-ocean ridges. *Geophysical Monograph American Geophysical Union* 71:281–310.

GULLINE, A. B. 1959. The underground water resources of the Smithton district. *Underground Water Supply Paper Tasmania* 5.

GUNN, R. J. 1999. *Exploration Report. Preliminary Technical Summary, Exploration Licences EL12/97, EL14/97 and EL61/94*. Ashton Mining Limited; Pacific-Nevada Mining Proprietary Limited [TCR 99-4323A].

GUNN, P. J.; MACKEY, T. E.; RICHARDSON, R. G.; SEYMOUR, D. B.; MCCLENAGHAN, M. P.; CALVER, C. R.; ROACH, M. J.; YEATES, A. N. 1996. The basement elements of Tasmania. *Record Australian Geological Survey Organisation* 1996/29.

HAMR, P. 1992. A revision of the Tasmanian freshwater crayfish genus *Astacopsis* Huxley (Decapoda: Parastacidae). *Papers and Proceedings Royal Society of Tasmania* 126:91–94.

HEITHERSAY, P. 1982. *Mineral lease 19M/76 — Balfour, Tasmania. Report for the twelve months ending 31st December 1981*. CRA Exploration Pty Ltd [TCR 82-1742].

HEY, M. H. 1954. A new review of the chlorites. *Mineralogical Magazine* 30:277–292.

HOFTO, V.; MORRISON, K. C. 1989. *Exploration Licence 53/88 — Mt Frankland. Annual report: year 1 (6 January, 1989–5 January, 1990).* Soloriens Mining Pty Ltd [TCR 89-3057].

HOLM, O. H.; BERRY, R. F. 2002. Structural history of the Arthur Lineament, northwest Tasmania: an analysis of critical outcrops. *Australian Journal of Earth Sciences* 49:167–185.

HUGHES, T. D. 1957*a*. Limestones in Tasmania. *Geological Survey Mineral Resources Tasmania* 10.

HUGHES, T. D. 1957*b*. Notes on alluvial chromite deposits near Montagu Swamp. *Technical Reports Department of Mines Tasmania* 1:16–19.

JACKAMAN, B. 1972. *The geology of The Clump prospect, Balfour, northwest Tasmania*. Australian Consolidated Industries Ltd [TCR74-1070A].

JACKSON, J. 1996. *Sediment hosted copper deposits – a literature review*. Master Economic Geology Ore Deposit Paper, University of Tasmania.

JAGO, J. B. 1976. Late Middle Cambrian agnostid trilobites from north-western Tasmania. *Palaeontology* 19:133–172.

JAGO, J. B. 1981. Possible Late Precambrian (Adelaidean) tillites of Tasmania, *in:* HAMBREY, M. J.; HARLAND, W. B. (ed.). *Earth's pre-Pleistocene glacial record*. 549–554. Cambridge University Press.

JAGO, J. B.; BAILLIE, P. W. 1992. An Idamean aglaspidid from northwestern Tasmania. *Alcheringa* 16:14.

JAGO, J. B.; BROWN, A. V. 1989. Middle to Upper Cambrian fossiliferous sedimentary rocks, *in:* BURRETT, C. F.; MARTIN, E. L. (ed.). Geology and mineral resources of Tasmania. *Special Publication Geological Society of Australia* 15:74–83.

JAGO, J. B.; BUCKLEY, J. H. 1971. An abrupt upper Middle Cambrian faunal change, Christmas Hills, Tasmania, Australia. *Papers and Proceedings Royal Society of Tasmania* 105:83–85.

JENKE, G. P. 2004. *EL8/2002 and EL10/2002 Balfour–Temma. Partial relinquishment report to 20/12/2003. EL9/2002 final report*. Ausvaal Projects Pty Ltd [TCR 04-4996].

JENNINGS, D. J. 1970. Chromite-bearing gravel deposits in the area south of Montagu Swamp. *Technical Reports Department of Mines Tasmania* 15:12–15.

JOHNSON, R. W.; DUGGAN, M. B. 1989. Rock classification and analytical data bases, *in:* JOHNSON, R. W.; KNUTSEN, J.; TAYLOR, S. R. (ed.). *Intraplate volcanism in Eastern Australia and New Zealand*. 12–13. Cambridge University Press.

KAMENETSKY, V. S.; CRAWFORD, A. J.; MEFFRE, S. 2001. Factors controlling chemistry of magmatic spinel: an empirical study of associated olivine, Cr-spinel and melt inclusions from primitive rocks. *Journal of Petrology* 42:655–671.

KINNANE, N. R. 1972. *Report on the geological reconnaissance and stream sediment sampling programme, north-west Tasmania*. Australian and New Zealand Exploration Company [TCR 72-869].

KOSSERIS, W. C. 1988. *Combined annual/final report for the period ended 24 February 1988. Exploration Licence 12/86, Montagu area, Tasmania*. BHP Minerals Exploration [TCR 88-2786].

LAAN, P. 1985. *Final report on EL15/84 at Balfour – 22nd August 1985*. [Letter to Director of Mines] [TCR 85-2482].

LANGSFORD, N. R. 1982. *Geology and mineralisation, Specimen Hill area. Balfour NW Tasmania*. CRA Exploration Pty Ltd [TCR 83-1932].

LARGE, R. R. 1982. *Annual report – EL25/85 Montagu. 1981 season*. Geopeko Limited [TCR 82-1793].

LARGE, R. 1996. Key features and ore deposit models for sediment-hosted Pb-Zn-Ag deposits, *in: Ore deposit studies and exploration models: sediment-hosted base metal deposits, sediment-hosted and MVT deposits*. 1.1–1.18. CODES Short Course Manual 2, University of Tasmania.

LEAKE, B. E.; *et al*. 1997. Nomenclature of amphiboles; report of the Subcommittee on Amphiboles of the International Mineralogical Association Commission on new minerals and mineral names. *Mineralogical Magazine* 61:295–321.

LEAMAN, D. E. 1988. *EL26/87, North Pedder River. Regional geophysical review for New Holland Mining NL*. Leaman Geophysics [TCR 88-2892A].

LEAMAN, D. E.; RICHARDSON, R. G. 1989. The granites of west and north-west Tasmania – a geophysical interpretation. *Bulletin Geological Survey Tasmania* 66.

LEAMAN, D. E.; RICHARDSON, R. G. 1992. A geophysical model of the major Tasmanian granitoids. *Report Department of Mines Tasmania* 1992/11.

LEAMAN, D. E.; RICHARDSON, R. G. 2003. A geophysical model of the major Tasmanian granitoids. *Record Tasmanian Geological Survey* 2003/11.

LE BAS, M. J. 2000. IUGS reclassification of the high-Mg and picritic volcanic rocks. *Journal of Petrology* 41:1467–1470.

LE MAITRE, R. W. (ed.). 1989. *Igneous rocks. A classification and glossary of terms*. Blackwell : Oxford.

LEGGE, P. J. 1980. *The lead zinc potential of the younger rocks (Precambrian) of North West Tasmania*. CRA Exploration Pty Ltd [TCR85-2349].

LENNOX, P. G.; CORBETT, K. D.; BAILLIE, P. W.; CORBETT, E. B.; BROWN, A. V. 1982. *Geological Atlas 1:50 000 Series. Sheet 21 (7916S). Smithton*. Department of Mines Tasmania.

LONGMAN, M. J. 1962. Petrological notes on the Bluff Point and Trowutta quadrangles. *Technical Reports Department of Mines Tasmania* 6:79–85.

LONGMAN, M. J.; MATTHEWS, W. L. 1962. The geology of the Bluff Point and Trowutta quadrangles. *Technical Reports Department of Mines Tasmania* 6:48–54.

MCCLENAGHAN, M. P.; FINDLAY, R. H. 1993. Geological Atlas 1:50 000 series. Sheet 64 (7913S). Macquarie Harbour. *Explanatory Report Geological Survey Tasmania.*

MCCLENAGHAN, M. P.; SEYMOUR, D. B. 1996. Combined interpretation of new aerial-survey geophysical datasets for northwestern Tasmania. *Record Tasmanian Geological Survey* 1996/16.

MACDONALD, G. A.; KATSURA, T. 1964. Chemical composition of Hawaiian lavas. *Journal of Petrology* 5:82–133.

MCEWEN, G. D. 1992. *Exploration Licence 29/90 Trowutta. Annual and final report for the period 15 February 1991 to 14 February 1992*. Newcrest Mining Ltd [TCR 92-3336].

MCINTYRE, M. H. 1972. *Mineral exploration in EL16/68, Balfour, Tasmania: summary report for field season 1971-71*. ACI Minerals Pty Ltd [TCR 74-1070D].

MCKAY, A. D.; FLIS, M. F. 1980. *Results of geophysical surveys in the Balfour area (NW Tas.)*. CRA Exploration Pty Ltd [TCR 81-1516].

MCNEIL, R. D. 1961. Geological reconnaissance of part of the Arthur River area. *Technical Reports Department of Mines Tasmania* 5:46–60.

MATTHEWS, W. L. 1961*a*. Geology of the Rapid River area. *Technical Reports Department of Mines Tasmania* 5:63–71.

MATTHEWS, W. L. 1961*b*. Geological reconnaissance, Trowutta area. *Plan Department of Mines Tasmania* 1891.

MENPES, S. A. 1995*a*. *Balfour EL4/94. Report on exploration for the first year of tenure 3/6/94 to 3/5/95*. CRA Exploration Pty Ltd [TCR 95-3734].

MENPES, S. A. 1995*b*. *Third annual report for the period ending 10 October 1995. EL18/92 Mt Frankland, Tasmania*. CRA Exploration Pty Ltd [TCR 95-3802].

MORIMOTO, N. 1988. Nomenclature of pyroxenes. *American Mineralogist* 73:1123–1133.

MORRISON, K. C. 1991*a*. *Exploration Licence 21/87 – Balfour. Relinquishment and final report*. Aureole Resources Pty Ltd [TCR 91-3316].

MORRISON, K. C. 1991*b*. *Exploration Licence 53/88, Mount Frankland. Annual report : year 3 (6 January 1991–5 January 1992)*. Soloriens Mining Pty Ltd [TCR 91-3315].

MORRISON, K. C. 1992. *EL 53/88 Mount Frankland. Annual report: year 4 (6 Jan 1992–5 Jan 1993)*. Soloriens Mining Pty Ltd [TCR 92-3403].

MUHLING, P. 1996. Carbonate-hosted Pb-Zn deposits, *in: Ore deposit studies and exploration models: sediment-hosted base metal deposits, sediment-hosted and MVT deposits*. 3.1–3.71. CODES Short Course Manual 2, University of Tasmania.

NEALE, R. C. 1974. *Exploration licence 2/73, Pieman River, Tasmania. Completion report*. Esso Australia Ltd [TCR 74-987].

NYE, P. B. 1975. *Report on SPL 142. Period June to September, 1975*. Mineral Holdings Australia Pty Ltd [TCR 75-1145].

NYE, P. B.; BLAKE, F. 1938. The geology and mineral deposits of Tasmania. *Bulletin Geological Survey Tasmania* 44.

NYE, P. B.; FINUCANE, K. J.; BLAKE, F. 1934. The Smithton district. *Bulletin Geological Survey Tasmania* 41.

PARKINSON, R. G. 1994. *Trowutta EL19/92, Tasmania. Report on exploration for the second year of tenure, 19/8/93 to 18/8/94, and final*. CRA Exploration Pty Ltd [TCR 94-3628].

PORTER, S. M.; KNOLL, A. H. 2000. Testate amoebae in the Neoproterozoic Era: evidence from vase-shaped microfossils in the Chuar Group, Grand Canyon. *Paleobiology* 26:360–385.

PORTER, T. M. 1980*a*. *EL1/77 Rocky Cape, north west Tasmania. Progress report, January 1 to December 31, 1979*. CRA Exploration Pty Ltd [TCR 80-1469].

PORTER, T. M. 1980*b*. *The Balfour–Specimen Hill program, six monthly report to December 26, 1979*. CRA Exploration Pty Ltd [TCR 80-1475].

REID, R.; WESTBROOK, S. 1998. *EL14/97 Lovells Creek. Report on exploration activity, 05-12-97 to 05-12-98*. Pacific Nevada Mining Pty Ltd [TCR 98-4234].

RICKARDS, R. B.; BAILLIE, P. W.; JAGO, J. B. 1990. An Upper Cambrian (Idamean) dendroid assemblage from near Smithton, northwestern Tasmania. *Alcheringa* 14:207–232.

ROLLINSON, H. R. 1993. *Using geochemical data: evaluation, presentation, interpretation*. Longman.

SAITO, Y.; TIBA, T.; MATSUBARA, S. 1988. Precambrian and Cambrian cherts in northwestern Tasmania. *Bulletin of the National Science Museum, Tokyo, Series C, Geology and Paleontology* 14(2):59–70.

SCOTT, B. 1954. The metamorphism of the Cambrian basic volcanic rocks of Tasmania and its relationship to the geosynclinal environment. *Papers and Proceedings Royal Society of Tasmania* 88:129–149.

SCOTT, C. M. 1997. *Sedimentology of the Arthur River area, northwest Tasmania*. B.Sc. (Hons) thesis, University of Tasmania.

SEYMOUR, D. B. 1997. A re-evaluation of the structural significance of the Boat Harbour Fault, northwestern Tasmania. *Record Tasmanian Geological Survey* 1997/09.

SEYMOUR, D. B. (comp.). 1989. Geological Atlas 1:50 000 Series. Sheet 36 (8015S). St Valentines. *Explanatory Report Geological Survey Tasmania*.

SEYMOUR, D. B.; BAILLIE, P. W. 1992. *Geological Atlas 1:50 000 Series. Sheet 20 (7816S). Woolnorth*. Department of Mines Tasmania.

SEYMOUR, D. B.; CALVER, C. R. 1995*a*. *NGMA TASGO Project. Sub-Project 1 — Geological Synthesis: Stratotectonic Elements Map of Tasmania*. Mineral Resources Tasmania, Australian Geological Survey Organisation.

SEYMOUR, D. B.; CALVER, C. R. 1995*b*. Explanatory notes for the Time-Space Diagram and Stratotectonic Elements Map of Tasmania. *Record Tasmanian Geological Survey* 1995/01.

SEYMOUR, D. B.; REED, A. R. 2003. *Geological Atlas 1:25 000 scale digital series. Sheet 3043, Temma*. Mineral Resources Tasmania.

SHARPLES, C. 1990. *The building and ornamental stone resources of Tasmania*. Tasmanian Development Authority; Tasmania Department of Resources and Energy.

SHARPLES, C. 1996. *A reconnaissance of landforms and geological sites of geoconservation significance in the Circular Head Forest District*. Unpublished report to Forestry Tasmania.

SPRY, A. 1955. The Tertiary volcanic rocks of Lower Sandy Bay, Hobart. *Papers and Proceedings Royal Society of Tasmania* 89:153–168.

SPRY, A. 1957. The Precambrian rocks of Tasmania, Part I, dolerites of the north-west coast of Tasmania. *Papers and Proceedings Royal Society of Tasmania* 91:81–93.

SPRY, A. 1962. The Precambrian rocks, *in:* SPRY, A.; BANKS, M. R. (ed.). 1962. The geology of Tasmania. *Journal of the Geological Society of Australia* 9(2):107–126.

SPRY, A. 1964. Precambrian rocks of Tasmania, Part VI, the Zeehan–Corinna area. *Papers and Proceedings Royal Society of Tasmania* 98:23–48.

SPRY, A.; FORD, R. 1957. A reconnaissance of the Corinna–Pieman Heads area — geology. *Papers and Proceedings Royal Society of Tasmania* 91:1–7.

SUMMONS, T. G. 1981. Silica in Tasmania. *Unpublished Report Department of Mines Tasmania* 1981/12.

SUTHERLAND, F. L. 1976. Cainozoic volcanic rocks, *in:* LEAMAN, D. E. Geological atlas 1:50 000 series. Sheet 82 (8312S). Hobart. *Explanatory Report Geological Survey Tasmania* 35–56.

TAHERI, J.; BOTTRILL, R. S. 2004. The nature and origins of copper and tin-tungsten deposits in the Balfour–Temma area, northwest Tasmania. *Record Tasmanian Geological Survey* 2004/5.

TEAR, S. J. 1996. *Fourth annual report for the period ending 5 October 1996, EL18/92 Mt Frankland, Tasmania*. CRA Exploration Pty Ltd [TCR 96-3931].

THREADER, V. 1992. *EL32/90 Montagu Plains, EL33/90 Brittons Swamp. Annual Report to the Dept of Mines and Mineral Holdings Australia Pty Ltd*. Vic Threader and Associates Pty Ltd [TCR 92-3348].

TURNER, N. J. (ed.). 1992. Corinna 1:50 000 geological map. Field guide to selected exposures. *Report Department of Mines Tasmania* 1992/06.

TURNER, N. J. 1993. K-Ar geochronology in the Arthur Metamorphic Complex, Ahrberg Group and Oonah Formation, Corinna district. *Report Mineral Resources Tasmania* 1993/27.

TURNER, N. J. 1994*a*. *Report on the stratigraphic and structural setting of rocks in EL18/92, Balfour district, north western Tasmania*. CRA Exploration Pty Ltd [TCR 96-3644A].

TURNER, N. J. 1994*b*. *Report on geological mapping and rock chip sampling around The Clump, Murrays Reward and other localities in EL18/92, Balfour district, north western Tasmania*. CRA Exploration Pty Ltd [TCR 95-3734A].

TURNER, N. J. 2000. *EL61/94 Arthur River. Partial relinquishment report at 9 June 2000*. Cominex Pty Ltd [TCR 00-4474].

TURNER, N. J. 2001. *EL61/1994 Arthur River. Annual report to 9th June 2001*. Cominex Pty Ltd [TCR 01-4560].

TURNER, N. J. 2003. *Roger River Project, Tasmania. ELs11/97, 12/97, 13/97, 14/97, 61/94 and 17/01, combined annual report to 18th December, 2002*. Morritt Holdings Pty Ltd [TCR 03-4841].

TURNER, N. J.; BLACK, L. P.; KAMPERMAN, M. 1995. Pre-Middle Cambrian stratigraphy, orogenesis and geochronology in western Tasmania, *in:* COOKE, D. R.; KITTO, P. A. (ed.). Contentious issues in Tasmanian geology. *Abstracts Geological Society of Australia* 39:51–56.

TURNER, N. J.; BLACK, L. P.; KAMPERMAN, M. 1998. Dating of Neoproterozoic and Cambrian orogenies in Tasmania. *Australian Journal of Earth Sciences* 45:789–806.

VESKA, L. 1993. *Geology, mineralisation and structure of the Balfour copper occurrence, northwestern Tasmania*. B.Sc. (Hons) thesis, University of Tasmania.

VIRGOE, K.; MATHISON, I. 1990. *EL46/89 Julius River. Report of exploration activity, January 1990 to November 1990 (relinquishment report)*. Geopeko Limited [TCR 91-3211].

VIRGOE, K.; MATHISON, I. 1991. *EL52/89 Balfour. Report of exploration activity, March 1990 to February 1991 (relinquishment report)*. Geopeko Limited [TCR 91-3229].

VOLKER, J. 1969. *Report on chromite areas, N. W. Tasmania*. Ocean Mining and Exploration NL [TCR 69-573].

WARD, L. K. 1911. The Mount Balfour mining field. *Bulletin Geological Survey Tasmania* 10.

WEAVER, B. L. 1991. The origin of ocean island basalt end-member compositions: trace element and isotopic constraints. *Earth and Planetary Science Letters* 104:381–397.

WEIR, D. J. 1982. *Rocky Cape EL1/77. Progress report, July 1981–June 30th, 1982*. CRA Exploration Pty Ltd [TCR 82-1811].

WEIR, D. J. 1983*a*. *Leigh River EL12/80. Progress report for year ending January 22nd, 1983*. CRA Exploration Pty Ltd [TCR 83-1923].

WEIR, D. J. 1983*b*. *Progress report, Rocky Cape EL1/77, Trowutta–Dempster Plains area, period ending 28th Feb. 1983*. CRA Exploration Pty Ltd [TCR 83-1959].

WEIR, D. J. 1983*c*. *Rocky Cape EL1/77, geochemical computer study, panned concentrates*. CRA Exploration Pty Ltd [TCR 83-1960].

WESTBROOK, S. 1999*a*. *EL61/94 Arthur River–Roger River. Report on exploration activity, 9-6-98 to 9-6-99*. Pacific Nevada Mining Pty Ltd [TCR 99-4323].

WESTBROOK, S. 1999*b*. *EL04/98 Balfour. Report on exploration activity, 10-7-98 to 10-7-99*. Pacific Nevada Mining Pty Ltd [TCR 99-4346].

WHITEHEAD, C. H. 1989. *Exploration Licence 19/88, Montagu River, N. W. Tasmania. Annual report 1988/89*. C. H. Whitehead [TCR 89-2985].

WHITEHEAD, C. H. 1990. *Relinquishment report, Exploration Licence 19/88, Montagu River – N. W. Tasmania*. C. H. Whitehead [TCR 90-3178].

WILLIAMS, E. 1979. *Tasman Fold Belt System in Tasmania. Explanatory notes for the 1:500 000 structural map of pre-Carboniferous rocks of Tasmania. Revised edition*. Department of Mines Tasmania.

WILLIAMS, E.; TURNER, N. J. 1973. *Geological Atlas 1:250 000 series. Sheet SK55-3. Burnie*. Department of Mines Tasmania.

YAXLEY, G. M. 1981. *The geology and mineralisation of the Balfour district – a mineralogical and fluid inclusion study*. B.Sc. (Hons) thesis, University of Tasmania.

APPENDIX 1

Detailed petrographic descriptions of the Black River Dolomite

J. L. Everard, C. R. Calver

Dolomite (Pssd)

Stromatolitic flakestone

This term is applied to a few samples with well preserved and sharply defined, tabular, generally micritic intraclasts.

Sample R005027, from near the base of the unit in the Arthur River, on the eastern limb of the Smithton Synclinorium, contains abundant (about 30–40%) tabular to platy, cream-coloured, stromatolitic intraclasts (up to 10 mm across and 0.2 to 2 mm thick) in a medium-grey matrix (about 60–70%). In thin section (Plate 42), the intraclasts are seen to be strongly microbanded dolomicrite with parallel internal lamination and rather diffuse margins. Most are aligned to define bedding, but a few are orientated obliquely. The matrix is fine to medium-grained sparry carbonate. The rock is a pure unsilicified carbonate with virtually no detrital impurities.

Sample R005029, from a similar stratigraphic position 1.6 km downstream, is similar, but the intraclasts are less well aligned. They consist of similar diffusely laminated alternations of dolomicrite, with some minute (40 μm) brown radiating fibrous ooids preserved, and fine-grained dolomicrosparite. The matrix is a coarse-grained (up to 2 mm) bladed dolospar cement.

Sample R005102 is from Lamprey Creek, further south and along strike from the other samples. It consists of similar randomly orientated, elongate to irregular, diffusely laminated, mainly micritic platy intraclasts (5–20 mm across and 1–4 mm wide) in a matrix of medium to coarse-grained (40–500 μm) sparry carbonate. Incipient slight silicification (<1%) is mainly restricted to the most coarse-grained sparry zones.

Other samples have a less well-preserved flakestone fabric, due to recrystallisation. Sample R005096, from a similar stratigraphic position on the lower reaches of the Rapid River, is a pale grey, cream-weathering dolomite with a streaky diffuse planar lamination. In thin section this is seen to be due to abundant wispy lenses of dolomicrite, probably remnant stromatolitic intraclasts, which are strongly aligned in an uneven-grained (10–400 μm, but typically 50–100 μm) dolomicrosparite matrix. The dolomite is nearly pure, with a very tenuous dissemination of opaque material and very rare small grains of detrital quartz, mainly associated with the intraclasts.

The only sample with flakestone fabric collected from the western limb of the synclinorium (sample R004831) is from well up in the Black River Dolomite. In hand specimen it is an apparently massive off-white dolomite, but in thin section a faint lamination is defined by diffusely wispy lenses and irregular patches of very fine-grained dolomicrosparite and dolomicrite. These may be remnant stromatolitic intraclasts. The matrix is a recrystallised coarse-grained (40–250 μm) dolomicrosparite.

Peloidal grainstone

This term is applied to samples with well preserved and sharply defined, ovoid or lenticular to irregularly shaped intraclasts.

A well preserved example (R005111, Plate 43), from the base of the Black River Dolomite in Lamprey Creek, contains abundant irregularly shaped micritic to very finely sparry peloids (500 μm–2 mm) with sharply defined margins. About 3–5% Rocky Cape Group detritus is present, including mostly well-rounded quartz grains (up to 1 mm) and minor elongate clasts of siliceous mudstone (with little sericite). The mainly micritic cement is partly recrystallised to fine-grained spar, producing a mottled appearance in thin section. A crude bedding is defined mainly by compaction flattening of the peloids, and also by orientation of the mudstone clasts. Another sample (R005110) from this vicinity is a similar but better bedded, slightly impure grainstone in which many grains have a clear, very fine-grained dolomicrosparite core and a darker dolomicritic rim. There are patches of coarse recrystallisation within the cement.

Sample R004829, from near the top of the unit in the west of the Smithton Synclinorium, lacks siliciclastic detritus, but is an otherwise similar peloidal grainstone. The irregularly shaped peloids (about 50%) are mainly very fine grained dolosparite, whilst the cement is slightly coarser spar with a locally fenestral fabric. There are a few narrow veinlets of coarse-grained spar and/or secondary silica.

Sample R005115, from the Horton River and also from near the top of the unit, is an impure, partly recrystallised peloidal grainstone with 1–2% detrital quartz. It was probably originally similar to R005111 and R005110, but has partly recrystallised (about 50%) to fine to medium-grained dolomicrosparite. Impurities, including opaque dust, have concentrated at the recrystallisation front between the dolomicrosparite and the mainly dolomicritic peloids.

Sample R004936 (Blackwater 1 road) contains about 40% crudely elliptical to irregular subrounded peloids (250–500 μm) of micritic to finely sparry carbonate. The cement is recrystallised sparry carbonate, generally

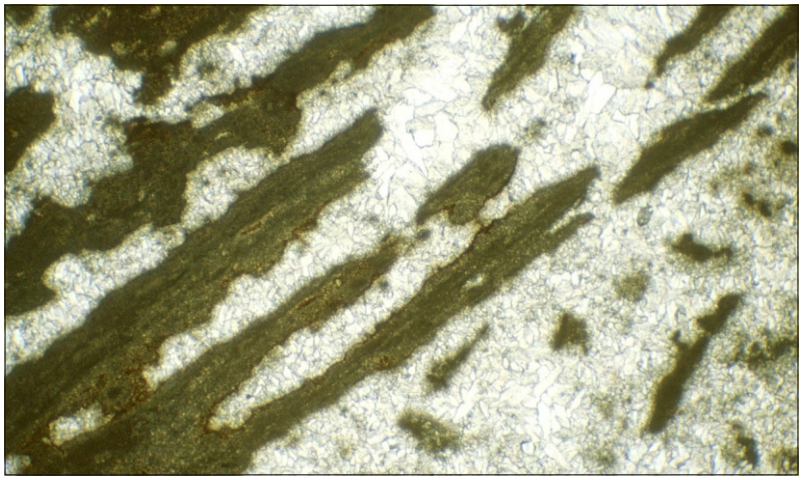

Plate 42

Photomicrograph of flakestone from Black River Dolomite (Pss), sample R005027 (Arthur River, 342 570 mE, 5 448 410 mN). Stromatolitic intraclasts of microbanded micrite in a sparry matrix. Plane polarised light, field of view 4.4 2.9 mm.

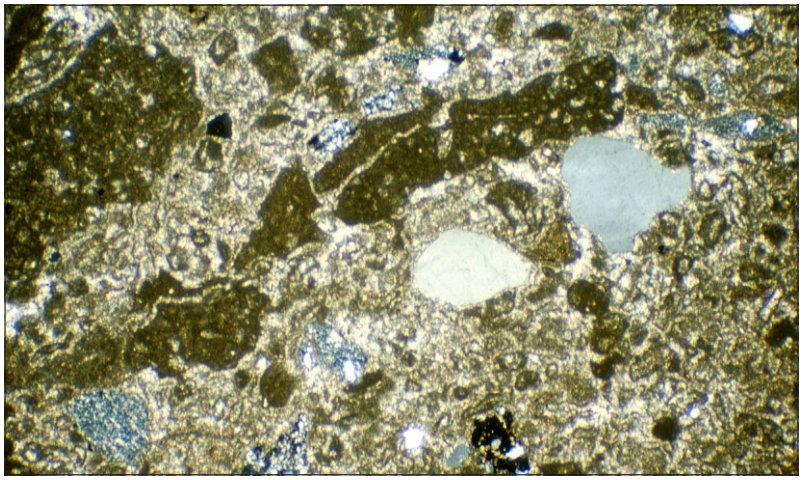

Plate 43

Photomicrograph of peloidal grainstone, Black River Dolomite (Pss), sample R005111 (Lamprey Creek, 340 090 mE, 5 440 390 mN). Note also detrital quartz grains and siliceous mudstone clasts. Crossed nicols, field of view 4.4 2.9 mm.

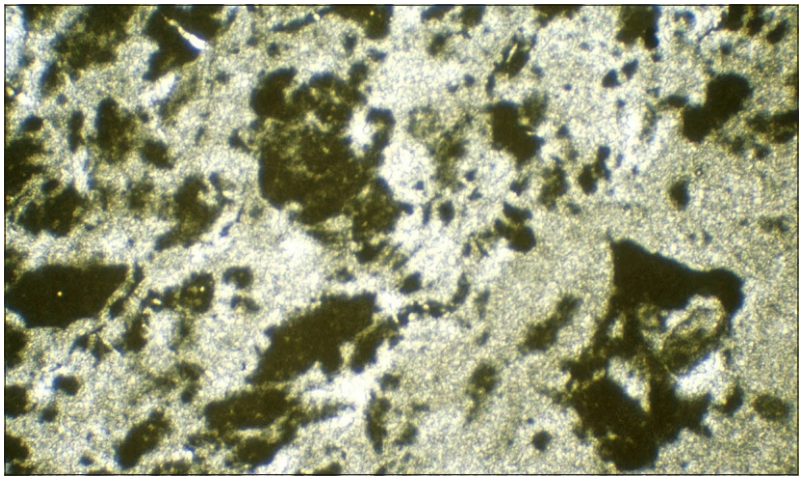

Plate 44

Photomicrograph of peloidal grainstone, Black River Dolomite (Pss), sample R005041 (Arthur River, 336 100 mE, 5 446 440 mN). Note micritic peloids, ooids (top right, lower right) with micritic cores and rims and microsparite mantles; and partly fenestral microsparite matrix. Plane polarised light, field of view 4.4 2.9 mm.

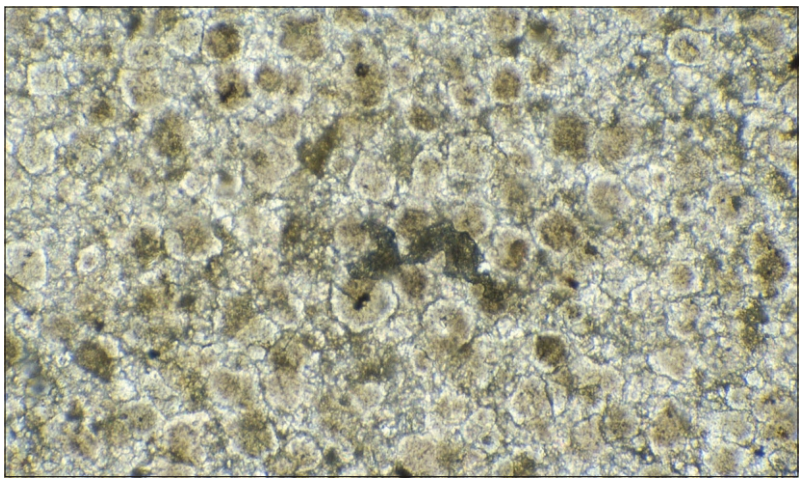

Plate 45

Photomicrograph of fine-grained grainstone, Black River Dolomite (Pss), sample R005091 (Sumac Rivulet, 338 010 mE, 5 440 980 mN). Plane polarised light, field of view 1.8 1.2 mm.

coarser, but variations in spar size define a diffuse banding. Sparse (1–2%) angular grains of detrital quartz anhedra are present; some are polycrystalline and probably derived from Rocky Cape Group quartzite.

Several samples of peloidal grainstone were collected from the Arthur River. Sample R005041 (Plate 44) contains abundant, irregular to lenticular peloids of dolomicrite. Ooids are common, typically 150–400 μm in diameter and usually with dark dolomicritic cores and rims and a clear mantle of fine-grained dolomicrosparite. The dolomicrosparite cement is fine to medium-grained (20–50 μm) and partly fenestral.

Sample R005030 is a similar, peloidal to intraclastic grainstone, although ooids are not preserved. The peloids are micritic and the matrix finely sparry. Some of the peloids are very elongate and in places the fabric is perhaps transitional to flakestone (see below).

Sample R005060 has a mesoscopically discernible coarse-grained grainstone fabric. In thin section the rock resembles R004936 and consists of abundant large (mostly 0.5–1.5 mm), generally well-rounded peloidal grains of fine-grained dolomicrosparite in a coarse-grained sparry cement. The rock is grain supported or nearly so. There are also scattered large crystals (0.5–1 mm) of late pseudopleochroic brown spar, without stress twinning. Detrital material is absent.

Fine-grained grainstone

Sample R005091 (Plate 45), a faintly bedded medium-grey dolomite from Sumac Rivulet, near the top of the formation, has an unusual fabric in thin section. It consists mainly of well-sorted, closely packed small equidimensional grains(?) (60–100 μm across), with large cores of turbid brown carbonate, surrounded by rims of almost clear carbonate. These are smaller than, and lack the concentric internal structure of, typical ooids. A diffuse lamination is defined by variations in the grain size and morphology of these grains. They are cemented by interstitial fine-grained (5–10 μm) spar. There are also a few branching veinlets, up to 200 μm wide, of interlocking clear spar (50–100 μm). Grain boundaries are commonly continuous across the margins of the veinlet, suggesting that the clear vein carbonate nucleated on adjacent grains of the wall rock.

Partly recrystallised intraclastic grainstone

In these samples the intraclasts are sparse or isolated ('floating') and poorly preserved, usually due to recrystallisation.

Sample R005093 (Sumac Rivulet, Plate 46) is a diffusely banded, fine-grained (5–10 μm) dolomicrosparite with fairly abundant ragged intraclasts (up to 1 mm) of relict dolomicrite, partly invasively recrystallised by the matrix. Some large (to 500 μm) aggregates of opaque grains, a few thin ferruginous seams and traces of detrital quartz are present.

Sample R004823 (Blackwater Rivulet) closely resembles R005093. Ragged dark micritic intraclasts (300 μm–1.5 mm), together with scattered anhedral grains of coarse-grained (50–200 μm) detrital spar, lie in a matrix of fine-grained, diffusely banded dolomicrosparite with rare small anhedra of detrital quartz.

Sample R004833 (Julius River) is similar. Abundant diffuse, irregularly shaped, dark micritic intraclasts include some with a clotted fabric which may be microbial mat fragments or catagraphs. The matrix is an unbedded, unsilicified, mostly fine-grained (10–20 μm) dolomicrosparite with some more coarsely recrystallised (to 100 μm) patches.

Sample R005094 (Rapid River) also contains floating ragged intraclasts of partly recrystallised dark dolomicrite, but in a much more coarsely recrystallised dolomicrosparite matrix (typically 50–200 μm with some finer-grained zones). Detrital quartz is absent and opaque material very sparse.

Sample R005090 (Sumac Rivulet bridge) similarly contains vaguely elongate to lenticular ragged intraclasts of dolomicrite, in places partly recrystallised to microspar, in a matrix of fine to medium grained (50–100 μm) dolomicrosparite, with minor (2–5%) intergranular, microcrystalline to cryptocrystalline chert.

In sample R005121 (Julius River tributary, Plate 47), poorly preserved micritic intraclasts are in places surrounded by a distinctive early cement phase about 150 μm thick of bladed, radiating brown spar, which is in turn coated with a thin layer of dolomicrite. The later cement is a clear fine-grained dolomicrosparite.

Two samples from Sumac Rivulet (R005105, R005106) contain diffuse wispy intraclasts of relict dolomicrite in a pure, uneven but mainly coarse-grained (up to 500 μm) dolomicrosparite matrix. In the former sample, some intraclasts are elongate and crudely aligned to define bedding, suggesting an original flakestone fabric.

Partly silicified intraclastic grainstone(?)

In sample R005081, isolated diffuse very irregular patches of dolomicrite up to 3 mm across comprise about 10–20% of the rock and may be remnant intraclasts. The remainder is cryptocrystalline to less commonly microcrystalline (up to 300 μm) chert, finely intergrown with subordinate fine-grained dolomicrosparite.

Dolomicrosparite

About one third of the dolomite samples sectioned are largely recrystallised to fine (10–20 μm) to medium (20–50 μm) and usually even grained dolomicrosparite. Commonly a few diffuse and sometimes faint finer-grained relict intraclasts are present (e.g. sample R004976 with 'floating' patches of remnant dolomicrite). Some samples have a well developed lamination defined by anastomosing brown impure

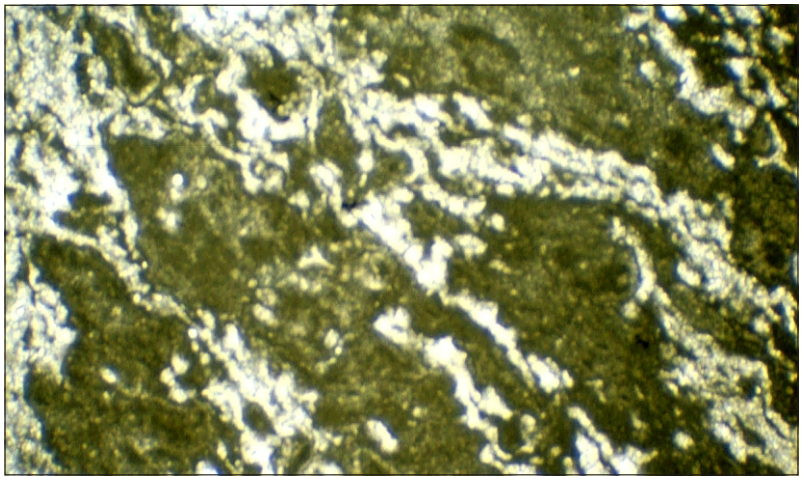

Plate 46

Photomicrograph of intraclastic grainstone, Black River Dolomite (Pss), sample R005093 (Sumac Rivulet, 339 300 mE, 5 441 650 mN). Ragged intraclasts of relict micrite, partly invasively recrystallised by the fine-grained microsparite matrix. Plane polarised light, field of view 4.4 2.9 mm.

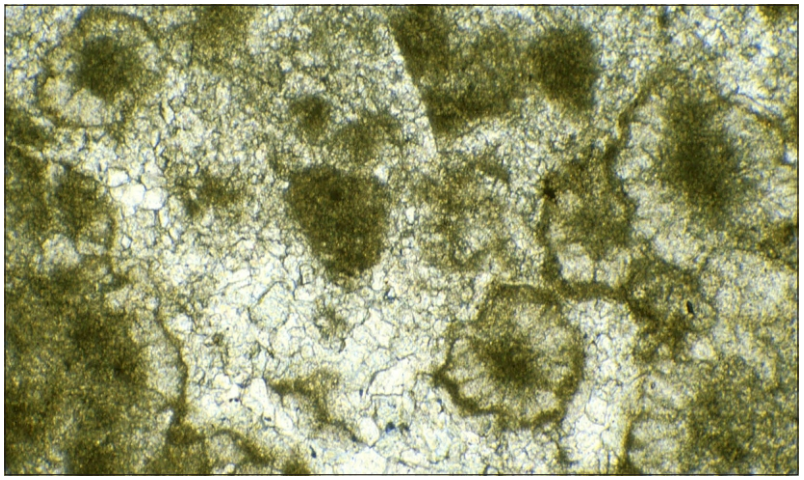

Plate 47

Photomicrograph of intraclastic grainstone, Black River Dolomite (Pss), sample R005121 (Julius River tributary, 333 560 mE, 5 439 970 mN). Note micritic intraclasts (e.g. top left, lower right) surrounded by radiating brown spar and with thin micritic rim, in a later cement of fine-grained microsparite. Plane polarised light, field of view 1.8 1.2 mm.

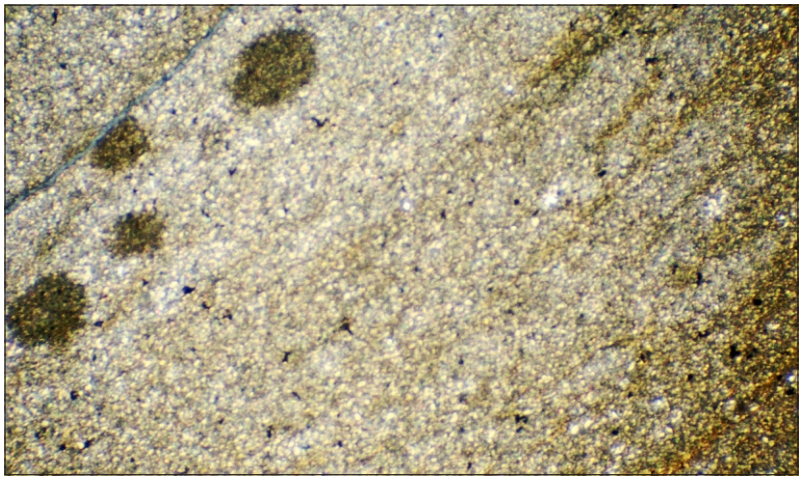

Plate 48

Photomicrograph of typical recrystallised fine-grained microsparite, Black River Dolomite (Pss), sample R006663 (328 790 mE, 5 430 170 mN). Note lamination defined by brown stylolitic seams. Crossed nicols, field of view 4.4 2.9 mm.

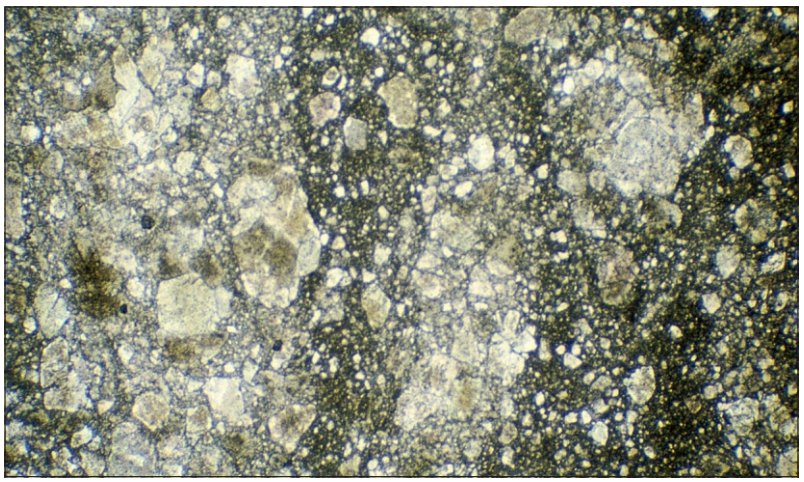

Plate 49

Photomicrograph of cataclastic microsparite, Black River Dolomite (Pss), sample R004834 (326 420 mE, 5 442 820 mN). Plane polarised light, field of view 4.4 2.9 mm.

(possibly partly sericitic) stylolitic seams (samples R006663; Plate 48, R005122). Others have a less well developed lamination defined by elongation of intraclasts (e.g. samples R005101, R005109) or subtle variations in grain size (sample R005107). A few samples (R006667, R006671) are thoroughly recrystallised, lack remnant intraclasts or bedding, and are very uneven-grained with domains of both fine (10–20 μm) and very coarse-grained (0.5–1.5 mm) spar. Most dolomicrosparites are pure except for a few hair-line stylolitic veinlets and a very tenuous dissemination of opaque material, but a few samples (notably R006663, R006673, R006676, R005122) contain rare detrital quartz. Sample R005031 has slight (1–2%) silicification, containing some microcrystalline chert mostly associated with coarser-grained sparry domains.

A critical sample (R006660) from the Leigh River outlier (333750/5426730) on the Balfour map sheet is a pale grey sparry dolomite with a diffuse streaky lamination, traversed by several cream-coloured, more coarsely crystalline veinlets. In thin section it is seen to be a fine to medium-grained (up to 30 μm) dolomicrosparite with well-developed stylolitic cleavage. There is a sparse dissemination of very fine-grained opaque material, and occasional larger grains of pyrite (one 2 mm across). On petrographic evidence it is difficult to assign this sample unequivocally to either the Black River or Smithton dolomites.

Cataclastic dolomicrosparite

Sample R005058 is a more coarsely (up to 500 μm) recrystallised cataclastic dolomicrosparite, collected from near an inferred thrust fault (325330/5447180). There is an irregular network of fractures filled with finer-grained carbonate, and associated with incipient silicification.

Another sample (R004834, Plate 49) from the vicinity of an inferred thrust (326420/5442820) contains probable clasts of coarse (up to 500 μm) brownish pseudopleochroic spar, one of which preserves a possible oolitic fabric. These grade down into a very uneven-grained matrix which includes very fine-grained, probably comminuted carbonate. There is no detrital material or secondary silicification.

Recrystallised conglomeratic dolomite

Sample R005558, from a small outlier in the Horton River (334260/5432420), is a medium-grey dolomite with numerous irregularly shaped, cream-coloured clasts up to 20 mm across, associated with minor outweathering silicification. In thin section (Plate 50) the clasts are seen to be rather diffuse but mainly coarse-grained (50–500 μm) dolomicrosparite. The matrix is mostly much finer grained dolomicrosparite approaching dolomicrite, but recrystallisation has obscured much of the fabric.

Dolomicrosparite with local botryoidal texture

Sample R005089 (Rapid River, Plate 51) is a mottled, uneven but mostly medium to coarse-grained (100–500 μm) dolomicrosparite. Highly irregular, cream to brown patches (5–20 mm long by a few millimetres wide) of much finer grained spar and dolomicrite define a crude banding. Some of the latter material has a botryoidal, concentric and radially fibrous fabric on a scale of 0.5–1 mm, probably of primary origin. There are also some patches of late clear coarsely sparry white calcite, which are associated with minor (1–2%) silicification.

Sample R006669 (Leigh River) is a massive pale grey dolomite with distinct irregular blotches (up to 10 mm) of bone-white carbonate, and smaller and more diffuse darker grey mottles. In thin section the rock is an uneven-grained dolomicrosparite (40–150 μm). The large pale blotches are seen to be pale-brown dolomicrite with a concentric to botryoidal fabric (similar to that of R005089) and the small darker patches are of structureless dolomicrite.

Dolomicrosparite with pelitic mudstone interbeds

Sample R005099, from a tributary of Sumac Rivulet, consists of pale grey to faintly olive-green dolomite beds up to 15 mm thick, alternating with thin planar interbeds of dark brown mudstone, 1–4 mm thick. In thin section (Plate 52) the dolomite is mainly a fine (c. 20 μm) and even-grained dolomicrosparite with some diffuse micritic patches, anastomosing thin seams of pelitic/ferruginous impurities, and very sparsely disseminated opaque grains. The mudstone interbeds contain small equant opaque grains (c. 40 μm) concentrated at both their tops and bottoms, a few small quartz grains (≤50 μm) and some detrital muscovite. The mainly sericitic matrix of the interbeds has a closely spaced penetrative cleavage.

Sample R005108, from the bridge over Sumac Rivulet, is a similar pale grey dolomite with darker grey interbeds (1–5 mm) of cleaved mudstone. Oxidation of the minor opaque material within the pelitic interbeds has imparted a pale greenish-brown staining.

Sample R004832, from the western limb of the Smithton Synclinorium, similarly consists of fine to medium-grained, pale to medium-grey dolomite (in thin section a fairly impure dolomicrosparite, 25–50 μm) with darker, planar to slightly anastomosing interbeds (0.5–2 mm) of cleaved pelitic mudstone.

Quartzose dolomite

Sample R005040 shows a transition, gradual on thin section scale (about 50 mm), between medium to dark grey quartzite and paler grey massive dolomite. The quartzite is well sorted (100–200 μm) with sutured grain boundaries and is fairly pure (95%) with only minor carbonate. The dolomite is a nearly pure medium-grained (50–100 μm) microsparite with a relict oolitic texture; many grains have darker

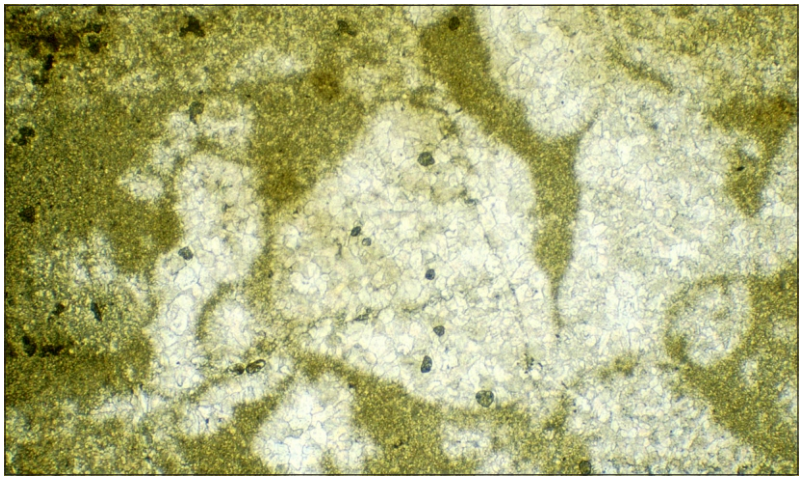

Plate 50

Photomicrograph of dolomitic conglomerate, Black River Dolomite (Pss), sample R005558 (Horton River, 334 260 mE, 5 432 420 mN). Recrystallised dolomite with relict conglomeratic texture; rather diffusely defined clasts of coarse-grained microsparite in a much finer-grained to micritic matrix. Plane polarised light, field of view 4.4 2.9 mm.

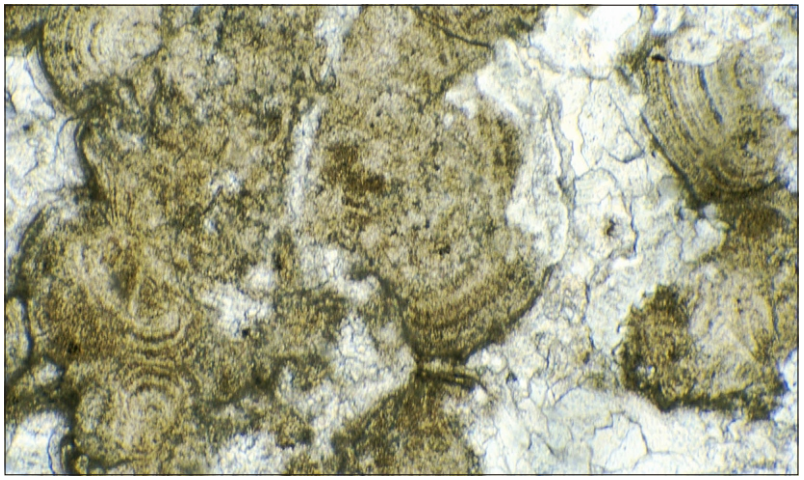

Plate 51

Photomicrograph of microsparite, Black River Dolomite (unit Pss), sample R005089 (Rapid River, 340 420 mE, 5 442 180 mN). Note botryoidal fabric of fine-grained spar and micrite; late coarse-grained spar also present. Plane polarised light, field of view 1.8 1.2 mm.

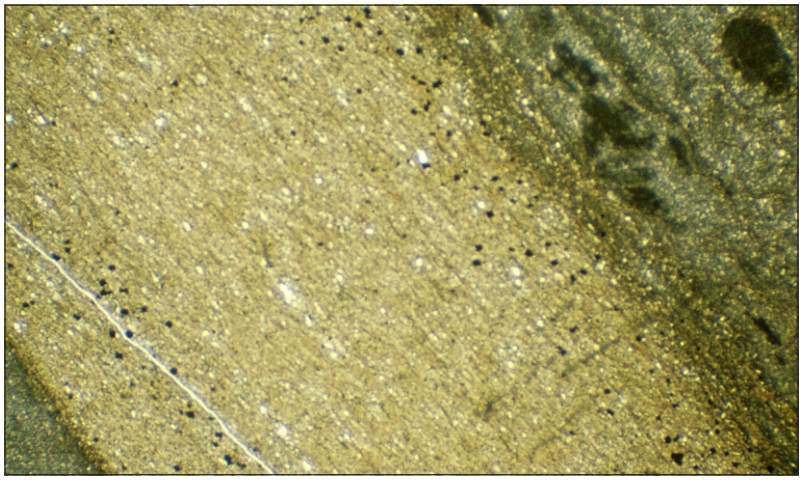

Plate 52

Photomicrograph of Black River Dolomite (Pss), sample R005099 (Sumac Rivulet tributary, 337 450 mE, 5 438 430 mN). Note pelitic mudstone interbed with detrital opaque grains (at top and bottom of bed), quartz and sericite; the enclosing fine-grained microsparite contains some relict micrite. Plane polarised light, field of view 4.4 2.9 mm.

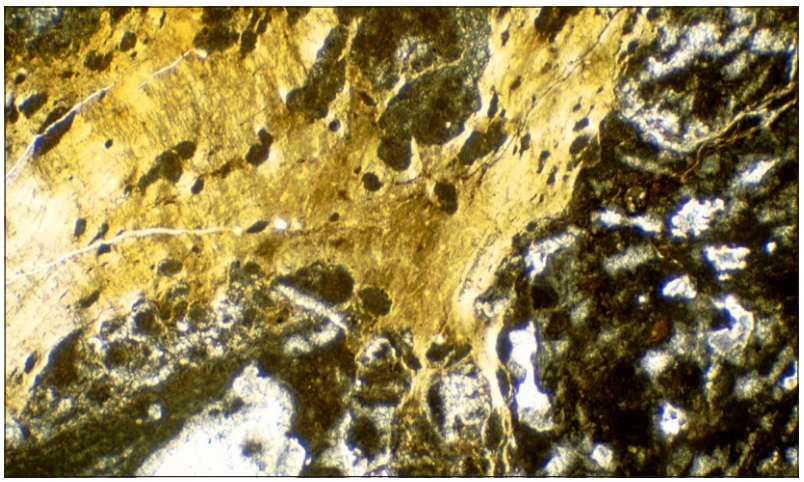

Plate 53

Photomicrograph of impure shaly dolomite, Black River Dolomite (Pss), sample R004824 (Blackwater Rivulet, 324 780 mE, 5 442 940 mN). Mottled to micronodular micrite and fine-grained sparite between anastomising bands of yellow-brown ferroan talc. Plane polarised light, field of view 4.4 2.9 mm.

pseudopleochroic cores. The centre of the slide is composed of subequal proportions of quartz and carbonate.

Impure talcose dolomite

Sample R004824, from Blackwater Rivulet (324780/5442940), is an impure shaly dolomite, parting along thin, anastomosing, wavy dark-grey to black bands up to 2 mm across. In thin section (Plate 53) these are seen to consist mainly of yellow-brown pleochroic ferroan talc (confirmed by x-ray diffraction). Between them is irregularly banded, mottled to micronodular dolomicrite and fine-grained dolosparite; some possible oolites (20–40 μm across) have dolomicritic cores and finely sparry mantles.

Pelitic mudstone

A typical sample (R005114), from a tributary of the Julius River, is a pale khaki-green to brown-green, hard, very finely planar laminated mudstone with a dull lustre and angular fracture. In thin section the rock consists of abundant tiny splinters (≤10 μm) of sericite, together with a sparse dissemination of small (10 μm) blebs of deep red oxidised opaque grains, in an indeterminate, very fine-grained, probably quartzose matrix. Both diffuse bedding, defined mainly by slight compositional variations, and a weak cleavage are present.

Other samples may have a stronger (e.g. R005098, R004827) or weaker (e.g. R005116) fabric, including both bedding and cleavage. The latter sample contains pale orange-brown discoid to lenticular structures, probably clay pellets, 2 to 5 mm across and about 0.5 mm thick, which have not survived thin section preparation. Sample R005098 (Sumac Road) is pale grey and less oxidised, with unaltered opaque blebs.

Another sample (R004816), from Blackwater Rivulet, is dark grey, less sericitic and transitional to fine-grained quartz siltstone. Fresh opaque grains, including pyrite euhedra up to 75 μm, are fairly abundant. There are a few larger grains (up to 100 μm) of detrital quartz. Bedding is defined mainly by diffuse, slightly carbonaceous bands, but there is no cleavage.

Sample R004814 (Blackwater 5-1 road) is a pale grey to off-white fissile silicified pelitic mudstone with a finely streaky lamination. In thin section it is poorly sorted, and contains scattered angular, irregular to elongate grains of microcrystalline chert, up to 2 mm long but mostly 500 μm, aligned in the bedding. At least some chert grains are secondary, rather than true clasts. The matrix is fine-grained to cryptocrystalline quartz, much of which is probably secondary. Scattered small splinters (up to 50 μm) of sericite and abundant but very small opaque blebs (mostly ≤5 μm) suggest that the rock is a silicified pelitic sediment rather than chert.

Dark grey to black carbonaceous siltstone and mudstone (Pssm)

Typical specimens (R005112, R005117, R006666) are black, weakly fissile carbonaceous mudstone with a conchoidal fracture and dull lustre, to subvitreous on bedding planes. In standard thickness thin sections they are almost opaque, but on the thinnest edges small angular quartz grains (up to 20 μm but commonly much smaller) and tiny splinters of mica (mostly ≤10 μm) can be resolved from a black carbonaceous matrix.

Chloritic siltstone wacke

An outcrop of medium to dark grey dolomitic siltstone, with convolute lamination suggesting soft-sediment deformation, occurs within a dolomite sequence in a small creek near Blackwater 5-2 spur road (326550/5442790). In thin section, a sample (R004835) is a siltstone wacke with a contorted foliation, containing sparse small grains of quartz in a matrix of mainly chlorite with opaque blebs and formless patches of dolomite. There are some possible clasts of finely sparry carbonate, around which the foliation wraps.

Flaggy black siliceous mudstone and siltstone (Pssf)

Typical samples (e.g. R004830, R005487, R005028, R005032, R006682, R005087) are platy to fissile, hard but brittle, fine-grained siltstone with a well developed finely streaky planar lamination. In thin section, typical specimens (R005487, R005028: Plate 54) contain scattered small (up to 40 μm) angular quartz grains and a few crudely aligned splinters (up to 100 μm by 10 μm) of detrital muscovite, very sparingly disseminated in a well laminated, dark coffee-brown, translucent matrix.

All these samples contain numerous chitinozoan-like microfossils, as previously described in the Black River Dolomite by Saito *et al*. (1988). They are ovoid or flask-shaped, 60–120 μm long, with thin clear, colourless possibly chalcedonic shell-like walls about 2 μm thick, and a dark interior (Plate 55). Many show brittle compaction fracture, and in some samples there are numerous curved or crescent-shaped fragments.

Some samples (R005028, R006682) contain small (up to 1 mm) irregular ragged lenses of finely microcrystalline chert, generally elongate parallel to the foliation. These samples are transitional to thinly laminated chert.

The amount of carbonaceous material varies considerably, and in darker samples largely obscures the mineralogy in thin section. A paler sample (R004826) from a tributary of Blackwater Rivulet consists of a very fine-grained pelitic aggregate of small (≤20 μm) muscovite splinters and low birefringence material, probably quartz. Carbonate is absent. Carbonaceous seams define both an anastomosing

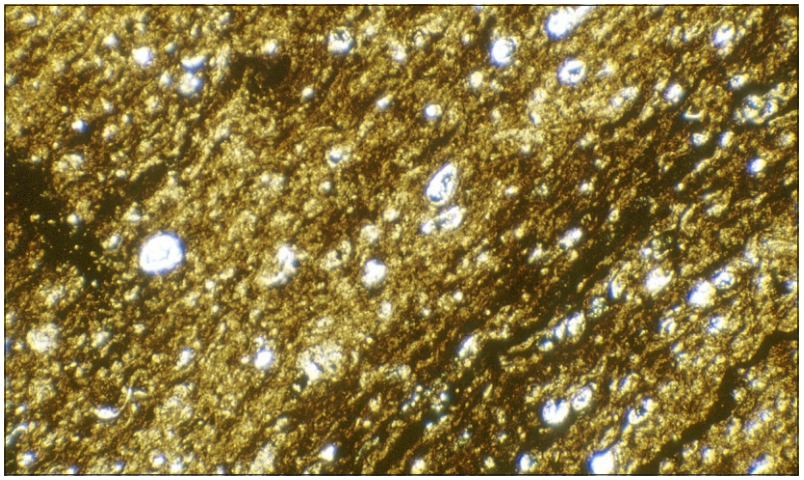

Plate 54

Photomicrograph of flaggy black siliceous mudstone (unit Pssf) from Black River Dolomite, sample R005028 (Arthur River, 342 450 mE, 5 448 220 mN). Note angular detrital quartz grains and chitinozoan-like microfossils. Plane polarised light, field of view 1.8 1.2mm.

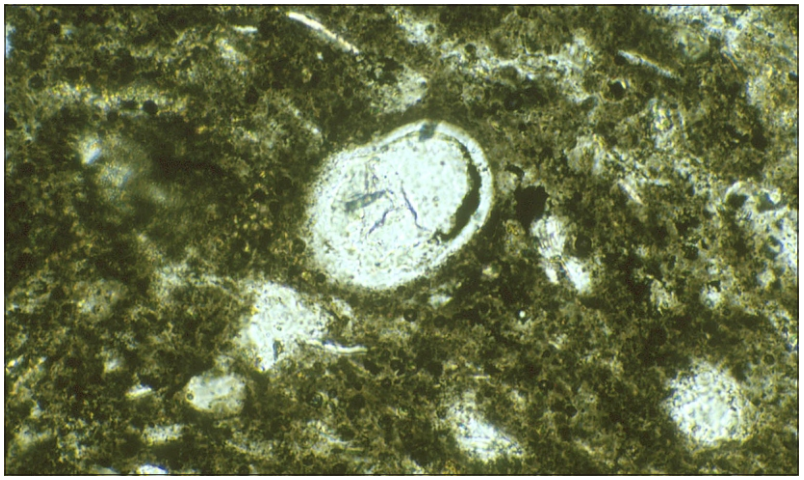

Plate 55

Photomicrograph (high magnification) of chitinozoan-like microfossil in flaggy black siliceous mudstone (unit Pssf) from Black River Dolomite, sample R006682 (336 910 mE, 5 426 670 mN). Plane polarised light, field of view 0.28 0.16mm.

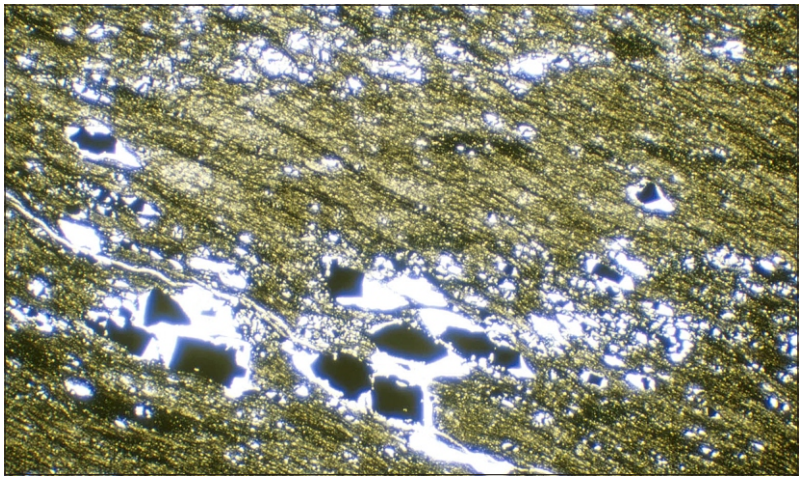

Plate 56

Photomicrograph of cleaved black pyritic siltstone (unit Pssf), from Black River Dolomite, sample R004828 (324 530 mE, 5 444 390 mN). Dominant fabric defined by carbonaceous seams is cleavage; bedding is horizontal on page and defined mainly by coarse-grained chlorite (clear) and pyrite. Plane polarised light, field of view 4.4 2.9 mm.

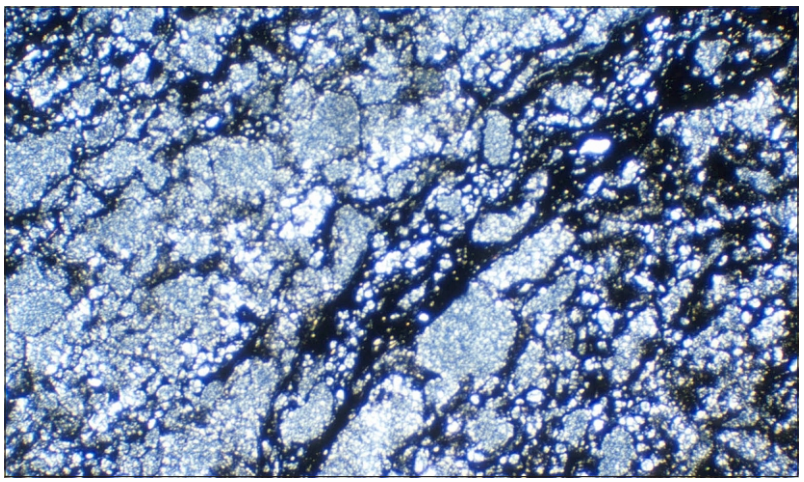

Plate 57

Photomicrograph of typical banded black chert (unit Pssc) from Black River Dolomite, sample R004817 (Blackwater Rivulet, 325 510 mE, 5 440 530 mN). Note patchy texture, uneven grain size and anastomising carbonaceous laminae. Crossed nicols, field of view 4.4 2.9 mm.

bedding lamination (dominant) and a penetrative cleavage. One pale grey interbed, 6 mm thick, is devoid of carbonaceous material, but contains small (up to 100 μm) equant opaque grains (pyrite?), concentrated along a particular horizon.

Sample R005087, closely associated with chert in a road cutting at Dempster Plains, closely resembles R004826 in thin section.

Another sample (R004828), from the same creek as R004826, is a black pyritic siltstone, somewhat resembling the Cowrie Siltstone, with fissility along both cleavage (dominant) and bedding. In thin section (Plate 56) it is a similar fine-grained pelitic siltstone. Bedding is defined mainly by thin (250 μm) coarser-grained laminae of chlorite and opaque grains, whilst seams of anastomosing carbonaceous material define the cleavage. Some shearing has occurred along cleavage planes and has begun to transpose bedding. Another sample (R004827) from the same locality is a pale grey, strongly cleaved fine-grained pelitic siltstone, with little carbonaceous material. Slightly coarser-grained aggregates of colourless chlorite occur in pressure shadows adjacent to the numerous small (up to 100 μm) pyrite grains.

Chert and related silicified rocks (Pssc)

Massive chert

Typical specimens (e.g. sample R005092, Sumac Rivulet, 338760/5441320) are thinly and diffusely laminated black cherts, sometimes with a well-spaced bedding fissility, but not closely fissile. Usually they are well jointed with an angular fracture and a subvitreous lustre. In thin section, R005092 consists of irregularly shaped patches (up to 1mm across) of clear microcrystalline silica, in a dark brown to almost opaque turbid matrix of similar silica and very fine-grained carbonaceous material. The clear patches have sharp to somewhat diffuse margins, and are probably a diagenetic feature, rather than clasts. Chitinozoan-like microfossils, similar to those described in lithology Pssf, are present.

Sample R005103 (Sumac Rivulet) is a dark grey chert consisting largely of an even-grained mosaic of clear microcrystalline (mostly 20–40 μm) silica. There are some zones of intimately intergrown chert and formless remnant finely sparry carbonate, near which the chert mosaic tends to be coarser grained (up to 100 μm).

Sample R006661 (Lindsay River tributary) is a bone white, irregularly blotchy chert. In thin section it consists of clear, microcrystalline to cryptocrystalline silica, transected by veinlets and irregular vugs of later quartz. Some of the latter have cores of interlocking coarsely anhedral (≤1 mm) quartz, and margins of bladed to radiating fibrous quartz.

Sample R006683, from the Leigh River inlier at the extreme southern end of the synclinorium, is a more uneven grained and less pure dark grey altered chert with some voids. It contains numerous tiny opaque blebs (≤5 μm) and scattered small splinters of detrital mica, and is traversed by a few anastomosing veinlets and stringers of black carbonaceous material and sericite.

Sample R005120 (Julius River tributary) is another highly altered, mottled to irregularly-banded creamy-white to medium-grey chert with a few small voids. The thin section shows an uneven grained silica mosaic, with some patches of intergrown relict carbonate. Silica grains are locally bladed or radiating, and there are some grains up to 500 μm across.

Banded chert

In thin section a typical sample (R004817, Blackwater Rivulet; Plate 57) of banded black chert also has a very uneven-grained patchy texture. Irregular patches (<50 μm to >1 mm) and larger elongate lenses of clear, cryptocrystalline to finely microcrystalline chert reside in a black carbonaceous cherty matrix, and are enveloped by thin wavy anastomosing carbonaceous laminae. There are also thicker (up to 1 mm) almost opaque carbonaceous bands. Rare grains of monocrystalline quartz and minute traces of detrital mica suggest a possible pelitic component to the protolith.

Other samples (R005036, R005088) are slightly less carbonaceous. The former (Plate 58) contains bands (up to 3 mm thick) of clear massive microcrystalline chert, as well as anastomosing carbonaceous and pseudoclastic chert bands.

Chitinozoan-like microfossils are visible in the less silicified parts of these samples.

Other specimens (sample R004812, R006685, R006668) are bone white, cream, grey to black, sometimes brown-weathering cherts with a generally slightly wavy, diffuse thin bedding lamination defined by anastomosing black bands, diffuse streaks and irregular blotches.

In thin section sample R004812 (Blackwater 1 road) consists of uneven-grained, microcrystalline to cryptocrystalline (<2 μm to 40 μm) clear silica, with a diffuse wavy lamination defined mainly by grain size variations. It is transected by dilational quartz veinlets.

Sample R006685, from a tributary of the Lindsay River, is similar apart from a few finer grained possible clasts, containing ovoid patches (500 μm–1 mm) of darker cryptocrystalline silica. This may be a relict peloidal fabric (Plate 59).

Sample R006668 (Leigh River) is a similar diffusely banded chert. In some brownish bands, chert is intergrown with finely sparry relict carbonate and oxidised opaque grains. There are also a few opaque stylolitic veinlets.

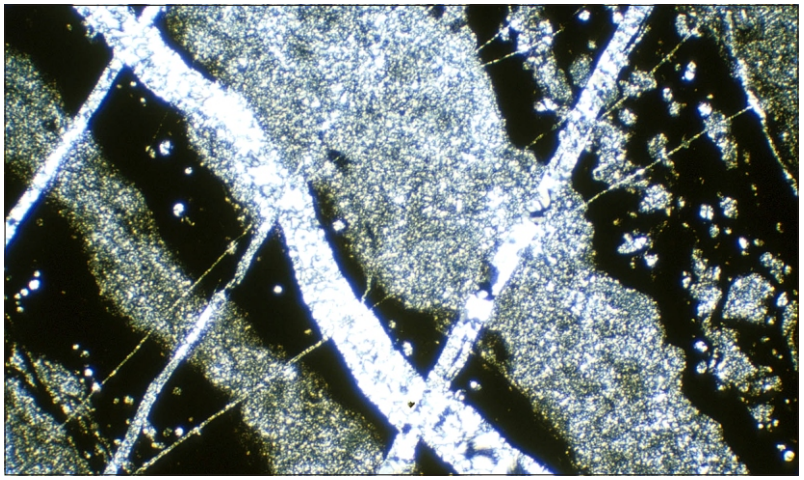

Plate 58

Photomicrograph of banded chert (unit Pssc) from Black River Dolomite, sample R005036 (Arthur River, 339 380 mE, 5 445 870 mN). Anastomising bands of clear massive microcrystalline and dark carbonaceous chert, cut by thin quartz veinlets. Crossed nicols, field of view 4.4 2.9 mm.

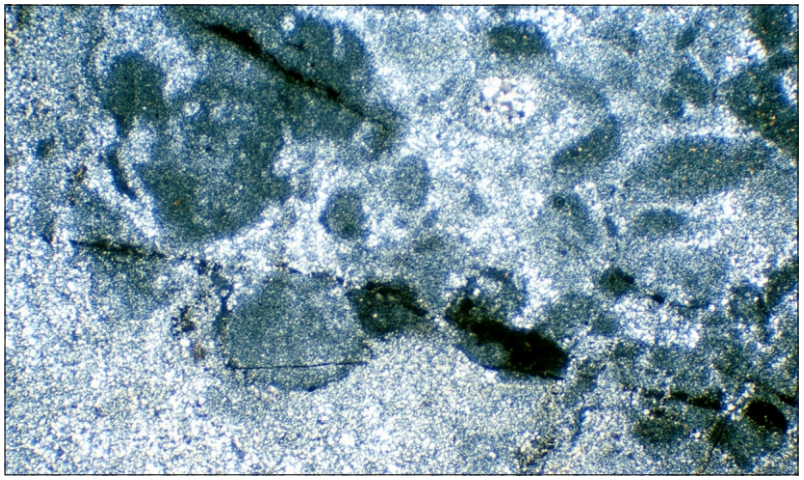

Plate 59

Photomicrograph of chert (unit Pssc) from Black River Dolomite, sample R006685 (331 430 mE, 5 430 320 mN). Possible relict peloidal fabric, now dark cryptocrystalline silica. Plane polarised light, field of view 4.4 2.9mm.

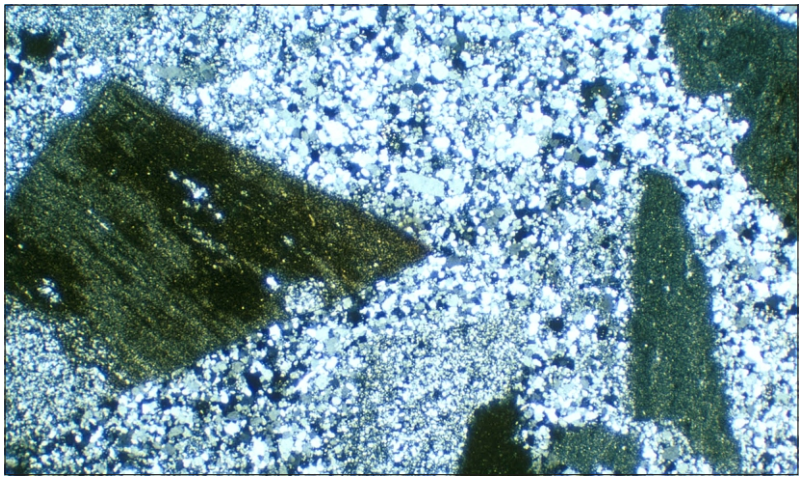

Plate 60

Photomicrograph of chert conglomerate (unit Pssc) from Black River Dolomite, sample R006769 (330 660 mE, 5 435 580 mN). Angular clasts of fine-grained chert (some banded) in a coarser-grained matrix. Crossed nicols, field of view 4.4 2.9 mm.

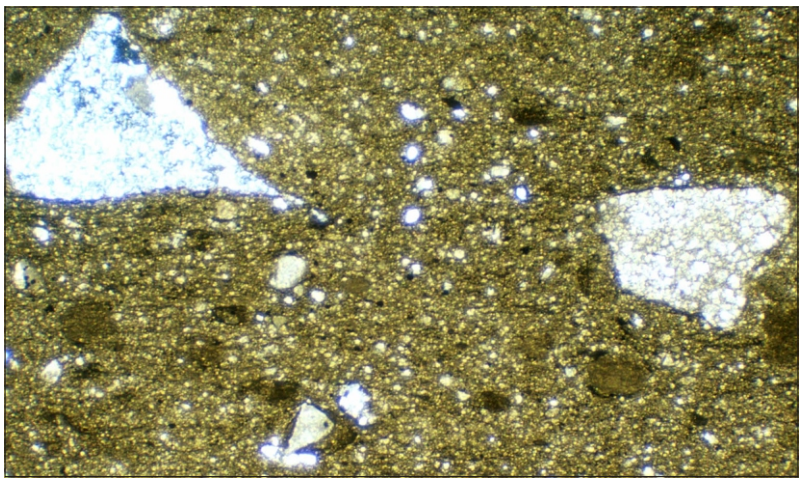

Plate 61

Photomicrograph of diamictite from Julius River Member (unit Pssr), sample R005128 (Julius River, 333 030 mE, 5 439 450 mN). The large clasts are polycrystalline chert (upper left) and sparry dolomite (right). Crossed nicols, field of view 4.4 2.9 mm.

Ferruginous chert

Two small isolated corroded outcrops of massive to diffusely laminated, dense, extremely tough orange-red ferruginous chert were noted on a minor tributary of the Lindsay River near the southern margin of the Dempster map sheet (329750/5430380, 331750/5430020). In thin section a sample (R006771) from the former locality consists mainly of a fine-grained (≤20 μm) orange-red goethite (confirmed by XRD), grading into diffuse, irregular patches of colourless, very fine to medium-grained (≤50 μm) chert. A sample (R006772) from the second locality is similar but paler and less ferruginous.

Sample R006696, from north of the Horton River (330160/5434500), is a mesoscopically similar rock. In thin section it consists mainly of diffuse ovoid patches (mostly 500 μm–1 mm long) of microcrystalline to cryptocrystalline clear chert, enveloped by a pervasive orange-brown anastomosing lamination. Equant angular grains, up to 150 μm across, of deep orange-red hematite are scattered throughout the rock, especially at the centres of the clearer patches, which may therefore be domains from which ferruginous material has been removed and re-aggregated.

These rocks all occur within tracts mapped as Black River Dolomite, and are probably derived from it by extreme silicification and lateritisation.

Chert conglomerate

Sample R006769 (Plate 60) (330660/5435580) consists of angular clasts, up to 10 mm across, of finely microcrystalline to cryptocrystalline chert, in an uneven grained but generally more coarsely microcrystalline mosaic (20–100 μm) of quartz, probably very fine-grained quartzarenite. Some of the clasts have sharp margins for part of their perimeter, and in other parts grade into the matrix. A few are very pale brown (possibly due to submicroscopic carbonaceous material) and weakly banded.

Sample R004820 (324310/5435190) is similar, but the matrix is coarser (typically 100–200 μm). This locality has been mapped within the Forest Conglomerate and Quartzite by D. B. Seymour (see discussion above), and sample R006769, which lies near the centre large tract of Black River Dolomite occupying a domal structure, could alternatively also be assigned to that formation.

Julius River Member

About twenty samples were examined in thin section. As many samples are essentially similar, a selected sample considered representative of the unit is described in detail. Comparative comments are made on some other noteworthy samples.

A typical sample (R005128, Plate 61) from the Julius River (333030/5439450) is a very poorly sorted and unbedded matrix-supported dolomitic diamictite. Clasts are mostly subangular, equi-dimensional and irregular to crudely elongate, and up to 10 mm but mostly less than 2 mm across. There is some tendency for the long axes of the more elongate clasts to be aligned, possibly but not necessarily representing bedding. The proportion of clasts is difficult to estimate as they grade in size down to the matrix, but is probably no more than 15% in this sample.

The dominant clast lithology is coarsely (50 μm) to finely sparry or micritic dolomite. The micritic clasts tend to be better rounded and are more diffusely defined with respect to the matrix. Subordinate clast types include diamictite (one clast comprising sparse grains of mostly sparry carbonate in a micritic matrix) and microcrystalline chert; the latter may be partly replaced by (or replacing?) coarsely sparry carbonate. Scattered small subangular grains of detrital quartz are volumetrically insignificant. The section has also intersected part of a small quartzite clast.

The matrix is a darker brownish-grey fine-grained sparry impure dolomite. Impurities have been apparently largely segregated into a weakly developed anastomosing stylolitic cleavage, subparallel to the foliation defined by long axes of the more elongate clasts. There is also a sparse but pervasive dissemination of subspherical to ellipsoidal opaque blebs (mostly <5 μm to 20 μm) and scattered larger (to 500 μm), irregular to lenticular opaque aggregates.

Other samples

All samples consist essentially of angular to subangular clasts of dominantly carbonate and subordinate chert, in a finely sparry to micritic, grey to pale yellow-brown weathering impure carbonate matrix. There is considerable variation in clast size and abundance and matrix texture. Some samples have very sparse clasts (5% or less) (R005127, R006674, R006676; see sample list for locations) and/or very small (1 mm or less) clasts (R006674, R005064), and grade into typical Black River Dolomite. Others (R006680, R004843) have very abundant (approximately 30–40%) clasts, although because of the very poor sorting it is not always possible to clearly distinguish clasts and matrix. All are open framework and matrix supported, with usually no suggestion of bedding.

The dolomite clasts are usually composed of coarse to fine-grained spar, and less commonly dolomicrite; the latter clasts are commonly smaller and slightly less angular. In sample R004841, several clasts have a diffuse stromatolitic banding, defined by laminae (100–200 μm thick) of alternately sparry and micritic carbonate. Sample R005080 (Plate 62) contains several clasts of thinly planar laminated dolomicrite, the long axes of which are subparallel to internal bedding within each clast, and define a crude probable bedding in the diamictite. Sample R005113 also contains similar, but unorientated, clasts of fine-grained laminated dolomite, in a dark, partly carbonaceous matrix. A dolomite clast in sample R006680 contains micritic intraclasts fringed by isopachous cement layers (Plate 63). Partial replacement of dolomite clasts by chert, pre-dating their incorporation into the diamictite, is occasionally evident.

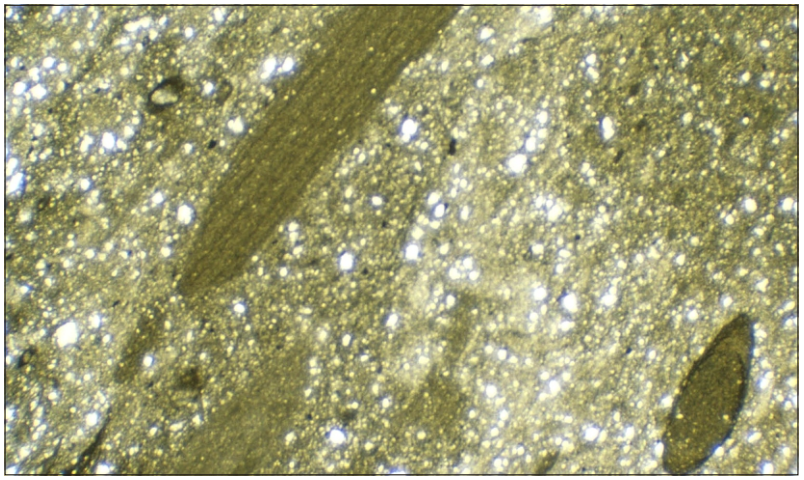

Plate 62

Photomicrograph of diamictite from Julius River Member (unit Pssr), sample R005080 (Arthur River, 322 680 mE, 5 446 000 mN). Note elongate clasts of thinly planar laminated dolomicrite. Plane polarised light, field of view 4.4 2.9 mm.

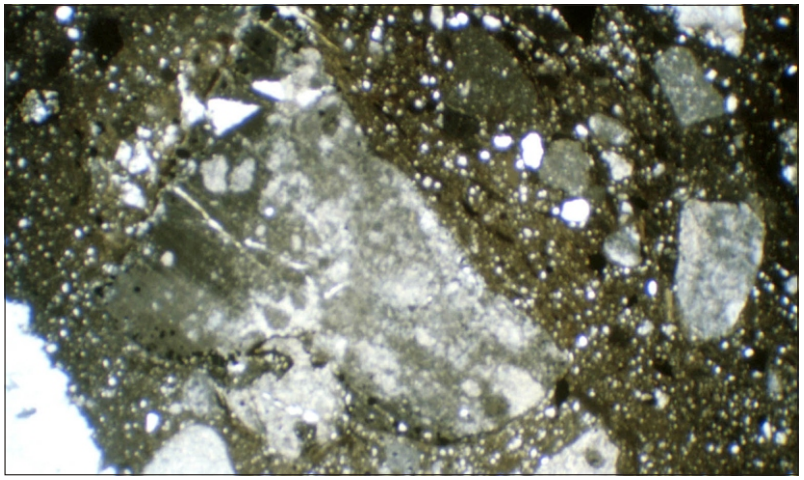

Plate 63

Photomicrograph of diamictite from Julius River Member (unit Pssr), sample R006680 (330 090 mE, 5 430 220 mN), showing dolomite clast with micritic intraclasts. Field of view 11.0 7.3 mm.

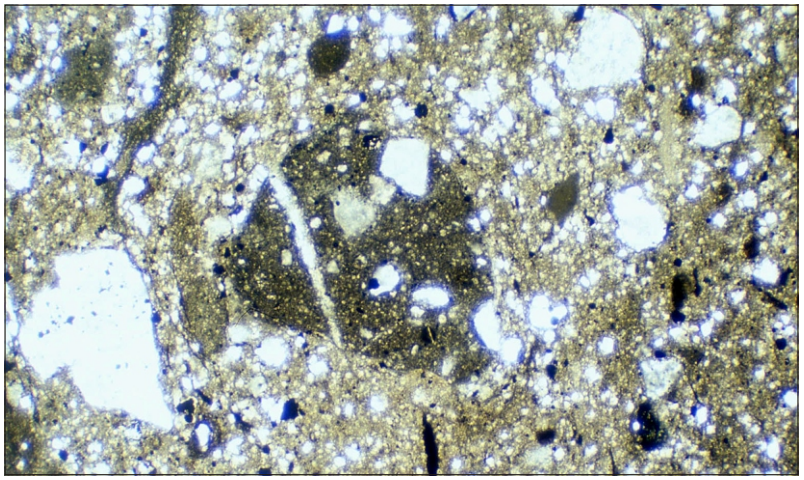

Plate 64

Photomicrograph of diamictite from Julius River Member (unit Pssr), also from sample R006680 (330 090 mE, 5 430 220 mN). Note cannibalistic clast of diamictite (centre), clast of dolosparite (left, pale) and small elongate clasts of carbonaceous shale (bottom). Field of view 11.0 7.3 mm.

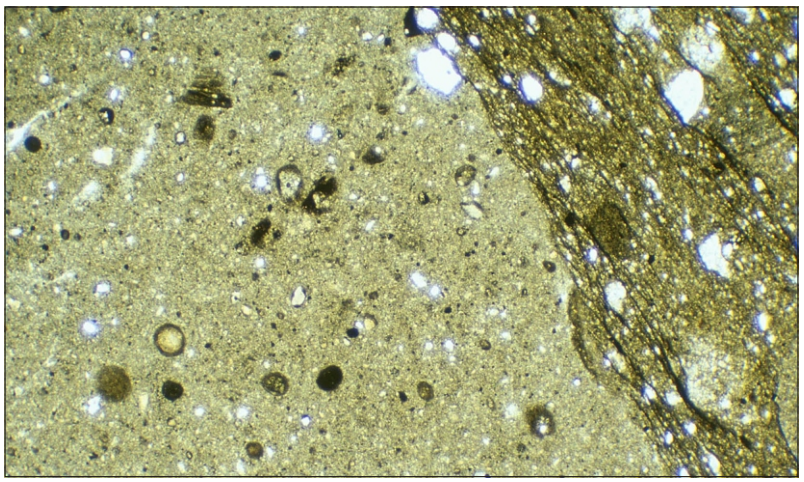

Plate 65

Photomicrograph of diamictite from Julius River Member (unit Pssr), sample R005125 (Julius River, 334 110 mE, 5 441 280 mN). Part of a large cannibalistic clast of wackestone diamictite contains spherical coated grains and simple ooids; matrix at right. Plane polarised light, field of view 4.4 2.9 mm.

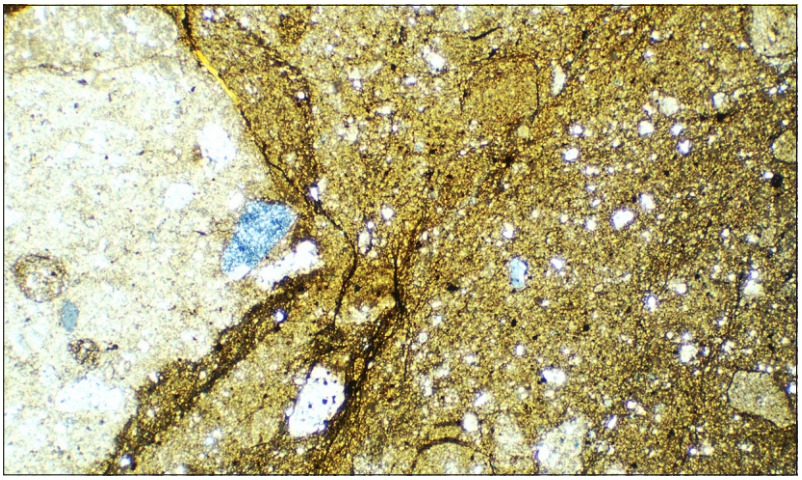

Plate 66

Photomicrograph of diamictite from Julius River Member (unit Pssr), sample R005042 (Arthur River, 335 860 mE, 5 445 530 mN). Cannibalistic clast of diamictite at left; note locally developed anastomising ferruginous stylolites in matrix. Plane polarised light, field of view 4.4 2.9 mm.

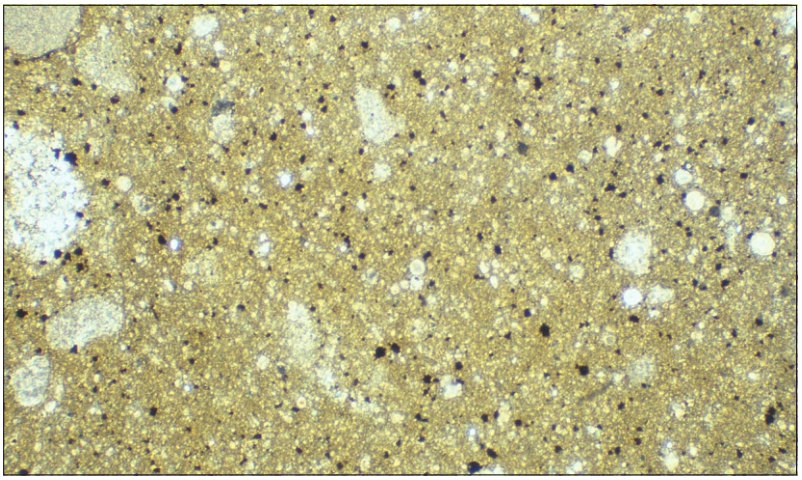

Plate 67

Photomicrograph of diamictite from Julius River Member (unit Pssr), sample R005129. Note possible ooids in matrix and marginal replacement of chert clast (at right) by carbonate. Plane polarised light, field of view 4.4 2.9 mm.

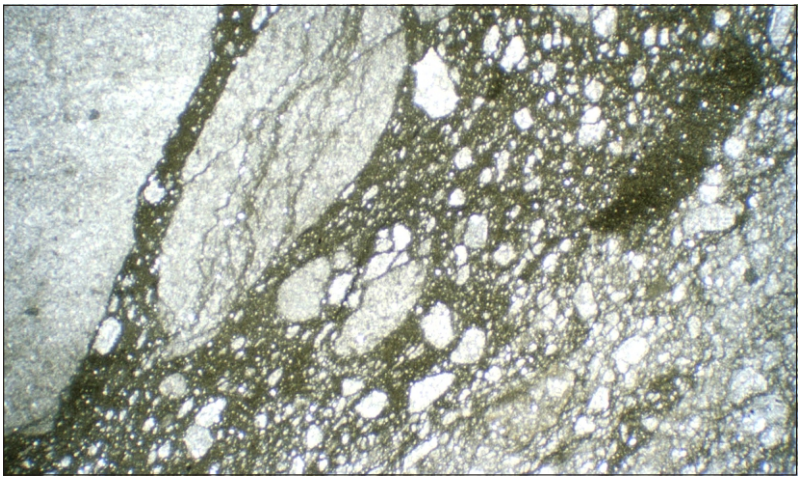

Plate 68

Photomicrograph of strongly stylolitised diamictite from Julius River Member (unit Pssr), sample R004839 (323 020 mE, 5 445 580 mN). Field of view 11.0 7.3 mm.

Some samples (R006680, Plate 64; R005125, Plate 65; R006664; R005042, Plate 66; R005080) contain clasts of dolomitic diamictite, similar to but generally with a finer grained matrix than the host, suggesting some 'cannibalistic' sedimentation.

Chert clasts are usually highly angular, and may show marginal replacement by carbonate, post-dating their incorporation into diamictite (R005104; R005129, Plate 67; R004841; R006679; R005043).

Sporadic to rare clast types include quartzite with sutured grain boundaries and undulose extinction (R005128, R005130, R006675) and carbonaceous mudstone or shale (R005125; R006680, Plate 64). These, together with rare but ubiquitous small quartz anhedra, could have been derived from the Rocky Cape Group.

Rare basalt or dolerite (R005125, R005130, R006680) clasts are identified by their relict igneous texture; they now consist of albite (?), colourless chlorite or clay minerals and iron oxides, and are partly replaced by carbonate.

Sample R005064, with only sparse and relatively small clasts, contains numerous well rounded, subspherical to ellipsoidal coated grains (20–200 μm long). These have a thin, darker, fine-grained rim or coating, composed of material resembling that of the anastomosing stylolitic cleavage. Some coated grains have developed around a nucleus grain of carbonate

spar, but most consist of dark fine-grained dolomicrite. Similar coated grains are also present in sample R005125, both in its matrix and in large (up to 10 mm or more) clasts of wackestone diamictite within it; the latter also contain simple ooids. Rare coated grains also occur in sample R005080.

Possible ooids occur in the matrix of sample R005129 (Plate 67). These are small (mostly 40–70 μm across) rounded monocrystalline carbonate grains, with 'hollow' micritic cores surrounded by a mantle with some suggestion of a radially fibrous texture.

The matrix of sample R005043 has many well-rounded grains with a brown core and clear rim. They are not ooids and this may be a secondary fabric.

The opaque impurities are rather variable in grain size and abundance; in some samples (R005043, R004841, R004843) they are sub-cubic to euhedral and are probably largely pyrite.

The anastomosing stylolitic cleavage is very weak in some samples (R005130, R004841, R005043, R006664) and well developed in others (R005113, R005125, R005126, R004839, R005080, R006670A). It is defined by segregated impurities, probably including clay minerals, iron oxides and carbonaceous material. In sample R005126, stylolitic veinlets have overprinted a thoroughly recrystallised sparry (50 μm) carbonate, although there is some suggestion of an original diamictite texture. In this and some other strongly stylolitised samples (R004839, Plate 68; R005124, R005129), it is locally difficult to distinguish primary diamictite textures from pseudobreccia textures. Ferruginous stylolitic veinlets may outline clasts, by passing around rather than through them (samples R005126, R005118, R005129, R005041, R005043, R006679).

APPENDIX 2

Detailed petrographic descriptions of the Keppel Creek Formation

J. L. Everard, M. P. McClenaghan

Coarse-grained lithicwacke sandstone

A specimen (R005056) from the central tract, exposed in the Arthur River, is a diffusely laminated, cleaved, grey to olive-green lithicwacke. In thin section (Plate 69) it is seen to be very polymict and extremely poorly sorted, with lithic clasts and crystals ranging from 5 mm down to granules in the yellow-green chloritic matrix. Common clast and grain types include basalt (in varying stages of alteration but commonly fine grained and plagioclase rich), microcrystalline chert, usually brown-weathered sedimentary rocks including mudstone and finer-grained lithicwacke, relatively well-rounded hematite grains, monocrystalline and polycrystalline quartz grains, rare quartz-mica schist and rare grains of chromite. Many of the clasts of sedimentary rocks are better rounded, ellipsoidal to elongate, and tend to be aligned parallel to bedding.

Another specimen (R005071) of coarse-grained lithicwacke, from the western tract exposed in the Arthur River below Hawkes Creek, is a massive, dark maroon rock with a hackly fracture. In thin section it is seen to be poorly sorted, but less so than R005056 and less polymict. The angular lithic clasts are typically 500 μm to 1 mm long, with some up to 7 mm. The dominant clast type is basalt, but there is a wide range of grain size, mineralogy and alteration. Most basalt clasts are fairly fine grained and very plagioclase rich, with a low proportion of ferromagnesian minerals. Some are nearly free of opaque phases, whilst in others the opaques are densely disseminated. Some basalt clasts contain chlorite-filled amygdales. Many have a pale pinkish-brown oxidation staining. Also present are ellipsoidal subrounded clasts of hematite(?), occasional subhedral grains of dark red-brown chlorite, rare crystals of fresh pyroxene, and rare mostly monocrystalline (volcanic?) quartz. The matrix of the lithicwacke consists of chlorite, secondary well-crystallised albite, and minor epidote and carbonate.

Coarse-grained lithic arenite

A massive greyish-blue-green rock (sample R005069) from the western tract in the Arthur River (322900/5424300) resembles the lithicwackes in hand specimen, but in thin section (Plate 70) it is seen to be very well sorted. It is clast supported with very well-rounded, subspherical to ellipsoidal lithic grains, nearly all between 500 μm and 1.5 mm across, in a fine-grained quartzofeldspathic matrix with abundant, probably secondary, carbonate. The alignment of long axes of the grains defines a bedding foliation. The dominant lithic grain lithology is fine to very fine-grained plagioclase-rich basalt. No primary ferromagnesian minerals remain except variably abundant, very sparse to densely disseminated opaque grains. Partial alteration to carbonate is very common. Some grains may be more felsic than basalt, but because of the fine grain size and alteration this is difficult to confirm. Also present are occasional to rare clasts of orthoquartzite, well-sorted quartz sandstone, quartz, sparry carbonate (dolomite?), possibly very fine-grained mudstone, and red-brown chromite. All are similar in grain size and roundness to the basalt clasts.

A somewhat similar sample (R006701) was collected from the eastern bank of the Lindsay River at 330580/5428610, from a small fault-bounded outlier on the Balfour map sheet. This sample is from a 500 mm bed of greenish lithic sandstone, ranging to granule conglomerate, interbedded with tough maroon, very fractured and probably tectonised siltstone. In thin section it consists mainly of tightly packed, generally well rounded but usually ellipsoidal to elongate grains (mostly 500 μm–1.5 mm long) of basalt, apparently flattened parallel to bedding. The basalt grains are very variable in grain size, texture and alteration, but are mostly fine grained, feldspathic and turbid; some are hematite altered and almost opaque. Occasional grains of felsic volcanic rocks, and rare small (150 μm) subangular grains of chromite, are also present. The mostly interstitial matrix consists mainly of basalt-derived feldspathic material (although coarser grained than in the clasts themselves). Chlorite and epidote are common metamorphic minerals, both in clasts and matrix. Quartzose material, primary carbonate and clastic sedimentary rock clasts are conspicuously absent. The rock differs from R005069 in being less well sorted and in its less varied provenance.

Medium to fine-grained lithicwacke sandstone

A typical, relatively fresh sample (R005055) from the Arthur River (326160/5447850) is a hard, faintly planar laminated, medium-dark grey to olive-grey rock with an angular fracture. In thin section it is seen to be a polymict wacke consisting of angular grains of quartz (50–200 μm) frequently with undulose extinction, turbid feldspar, pale yellow fine-grained chlorite, both fine-grained and sparry carbonate and oxidised opaque grains. A crude bedding fabric is defined by the preferred orientation of the long axes of clasts. A mixed provenance from the Rocky Cape Group siliciclastic

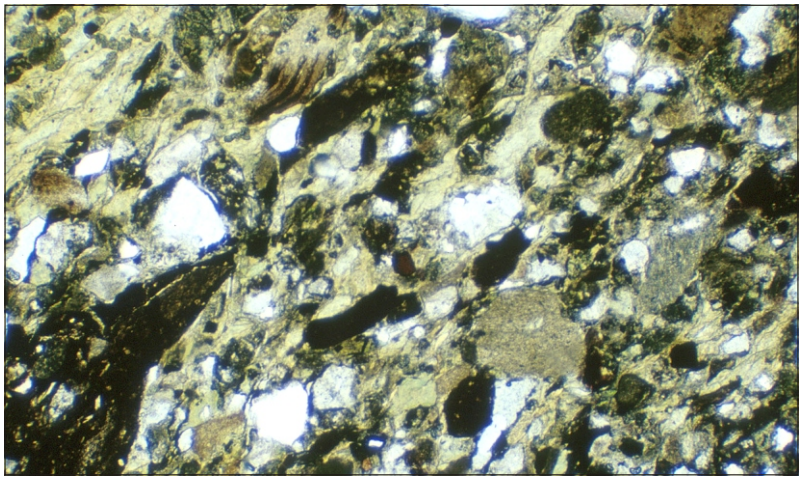

Plate 69

Photomicrograph of coarse-grained lithicwacke sandstone, Keppel Creek Formation (unit Psvw), sample R005056 (Arthur River, 325 680 mE, 5 447 030 mN). Note poor sorting and polymict composition. Plane polarised light, field of view 4.4 2.9 mm.

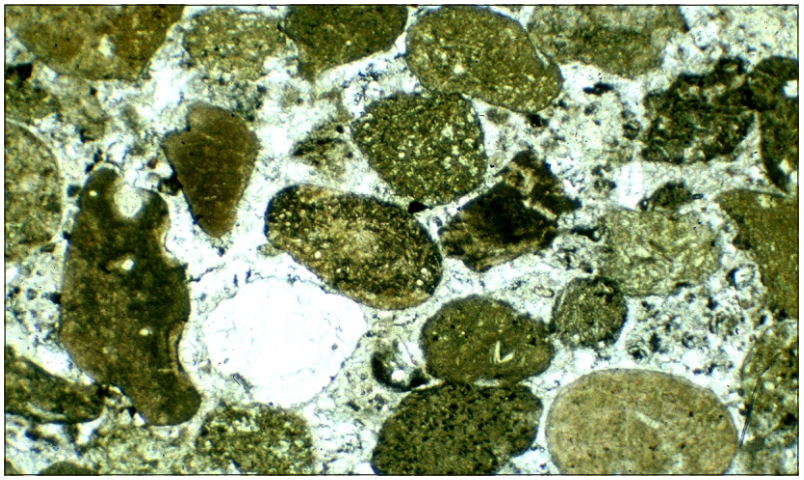

Plate 70

Photomicrograph of coarse-grained lithic arenite, Keppel Creek Formation (unit Psvw), sample R005069 (Arthur River, 322 920 mE, 5 446 300 mN). Note well-sorted and mostly well-rounded clasts, mainly of fine-grained leucocratic basalt, but also of orthoquartzite (lower left). Plane polarised light, field of view 4.4 2.9 mm.

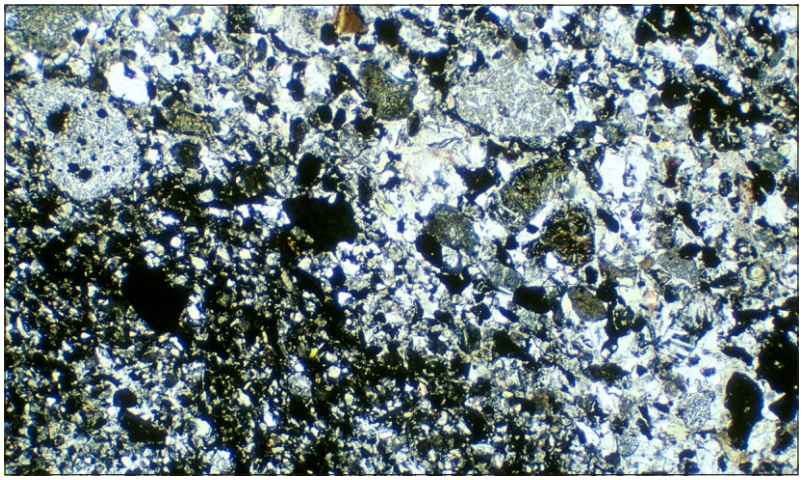

Plate 71

Photomicrograph of sample R004868 (upper Keppel Creek, 331 800 mE, 5 440 040 mN), Keppel Creek Formation (unit Psvwi). Hematitic medium to fine-grained lithicwacke sandstone. Note well rounded clasts of leucocratic basalt. Plane polarised light, field of view 4.4 2.9 mm.

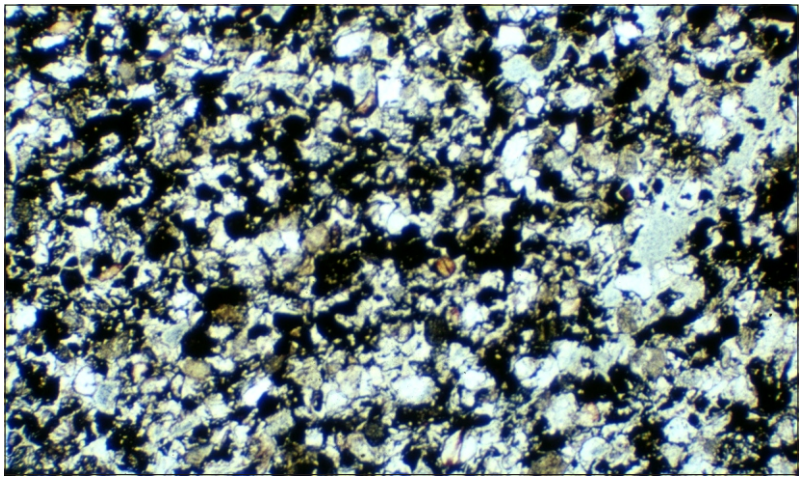

Plate 72

Photomicrograph of sample R004856 (Stephens Rivulet tributary, 328 520 mE, 5 442 480 mN), Keppel Creek Formation (unit Psvw). Hematitic fine-grained lithic arenite, consisting of basalt-derived clasts and grains, minor detrital quartz, and hematite. Plane polarised light, field of view 4.4 2.9 mm.

rocks, Black River Dolomite and basaltic volcanic rocks is evident.

Sample R006700 from 327320/5432940, 15 km to the south on the Dempster map sheet, is from near the top of the formation, just below the contact with the Smithton Dolomite. It is similar to R005055, but slightly fresher and finer grained. Grain types include abundant angular quartz (up to 150 μm), usually turbid but sometimes clear and multiply-twinned feldspar (plagioclase), pale green chlorite, abundant opaque grains, brown impure fine-grained carbonate and rare chromite. Bedding is defined by both clast long axis orientation and compositional banding (e.g. some bands are richer in opaque grains).

Other samples are maroon in colour and distinctly hematitic in thin section. Perhaps the freshest is R004868 (Plate 71), collected from upper Keppel Creek (331800/5440040) and stratigraphically just below the contact with the Spinks Creek Volcanics. This rock displays diffuse planar lamination defined by compositional banding, but is very poorly sorted. A few moderately well rounded but irregularly shaped clasts up to 3 mm across of fairly fresh basalt, usually but not always relatively leucocratic (feldspathic), are present. Other grain types include opaque grains, hematite, fresh clinopyroxene, both fresh plagioclase and turbid indeterminate feldspar fragments, pale yellow-green chlorite and rare chromite. There is no well-defined matrix, but the colourless low birefringence intergranular material is probably mainly chlorite and/or clay minerals. Detrital quartz and carbonate are absent and the provenance seems wholly basaltic.

Sample R004866, from a minor tributary of Stephens Rivulet (328570/5442870), is a massive to faintly and diffusely laminated, maroon (greyish-red to purple) rock with an uneven to subconchoidal fracture. In thin section it lacks the compositional banding of R004868, and has a better developed hematitic matrix. The mostly highly angular grains (up to 200 μm across) include clear plagioclase, fine-grained colourless to rarely blue-green chlorite, abundant hematite, rare chromite and some detrital quartz. Sample R004855, from the same general area (327930/5443170), is a similar, slightly coarser-grained and more weathered rock.

Fine-grained hematitic lithic arenite

Sample R006689, from the lower Leigh River (331510/5427740) on the Balfour map sheet, is better sorted than most samples from the Keppel Creek Formation. In the field it is a hard, tough, massive, grey-green to maroon-weathering rock with closely spaced jointing, difficult to distinguish from the basalt with which it is closely associated. In thin section it is seen to be a polymict lithic arenite, with angular to well-rounded grains and clasts mostly in the 100–200 μm size range but up to 300 μm, and little matrix. There is little compositional banding, and bedding is mostly defined by alignment of the long axes of the more elongate grains and clasts. Most lithic clasts are of fine-grained leucocratic basalt, internally consisting of turbid feldspar, fine-grained chlorite and occasional clinopyroxene. Other grain types include dark deep reddish to almost black hematite, pale green chlorite, less abundant clear plagioclase, and rare fresh clinopyroxene, rare subangular chromite and traces of epidote. Quartz is absent. Thin rims of deep red-brown hematite form outlines around many other grains. Its provenance is apparently wholly basaltic.

Sample R004856 (Plate 72), collected from a tributary of Stephens Rivulet about 25 km further north, is another relatively well-sorted, maroon, hematitic lithic arenite, similar to R006689. It differs mainly in being less well laminated and in containing some detrital quartz.

Fine-grained quartz arenite(?)

Sample R006688, from the lower Lindsay River area in the south of the Dempster map sheet (328940/5430420), is highly atypical of the formation. In hand specimen it is a tough, massive, medium grey-green fine-grained sandstone, resembling some Rocky Cape Group lithologies, with a friable dark red-brown weathering rind. It contains abundant disseminated pyrite, the grains of which weather out to leave small voids. In thin section it consists of an even-grained mosaic of irregularly-shaped but annealed anhedral quartz grains (mostly 100–200 μm, rarely 1 mm across; about 70%), ragged grains of clear pale green chlorite (typically 50–150 μm; about 30%) and minor (1%) equant irregular opaque grains, including deep red hematite as well as probable pyrite. Traces of zircon are also present, supporting a clastic origin for the rock, but some hydrothermal influence seems likely in view of the annealed quartz, clear chlorite and disseminated pyrite.

Very fine-grained lithicwacke sandstone

The freshest sample (R004864), from a tributary of Blackwater Rivulet (327100/5439840), is a tough grey-green rock with occasional faint but definite bedding, otherwise resembling basalt. In thin section (Plate 73) it is seen to consist of poorly-sorted, close-packed, angular anhedral grains of fresh pyroxene (mostly ≤75 μm), very turbid feldspar, chlorite and rare chromite, together with scattered small, irregularly shaped clasts of basalt. There are also sporadic ellipsoidal to strongly flattened, spindle-shaped clasts (500 μm–1 mm across) of very fine-grained, unresolvable golden-brown material. Some of these have a banded to vaguely concentric texture; they may be spherules of basaltic glass (Pele's tears). The possible spherules are orientated obliquely to a faint diffuse banding, which itself is parallel to a few minor prehnite veinlets and may be a secondary feature. In any case the rock lacks quartz or carbonate and is of wholly basaltic provenance.

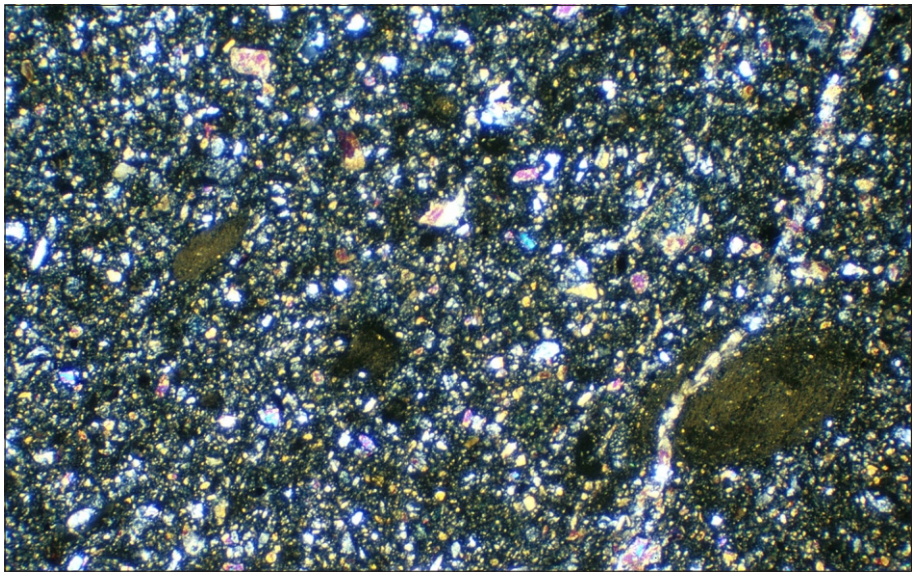

Plate 73

Photomicrograph of sample R004864 (327 100 mE, 5 439 840 mN), Keppel Creek Formation (unit Psvw). Very fine-grained lithicwacke sandstone with much fresh detrital pyroxene, and possible Peles beads (lower right). Plane polarised light, field of view 4.4 2.9 mm.

Less fresh, but mineralogically and texturally more typical samples, commonly contain detrital quartz. Sample R004845, from the start of Blackwater 5-1-1 road (325730/5442120), contains fairly abundant, equi-dimensional but angular grains of quartz (50–100 μm) and subrounded opaque grains (40–80 μm) partly altered to sphene, together with more sparsely distributed grains of very turbid feldspar and subangular chromite, in a chloritic matrix. There are also rare shreds (up to 100 μm) of altered but still pleochroic (yellow-brown to pale yellow-brown) biotite. The matrix comprises 60–70% of the rock, but itself appears to be an aggregate of altered ferromagnesian grains, replaced by pale yellow-green chlorite.

Sample R004858, from a minor creek just south of the Arthur River (325840/5446770), is similar but finer grained and more weathered than R004845. Numerous cross-cutting veinlets of early actinolite (fibrous, perpendicular to veinlet axes) and later carbonate (in veinlet axes or later cross-cutting veinlets) are present.

Samples R004860 and R004859 (Stephens Rivulet tributary, 327390/5441510, 327230/5441050) are well laminated but weathered rocks with angular grains (mostly ≤150 μm) of identifiable quartz, hematite and rare chromite; many other grains are altered to fine-grained colourless clay minerals.

Sample R006707 (Frankland River tributary at 326780/5431570) is a slightly weathered, poorly laminated, very fine-grained lithicwacke sandstone, grading to coarse-grained lithicwacke siltstone. The main grain types are fine-grained chlorite, feldspar and altered opaque grains. Minor detrital quartz is present but the provenance is mainly basaltic.

Sample R006690 (lower Leigh River, 331490/5427700) is similar, with a faint diffuse bedding lamination, defined mainly by grain alignment. Quartz is a more abundant grain type and impure carbonate is also present. There is a weak hematitic alteration.

Several maroon-coloured hematitic samples were collected from either stratigraphically just below the basalt of the Spinks Creek Volcanics (R005131, lower Horton River, 332500/5431660; R004863, 326900/5440390), intercalated within the basalt (R006692, 330190/5433310), or from roughly the same horizon as the basalt (R004861, 325990/5441130). The latter sample contains abundant but small (≤100 μm), equant but angular quartz grains and more elongate chlorite grains, aligned to define a foliation, in a deep red hematite-impregnated matrix. Small clasts of hematite are discernible in thin section. Samples R005131, R004861 and R006692 are similar but have better developed lamination, defined by both compositional and grain-size variations between laminae. Sample R006692 contains rare fresh pyroxene and lacks detrital quartz.

Sample R006699, from 3.7 km northeast of Balfour (327100/5432880), is a medium dull bluish-grey, hard but brittle rock with a faint planar bedding lamination and a subconchoidal fracture. In thin section it is poorly sorted, with no well-defined matrix. Grains are mostly ≤100 μm across and include dominant feldspar and subordinate quartz, colourless chlorite, opaques, fine-grained to sparry carbonate and rare chromite. It resembles R006707 from the same general area, except for the presence of carbonate. The stratigraphic position of the sample, at the top of the formation, and the presence of carbonate may indicate a transition to the overlying Smithton Dolomite, which crops out 20 m downstream in the same small creek.

Coarse to medium-grained lithicwacke siltstone

A sample (R004867) from upper Keppel Creek (331900/5440210), not far below the contact with the basalt of the Spinks Creek Volcanics, is a dark to olive-grey siltstone with a well-developed planar lamination, including some pyritic laminae. In thin section (Plate 74), thinner (500 μm), darker, finer grained, slightly anastomosing, carbonaceous laminae alternate with thicker (≤10 mm), paler, coarser-grained laminae consisting of poorly-sorted angular

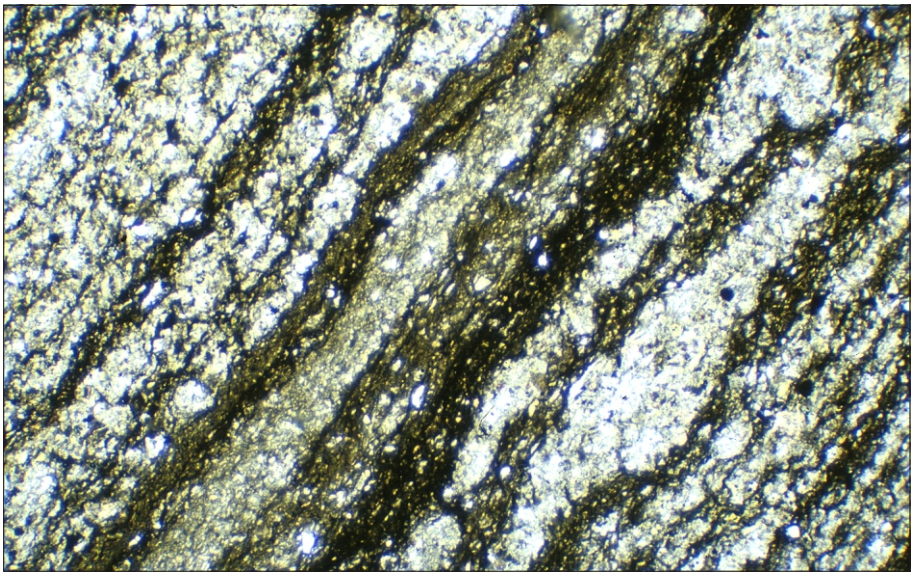

Plate 74

Photomicrograph of sample R004867 (upper Keppel Creek, 331 900 mE, 5 440 210 mN), Keppel Creek Formation (unit Psvw). Medium to fine-grained lithicwacke siltstone. Note thick laminae of mainly detrital pyroxene and plagioclase (pale), alternating with thinner anastomising finer-grained carbonaceous laminae (dark). Plane polarised light, field of view 4.4 2.9 mm.

plagioclase and pyroxene fragments (up to 200 μm, but mostly <50 μm). These grade down to an indeterminate but probably feldspathic matrix. Scattered opaque grains, minor pale yellow chlorite and rare chromite are also present. Quartz is absent. The rock is an unusually fresh basaltic wacke.

Sample R005568, from a similar stratigraphic position on the Horton River eight kilometres to the south (331030/5432590), is a similar well-laminated basaltic wacke with abundant fresh pyroxene. It differs mainly in also containing irregular patches of fine-grained carbonate, which are probably of secondary rather than detrital origin.

Sample R005575, also from the Horton River (330540/5432000) and closely associated with basalt, is finer grained and nearly massive, but is similar in containing abundant angular fragments of fresh pyroxene and plagioclase, in an indeterminate, mostly low birefringence matrix with some secondary carbonate.

Sample R006691, from a tributary of the Horton River (330180/5433300), is a hard, tough, medium khaki-green, pale orange-brown weathering coarse-grained lithicwacke siltstone with a thin wavy bedding lamination. In thin section it is seen to largely consist of epidote and chlorite, with opaque grains largely altered to fuzzy sphene and hematite. The lamination is defined both by grain size and composition, as the coarser-grained laminae tend to be more epidote rich. The outcrop is closely associated with, and probably intercalated within, basalt, and the provenance seems wholly basaltic.

Sample R005572 (330970/5432270) from the same general area, but stratigraphically further below the basalt, contains abundant angular to irregular grains of fine-grained to coarse and sparry carbonate. Most are <50 μm across, but others are 250 μm or more, and clearly detrital. The likely source is the underlying Black River Dolomite; this is supported by the presence of occasional polycrystalline grains of unstrained quartz, probably chert. Occasional plagioclase grains, rare small basalt fragments and rare small chromite grains indicate that volcanism had already commenced somewhere within the basin when this rock was deposited. These grain and clast types grade down to a colourless, very fine-grained indeterminate matrix with low birefringence.

Sample R005563 (333150/5432320) is similar to other samples from the Horton River. It is a poorly sorted, rather weathered pale grey-green coarse-grained lithicwacke siltstone containing angular grains of feldspar, oxidised opaque grains, rare detrital quartz and splintery fragments of white mica in a diffusely laminated chloritic matrix. In a dark maroon cuboidal weathering variant (R005564), collected from a few metres away, the matrix is impregnated with reddish-purple hematite and minor fresh clinopyroxene is present.

Sample R005584 from the lower Lindsay River (328280/5430730), stratigraphically not far above the Black River Dolomite, is an atypical lithology, shaly black carbonaceous siltstone. In thin section the rock is poorly sorted, with former angular grains, up to 100 μm but more commonly 10–50 μm across, largely altered to clay or left as voids. A little very fine-grained detrital white mica is present. The diffusely laminated matrix is black to very dark brown. There is no indication of any basaltic or carbonate component.

Sample R006702 is another atypical rock from the lower Lindsay River area (329820/5430040). It is a thinly banded dark grey pyritic rock with ferruginous crusts, consisting mainly of finely granular opaque grains with interstitial fine-grained colourless chlorite.

Two samples from the Blackwater Rivulet area (R004852, 325080/5444360; R004854, 324740/5444590), on the western limb of the Smithton Synclinorium and both stratigraphically above the thin basalt unit, are hard, tough, massive to diffusely laminated pale yellowish-green to grey-green coarse-grained lithicwacke siltstones. In thin section both contain abundant small grains of quartz and plagioclase (generally ≤75 μm) and smaller opaque grains partly

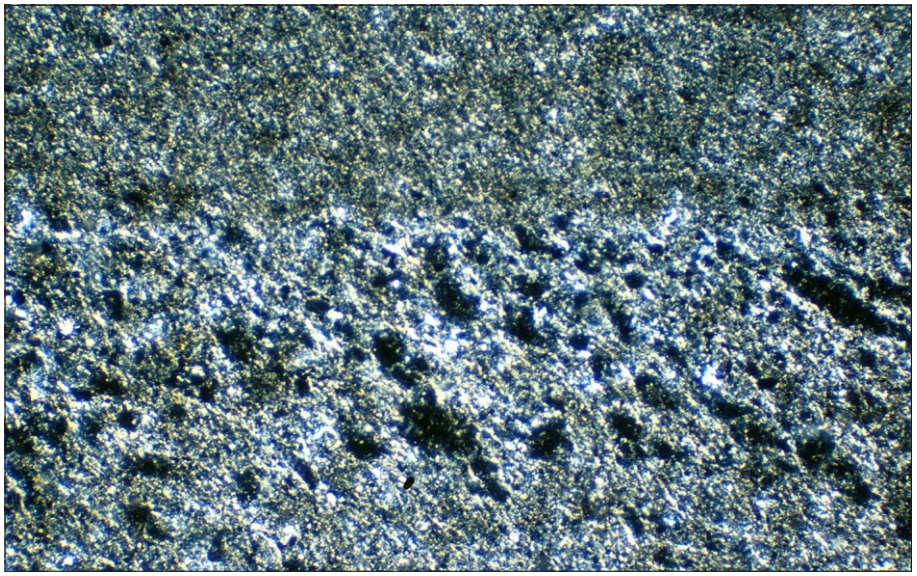

Plate 75

Photomicrograph of sample R004850 (326 020 mE, 5 441 290 mN), Keppel Creek Formation (unit Psvw). Cleaved, relatively pelitic, coarse to medium-grained lithicwacke siltstone. Note bedding (horizontal on page) and cleavage (oblique) defined by sericitic shreds. Crossed nicols, field of view 4.4 2.9 mm.

altered to sphene, in a largely chloritic groundmass. Fine-grained impure carbonate, probably secondary, is also present, particularly in R004854.

Another sample (R005068, 322900/5446480), from the western limb and close to the top of the Keppel Creek Formation, is more pelitic. In thin section it consists of sparsely distributed subrounded grains (mostly ≤100 μm) of clear quartz (some strained), turbid feldspar and equant opaque grains in a well-laminated sericitic (?) matrix. There is some compositional banding, with alternating quartz-rich and quartz-poor laminae.

Sample R004850 (Plate 75), from a small tributary of Blackwater Rivulet (326020/5441290), is a similar pelitic rock, but contains less detrital quartz. In this sample sericitic shreds define a penetrative cleavage strongly oblique to a well-defined bedding lamination.

A nearby sample (R005057, 325560/5447130) from the Arthur River is more mixed in provenance. In thin section the coarser-grained bed is relatively well sorted and comprises grains of subangular quartz (≤ 75 μm), fine-grained carbonate, pale yellow chlorite, scaly opaque grains, and occasional small splinters of detrital white mica. This bed rests on a much finer grained (>25 μm) but mineralogically similar siltstone.

Sample R006710, from Blackwater 6B road (326630/5439200), is a rather hard, weathered, off white to cream-coloured lithicwacke siltstone, with zones of thin pale purple laminae. In thin section it is seen to mainly consist of chlorite, altered opaque minerals and turbid feldspar, with minor detrital quartz. A sample (R006715) from the lower Lindsay River area (329410/5429950) is a similar, dull olive-green, rather brittle rock with a cuboidal fracture and a thin faint bedding lamination. In thin section it consists of feldspar grains (mostly 40–100 μm, although up to 170 μm), chlorite and oxidised opaque minerals, and some detrital quartz.

A sample (R006703) from a small creek south of the Frankland River (327550/5430780) is a dull bluish grey, hard but brittle rock with a fine planar bedding lamination. The thin section shows it to be a generally medium grained but very poorly-sorted pebbly lithicwacke siltstone, perhaps transitional to basaltic diamictite (Psvx). Angular clasts of altered basalt (up to 2 mm across) grade down to feldspar grains and into a low birefringence matrix with very sparse opaque grains.

Fine to very fine-grained siltstone

These are samples with a mean grain size of less than about 16 μm. Typical specimens (R005077, R005044) have a planar lamination defined by slight variations in grain size and mineralogy. In some samples (R004862, R005070) the lamination is slightly wavy.

In R005077, from the western tract and stratigraphically below the basalt flows (Spinks Creek Volcanics) in the Arthur River section, there are well defined laminae and lenses particularly rich in opaque minerals, but otherwise there is no component of obviously mafic provenance. This sample contains 1–2% irregular grains of albite (500 μm–2 mm) and opaque grains and aggregates up to 50 μm, in a matrix of mainly quartzofeldspathic material with crudely aligned splinters (5–20 μm) of detrital white mica, probably derived from the Rocky Cape Group.

In sample R005070, stratigraphically further up in the river section and above the basalt, the lamination is defined by distinct, coarser grained dark laminae and lenses of coarser grained greenish chlorite which imparts an olive to yellow-brown colour in thin section.

Detrital sericite is also discernible in some samples (e.g. R004862, R005044, R004844), all of which lie stratigraphically below the basalt. In the relatively oxidised sample R004862, similar splinters (≤ 20 μm) of a reddish-brown very weakly pleochroic phyllosilicate mineral (possibly stilpnomelane) are resolvable under high magnification and strong illumination.

In sample R005065, from the central tract, 1–2% subrounded grains of quartz (10–30 μm) are present, concentrated in particular laminae, together with both

equant euhedral (≤40 μm) and elongate to acicular opaque grains. The matrix contains about 40% carbonate.

Fine-grained carbonate is also abundant (60%) in the matrix of sample R004853, together with a few per cent of subrounded detrital grains (≤100 μm) of quartz and feldspar, and smaller blebs of opaque minerals. Lenticular laminae and scouring indicate some tractional sedimentation. This sample, from the western tract in a tributary of Blackwater Rivulet, is stratigraphically just below and lithologically transitional to the Smithton Dolomite.

Sample R005053, from just below Kanunnah Bridge but east of the Roger River Fault, is a slightly coarser grained, poorly-sorted and poorly-laminated maroon siltstone, affected by hematitic alteration probably due to the proximity of thick basalt.

The pale orange-red colour of R004844 (325910/5446190), a well-laminated very fine-grained siltstone, is probably caused by weathering. Sample R005184 (337140/5439410) is a similar rock, in which remnant aggregates of altered opaque grains are surrounded by colourless reduction haloes in an otherwise orange-red, very fine-grained indeterminate matrix.

Mudstone

Sample R006697, from a small creek north of the Horton River (328710/5432110), is one of the few samples from the Keppel Creek Formation that approach mudstone (<4 μm) in grain size. This brittle, cuboidally weathering, khaki-brown rock has a thin faint planar lamination with laminae mostly between 100 μm and 3 mm thick. In thin section its mineralogy is difficult to determine because of alteration and fine grain size, but unoxidised zones have generally low birefringence and may consist mainly of feldspar, colourless chlorite and traces of white mica.

Impure dolomite

The only sample (R005593) sectioned, from the Horton River at 327080/5431550, lies at the top of the Keppel Creek Formation and is transitional to the Smithton Dolomite. In thin section it is seen to contain about 10% well-rounded to subrounded grains of detrital quartz (≤100 μm), sparse small opaque grains and rare chlorite grains in a diffusely laminated fine-grained matrix of recrystallised carbonate. It effervesces weakly in dilute hydrochloric acid and therefore the carbonate is probably dolomite.

Sheared altered wacke

Sample R006708, from the lower Leigh River (331510/5427610), is a dark green, poorly-sorted fine-grained wacke, interbedded with impure carbonate (calcite). Much of the rock consists of scattered small angular grains of quartz, pyroxene, chlorite, opaque minerals and feldspar in a very fine-grained, low birefringence, sheared matrix with formless patches of probably secondary carbonate. There are also bands of finely sparry impure carbonate with similar grain types, traversed by veinlets of more coarsely sparry carbonate. The rock is probably of mixed basaltic and siliciclastic provenance.

Basaltic tuff(?)

A sample (R004851) of moderately weathered, diffusely bedded maroon rock was collected from stratigraphically just below the Spinks Creek Volcanics in Blackwater Rivulet (325080/5443200). In thin section it consists mainly of flattened clasts up to 5 mm across of basalt, generally fine grained to glassy, in a very altered matrix which includes angular grains of hematite, prehnitised plagioclase, chlorite and epidote. Parts of the matrix display well developed compositional banding, whilst other parts appear chaotic.

Altered (oxidised) rocks

A strongly altered sample (R004847) of fine-grained siltstone(?) from Blackwater 5-1-1 road (325420/5442560), in close proximity to basalt, consists of scattered basalt clasts (up to 1 mm) in an orange-red stained, fine-grained matrix in which small (≤50 μm) grains of oxidised opaque minerals and possibly clay-altered feldspar are present. Quartz is absent.

Another thoroughly altered sample (R004846) from a few metres away (325450/5442500) now largely consists of fine to coarse-grained epidote, patches of microcrystalline silica, and hematite. The latter mineral occurs both as a dense fine-grained impregnation and as bands of subrounded grains up to 200 μm across cemented by silica. The compositional banding may represent original bedding. A few narrow quartz veinlets cross the thin section.

APPENDIX 3

Mineral chemistry of detrital spinel in the Kanunnah Subgroup and Scopus Formation

J. L. Everard

Introduction

A reconnaissance electron microprobe study of detrital spinel from Neoproterozoic and Cambrian lithicwacke was undertaken as a pilot project to determine whether this technique could yield useful information about the provenance of these units. Sixteen spinel grains from three separate samples (R004864, R005056, R006689) of the Keppel Creek Formation, a single grain from the Croles Hill Diamictite (sample R005137), and seven grains from one sample (R002872) of the Scopus Formation were analysed using the Cameca SX-50 electron microprobe at the University of Tasmania.

Results

Results are given in Table 14. The analyses are relatively uncontaminated by silicate material (all but one having <0.30% SiO_2 and 19 out of 25 with <0.10% SiO_2). Cation numbers were calculated to the standard spinel formula by distributing iron to Fe^3 and Fe^2 as required. Individual grains appear to be optically and chemically homogeneous (e.g. see analyses R002872/R7/1 and 7/2).

Spinels from both units exhibit a very large and overlapping range in Cr# (atomic 100*Cr/(Cr + Al)), with those from the Keppel Creek Formation (32–92) extending to higher values and those from the Scopus Formation (17–66) including a very aluminous composition. It is noteworthy that, in transmitted light, the most chromian spinels are very dark red to almost opaque, whilst the more aluminous spinels are amber yellow.

Mg# (atomic 100*Mg/(Mg +Fe^2)) also has a large range (Keppel Creek Formation 40–71; Scopus Formation 39–68). It should perhaps be noted that Mg/Fe^2 in spinel is more susceptible to alteration than Cr/Al, both by early post-magmatic interchange with host olivine (e.g. Kamenetsky *et al*., 2001) and by metamorphism and weathering (e.g. Brown, 1986, p.85–89).

A good negative correlation between Mg# and Cr# is evident, particularly in spinels from the Scopus Formation (fig. 28*a*). This is a very common feature in chrome spinels from many igneous suites, and is due to the greater thermodynamic stability of $MgAl_2O_4$ and $FeCr_2O_4$ relative to other possible end members. Thus the Mg/Fe^2 distribution coefficient between spinel and olivine (or spinel and melt) increases with spinel Cr# (e.g. Dick and Bullen, 1984). Data from the Keppel Creek Formation are more scattered, show a cruder correlation, and tend to have a lower Mg# at a given Cr#. This could be due to slower cooling in the igneous protolith, or simply be a function of melt composition (e.g. Kamenetsky *et al*., 2001).

Titanium is low in these spinels, but has a larger range (up to 0.272% TiO_2) in the Keppel Creek Formation than in the Scopus Formation (up to 0.097% TiO_2). In the latter unit it may correlate negatively with Mg# and positively with Cr#, but more data are needed. The most titaniferous spinels in the Keppel Creek Formation all have moderate to high Mg#.

Ni and Mn respectively show crude positive and negative correlations with Mg#, as is commonly observed. Zn and V do not appear to show any systematic relationships with other elements. However Zn appears to be generally higher (0.17–0.36% ZnO) in the Scopus Formation than the Keppel Creek Formation (0–0.24% ZnO) (fig. 28*b*).

The single grain from the Croles Hill Diamictite is similar to typical grains from the approximately coeval Keppel Creek Formation.

Comparison with spinels in Cambrian mafic/ultramafic complexes

The fields of chrome spinel from some mafic and ultramafic units in the Zeehan–Waratah area ('Dundas Trough') are also plotted in Figure 28*a* (data from Brown, 1986). The spinels in the Scopus Formation have consistently lower Cr# than those from Dundas Trough boninites (termed high magnesium andesites by Brown) and their inferred cumulates, the Layered Dunite and Harzburgite (LDH) succession.

The other two ultramafic associations identified by Brown (1986) are the Layered Peridotite and Dunite (LPD) and Layered Pyroxenite-Peridotite and associated Gabbro (LPG) successions, which have similar and distinctive spinel compositions. Some Scopus Formation spinels are similar in both Cr# and Mg# to those from the LPD and LPG successions, but others extend to much lower Cr#.

The Keppel Creek Formation (650–580 Ma) does contain a few refractory spinels with very high Cr# (with rather low Mg#, thus more akin to the LDH ultramafic rocks than boninites). The bulk of the population has lower Cr#, similar to the LPD field, but at slightly higher Mg#. However the western Tasmanian mafic/ultramafic complexes, thought to be emplaced in the Early Cambrian (e.g. Berry and Crawford, 1988; Seymour and Calver, 1995*a*, *b*), are too young to have been the source.

Unfortunately no data for Zn in spinels from the mafic/ultramafic complexes is available.

Implications of spinel composition for tectonic setting of provenance

The spinel compositions are also plotted on discrimination diagrams (TiO_2 and Fe^2/Fe^3 against Al_2O_3) for volcanic and peridotitic spinels from various tectonic settings (fig. 28*c, d, e*; slightly modified after Kamenetsky *et al*., 2001). These show clearly that these spinels, from both the Keppel Creek Formation and Scopus Formation, are unlike those from the volcanic fields, and are therefore unlikely to have been locally derived from the Spinks Creek Volcanics (in which spinel has not been found). Their low TiO_2 contents and high Fe^2/Fe^3 ratios, at moderately high Al_2O_3, are similar to spinel from mantle peridotites, perhaps particularly those from a supra-subduction zone (rather than MORB) setting. In the case of the Scopus Formation, this is in accord with the presence of other ultramafic debris, such as abundant serpentinite clasts.

Spinels from western Tasmanian boninites and ultramafic rocks plot in appropriate fields on these diagrams.

Discussion

Berry *et al.* (1997) analysed spinels from the Keppel Creek Formation (two localities near Smithton) and the Scopus Formation (five on the Woolnorth map sheet including the Stony Point, Scopus and Christmas Hill fossil localities). Their data show that, at these localities in the northern part of the Smithton Synclinorium, the spinels are compositionally more variable. Both low TiO_2 (ultramafic) and high TiO_2 (volcanic/tholeiitic) spinels are present in both units. Volcanic spinels are the dominant component at one of the Smithton localities (Keppel Creek Formation) and at Barcoo Road (lower part of the Scopus Formation). Most spinels from the younger, deeper water parts of the Scopus Formation appear to be ultramafic derived, and some have very high Cr# (>80) and low TiO_2 consistent with an LDH (and/or boninitic) source. In contrast, very few spinels from the Keppel Creek Formation have such high Cr# (although our new data includes two more).

The data suggest that the source of the low TiO_2 spinels dominant at the other Smithton locality (Keppel Creek Formation) was picritic rather than ultramafic. Picrites are present in the Smithton Synclinorium (see below) but available compositional data from spinels (Brown, 1989*a*, p.65–67) shows that they have high TiO_2 (0.65–6.90%). S. Meffre (R. F. Berry, pers. comm.) has reported low TiO_2 spinels from picrites on King Island.

Our new data suggests that, in the southern part of the Smithton Synclinorium, spinels from both the Keppel Creek Formation and Scopus Formation are derived from ultramafic rocks, possibly those from a subduction setting. No evidence for the volcanic component seen in the north was found, even though the Scopus Formation sample R002872 probably comes from the lower part of that unit, like the Barcoo Road sample.

Known Tasmanian ultramafic rocks are an improbable source for spinels from the Neoproterozoic Keppel Creek Formation, as they were probably emplaced too late (in the Early Cambrian). The alternative suggestion of Berry *et al.* (1997), that their source was instead picritic, could obviate the need to postulate a source terrain containing older ultramafic rocks, for which there is little other evidence, at least within Tasmania.

An LPD/LPG ultramafic source for spinels from the Scopus Formation sample R002872 seems possible, but no high Cr# (LDH/boninitic) spinels were found, and another source component seems likely. Derivation of these by reworking of Keppel Creek Formation spinels seems precluded by the lower Zn content of the latter, but more work is needed.

Table 14

Electron microprobe analyses, spinel grains from Keppel Creek Formation, Croles Hill Diamictite and Scopus Formation

Unit	Keppel Creek Formation					Keppel Creek Formation				
Sample	FJ852					AR131				
Reg. No.	R004864					R005056				
AMG (mE)	327100					325680				
AMG (mN)	5439840					5447030				
Analysis	R1	R2	R3	R4/1	R4/2	R1	R2	R3	R4/2	R5/3
SiO_2	0.161	0.108	0.071	1.312	0.273	0.026	0.000	0.006	0.037	0.046
TiO_2	0.097	0.095	0.272	0.131	0.116	0.034	0.137	0.014	0.014	0.051
Al_2O_3	27.893	21.795	26.839	32.570	31.077	39.427	26.677	5.803	4.271	12.040
Cr_2O_3	39.539	47.263	41.634	33.011	33.910	27.923	39.307	66.198	66.261	58.116
V_2O_3	0.111	0.048	0.370	0.233	0.186	0.124	0.168	0.191	0.096	0.041
FeO	16.212	14.728	17.686	20.039	21.359	16.657	21.589	17.958	20.787	19.347
MnO	0.124	0.146	0.222	0.243	0.201	0.061	0.171	0.218	0.292	0.089
ZnO	0.016	0.119	0.060	0.172	0.210	0.065	0.186	0.143	0.031	0.238
NiO	0.152	0.157	0.070	0.124	0.062	0.214	0.193	0.023	0.000	0.081
MgO	14.803	15.470	13.413	12.821	12.541	15.306	12.120	9.930	7.686	9.783
CaO	0.046	0.067	0.049	0.012	0.037	0.003	0.012	0.000	0.000	0.000
TOTAL	**99.154**	**99.994**	**100.686**	**100.667**	**99.974**	**99.839**	**100.561**	**100.484**	**99.474**	**99.830**
Ions calculated on the basis of (O) = 4, cation total = 3										
Si	excl	excl	excl	excl	excl	excl	excl	excl	excl	excl
Ti	0.0022	0.0022	0.0061	0.0029	0.0026	0.0007	0.0031	0.0004	0.0004	0.0013
Al	0.9841	0.7788	0.9473	1.1392	1.0917	1.3190	0.9496	0.2293	0.1743	0.4663
Cr	0.9359	1.1329	0.9858	0.7746	0.7991	0.6266	0.9386	1.7549	1.8144	1.5100
V	0.0027	0.0012	0.0089	0.0055	0.0045	0.0028	0.0041	0.0051	0.0027	0.0011
Fe^3	0.0729	0.0828	0.0458	0.0749	0.0995	0.0501	0.1015	0.0099	0.0079	0.0201
Fe^2	0.3329	0.2906	0.3971	0.4225	0.4330	0.3453	0.4438	0.4936	0.5942	0.5116
Mn	0.0031	0.0037	0.0056	0.0061	0.0051	0.0015	0.0044	0.0062	0.0086	0.0025
Zn	0.0004	0.0027	0.0013	0.0038	0.0046	0.0014	0.0042	0.0035	0.0008	0.0058
Ni	0.0037	0.0038	0.0017	0.0030	0.0015	0.0049	0.0047	0.0006	0.0000	0.0021
Mg	0.6607	0.6992	0.5988	0.5672	0.5573	0.6477	0.5457	0.4964	0.3968	0.4793
Ca	0.0015	0.0022	0.0016	0.0004	0.0012	0.0001	0.0004	0.0000	0.0000	0.0000
Mg#	66.49	70.64	60.12	57.31	56.28	65.23	55.15	50.14	40.04	48.37
Cr#	48.74	59.26	51.00	40.47	42.26	32.21	49.71	88.44	91.23	76.40

Mg# is $100Mg/(Mg + Fe^2)$, Cr# is $100Cr/(Cr + Al)$

Analyses by Cameca SX-50 electron microprobe, Central Science Laboratory, University of Tasmania.

Analyst: J. L. Everard

Table 14 *(continued)*

Unit	Keppel Creek Formation						Croles Hill Diamictite
Sample	MJ548						TJ785Y
Reg. No.	R006689						R005137
AMG (mE)	331510						336740
AMG (mN)	5427740						5440760
Analysis	R1	R2	R3	R4	R5/1	R5/2	R2/1
SiO_2	0.063	0.151	0.098	0.055	0.066	0.075	0.118
TiO_2	0.080	0.093	0.144	0.153	0.159	0.020	0.144
Al_2O_3	24.799	23.329	23.267	21.405	26.782	28.629	25.332
Cr_2O_3	43.370	44.999	43.659	44.016	39.066	37.834	43.657
V_2O_3	0.152	0.130	0.102	0.147	0.176	0.134	0.084
FeO	17.317	14.472	17.860	20.177	18.872	17.893	14.650
MnO	0.171	0.116	0.065	0.209	0.214	0.119	0.098
ZnO	0.052	0.135	0.000	0.059	0.175	0.012	0.037
NiO	0.180	0.229	0.165	0.110	0.139	0.256	0.187
MgO	13.930	15.456	14.379	13.053	13.944	13.819	15.479
CaO	0.026	0.021	0.000	0.002	0.008	0.047	0.014
TOTAL	**100.139**	**99.130**	**99.738**	**99.385**	**99.599**	**98.837**	**99.798**
Ions calculated on the basis of (O) = 4, cation total = 3							
Si	excl	excl	excl	excl	excl	excl	excl
Ti	0.0018	0.0021	0.0033	0.0036	0.0036	0.0005	0.0032
Al	0.8830	0.8349	0.8336	0.7810	0.9497	1.0152	0.8943
Cr	1.0359	1.0803	1.0493	1.0774	0.9293	0.9000	1.0340
V	0.0037	0.0032	0.0025	0.0036	0.0043	0.0032	0.0020
Fe^3	0.0738	0.0773	0.1081	0.1309	0.1096	0.0806	0.0632
Fe^2	0.3637	0.2902	0.3460	0.3915	0.3652	0.3696	0.3038
Mn	0.0044	0.0030	0.0017	0.0055	0.0055	0.0030	0.0025
Zn	0.0012	0.0030	0.0000	0.0013	0.0039	0.0003	0.0008
Ni	0.0044	0.0056	0.0040	0.0027	0.0034	0.0062	0.0045
Mg	0.6274	0.6997	0.6516	0.6024	0.6254	0.6199	0.6912
Ca	0.0008	0.0007	0.0000	0.0001	0.0003	0.0015	0.0004
Mg#	63.30	70.68	65.32	60.61	63.13	62.65	69.47
Cr#	53.99	56.41	55.73	57.97	49.46	46.99	53.62

Table 14 *(continued)*

Unit	Scopus Formation							
Sample	MRS30							
Reg. No.	R002872							
AMG (mE)	331300							
AMG (mN)	5458000							
Analysis	R1	R2	R3	R4	R5	R6	R7/1	R7/2
SiO_2	0.023	0.025	0.026	0.028	0.023	0.018	0.025	0.000
TiO_2	0.090	0.048	0.043	0.053	0.097	0.025	0.055	0.056
Al_2O_3	17.287	33.193	20.340	13.037	19.111	50.364	33.455	32.611
Cr_2O_3	50.107	34.530	46.947	56.436	46.285	15.477	32.774	33.273
V_2O_3	0.210	0.096	0.163	0.059	0.239	0.042	0.151	0.172
FeO	22.025	18.306	20.248	22.190	23.161	16.652	19.630	19.470
MnO	0.274	0.144	0.207	0.182	0.228	0.125	0.180	0.146
ZnO	0.176	0.352	0.260	0.226	0.255	0.286	0.320	0.239
NiO	0.041	0.098	0.061	0.051	0.087	0.255	0.135	0.059
MgO	8.773	12.887	11.340	7.950	9.550	16.421	12.964	12.488
CaO	0.000	0.020	0.000	0.000	0.000	0.000	0.023	0.020
TOTAL	**99.007**	**99.701**	**99.635**	**100.211**	**99.036**	**99.664**	**99.709**	**98.534**
Ions calculated on the basis of (O) = 4, cation total = 3								
Si	excl	excl	excl	excl	excl	excl	excl	excl
Ti	0.0022	0.0011	0.0010	0.0013	0.0023	0.0005	0.0012	0.0013
Al	0.6635	1.1558	0.7530	0.5074	0.7232	1.6104	1.1623	1.1508
Cr	1.2902	0.8066	1.1659	1.4735	1.1749	0.3320	0.7639	0.7877
V	0.0055	0.0023	0.0041	0.0016	0.0062	0.0009	0.0036	0.0041
Fe^3	0.0364	0.0331	0.0749	0.0148	0.0911	0.0557	0.0678	0.0548
Fe^2	0.5634	0.4192	0.4570	0.5980	0.5308	0.3222	0.4161	0.4327
Mn	0.0076	0.0036	0.0055	0.0051	0.0062	0.0029	0.0045	0.0037
Zn	0.0042	0.0077	0.0060	0.0055	0.0060	0.0057	0.0070	0.0053
Ni	0.0011	0.0023	0.0016	0.0013	0.0022	0.0056	0.0032	0.0014
Mg	0.4259	0.5676	0.5310	0.3914	0.4571	0.6642	0.5697	0.5574
Ca	0.0000	0.0006	0.0000	0.0000	0.0000	0.0000	0.0007	0.0007
Mg#	43.05	57.52	53.75	39.56	46.27	67.34	57.79	56.30
Cr#	66.04	41.10	60.76	74.39	61.90	17.09	39.66	40.63

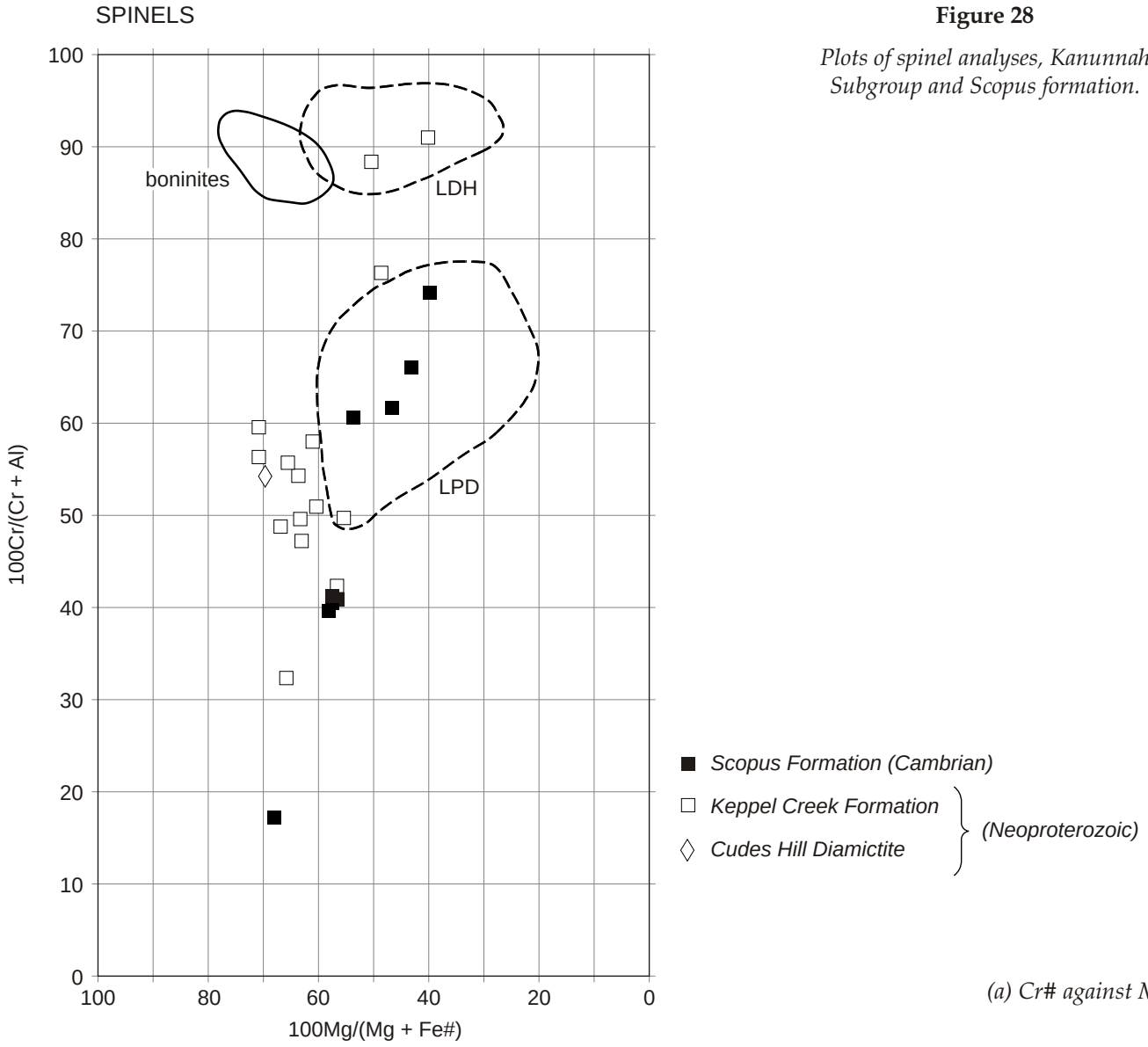

Figure 28

Plots of spinel analyses, Kanunnah Subgroup and Scopus formation.

(a) Cr# against Mg#

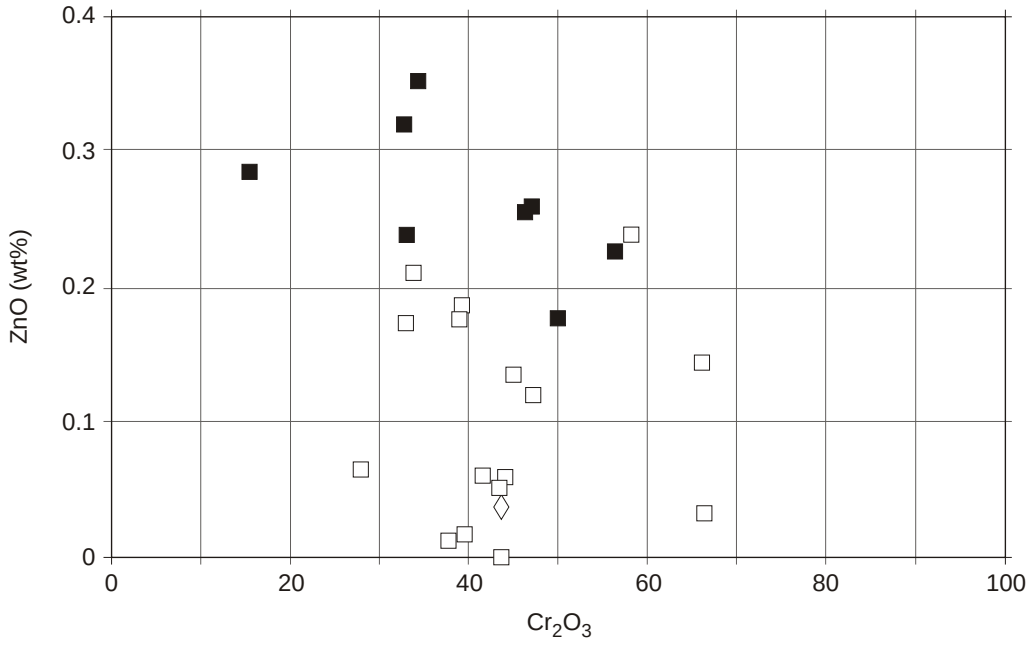

(b) Zn against Cr_2O_3

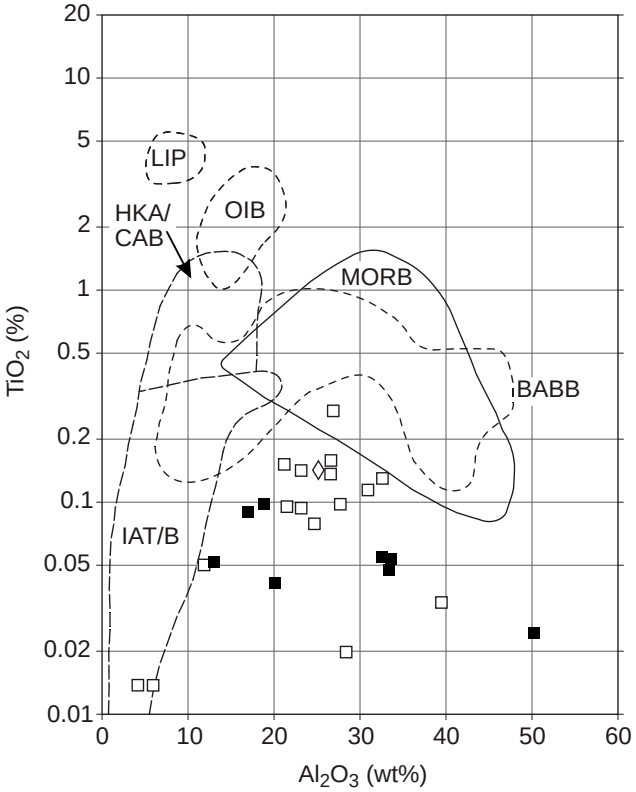

(c) TiO_2 against Al_2O_3, fields for volcanic spinels after Kamenetsky et al. (2001)

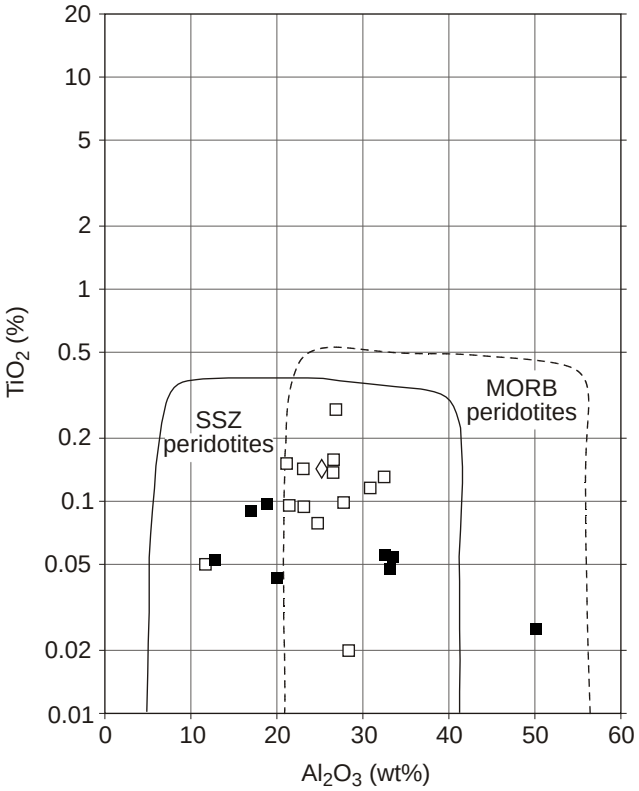

(d) TiO_2 against Al_2O_3, fields for volcanic spinels after Kamenetsky et al. (2001)

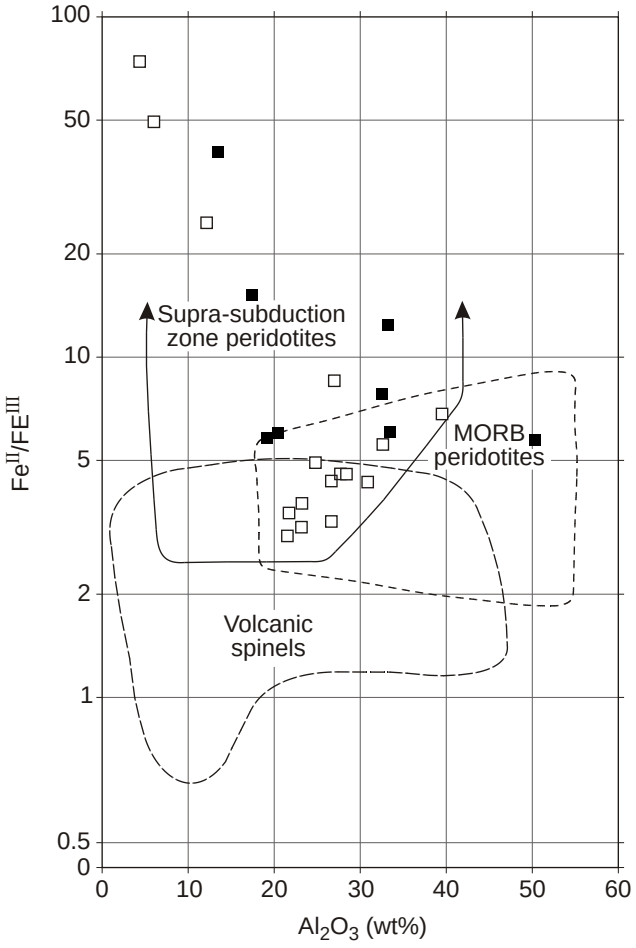

(e) FeII/FeIII against Al_2O_3, spinel fields after Kamenetsky et al. (2001)

Figure 28

Plots of spinel analyses, Kanunnah Subgroup and Scopus formation.

APPENDIX 4

Chemical analyses and summary of petrography, Spinks Creek Volcanics

Table 15*a*

New chemical analyses, Spinks Creek Volcanics

Field No.	AR164	FJ790A	AR100	FJ162	FJ826	FJ1111	MJ725	TJ926	TJ1586	TJ2144
Reg. No.	R005078	R004904	R005046	R004875	R004908	R004922	R006740	R005157	R005164	R005171
Anal. No.	920468	961010	920458	960992	961014	961025	980392	902542	902557	902567
AMG (mE)	322780	322940	333880	327850	330000	331770	328870	333920	331910	332560
AMG (mN)	5446060	5445690	5446880	5441060	5439690	5439940	5432790	5426870	5431860	5438470
Group	P	P	A	A	A	A	A	B	B	B
SiO_2 (%)	48.61	48.84	47.63	48.25	47.68	47.71	49.11	46.85	46.90	47.87
TiO_2	0.58	0.58	0.69	0.72	0.70	0.68	0.68	1.06	1.02	1.03
Al_2O_3	14.69	14.79	14.24	14.63	14.69	14.68	14.26	14.53	14.49	14.20
Fe_2O_3	1.67	0.95	2.63	2.48	3.18	3.74	3.24	3.11	3.07	3.76
FeO	8.06	8.13	10.83	9.80	8.96	8.34	8.33	8.31	7.70	7.57
MnO	0.17	0.18	0.22	0.22	0.20	0.23	0.20	0.19	0.19	0.20
MgO	8.87	9.21	7.55	8.05	7.89	7.88	7.49	8.26	7.81	7.75
CaO	11.33	12.00	11.40	10.50	9.74	10.39	9.18	10.04	11.00	9.23
Na_2O	1.91	1.61	2.26	2.13	2.99	2.55	3.78	3.67	3.50	4.87
K_2O	0.73	0.63	0.28	0.43	0.22	0.36	0.43	0.33	0.24	0.10
P_2O_5	0.19	0.21	0.21	0.19	0.18	0.20	0.21	0.14	0.11	0.12
SO_3 (tot)	0.09	0.09	0.07	0.07	0.08	0.08	0.12			
SO_3 (ate)								0.02	0.01	0.02
SO_3 (ide)								0.53	0.14	0.15
CO_2	0.07	0.05	0.08	0.09	0.14	0.09	0.04	0.02	0.08	0.04
H_2O^+	2.74	2.41	1.43	2.14	2.78	2.31	3.01	3.56	3.88	3.35
TOTAL	**99.70**	**99.68**	**99.52**	**99.69**	**99.41**	**99.24**	**100.07**	**100.62**	**100.14**	**100.26**
Sc (ppm)	24	41	33	49	49	49	51	37	38	37
V	195	230	290	280	290	290	270	250	230	240
Cr	440	420	130	135	135	145	140	185	185	195
Co	39	45	46	53	57	60	47	50	49	47
Ni	160	150	165	120	115	115	105	94	95	92
Cu	65	36	88	98	99	37	350	220	100	85
Zn	76	96	93	97	97	98	89	78	76	77
Ga	11	13	15	14	15	16	16	16	16	12
As	<20	<20	<20	<20	<20	<20	<20	<20	<20	<20
Rb	20	23	6	18	11	14	15	8	8	<5
Sr	140	135	120	115	135	115	140	140	140	270
Y	19	20	22	24	25	25	21	19	17	17
Zr	58	67	51	60	59	59	52	62	60	58
Nb	10	14	9	14	14	14	12	3	<3	<3
Mo	<5	<5	6	<5	<5	<5	<5	<5	<5	<5
Sn	<9	<9	<9	<9	<9	<9	<9	<9	<9	<9
Ba	220	330	91	125	100	110	145	155	135	125
La	<20	<20	<20	<20	<20	<20	<20	<20	<20	<20
Ce	<28	31	<28	<28	30	<28	<28	20	25	37
Nd	28	<20	<20	<20	<20	<20	<20	<20	<20	<20
W	<10	<10	<10	<10	<10	<10	<10	<10	<10	<10
Pb	15	<10	14	<10	<10	<10	<10	<5	<5	<5
Bi	<5	<5	<5	6	<5	5	<5	<5	<5	<5
Th	<10	<10	<10	<10	<10	<10	12	<10	<10	<10
U	<10	<10	<10	<10	<10	<10	<10	<10	<10	<10
FeOt	9.56	8.98	13.20	12.03	11.82	11.71	11.25	11.11	10.46	10.95
Nb/Zr	0.172	0.209	0.176	0.233	0.237	0.237	0.231	0.048		
Mg# (0.20)	66.11	68.32	54.62	58.46	58.40	58.61	58.35	61.00	61.09	59.81

Mg# (0.20) is 100Mg/(Mg + Fe_2) calculated at $Fe_2O_3/FeO = 0.20$

Analyses at Mineral Resources Tasmania Laboratories. Analyst: L. M. Hay

Table 15*a* (*continued*)

Field No.	TJ3092	FJ143	FJ322	FJ865	FJ1091	HR35	HR47	HR49	HR60	HR63
Reg. No.	R005175	R004871	R004882	R004910	R004921	R005567	R005573	R005574	R005579	R005580
Anal. No	920455	960990	960998	961016	961024	980367	980368	980369	980373	980374
AMG (mE)	335330	325880	324670	327190	333200	331000	330760	330600	330590	330060
AMG (mN)	5439440	5439890	5435280	5439480	5441820	5432650	5432180	5432040	5432440	5432610
Group	B	B	B	B	B	B	B	B	B	B
SiO_2 (%)	47.07	46.64	47.44	47.57	46.27	47.15	49.75	48.35	47.25	46.88
TiO_2	1.03	1.07	1.05	1.07	1.06	1.06	1.09	1.09	1.07	1.06
Al_2O_3	14.66	15.42	15.02	14.97	15.36	14.83	14.79	15.27	15.11	14.97
Fe_2O_3	1.49	4.38	3.64	4.85	3.65	2.03	1.64	1.75	2.25	3.04
FeO	11.10	6.88	7.44	6.46	7.57	9.10	9.23	8.46	8.85	8.07
MnO	0.20	0.17	0.19	0.20	0.18	0.21	0.20	0.20	0.22	0.20
MgO	6.99	7.25	7.52	7.03	7.31	7.19	7.86	7.82	7.67	7.37
CaO	10.09	10.28	10.45	10.30	11.05	10.27	6.92	7.62	8.82	10.85
Na_2O	3.46	3.58	3.50	3.61	3.15	3.29	4.35	4.26	3.88	3.25
K_2O	0.07	0.05	0.11	0.24	0.10	0.06	0.17	0.04	0.04	0.05
P_2O_5	0.19	0.16	0.18	0.18	0.19	0.19	0.19	0.19	0.20	0.19
SO_3 (tot)	0.08	0.09	0.08	0.09	0.08	0.13	0.15	0.13	0.10	0.13
SO_3 (ate)										
SO_3 (ide)										
CO_2	0.18	0.03	0.06	0.10	0.12	0.08	0.09	0.10	0.07	0.05
H_2O^+	2.98	3.80	3.17	2.90	3.43	3.96	3.83	4.21	4.17	4.04
TOTAL	**99.59**	**99.80**	**99.85**	**99.55**	**99.52**	**99.53**	**100.26**	**99.49**	**99.71**	**100.15**
Sc (ppm)	28	40	42	41	43	47	46	44	46	46
V	310	340	320	320	340	340	340	340	340	340
Cr	185	210	200	230	195	220	220	210	210	210
Co	45	46	48	50	52	44	42	41	43	42
Ni	175	105	115	98	100	96	95	96	95	95
Cu	140	32	139	155	96	48	145	105	29	220
Zn	91	100	96	93	96	96	95	91	93	93
Ga	18	20	16	18	19	18	18	18	18	20
As	<20	<20	<20	<20	<20	<20	<20	<20	<20	<20
Rb	<5	<5	8	10	<5	5	7	<5	<5	7
Sr	180	140	145	250	200	160	288	95	58	155
Y	17	28	22	22	22	19	20	21	17	19
Zr	61	76	75	71	73	68	77	69	63	71
Nb	4	6	7	5	5	6	5	6	6	6
Mo	<5	<5	<5	<5	<5	<5	<5	<5	<5	<5
Sn	<9	<9	<9	<9	<9	<9	<9	<9	<9	<9
Ba	66	68	76	94	56	105	145	83	73	99
La	<20	<20	<20	<20	<20	<20	<20	<20	<20	<20
Ce	<28	<28	<28	<28	<28	<28	<28	<28	<28	<28
Nd	24	<20	<20	<20	<20	<20	<20	<20	<20	<20
W	<10	<10	<10	<10	<10	<10	<10	<10	<10	<10
Pb	16	<10	<10	<10	<10	<10	<10	<10	<10	<10
Bi	6	6	<5	<5	<5	<5	<5	<5	<5	<5
Th	<10	<10	<10	<10	<10	11	15	<10	<10	14
U	<10	<10	<10	<10	<10	<10	<10	<10	<10	<10
FeOt	12.44	10.82	10.72	10.82	10.85	10.93	10.71	10.03	10.87	10.81
Nb/Zr	0.066	0.079	0.093	0.070	0.068	0.088	0.065	0.087	0.095	0.085
Mg# (0.20)	54.17	58.49	59.61	57.74	58.62	58.05	60.70	62.11	59.73	58.93

Table 15*a* *(continued)*

Field No.	HR114	MJ547	MJ549	MJ582	MJ598	MJ641	MJ709	MJ880	MJ965	MJ1028
Reg. No.	R005588	R006724	R006725	R006728	R006729	R006732	R006739	R006745	R006747	R006752
Anal. No	980376	980381	980382	980384	980385	980388	980391	980396	980398	980403
AMG (mE)	328070	331490	331510	330190	330160	329910	329170	331290	331450	330910
AMG (mN)	5431120	5427700	5427760	5432990	5433220	5431450	5433130	5430320	5430920	5430180
Group	B	B	B	B	B	B	B	B	B	B
SiO_2 (%)	45.94	46.23	48.75	48.17	45.54	47.45	46.70	47.95	47.76	48.09
TiO_2	1.05	1.03	1.10	1.04	1.02	1.05	1.03	1.10	1.04	1.08
Al_2O_3	15.27	15.22	14.90	14.91	14.64	14.92	14.88	14.94	15.12	15.02
Fe_2O_3	2.66	3.64	3.59	3.04	3.20	1.91	3.11	3.73	2.23	3.64
FeO	7.68	6.59	7.88	7.94	7.81	9.36	7.81	6.91	8.07	7.62
MnO	0.17	0.18	0.20	0.19	0.23	0.20	0.20	0.19	0.19	0.22
MgO	7.50	7.05	8.09	7.55	7.31	7.43	7.05	6.84	7.62	7.50
CaO	11.63	12.32	7.96	9.14	12.66	10.72	11.63	10.00	9.76	9.74
Na_2O	2.95	3.23	3.41	3.77	2.62	2.74	3.19	3.68	3.69	3.00
K_2O	0.01	0.04	1.06	0.17	0.02	0.60	0.02	0.06	0.06	1.01
P_2O_5	0.19	0.19	0.20	0.19	0.19	0.20	0.20	0.19	0.19	0.20
SO_3 (tot)	0.18	0.19	0.10	0.10	0.10	0.09	0.39	0.15	0.15	0.09
SO_3 (ate)										
SO_3 (ide)										
CO_2	0.04	0.04	0.06	0.06	0.13	0.09	0.11	0.03	0.06	0.07
H_2O^+	4.61	3.83	2.81	3.33	4.21	3.07	4.01	4.04	3.95	2.66
TOTAL	**99.90**	**99.79**	**100.09**	**99.59**	**99.68**	**99.81**	**100.33**	**99.82**	**99.89**	**99.93**
Sc (ppm)	48	44	41	43	44	44	45	48	43	43
V	340	320	340	320	320	330	330	350	330	330
Cr	230	200	190	190	200	210	210	200	210	210
Co	40	43	44	43	40	40	45	42	44	45
Ni	98	96	103	94	96	96	105	93	100	97
Cu	230	440	93	170	18	80	24	30	590	67
Zn	86	89	91	91	70	92	99	100	105	96
Ga	19	22	17	17	19	18	21	18	19	19
As	<20	<20	<20	<20	<20	<20	<20	<20	<20	<20
Rb	5	<5	38	7	<5	22	<5	6	6	35
Sr	38	40	145	270	35	250	81	130	145	250
Y	18	20	21	19	18	20	22	20	22	20
Zr	61	64	72	74	60	77	67	72	69	76
Nb	7	6	6	6	6	5	6	6	6	6
Mo	<5	<5	<5	<5	<5	<5	<5	<5	<5	<5
Sn	<9	<9	<9	<9	<9	<9	<9	<9	<9	<9
Ba	87	92	200	125	73	140	88	110	87	175
La	<20	<20	<20	<20	<20	<20	<20	<20	<20	<20
Ce	<28	<28	<28	<28	<28	<28	<28	<28	<28	<28
Nd	<20	<20	<20	<20	<20	<20	<20	<20	<20	<20
W	<10	<10	<10	<10	<10	<10	<10	<10	<10	<10
Pb	<10	<10	<10	<10	<10	<10	<10	<10	<10	<10
Bi	<5	<5	<5	<5	<5	<5	<5	<5	<5	<5
Th	<10	12	14	13	12	12	10	16	12	11
U	<10	<10	<10	<10	<10	<10	<10	<10	<10	<10
FeOt	10.07	9.87	11.11	10.68	10.69	11.08	10.61	10.27	10.08	10.90
Nb/Zr	0.115	0.094	0.083	0.081	0.100	0.065	0.090	0.083	0.087	0.079
Mg# (0.20)	61.03	60.05	60.50	59.80	58.99	58.52	58.30	58.36	61.40	59.15

Table 15*a* (*continued*)

Field No.	MJ1613	MJ2559	AR103	AR106	AR112	AR113	TJ984	TJ988	TJ1582	TJ2101
Reg. No.	R006758	R006761	R005047	R005048	R005051	R005052	R005158	R005160	R005162	R005167
Anal. No	990462	990472	920459	920460	920462	920463	902543	902544	902556	902563
AMG (mE)	334060	334590	333510	332960	331040	330680	332600	332520	332110	333440
AMG (mN)	5427070	5426610	5446770	5446960	5446310	5446340	5432070	5431660	5431750	5435080
Group	B	B	C	C	C	C	C	C	C	C
SiO_2 (%)	48.64	46.68	49.37	46.89	48.09	47.58	48.80	48.44	47.58	47.32
TiO_2	1.07	1.03	1.66	1.53	1.63	1.61	1.70	1.65	1.60	1.51
Al_2O_3	14.18	14.66	14.61	15.02	13.86	13.68	13.60	13.82	13.71	13.46
Fe_2O_3	4.49	4.76	3.55	4.97	4.62	5.60	7.44	8.45	2.69	4.51
FeO	6.59	6.08	8.19	8.13	8.92	8.19	6.36	5.56	9.85	8.71
MnO	0.20	0.16	0.16	0.22	0.19	0.20	0.18	0.19	0.20	0.25
MgO	7.15	6.78	6.62	7.15	6.65	6.34	6.93	6.69	7.10	7.21
CaO	9.91	12.46	10.67	7.69	9.21	8.54	6.81	6.83	9.58	8.83
Na_2O	4.05	2.99	2.49	4.25	3.07	4.34	4.50	4.64	3.78	4.94
K_2O	0.15	0.05	0.36	0.31	0.53	0.39	0.25	0.62	0.30	0.43
P_2O_5	0.14	0.12	0.23	0.21	0.22	0.24	0.19	0.19	0.18	0.18
SO_3 (tot)	0.06	0.13	0.10	0.08	0.07	0.09				
SO_3 (ate)							0.01	0.01	0.00	0.05
SO_3 (ide)							0.14	0.10	0.10	0.13
CO_2	0.10	0.03	0.12	0.18	0.08	0.47	0.17	0.10	0.07	0.04
H_2O^+	3.05	3.83	2.40	3.00	2.27	2.08	3.07	2.42	3.25	2.70
TOTAL	**99.77**	**99.74**	**100.54**	**99.63**	**99.40**	**99.34**	**100.15**	**99.71**	**99.99**	**100.27**
Sc (ppm)	43	43	26	26	23	22	37	39	35	37
V	320	340	380	370	360	370	280	290	280	290
Cr	210	220	165	75	93	110	97	97	175	70
Co	43	38	46	47	47	51	54	48	45	47
Ni	95	97	135	110	115	120	89	85	94	83
Cu	26	185	96	54	92	140	125	89	74	130
Zn	98	90	93	115	110	115	95	94	89	92
Ga	18	20	20	21	21	20	17	18	20	18
As	<20	<20	<20	<20	<20	<20	<20	<20	<20	<20
Rb	5	<5	<5	<5	7	6	<5	10	5	5
Sr	180	38	230	220	220	180	105	170	260	220
Y	19	18	22	20	21	21	46	29	22	23
Zr	71	59	105	89	95	93	100	100	91	94
Nb	6	6	5	4	4	5	5	5	<3	<3
Mo	<5	<5	<5	<5	<5	5	<5	<5	<5	<5
Sn	<9	<9	<9	<9	<9	<9	<9	<9	<9	63
Ba	86	32	68	75	130	82	190	300	135	175
La	<20	<20	<20	<20	<20	<20	<20	<20	<20	<20
Ce	<28	<28	<28	17	<28	29	56	41	51	49
Nd	<20	<20	27	42	<20	23	28	21	<20	<20
W	<10	<10	<10	<10	<10	<10	<10	<10	<10	<10
Pb	<10	<10	17	18	15	17	<5	<5	<5	<5
Bi	<5	<5	<5	5	<5	6	<5	<5	<5	<5
Th	10	12	<10	<10	<10	<10	<10	<10	<10	<10
U	<10	<10	<10	<10	<10	<10	<10	<10	<10	<10
FeOt	10.63	10.36	11.38	12.60	13.08	13.23	13.05	13.16	12.27	12.77
Nb/Zr	0.085	0.102	0.048	0.045	0.042	0.054	0.050	0.050		
Mg# (0.20)	58.61	57.91	55.02	54.41	51.68	50.20	52.75	51.67	54.90	54.29

Table 15*a* *(continued)*

Field No.	TJ2103	TJ2105	TJ2142	TJ2147	TJ3085	TJ3116	TJ3238	TJ3246	TJ3384	TJ3388
Reg. No.	R005168	R005169	R005170	R005172	R005174	R005178	R005179	R005180	R005182	R005183
Anal. No	902564	902565	902566	902568	920454	920456	930631	930632	930637	930638
AMG (mE)	333130	333710	332580	333230	336900	335110	335660	334100	332450	332330
AMG (mN)	5435260	5435440	5438180	5433190	5439420	5437820	5439960	5438050	5440590	5440110
Group	C	C	C	C	C	C	C	C	C	C
SiO_2 (%)	48.65	47.81	47.64	47.84	49.17	49.19	48.05	47.80	48.21	49.10
TiO_2	1.70	1.44	1.60	1.60	1.65	1.60	1.57	1.52	1.62	1.63
Al_2O_3	13.78	14.29	13.74	13.71	13.96	14.16	13.98	14.00	14.41	13.86
Fe_2O_3	3.26	2.77	3.46	3.79	2.70	2.16	2.60	4.52	3.61	3.46
FeO	9.18	9.31	9.31	8.71	9.51	9.78	9.84	8.26	8.72	8.85
MnO	0.22	0.27	0.23	0.21	0.21	0.21	0.21	0.20	0.21	0.19
MgO	6.96	7.67	7.38	7.15	6.08	5.95	6.61	6.67	6.90	6.78
CaO	10.06	9.90	10.31	10.86	7.99	8.71	9.10	9.31	10.42	10.48
Na_2O	3.20	3.24	3.21	2.76	4.57	4.31	3.82	3.90	2.32	2.81
K_2O	0.83	0.58	0.63	0.47	0.08	0.18	0.07	0.07	0.27	0.15
P_2O_5	0.20	0.17	0.19	0.18	0.23	0.26	0.21	0.21	0.21	0.21
SO_3 (tot)					0.09	0.12	0.08	0.10	0.07	0.05
SO_3 (ate)	0.01	0.01	0.01	0.00						
SO_3 (ide)	0.09	0.13	0.08	0.09						
CO_2	0.04	0.12	0.09		0.13	0.09	0.14	0.01	0.03	0.03
H_2O^+	2.15	3.11	2.29	2.60	3.19	2.97	3.70	3.58	2.73	2.39
TOTAL	**100.33**	**100.82**	**100.17**	**99.97**	**99.56**	**99.70**	**99.99**	**100.15**	**99.73**	**99.97**
Sc (ppm)	37	38	40	40	27	26	43	44	48	43
V	280	270	290	290	400	370	360	367	344	357
Cr	170	200	175	190	51	67	82	85	187	186
Co	47	48	50	53	44	45	47	45	43	46
Ni	85	97	88	91	110	120	72	73	85	85
Cu	145	200	145	135	160	64	23	137	52	94
Zn	95	92	96	98	120	110	72	95	96	95
Ga	19	19	18	19	16	21	15	18	19	19
As	<20	<20	<20	<20	<20	<20	<20	<20	<20	<20
Rb	17	8	15	11	<5	<5	<10	<10	<10	<10
Sr	220	195	220	230	43	145	130	93	220	200
Y	22	21	23	21	28	25	27	27	27	29
Zr	97	80	95	93	110	96	110	110	100	100
Nb	3	3	3	3	7	5	10	10	7	7
Mo	<5	<5	<5	<5	<5	5	<5	<5	<5	<5
Sn	<9	<9	<9	<9	<9	<9	<9	<9	<9	<9
Ba	140	175	145	130	<23	49	30	24	48	33
La	<20	<20	<20	<20	<20	<20	<20	<20	26	<20
Ce	41	39	40	52	<28	<28	<28	<28	<28	<28
Nd	21	<20	<20	21	24	<20	20	<20	<20	<20
W	<10	<10	<10	<10	<10	<10	<10	<10	<10	<10
Pb	<5	<5	<5	<5	12	14	<10	<10	<10	<10
Bi	<5	<5	<5	<5	<5	<5	<5	<5	<5	<5
Th	<10	<10	<10	<10	<10	<10	<10	<10	<10	<10
U	<10	<10	<10	<10	<10	<10	<10	<10	<10	<10
FeOt	12.11	11.80	12.42	12.12	11.94	11.72	12.18	12.33	11.97	11.96
Nb/Zr	0.031	0.038	0.032	0.032	0.064	0.052	0.091	0.091	0.070	0.070
Mg# (0.20)	54.72	57.75	55.55	55.37	51.72	51.63	53.30	53.23	54.81	54.38

Table 7*a* (*continued*)

Field No.	FJ89	FJ165	FJ168	FJ315	FJ317	FJ460	FJ593	FJ603	FJ641	FJ731
Reg. No.	R004869	R004876	R004877	R004880	R004881	R004888	R004894	R004896	R004900	R004902
Anal. No	960988	960993	960994	960996	960997	961002	961006	961007	961008	961009
AMG (mE)	325720	328380	328630	324550	324690	325110	328180	328290	329690	325960
AMG (mN)	5441820	5441150	5441480	5436500	5436040	5443200	5442290	5441870	5441460	5440630
Group	C	C	C	C	C	C	C	C	C	C
SiO_2 (%)	47.12	48.28	48.24	46.35	47.07	46.52	46.23	48.39	48.02	47.47
TiO_2	1.74	1.56	1.61	1.69	1.75	1.58	1.66	1.60	1.58	1.67
Al_2O_3	14.77	14.70	14.30	14.55	14.54	15.01	14.82	14.18	14.20	14.41
Fe_2O_3	6.42	3.31	3.61	6.41	5.50	4.14	3.45	5.04	5.03	3.79
FeO	7.57	8.69	9.38	6.88	8.13	8.27	9.94	7.57	8.27	8.96
MnO	0.22	0.20	0.21	0.20	0.21	0.24	0.25	0.19	0.21	0.20
MgO	6.94	6.84	6.84	7.45	6.74	8.00	7.13	6.60	6.11	6.80
CaO	7.30	10.58	9.88	9.45	8.70	6.93	7.71	9.73	8.35	9.48
Na_2O	4.31	2.47	2.41	3.16	3.69	4.18	3.71	3.06	4.23	3.31
K_2O	0.12	0.24	0.16	0.05	0.15	0.22	0.10	0.21	0.06	0.10
P_2O_5	0.18	0.24	0.25	0.23	0.22	0.20	0.21	0.22	0.22	0.15
SO_3 (tot)	0.08	0.08	0.08	0.08	0.07	0.08	0.07	0.07	0.09	0.23
SO_3 (ate)										
SO_3 (ide)										
CO_2	0.06	0.06	0.10	0.06		0.05	0.14	0.07	0.10	0.08
H_2O^+	3.23	2.54	2.20	3.20	3.17	3.73	4.09	2.43	3.06	3.03
TOTAL	**100.04**	**99.77**	**99.26**	**99.75**	**99.94**	**99.15**	**99.51**	**99.35**	**99.52**	**99.67**
Sc (ppm)	40	38	37	41	39	42	45	35	42	42
V	380	370	390	390	400	390	420	400	400	400
Cr	110	175	61	110	98	91	73	105	69	100
Co	52	44	51	52	54	50	53	50	50	51
Ni	94	93	83	88	90	89	86	87	83	95
Cu	55	41	155	36	40	21	39	500	210	250
Zn	130	105	120	120	125	115	125	105	120	110
Ga	20	21	22	19	20	20	21	21	22	22
As	<20	<20	<20	<20	<20	<20	<20	<20	<20	<20
Rb	7	7	7	5	7	8	5	7	5	8
Sr	165	200	180	210	160	200	155	165	96	230
Y	30	27	27	27	29	26	26	26	30	26
Zr	115	99	105	115	115	105	105	105	110	110
Nb	9	7	9	9	10	7	8	9	9	9
Mo	<5	<5	<5	<5	<5	<5	<5	<5	<5	<5
Sn	<9	<9	<9	<9	<9	<9	<9	<9	<9	<9
Ba	37	65	65	55	81	240	37	69	38	72
La	<20	<20	<20	<20	<20	<20	<20	<20	<20	<20
Ce	<28	<28	<28	<28	36	<28	<28	<28	31	<28
Nd	25	<20	<20	22	<20	<20	<20	<20	20	20
W	<10	<10	<10	<10	<10	<10	<10	<10	<10	<10
Pb	<10	<10	<10	<10	<10	<10	<10	<10	<10	<10
Bi	5	7	<5	5	<5	<5	<5	<5	<5	5
Th	<10	<10	<10	<10	<10	<10	<10	<10	<10	<10
U	<10	<10	<10	<10	<10	<10	<10	<10	<10	<10
FeOt	13.35	11.67	12.63	12.65	13.08	12.00	13.04	12.10	12.80	12.37
Nb/Zr	0.078	0.071	0.086	0.078	0.087	0.067	0.076	0.086	0.082	0.082
Mg# (0.20)	52.24	55.22	53.26	55.34	52.01	58.38	53.48	53.42	50.11	53.62

Table 15*a* *(continued)*

Field No.	FJ808	FJ812	FJ821	FJ833	FJ892	FJ906	FJ955	FJ963	FJ964	FJ978
Reg. No.	R004905	R004906	R004907	R004909	R004912	R004913	R004916	R004917	R004918	R004919
Anal. No	961011	961012	961013	961015	961018	961019	961020	961021	961022	961023
AMG (mE)	328830	329160	329410	326960	329290	330110	332690	331880	331630	331690
AMG (mN)	5441210	5441150	5440430	5440290	5443010	5442290	5443760	5444070	5444020	5442520
Group	C	C	C	C	C	C	C	C	C	C
SiO_2 (%)	49.16	48.85	47.02	47.69	48.48	48.13	48.96	48.94	48.59	46.60
TiO_2	1.68	1.69	1.58	1.57	1.62	1.63	1.53	1.67	1.60	1.64
Al_2O_3	14.78	14.50	14.94	14.23	14.30	13.98	14.36	14.15	14.08	14.67
Fe_2O_3	7.33	8.21	5.72	4.38	4.30	6.27	5.07	3.58	7.61	3.74
FeO	5.63	5.07	7.02	8.13	8.41	6.88	7.57	9.52	5.63	9.24
MnO	0.22	0.24	0.15	0.21	0.21	0.21	0.20	0.21	0.20	0.19
MgO	6.30	6.89	6.46	6.58	6.82	6.71	6.29	6.70	6.19	6.83
CaO	7.78	7.48	10.10	9.60	9.98	8.64	10.50	10.54	8.85	8.73
Na_2O	3.49	3.89	2.70	3.88	2.73	3.99	2.41	2.34	3.53	3.74
K_2O	0.44	0.51	0.50	0.07	0.14	0.33	0.23	0.16	0.51	0.10
P_2O_5	0.23	0.22	0.22	0.22	0.24	0.22	0.23	0.24	0.23	0.20
SO_3 (tot)	0.08	0.07	0.08	0.09	0.08	0.07	0.08	0.07	0.08	0.08
SO_3 (ate)										
SO_3 (ide)										
CO_2	0.05	0.04	0.19	0.18	0.08	0.12	0.19	0.10	0.16	0.17
H_2O^+	2.04	2.41	2.46	3.23	2.19	2.21	1.94	1.79	2.04	3.48
TOTAL	**99.20**	**100.05**	**99.13**	**100.07**	**99.57**	**99.40**	**99.56**	**100.01**	**99.31**	**99.39**
Sc (ppm)	41	41	36	40	38	35	40	36	38	40
V	390	370	350	390	390	400	390	390	380	390
Cr	110	105	180	75	100	110	75	100	100	73
Co	50	51	55	54	49	43	51	54	45	48
Ni	99	90	100	84	83	86	95	91	81	83
Cu	18	28	125	49	260	15	22	240	130	24
Zn	125	120	105	110	105	110	110	115	91	115
Ga	24	22	21	22	20	21	21	21	21	22
As	<20	<20	<20	<20	<20	<20	<20	<20	<20	<20
Rb	9	12	13	5	5	10	8	6	10	6
Sr	170	195	230	165	180	190	180	175	210	270
Y	27	27	29	26	26	25	27	25	27	25
Zr	110	110	99	100	105	105	98	105	105	105
Nb	9	8	7	7	7	7	7	7	8	7
Mo	<5	<5	<5	<5	<5	<5	<5	<5	<5	<5
Sn	<9	<9	<9	<9	<9	<9	<9	<9	<9	<9
Ba	115	170	120	31	73	105	71	69	150	40
La	<20	<20	<20	<20	<20	<20	<20	<20	<20	<20
Ce	<28	<28	28	<28	29	<28	<28	<28	<28	<28
Nd	<20	<20	23	20	<20	21	<20	<20	<20	20
W	<10	<10	<10	<10	<10	<10	<10	<10	<10	<10
Pb	<10	<10	<10	<10	<10	<10	<10	<10	<10	<10
Bi	<5	<5	6	6	5	5	<5	5	6	<5
Th	<10	<10	<10	<10	<10	<10	<10	<10	<10	<10
U	<10	<10	<10	<10	<10	<10	<10	<10	<10	<10
FeOt	12.23	12.46	12.17	12.07	12.28	12.52	12.13	12.74	12.48	12.61
Nb/Zr	0.082	0.073	0.071	0.070	0.067	0.067	0.071	0.067	0.076	0.067
Mg#0.20	52.01	53.78	52.76	53.41	53.88	52.99	52.16	52.52	51.06	53.26

Table 15*a* (*continued*)

Field No.	FJ1122	HR15	HR52	HR53	HR57	HR118	HR122	HR125	MJ560	MJ628
Reg. No.	R004923	R005565	R005576	R005577	R005578	R005589	R005590	R005592	R006727	R006730
Anal. No	961026	980366	980370	980371	980372	980377	980378	980379	980383	980386
AMG (mE)	331250	332990	330510	330520	330510	327690	327460	327200	331110	330790
AMG (mN)	5440760	5432400	5432070	5432070	5432440	5431080	5431060	5431130	5428380	5432870
Group	C	C	C	C	C	C	C	C	C	C
SiO_2 (%)	48.80	47.15	48.71	47.34	48.21	47.29	48.81	49.99	50.40	48.76
TiO_2	1.56	1.60	1.63	1.64	1.62	1.66	1.65	1.77	1.57	1.62
Al_2O_3	14.48	14.18	13.83	14.36	14.62	14.46	14.28	14.79	13.52	13.97
Fe_2O_3	4.24	5.74	4.24	2.49	3.06	3.12	4.51	8.14	6.05	3.94
FeO	8.55	7.43	8.27	9.30	9.23	9.36	8.07	5.42	6.78	9.23
MnO	0.20	0.22	0.18	0.19	0.21	0.24	0.21	0.28	0.20	0.20
MgO	6.75	5.75	6.70	6.48	6.79	6.95	6.57	6.53	6.15	6.79
CaO	10.58	9.89	9.77	10.49	11.29	9.52	9.86	4.59	7.44	10.38
Na_2O	2.28	2.95	3.10	3.24	2.22	3.51	2.86	4.07	4.73	2.51
K_2O	0.20	0.08	0.24	0.09	0.13	0.11	0.35	0.34	0.25	0.43
P_2O_5	0.22	0.24	0.23	0.24	0.24	0.25	0.26	0.22	0.24	0.25
SO_3 (tot)	0.07	0.11	0.11	0.13	0.10	0.11	0.10	0.11	0.10	0.09
SO_3 (ate)										
SO_3 (ide)										
CO_2	0.06	0.18	0.21	0.08	0.08	0.13	0.03	0.31	0.04	0.02
H_2O^+	1.84	4.20	3.12	3.46	2.18	3.07	2.19	3.26	2.24	1.79
TOTAL	**99.81**	**99.71**	**100.34**	**99.53**	**99.96**	**99.78**	**99.73**	**99.81**	**99.69**	**99.97**
Sc (ppm)	35	48	40	42	39	44	41	44	38	41
V	390	420	370	400	380	410	400	420	370	390
Cr	73	87	185	195	185	79	115	130	115	74
Co	43	43	44	44	41	48	47	44	42	40
Ni	85	90	90	89	93	85	83	82	79	76
Cu	105	83	120	450	120	390	55	105	130	46
Zn	110	125	105	105	110	115	110	130	110	110
Ga	22	24	21	21	21	21	21	20	18	20
As	<20	<20	<20	<20	<20	<20	<20	<20	<20	<20
Rb	6	6	8	<5	5	6	9	9	8	12
Sr	175	73	220	300	170	290	180	195	260	190
Y	25	33	26	24	23	23	23	26	21	25
Zr	100	105	108	115	94	110	105	115	100	100
Nb	7	8	7	7	7	7	8	8	6	7
Mo	<5	<5	<5	<5	<5	<5	<5	<5	<5	<5
Sn	<9	<9	<9	<9	<9	<9	<9	<9	<9	<9
Ba	63	70	100	87	94	105	130	165	175	100
La	<20	<20	<20	<20	<20	<20	<20	<20	<20	<20
Ce	<28	<28	<28	<28	<28	<28	<28	<28	<28	<28
Nd	<20	<20	<20	<20	<20	<20	<20	<20	<20	<20
W	<10	<10	<10	<10	<10	<10	<10	<10	<10	<10
Pb	<10	<10	<10	<10	<10	<10	<10	<10	<10	<10
Bi	5	<5	<5	<5	<5	<5	<5	<5	<5	<5
Th	<10	14	<10	15	13	11	<10	<10	10	13
U	<10	<10	<10	<10	<10	<10	<10	<10	<10	<10
FeOt	12.37	12.59	12.09	11.54	11.98	12.17	12.13	12.74	12.22	12.78
Nb/Zr	0.070	0.076	0.065	0.061	0.074	0.064	0.076	0.070	0.060	0.070
Mg# (0.20)	53.45	48.99	53.83	54.15	54.38	54.58	53.26	51.87	51.41	52.78

Table 15*a* *(continued)*

Field No.	MJ634	MJ647	MJ673	MJ855	MJ966	MJ994	MJ1032	MJ1088	MJ1455	MRS9
Reg. No.	R006731	R006733	R006735	R006744	R006748	R006749	R006754	R006755	R006757	R002851
Anal. No	980387	980389	980390	980380	980399	980400	980404	980406	990451	960785
AMG (mE)	330720	331400	330220	329810	331560	333060	331420	327520	334710	332150
AMG (mN)	5432370	5431890	5433080	5429970	5430730	5432870	5430560	5430850	5426740	5448800
Group	C	C	C	C	C	C	C	C	C	C
SiO_2 (%)	47.88	47.60	48.74	47.61	50.27	48.71	49.33	48.91	48.78	49.20
TiO_2	1.49	1.63	1.63	1.65	1.63	1.64	1.67	1.66	1.59	1.66
Al_2O_3	14.60	14.14	14.17	14.66	13.68	13.93	13.50	14.08	13.99	13.80
Fe_2O_3	3.74	5.26	3.64	4.69	7.08	4.13	6.54	3.61	5.04	4.20
FeO	7.94	7.43	8.72	9.23	6.13	8.46	6.78	8.52	7.36	8.62
MnO	0.18	0.18	0.21	0.27	0.18	0.20	0.24	0.16	0.18	0.22
MgO	7.09	6.77	6.81	6.10	6.01	6.31	6.25	6.09	6.46	6.87
CaO	11.04	9.10	10.21	6.80	9.79	10.95	10.41	9.11	9.48	10.50
Na_2O	2.68	3.95	2.65	4.66	2.91	2.53	2.96	4.12	3.11	2.48
K_2O	0.28	0.11	1.10	0.08	0.52	0.27	0.32	0.22	0.56	0.31
P_2O_5	0.24	0.24	0.25	0.23	0.26	0.26	0.25	0.23	0.18	0.25
SO_3 (tot)	0.09	0.10	0.10	0.22	0.10	0.10	0.09	0.11	0.05	0.08
SO_3 (ate)										
SO_3 (ide)										
CO_2	0.04	0.13	0.04	0.33	0.16	0.08	0.09	0.19	0.06	0.10
H_2O^+	2.58	3.29	2.11	3.59	1.64	2.36	1.74	3.03	3.05	1.91
TOTAL	**99.87**	**99.92**	**100.37**	**100.13**	**100.36**	**99.92**	**100.17**	**100.05**	**99.87**	**100.20**
Sc (ppm)	38	40	41	42	39	39	39	41	41	39
V	350	370	380	400	400	370	400	390	380	400
Cr	200	180	185	80	115	165	120	180	190	110
Co	41	41	42	35	41	40	44	40	41	47
Ni	94	88	86	73	87	86	83	88	87	88
Cu	46	52	340	86	33	250	79	86	61	540
Zn	110	120	115	135	110	110	115	105	110	115
Ga	21	20	21	20	20	20	21	21	20	17
As	<20	<20	<20	<20	<20	<20	<20	<20	<20	<20
Rb	7	<5	27	6	10	9	9	8	14	9
Sr	240	96	240	90	190	230	200	150	250	210
Y	21	25	26	26	23	24	24	24	23	29
Zr	92	95	110	100	105	100	110	105	99	110
Nb	6	7	7	8	7	7	8	8	6	9
Mo	<5	<5	<5	<5	<5	<5	<5	<5	<5	<5
Sn	<9	<9	<9	<9	<9	<9	<9	<9	<9	<9
Ba	100	80	130	78	120	87	110	125	105	78
La	<20	<20	<20	<20	<20	<20	<20	<20	<20	<20
Ce	<28	<28	<28	<28	<28	<28	<28	<28	<28	23
Nd	<20	<20	<20	<20	<20	<20	<20	<20	<20	19
W	<10	<10	<10	<10	<10	<10	<10	<10	<10	<10
Pb	<10	<10	<10	<10	<10	<10	<10	<10	<10	<10
Bi	<5	<5	<5	<5	<5	<5	<5	<5	<5	<5
Th	13	11	14	12	13	<10	16	11	13	15
U	<10	<10	<10	<10	<10	<10	<10	<10	<10	<10
FeOt	11.31	12.16	12.00	13.45	12.50	12.18	12.66	11.77	11.90	12.40
Nb/Zr	0.065	0.074	0.064	0.080	0.067	0.070	0.073	0.076	0.061	0.082
Mg# (0.20)	56.88	53.93	54.42	49.50	50.28	52.15	50.93	52.12	53.31	53.82

Table 15*a* (*continued*)

Field No.	MRS20	MRS26	MRS31	MRS39	-	-	-	AR111	FJ99A	FJ464
Reg. No.	R002862	R002868	R002873	R002881	G401349	G401350	G401351	R005050	R004870	R004889
Anal. No	960786	960787	960788	960790	891862	891863	891864	920461	960989	980407
AMG (mE)	330440	332740	332010	331900	330580	330580	329300	331280	325420	325160
AMG (mN)	5446430	5447040	5449040	5449830	5446280	5446280	5446200	5446260	5442560	5443240
Group	C	C	C	C	C	C	C	D	D	D
SiO_2 (%)	47.83	48.19	48.41	48.08	50.50	46.04	47.84	50.89	46.53	48.78
TiO_2	1.67	1.56	1.67	1.68	1.60	1.65	1.59	2.18	2.32	2.27
Al_2O_3	13.69	14.12	14.27	14.15	13.40	14.35	13.82	13.15	14.51	13.78
Fe_2O_3	6.13	5.54	4.62	6.47	4.06	4.60	3.97	5.12	4.84	4.96
FeO	6.88	7.30	8.55	6.53	9.33	9.79	9.33	8.39	8.13	8.07
MnO	0.23	0.18	0.26	0.23	0.12	0.20	0.13	0.19	0.23	0.21
MgO	6.19	6.59	6.37	6.31	5.86	8.50	5.61	5.54	6.77	5.91
CaO	9.33	10.52	8.88	8.57	3.53	5.25	4.44	7.43	8.44	9.85
Na_2O	4.34	2.26	3.51	4.60	4.94	4.15	5.44	3.44	3.74	2.76
K_2O	0.09	0.28	0.43	0.13	0.05	0.03	0.05	0.65	0.11	0.54
P_2O_5	0.21	0.25	0.25	0.22	0.14	0.13	0.16	0.26	0.30	0.33
SO_3 (tot)	0.09	0.08	0.08	0.08	0.27	0.13	0.35	0.08	0.09	0.09
SO_3 (ate)										
SO_3 (ide)										
CO_2	0.23	0.07	0.14	0.06	1.70	0.59	1.95	0.10	0.04	0.05
H_2O^+	2.94	2.15	2.41	2.51	5.15	4.95	5.62	1.90	3.54	2.41
TOTAL	**99.85**	**99.07**	**99.84**	**99.62**	**100.65**	**100.36**	**100.30**	**99.32**	**99.58**	**100.02**
Sc (ppm)	43	44	44	46	49	51	49	23	36	37
V	400	390	400	410	230	290	240	390	440	450
Cr	120	83	105	120	115	120	120	87	100	100
Co	45	45	50	47	36	43	40	43	52	41
Ni	87	87	93	85	60	70	59	120	83	78
Cu	54	200	225	13	200	145	155	115	330	130
Zn	105	96	115	110	74	88	68	77	120	125
Ga	19	19	18	16	13	14	14	19	24	21
As	<20	<20	<20	<20	8			<20	<20	<20
Rb	6	10	10	7				8	7	14
Sr	120	195	235	215	22	71	16	230	15	280
Y	29	24	26	26	25	22	24	23	33	27
Zr	120	105	110	115	92	93	95	135	160	150
Nb	10	7	7	9	6	5	7	12	17	15
Mo	<5	<5	<5	<5				<5	<5	<5
Sn	<9	11	9	21				<9	<9	<9
Ba	67	78	175	78	84	89	92	230	70	260
La	<20	<20	<20	<20	10		8	<20	<20	<20
Ce	26	19	26	27	46	46	37	42	51	42
Nd	16	18	27	14	17	17	15	32	23	20
W	<10	<10	<10	<10	9	8		<10	<10	<10
Pb	<10	<10	<10	<10				18	<10	<10
Bi	<5	<5	<5	<5	5	6		<5	<5	<5
Th	20	15	13	16				<10	<10	13
U	<10	<10	<10	<10				<10	<10	<10
FeOt	12.40	12.28	12.71	12.35	12.98	13.93	12.90	13.00	12.49	12.53
Nb/Zr	0.083	0.067	0.064	0.078	0.065	0.054	0.074	0.089	0.106	0.100
Mg# (0.20)	51.23	53.01	51.32	51.80	48.70	56.21	47.77	47.27	53.28	49.80

Table 15*a* *(continued)*

Field No.	FJ473	FJ477	FJ542	MRS8	MRS35	HR112	MJ998	MJ1009	MJ1617	MJ1618
Reg. No.	R004890	R004891	R004893	R002850	R002877	R005587	R006750	R006751	R006759	R006760
Anal. No	961003	980408	961005	960784	960789	980375	980401	980402	990463	990464
AMG (mE)	325100	325150	324680	330450	331900	328240	332570	333010	334030	333840
AMG (mN)	5443640	5443890	5444500	5446540	5449830	5431210	5432290	5431870	5427000	5426800
Group	D	D	D	D	D	E	E	E	E	E
SiO_2 (%)	48.31	46.29	47.35	49.05	46.72	49.59	51.86	54.07	51.98	52.46
TiO_2	2.25	2.35	2.12	2.39	2.32	2.14	2.06	2.22	1.98	1.99
Al_2O_3	13.92	13.98	14.99	13.88	13.80	13.19	12.73	13.56	12.47	12.37
Fe_2O_3	4.68	5.90	3.99	4.95	4.39	2.58	5.05	2.27	6.76	4.37
FeO	8.13	7.81	8.96	7.37	9.03	13.43	10.65	10.65	9.28	10.69
MnO	0.20	0.20	0.32	0.37	0.42	0.29	0.30	0.22	0.28	0.26
MgO	6.21	6.24	6.40	6.83	7.82	3.18	3.16	2.73	3.16	2.45
CaO	9.01	9.18	5.87	6.12	5.41	8.26	6.16	4.34	4.75	5.31
Na_2O	3.12	4.03	4.54	4.95	4.53	2.76	2.99	4.89	4.71	5.10
K_2O	0.19	0.05	0.27	0.13	0.08	0.79	2.09	1.24	1.08	1.43
P_2O_5	0.30	0.30	0.26	0.25	0.26	0.74	0.74	0.72	0.68	0.65
SO_3 (tot)	0.08	0.12	0.07	0.07	0.08	0.11	0.11	0.11	0.05	0.05
SO_3 (ate)										
SO_3 (ide)										
CO_2	0.03	0.08	0.23	0.05	0.27	0.14	0.13	0.23	0.02	0.02
H_2O^+	3.27	3.40	3.92	3.08	4.09	2.44	2.14	2.92	2.38	2.41
TOTAL	**99.71**	**99.93**	**99.29**	**99.49**	**99.21**	**99.63**	**100.16**	**100.16**	**99.59**	**99.57**
Sc (ppm)	35	39	30	40	38	42	39	39	36	36
V	420	470	450	440	430	185	180	180	170	170
Cr	91	105	86	100	105	13	11	13	13	11
Co	47	37	37	42	46	19	23	31	15	14
Ni	80	80	75	79	87	12	10	15	8	8
Cu	155	38	49	59	18	13	14	120	12	21
Zn	110	120	105	110	120	175	185	160	160	155
Ga	23	22	22	18	20	21	19	19	18	17
As	<20	<20	<20	<20	<20	<20	<20	<20	<20	<20
Rb	6	6	8	5	8	22	39	42	20	43
Sr	370	75	94	205	110	240	165	89	69	96
Y	30	29	39	30	32	55	54	56	52	53
Zr	155	155	150	160	165	220	210	220	200	200
Nb	15	17	16	18	20	62	57	66	59	58
Mo	<5	<5	<5	<5	<5	5	<5	<5	<5	<5
Sn	<9	<9	<9	<9	<9	<9	<9	<9	<9	<9
Ba	165	87	320	80	38	600	530	350	360	480
La	<20	<20	<20	<20	<20	47	41	37	57	59
Ce	47	39	42	39	48	100	96	91	87	105
Nd	20	21	<20	23	31	37	43	33	33	36
W	<10	<10	<10	<10	<10	<10	<10	<10	<10	<10
Pb	<10	<10	<10	<10	<10	12	11	14	<10	<10
Bi	5	<5	5	<5	<5	<5	<5	<5	<5	<5
Th	<10	14	<10	15	22	28	28	21	25	25
U	<10	<10	<10	<10	<10	<10	<10	<10	<10	<10
FeOt	12.34	13.12	12.55	11.82	12.98	15.75	15.19	12.69	15.36	14.62
Nb/Zr	0.097	0.110	0.107	0.113	0.121	0.282	0.271	0.300	0.295	0.290
Mg# (0.20)	51.42	50.01	51.75	54.85	55.89	29.81	30.43	31.15	30.17	26.05

Table 15*a* (*continued*)

Field No.	AR160C	FJ145	FJ284	FJ360	FJ363	FJ481	AR161
Reg. No.	R005074	R004872	R004878	R004883	R004884	R004892	R005076
Anal. No	920465	960991	960995	960999	961000	961004	920467
AMG (mE)	322900	325670	325460	325750	325590	325160	322870
AMG (mN)	5446240	5439830	5440520	5441060	5441260	5444050	5446160
Group	F	F	F	F	F	F	VLT
SiO_2 (%)	49.43	45.55	45.92	47.31	46.47	45.37	48.24
TiO_2	0.85	1.22	0.88	0.85	0.81	0.84	0.45
Al_2O_3	16.90	18.07	16.95	16.95	16.41	17.06	15.27
Fe_2O_3	3.93	2.16	3.72	1.49	1.77	3.13	1.17
FeO	8.32	8.96	6.18	7.92	7.02	10.08	9.65
MnO	0.19	0.18	0.65	0.18	0.18	0.20	0.24
MgO	5.22	3.88	5.98	7.08	8.50	6.44	8.97
CaO	5.84	10.51	10.22	8.52	9.65	7.66	8.15
Na_2O	4.32	3.57	3.24	3.30	2.55	2.95	3.82
K_2O	0.46	0.71	0.94	2.37	1.64	1.05	0.31
P_2O_5	0.38	0.71	0.49	0.38	0.39	0.35	0.16
SO_3 (tot)	0.09	0.09	0.10	0.11	0.07	0.08	0.09
SO_3 (ate)							
SO_3 (ide)							
CO_2	0.39	0.08	0.69	0.30	0.05	0.02	0.13
H_2O^+	3.18	3.95	3.63	3.05	3.60	4.06	3.09
TOTAL	**99.49**	**99.62**	**99.58**	**99.80**	**99.10**	**99.30**	**99.75**
Sc (ppm)	13	23	34	34	36	18	25
V	130	260	190	175	200	125	175
Cr	33	11	180	240	390	12	420
Co	38	39	35	36	40	49	41
Ni	120	28	70	78	115	56	220
Cu	480	63	68	57	52	84	97
Zn	72	99	79	81	70	80	76
Ga	12	17	16	16	13	14	12
As	<20	<20	<20	<20	<20	<20	<20
Rb	14	20	22	67	48	24	9
Sr	195	580	500	530	740	280	155
Y	26	38	33	32	30	30	16
Zr	93	140	145	150	130	110	52
Nb	40	64	68	65	58	48	<3
Mo	<5	<5	<5	<5	<5	<5	5
Sn	<9	<9	<9	<9	<9	<9	<9
Ba	260	470	350	670	640	720	1900
La	35	64	59	58	52	35	<20
Ce	71	105	105	100	79	64	33
Nd	34	33	38	36	31	<20	<20
W	<10	<10	<10	<10	<10	<10	<10
Pb	21	<10	<10	<10	<10	<10	12
Bi	<5	5	<5	<5	<5	<5	<5
Th	<10	<10	12	<10	10	11	<10
U	<10	<10	<10	<10	<10	<10	<10
FeOt	11.86	10.90	9.53	9.26	8.61	12.90	10.70
Nb/Zr	0.430	0.457	0.469	0.433	0.446	0.436	
Mg# (0.20)	48.08	42.81	56.90	61.66	67.49	51.23	63.81

Table 15*a* *(continued)*

Field No.	AR137C	FJ448	AR160D	FJ880
Reg. No.	R005063	R004886	R005075	R004911
Anal. No	920464	961001	920466	961017
AMG (mE)	325250	324660	322900	328900
AMG (mN)	5446920	5442900	5446240	5442030
Group	picrite	picrite	altered	altered
SiO_2 (%)	33.95	38.75	41.51	59.22
TiO_2	2.95	0.30	0.99	1.94
Al_2O_3	6.26	7.28	16.80	16.09
Fe_2O_3	3.55	6.46	2.41	9.91
FeO	9.84	5.63	7.86	1.74
MnO	0.12	0.18	0.17	0.09
MgO	17.19	26.33	7.28	0.66
CaO	9.12	4.72	8.02	1.96
Na_2O	0.07	0.10	3.73	6.08
K_2O	0.65	0.19	0.53	0.36
P_2O_5	0.66	0.21	0.46	0.21
SO_3 (tot)	0.33	0.08	0.08	0.07
SO_3 (ate)				
SO_3 (ide)				
CO_2	8.08	0.09	3.98	0.13
H_2O^+	6.52	8.94	5.81	1.28
TOTAL	**99.29**	**99.27**	**99.64**	**99.72**
Sc (ppm)	12	21	20	45
V	260	110	210	360
Cr	630	1800	65	120
Co	81	100	54	20
Ni	700	1050	115	50
Cu	85	27	43	9
Zn	115	64	115	92
Ga	17	6	16	17
As	<20	<20	<20	<20
Rb	37	15	15	7
Sr	520	34	65	165
Y	18	11	20	24
Zr	180	61	74	125
Nb	42	25	21	9
Mo	<5	<5	<5	<5
Sn	<9	<9	<9	<9
Ba	360	130	260	125
La	32	21	22	<20
Ce	102	35	50	<28
Nd	64	<20	32	<20
W	<10	<10	<10	<10
Pb	19	<10	16	<10
Bi	7	<5	5	<5
Th	<10	10	<10	<10
U	<10	<10	<10	<10
FeOt	13.03	11.44	10.03	10.66
Nb/Zr	0.233	0.410	0.284	0.072
Mg# (0.20)	73.50	82.88	60.43	11.53

Table 15*b*

Previously published analyses, Spinks Creek Volcanics

Field No.	ABS36	ABS37	ABS38	42167	42168	42159	42165	42169	42176	42181
Reg. No.	85/0081	85/0083	85/0082	-	-	-	-	-	-	-
Anal. No	814100	814102	814101	-	-	-	-	-	-	-
AMG (mE)	343200	343200	343200	334170	334170	333990	334080	333720	338510	338240
AMG (mN)	5479350	5479450	5479600	5446720	5446720	5446900	5446720	5446980	5451150	5451600
Group	P	P	P	P	P	A	A	A	A	A
SiO_2 (%)	45.87	46.69	47.03	50.10	49.59	49.59	48.12	49.55	48.86	49.21
TiO_2	0.66	0.68	0.67	0.67	0.65	0.70	0.69	0.69	0.71	0.70
Al_2O_3	14.44	14.48	14.76	13.72	12.30	13.97	13.67	14.33	14.12	14.20
Fe_2O_3	3.68	3.18	2.71	10.22	10.58	13.56	13.91	13.12	12.94	13.49
FeO	6.04	6.27	6.72	nd	nd	nd	nd	nd	nd	nd
MnO	0.19	0.17	0.16	0.18	0.26	0.21	0.28	0.24	0.22	0.23
MgO	10.67	10.04	10.11	8.67	10.98	7.32	7.48	8.13	7.75	7.79
CaO	9.95	10.30	9.87	7.51	9.01	11.04	11.63	9.71	10.70	10.39
Na_2O	2.61	2.70	2.13	3.79	2.94	3.02	2.41	3.48	2.66	2.74
K_2O	0.14	0.15	0.63	0.58	0.53	0.46	0.30	0.40	0.23	0.32
P_2O_5	0.16	0.16	0.17	0.15	0.14	0.15	0.13	0.13	0.13	0.13
SO_3	nd	nd	nd	nd	nd	nd	nd	nd	nd	nd
CO_2	0.08	0.04	0.07	nd	nd	nd	nd	nd	nd	nd
H_2O^+	4.62	4.32	4.20	nd	nd	nd	nd	nd	nd	nd
H_2O^-	0.23	0.22	0.26	nd	nd	nd	nd	nd	nd	nd
LOI	-	-	-	3.57	4.30	1.59	1.90	1.97	2.53	1.98
TOTAL	**99.34**	**99.40**	**99.49**	**99.16**	**101.28**	**101.61**	**100.52**	**101.75**	**100.85**	**101.18**
Sc (ppm)	50	48	46	nd	nd	nd	nd	nd	nd	nd
V	210	220	220	236	295	349	370	354	323	293
Cr	952	777	767	789	876	165	172	163	171	123
Co	nd	nd	nd	nd	nd	nd	nd	nd	nd	nd
Ni	297	226	230	308	259	105	104	105	105	107
Cu	nd	nd	nd	nd	nd	nd	nd	nd	nd	nd
Zn	nd	nd	nd	nd	nd	nd	nd	nd	nd	nd
Ga	nd	nd	nd	nd	nd	nd	nd	nd	nd	nd
As	nd	nd	nd	nd	nd	nd	nd	nd	nd	nd
Rb	nd	nd	9	10	18	13	6	10	3	10
Sr	566	532	140	188	114	164	172	28	151	241
Y	15	15	18	23	26	24	23	25	24	22
Zr	72	71	65	93	91	66	58	69	60	65
Nb	15	13	13	nd	nd	nd	nd	nd	nd	nd
Ag	nd	nd	nd	nd	nd	nd	nd	nd	nd	nd
Sb	nd	nd	nd	nd	nd	nd	nd	nd	nd	nd
Ba	420	490	830	512	208	143	147	162	117	133
La	nd	nd	nd	nd	nd	nd	nd	nd	nd	nd
Ce	nd	nd	nd	nd	nd	nd	nd	nd	nd	nd
Nd	nd	nd	nd	nd	nd	nd	nd	nd	nd	nd
W	nd	nd	nd	nd	nd	nd	nd	nd	nd	nd
Bi	nd	nd	nd	nd	nd	nd	nd	nd	nd	nd
Th	nd	nd	nd	nd	nd	nd	nd	nd	nd	nd
U	nd	nd	nd	nd	nd	nd	nd	nd	nd	nd
FeOt	9.35	9.13	9.16	9.20	9.52	12.20	12.52	11.81	11.64	12.14
Nb/Zr	0.208	0.183	0.200	nd	nd	nd	nd	nd	nd	nd
Mg# (0.20)	70.59	69.81	69.90	66.48	70.81	55.79	55.69	59.16	58.33	57.44

Analyses from Griffin (1974), Brown (1985, 1989*a*) and R. G. Richardson and J. W. Hudspeth (data in MRT ROCKCHEM database)

Table 15*b* *(continued)*

Field No.	-	42144	42171	42185	ABS20	ABS21	ABS28	ABS40	SB11	SB16
Reg. No.	G401285	-	-	-	85/0780	85/0781	85/0779	85/0084	85/0782	85/0079
Anal. No	891796	-	-	-	814087	814088	814094	814104	813132	813133
AMG (mE)	347000	333620	333900	340060	340900	340800	342600	341900	349200	348750
AMG (mN)	5476850	5446900	5446900	5451720	5462400	5468450	5478500	5472450	5471250	5471400
Group	B	B	B	B	C	C	C	C	C	C
SiO_2 (%)	48.31	48.08	48.65	48.64	47.41	48.29	48.58	47.74	49.72	47.23
TiO_2	1.12	1.06	1.06	1.07	1.69	1.74	1.68	1.56	1.57	1.67
Al_2O_3	14.60	14.00	14.16	14.96	13.81	13.83	14.32	13.96	14.12	14.27
Fe_2O_3	4.92	12.39	12.60	12.72	5.54	5.01	4.50	4.70	7.60	5.23
FeO	7.32	nd	nd	nd	7.63	7.33	7.94	7.94	4.68	7.18
MnO	0.21	0.18	0.19	0.20	0.17	0.20	0.25	0.20	0.15	0.18
MgO	7.46	5.95	5.99	7.57	6.49	6.60	6.88	6.66	4.65	6.51
CaO	9.77	11.57	11.56	8.18	10.01	8.32	10.58	10.46	7.73	11.24
Na_2O	3.42	2.71	2.06	2.81	2.67	2.87	2.12	2.45	0.21	2.28
K_2O	0.66	-	0.01	0.29	0.35	0.16	0.13	0.56	0.15	0.22
P_2O_5	0.03	0.11	0.11	0.14	0.19	0.19	0.21	0.20	0.16	0.20
SO_3	0.12	nd	nd	nd	nd	nd	nd	nd	nd	nd
CO_2	0.15	nd	nd	nd	0.05	0.05	0.05	0.28	0.85	0.15
H_2O^+	2.46	nd	nd	nd	3.29	4.36	2.37	2.77	6.79	2.79
H_2O^-	nd	nd	nd	nd	0.04	0.06	0.15	0.10	1.18	0.29
LOI	-	4.16	1.27	2.96	-	-	-	-	-	-
TOTAL	**100.55**	**100.21**	**97.66**	**99.54**	**99.34**	**99.01**	**99.76**	**99.58**	**99.56**	**99.44**
Sc (ppm)	39	nd	nd	nd	41	44	39	44	nd	40
V	290	424	202	872	370	370	350	350	nd	350
Cr	210	259	127	244	161	161	249	169	227	260
Co	56	nd	nd	nd	nd	nd	nd	nd	nd	45
Ni	110	95	98	99	81	83	95	87	84	92
Cu	74	nd	nd	nd	nd	nd	nd	nd	nd	nd
Zn	98	nd	nd	nd	nd	nd	nd	nd	nd	nd
Ga	23	nd	nd	nd	nd	nd	nd	nd	nd	nd
As	11	nd	nd	nd	nd	nd	nd	nd	nd	nd
Rb	10	nd	11	nd	5	nd	nd	4	4	nd
Sr	260	28	314	219	225	243	176	210	24	290
Y	19	19	22	21	20	22	20	20	29	23
Zr	55	84	126	102	95	98	100	93	84	97
Nb	nd	nd	nd	nd	6	7	7	5	8	7
Ag	9	nd	nd	nd	nd	nd	nd	nd	nd	nd
Sb	nd	nd	nd	nd	nd	nd	nd	nd	nd	nd
Ba	120	82	134	112	200	260	200	290	nd	240
La	nd	nd	nd	nd	nd	nd	nd	nd	nd	nd
Ce	16	nd	nd	nd	nd	nd	nd	nd	nd	nd
Nd	17	nd	nd	nd	nd	nd	nd	nd	nd	nd
W	nd	nd	nd	nd	nd	nd	nd	nd	nd	nd
Bi	7	nd	nd	nd	nd	nd	nd	nd	nd	nd
Th	nd	nd	nd	nd	nd	nd	nd	nd	nd	nd
U	nd	nd	nd	nd	nd	nd	nd	nd	nd	nd
FeOt	11.75	11.15	11.34	11.45	12.61	11.84	11.99	12.17	11.52	11.89
Nb/Zr	nd	nd	nd	nd	0.063	0.071	0.070	0.054	0.095	0.072
Mg# (0.20)	57.19	52.89	52.64	58.18	51.97	53.97	54.69	53.51	45.92	53.53

Table 15*b* (*continued*)

Field No.	SB18	-	42146	42150	42154	42155	42156	42164	42170	42172
Reg. No.	85/0783	G401286	-	-	-	-	-	-	-	-
Anal. No	813134	891797	-	-	-	-	-	-	-	-
AMG (mE)	348800	346900	333170	337330	333530	330700	330700	330800	332980	332800
AMG (mN)	5471650	5477600	5446890	5451050	5446800	5446400	5446400	5446310	5447070	5446880
Group	C	C	C	C	C	C	C	C	C	C
SiO_2 (%)	46.78	49.25	48.25	50.37	49.25	48.69	48.63	50.07	49.34	49.41
TiO_2	1.63	1.71	1.62	1.49	1.61	1.71	1.69	1.66	1.59	1.60
Al_2O_3	13.87	13.93	13.61	13.55	13.86	13.71	13.83	13.39	13.90	13.68
Fe_2O_3	7.80	6.96	14.27	13.02	14.15	13.94	13.73	13.85	13.95	14.50
FeO	5.28	6.65	nd	nd	nd	nd	nd	nd	nd	nd
MnO	0.17	0.25	0.23	0.19	0.22	0.17	0.18	0.19	0.18	0.24
MgO	5.64	6.42	6.63	5.06	6.50	6.05	6.36	5.97	6.05	6.33
CaO	7.79	8.97	11.01	9.85	10.42	8.69	9.10	8.34	9.48	7.97
Na_2O	3.71	3.49	2.06	2.69	3.10	3.95	4.07	4.81	3.84	4.13
K_2O	0.20	0.75	0.17	0.02	0.52	0.42	0.18	0.15	0.54	0.47
P_2O_5	0.19	0.03	0.17	0.17	0.18	0.17	0.19	0.18	0.17	0.19
SO_3	nd	0.18	nd	nd	nd	nd	nd	nd	nd	nd
CO_2	0.23	0.23	nd	nd	nd	nd	nd	nd	nd	nd
H_2O^+	3.24	1.93	nd	nd	nd	nd	nd	nd	nd	nd
H_2O^-	0.48	nd	nd	nd	nd	nd	nd	nd	nd	nd
LOI	-	-	2.27	4.11	1.47	2.67	2.82	2.35	2.36	2.46
TOTAL	**97.01**	**100.75**	**100.29**	**100.52**	**101.28**	**100.17**	**100.78**	**100.96**	**101.40**	**100.98**
Sc (ppm)	42	38	nd	nd	nd	nd	nd	nd	nd	nd
V	370	340	448	498	572	429	577	547	494	173
Cr	150	100	116	112	226	140	148	148	116	116
Co	47	58	nd	nd	nd	nd	nd	nd	nd	nd
Ni	82	88	75	66	85	78	79	77	78	78
Cu	nd	51	nd	nd	nd	nd	nd	nd	nd	nd
Zn	nd	120	nd	nd	nd	nd	nd	nd	nd	nd
Ga	nd	23	nd	nd	nd	nd	nd	nd	nd	nd
As	nd	nd	nd	nd	nd	nd	nd	nd	nd	nd
Rb	5	9	nd	nd	5	nd	1	nd	4	2
Sr	142	200	134	32	192	188	196	130	94	266
Y	22	24	25	26	25	25	23	26	24	25
Zr	98	97	122	111	132	126	131	138	54	124
Nb	9	6	nd	nd	nd	nd	nd	nd	nd	nd
Ag	nd	11	nd	nd	nd	nd	nd	nd	nd	nd
Sb	nd	nd	nd	nd	nd	nd	nd	nd	nd	nd
Ba	350	200	nd	nd	nd	nd	nd	nd	nd	nd
La	nd	nd	nd	nd	nd	nd	nd	nd	nd	nd
Ce	nd	43	nd	nd	nd	nd	nd	nd	nd	nd
Nd	nd	12	nd	nd	nd	nd	nd	nd	nd	nd
W	nd	75	nd	nd	nd	nd	nd	nd	nd	nd
Bi	nd	7	nd	nd	nd	nd	nd	nd	nd	nd
Th	nd	nd	nd	nd	nd	nd	nd	nd	nd	nd
U	nd	nd	nd	nd	nd	nd	nd	nd	nd	nd
FeOt	12.30	12.91	12.84	11.72	12.73	12.54	12.35	12.46	12.55	13.05
Nb/Zr	0.092	0.062	nd	nd	nd	nd	nd	nd	nd	nd
Mg# (0.20)	49.10	51.12	52.06	47.60	51.78	50.36	51.99	50.19	50.34	50.51

Table 15*b* *(continued)*

Field No.	42173	42174	42175	42177	42178	ABS22	ABS23	ABS24	ABS25	ABS26
Reg. No.	-	-	-	-	-	-	-	-	-	85/0785
Anal. No	-	-	-	-	-	814089	814090	814091	814092	814093
AMG (mE)	332620	339430	336660	338240	335930	324300	324100	320850	321150	342300
AMG (mN)	5446520	5451440	5452870	5451600	5453050	5483600	5483550	5486050	5485150	5479400
Group	C	C	C	C	C	D	D	D	D	D
SiO_2 (%)	48.25	48.29	47.80	47.66	48.55	48.65	48.48	48.05	48.20	48.44
TiO_2	1.78	1.64	1.66	1.61	1.60	2.34	2.31	2.39	2.35	2.32
Al_2O_3	13.43	13.44	13.49	14.17	13.14	13.44	13.45	13.47	13.66	13.25
Fe_2O_3	14.30	13.92	13.81	13.70	14.23	4.77	5.85	4.76	5.38	5.57
FeO	nd	nd	nd	nd	nd	8.16	7.63	8.62	7.86	7.71
MnO	0.18	0.21	0.20	0.23	0.17	0.21	0.21	0.20	0.19	0.21
MgO	6.10	6.76	6.53	6.85	5.90	6.11	5.66	5.85	5.73	6.43
CaO	6.12	9.85	10.28	8.56	10.84	8.31	9.48	10.32	10.49	8.08
Na_2O	4.99	2.46	2.49	2.81	2.72	3.76	3.12	2.30	2.51	3.27
K_2O	0.28	0.36	0.39	0.01	0.18	0.24	0.56	0.23	0.36	0.12
P_2O_5	0.19	0.18	0.18	0.18	0.16	0.26	0.27	0.29	0.29	0.25
SO_3	nd	nd	nd	nd	nd	nd	nd	nd	nd	nd
CO_2	nd	nd	nd	nd	nd	0.11	0.17	0.06	0.09	0.08
H_2O^+	nd	nd	nd	nd	nd	2.95	2.33	2.62	2.64	3.57
H_2O^-	nd	nd	nd	nd	nd	0.13	0.10	0.10	0.14	0.26
LOI	2.60	2.36	1.68	4.55	2.43	-	-	-	-	-
TOTAL	**98.22**	**99.47**	**98.51**	**100.33**	**99.92**	**99.44**	**99.62**	**99.26**	**99.89**	**99.56**
Sc (ppm)	nd	nd	nd	nd	nd	nd	nd	nd	nd	35
V	498	499	453	497	504	nd	nd	nd	nd	380
Cr	124	112	149	122	112	143	142	152	161	161
Co	nd	nd	nd	nd	nd	nd	nd	nd	nd	nd
Ni	73	76	81	70	73	82	76	84	88	85
Cu	nd	nd	nd	nd	nd	nd	nd	nd	nd	nd
Zn	nd	nd	nd	nd	nd	nd	nd	nd	nd	nd
Ga	nd	nd	nd	nd	nd	nd	nd	nd	nd	nd
As	nd	nd	nd	nd	nd	nd	nd	nd	nd	nd
Rb	1	nd	nd	nd	nd	7	15	6	9	4
Sr	158	188	214	32	197	297	266	224	245	293
Y	18	25	27	22	22	24	23	24	23	22
Zr	150	130	123	127	113	147	148	148	144	139
Nb	nd	nd	nd	nd	nd	14	17	15	15	15
Ag	nd	nd	nd	nd	nd	nd	nd	nd	nd	nd
Sb	nd	nd	nd	nd	nd	nd	nd	nd	nd	nd
Ba	nd	nd	nd	nd	nd	nd	nd	nd	nd	250
La	nd	nd	nd	nd	nd	nd	nd	nd	nd	nd
Ce	nd	nd	nd	nd	nd	nd	nd	nd	nd	nd
Nd	nd	nd	nd	nd	nd	nd	nd	nd	nd	nd
W	nd	nd	nd	nd	nd	nd	nd	nd	nd	nd
Bi	nd	nd	nd	nd	nd	nd	nd	nd	nd	nd
Th	nd	nd	nd	nd	nd	nd	nd	nd	nd	nd
U	nd	nd	nd	nd	nd	nd	nd	nd	nd	nd
FeOt	12.87	12.53	12.43	12.33	12.80	12.45	12.89	12.90	12.70	12.72
Nb/Zr	nd	nd	nd	nd	nd	0.095	0.115	0.101	0.104	0.108
Mg# (0.20)	49.93	53.17	52.50	53.89	49.22	50.79	48.01	48.81	48.69	51.53

Table 15*b* (*continued*)

Field No.	-	42147	ABS6	ABS44	ABS52	42145
Reg. No.	G401287	-	85/0784	85/0785	85/0788	-
Anal. No	891798	-	814081	830782	830784	-
AMG (mE)	342350	331440	352750	352740	352740	334080
AMG (mN)	5478550	5446140	5479850	5480110	5480110	5446720
Group	D	D	E	E	VHT	VLT
SiO_2 (%)	51.88	49.28	49.44	50.99	45.22	50.78
TiO_2	2.22	2.32	1.63	1.75	3.59	0.44
Al_2O_3	14.02	13.33	12.67	11.40	12.30	17.22
Fe_2O_3	7.10	14.24	5.60	4.70	1.93	10.60
FeO	5.92	nd	11.28	11.87	13.06	nd
MnO	0.20	0.18	0.24	0.27	0.20	0.21
MgO	5.57	6.02	4.53	4.17	5.81	7.19
CaO	5.73	7.43	7.91	7.15	8.21	5.09
Na_2O	4.30	3.79	2.73	2.80	2.96	3.74
K_2O	0.68	0.63	0.80	0.77	0.19	1.23
P_2O_5	0.05	0.28	0.32	0.40	0.44	0.10
SO_3	0.09	nd	nd	nd	nd	nd
CO_2	0.27	nd	0.08	0.11	0.42	nd
H_2O^+	2.41	nd	2.68	2.86	4.09	nd
H_2O^-	nd	nd	nd	0.14	0.19	nd
LOI	-	4.57	-	-	-	3.53
TOTAL	**100.44**	**102.07**	**99.91**	**99.38**	**98.61**	**100.13**
Sc (ppm)	29	nd	51	53	26	nd
V	360	465	410	420	410	238
Cr	135	136	84	50	30	46
Co	57	nd	nd	42	45	nd
Ni	86	74	42	34	54	53
Cu	14	nd	nd	nd	nd	nd
Zn	125	nd	nd	nd	nd	nd
Ga	27	nd	nd	nd	nd	nd
As	nd	nd	nd	nd	nd	nd
Rb	11	1	18	25	10	37
Sr	250	265	177	110	145	249
Y	32	31	43	49	33	15
Zr	165	200	119	130	230	47
Nb	15	nd	29	27	28	nd
Ag	9	nd	nd	nd	nd	nd
Sb	nd	nd	nd	nd	nd	nd
Ba	300	nd	720	290	75	572
La	6	nd	nd	nd	nd	nd
Ce	53	nd	nd	nd	nd	nd
Nd	26	nd	nd	nd	nd	nd
W	nd	nd	nd	nd	nd	nd
Bi	6	nd	nd	nd	nd	nd
Th	nd	nd	nd	7	5	nd
U	11	nd	nd	nd	nd	nd
FeOt	12.31	12.81	16.32	16.10	14.80	9.54
Nb/Zr	0.091	nd	0.244	0.208	0.122	nd
Mg# (0.20)	48.77	49.70	36.86	35.27	45.23	61.32

Table 15*c*

INAA and ICPMS analyses, Spinks Creek Volcanics

Field No.	AR164	ABS36	ABS37	ABS38	AR100	FJ162	FJ826	TJ926	TJ1586	FJ1091	AR106
Reg. No.	R005078	85/0081	85/0082	85/0083	R005046	R004875	R004908	R005157	R005164	R004921	R005048
Group	P	P	P	P	A	A	A	B	B	B	C
Method	INAA	INAA	INAA	INAA	ICPMS	ICPMS	INAA	ICPMS	INAA	ICPMS	ICPMS
La (ppm)	10.07	13.04	13.74	12.67	8.22	8.18	7.55	5.83	4.30	5.64	7.11
Ce	19.54	27.92	29.12	26.85	15.2	15.5	14.80	13.6	10.80	13.2	17.9
Pr	nd	nd	nd	nd	1.87	1.91	nd	2.01	nd	1.97	2.81
Nd	9.28	11.89	12.36	12.55	6.9	7.1	6.77	8.6	8.02	8.6	12.7
Sm	2.25	2.57	2.71	2.54	1.8	1.8	1.82	2.5	2.39	2.5	3.6
Eu	0.71	0.76	0.79	0.74	0.61	0.62	0.66	0.82	0.84	0.80	1.13
Gd	nd	2.57	2.82	2.67	3.3	3.2	nd	3.7	nd	3.6	5.0
Tb	0.41	0.44	0.56	0.51	1.13	1.06	0.47	1.11	0.49	1.08	1.37
Dy	nd	nd	nd	nd	3.9	3.8	nd	3.8	nd	3.8	4.9
Ho	0.64	0.76	0.86	0.75	0.91	0.88	0.80	0.79	0.67	0.80	1.01
Er	nd	nd	nd	nd	3.7	3.5	nd	2.9	nd	2.8	3.4
Tm	nd	0.34	0.37	0.40	0.47	0.47	nd	0.36	nd	0.36	0.42
Yb	1.98	2.63	2.45	2.59	2.8	2.7	2.65	2.0	1.72	2.0	2.4
Lu	0.30	0.42	0.37	0.42	0.4	0.4	0.42	0.3	0.24	0.3	0.3
(La/Yb)N	3.43	3.34	3.78	3.30	1.98	2.04	1.92	1.97	1.69	1.90	2.00
Ta	0.71	nd	nd	nd	1.6	5.0	1.11	3.4	<0.50	5.3	1.2
Hf	1.40	nd	nd	nd	2.9	2.7	1.23	3.7	1.45	3.8	5.5
Th	2.37	nd	nd	nd	1.50	1.44	0.88	0.65	0.89	0.65	0.67
Nb	nd	nd	nd	nd	16.5	30.2	nd	16.5	nd	24.1	10.2
Sc	nd	nd	nd	nd	nd	nd	54.8	nd	nd	nd	nd
Au	nd	nd	nd	nd	nd	nd	<0.003	nd	nd	nd	nd

Field No.	TJ1582	TJ2105	TJ2142	FJ460	MRS31	MRS39	SB16	ABS40	FJ473	MRS8	ABS25
Reg. No.	R005162	R002565	R005170	R004888	R002873	R002881	85/0079	85/0078	R004890	R002850	85/0079
Group	C	C	C	C	C	C	C	C	D	D	D
Method	INAA	ICPMS	ICPMS	ICPMS	ICPMS	ICPMS	INAA	INAA	ICPMS	ICPMS	INAA
La (ppm)	6.06	6.27	7.37	6.76	8.57	9.10	7.26	8.13	18.4	16.2	14.73
Ce	14.22	15.9	18.6	17.8	21.6	22.5	18.01	19.89	41.0	38.6	35.36
Pr	nd	2.51	2.89	2.76	3.15	3.29	nd	nd	5.59	5.48	nd
Nd	11.23	11.2	12.9	12.6	14.0	14.4	12.11	12.51	22.7	22.8	20.48
Sm	3.51	3.3	3.7	3.7	3.9	4	3.84	3.18	5.4	5.6	5.22
Eu	1.32	1.05	1.17	1.18	1.22	1.21	1.41	1.38	1.64	1.58	1.74
Gd	nd	4.7	5.2	5.1	5.1	5.5	4.60	4.16	6.4	6.5	5.54
Tb	0.79	1.34	1.48	1.46	1.43	1.56	0.84	0.70	1.49	1.50	0.90
Dy	nd	4.4	5.0	4.9	5.0	5.2	nd	nd	5.8	5.9	nd
Ho	1.08	0.89	1.03	0.98	1.03	1.04	1.22	0.97	1.14	1.18	0.99
Er	nd	3.1	3.5	3.2	3.4	3.5	nd	nd	3.4	3.5	nd
Tm	nd	0.38	0.44	0.40	0.43	0.44	0.40	0.35	0.45	0.47	0.40
Yb	2.20	2.0	2.4	2.1	2.4	2.4	2.81	2.61	2.5	2.5	2.49
Lu	0.24	0.3	0.3	0.3	0.3	0.3	0.43	0.38	0.3	0.3	0.37
(La/Yb)N	1.86	2.11	2.07	2.17	2.41	2.56	1.74	2.10	4.96	4.37	3.99
Ta	0.74	2.7	3.2	4.7	1.7	2.3	nd	nd	4.1	2.5	nd
Hf	2.27	4.6	5.6	5.0	5.5	6.2	nd	nd	8.1	8.5	nd
Th	0.92	0.6	0.69	0.78	0.78	0.83	nd	nd	1.84	1.79	nd
Nb	nd	14.8	16.8	28.9	13.7	16.1	nd	nd	30.7	24.8	nd
Sc	nd	nd	nd	nd	nd	nd	nd	nd	nd	nd	nd
Au	nd	nd	nd	nd	nd	nd	nd	nd	nd	nd	nd

Analyses prefixed by ABS and SB presented by Brown (1986), remainder are new data
INAA analyses by Becquerel Laboratories, NSW
ICPMS analyses by Analabs, WA

Table 15*c* (*continued*)

Field No.	ABS26	HR112	MJ1617	AR160C	FJ145	FJ360	FJ481	AR161	FJ448
Reg. No.	85/0080	R005587	R006759	R005074	R004872	R004883	R004892	R005076	R004886
Group	D	E	E	F	F	F	F	VLT	Picrite
Method	INAA	INAA	INAA	ICPMS	INAA	ICPMS	ICPMS	ICPMS	ICPMS
La (ppm)	15.36	45.90	46.30	35.9	52.00	50.5	33.1	11.2	18.5
Ce	36.71	87.30	85.80	68.2	91.90	90.7	61.7	24.9	33.8
Pr	nd	nd	nd	7.56	nd	9.80	6.86	3.14	3.74
Nd	22.20	37.80	36.20	24.5	36.10	32.1	22.8	11.5	12.7
Sm	5.34	7.09	6.80	4.2	5.98	5.3	3.9	2.5	2.2
Eu	1.60	2.00	1.97	1.28	1.72	1.68	1.43	1.38	0.61
Gd	5.54	nd	nd	4.1	nd	4.8	4.2	2.8	2.0
Tb	0.98	1.41	1.14	0.61	0.96	0.63	0.79	0.72	0.29
Dy	nd	nd	nd	5.2	nd	5.4	4.8	3.5	2.2
Ho	1.10	2.22	1.78	1.18	1.33	1.19	1.09	0.81	0.47
Er	nd	nd	nd	3.9	nd	3.8	3.8	3.1	1.5
Tm	0.39	nd	nd	0.58	nd	0.57	0.55	0.43	0.22
Yb	2.50	6.47	6.04	3.6	3.75	3.6	3.3	2.7	1.4
Lu	0.38	1.00	0.97	0.5	0.57	0.5	0.5	0.4	0.2
(La/Yb)N	4.14	4.78	5.17	6.72	9.35	9.46	6.76	2.80	8.91
Ta	nd	4.33	4.37	3.6	4.48	8.6	7.8	2.7	2.2
Hf	nd	5.39	5.03	4.4	3.67	6.3	4.8	3.6	2.5
Th	nd	8.45	8.20	4.57	8.45	8.38	4.17	3.47	2.74
Nb	nd	nd	nd	58.9	nd	93.5	77.8	22.0	28.0
Sc	nd	42.8	39.5	nd	24.4	nd	nd	nd	nd
Au	nd	<0.003	<0.003	nd	<0.003	nd	nd	nd	nd

Table 16

Summary of petrography, Spinks Creek Volcanics

Field No.	Reg. No.	Suite	TiO_2 (%)	X ($\times 10^{-3}$)	grain size	phenocrysts plag	cpx	ol	Opaques	Comments
MRS8	R002850	D	2.39		c	r	r		mostly fresh	
MRS9	R002851	C	1.66		mc		r		large (to 700 μm), skeletal, partly oxidised	
MRS20	R002862	C	1.67		f	c			very fine grained, fresh	turbid groundmass with altered cpx; chlorite amygdales
MRS26	R002868	C	1.56		m		r		slightly oxidised	
MRS31	R002873	C	1.67		m	s	r		large (to 500 μm), skeletal, fresh	amygdales of prehnite, vf grained silica (?)
MRS35	R002877	D	2.32		mc	r			mostly fresh	large (13 mm) amygdale (prehnite)
MRS39	R002881	C	1.68		f	s			mostly fresh	irregular amygdales of yellow-green chlorite
FJ89	R004869	C	1.78	51.4	mf	c	r		fresh	large (3 mm) amygdale of albite-prehnite-epidote
FJ99A	R004870	D	2.38	59.4	m	r	r		mostly fresh	scattered amygdales (fine-grained green chlorite)
FJ143	R004871	B	1.10	23.0	m/vf	a	c	s	mostly fresh	microporphyritic groundmass
FJ145	R004872	F	1.26	0.63	g				mostly sphene	microgabbroic, ophitic
FJ162	R004875	A	0.73	16.2	mf	s	r	s	fresh	pumpellyite replacing olivine
FJ165	R004876	C	1.59	25.0	c				large (to 500 μm), fresh	aphyric; amygdale (2.5 mm) of pale green chlorite
FJ168	R004877	C	1.63	41.7	m	r			fresh	amygdale (1 mm) of chlorite
FJ284	R004878	F	0.91	0.45	g				mostly sphene	microgabbroic, ophitic
FJ315	R004880	C	1.73	45.7	vf				very fine grained	amygdales of pale green chlorite
FJ317	R004881	C	1.79	42.3	mf	c			partly altered	very turbid plagioclase; epidote grains and veinlets
FJ322	R004882	B	1.08	23.5	m/vf	a	c	r	fresh	microporphyritic groundmass
FJ360	R004883	F	0.87	1.73	g				mostly sphene	microgabbroic, ophitic
FJ363	R004884	F	0.83	0.54	g				mostly sphene	microgabbroic, ophitic
FJ448	R004886		0.33	50.7					mostly fresh, some oxidised	picrite
FJ460	R004888	C	1.63	41.8	m	c	s		partly altered	abundant pale green chlorite in groundmass
FJ464	R004889	D	2.27	49.6	m		r		mostly fresh	
FJ473	R004890	D	2.31	>25.9	m		r		fresh	
FJ477	R004891	D	2.35	79.3	mc	r	r		partly altered	pumpellyite confirmed
FJ481	R004892	F	0.87	9.07	m	c			fresh	fluidal, ophitic
FJ542	R004893	D	2.19	54.5	m				partly altered	numerous amygdales (chlorite, albite, epidote)
FJ593	R004894	C	1.71	35.5	f	c	r		mostly fresh	
FJ603	R004896	C	1.63	32.1	m	s	r		mostly fresh	
FJ641	R004900	C	1.62	71.7	f	c		?	very fine grained, fresh	amygdaloidal zones with chlorite
FJ731	R004902	C	1.71	21.7	m	s			partly altered	
FJ790A	R004904	P	0.59	0.56	vc				partly altered to sphene	very pale yellow chlorite present
FJ808	R004905	C	1.70	78.4	f	s			fresh	turbid groundmass with altered cpx (to sphene?)
FJ812	R004906	C	1.72	0.89	m	s			large (to 500 μm), partly altered, oxidised	opaques probably recrystallised
FJ821	R004907	C	1.61	10.3	mc	s	s	s	partly oxidised	very turbid groundmass with hematitic alteration
FJ826	R004908	A	0.71	15.7	mf	r		s	mostly fresh	abundant pale yellow-green chlorite
FJ833	R004909	C	1.61	53.6	m	c	s	r	rimmed by sphene	
FJ865	R004910	B	1.09	47.6	mc	a	c	s	partly altered to sphene	
FJ880	R004911		1.96	13.2	mf	s			partly oxidised	altered
FJ892	R004912	C	1.64	44.3	m	s			large (to 700 μm), skeletal, fresh	

Field No.	Reg. No.	Suite	TiO_2 (%)	X ($\times 10^{-3}$)	grain size	phenocrysts plag	cpx	ol	Opaques	Comments
FJ906	R004913	C	1.66	43.2	mf	s			mostly fresh	
FJ955	R004916	C	1.55	63.2	m	c	s		mostly fresh	very turbid plagioclase
FJ963	R004917	C	1.68	29.9	c	s			large (to 1 mm), skeletal, fresh	
FJ964	R004918	C	1.63	7.63	mf	c		r	partly oxidised	hematitic alteration in groundmass
FJ978	R004919	C	1.68	29.1	m	s		r	mostly fresh	
FJ1091	R004921	B	1.09	44.5	m	s	c	s	fresh	abundant yellow-green chlorite in groundmass
FJ1111	R004922	A	0.69	13.3	mf			r	partly oxidised	some oxidation
FJ1122	R004923	C	1.57	41.6	m	s			mostly fresh	
AR100	R005046	A	0.69	19.7	m		r	c	fresh	pumpellyite(?) present, partly oxidised
AR103	R005047	C	1.66	>23.1	mc	s	c	s	partly oxidised	hematite in groundmass
AR106	R005048	C	1.53	>23.8	f	c	s	?	partly oxidised	
AR111	R005050	D	2.18	>43.9	mc	r	r		mostly fresh	
AR112	R005051	C	1.63	>36.3	m	c		c	large (to 1 mm), skeletal, fresh	amygdales (to 2.5 mm) of prehnite
AR113	R005052	C	1.61	105	f	s		r	very fine grained, fresh	
AR137C	R005063		2.95	>3.90	c				partly altered to sphene, some oxidised	altered picrite
AR160C	R005074	F	0.85	44.8	m		?		partly altered	
AR160D	R005075	F?	0.99	>3.91	m?				mostly fresh	altered
AR161	R005076	VLT	0.45	>0.52	mf				very sparse, opaques and sphene	
AR164	R005078	P	0.58	0.56	g				mostly sphene	
TJ926	R005157	B	1.06	24.6	mc	c	s		fresh	large (6 mm) chlorite amygdale
TJ984	R005158	C	1.70	>>14.2	mf	c			partly oxidised	very turbid groundmass; epidote veinlets present
TJ988	R005160	C	1.65		m	c	r	r	large (to 400 m), partly oxidised	
TJ1582	R005162	C	1.60	>>0.36	c	c	c		mostly altered to sphene	
TJ1586	R005164	B	1.02	>5.34	c	c	s	r	partly sphene	abundant yellow-green chlorite in groundmass
TJ2101	R005167	C	1.51	>29.4	m	r	r	r	fresh	
TJ2103	R005168	C	1.70	>28.3	m	c	c		fresh	very turbid plagioclase
TJ2105	R005169	C	1.44	>13.5	m	s	c		fresh	
TJ2142	R005170	C	1.60	>24.9	m	s	c	r	fresh	very turbid plagioclase
TJ2144	R005171	B	1.03	38.3	mc	a	c	s	mostly fresh	abundant yellow-green chlorite in groundmass
TJ2147	R005172	C	1.60	>17.3	m		c		mostly fresh	unusual amygdale present
TJ3085	R005174	C	1.65	>30.1	c	c	c		mostly fresh	abundant irregular amygdales of yellow-green chlorite
TJ3092	R005175	B	1.03	0.51	mc	a	c	s	sphene	abundant yellow-green chlorite in groundmass
TJ3116	R005178	C	1.60	>28.7	m	?	s		mostly fresh	abundant green chlorite in groundmass
TJ3238	R005179	C	1.61	0.66	c	a	c	r	altered to sphene	abundant yellow-green chlorite in groundmass
TJ3246	R005180	C	1.56	48.3	c	a	c		mostly fresh	abundant green chlorite in groundmass
TJ3384	R005182	C	1.65	23.7	m		c		large (to 500 m), mostly fresh	abundant green chlorite in groundmass
TJ3388	R005183	C	1.65	28.4	m	s	r	r	mostly fresh	very turbid groundmass
HR15	R005565	C	1.60	0.46	vf	s	r		altered, oxidised	
HR35	R005567	B	1.06	0.52	mc	a	s	c	sphene	
HR47	R005573	B	1.09	0.43	m	a	s	r	mostly sphene	intergranular groundmass with fresh plagioclase
HR49	R005574	B	1.09	0.34	mf	c	c	c	sphene	
HR52	R005576	C	1.63	21.2	m		s	r	fresh	
HR53	R005577	C	1.63	0.54	m	c	s		altered to sphene	
HR57	R005578	C	1.62	22.9	mc		r	r	mostly fresh	

Field No.	Reg. No.	Suite	TiO_2 (%)	X ($\times 10^{-3}$)	grain size	phenocrysts plag	cpx	ol	Opaques	Comments
HR60	R005579	B	1.07	21.1	m	c	c	r	sphene	large (4 3 mm) chlorite amygdale
HR63	R005580	B	1.06	10.8	mc	a	c	s	fresh	amygdale with chlorite and prehnite
HR112	R005587	E	2.14	2.79	m	c	r		partly altered	
HR114	R005588	B	1.05	0.47	mc	a	c	s	mostly sphene	
HR118	R005589	C	1.66	29.6	mf	c			mostly fresh	round amygdale (1 mm) with carbonate, zeolite
HR122	R005590	C	1.65	39.5	f	s		r?	fresh	
HR125	R005592	C	1.77	34.7	vf	s		r?	partly altered to sphene	vesicular
MJ547	R006724	B	1.03	14.0	mc	a	c	c	fresh	microporphyritic groundmass with abundant pale green chlorite
MJ549	R006725	B	1.10	31.3	mc	a	c	c	mostly fresh	
MJ560	R006727	C	1.57	53.5	f	r			partly altered to sphene	pale green chlorite amygdales, albite-epidote veinlets
MJ582	R006728	B	1.04	17.8	mc	c	s	r	fresh	
MJ598	R006729	B	1.02	0.55	mc	a	c	s	sphene	abundant yellowish chlorite in groundmass
MJ628	R006730	C	1.62	32.2	m	c			fresh	altered plagioclase phenocrysts; abundant yellow-green chlorite
MJ634	R006731	C	1.49	25.2	m	c	c	s	fresh	
MJ641	R006732	B	1.05	0.45	m	c	c		sphene	
MJ647	R006733	C	1.63	26.9	c	a	c		fresh	pale yellow-green chlorite in groundmass
MJ673	R006735	C	1.63	28.1	m	c?	c	r	fresh	metamorphic groundmass with pumpellyite
MJ709	R006739	B	1.03	6.31	mc	a	c	s	mostly fresh	microporphyritic groundmass
MJ725	R006740	A	0.68	7.16	mf		r	c	mostly fresh	some oxidation; pumpellyite(?) present
MJ855	R006744	C	1.65	38.0	f	c	s		fresh	chlorite amygdales
MJ880	R006745	B	1.10		m	a	c	s	sphene	hematitic veinlets present
MJ965	R006747	B	1.04	0.52	m	a	c	s	mostly sphene	
MJ966	R006748	C	1.63	108	f	c			fresh	irregular amygdales with carbonate, chlorite
MJ994	R006749	C	1.64	32.4	mc	c	c		mostly fresh	
MJ998	R006750	E	2.06	48.1	m	c	s		mostly fresh	
MJ1009	R006751	E	2.22	2.27	mc	s	r	r	mostly sphene	
MJ1028	R006752	B	1.08	43.7	mc	a	c	r	partly sphene	
MJ1032	R006754	C	1.67	94.7	f	c	s		fresh	minor epidote
MJ1088	R006755	C	1.66	23.7	mc	c			partly sphene, also oxidised	
MJ1455	R006757	C			c	s	s	s	nearly fresh	almost microporphyritic, very altered plagioclase
MJ1613	R006758	B			mc/vf	ab	c	s	partly altered to sphene	microporphyritic, epidote present, albite veinlets
MJ1617	R006759	E			c	c	r		nearly fresh	groundmass very feldspathic, some yellow-green chlorite
MJ1618	R006760	E			mc	c			partly altered and oxidised	groundmass, feldspathic, altered
Samples not analysed										
004283	R004283				mf				hematite	amygdaloidal, altered
004284	R004284				mf	r			partly altered to sphene	
004289	R004289				f	s?		s		leucocratic, altered
004290	R004290				mf	s?			hematite?	cleaved, altered
004291	R004291				f	r			mostly fresh	
004292	R004292				f	s?			mostly fresh	
004293	R004293	C?			mf	c			partly sphene	see FJ317 (same locality)
FJ154A	R004873				c				oxidised	very altered; silica amygdales, may have goethite(?) cores
FJ160	R004874	A?		15.9	f	s	r	s	mostly fresh	altered to prehnite, similar to FJ162

Field No.	Reg. No.	Suite	TiO_2 (%)	X ($\times 10^{-3}$)	grain size	phenocrysts plag	cpx	ol	Opaques	Comments
FJ312	R004879			0.56	vf		?		altered to sphene	very altered epidote-rich groundmass; quartz veinlets
FJ447	R004885				g				very sparse, fresh	picrite; see description in text
FJ456	R004887	A?		0.48	m			c	very sparse and altered to sphene	
FJ596	R004895	C?		26.9	mc	s			fresh	relatively fresh groundmass with minor yellow-green chlorite
FJ606	R004897	C?		>28.4	m	ab	r	?	large (to 500 m), skeletal, mostly fresh	abundant yellow-green chlorite
FJ625	R004899	C?		37.5	m	s			large (to 1.5 mm), skeletal, mostly fresh	abundant yellow-green chlorite, similar to FJ892
FJ680	R004901	C?		0.64	m	c	s	r	altered to sphene	
FJ746	R004903	F?		0.32	g				almost all altered to sphene	weathered equivalent of FJ360
FJ917	R004914			0.37	f	c?			fine-grained, recrystallised	very altered, unidentified pink secondary mineral
FJ920	R004915	C?		4.74	f	c		r	fresh to slightly oxidised	
FJ983	R004920				mc	c			oxidised	extremely weathered
TJ1649	R005145				mc				very sparse	aphyric, subophitic, clast in diamictite
TJ925	R005156	E?		69.9	c	c	r		mostly fresh	groundmass cpx mostly oxidised; yellow-green chl amygdales
TJ987	R005159	C?		56.1	vf	c	r		fresh, small (<25 m)	quartz in amygdales; plagioclase phenocrysts very altered
TJ1580	R005161	C?		84.1	f	c	r		fresh to oxidised, small (<30 m)	plag. phenocrysts altered to prehnite, minor chlorite, epidote
TJ1583	R005163	B?		0.52	m/vf	ab	c	?	altered to sphene	microporphyritic, chlorite amygdales, carbonate alteration
TJ1643	R005165	B?		0.66	mc	ab	c	s	altered to sphene	abundant greenish-brown chlorite
TJ2099	R005166			0.55	mf/vf	ab	c		altered to sphene	microporphyritic, ab chl carb in groundmass and amygdales
TJ2156	R005173	C?		>0.38	m		r		mostly altered to sphene	abundant yellow-green chlorite
TJ3099	R005176	B?		39.0	mc	s	s		mostly fresh	abundant yellow-green chlorite
TJ3105	R005177	C?		45.5	m	s	s		mostly fresh	abundant green chl in groundmass, with prehnite in amygdales
TJ3379	R005181	B?		25.0	mc	c	c		mostly fresh	abundant very pale green chlorite in groundmass
HR123	R005591			40.3	mc	s			large (to 500 m), skeletal, mostly fresh	pale green chlorite (partly after olivine) in groundmass
006002	R006002	B?			m/vf	c	c	s	mostly sphene	microporphyritic, see FJ143 (same locality)
006006	R006006				f				fine grained, recrystallised	amygdaloidal, very altered
006011	R006011				mf				fine grained, recrystallised	metabasalt with actinolite
MJ1112X	R006704				mf	r?	r?		turbid sphene and hematite	altered, oxidised, epidote present
MJ550	R006726			1.65	mf	c	c		sparse, mostly altered to sphene	coarse-grained epidote-quartz veinlets
MJ674	R006736	C		24.5	mc		s		fresh	glassy patches in groundmass; chl, minor pumpellyite, cf. TJ2147
MJ731	R006741	C?		18.0	mc	ab	c	s	oxidised	altered with prehnite, yellow-green chlorite
MJ758	R006742	C?		9.70	c	c	s		partly altered to sphene	abundant yellow-green chlorite
MJ815	R006743	B?		0.23	m	s			altered to sphene	altered groundmass with epidote veinlets
MJ1031	R006753	B?		>0.97	m	c	s		almost all altered to sphene	abundant pale yellow chlorite
MJ1104X	R006756	C?		>9.4	m	s	r		large (<700 m), mostly fresh	altered groundmass with much prehnite

vf	very fine grained	r	rare
f	fine grained	s	sparse
mf	medium to fine-grained	c	common
mf	medium grained	ab	abundant
mc	medium to coarse grained		
c	coarse grained		
vc	very coarse grained	X = magnetic susceptibility 10^{-3} SI	
g	gabbroic		

Table 17

Pyroxene, Spinks Creek Volcanics: electron microprobe analyses

Group	P					P						A			
Field No.	AR164					FJ790A						FJ162			
Reg. No.	R005078					R004904						R004874			
AMG (mE)	322780					322940						327850			
AMG (mN)	5446060					5445700						5441060			
Analysis	R1/2	R2	R3/1	R3/2	R4	R1/1	R2/1	R3/1	R4/1	R5/3	R5/4	R4/2	R3	R2/1	R1/2
Form	granule	platelet	platelet	platelet	platelet	granule	granule	granule	platelet	granule	granule	micro	micro	micro	granule
SiO_2	53.730	53.344	53.545	51.554	53.945	52.640	53.161	51.368	51.917	51.400	53.112	49.062	52.274	52.723	52.790
TiO_2	0.243	0.236	0.193	0.595	0.261	0.187	0.279	0.701	0.305	0.454	0.197	0.231	0.297	0.279	0.204
Al_2O_3	2.213	1.804	2.144	1.935	1.843	2.404	1.797	1.717	3.422	1.101	2.230	2.852	1.791	2.148	0.979
Cr_2O_3	0.430	0.044	0.399	0.158	0.079	0.729	-	-	1.062	-	0.729	0.029	0.047	0.210	0.017
V_2O_3	nd	nd	nd	nd	nd	nd	nd	nd	nd	nd	nd	nd	nd	nd	nd
FeOt	5.429	7.979	5.444	13.132	7.196	5.067	6.499	13.160	5.205	19.905	5.133	21.377	10.496	8.618	19.593
MnO	0.158	0.269	0.128	0.396	0.221	0.098	0.212	0.339	0.155	0.487	0.169	0.589	0.259	0.214	0.504
ZnO	nd	nd	nd	nd	nd	nd	nd	nd	nd	nd	nd	nd	nd	nd	nd
NiO	nd	nd	nd	nd	nd	nd	nd	nd	nd	nd	nd	nd	nd	nd	nd
MgO	17.777	16.880	17.508	14.460	17.534	17.300	17.397	14.234	17.012	18.187	17.658	16.999	15.973	16.941	20.981
CaO	21.098	19.938	21.423	18.413	19.987	20.815	20.647	18.263	21.008	7.690	21.341	6.853	18.705	19.157	4.798
Na_2O	0.170	0.164	0.154	0.221	0.166	0.167	0.140	0.243	0.173	0.108	0.152	0.142	0.204	0.158	0.073
K_2O	0.012	-	0.003	-	0.008	0.012	0.005	0.006	-	-	-	-	-	0.012	-
TOTAL	**101.259**	**100.658**	**100.942**	**100.862**	**101.241**	**99.419**	**100.137**	**100.030**	**100.259**	**99.331**	**100.720**	**98.133**	**100.047**	**100.459**	**99.940**
Cations calculated on the basis of Z = 4, (O) = 6															
Si	1.9365	1.9499	1.9374	1.9195	1.9533	1.9328	1.9430	1.9297	1.8929	1.9459	1.9246	1.8878	1.9380	1.9327	1.9646
$Al^{(iv)}$	0.0635	0.0501	0.0626	0.0805	0.0467	0.0672	0.0570	0.0703	0.1071	0.0491	0.0754	0.1122	0.0620	0.0673	0.0354
$Ti^{(iv)}$	-	-	-	-	-	-	-	-	-	0.0050	-	-	-	-	-
$Al^{(vi)}$	0.0305	0.0277	0.0288	0.0044	0.0320	0.0368	0.0204	0.0057	0.0400	-	0.0199	0.0171	0.0163	0.0254	0.0075
$Ti^{(vi)}$	0.0066	0.0065	0.0053	0.0167	0.0071	0.0052	0.0077	0.0198	0.0083	0.0079	0.0054	0.0067	0.0083	0.0077	0.0057
V	nd	nd	nd	nd	nd	nd	nd	nd	nd	nd	nd	nd	nd	nd	nd
Cr	0.0122	0.0013	0.0114	0.0046	0.0023	0.0212	-	-	0.0306	-	0.0209	0.0009	0.0014	0.0061	0.0005
Fe^3	0.0201	0.0198	0.0229	0.0542	0.0103	0.0114	0.0314	0.0430	0.0321	0.0412	0.0346	0.0914	0.0425	0.0322	0.0213
Fe^2	0.1435	0.2241	0.1419	0.3547	0.2077	0.1442	0.1673	0.3705	0.1267	0.5890	0.1210	0.5965	0.2830	0.2320	0.5885
Zn	nd	nd	nd	nd	nd	nd	nd	nd	nd	nd	nd	nd	nd	nd	nd
Mn	0.0048	0.0083	0.0039	0.0125	0.0068	0.0031	0.0066	0.0108	0.0048	0.0156	0.0052	0.0192	0.0081	0.0066	0.0159
Ni	nd	nd	nd	nd	nd	nd	nd	nd	nd	nd	nd	nd	nd	nd	nd
Mg	0.9552	0.9199	0.9444	0.8026	0.9465	0.9469	0.9479	0.7971	0.9247	1.0264	0.9539	0.9751	0.8828	0.9258	1.1640
Ca	0.8147	0.7809	0.8305	0.7345	0.7754	0.8189	0.8086	0.7351	0.8207	0.3119	0.8286	0.2825	0.7430	0.7524	0.1913
Na	0.0119	0.0116	0.0108	0.0159	0.0117	0.0119	0.0099	0.0177	0.0122	0.0079	0.0107	0.0106	0.0147	0.0112	0.0053
K	0.0006	-	0.0001	-	0.0004	0.0006	0.0002	0.0003	-	-	-	-	-	0.0006	-
Mg#	86.94	80.41	86.94	69.35	82.01	86.78	85.00	68.27	87.95	63.54	88.75	62.05	75.73	79.96	66.42
wo	42.58	40.57	43.33	38.83	40.19	42.87	42.03	38.63	43.84	16.18	43.53	14.52	38.08	38.74	9.74
en	49.92	47.79	49.27	42.42	49.05	49.58	49.27	41.90	49.39	53.26	50.11	50.12	45.24	47.66	59.23
fs	7.50	11.64	7.40	18.75	10.76	7.55	8.69	19.47	6.77	30.56	6.36	35.36	16.68	13.60	31.03

Table 17 (*continued*)

Group	A			B				B					
Field No.	MJ725			TJ2144				FJ143					
Reg. No.	R006740			R005171				R004871					
AMG (mE)	328870			333230				325880					
AMG (mN)	5432790			5433200				5439890					
Analysis	R2	R4	R6	R1/3	R1/4	R3/2	R5/1	R5/2	R4/1	R4/2	R2/1	R2/2	R1/1
Form	micro	granule	micro	micro	granule	glom	granule	granule	glom	glom	glom	glom	granule
SiO_2	53.011	52.844	51.863	51.509	51.940	52.117	51.973	52.574	51.944	52.112	51.092	51.038	51.415
TiO_2	0.224	0.216	0.305	0.424	0.377	0.391	0.333	0.259	0.349	0.327	0.421	0.475	0.380
Al_2O_3	2.353	1.997	3.740	4.202	2.577	3.239	3.565	2.180	2.925	2.606	4.036	3.984	3.854
Cr_2O_3	0.249	0.180	0.433	0.608	0.224	0.534	0.469	0.419	0.536	0.489	0.671	0.720	0.593
V_2O_3	nd	nd	nd	nd	nd	nd	nd	nd	nd	nd	nd	nd	nd
FeOt	8.035	8.149	7.731	7.744	8.537	6.647	6.714	7.468	6.310	6.284	7.067	6.902	7.190
MnO	0.201	0.141	0.201	0.187	0.193	0.155	0.120	0.212	0.217	0.136	0.203	0.179	0.098
ZnO	nd	nd	nd	nd	nd	nd	nd	nd	nd	nd	nd	nd	nd
NiO	nd	nd	nd	nd	nd	nd	nd	nd	nd	nd	nd	nd	nd
MgO	16.947	16.626	17.042	17.280	16.928	17.068	16.923	18.154	16.703	16.935	16.355	16.249	16.774
CaO	19.769	20.277	19.026	18.528	20.141	19.854	20.314	18.217	20.946	21.017	20.422	20.433	19.809
Na_2O	0.188	0.146	0.196	0.235	0.223	0.258	0.218	0.194	0.238	0.231	0.231	0.210	0.239
K_2O	-	0.003	-	-	0.005	-	0.010	-	-	-	0.011	-	0.001
TOTAL	**100.976**	**100.578**	**100.538**	**100.717**	**101.143**	**100.262**	**100.638**	**99.677**	**100.169**	**100.137**	**100.507**	**100.189**	**100.354**
Cations calculated on the basis of Z = 4, (O) = 6													
Si	1.9304	1.9351	1.8919	1.8737	1.8888	1.9028	1.8910	1.9284	1.9002	1.9054	1.8663	1.8711	1.8781
$Al^{(iv)}$	0.0696	0.0649	0.1081	0.1263	0.1104	0.0972	0.1090	0.0716	0.0998	0.0946	0.1337	0.1289	0.1219
$Ti^{(iv)}$	-	-	-	-	0.0007	-	-	-	-	-	-	-	-
$Al^{(vi)}$	0.0313	0.0213	0.0527	0.0538	-	0.0422	0.0438	0.0226	0.0263	0.0177	0.0401	0.0433	0.0440
$Ti^{(vi)}$	0.0061	0.0059	0.0084	0.0116	0.0096	0.0107	0.0091	0.0071	0.0096	0.0090	0.0116	0.0131	0.0104
V	nd	nd	nd	nd	nd	nd	nd	nd	nd	nd	nd	nd	nd
Cr	0.0072	0.0052	0.0125	0.0175	0.0064	0.0154	0.0135	0.0122	0.0155	0.0141	0.0194	0.0209	0.0171
Fe^3	0.0322	0.0371	0.0400	0.0483	0.1008	0.0364	0.0493	0.0363	0.0556	0.0611	0.0679	0.0535	0.0568
Fe^2	0.2125	0.2125	0.1958	0.1872	0.1588	0.1666	0.1549	0.1927	0.1375	0.1310	0.1480	0.1581	0.1628
Zn	nd	nd	nd	nd	nd	nd	nd	nd	nd	nd	nd	nd	nd
Mn	0.0062	0.0044	0.0062	0.0058	0.0059	0.0048	0.0037	0.0066	0.0067	0.0042	0.0063	0.0056	0.0030
Ni	nd	nd	nd	nd	nd	nd	nd	nd	nd	nd	nd	nd	nd
Mg	0.9199	0.9076	0.9268	0.9371	0.9177	0.9290	0.9179	0.9927	0.9109	0.9231	0.8907	0.8881	0.9135
Ca	0.7713	0.7955	0.7436	0.7221	0.7848	0.7767	0.7919	0.7159	0.8210	0.8234	0.7993	0.8026	0.7753
Na	0.0132	0.0104	0.0139	0.0165	0.0157	0.0183	0.0154	0.0138	0.0169	0.0164	0.0164	0.0150	0.0169
K	-	0.0001	-	-	0.0002	-	0.0005	-	-	-	0.0005	-	0.0001
Mg#	81.23	81.03	82.55	83.35	85.25	84.80	85.56	83.74	86.89	87.57	85.76	84.89	84.87
wo	40.51	41.53	39.85	39.11	42.16	41.48	42.47	36.95	42.65	42.47	41.94	42.19	40.63
en	48.32	47.38	49.66	50.75	49.31	49.62	49.22	51.23	47.32	47.62	46.73	46.68	47.87
fs	11.16	11.09	10.49	10.14	8.53	8.90	8.31	11.82	10.03	9.91	11.33	11.12	11.51

Table 17 *(continued)*

Group	Group C				C			Group D			Group E	
Field No.	FJ593				MJ673			FJ477			HR112	
Reg. No.	R004894				R006793			R004891			R005587	
AMG (mE)	328180				327840			325150			328240	
AMG (mN)	5442300				5434370			5443890			5431210	
Analysis	R1/1	R3/2	R4/2	R5/1	R1/4	R2/2	R3/3	R5	R3	R1/1	R3	R5
Form	granule	granule	glom	granule	granule	granule	granule	glom	glom	granule	micro	granule
SiO_2	49.354	51.398	52.892	51.165	51.473	53.302	51.364	51.093	51.455	51.038	49.824	49.630
TiO_2	0.531	0.654	0.412	0.664	0.570	0.448	0.626	0.847	0.687	0.742	0.719	1.034
Al_2O_3	3.688	3.629	2.208	3.479	3.234	1.947	2.220	2.540	2.321	2.750	1.983	2.709
Cr_2O_3	0.040	0.144	0.168	0.216	0.324	0.354	0.126	0.140	0.138	0.092	-	0.011
V_2O_3	nd	nd	nd	nd	nd	nd	nd	nd	nd	nd	nd	nd
FeOt	13.361	8.571	7.608	8.601	8.509	8.158	11.297	9.814	10.252	9.835	15.857	15.350
MnO	0.338	0.203	0.212	0.157	0.255	0.285	0.259	0.284	0.275	0.246	0.411	0.441
ZnO	nd	nd	nd	nd	nd	nd	nd	nd	nd	nd	nd	nd
NiO	nd	nd	nd	nd	nd	nd	nd	nd	nd	nd	nd	nd
MgO	15.327	15.992	17.199	16.031	16.561	17.828	15.702	15.913	16.603	16.213	12.847	12.050
CaO	15.780	19.869	19.895	19.884	19.183	18.423	18.461	19.084	18.225	18.533	16.936	18.199
Na_2O	0.223	0.274	0.230	0.227	0.239	0.208	0.233	0.277	0.246	0.253	0.226	0.215
K_2O	0.019	0.027	0.022	-	0.024	0.013	0.010	0.019	0.006	0.016	-	0.001
TOTAL	**98.661**	**100.760**	**100.846**	**100.425**	**100.369**	**100.965**	**100.297**	**100.008**	**100.207**	**99.718**	**98.803**	**99.639**
Cations calculated on the basis of Z = 4, (O) = 6												
Si	1.8658	1.8808	1.9250	1.8793	1.8883	1.9380	1.9047	1.8922	1.8990	1.8924	1.9154	1.8961
$Al^{(iv)}$	0.1342	0.1192	0.0750	0.1207	0.1117	0.0620	0.0953	0.1078	0.1010	0.1076	0.0846	0.1039
$TiO^{(iv)}$	-	-	-	-	-	-	-	-	0.0001	-	-	-
$Al^{(vi)}$	0.0302	0.0372	0.0196	0.0299	0.0281	0.0214	0.0017	0.0030	-	0.0126	0.0052	0.0180
$Ti^{(vi)}$	0.0151	0.0180	0.0113	0.0183	0.0157	0.0122	0.0175	0.0236	0.0190	0.0207	0.0208	0.0297
V	nd	nd	nd	nd	nd	nd	nd	nd	nd	nd	nd	nd
Cr	0.0012	0.0042	0.0048	0.0063	0.0094	0.0102	0.0037	0.0041	0.0040	0.0027	0.0000	0.0003
Fe3	0.0899	0.0625	0.0453	0.0641	0.0608	0.0212	0.0722	0.0743	0.0769	0.0699	0.0546	0.0422
Fe2	0.3325	0.1998	0.1863	0.2001	0.2003	0.2269	0.2781	0.2296	0.2396	0.2350	0.4552	0.4483
Zn	nd	nd	nd	nd	nd	nd	nd	nd	nd	nd	nd	nd
Mn	0.0108	0.0063	0.0065	0.0049	0.0079	0.0088	0.0081	0.0089	0.0086	0.0077	0.0134	0.0143
Ni	nd	nd	nd	nd	nd	nd	nd	nd	nd	nd	nd	nd
Mg	0.8638	0.8724	0.9331	0.8778	0.9057	0.9664	0.8680	0.8785	0.9135	0.8962	0.7363	0.6863
Ca	0.6392	0.7790	0.7758	0.7825	0.7540	0.7177	0.7335	0.7572	0.7206	0.7363	0.6976	0.7450
Na	0.0164	0.0194	0.0162	0.0162	0.0170	0.0147	0.0167	0.0199	0.0176	0.0182	0.0169	0.0160
K	0.0009	0.0012	0.0010	-	0.0011	0.0006	0.0005	0.0009	0.0003	0.0008	-	-
Mg#	72.20	81.36	83.36	81.43	81.89	80.99	75.73	79.28	79.22	79.22	61.80	60.49
wo	33.20	40.71	39.98	40.66	40.54	37.56	39.02	39.04	36.95	38.00	35.89	38.77
en	44.86	45.59	48.09	45.61	48.69	50.57	46.18	45.29	46.83	46.26	37.88	35.71
fs	21.94	13.71	11.93	13.73	10.77	11.87	14.80	15.67	16.22	15.74	26.23	25.52

Table 17 *(continued)*

Group	F							Picrite					VLT		
Field No.	FJ360				FJ481			FJ447A				FJ447	AR161		
Reg. No.	R004883				R004892			R006799				R004885	R005076		
AMG (mE)	325750				325160			324640				324640	322850		
AMG (mN)	5441070				5444050			5442890				5442890	5446160		
Analysis	R1	R2	R3/1	R4	R2/1	R3/1	R4	R2/1	R3/2	R4/1	R4/2	R1/2	R1	R2/1	R2/2
Form	platelet	platelet	platelet	platelet	ophitic	granule	granule	platelet	platelet	platelet	platelet	platelet	granule	micro	granule
SiO_2	51.985	50.639	50.662	50.884	48.030	49.489	48.716	46.843	49.234	49.111	49.324	46.316	52.807	51.462	50.193
TiO_2	0.464	0.512	0.603	0.596	1.477	1.198	1.452	1.928	1.603	0.916	0.861	2.201	0.122	0.261	0.285
Al_2O_3	2.553	4.469	4.762	4.254	4.868	3.185	3.726	6.198	4.253	5.481	5.310	7.161	5.972	2.771	2.852
Cr_2O_3	-	1.113	0.870	0.317	0.022	0.030	0.003	0.273	0.171	0.846	0.925	0.084	0.391	0.784	0.513
V_2O_3	nd	nd	nd	0.035	nd	nd	nd	nd	nd	nd	nd	nd	nd	nd	nd
FeOt	6.449	4.786	5.142	5.554	12.171	13.221	12.830	7.148	6.170	5.402	4.943	7.619	6.430	6.389	6.603
MnO	0.090	0.090	0.060	0.117	0.242	0.290	0.247	0.113	0.182	0.177	0.078	0.119	0.171	0.215	0.111
ZnO	nd	nd	nd	0.101	nd	nd	nd	nd	nd	nd	nd	nd	nd	nd	nd
NiO	nd	nd	nd	0.032	nd	nd	nd	nd	nd	nd	nd	nd	nd	nd	nd
MgO	15.212	15.089	14.958	14.909	10.931	10.936	10.749	13.050	14.199	13.925	14.451	12.118	14.359	17.628	16.135
CaO	23.274	23.375	23.647	23.588	21.805	21.873	21.567	22.861	23.154	23.399	23.195	23.182	14.012	18.367	19.079
Na_2O	0.225	0.248	0.275	nd	0.548	0.591	0.569	0.458	0.466	0.353	0.306	0.473	1.864	0.119	0.153
K_2O	0.006	-	0.001	-	0.003	0.004	0.002	-	0.009	0.002	0.007	-	0.112	-	-
TOTAL	**100.257**	**100.320**	**100.981**	**100.386**	**100.097**	**100.817**	**99.861**	**98.871**	**99.442**	**99.612**	**99.400**	**99.272**	**96.240**	**97.996**	**95.925**
Cations calculated on the basis of Z = 4, (O) = 6															
Si	1.9100	1.8537	1.8433	1.8679	1.8124	1.8612	1.8492	1.7557	1.8270	1.8170	1.8241	1.7352		1.9192	1.9198
$Al^{(iv)}$	0.0900	0.1463	0.1567	0.1321	0.1876	0.1388	0.1508	0.2443	0.1730	0.1830	0.1759	0.2648		0.0808	0.0802
$Ti^{(iv)}$	-	-	-	-	-	-	-	-	-	-	-	-		-	-
$Al^{(vi)}$	0.0206	0.0466	0.0475	0.0519	0.0289	0.0024	0.0159	0.0295	0.0130	0.0560	0.0556	0.0513		0.0410	0.0483
$Ti^{(vi)}$	0.0128	0.0141	0.0165	0.0164	0.0419	0.0339	0.0414	0.0543	0.0447	0.0255	0.0239	0.0620		0.0073	0.0082
V	nd	nd	nd	0.0010	nd	nd	nd	nd	nd	nd	nd	nd		nd	nd
Cr	0.0000	0.0322	0.0250	0.0092	0.0007	0.0009	0.0001	0.0081	0.0050	0.0247	0.0271	0.0025		0.0231	0.0155
Fe^3	0.0601	0.0569	0.0706	0.0371	0.1146	0.1110	0.0940	0.1313	0.0995	0.0767	0.0676	0.1213		0.0106	0.0114
Fe^2	0.1381	0.0896	0.0859	0.1334	0.2695	0.3048	0.3133	0.0927	0.0920	0.0905	0.0853	0.1174		0.1887	0.1998
Zn	nd	nd	nd	0.0027	nd	nd	nd	nd	nd	nd	nd	nd		nd	nd
Mn	0.0028	0.0028	0.0018	0.0036	nd	nd	nd	0.0036	0.0057	0.0055	0.0024	0.0038		0.0068	0.0036
Ni	nd	nd	nd	0.0010	nd	nd	nd	nd	nd	nd	nd	nd		nd	nd
Mg	0.8332	0.8235	0.8114	0.8159	0.6149	0.6131	0.6082	0.7292	0.7855	0.7681	0.7967	0.6768		0.9800	0.9200
Ca	0.9162	0.9168	0.9218	0.9277	0.8816	0.8814	0.8771	0.9181	0.9206	0.9276	0.9191	0.9305		0.7339	0.7819
Na	0.0160	0.0176	0.0194	nd	0.0401	0.0431	0.0419	0.0333	0.0335	0.0254	0.0219	0.0344		0.0086	0.0114
K	0.0003	-	-	-	0.0002	0.0002	0.0001	-	0.0004	0.0001	0.0003	-		-	-
Mg#	85.78	90.19	90.43	85.95	69.53	66.79	66.00	0.8872	0.8952	0.8946	0.9033	0.8522		83.86	82.16
wo	47.04	48.59	48.78	48.47	46.88	46.14	46.34	49.06	48.51	49.80	49.18	50.41		38.57	41.11
en	42.78	43.64	42.94	42.62	32.70	32.10	32.14	38.97	41.40	41.23	42.64	36.66		51.51	48.38
fs	10.17	7.77	8.28	8.91	20.42	21.77	21.52	11.97	10.09	8.97	8.18	12.93		9.92	10.51

nd = not determined; micro = microphenocryst; glom = glomerocryst; Mg# = 100Mg/(Mg + Fe^2); wo:en:fs is Ca:Mg:Fe^2.
Analyses by Cameca SX-50 electron microprobe, Central Science Laboratory, University of Tasmania. Analyst: J. L. Everard

Cations not calculated for analysis AR161/R1 due to probable contamination by feldspar

Table 18

Feldspars, Spinks Creek Volcanics: electron microprobe analyses

Group	P					A		B				
Field No.	AR164	FJ790A				FJ162	MJ725	TJ2144		FJ143		
Reg. No.	R005078	R004904				R004874	R006740	R005171		R004871		
AMG (mE)	322780	322940				327850	328870	333230		325880		
AMG (mN)	5446060	5445700				5441060	5432790	5433200		5439890		
Analysis	R1/5	R1/2	R2/3	R3/2	R5/1	R4/1	R4/2	R3/1	R5/2	R5/1	R4/3	R3
SiO_2	68.266	50.604	51.708	53.628	56.938	56.433	64.749	70.154	68.810	68.901	68.873	68.295
TiO_2	-	0.034	0.028	0.064	0.051	0.073	0.007	-	-	-	-	-
Al_2O_3	20.800	31.183	30.072	29.217	27.349	27.791	22.571	21.343	20.756	20.351	20.517	20.497
FeO	0.242	0.912	0.982	1.013	0.602	0.884	0.370	0.048	0.134	0.050	0.068	0.080
MnO	0.083	-	0.036	0.027	0.060	0.022	0.006	-	0.055	-	0.028	0.030
MgO	0.005	0.067	0.095	0.088	0.023	0.086	0.096	0.021	-	0.021	0.002	-
CaO	0.718	14.462	13.481	12.086	9.383	10.175	0.442	0.732	0.508	0.225	0.653	0.508
Na_2O	11.075	3.288	3.822	4.515	5.725	5.401	9.765	7.511	11.306	11.205	10.028	10.889
K_2O	0.058	0.191	0.244	0.348	0.535	0.465	1.202	0.071	0.034	0.128	0.097	0.072
BaO	0.056	0.008	0.016	-	0.105	0.085	-	0.005	-	0.020	-	0.010
P_2O_5	0.030	-	0.002	0.076	-	0.024	0.006	0.046	-	0.005	0.020	0.040
TOTAL	**101.332**	**100.748**	**100.487**	**101.062**	**100.771**	**101.438**	**99.212**	**99.929**	**101.602**	**100.907**	**100.286**	**100.423**
Cations on the basis of (O) = 8												
Si	2.9487	2.2994	2.3513	2.4141	2.5465	2.5158	2.8684	3.0122	2.9596	2.9788	2.9847	2.9676
Ti	-	0.0011	0.0010	0.0022	0.0017	0.0025	0.0002	-	-	-	-	-
Al	1.0589	1.6700	1.6116	1.5501	1.4416	1.4602	1.1785	1.0800	1.0522	1.0370	1.0479	1.0497
Fe^2	0.0087	0.0346	0.0374	0.0381	0.0225	0.0330	0.0137	0.0017	0.0048	0.0018	0.0025	0.0029
Mn	0.0030	-	0.0014	0.0010	0.0023	0.0008	0.0002	-	0.0020	-	0.0010	0.0011
Mg	0.0003	0.0046	0.0065	0.0059	0.0016	0.0057	0.0063	0.0013	-	0.0014	0.0001	-
Ca	0.0332	0.7041	0.6568	0.5829	0.4496	0.4860	0.0210	0.0337	0.0234	0.0104	0.0303	0.0237
Na	0.9275	0.2897	0.3370	0.3941	0.4964	0.4669	0.8387	0.6253	0.9428	0.9393	0.8426	0.9174
K	0.0032	0.0111	0.0142	0.0200	0.0305	0.0264	0.0679	0.0039	0.0019	0.0071	0.0053	0.0040
Ba	0.0010	0.0001	0.0003	-	0.0018	0.0015	-	0.0001	-	0.0003	-	0.0002
P	0.0011	-	0.0001	0.0029	-	0.0009	0.0002	0.0017	-	0.0002	0.0007	0.0015
TOTAL	**4.9856**	**5.0148**	**5.0174**	**5.0113**	**4.9945**	**4.9996**	**4.9952**	**4.7598**	**4.9867**	**4.9762**	**4.9152**	**4.9681**
an	3.4	70.1	65.1	58.5	46.0	49.6	2.3	5.1	2.4	1.1	3.5	2.5
ab	96.1	28.8	33.4	39.5	50.7	47.6	90.4	94.3	97.4	98.1	95.9	97.1
or	0.3	1.1	1.4	2.0	3.1	2.7	7.3	0.6	0.2	0.7	0.6	0.4
cs	0.1	-	-	-	0.2	0.2	-	-	-	-	-	-

an:ab:or:cs = Ca:Na:K:Ba

Analyses by Cameca SX-50 electron microprobe, Central Science Laboratory, University of Tasmania

Analyst: J. L. Everard

Cations for MJ763/R3/4 not calculated due to substantial impurities (e.g. Fe)

Table 18 (*continued*)

Group	Group C				D	E			F		
Field No.	FJ593		MJ673		FJ477	HR112			FJ481		FJ360
Reg. No.	R004894		R006793		R004891	R005587			R004892		R004883
AMG (mE)	328180		327840		325150	328240			325160		325750
AMG (mN)	5442300		5434370		5443890	5431210			5444050		5441070
Analysis	R3/1	R4/1	R3/4	R5/1	R4	R1	R2	R4	R1	R2/3	R3/2
SiO_2	68.723	68.773	52.308	52.549	68.184	55.664	53.961	54.453	57.459	54.514	50.174
TiO_2	0.049	0.007	0.104	0.139	0.034	0.196	0.067	0.009	0.003	0.027	0.055
Al_2O_3	20.322	20.330	27.322	29.516	20.302	24.072	29.059	28.840	27.739	29.199	29.507
FeO	0.312	0.043	2.957	1.344	0.116	3.456	0.828	0.946	1.783	1.116	4.154
MnO	0.014	0.047	0.025	0.071	0.052	0.193	0.006	0.041	-	0.027	0.103
MgO	0.090	-	0.707	0.127	-	1.106	0.115	0.121	0.690	0.083	2.346
CaO	0.304	0.365	10.787	12.741	0.239	9.578	11.994	11.585	1.369	11.236	0.637
Na_2O	10.864	11.126	4.798	4.170	10.798	5.164	4.575	4.597	4.195	4.768	1.444
K_2O	0.064	0.052	0.153	0.131	0.384	0.462	0.279	0.438	6.641	0.556	8.411
BaO	-	0.024	-	-	0.053	0.017	0.060	0.048	0.149	-	0.008
P_2O_5	0.045	0.065	0.016	-	0.005	-	-	0.043	0.015	0.014	-
TOTAL	**100.787**	**100.831**	**99.176**	**100.788**	**100.167**	**99.907**	**100.944**	**101.122**	**100.042**	**101.540**	**96.840**
Cations on the basis of (O) = 8											
Si	2.9751	2.9764		2.3800	2.9738		2.4289	2.4459		2.4391	
Ti	0.0016	0.0002		0.0047	0.0011		0.0023	0.0003		0.0009	
Al	1.0368	1.0370		1.5755	1.0436		1.5416	1.5268		1.5397	
Fe^2	0.0113	0.0015		0.0509	0.0042		0.0312	0.0355		0.0417	
Mn	0.0005	0.0017		0.0027	0.0019		0.0002	0.0016		0.0010	
Mg	0.0058	-		0.0086	-		0.0077	0.0081		0.0055	
Ca	0.0141	0.0169		0.6183	0.0112		0.5784	0.5575		0.5386	
Na	0.9118	0.9336		0.3661	0.9131		0.3993	0.4004		0.4136	
K	0.0036	0.0029		0.0076	0.0214		0.0160	0.0251		0.0317	
Ba	-	0.0004		-	0.0009		0.0011	0.0009		-	
P	0.0016	0.0024		-	0.0002		-	0.0016		0.0005	
TOTAL	**4.9622**	**4.9730**		**5.0144**	**4.9714**		**5.0067**	**5.0036**		**5.0126**	
an	1.5	1.8		62.3	1.2		58.1	56.7		54.7	
ab	98.1	97.9		36.9	96.5		40.1	40.7		42.0	
or	0.4	0.3		0.8	2.3		1.6	2.6		3.2	
cs	-	-		-	0.1		0.1	0.1		-	

Table 19

Opaque minerals, Spinks Creek Volcanics: electron microprobe analyses

Group	P		A	B		C		D	F	
Field No.	FJ790A		FJ162	FJ143		MJ673		FJ477	FJ481	
Reg. No.	R004904		R004874	R004871		R004894		R004891	R004892	
AMG (mE)	322940		327850	325880		328280		325150	325160	
AMG (mN)	5445700		5441060	5439890		5442300		5443890	5444050	
Analysis	R1/3	R3/3	R2/2	R1/2	R1/3	R2/4	R3/2	R1/2	R2/2	R3/2
SiO_2	0.027	0.015	2.421	1.395	4.588	6.716	7.366	3.308	0.154	0.185
TiO_2	48.041	49.268	13.679	9.120	11.248	23.477	22.658	4.659	11.046	13.727
ZrO_2	0.128	0.209	-	-	-	0.060	0.069	-	-	-
Al_2O_3	0.077	0.018	0.421	0.337	1.071	0.849	1.282	1.418	4.085	4.844
Cr_2O_3	-	-	0.060	0.028	0.026	0.042	0.097	0.088	0.111	0.055
V_2O_3	-	-	0.023	-	0.081	-	0.194	-	-	-
FeOt	45.644	45.582	72.466	79.908	71.896	56.976	55.150	79.560	76.749	72.862
MnO	3.147	3.317	0.087	0.019	0.095	0.015	-	0.083	0.028	1.341
ZnO	-	-	-	0.064	-	-	-	0.110	-	0.004
NiO	-	0.015	-	0.057	0.062	0.077	0.040	0.040	0.087	-
MgO	0.033	0.054	-	0.023	0.074	0.014	0.314	1.063	-	0.052
CaO	0.103	0.058	2.000	0.700	3.596	6.132	5.880	0.435	0.019	0.040
TOTAL	**97.200**	**98.536**	**91.158**	**91.650**	**92.736**	**94.356**	**93.048**	**90.765**	**92.279**	**93.109**
Cations calculated on the basis of:										
	Z = 2								**Z = 3**	
	(O) = 3								**(O) = 4**	
Si	excl	excl							excl	excl
Ti	0.9350	0.9469							0.3215	0.3957
Zr	0.0016	0.0026							-	-
Al	0.0024	0.0005							0.1864	0.2188
Cr	-	-							0.0034	0.0017
V	-	-							-	-
Fe^3	0.1244	0.1005							1.1672	0.9882
Fe^2	0.8635	0.8737							1.3171	1.3474
Mn	0.0690	0.0718							0.0009	0.0435
Zn	-	-							-	0.0001
Ni	-	0.0003							0.0027	-
Mg	0.0013	0.0021							-	0.0030
Ca	0.0028	0.0016							0.0008	0.0016
Molar % end members:										
ilmenite	86.35	87.37						magnetite	58.09	44.66
$MnTiO_3$	6.90	7.18						ulvospinel	32.15	39.57
hematite	6.22	5.03						hercynite	9.32	10.94
other	0.53	0.42						other	0.44	4.83
TOTAL	**100.00**	**100.00**						**Total**	**100.00**	**100.00**

Cations for remaining analyses are not calculated due to the presence of substantial silicate impurities.
Analyses by Cameca SX-50 electron microprobe, Central Science Laboratory, University of Tasmania
Analyst: J. L. Everard

Table 20

Epidote, Spinks Creek Volcanics: electron microprobe analyses

Group		A		C	
Field No.		MJ725		MJ673	
Reg. No.		R006740		R006793	
AMG (mE)		328870		327840	
AMG (mN)		5432790		5434370	
Analysis		R1/1	R3	R4/3	
SiO_2		37.867	37.535	36.437	
TiO_2		0.037	-	0.008	
ZrO_2		0.087	-	-	
Al_2O_3		25.232	24.481	21.268	
Cr_2O_3		0.061	-	-	
La_2O_3		nd	nd	0.932	
Ce_2O_3		nd	nd	0.994	
Y_2O_3		nd	0.071	0.040	
FeO		10.374	11.347	14.195	
MnO		0.113	0.054	0.101	
MgO		0.190	0.250	0.256	
CaO		23.977	23.946	21.600	
BaO		0.035	-	-	
Na_2O		0.038	-	-	
K_2O		0.001	-	0.000	
F		0.037	0.015	0.024	
Cl		0.011	0.013	-	
TOTAL		**98.060**	**97.712**	**95.855**	
Cations on the basis of (O) = 12, (OH) = 1, all iron as Fe^3					
	site				ideal
Si	Z	2.9641	2.9562	2.9769	
$Al^{(iv)}$	Z	0.0359	0.0438	0.0231	
Total	**Z**	**3.0000**	**3.0000**	**3.0000**	**3**
$Al^{(iv)}$	Y	2.2920	2.2286	2.0249	
Fe^3	Y	0.6791	0.7474	0.9699	
Ti	Y	0.0022	-	0.0005	
Zr	Y	0.0033	-	-	
Cr	Y	0.0037	-	-	
Mn	Y	0.0075	0.0036	0.0070	
Mg	Y	0.0222	0.0293	0.0311	
Total	**Y**	**3.0100**	**3.0088**	**3.0334**	**3**
La	X	nd	nd	0.0281	
Ce	X	nd	nd	0.0297	
Y	X	nd	0.0030	0.0017	
Ca	X	2.0110	2.0206	1.8909	
Ba	X	0.0011	-	-	
Na	X	0.0057	-	-	
K	X	0.0001	-	-	
Total	**X**	**2.0179**	**2.0236**	**1.9504**	**2**
F		0.0093	0.0036	0.0062	
Cl		0.0014	0.0017	0.0000	
(OH)		0.9893	0.9946	0.9938	1

Analyses by Cameca SX-50 electron microprobe, Central Science Laboratory, University of Tasmania. Analyst: J. L. Everard

Table 21

Pumpellyite, Spinks Creek Volcanics: electron microprobe analyses

Group		P	A		B			C		D	
Field No.		AR164	FJ162		TJ2144			MJ673		FJ477	
Reg. No.		R005078	R004874		R005171			R006793		R004891	
AMG (mE)		322780	327850		333230			327840		325150	
AMG (mN)		5446060	5441060		5433200			5434370		5443890	
Analysis		R1/1	R1/1	R1/3	R1/1	R2	R4/1	R1/1	R1/2	R2	
SiO_2		36.475	36.755	36.649	36.915	37.276	36.811	36.072	35.767	34.764	
TiO_2		0.012	0.001	0.002	0.080	0.092	0.070	-	-	0.231	
ZrO_2		nd	nd	nd	0.052	0.026	0.063	nd	nd	nd	
Al_2O_3		20.265	20.435	20.625	21.905	22.506	22.086	18.789	17.073	20.178	
Cr_2O_3		-	0.024	0.010	0.034	0.067	-	-	0.044	0.043	
La_2O_3		nd	0.005	nd	nd	nd	nd	nd	nd	nd	
Ce_2O_3		nd	0.019	nd	nd	nd	nd	nd	nd	nd	
Y_2O_3		nd	0.029	nd	nd	nd	nd	nd	nd	nd	
FeO		12.160	11.820	11.182	9.239	8.937	9.106	13.779	16.423	12.393	
MnO		0.046	0.046	0.011	0.086	0.140	0.248	0.019	0.104	0.243	
MgO		1.602	1.778	1.884	2.609	2.438	2.595	1.779	1.277	4.656	
CaO		22.554	22.219	22.205	22.115	22.110	21.707	22.915	22.610	18.752	
BaO		nd	nd	nd	nd	nd	0.034	nd	nd	nd	
Na_2O		0.062	-	0.036	0.036	0.054	0.054	0.019	0.026	0.053	
K_2O		-	-	0.001	-	0.015	-	0.010	0.009	0.007	
F		nd	-	nd	0.027	0.039	-	nd	nd	nd	
Cl		nd	0.015	nd	0.004	0.006	0.002	nd	nd	nd	
TOTAL		**93.176**	**93.144**	**92.603**	**93.104**	**93.707**	**92.777**	**93.383**	**93.332**	**91.321**	
Cations calculated on the basis of 16 cations, (O) = 21, (OH) = 7											
	site										*ideal*
Si	Z	6.0011	6.0463	6.0454	6.0086	6.0258	6.0103	5.9494	5.9651	5.7658	
$Al^{(iv)}$	Z	-	-	-	-	-	-	0.0506	0.0349	0.2342	
Total		**6.0011**	**6.0463**	**6.0454**	**6.0086**	**6.0258**	**6.0103**	**6.0000**	**6.0000**	**6.0000**	**6**
Ti	Y	0.0015	0.0001	0.0003	0.0098	0.0111	0.0086	-	-	0.0288	
Zr	Y	nd	nd	nd	0.0041	0.0021	0.0050	nd	nd	nd	
Cr	Y	-	0.0031	0.0013	0.0044	0.0086	-	-	0.0059	0.0057	
La	Y	nd	0.0003	nd	nd	nd	nd	nd	nd	nd	
Ce	Y	nd	0.0011	nd	nd	nd	nd	nd	nd	nd	
Y	Y	nd	0.0025	nd	nd	nd	nd	nd	nd	nd	
Fe^3	Y	1.0851	0.9382	0.9096	0.7598	0.6454	0.7193	1.4572	1.7183	1.4792	
Al (Y)	Y	2.9134	3.0546	3.0889	3.2218	3.3328	3.2671	2.5428	2.2758	2.4864	
Total	**Y**	**4.0000**	**4.0000**	**4.0000**	**4.0000**	**4.0000**	**4.0000**	**4.0000**	**4.0000**	**4.0000**	4
Al (X)	X	1.0161	0.9074	0.9208	0.9804	0.9552	0.9829	1.0589	1.0452	1.2239	
Fe^2	X	0.5880	0.6878	0.6329	0.4979	0.5627	0.5241	0.4434	0.5723	0.2398	
Mn	X	0.0064	0.0063	0.0015	0.0119	0.0192	0.0343	0.0026	0.0147	0.0342	
Mg	X	0.3928	0.4360	0.4632	0.6331	0.5875	0.6317	0.4375	0.3174	1.1513	
Total	**X**	**2.0033**	**2.0376**	**2.0184**	**2.1232**	**2.1246**	**2.1731**	**1.9423**	**1.9495**	**2.6492**	2
Ca	W	3.9758	3.9162	3.9244	3.8567	3.8295	3.7974	4.0493	4.0402	3.3323	
Ba	W	nd	nd	nd	nd	nd	0.0022	nd	nd	nd	
Na	W	0.0198	—	0.0116	0.0115	0.0169	0.0171	0.0062	0.0084	0.0170	
K	W	-	-	0.0001	-	0.0031	-	0.0021	0.0019	0.0015	
Total	**W**	**3.9956**	**3.9162**	**3.9362**	**3.8682**	**3.8496**	**3.8167**	**4.0577**	**4.0505**	**3.3508**	4
F		nd	-	nd	0.0138	0.0198	-	nd	nd	nd	
Cl		nd	0.0040	nd	0.0010	0.0017	0.0005	nd	nd	nd	
(OH)		[3.0000]	[2.9960]	[3.0000]	2.9852	2.9785	2.99950192	[3.0000]	[3.0000]	[3.0000]	3
Mg#		40.05	38.80	42.26	55.98	51.08	54.66	49.67	35.68	82.76	

Analyses by Cameca SX-50 electron microprobe, Central Science Laboratory, University of Tasmania.
Analyst: J. L. Everard

Table 22

Chlorite, Spinks Creek Volcanics: electron microprobe analyses

Group	P				B			C			
Field No.	FJ790A			AR164	TJ2144			MJ673			
Reg. No.	R004904			R005078	R005171			R004894			
AMG (mE)	322940			322780	333230			328280			
AMG (mN)	5445700			5446060	5433200			5442300			
Analysis	R1/3	R2/4	R4/2	R1/4	R1/2	R4/2	R4/3	R2	R2/3	R3/1	R4/1
Form*	p'morph	grain	gmass	grain	p'morph	p'morph	gmass	gmass	gmass	gmass	amyg
SiO_2	30.530	29.490	29.520	29.085	30.250	30.359	30.213	29.499	29.075	28.485	28.617
TiO_2	0.007	-	0.037	0.004	-	-	-	0.029	0.038	-	-
Al_2O_3	15.916	16.971	16.667	17.235	15.281	15.753	15.478	16.143	16.523	16.068	16.188
Cr_2O_3	-	0.006	-	-	-	0.029	0.025	0.004	-	0.011	0.007
FeO	23.246	24.310	24.055	27.347	25.220	25.237	25.164	30.076	30.462	29.980	31.129
MnO	0.152	0.217	0.206	0.392	0.354	0.253	0.323	0.237	0.316	0.268	0.288
ZnO	-	0.142	-	-	0.081	0.053	0.125	-	0.036	0.116	0.192
NiO	0.016	0.123	0.026	-	0.008	0.026	0.042	-	0.026	-	0.031
MgO	17.270	16.456	16.297	14.432	16.704	16.458	16.596	11.531	11.656	11.486	11.596
CaO	0.276	0.449	0.296	0.208	0.227	0.230	0.249	0.393	0.380	0.254	0.277
Na_2O	0.012	0.025	0.031	0.035	0.007	0.006	0.023	0.012	0.021	0.010	0.004
K_2O	0.024	0.034	0.034	0.017	-	0.012	-	0.043	0.041	0.021	0.016
TOTAL	**87.448**	**88.223**	**87.170**	**88.755**	**88.132**	**88.415**	**88.238**	**87.968**	**88.573**	**86.698**	**88.345**
Cations on the basis of (O) = 10, (OH) = 8											
Si	3.1694	3.0635	3.0948	3.0471	3.1575	3.1535	3.1497	3.1625	3.1063	3.1109	3.0842
$Al^{(iv)}$	0.8306	0.9365	0.9052	0.9529	0.8425	0.8465	0.8503	0.8375	0.8937	0.8891	0.9158
$Al^{(vi)}$	1.1168	1.1414	1.1542	1.1752	1.0374	1.0821	1.0515	1.2022	1.1869	1.1791	1.1403
Ti	0.0005	0.0000	0.0029	0.0003	0.0000	0.0000	0.0000	0.0024	0.0030	0.0000	0.0000
Cr	0.0000	0.0005	0.0000	0.0000	0.0000	0.0024	0.0021	0.0004	0.0000	0.0009	0.0006
Fe^2	2.0182	2.1120	2.1091	2.3960	2.2015	2.1924	2.1939	2.6965	2.7218	2.7382	2.8057
Mn	0.0133	0.0190	0.0183	0.0347	0.0313	0.0222	0.0285	0.0215	0.0286	0.0247	0.0263
Zn	0.0000	0.0109	0.0000	0.0000	0.0062	0.0040	0.0097	0.0000	0.0028	0.0094	0.0153
Ni	0.0013	0.0103	0.0022	0.0000	0.0007	0.0022	0.0035	0.0000	0.0022	0.0000	0.0027
Mg	2.6727	2.5485	2.5471	2.2540	2.5993	2.5487	2.5792	1.8429	1.8565	1.8700	1.8631
Ca	0.0307	0.0500	0.0333	0.0234	0.0254	0.0256	0.0278	0.0452	0.0435	0.0297	0.0320
Na	0.0024	0.0050	0.0063	0.0072	0.0014	0.0012	0.0047	0.0025	0.0044	0.0020	0.0008
K	0.0032	0.0045	0.0046	0.0023	0.0000	0.0015	0.0000	0.0059	0.0056	0.0029	0.0022
cation tot	9.8592	9.9021	9.8780	9.8932	9.9032	9.8823	9.9007	9.8193	9.8553	9.8570	9.8890
Mg#	56.98	54.68	54.70	48.47	54.14	53.76	54.04	40.60	40.55	40.58	39.91

* p'morph = pseudomorph, gmass = groundmass, grain = large grain in coarse intrusive, amyg = amygdale

Table 23a

Electron microprobe analyses of amphibole and biotite from picrite

		AMPHIBOLE (KAERSUTITE)		BIOTITE			
Field No.		FJ447A		FJ447A			
Reg. No.		R006799		R006799			
AMG (mE)		324640		324640			
AMG (mN)		5442890		5442890			
Analysis		R5		R2/2	R3/1	R5/2	R1
SiO_2		39.4183		37.0645	35.2155	35.0189	35.5129
TiO_2		6.8092		6.4646	8.7927	9.0087	7.6178
ZrO_2		nd		nd	nd	0.0424	nd
Al_2O_3		12.8360		14.2993	14.7906	14.4642	15.2517
V_2O_3		0.0517		-	-	nd	-
Cr_2O_3		0.0148		0.0073	0.0192	-	0.0052
FeO		9.9121		10.0532	10.3641	12.4458	11.591
ZnO		0.1392		-	-	nd	-
MnO		0.1283		0.1062	0.0569	0.1107	0.0758
NiO		0.0294		0.0613	0.0901	nd	0.0875
MgO		12.8032		17.6149	15.2047	13.5736	14.8352
CaO		11.9404		0.0048	0.0002	0.029	0.0284
BaO		0.125		0.5865	1.6398	1.8204	1.9831
Na_2O		2.6661		0.4663	0.7613	0.8232	1.0289
K_2O		1.1361		8.7911	8.1345	7.9697	7.8237
F		0.5317		0.0782	0.0564	0.0319	0.7218
Cl		0.0568		0.0241	0.0207	0.0271	0.0493
TOTAL		**98.5983**		**95.6225**	**95.1469**	**95.3658**	**96.6125**
**See note*				*Cations on the basis of (O)=20, (OH, F,Cl) = 4*			
Si	T	5.8677		Si	5.4274	5.2400	5.2580	5.2721
$Al^{(iv)}$	T	2.1323		Al	2.4678	2.5939	2.5596	2.6686
$Al^{(vi)}$	C	0.1197		$Ti^{(iv)}$	0.1048	0.1661	0.1823	0.0593
Ti	C	0.7622		**Total**	**8.0000**	**8.0000**	**8.0000**	**8.0000**
V	C	0.0062		$Ti^{(vi)}$	0.6071	0.8178	0.8349	0.7911
Cr	C	0.0017		Zr	nd	nd	0.0003	nd
Zn	C	0.0153		Cr	0.0008	0.0023	-	0.0006
Mg	C	2.8412		V	-	-	nd	-
Ni	C	0.0035		Fe^2	1.2311	1.2897	1.5628	1.4391
Fe^2	C	1.2340		Zn	-	-	nd	-
Mn	C	0.0162		Mn	0.0132	0.0072	0.0141	0.0095
Ca	B	1.9044		Ni	0.0072	0.0108	nd	0.0104
Na	B	0.0956		Mg	3.8453	3.3728	3.0383	3.2833
Na	A	0.6739		**Total**	**5.7047**	**5.5005**	**5.4504**	**5.5340**
Ba	A	0.0073		Ca	0.0008	-	0.0047	0.0045
K	A	0.2158		Ba	0.0337	0.0956	0.1071	0.1154
(O)		22.3284		Na	0.1324	0.2196	0.2396	0.2962
(OH)		1.4069		K	1.6423	1.5442	1.5266	1.4817
F		0.2503		**Total**	**1.8090**	**1.8594**	**1.8780**	**1.8978**
Cl		0.0143		F	0.0362	0.0265	0.0151	0.3389
				Cl	0.0060	0.0052	0.0069	0.0124
Mg#		69.72		(OH)	1.9578	1.9682	1.9780	1.6487
T sites		8.0000						
C sites		5.0000		Mg#	75.75	72.34	66.03	69.53
B sites		2.0000						
A sites		0.8969						
cations		15.8969						

* Cations calculated on the basis of (Si, Al, Ti, V, Cr, Zn, Mg, Ni, Fe, Mn) = 13 and (O, OH, F, Cl) = 24 with all iron as Fe^2

Table 23b

Electron microprobe analyses of olivine from picrite

Field No.	FJ447A	
Reg. No.	R006799	
AMG (mE)	324640	
AMG (mN)	5442890	
Analysis	R1/1	R1/2
SiO_2	39.415	40.069
TiO_2	0.030	0.025
Al_2O_3	0.035	0.037
Cr_2O_3	0.029	0.076
FeO	17.679	15.353
MnO	0.219	0.245
NiO	0.202	0.143
MgO	41.876	43.954
CaO	0.175	0.360
TOTAL	**99.659**	**100.261**
Ions calculated on the basis of (O) =4		
Si	1.0060	1.0055
Ti	0.0006	0.0005
Al	0.0011	0.0011
Cr	0.0006	0.0015
Fe	0.3774	0.3222
Mn	0.0047	0.0052
Ni	0.0041	0.0029
Mg	1.5934	1.6443
Ca	0.0048	0.0097
Cations	2.9926	2.9928
Mg#	80.85	83.62

Analyses by Cameca SX-50 electron microprobe,
Central Science Laboratory, University of Tasmania.
Analyst: J. L. Everard

Table 24

Average, minimum and maximum copper content by chemical group, Spinks Creek Volcanics

Group	No*	Average (ppm Cu)	Minimum (ppm Cu)	Maximum (ppm Cu)	Highest sample		AMG of highest	
					Reg. No.	Field No.	mE	mN
P	2	50	36	65	R005078	AR164	322780	5446060
A	5	134	37	350	R006740	MJ725	328870	5432790
B	27	127	11	590	R006747	MJ965	331450	5430920
C	61	128	13	540	R002851	MRS9	332150	5448800
D	19	106	14	330	R004870	FJ99A	325420	5442560
E	3	49	13	120	R006751	MJ1009	333010	5431870
F	6	134	52	480	R005074	AR160C	322900	5446240

* Number of samples analysed for copper
Source: Table 15*a*, this report

APPENDIX 5

Phase relationships of the Spinks Creek Volcanics

J. L. Everard

Grove *et al*. (1992) described a method for calculating liquidus mineralogy (and hence potentially fractionation trends) as a function of pressure (from 0.1 MPa to 100 MPa; i.e. 1 bar to 10 kb) and melt composition. Although this algorithm was developed for mid-ocean ridge basalts (MORB), it is probably also applicable to the Spinks Creek Volcanics, which have major element chemistry similar to many MORB. As most lava samples contain only a few per cent phenocrysts, they are considered to approximate melt compositions (apart from Fe_2O_3/FeO ratios and volatile contents, which are not incorporated in the algorithm). Some caution is required due to the likelihood of element mobility (particularly of Na_2O) during low-grade metamorphism.

Each analysed sample was plotted on the two projection schemes used by Grove *et al*. (1992), normative olivine-clinopyroxene-quartz (not illustrated) and plagioclase-clinopyroxene-olivine (fig. 29*a*–*g*). The average compositions of chemical groups (P, A, B, C, D and F) were used to calculate the positions of the olivine-plagioclase-augite-low Ca pyroxene melt (OPALM) and olivine-plagioclase-augite-melt equilibria, at pressures of 0.1, 20, 50 and 100 MPa. This was also done for selected and representative individual analyses, including samples R005587 and R006760 from Group E (fig. 29*f*). From this information it is possible to estimate the liquidus phase or phases and compare them with the observed phenocryst mineralogy. It should be noted that the main effect of pressure is to increase the stability of clinopyroxene, whilst the position of the plagioclase-olivine cotectic is little affected.

Group P samples (fig. 29*a*) appear to have olivine as their liquidus phase at low pressures, but it is replaced by augite above variously 50 MPa (R005078), 85 MPa (average Group P) or 110 MPa (ABS38). Most samples plot just to the right of the plagioclase-olivine cotectic, suggesting that plagioclase is not a liquidus phase at any pressure. However low Ca-pyroxene (orthopyroxene and/or pigeonite), in addition to olivine and augite, seems possible at higher pressures for sample ABS38. The two samples collected during this study (R005078 and R004904), from an intrusion near the Arthur River, are both equigranular doleritic to gabbroic rocks with locally developed cumulate textures, and may not represent melt compositions. However they contain coarse-grained augite and altered olivine. Sample ABS38 from the Smithton foreshore was reportedly olivine-phyric (Brown, 1989*a*), in accord with calculated phase relationships below about 110 MPa.

Group A (fig. 29*b*) samples have similar phase relationships to Group P. The liquidus phase is generally olivine at low pressures and augite at higher pressures, never plagioclase (or low Ca-pyroxene). The pressure of the olivine-augite cotectic is highly variable between samples, from near 0.1 MPa (42165) to 45 MPa (average composition) and 65 MPa (R004875). This is broadly consistent with the essentially olivine-phyric character of Group A samples, although rare clinopyroxene (three samples) and plagioclase (two samples) phenocrysts were noted in this study. Fractionation therefore probably took place at moderate to shallow depths (20 km and less).

Group B samples (fig. 29*c*), although generally also having olivine or augite on their calculated liquidii, plot in a broad subvertical band, very close to the respective cotectics with plagioclase. Most individual compositions lie near the three-phase olivine-augite-plagioclase cotectic, at some pressure between 0.1 MPa and about 120 MPa. This suggests that Group B compositions were modified by polybaric fractionation of plagioclase, augite and olivine. These three minerals co-exist as phenocryst phases in 22 out of the 24 Group B samples examined petrographically during this study.

Group C (fig. 29*d*) and Group D (fig. 29*e*) compositions have similar phase relationships to Group B. Individual compositions plot in a subvertical band, close to the olivine-augite-plagioclase cotectic but at a wide range of pressures. A few compositions (mostly with low CaO) plot away from the OPALM point away from clinopyroxene and towards normative quartz in the olivine-clinopyroxene-quartz projection, and thus potentially could be saturated in a low Ca-pyroxene. Most group C and D rocks contain plagioclase and clinopyroxene phenocrysts, and many contain (subordinate) altered olivine.

The relatively rare Group E (fig. 29*f*) lavas show more dispersal when plotted on the normative plagioclase-clinopyroxene-olivine projection. For these strongly evolved rocks, the liquidus fields are strongly composition dependent, and are shown in Figure 29*f* for two representative samples, rather than the average Group E composition. This, in addition to equilibration at a range of pressures, may account for the dispersal of the data.

Group F (fig. 29*g*), which comprises both generally aphyric to plagioclase-phyric lavas and coarse-grained intrusive rocks, has rather variable phase relationships. The average Group F composition plots near the plagioclase-olivine cotectic, and clinopyroxene does not appear on the liquidus below about 120 MPa. The relatively fresh, plagioclase-phyric lava has similar

phase relationships. The microgabbroic sample R004878, on the other hand, plots close to olivine-augite-plagioclase at around 70 MPa.

In summary, the calculated phase relationships of the Spinks Creek Volcanics are generally in accord with their observed phenocryst assemblages. They preserve evidence that fractionation took place at a wide range of depths and pressures up to 120 MPa , not merely in shallow subvolcanic levels.

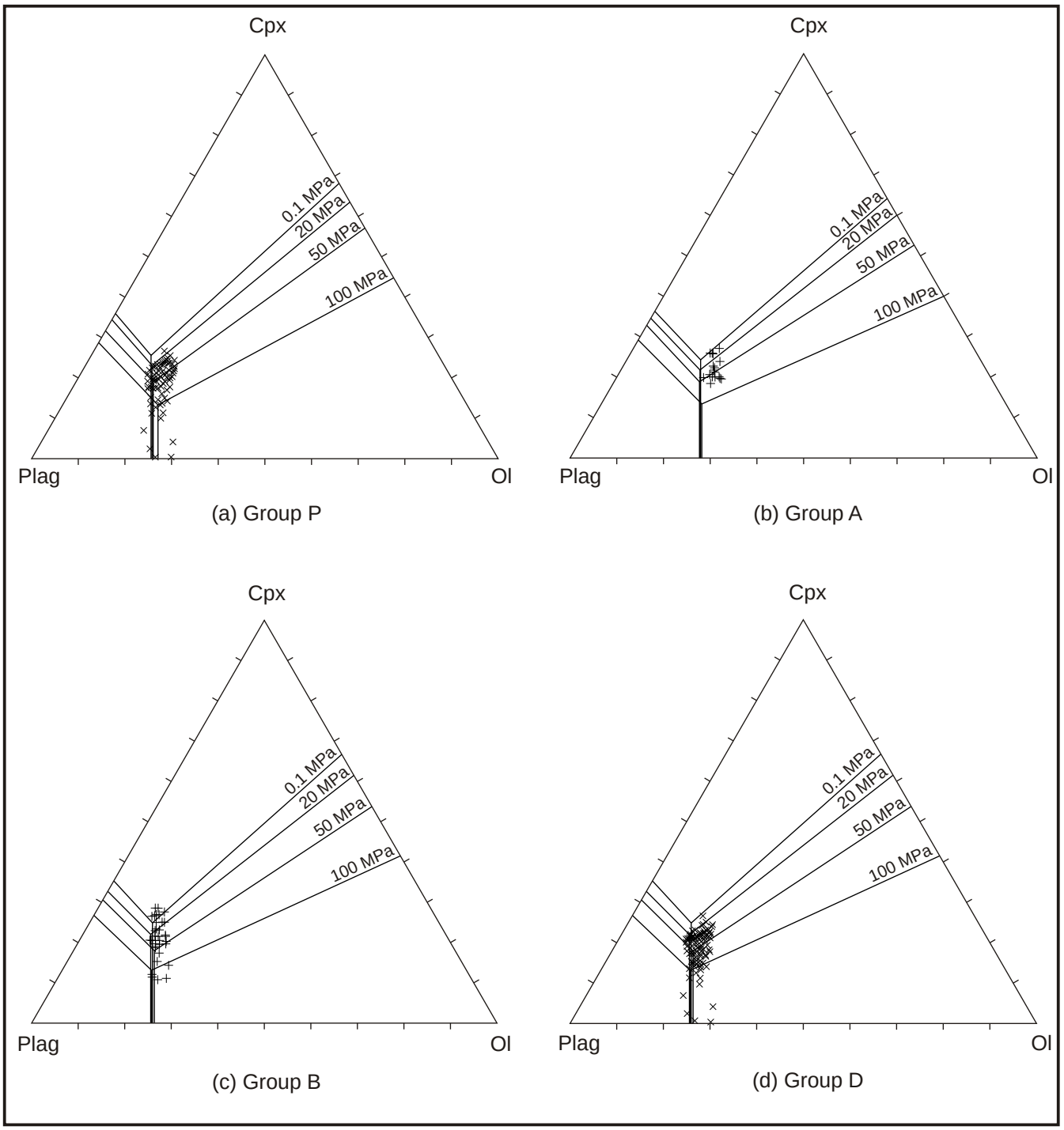

Figure 29

Major element composition of basalts, Spinks Creek Volcanics, projected on to the system plagioclase-clinopyroxene-olivine by the method of Grove et al. (1992). Calculated liquidus field boundaries for average compositions (except for Group E) at 100, 50, 20 and 0.1 MPa also shown.

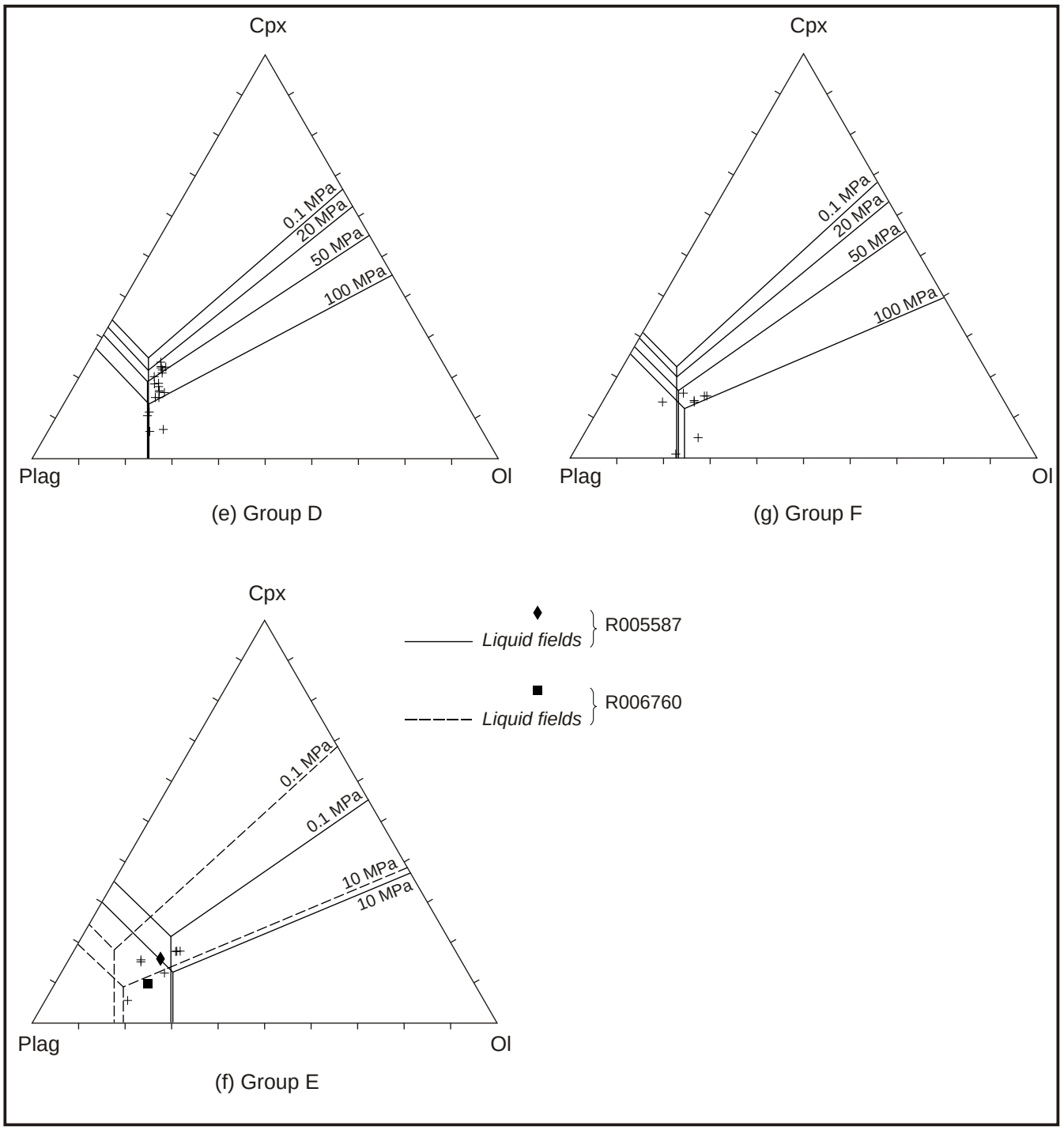

Figure 29

Major element composition of basalts, Spinks Creek Volcanics, projected on to the system plagioclase-clinopyroxene-olivine by the method of Grove et al. (1992). Calculated liquidus field boundaries for average compositions (except for Group E) at 100, 50, 20 and 0.1 MPa also shown.

APPENDIX 6

Listing of rock samples

Reg. No.	Field No.	AMG (mE)	AMG (mN)	Locality	Unit	Comments	TS	CA	X
R002843	MRS1	331350	5457620	Gravel quarry, Christmas Hills area	Psr	Chert	1		
R002844	MRS2	328120	5457520	Christmas Hills area	Psd	Chert, float	1		
R002845	MRS3	330650	5446250	Arthur River area	Psb	Weathered basalt	1		
R002846	MRS4	330600	5446250	Arthur River area	Psb	Basalt	1		
R002847	MRS5	328800	5445300	Keppel Creek area	Psvw	Siltstone	1		
R002848	MRS6	328700	5445300	Keppel Creek area	Psd	Chert	1		
R002849	MRS7	330500	5446450	Arthur River area	Psb	Basalt	1		
R002850	MRS8	330450	5446540	Arthur River area	Psb	Basalt	1	1	
R002851	MRS9	332150	5448800	Ekberg Creek area	Psb	Basalt	1	1	
R002852	MRS10	330300	5458200	Christmas Hills area	Psr	Chert	1		
R002853	MRS11	330500	5448700	Chester Creek	Psd	Chert	1		
R002854	MRS12	330840	5446960	Arthur River area	Psb	Basalt	1		
R002855	MRS13	331170	5444460	Keppel Creek area	Psb	Basalt	1		
R002856	MRS14	331170	5444460	Keppel Creek area	Psb	Basalt	1		
R002857	MRS15	329960	5444250	Keppel Creek area	Psvwl	Impure limestone	1		
R002858	MRS16	330980	5444270	Keppel Creek area	Psvw	Siltstone/sandstone	1		
R002859	MRS17	331140	5444030	Keppel Creek area	Psb	Basalt	1		
R002860	MRS18	330300	5453610	Montagu River area	Psd	Dolomite	1		
R002861	MRS19	329300	5445750	Keppel Creek area	Psvw	Siltstone	1		
R002862	MRS20	330440	5446430	Arthur River area	Psb	Basalt	1	1	
R002863	MRS21	328510	5442320	Keppel Creek area	Psb	Basalt	1		
R002864	MRS22	328510	5442320	Keppel Creek area	Psvwi	Ironstone	1	1	
R002865	MRS23	328460	5443390	Keppel Creek area	Ps	Basalt	1		
R002866	MRS24	329310	5445170	Keppel Creek area	Psvwl	Impure limestone	1		
R002867	MRS25	332910	5446960	Arthur River	Psb	Basalt	1		
R002868	MRS26	332740	5447040	Arthur River	Psb	Basalt	1	1	
R002869	MRS27	328120	5457520	Christmas Hills area	Psd	Silicified dolomite			
R002870	MRS28	332480	5458890	Christmas Hills area	Cm	Siltstone	1		
R002871	MRS29	332600	5458930	Christmas Hills area	Cm	Sandstone	1		
R002872	MRS30	332650	5458930	Christmas Hills area	Cm	Coarse sandstone	1		
R002873	MRS31	332010	5449040	Ekberg Creek area	Psb	Basalt	1	1	
R002874	MRS32	331920	5449320	Ekberg Creek area	Psvwi	Ironstone	1	1	
R002875	MRS33	331930	5449640	Ekberg Creek area	Psvwi	Ironstone	1		
R002876	MRS34	331830	5449820	Ekberg Creek area		Quartz vein			
R002877	MRS35	331900	5449830	Ekberg Creek area	Psb	Basalt	1	1	
R002878	MRS36	331850	5449900	Ekberg Creek area	Psb	Basalt	1		
R002879	MRS37	332220	5450560	Ekberg Creek area	Cm	Quartz vein			
R002880	MRS38	330540	5443400	Keppel Creek area	Psb	Basalt	1		
R002881	MRS39	330300	5443220	Keppel Creek area	Psb	Basalt	1	1	
R002882	MRS40	329370	5443500	Keppel Creek area	Psb	Basalt	1		
R002883	MRS41	330190	5443860	Keppel Creek area	Psvw	Siltstone	1		
R002884	MRS42	329510	5443720	Keppel Creek area	Psb	Basalt	1		
R002885	MRS43	330260	5456580	Christmas Hills area	Psr	Siltstone	1		
R004245	RS465A	324920	5448210	Float	Pss	Pale grey chert			
R004246	RS465B	324920	5448210	Float	Pss	Grey oolitic chert			
R004247	RS467	324770	5448420	Creek outcrop	Pss	Buff-coloured dolomite			
R004248	RS475	325050	5447780	Float	Pss	Grey oolitic chert			
R004249	RS477	325150	5447500	Creek outcrop	Pss	Sheared grey ?dolomite			
R004250	RS155	321860	5446410	Creek outcrop	Pssc	Grey chert, quartz ovoids			
R004251	RS162	321930	5446680	Creek outcrop	Pssr	Diamictite			
R004252	RS169A	322440	5446900	Creek outcrop	Psb	Basalt			
R004253	RS169B	322440	5446900	Creek outcrop	Psb	Basalt			
R004254	RS169C	322440	5446900	Creek outcrop	Psb	Basalt			
R004255	RS169D	322440	5446900	Creek outcrop	Psb	Amygdaloidal basalt			
R004256	RS176A	322060	5447440	Creek outcrop	Psb	Silicified basalt			
R004257	RS176B	322060	5447440	Creek outcrop	Psb	Amygdaloidal basalt			
R004258	RS177	322110	5447490	Waterfall outcrop	Psb	Basalt			
R004259	RS409	324110	5448990	Creek outcrop	Psb	Altered basalt			
R004260	RS428	323760	5449520	Creek outcrop	Psb	Basalt			
R004261	RS426	323650	5449430	Creek outcrop	Psvwi	?Hematitic ironstone			
R004262	RS76	324020	5448990	Float	Psvwi	?Hematitic ironstone			
R004263	RS399A	321840	5447360	Blocky float	Psvw	?Diamictite			

Reg. No.	Field No.	AMG (mE)	AMG (mN)	Locality	Unit	Comments	TS	CA	X
R004264	RS399B	321840	5447360	Blocky float	Psvw	?Diamictite			
R004265	RS150	321680	5446090	Creek outcrop	Prc	Grey, massive quartz sltst			
R004266	RS217	322330	5448620	Creek outcrop	Psd	Massive dolomite			
R004267	RS110A	323410	5448390	Float	Psr	Grey silicified lam sltst			
R004268	RS110B	323410	5448390	Float	Psr	Grey silicified lam sltst			
R004269	RS110C	323410	5448390	Float	Psr	Grey silicified lam sltst			
R004270	RS115A	323910	5447420	Float	Psr	Grey-black silfd lam sltst			
R004271	RS115B	323910	5447420	Float	Psr	Grey-black silfd lam sltst			
R004272	RS115C	323910	5447420	Float	Psr	Grey-black silfd lam sltst			
R004273	RS209A	322380	5449840	Quarry outcrop	Psr	Grey silicified lam sltst			
R004274	RS209B	322380	5449840	Quarry outcrop	Psr	Grey silicified lam sltst			
R004275	RS209C	322380	5449840	Quarry outcrop	Psr	Grey silicified lam sltst			
R004276	RS500	322810	5449340	Creek outcrop	Psd	Dolomite			
R004277	RS501A	322780	5449340	Creek outcrop	Psd	Dolomite			
R004278	RS501B	322780	5449340	Creek outcrop	Psd	Dolomite			
R004279	RS290	321110	5448510	Creek outcrop	Psbz	?Gabbro			
R004280	RS212	322330	5449290	Bouldery float	Tsgs	Siliciclastic conglomerate			
R004283	DM3	325980	5439780	Creek outcrop	Psb?	Spotted maroon sltst			
R004284	DM4	325980	5439780	Creek outcrop	Psb?	Blue-grey ?sltst/?basalt			
R004285	DM15	324930	5440140	Creek outcrop	Prc	Massive qtz-rich sltst			
R004286	DM17	324900	5440090	Creek outcrop	Prc	Fissile, ?gphitic sltst/shale			
R004287	DM22	321940	5438190	Creek outcrop	Prbg	Banded sltst/mst			
R004288	DM29	322290	5438300	Creek outcrop	Prbs	Banded sltst, chloritic spots			
R004289	DM43	324450	5436560	Float	Psvx?	Basaltic breccia			
R004290	DM44	324460	5436540	Float	Psb?	?Leached basalt			
R004291	DM45	324470	5436520	Float	Psb?	Basalt			
R004292	DM48	324630	5436230	Float	Psb?	Massive fine-grained basalt			
R004293	DM50	324650	5436200	Track outcrop	Psb?	Massive fine-grained basalt			
R004294	DM53	324380	5435300	Float	Pss	Chert breccia			
R004295	DM54	324330	5435300	Float	Pscb	Pebble conglomerate			
R004296	DM55	324290	5435350	Float	Pscb	Lam, m-grained quartzarenite			
R004297	DM68	321920	5438680	Road cut	Prbs	Olive green sltst			
R004298	DM81	323380	5439940	Road cut	Prc	?spotted graphitic shale			
R004299	DM94A	325600	5439890	Float	Pscb	Breccia			
R004300	DM94B	325600	5439890	Float	Pscb	Pale grey quartzarenite			
R004801	FJ66	326860	5443060	Blackwater 4 road	Prc	Black, pyritic	1		>0.14
R004802	FJ131	326840	5440730	Blackwater Road	Prc		1		0.09
R004803	FJ280	325360	5440440	Upper Blackwater Rivulet	Prc	Purplish	1		>0.24
R004804	FJ295	325500	5441030	Upper Blackwater Rivulet	Prc		1		0.16
R004805	FJ300	326430	5441190	Blackwater Rivulet tributary junction	Prc		1		0.03
R004806	FJ331	326660	5444100	'Cowrie Ridge'	Prc?		1		0.11
R004807	FJ392	325190	5441200	Middle Blackwater Rivulet	Prc		1		0.14
R004808	FJ428	325000	5442180	Middle Blackwater Rivulet	Prc		1		0.14
R004809	FJ573	324060	5444150	Western trib. of Blackwater Rivulet	Prc		1		0.10
R004810	FJ776	322940	5445200	Small tributary of Arthur River	Prc		1		0.06
R004811	FJ1028	326610	5444170	Gully, west side of 'Cowrie Ridge'	Prc		1		0.03
R004812	FJ4	326240	5446200	Blackwater 1 road	Pssc	Blotchy chert	1		0.02
R004813	FJ5	326150	5446040	Blackwater 1 road	Pssc	Laminated black chert			0.02
R004814	FJ96	325540	5441460	Blackwater 5-1 road	Pssc	Silicified pelitic mst	1		0.03
R004815	FJ283	325410	5440500	Upper Blackwater Rivulet	Pssc	Massive chert			0.01
R004816	FJ285	325480	5440520	Upper Blackwater Rivulet	Pssm	Pelitic mudstone	1		0.11
R004817	FJ286	325510	5440530	Upper Blackwater Rivulet	Pssm	Banded chert	1		>0.14
R004818	FJ292A	325620	5440960	Upper Blackwater Rivulet	Pss		1		>0.02
R004819	FJ292B	325620	5440960	Upper Blackwater Rivulet	Pssc	Laminated chert			0.01
R004820	FJ320	324310	5435190	West of Old Balfour track	Pssc	Chert conglomerate	1		0.01
R004821	FJ426	325050	5442130	Middle Blackwater Rivulet	Psc	Granule conglomerate	1		0.14
R004822	FJ431	324990	5442340	Middle Blackwater Rivulet	Psc?	Chert conglomerate			>0.02
R004823	FJ450A	324780	5442940	Middle Blackwater Rivulet	Pssd		1		0.02
R004824	FJ450B	324780	5442940	Middle Blackwater Rivulet	Pssm	Talcose dolomite	1		>0.02
R004825	FJ454	324830	5443040	Middle Blackwater Rivulet	Pss		1		0.02
R004826	FJ549	324590	5444430	Western trib. of Blackwater Rivulet	Pssm		1		0.12
R004827	FJ553A	324530	5444400	Western trib. of Blackwater Rivulet	Pss	Pelitic mudstone	1		0.05
R004828	FJ553B	324530	5444390	Western trib. of Blackwater Rivulet	Pss		1		0.05
R004829	FJ557	324390	5444420	Western trib. of Blackwater Rivulet	Pss		1		0.02
R004830	FJ570	324170	5444320	Western trib. of Blackwater Rivulet	Pssc		1		0.02

Reg. No.	Field No.	AMG (mE)	AMG (mN)	Locality	Unit	Comments	TS	CA	X
R004831	FJ760	324250	5444580	W sub-trib. of Blackwater Rivulet	Pss	stromatolitic flakestone?	1		>0.03
R004832	FJ762	324180	5444650	W sub-trib. of Blackwater Rivulet	Pss		1		>0.05
R004833	FJ1052	334980	5443350	Julius River	Pss		1		>0.01
R004834	FJ1079	326420	5442820	Creek east of Blackwater 5 road	Pss		1		>0.01
R004835	FJ1084	326550	5442790	Creek east of Blackwater 5 road	Pssm	chloritic siltstone wacke	1		0.48
R004836	FJ302B	325700	5440500	South tributary, Blackwater Rivulet	Pssr		1		0.29
R004837	FJ303	325960	5440460	South tributary, Blackwater Rivulet	Psvx?	altered basalt clast	1		0.51
R004838	FJ548	324580	5444440	West tributary of Blackwater Rivulet	Pssr	hematitic			>0.16
R004839	FJ788	323020	5445580	Small tributary of Arthur River	Pssr		1		0.06
R004840	FJ791	322890	5445760	Small tributary of Arthur River	Pssr		1		>0.06
R004841	FJ1031	326510	5444210	Gully, west side of 'Cowrie Ridge'	Psvx		1		>0.38
R004842	FJ1032	326480	5444220	Gully, west side of 'Cowrie Ridge'	Psvx		1		0.31
R004843	FJ1067	334460	5443670	Julius River	Pssr		1		0.12
R004844	FJ8	325810	5446250	NW of Blackwater 1 road	Psvw		1		0.12
R004845	FJ85	325730	5442120	Blackwater 5-1-1 road: start	Psvw		1		0.77
R004846	FJ98	325450	5442500	Blackwater 5-1 road	Psvw	altered, oxidised	1		0.48
R004847	FJ99	325420	5442560	Blackwater 5-1-1 road	Psvw	altered, oxidised	1		0.28
R004848	FJ140	326240	5440030	Blackwater Road	Psvw				0.13
R004849	FJ157	327400	5440760	Blackwater 6 road	Psvw		1		
R004850	FJ348	326020	5441290	East tributary of Blackwater Rivulet	Psvw		1		0.20
R004851	FJ459	325080	5443200	Middle Blackwater Rivulet	Psvw	basaltic tuff	1		0.41
R004852	FJ489	325080	5444360	Middle Blackwater Rivulet	Psvw		1		>0.55
R004853	FJ534	324750	5444640	West tributary of Blackwater Rivulet	Psvw		1		0.35
R004854	FJ536	324740	5444590	West tributary of Blackwater Rivulet	Psvw		1		0.80
R004855	FJ575	327930	5443170	Middle Stephens Rivulet	Psvw	hematitic	1		2.33
R004856	FJ620	328520	5442480	East tributary, Stephens Rivulet	Psvw	hematitic	1		1.02
R004857	FJ656	325940	5446790	Small creek near BW 1 road	Psvw				>0.15
R004858	FJ659	325840	5446770	Small creek near BW 1 road	Psvw		1		>0.24
R004859	FJ685	327230	5441050	Southern tributary, Stephens Rivulet	Psvw	weathered	1		2.81
R004860	FJ689	327390	5441510	Southern tributary, Stephens Rivulet	Psvw		1		0.38
R004861	FJ733	325990	5441130	North of Blackwater Road	Psvw	hematitic	1		0.34
R004862	FJ757	324370	5444720	Ridge NW of Blackwater Rivulet	Psvw		1		>0.04
R004863	FJ831	326900	5440390	East tributary of Blackwater Rivulet	Psvw	hematitic, weathered	1		
R004864	FJ852	327100	5439840	East tributary of Blackwater Rivulet	Psvw		1		
R004865	FJ879	328960	5442000	Small south trib. of Stephens Rivulet	Psvw				
R004866	FJ928	328570	5442870	Steep east trib. of Stephens Rivulet	Psvw	hematitic	1		
R004867	FJ1106	331900	5440210	Upper Keppel Creek	Psvw		1		0.37
R004868	FJ1110	331800	5440040	Upper Keppel Creek	Psvw	hematitic	1		0.59
R004869	FJ89	325720	5441820	Blackwater 5-1 road	Psbc		1	1	51.4
R004870	FJ99A	325420	5442560	Blackwater 5-1-1 road	Psbd		1	1	59.4
R004871	FJ143	325880	5439890	Blackwater Road	(Psbb)	clasts in wacke	1	1	23.0
R004872	FJ145	325670	5439830	Blackwater Road	Psbz		1	1	0.63
R004873	FJ154A	327140	5440650	Blackwater 6 Road	Psb		1		
R004874	FJ160	327660	5441040	Blackwater 6 Road	Psb		1		15.9
R004875	FJ162	327850	5441060	Blackwater 6 Road	Psba		1	1	16.2
R004876	FJ165	328380	5441150	Blackwater 6 Road	Psbc		1	1	25.0
R004877	FJ168	328630	5441480	Blackwater 6 Road	Psbc		1	1	41.7
R004878	FJ284	325460	5440520	Upper Blackwater Rivulet	Psbz		1	1	0.45
R004879	FJ312	324380	5436690	Old Balfour track	Psb		1		0.56
R004880	FJ315	324550	5436510	Old Balfour track	Psbc		1	1	45.7
R004881	FJ317	324690	5436040	Old Balfour track	Psbc		1	1	42.3
R004882	FJ322	324670	5435290	Old Balfour track	Psbb		1	1	23.5
R004883	FJ360	325750	5441070	East tributary of Blackwater Rivulet	Psbz		1	1	1.73
R004884	FJ363	325590	5441260	East tributary of Blackwater Rivulet	Psbz		1	1	0.54
R004885	FJ447	324640	5442890	Middle Blackwater Rivulet	Psbzp		1		1.85
R004886	FJ448	324660	5442900	Middle Blackwater Rivulet	Psb		1	1	50.7
R004887	FJ456	325000	5443170	Middle Blackwater Rivulet	Psb		1		0.48
R004888	FJ460	325110	5443210	Middle Blackwater Rivulet	Psbc		1	1	41.8
R004889	FJ464	325160	5443240	Middle Blackwater Rivulet	Psbd		1		49.9
R004890	FJ473	325100	5443640	Middle Blackwater Rivulet	Psbd		1	1	>25.9
R004891	FJ477	325150	5443890	Middle Blackwater Rivulet	Psbd		1		79.3
R004892	FJ481	325160	5444050	Middle Blackwater Rivulet	Psbf		1	1	9.07
R004893	FJ542	324680	5444500	West tributary of Blackwater Rivulet	Psbd		1	1	54.5
R004894	FJ593	328180	5442300	Middle Stephens Rivulet	Psbc		1	1	35.5
R004895	FJ596	328270	5442150	Middle Stephens Rivulet	Psb		1		26.9
R004896	FJ603	328290	5441880	Middle Stephens Rivulet	Psbc	native Cu present	1	1	32.1

Reg. No.	Field No.	AMG (mE)	AMG (mN)	Locality	Unit	Comments	TS	CA	X
R004897	FJ606	328360	5441750	Middle Stephens Rivulet	Psb		1		>28.4
R004898	FJ615	328310	5441310	Middle Stephens Rivulet	Psb	calcite amygdales			35.8
R004899	FJ625	328780	5442500	Eastern tributary, Stephens Rivulet	Psb		1		37.5
R004900	FJ641	329690	5441460	Stephens Rivulet tributary headwaters	Psbc		1	1	71.7
R004901	FJ680	327260	5440890	Southern tributary, Stephens Rivulet	Psb		1		0.64
R004902	FJ731	325960	5440640	North of Blackwater Road	Psbc		1	1	21.70
R004903	FJ746	325570	5441220	Ridge NW of Blackwater Rivulet	Psbz	weathered	1		0.32
R004904	FJ790A	322940	5445700	Small tributary of Arthur River	Psbp		1	1	0.56
R004905	FJ808	328830	5441210	Upper Stephens Rivulet	Psbc		1	1	78.4
R004906	FJ812	329160	5441160	Upper Stephens Rivulet	Psbc		1	1	0.89
R004907	FJ821	329410	5440430	Upper Stephens Rivulet	Psbc		1	1	10.3
R004908	FJ826	330000	5439690	Upper Stephens Rivulet	Psba		1	1	15.7
R004909	FJ833	326960	5440300	Eastern trib. of Blackwater Rivulet	Psbc		1	1	53.6
R004910	FJ865	327190	5439490	Eastern trib. of Blackwater Rivulet	Psbb		1	1	47.6
R004911	FJ880	328900	5442040	Small S tributary of Stephens Rivulet	Psb	weathered, felspathic	1	1	13.2
R004912	FJ892	329290	5443020	Hill north of Stephens Rivulet	Psbc		1	1	44.3
R004913	FJ906	330110	5442290	Eastern tributary, Stephens Rivulet	Psbc		1	1	43.2
R004914	FJ917	328730	5442370	South of E tributary, Stephens Rivulet	Psb		1		0.37
R004915	FJ920	328660	5442300	Small tributary of Stephens Rivulet	Psb		1		4.74
R004916	FJ955	332690	5443760	Upper Keppel Creek	Psbc		1	1	63.2
R004917	FJ963	331880	5444080	Upper Keppel Creek	Psbc		1	1	29.9
R004918	FJ964	331630	5444020	Upper Keppel Creek – falls	Psbc		1	1	7.63
R004919	FJ978	331690	5442520	West of Sumac Road	Psbc		1	1	29.1
R004920	FJ983	328170	5442100	Ridge north of Blackwater 6 road	Psb	weathered	1		3.33
R004921	FJ1091	333200	5441820	West of Sumac Road	Psbb		1	1	44.5
R004922	FJ1111	331770	5439950	Upper Keppel Creek	Psba		1	1	13.3
R004923	FJ1122	331250	5440760	West of upper Keppel Creek	Psbc		1	1	41.6
R004924	FJ349	325940	5441270	East tributary of Blackwater Rivulet	Psvx		1		0.38
R004925	FJ356	325920	5441160	East tributary of Blackwater Rivulet	Psvx		1		0.26
R004926	FJ357	325900	5441130	East tributary of Blackwater Rivulet	Psvx		1		0.42
R004927	FJ723	325570	5441990	Near Blackwater 5-1 road	Psvx		1		1.03
R004928	FJ823	329850	5439810	Upper Stephens Rivulet	Psvx		1		2.01
R004929	FJ828	329530	5439800	Gully near Upper Stephens Rivulet	Psvx		1		
R004930	FJ842	327190	5440200	East tributary of Blackwater Rivulet	Psvx		1		
R004931	FJ850	327170	5439910	East tributary of Blackwater Rivulet	Psvx		1		
R004932	FJ1006	327480	5440770	Creek south of Blackwater 6 road	Psvx		1	1	6.79
R004933	FJ1033	326450	5444230	Gully, west side of 'Cowrie Ridge'	Psvx		1	-	0.66
R004934	FJ1093	332030	5441520	Upper Keppel Creek	Psvx		1	-	0.73
R004935	FJ1104	332060	5440500	Upper Keppel Creek	Psvx		1	1	2.47
R004936	FJ36	327570	5446850	Blackwater 1 road	Psd		1		0.02
R004937	FJ37	327560	5446890	Blackwater 1 road	Psd?	leached?			>0.01
R004938	FJ68	325900	5444450	Blackwater 5 road	Psd				0.02
R004939	FJ123	325470	5444520	Small creek near BW 5-3 road	Psd		1		0.04
R004940	FJ124	325360	5444560	End of Blackwater 5-3 road	Psd		1		>0.01
R004941	FJ126	326310	5443170	Blackwater 5-2 road	Psdc?		1		0.01
R004942	FJ134	326770	5440540	Blackwater Road	Psdc?		1		>0.01
R004943	FJ202	327780	5443870	Opposite start of BW 3A road	Psd		1		0.02
R004944	FJ265	328030	5444550	Stephens Rivulet	Psd		1		>0.02
R004945	FJ325A	328290	5445120	Low hill east of lwr Stephens Rivulet	Pssc	botryoidal			0.03
R004946	FJ335	326450	5440970	East tributary of Blackwater Rivulet	Pssc		1		0.01
R004947	FJ338	326350	5440990	East tributary of Blackwater Rivulet	Psd		1		0.02
R004948	FJ343	326190	5441350	East tributary of Blackwater Rivulet	Psd		1		0.02
R004949	FJ492	325190	5444440	Lower Blackwater Rivulet	Psd		1		0.04
R004950	FJ505	324960	5445030	Lower Blackwater Rivulet	Psd				>0.00
R004951	FJ514	324420	5445770	Lower Blackwater Rivulet	Psd		1		0.01
R004952	FJ531	324820	5444720	West tributary of Blackwater Rivulet	Psd		1		0.14
R004953	FJ671	327890	5443620	Middle Stephens Rivulet	Psd	silicified	1		0.02
R004954	FJ1034	326340	5444270	Gully east of Blackwater 5 road	Psd		1		>0.01
R004955	FJ1047	326560	5443330	Gully east of Blackwater 5 road	Psd		1		>0.01
R004956	FJ1145	328680	5445270	Lower Keppel Creek	Psd		1		>0.06
R004957	FJ1175	326430	5442600	Creek east of Blackwater 5 road	Psd		1		
R004958	FJ1176	326340	5442710	Creek east of Blackwater 5 road	Psd		1		
R004959	FJ1177	326580	5443580	Gully, west side of 'Cowrie Ridge'	Psd		1		
R004960	FJ1076	326330	5442890	Creek east of Blackwater 5 road	Psd		1		
R004962	FJ30	325000	5430320	Balfour	Tbr		1	1	6.88
R004964	FJ321	324360	5435260	Old Balfour track	Tbr		1	1	3.14

Reg. No.	Field No.	AMG (mE)	AMG (mN)	Locality	Unit	Comments	TS	CA	X
R004965	FJ1113	331360	5439990	West of upper Keppel Creek	Tba		1	1	4.58
R004966	FJ1117	330960	5440020	West of upper Keppel Creek	Tb		1		13.9
R004968	FJ2	326440	5446530	Blackwater 1 road	Tsgs	silcrete?	1		0.04
R004969	FJ726	326060	5442070	Near Blackwater 5-1 road	Tsgs	siliceous conglomerate			0.02
R004970	FJ873	328090	5440770	South of Blackwater 6		laterite	1		
R004974	FJ138	326420	5440160	Blackwater Road	Psdc	silica sand	1	1	
R004975	FJ200	327720	5443650	Blackwater Road	Psdc	silica sand	1	1	
R004976	FJ1135	326410	5444750	West side of 'Cowrie Ridge'	Pss		1		>0.02
R005025	AR1	343760	5450150	Arthur River	Prcs	'quartzite'	1	1	
R005026	AR9	342890	5449620	Arthur River	Prc	granule conglomerate	1		
R005027	AR23	342570	5448410	Arthur River	Pssd	stromatolitic flakestone	1		
R005028	AR25	342450	5448220	Arthur River	Pssm		1		
R005029	AR33	342010	5446890	Arthur River	Pssd	stromatolitic flakestone	1		
R005030	AR38	341580	5446540	Arthur River	Pssd		1	1	
R005031	AR41	341260	5446360	Arthur River	Pssd		1		
R005032	AR49	340330	5445890	Arthur River	Pssm		1		
R005033	AR51	340080	5445960	Arthur River	Prcs	'quartzite'	1		
R005034	AR53	339970	5445940	Arthur River	Prcs	pink 'quartzite'	1		
R005035	AR59	339590	5445990	Arthur River	Prc		1		
R005036	AR61	339380	5445870	Arthur River	Pssc	black chert	1		
R005037	AR65	338940	5445660	Arthur River	Pssd		1		
R005038	AR68A	338750	5445730	Arthur River	Pssm		1		
R005039	AR68B	338750	5445730	Arthur River	Pssc				
R005040	AR76	337160	5445790	Arthur River	Pssd	impure quartzose dolomite	1		
R005041	AR84	336100	5446440	Arthur River	Pssd		1	1	
R005042	AR86	335860	5445530	Arthur River	Pssr		1		
R005043	AR93	334850	5446950	Arthur River	Pssr		1		
R005044	AR96	334460	5446780	Arthur River below Julius River	Psvw		1		
R005045	AR99	334060	5446750	Arthur River below Julius River	Psvx		1		
R005046	AR100	333880	5446880	Arthur River above Kanunnah Bridge	Psba		1	1	19.7
R005047	AR103	333510	5446770	Arthur River above Kanunnah Bridge	Psbc		1	1	>23.1
R005048	AR106	332960	5446960	Arthur River below Kanunnah Bridge	Psbc		1	1	>23.8
R005049	AR109	332690	5446570	Arthur River above Kanunnah Bridge	Psvw		1		0.41
R005050	AR111	331280	5446260	Arthur River above Kanunnah Bridge	Psbd		1	1	>43.9
R005051	AR112	331040	5446310	Arthur River above Kanunnah Bridge	Psbc		1	1	>36.3
R005052	AR113	330680	5446340	Under Kanunnah Bridge	Psbc		1	1	105
R005053	AR116	330010	5446750	Arthur River below Kanunnah Bridge	Psvw		1		
R005054	AR122	326480	5448500	Arthur River below Kanunnah Bridge	Psd		1	1	
R005055	AR125	326160	5447850	Arthur River below Ekberg Creek	Psvw		1		
R005056	AR131	325680	5447030	Arthur River below Ekberg Creek	Psvw	coarse-gr lithicwacke sst	1		
R005057	AR133	325560	5447130	Arthur River below Ekberg Creek	Psvw		1		
R005058	AR134	325330	5447180	Arthur River below Ekberg Creek	Psd	cataclastic texture	1		
R005059	AR134B	325330	5447180	Arthur River below Ekberg Creek	Psd				
R005060	AR134C	325330	5447180	Arthur River below Ekberg Creek	Psd		1		
R005061	AR137A	325250	5446920	Arthur River below Ekberg Creek	Pssd				
R005062	AR137B	325250	5446920	Arthur River below Ekberg Creek	Psb	weathered, vesicular	1		>0.87
R005063	AR137C	325250	5446920	Arthur River below Ekberg Creek	Psb	massive weath'd picrite	1	1	>3.90
R005064	AR140	325330	5446660	Arthur River below Ekberg Creek	Pssr		1		
R005065	AR143	325340	5446490	Arthur River below Ekberg Creek	Psvw		1		
R005066	AR146	324050	5446170	Arthur River below Ekberg Creek	Psd		1		
R005067	AR150	323860	5446410	Arthur River below Ekberg Creek	Psd		1		
R005068	AR157	322900	5446480	Arthur River below Hawkes Creek	Psvw		1		
R005069	AR159A	322920	5446300	Arthur River below Hawkes Creek	Psvw	coarse-grain lithicwacke	1		
R005070	AR159B	322920	5446300	Arthur River below Hawkes Creek	Psvw		1		
R005071	AR160	322900	5446240	Arthur River below Hawkes Creek	Psvw	c-grain lithicwacke sst	1		
R005072	AR160A	322900	5446240	Arthur River below Hawkes Creek	Psvw-clast	felsic volcanic clast	1		
R005073	AR160B	322900	5446240	Arthur River below Hawkes Creek	Psvw-clast	basalt clast	1		
R005074	AR160C	322900	5446240	Arthur River below Hawkes Creek	Psbf	bottom flow	1	1	44.8
R005075	AR160D	322900	5446240	Arthur River below Hawkes Creek	Psb	top flow	1	1	>3.91
R005076	AR161	322870	5446160	Arthur River below Hawkes Creek	Psb (VLT)		1	1	>0.52
R005077	AR162	322850	5446120	Arthur River below Hawkes Creek	Psvw		1		
R005078	AR164	322780	5446060	Arthur River below Hawkes Creek	Psbz		1	1	0.56
R005079	AR164B	322780	5446060	Arthur River below Hawkes Creek	Psbz	pegmatitic	1		0.57
R005080	AR167	322680	5446000	Arthur River below Hawkes Creek	Pssr		1		
R005081	AR168	322640	5445950	Arthur River below Hawkes Creek	Pssc		1		

Reg. No.	Field No.	AMG (mE)	AMG (mN)	Locality	Unit	Comments	TS	CA	X
R005082	AR174	322370	5445620	Arthur River below Hawkes Creek	Prc		1		
R005083	TJ1A	340490	5442100	Rapid River near bridge	Psc	clasts in conglomerate			
R005084	TJ1B	340490	5442100	Rapid River near bridge	Psc	clasts in conglomerate			
R005085	TJ1C	340490	5442100	Rapid River near bridge	Psc	clasts in conglomerate			
R005086	TJ1D	340490	5442100	Rapid River near bridge	Psc	clasts in conglomerate			
R005087	TJ48	337990	5437810	Dempsters Lookout	Pssc	laminated chert	1		
R005088	TJ481	339840	5440770	Rapid Quarry	Pssc	laminated chert	1		
R005089	TJ491	340420	5442180	Rapid River	Pssd	botryoidal microfabric	1		
R005090	TJ501	337930	5440920	Sumac Rivulet	Pssd		1		
R005091	TJ502	338010	5440980	Sumac Rivulet bridge	Pssd		1	1	
R005092	TJ506	338760	5441320	Sumac Rivulet	Pssc	black chert	1		
R005093	TJ509	339300	5441650	Sumac Rivulet	Pssd		1		
R005094	TJ516	339750	5443170	Rapid River	Pss		1	1	
R005095	TJ621	340500	5443000	Rapid River	Pssd	banded			
R005096	TJ625	340680	5445400	Rapid River	Pssd	stromatolitic flakestone	1		
R005097	TJ704	336980	5441700	Sumac Road	Pssd	weathered, puggy			
R005098	TJ707	336460	5441840	Sumac Road	Pss	sericitic mudstone	1		
R005099	TJ772	337450	5438430	Sumac Rivulet tributary	Pssd	pelitic mst interbeds	1		
R005101	TJ942	340420	5441660	Lamprey Creek	Pssd		1	1	
R005102	TJ943	340460	5441750	Lamprey Creek	Pssd	stromatolitic flakestone	1		
R005103	TJ1013	337250	5439600	Sumac Rivulet	Pssc		1		
R005104	TJ1014	337330	5439990	Sumac Rivulet	Pssr		1		
R005105	TJ1016	337510	5440500	Sumac Rivulet	Pssd		1		
R005106	TJ1018	337640	5440680	Sumac Rivulet	Pssd		1		
R005107	TJ1018B	337640	5440680	Sumac Rivulet	Pssd		1		
R005108	TJ1020	337860	5440900	Sumac Rivulet near bridge	Pssd	pelitic mudstone interbeds	1		
R005109	TJ1079	340110	5440510	Lamprey Creek	Pssd		1		
R005110	TJ1082	340100	5440440	Lamprey Creek	Pssd		1		
R005111	TJ1083A	340090	5440390	Lamprey Creek	Pssd		1		
R005112	TJ1095	333610	5440810	Julius River	Pssm		1	1	
R005113	TJ1100	333130	5439700	Julius River	Pssr		1		
R005114	TJ1375	335560	5441000	Tributary, Julius River	Pss	pelitic mudstone	1		
R005115	TJ1589	331940	5432400	Horton River	Pssd		1		
R005116	TJ1598	333290	5440420	Julius River	Pssm		1		
R005117	TJ1601	332860	5439300	Julius River	Pssm		1		
R005118	TJ1644	332550	5433650	Lagunta Creek	Pssr		1		
R005119	TJ3255	333630	5439720	Little Julius River	Pssd	impure, khaki coloured	1		0.05
R005120	TJ3256	333590	5439880	Little Julius River	Pssc		1		0.23
R005121	TJ3258	333560	5439970	Little Julius River	Pssd		1		0.03
R005122	TJ3394	333370	5440170	Little Julius River	Pssd		1	1	0.15
R005123	-	336100	5442100	Sumac Quarry	Pssc		1		
R005124	TJ1590	331890	5432280	Horton River	Pssr		1		
R005125	TJ1596	334110	5441280	Julius River	Pssr		1		
R005126	TJ1597	333930	5441080	Julius River	Pssr		1		
R005127	TJ1599	333150	5439730	Julius River	Pssr		1		
R005128	TJ1600	333030	5439450	Julius River	Pssr		1		
R005129	TJ1645	332650	5433900	Lagunta Creek	Pssr		1		
R005130	TJ3254	333780	5439560	Little Julius River	Pssr		1		0.17
R005131	TJ989	332500	5431600	Horton River	Psvw	hematitic	1		
R005132	TJ2096	334180	5434350	East of Lagunta Creek	Psvw	weathered			
R005133	TJ2097	334180	5434430	East of Lagunta Creek	Psvw	weathered			
R005134	TJ2140	332130	5438400	Julius River	Psvw	weathered, pale			
R005135	TJ2149	332990	5432700	Ridge north of Horton River	Psvw	weathered, pale			
R005136	TJ2150	332590	5432310	Horton River	Psvw	weathered			
R005137	TJ785Y	336740	5440760	Unnamed Sumac spur road	Psvx		1		
R005138	TJ786Y	336410	5441210	Unnamed Sumac spur road	Psvx		1		
R005139	TJ789A	336260	5441310	Sumac 3 road	Psvx		1		
R005140	TJ789B	336260	5441310	Sumac 3 road	Psvx		1		
R005141	TJ979	333170	5432250	Horton River	Psvx		1		
R005142	TJ1106	332660	5439030	Julius River	Psvx		1		
R005143	TJ1108	332520	5438730	Julius River	Psvx		1		
R005144	TJ1109	332520	5438650	Julius River	Psvx		1		
R005145	TJ1649	332600	5435150	Lagunta Creek	Psvx	basalt clast	1		
R005146	TJ1650	332650	5435250	Lagunta Creek	Psvx		1		
R005147	TJ1652	333300	5435250	Lagunta Creek	Psvx				
R005148	TJ2132	332740	5439110	Julius River	Psvx		1		

Reg. No.	Field No.	AMG (mE)	AMG (mN)	Locality	Unit	Comments	TS	CA	X
R005149	TJ2133	332600	5438910	Julius River	Psvx		1		
R005150	TJ2137	332530	5438680	Julius River	Psvx		1		
R005151	TJ3097	334850	5439580	East of Little Julius River	Psvx		1		
R005152	TJ3120	334330	5436900	NE of Lagunta Creek	Psvx		1		
R005153	TJ3121	334320	5436640	NE of Lagunta Creek	Psvx				
R005154	TJ3234	335830	5440720	East tributary of Julius River	Psvx		1		0.46
R005155	TJ3250	333800	5438540	Little Julius River	Psvx		1		0.30
R005156	TJ925	334550	5426820	Sumac 10 spur	Psb	weathered	1		69.9
R005157	TJ926	333920	5426870	Leigh River bridge	Psbb		1	1	24.6
R005158	TJ984	332600	5432080	Horton River	Psbc		1	1	>>14.2
R005159	TJ987	332540	5431750	Horton River	Psb		1		56.1
R005160	TJ988	332520	5431670	Horton River	Psbc		1	1	
R005161	TJ1580	332450	5431600	Horton River	Psb		1		84.1
R005162	TJ1582	332110	5431750	Horton River	Psbc		1	1	>0.36
R005163	TJ1583	331960	5431710	Horton River	Psb		1		0.52
R005164	TJ1586	331910	5431870	Horton River	Psbb		1	1	>5.34
R005165	TJ1643	333000	5433500	East of Lagunta Creek	Psb	weathered float	1		0.66
R005166	TJ2099	333900	5434550	East of Lagunta Creek	Psb	amygdaloidal	1		0.55
R005167	TJ2101	333440	5435080	East of Lagunta Creek	Psbc		1	1	>29.4
R005168	TJ2103	333130	5435260	East of Lagunta Creek	Psbc		1	1	>28.3
R005169	TJ2105	333710	5435450	East of Lagunta Creek	Psbc		1	1	>13.5
R005170	TJ2142	332580	5438180	Upper Julius River	Psbc	float	1	1	>24.9
R005171	TJ2144	332560	5438470	Near upper Julius River	Psbb		1	1	38.3
R005172	TJ2147	333230	5433200	North of Horton River	Psbc		1	1	>17.3
R005173	TJ2156	333040	5432410	Horton River	Psb		1		>0.38
R005174	TJ3085	336900	5439430	West of Sumac Rivulet	Psbc		1	1	>30.1
R005175	TJ3092	335330	5439450	West of Sumac Rivulet	Psbb		1	1	0.51
R005176	TJ3099	334950	5439330	Ridge east of Little Julius River	Psb		1		39.0
R005177	TJ3105	334720	5438810	Ridge east of Little Julius River	Psb		1		45.5
R005178	TJ3116	335110	5437830	West of Sumac Rivulet	Psbc		1	1	>28.7
R005179	TJ3238	335660	5439970	East tributary of Julius River	Psbc		1	1	0.66
R005180	TJ3246	334100	5438060	Little Julius River source	Psbc		1	1	48.3
R005181	TJ3379	332980	5441550	West of Julius River	Psb		1		25.0
R005182	TJ3384	332450	5440590	West of Julius River	Psbc		1	1	23.7
R005183	TJ3388	332330	5440120	West of Julius River	Psbc		1	1	28.4
R005184	TJ3083	337140	5439410	Near Sumac Rivulet	Pssm?		1		
R005185	TJ50	337490	5437420	Sumac Road	Prc				
R005186	TJ71	342440	5437380	'Mt Bertha' quarry	Prc		1	1	
R005187	TJ148	342710	5435160	Horton Loop Road	Prc		1	1	
R005195	TJ519	340940	5442130	Rapid River	Prcs	'quartzite'	1		
R005197	TJ571	344100	5441850	Tayatea Road Spur 8	Prc		1	1	
R005198	TJ636	334560	5432440	Horton River bridge	Prc		1		
R005199	TJ639	335100	5432450	Horton River	Prc		1		
R005200	TJ641	335120	5432460	Horton River	Prc		1		
R005201	TJ647	335930	5432050	Horton River	Prc		1		
R005206	TJ714	334520	5432010	Sumac Road	Prc		1		
R005207	TJ752A	337570	5437260	Sumac Road	Prcs	'quartzite'			
R005208	TJ752B	337570	5437260	Sumac Road	Prcs	'quartzite'	1		
R005211	TJ921	336450	5435690	Dempster Plains	Prc		1		
R005212	TJ928	340220	5441070	Lamprey Creek	Prc		1		
R005213	TJ929	340190	5441130	Lamprey Creek	Prcs	'quartzite'	1		
R005214	TJ935	340230	5441400	Lamprey Creek	Prcs	'quartzite'	1		
R005215	TJ953	342130	5432970	Dempster Plains	Prc		1		
R005216	TJ960	337110	5432150	Dempster Plains	Prc		1		
R005217	TJ966	334360	5432250	Horton River	Prc		1		
R005218	TJ975	333730	5432440	Horton River	Prc		1		
R005222	TJ1081B	340100	5440460	Lamprey Creek	Prcs	'quartzite'	1		
R005223	TJ1083B	340090	5440390	Lamprey Creek	Prcs	'quartzite'	1		
R005224	TJ1085	340100	5440260	Lamprey Creek	Prc		1		
R005228	TJ1192	338430	5433330	Trias Creek	Prc		1		
R005230	TJ1226	340130	5440340	Tributary, Lamprey Creek	Prcs		1		
R005237	TJ1492	336560	5434330	Whitehead Creek	Prc		1		
R005238	TJ1494	336380	5434290	Whitehead Creek	Prc	pseudobreccia	1		
R005239	TJ1500	335800	5434100	Whitehead Creek	Prc		1		
R005240	TJ1523	335050	5432990	Whitehead Creek	Prc		1		
R005241	TJ1541	337940	5435120	Whitehead Creek	Prc	spotted	1		

Reg. No.	Field No.	AMG (mE)	AMG (mN)	Locality	Unit	Comments	TS	CA	X
R005242	TJ1604	340910	5443740	Creek near Red Hat Hill	Prc		1		
R005243	TJ1609	341280	5443640	Creek near Red Hat Hill	Prc		1		
R005244	TJ1629	341110	5444050	Creek near Colemans Hill	Prcs	'quartzite'	1		
R005245	TJ1640	342410	5444430	Creek near Colemans Hill	Prc		1		
R005247	TJ1687	341520	5445070	Unnamed creek	Prc		1		
R005251	TJ1944	341610	5445930	Joy Creek	Prc		1		
R005252	TJ1954	342020	5445560	Joy Creek	Prc		1		
R005253	TJ1956	342140	5445560	Joy Creek	Prc		1		
R005254	TJ1962	342380	5445600	Joy Creek	Prc		1		
R005373	TJ3600	332470	5457770	Molompto Road	Tb	nepheline mugearite	1	1	
R005487	FJ780	323000	5445320	Small tributary of Arthur River	Pssc		1		0.04
R005488	FJ26	326400	5447650	Track north of Blackwater 1 Road	Psvw				0.14
R005558	HR1	334260	5432420	Horton River	Pssd	dolomitic conglomerate	1		
R005559	HR9	333410	5432220	Horton River	Pssc				0.00
R005560	HR10	333280	5432180	Horton River	Psvx		1		0.34
R005561	HR11	333220	5432190	Horton River	Psvx		1		0.19
R005562	HR12	333170	5432240	Horton River	Psvx		1		0.24
R005563	HR13	333150	5432320	Horton River	Psvw	wavy laminated	1		0.39
R005564	HR13B	333150	5432320	Horton River	Psvw		1		0.50
R005565	HR15	332990	5432400	Horton River	Psbc		1	1	0.46
R005566	HR33	331200	5432600	Horton River	Psvx	basalt clast, altered	1		0.33
R005567	HR35	331000	5432650	Horton River	Psbb		1	1	0.52
R005568	HR37	331030	5432590	Horton River	Psvw		1		0.47
R005569	HR39	331070	5432550	Horton River	Psvw	lost?			0.15
R005570	HR40	331090	5432530	Horton River	Psvx?	dolomitic, trans to Pssr?	1		0.36
R005571	HR41	331090	5432480	Horton River	Psvx		1		0.44
R005572	HR44	330970	5432270	Horton River	Psvw		1		6.09
R005573	HR47	330760	5432180	Horton River	Psbb		1	1	0.43
R005574	HR49	330600	5432040	Horton River	Psbb		1	1	0.34
R005575	HR50	330540	5432000	Horton River	Psvw		1		0.41
R005576	HR52	330510	5432070	Horton River	Psbc		1	1	21.2
R005577	HR53	330520	5432210	Horton River	Psbc		1	1	0.54
R005578	HR57	330590	5432440	Horton River	Psbc		1	1	27.9
R005579	HR60	330200	5432660	Horton River	Psbb		1	1	21.1
R005580	HR63	330060	5432610	Horton River	Psbb		1	1	10.8
R005581	HR74	329500	5432360	Horton River	Psvx		1		0.42
R005582	HR82	328960	5431830	Horton River	Psvw				0.38
R005583	HR93	328800	5431200	Horton River	Psvx		1		0.37
R005584	HR98	328780	5430730	Lower Lindsay River	Psvw		1		>0.04
R005585	HR105	328630	5431120	Frankland River	Psvx		1		0.47
R005586	HR109	328290	5430920	Frankland River	Psvw		1		0.42
R005587	HR112	328240	5431210	Frankland River	Psbe		1	1	2.79
R005588	HR114	328070	5431120	Frankland River	Psbb		1	1	0.47
R005589	HR118	327690	5431080	Frankland River	Psbc		1	1	29.6
R005590	HR122	327460	5431060	Frankland River	Psbc		1	1	39.5
R005591	HR123	327380	5431050	Frankland River	Psb		1		40.3
R005592	HR125	327200	5431130	Frankland River	Psbc		1	1	34.7
R005593	HR130	327080	5431550	Frankland River	Psvwd	impure dolomite	1		0.76
R005594	HR132	326990	5431440	Frankland River	Psvw				
R005595	HR134	326680	5431250	Frankland River	Prc	tourmaline present	1		0.14
R005596	HR135	326620	5431130	Frankland River	Prc		1		0.08
R005597	HR139	326220	5431370	Frankland River	Prc	tourmaline present	1		0.12
R005100	TJ783X	340210	5439120	Near Forked Tree Hill	Pssc	chert breccia			
R006001	DM95	325670	5439830	Road cut	Psbzf	dolerite			
R006002	DM97	325850	5439880	Road cut	Psb	basalt			
R006003	DM135	325410	5437940	Creek outcrop	Pss	silicified ooidal dolomite			
R006004	DM139	325400	5437530	Creek outcrop	Psd	finely xtalline dolomite			
R006005	DM142	325520	5437360	Creek outcrop	Psd	agate-textured silica			
R006006	DM149	324270	5436560	Creek outcrop	Psvx?	diamictite, basalt clasts ?			
R006007	DM152	324140	5436490	Creek outcrop	Pss	thin bedded, f-gr dolomite			
R006008	DM153	324020	5436460	Creek outcrop	?	dark spotted, mafic rock			
R006009	DM157	323490	5436440	Creek outcrop	Prbs	banded spotted sltst			
R006010	DM171	325230	5431510	Creek outcrop	Pmf	dolerite			
R006011	DM185	324950	5432050	Creek outcrop	Psb	amygdaloidal basalt			
R006012	DM199	326040	5437350	Creek outcrop	Tsgs?	siliceous conglomerate			
R006074		328130	5457500	Quarry	Psd	silicified oolitic dolomite			

Reg. No.	Field No.	AMG (mE)	AMG (mN)	Locality	Unit	Comments	TS	CA	X
R006574	MJ60	333770	5427630	Leigh River	Prc		1		
R006575	MJ67	333440	5427820	Leigh River	Prc		1		
R006577	MJ341	332070	5428020	Lower Leigh River	Prc		1		
R006578	MJ346	331880	5428060	Lower Leigh River	Prc		1		
R006584	MJ446	333760	5430490	Sumac Spur 7	Prc		1		
R006585	MJ453	333500	5430290	Sumac Spur 7	Prc		1		
R006586	MJ488	336820	5429780	Horton River	Prc		1		0.08
R006587	MJ498	336690	5430640	Horton River	Prc		1		0.07
R006588	MJ501	336420	5430560	Horton River	Prc		1		0.13
R006589	MJ505A	336040	5430700	Horton River	Prc	concretion	1		>0.18
R006590	MJ512	336300	5431170	Horton River	Prc		1		0.08
R006591	MJ513	336310	5431260	Horton River	Prc		1		0.13
R006592	MJ530	328530	5429880	'Eel Creek'	Prc		1		0.10
R006593	MJ555	331520	5428050	Lower Leigh River	Prc		1		0.07
R006594	MJ580	330370	5429370	Lower Leigh River	Prc	silicified?	1		0.00
R006595	MJ820	330300	5428910	Lindsay River	Prc		1		0.04
R006596	MJ846	329970	5429400	Lindsay River	Prc	spotted	1		0.12
R006597	MJ927	339450	5430140	Dempster Plains	Prc		1		0.06
R006598	MJ1035	338030	5426200	Hill east of Sumac Spur 10	Prc		1		>0.02
R006599	MJ1063	330280	5428470	Lindsay River	Prc		1		0.19
R006600	MJ1176X	326770	5431380	Frankland River	Prc	wavy laminated	1		0.10
R006602	MJ1126Y	338860	5426500	Horton River	Prc		1		
R006603	MJ1146Y	336380	5428720	Horton River	Prc		1		
R006604	MJ1160Y	336890	5427610	Horton River	Prc		1		
R006606	MJ1226	334270	5429030	Sumac Spur 7A	Prc		1		
R006608	MJ1395	336180	5427030	Sumac Road	Prc		1		
R006609	MJ1401	330190	5426410	Lindsay River	Prc		1		
R006610	MJ1404	330130	5426320	Lindsay River	Prc	sulfide present	1	1	
R006611	MJ1407	330110	5426260	Lindsay River	Prc		1		
R006612	MJ1424	330280	5427500	Lindsay River	Prc		1		
R006613	MJ1432	330140	5427710	Lindsay River	Prc		1		
R006615	MJ1463	333940	5426250	Leigh River	Prc		1		
R006621	MJ1523A	330040	5426530	Lindsay River	Prc		1		
R006622	MJ1523B	330040	5426530	Lindsay River	Prc		1		
R006623	MJ1523C	330040	5426530	Lindsay River	Prc	phyllitic	1		
R006624	MJ1529	329880	5426490	Lindsay River	Prs	quartzite	1		
R006649	MJ2224	332980	5428540	Clearfell, end of Sumac Spur 7	Prc		1		
R006659	MJ2661	331350	5427720	Hill north of Sumac Spur 10-1	Prc?		1		
R006660	MJ151	333750	5426730	Leigh River	Pssd		1	1	
R006661	MJ531	328620	5430000	'Eel Creek'	Pssc		1		0.00
R006662	MJ533	328620	5430030	'Eel Creek'	Pssd		1		
R006663	MJ537	328790	5430170	'Eel Creek'	Pssd	laminated	1		0.07
R006664	MJ539	328890	5430190	'Eel Creek'	Pssr		1		0.09
R006665	MJ540	328920	5430280	'Eel Creek'	Pssr				0.04
R006666	MJ541	328940	5430370	'Eel Creek'	Pssm		1		0.05
R006667	MJ563	331000	5428730	Lower Leigh River	Pssd		1		0.02
R006668	MJ577	330490	5429440	Lower Leigh River	Pssc		1		0.06
R006669	MJ579	330350	5429420	Lower Leigh River	Pssr		1		0.02
R006670A	MJ609	330190	5433570	'Misty Creek'	Pssr		1		0.13
R006670B	MJ800	327040	5432890	'Slides Creek'	Psd		1		0.25
R006671	MJ812	330560	5428680	Lindsay River	Pssd		1		0.01
R006672	MJ860	329680	5430040	Lindsay River	Pssd		1		0.01
R006673	MJ861	329440	5430030	Lindsay River	Pssd		1		0.03
R006674	MJ864	329360	5430130	Lindsay River	Pssr	clast poor	1		0.07
R006675	MJ866	329330	5430170	Lindsay River	Pssr		1		0.02
R006676	MJ868	329570	5430230	'Tiger Snake Creek'	Pssr		1		0.09
R006677	MJ897	330430	5429950	'Tiger Snake Creek' — south branch	Pssd				
R006678	MJ898	330460	5429980	'Tiger Snake Creek' — south branch	Pssr				
R006679	MJ903	330390	5430270	'Tiger Snake Creek' — south branch	Pssr		1		
R006680	MJ906	330090	5430220	'Tiger Snake Creek' — south branch	Pssr		1		0.15
R006681	MJ944	329720	5430310	'Tiger Snake Creek' — north branch	Pssd				
R006682	MJ2477	336910	5426670	Near Sumac Spur 10	Pssc	black chert	1		
R006683	MJ2555	334010	5426700	Small creek south of Sumac Spur 10	Pssc?		1		
R006684	MJ2619	329850	5429320	West of lower Lindsay River	Pssc				
R006685	MJ877	331430	5430320	'Tiger Snake Creek' — south branch	Pssc		1		0.03
R006686	MJ9	335270	5426620	Leigh River Road	Psvw	lost?			

Reg. No.	Field No.	AMG (mE)	AMG (mN)	Locality	Unit	Comments	TS	CA	X
R006687	MJ54	333940	5427250	Leigh River	Psvw				
R006688	MJ542	328940	5430420	'Eel Creek'	Psvw?	fine-gr pyritic quartzarenite	1		0.17
R006689	MJ548	331510	5427740	Lower Leigh River	Psvw	hematitic	1		9.06
R006690	MJ554	331470	5427980	Lower Leigh River	Psvw		1		3.20
R006691	MJ600	330180	5433300	'Misty Creek'	Psvw		1		1.12
R006692	MJ601	330190	5433310	'Misty Creek'	Psvw		1		2.49
R006693	MJ644	330750	5431620	West of saddle	Psvw	orange-red, soft, weathered			0.13
R006694	MJ650	332420	5432080	Ridge north of Horton River	Psvw				>0.13
R006695	MJ655	330070	5434150	Low hill west of 'Misty Creek'	Psvw				1.17
R006696	MJ657	330160	5434500	Low hill west of 'Misty Creek'	Pssc?	ferruginous chert	1		1.02
R006697	MJ721	329060	5432860	South tributary of 'Laurel Creek'	Psvw	mudstone	1		0.27
R006698	MJ753	328910	5433340	Upper 'Laurel Creek'	Psvw				1.31
R006699	MJ803	327100	5432880	'Slides Creek'	Psvw		1		0.59
R006700	MJ808	327320	5432940	'Slides Creek'	Psvw		1		0.80
R006701	MJ811	330580	5428610	Lindsay River	Psvw	coarse-grain lithicwacke	1		0.82
R006702	MJ857	329820	5430040	Lindsay River	Pssc?	chert +opaques	1		0.05
R006703	MJ1085	327550	5430780	Small creek south of Frankland River	Psvw		1		>0.34
R006704	MJ1112X	327980	5431920	Small creek, SW basalt plateau	Psb?	altered	1		>0.24
R006705	MJ1115X	327750	5431700	Small creek, SW basalt plateau	Psvw				0.97
R006706	MJ1118X	327680	5431660	Small creek, SW basalt plateau	Psvw				3.25
R006707	MJ1175X	326780	5431570	'Agate Creek'	Psvw		1		
R006708	MJ1457	331510	5427610	Lower Leigh River	Psvw	altered sheared wacke	1		
R006709	MJ1458	331750	5427790	Lower Leigh River	Psvw		1		
R006710	MJ2170	326630	5439200	Blackwater Spur 6B	Psvw		1		
R006711	MJ2483	331100	5428280	Minor tributary of Leigh River	Prc?	altered	1		
R006712	MJ2484	331090	5428240	Minor tributary of Leigh River	Prc?	altered	1		
R006713	MJ2485	331090	5428220	Minor tributary of Leigh River	Prc?	altered	1		
R006714	MJ2567	330640	5428540	NW of end of Sumac Spur 10	Psvw		1		
R006715	MJ2632	329410	5429950	Small creek W of lower Lindsay River	Psvw		1		
R006716	MJ1060	330510	5428550	Lindsay River	Psvw		1		0.62
R006717	MJ603	330190	5433360	'Misty Creek'	Psvx		1		0.30
R006718	MJ604	330180	5433370	'Misty Creek'	Psvx				0.47
R006719	MJ606	330200	5433390	'Misty Creek'	Psvx		1		0.59
R006720	MJ972	332810	5431060	Small creek south of Horton River	Psvx				
R006721	MJ975	332730	5431280	Small creek south of Horton River	Psvx		1		
R006722	MJ980	332320	5431510	Small creek south of Horton River	Psvx				
R006723	MJ1003	332950	5432090	Ridge east of Lagunta Creek	Psvx		1		>0.74
R006724	MJ547	331490	5427700	Lower Leigh River	Psbb		1	1	14.0
R006725	MJ549	331510	5427760	Lower Leigh River	Psbb		1	1	31.3
R006726	MJ550	331470	5427810	Lower Leigh River	Psb	altered	1		1.65
R006727	MJ560	331110	5428380	Lower Leigh River	Psbc		1	1	53.5
R006728	MJ582	330190	5432990	'Misty Creek'	Psbb		1	1	17.8
R006729	MJ598	330160	5433220	'Misty Creek'	Psbb		1	1	0.55
R006730	MJ628	330790	5432870	Ridge east of 'Misty Creek'	Psbc		1	1	32.2
R006731	MJ634	330720	5432370	Ridge east of 'Misty Creek'	Psbc		1	1	25.2
R006732	MJ641	329910	5431450	Hill south of Horton River	Psbb		1	1	0.45
R006733	MJ647	331400	5431890	Hill SW of Horton River	Psbc		1	1	26.9
R006734	MJ651	332540	5432270	Ridge north of Horton River	Psb	weathered			39.7
R006735	MJ673	330220	5433080	Near 'Misty Creek'	Psbc		1	1	28.1
R006736	MJ674	333230	5433200	Access track — ridge top	Psb		1		24.5
R006737	MJ678	333970	5433200	Access track	Psb	weathered			6.69
R006738	MJ680	333850	5433200	Access track	Psb				5.19
R006739	MJ709	329170	5433130	'Laurel Creek'	Psbb		1	1	6.31
R006740	MJ725	328870	5432790	South tributary of 'Laurel Creek'	Psba		1	1	7.16
R006741	MJ731	328710	5432110	Southern basalt plateau	Psb		1		18.0
R006742	MJ758	328640	5433200	Headwaters, 'Laurel Creek'	Psb		1		9.70
R006743	MJ815	330290	5428740	Lindsay River	Psb	altered	1		0.23
R006744	MJ855	329810	5429970	Lindsay River	Psbc		1	1	38.0
R006745	MJ880	331290	5430320	'Tiger Snake Creek' — south branch	Psbb		1	1	
R006746	MJ962	331350	5430770	Head of north 'Tiger Snake Creek'	Psb				
R006747	MJ965	331450	5430920	Head of north 'Tiger Snake Creek'	Psbb		1	1	0.52
R006748	MJ966	331560	5430730	Head of north 'Tiger Snake Creek'	Psbc		1	1	108
R006749	MJ994	333060	5432870	Ridge east of Lagunta Creek	Psbc		1	1	32.4
R006750	MJ998	332570	5432290	Ridge east of Lagunta Creek	Psbe		1	1	48.1
R006751	MJ1009	333010	5431870	Ridge east of Lagunta Creek	Psbe		1	1	2.27
R006752	MJ1028	330910	5430180	Ridge south of 'Tiger Snake Creek'	Psbb		1	1	43.7

Reg. No.	Field No.	AMG (mE)	AMG (mN)	Locality	Unit	Comments	TS	CA	X
R006753	MJ1031	331170	5430440	Ridge south of 'Tiger Snake Creek'	Psb		1		>0.97
R006754	MJ1032	331420	5430560	Ridge south of 'Tiger Snake Creek'	Psbc		1	1	94.7
R006755	MJ1088	327520	5430850	Small creek south of Frankland River	Psbc		1	1	23.7
R006756	MJ1104X	329000	5432650	Small creek south of Frankland River	Psb		1		>9.40
R006757	MJ1455	334710	5426740	South of Sumac Spur 10	Psbc		1	1	
R006758	MJ1613	334060	5427070	Leigh River	Psbb		1	1	
R006759	MJ1617	334030	5427000	Leigh River	Psbe		1	1	
R006760	MJ1618	333840	5426800	Leigh River	Psbe		1	1	
R006761	MJ2559	334590	5426610	Coupe south of Sumac Spur 10	Psbb		1	1	
R006762	MJ1134X	327280	5433870	Sinkhole, 'Agate Flats'	Psdc				
R006763	MJ1136X	326230	5433800	Small creek, 'Agate Flats'	Psd				
R006764	MJ1139X	326200	5433690	'Agate Creek'	Psd		1		
R006765	MJ1140X	326230	5433700	'Agate Creek'	Psd		1		0.03
R006766	MJ1143X	326350	5433670	'Agate Creek'	Psd		1		
R006767	MJ1172X	326280	5432470	Small creek, 'Agate Flats'	Psdc	agate			
R006768	MJ1174X	326550	5432000	'Agate Creek'	Psdc		1		
R006769	MJ665	330660	5435580	Upper 'Misty Creek'	Pssc	chert conglomerate	1		>0.02
R006770	MJ935	339320	5430950	Dempster Plains		limonite			
R006771	MJ946	329750	5430380	'Tiger Snake Creek' — north branch	Pssc?	ferruginous chert	1		
R006772	MJ953	331750	5430020	'Tiger Snake Creek' — north branch	Pssc?	ferruginous chert	1		
R006778	MJ925	339130	5430170	Dempster Plains	Pmd		1	1	11.0
R006779	MJ1022	333110	5430540	NW of Sumac Spur 7	Pmd?	altered	1		>0.26
R006780	MJ1057	330530	5427520	End of Sumac Spur 10	Pmd		1	1	33.0
R006782	MJ1272	337910	5428260	Near end of Horton Spur 5	Pmd		1	1	
R006783	MJ1425A	330260	5427540	Lindsay River	Pmd	chilled, upstream contact			
R006784	MJ1425B	330260	5427540	Lindsay River	Pmd	chilled, downstream contact			
R006785	MJ1425	330260	5427540	Lindsay River	Pmd	centre of dyke	1	1	
R006787	MJ2552	336960	5426970	NE of Sumac Road near spur 10	Pmd		1	1	
R006790	MJ662	330010	5435240	Incorrect	Tb		1		0.74
R006791	MJ729	328380	5432200	Southern basalt plateau	Tbb		1	1	4.73
R006792	MJ760	328350	5434010	Northern basalt plateau	Tb		1		>2.95
R006793	MJ763	327840	5434370	Small creek, NW basalt plateau	Tbb		1	1	8.18
R006794	MJ790	327570	5432670	Small creek, west basalt plateau	Tb		1		5.52
R006795	MJ1109X?	328200	5432970	Small creek, SW basalt plateau	Psb	altered, labelled MJ1108	1		>0.23
R006798	MJ2173	330270	5438630	Hill, Stephens Rivulet headwaters	Tbh		1	1	
R006799	FJ447A	324640	5442890	Middle Blackwater Rivulet	Psbzp		1		
R006800	FJ447B	324640	5442890	Middle Blackwater Rivulet	Psbzp		1		
-	MJ1455A	334710	5426740	South of Sumac Spur 10		quartz-hematite vein rock	1		
-	MJ2658	331240	5428510	Between Leigh River & Sumac 7	Psb?	weathered basalt?			
-	MJ2659	331190	5428510	Between Leigh River & Sumac 7	Psb?	weathered basalt?			

Sorted by Registered Number
Geographic limits: 320 000 mE to 340 000 mE; 5 426 000 mN to 5 460 000 mN
Also includes other samples mentioned in text
TS = thin section; CA = chemical analysis: X = magnetic susceptibility 10^{-3} SI